AN EXPERIMENTAL STUDY OF

HEAT DRIVEN ABSORPTION COOLING SYSTEMS

by

ROBERTO BEST Y BROWN

Thesis submitted for the degree of Ph.D.

Department of Chemical & Gas Engineering

University of Salford

ENGLAND

1990.

TO THE MEMORY

OF MY MOTHER

CONTENTS

		Page No.
NOMENCLATURE		i
LIST OF TABLES		v
LIST OF FIGURES		viii
ACKNOWLEDGMENTS		xix
ABSTRACT		xxi
CHAPTER 1	INTRODUCTION AND PERSPECTIVES FOR HEAT PUMPS IN MEXICO	1
	1.1 ENERGY RESERVES	1
	1.2 NEED FOR HEAT PUMP TECHNOLOGY	1
	1.3 SOLAR COOLING	2
	1.4 GEOTHERMAL COOLING	3
	1.5 PROSPECTS FOR HEAT PUMPS	4
	1.6 REFERENCES	6
CHAPTER 2	HEAT PUMPS	7
	2.1 TYPES OF HEAT PUMPS	7
	2.1.1 Vapour compression heat pumps	7
	2.1.2 Vapour jet heat pumps	7
	2.1.3 Thermoelectric heat pumps	8
	2.1.4 Absorption heat pumps	8
	2.1.5 Compression-absorption heat pumps	8
	2.1.6 Absorption-resorption heat pumps	9
	2.1.7 Heat of reaction chemical heat pumps	9

Page No.

2.2 HEAT PUMPS IN PROCESS APPLICATIONS 10

2.3 SOLAR ENERGY AS HEAT SOURCE FOR ABSORPTION COOLING SYSTEMS 10

2.4 GEOTHERMAL ENERGY AS HEAT SOURCE FOR ABSORPTION COOLING SYSTEMS 12

2.5 REFERENCES 13

CHAPTER 3 THERMODYNAMIC CONSIDERATIONS FOR ABSORPTION HEAT PUMPS 21

3.1 HEAT PUMPS 21

3.2 MECHANICAL VAPOUR COMPRESSION SYSTEMS 22

3.3 HEAT DRIVEN ABSORPTION SYSTEMS 23

3.3.1 Conventional absorption heat pumps 23

3.3.2 Ideal coefficient of performance of an absorption system 25

3.3.3 Enthalpy based coefficient of performance 26

3.4 HEAT TRANSFORMERS 28

3.5 WORKING FLUID PAIRS FOR ABSORPTION SYSTEMS 29

3.5.1 Working fluid-absorbent combinations 29

3.5.2 Properties of the working fluid 29

3.5.3 Properties of the absorbent 30

3.5.4 Criteria common to all fluids 31

3.6 REFERENCES 33

Page No.

CHAPTER 4 THERMODYNAMIC DESIGN DATA FOR ABSORPTION HEAT PUMPS 38

4.1 INTRODUCTION 38

4.2 IDEAL COEFFICIENT OF PERFORMANCE OF AN ABSORPTION COOLING SYSTEM 39

4.3 IDEAL COEFFICIENT OF PERFORMANCE OF AN ABSORPTION HEATING SYSTEM 40

4.4 COEFFICIENT OF PERFORMANCE OF AN ABSORPTION HEAT TRANSFORMER 40

4.5 THERMODYNAMIC PROCESS DESIGN DATA FOR AMMONIA-WATER FOR COOLING 41

4.6 THERMODYNAMIC PROCESS DESIGN DATA FOR AMMONIA-WATER FOR HEATING 42

4.7 THERMODYNAMIC PROCESS DESIGN DATA FOR AMMONIA-WATER FOR COOLING AND SIMULTANEOUS HEATING 43

4.8 THERMODYNAMIC PROCESS DESIGN DATA FOR AMMONIA-LITHIUM NITRATE FOR COOLING 44

4.9 THERMODYNAMIC PROCESS DESIGN DATA FOR AMMONIA-LITHIUM NITRATE FOR HEATING 44

4.10 THERMODYNAMIC PROCESS DESIGN DATA FOR AMMONIA-LITHIUM NITRATE FOR COOLING AND SIMULTANEOUS HEATING 45

4.11 THERMODYNAMIC PROCESS DESIGN DATA FOR AMMONIA-WATER FOR HEAT TRANSFORMERS 45

4.12 THERMODYNAMIC PROCESS DESIGN DATA FOR AMMONIA-LITHIUM NITRATE FOR HEAT TRANSFORMERS 46

Page No.

4.13 DISCUSSION OF THERMODYNAMIC PROCESS DESIGN DATA 47

4.14 THE IMPORTANCE OF DERIVED THERMODYNAMIC DATA 47

4.15 CONCLUSIONS 48

4.16 REFERENCES 49

CHAPTER 5 MODELLING OF CONTINUOUS ABSORPTION COOLING SYSTEMS 78

5.1 INTRODUCTION 78

5.2 THERMODYNAMIC CONSIDERATIONS 78

5.3 THERMODYNAMIC PROPERTIES OF THE AMMONIA-WATER MIXTURES 81

5.4 MASS AND ENERGY BALANCES FOR THE AMMONIA-WATER ABSORPTION SYSTEM 81

5.5 MASS AND ENERGY BALANCES FOR THE AMMONIA-LITHIUM NITRATE ABSORPTION SYSTEM 84

5.6 RESULTS AND DISCUSSION 87

5.7 CONCLUSIONS 90

5.8 REFERENCES 92

CHAPTER 6 EXPERIMENTAL STUDIES ON THE PERFORMANCE OF THE ABSORBER OF AN ABSORPTION COOLING SYSTEM 105

6.1 INTRODUCTION 105

6.2 THERMODYNAMIC CONSIDERATIONS 106

6.3 EXPERIMENTAL 108

6.4 RESULTS 109

6.5 CONCLUSIONS 110

6.6 REFERENCES 111

Page No.

CHAPTER 7 A STUDY ON THE OPERATING CHARACTERISTICS OF AN EXPERIMENTAL ABSORPTION COOLER USING TERNARY SYSTEMS 118

7.1 INTRODUCTION 118

7.2 EXPERIMENTAL 120

7.3 RESULTS AND DISCUSSION 121

7.4 CONCLUSIONS 123

7.5 REFERENCES 125

CHAPTER 8 EXPERIMENTAL STUDIES WITH AN AMMONIA-WATER ABSORPTION SYSTEM USING A FALLING FILM GENERATOR FOR SOLAR COOLING 137

8.1 INTRODUCTION 137

8.2 DESIGN CONSIDERATIONS 138

8.3 EQUIPMENT DETAILS 138

8.4 EXPERIMENTAL PROCEDURE 141

8.5 RESULTS AND DISCUSSION 141

8.6 CONCLUSIONS 143

8.7 REFERENCES 144

CHAPTER 9 EXPERIMENTAL STUDIES WITH AN AMMONIA-WATER ABSORPTION SYSTEMS OPERATING ON LOW ENTHALPY GEOTHERMAL ENERGY 157

9.1 INTRODUCTION 157

9.2 EXPERIMENTAL FOR INSTALLATION AT LOS AZUFRES 158

9.2.1 Equipment 158

9.2.2 Experimental procedure 160

Page No.

9.2.3 Results and discussion for installation at Los Azufres 161

9.3 EXPERIMENTAL FOR INSTALLATION AT CERRO PRIETO 163

9.3.1 Equipment 163

9.3.2 Results and discussion for installation at Cerro Prieto 164

9.4 CONCLUSIONS 166

9.5 REFERENCES 167

CHAPTER 10 CONCLUSIONS AND RECOMMENDATIONS 185

10.1 CONCLUSIONS 185

10.2 RECOMMENDATIONS 188

APPENDIX 1 DERIVED THERMODYNAMIC DESIGN DATA FOR ABSORPTION HEAT PUMP SYSTEMS 190

APPENDIX 2 RAW EXPERIMENTAL DATA 287

BIBLIOGRAPHY 348

AUTHOR'S PUBLICATIONS 361

NOMENCLATURE

A	cross sectional area of absorber, m^2
C_L	heat capacity per unit mass of solution, kJ kg^{-1} K^{-1}
(COP)	coefficient of performance, dimensionless
$(COP)_A$	actual coefficient of performance, dimensionless
$(COP)_{ACL}$	actual coefficient of performance for cooling, dimensionless
$(COP)_{AH}$	actual coefficient of performance for heating, dimensionless
$(COP)_{AT}$	actual coefficient of performance for a heat transformer, dimensionless
$(COP)_C$	Carnot coefficient of performance, dimensionless
$(COP)_{CL}$	coefficient of performance for cooling, dimensionless
$(COP)_{CCL}$	Carnot coefficient of performance for cooling, dimensionless
$(COP)_{CH}$	Carnot coefficient of performance for heating, dimensionless
$(COP)_{CT}$	Carnot coefficient of performance for a heat transformer, dimensionless
$(COP)_{ECL}$	enthalpy based coefficient of performance for cooling, dimensionless
$(COP)_{EH}$	enthalpy based coefficient of performance for heating, dimensionless
$(COP)_{ET}$	enthalpy based coefficient of performance for a heat transformer, dimensionless
$(COP)_H$	coefficient of performance for heating, dimensionless
(CR)	compression ratio, dimensionless

ETA1	economiser efficiency, dimensionless
ETA2	precooler efficiency, dimensionless
$(FR)_A$	actual flow ratio, dimensionless
(FR)	flow ratio, dimensionless
H	enthalpy per unit mass, kJ kg^{-1}
K	mass transfer coefficient, mh^{-1}
M	mass flow rate, kg s^{-1} or kg h^{-1}
M_{AM}	mass flow rate of ammonia, kg s^{-1}
M_L	mass flow rate of solution, kg h^{-1}
M_W	mass flow rate of water as working fluid kg h^{-1}
N_D	refractive index, dimensionless
$(N)_{GE}$	generator efficiency, dimensionless
$(N)_{REC}$	recuperator (economiser) efficiency, dimensionless
P	pressure, bar or MPa
P_{AB}	pressure in absorber, bar
P_{CO}	pressure in condenser, bar
P_{EV}	pressure in evaporator, bar
P_{GE}	pressure in generator, bar
P_R	pressure of refrigerant, bar
P_{REC}	pressure in rectifier, bar
Q	heat load, W or kW
Q_{AB}	heat load in absorber, W or kW
Q_{CO}	heat load in condenser, W or kW
Q_{EV}	heat load in evaporator W or kW
Q_{GE}	heat load in generator W or kW
Q_{REC}	heat load in rectifier, W or kW
Q_1	heat load in economiser, W or kW
Q_{11}	heat load in precooler, W or kW
T	temperature, °C or K

T_L	solution temperature, °C or K
T'	refrigerant temperature, °C
T_{AB}	temperature in absorber, °C
T_{CO}	temperature in condenser, °C
T_{EV}	temperature in evaporator, °C
T_{GE}	temperature in generator, °C
T_{REC}	temperature in rectifier, °C
W	rate of work delivered to the shaf of compressor, W or kW
W_P	rate of work delivered by solution pump, W or kW
X	weight fraction, or weight percent, dimensionless
X^*	equilibrium concentration of water at the bulk absorber solution temperature and pressure, weight fraction, dimensionless
X_B	actual concentration of water at the bulk absorber solution temperature and pressure, weight fraction, dimensionless
X_R	concentration of refrigerant at condenser outlet, weight fraction, dimensionless

GREEK LETTERS

ρ	density, kg m^{-3}
η	absorption ratio, dimensionless

SUBSCRIPTS

A	actual
AB	absorber
AM	ammonia
CO	condenser
GS	cold storage
DE	desorption
E	enthalpy
FD	feed solution to absorber
EV	evaporator
GE	generator
H	heating
HS	heat source
L	solution
R	refrigerant
RE	resorption
REC	rectifier
RF	reflux
W	water
WAB	water to absorber
WCO	water to condenser

LIST OF TABLES

		Page No.
Table 8.1	Operating conditions of the ammonia-water refrigeration prototype.	146
Table A1.1	Derived thermodynamic design data for absorption systems operating on ammonia-water for cooling.	190
Table A1.2	Derived thermodynamic design data for absorption systems operating on ammonia-water for heating.	201
Table A1.3	Derived thermodynamic design data for absorption systems operating on ammonia-water for cooling and simultaneous heating.	210
Table A1.4	Derived thermodynamic design data for absorption systems operating on ammonia-lithium nitrate for cooling.	219
Table A1.5	Derived thermodynamic design data for absorption systems operating on ammonia-lithium nitrate for heating.	240
Table A1.6	Derived thermodynamic design data for absorption systems operating on ammonia-lithium nitrate for cooling and simultaneous heating.	250

		Page No.
Table A1.7	Derived thermodynamic design data for absorption heat transformers operating on ammonia-water.	266
Table A1.8	Derived thermodynamic design data for absorption heat transformers operating on ammonia-lithium nitrate.	274
Table A2.1	Raw experimental performance data for the operating characteristics of the water-lithium bromide absorption cooler.	287
Table A2.2	Raw experimental performance data for the operating characteristics of the water-lithium bromide-zinc bromide absorption cooler.	290
Table A2.3	Raw experimental performance data for the operating characteristics of the water-lithium bromide-lithium iodide absorption cooler.	294
Table A2.4	Raw experimental performance data for the operating characteristics of the ammonia-water absorption refrigerator operated with geothermal steam at Los Azufres, Michoacán, México.	297

Page No.

Table A2.5 Raw experimental performance data for the operating characteristics of the ammonia-water absorption system at UNAM. 302

Table A2.6 Raw experimental performance data for the operating characteristics of the ammonia-water absorption refrigerator at the Cerro Prieto geothermal field. 318

LIST OF FIGURES

		Page No.
2.1	Mechanical vapour compression heat pump	16
2.2	Vapour jet heat pump	17
2.3	Absorption heat pump	18
2.4	Resorption heat pump	19
2.5	Absorption-resorption heat pump	20
3.1	Mechanical vapour compression heat pump	34
3.2	Absorption heat pump	35
3.3	Schematic diagram for a conventional absorption heat pump	36
3.4	Simplified block diagram for a basic absorption heat transformer	37
4.1	Simplified block diagram for a basic absorption heat pump	51
4.2	Absorption cycle on an equilibrium chart for the ammonia-water system	52
4.3	Simplified block diagram for a basic absorption heat transformer	53
4.4	Plot of coefficients of performance and flow ratio against generator temperature at three different absorber temperatures	54
4.5	Plot of coefficients of performance and flow ratio against condenser temperature at three different absorber temperatures	55
4.6	Plot of coefficients of performance and flow ratio against evaporator temperature at three different absorber temperatures	56

Page No.

4.7	Plot of coefficients of performance and flow ratio against generator temperature at three different absorber temperatures	57
4.8	Plot of coefficients of performance and flow ratio against condenser temperature at three different absorber temperatures	58
4.9	Plot of coefficients of performance and flow ratio against evaporator temperature at three different absorber temperatures	59
4.10	Plot of coefficient of performance and flow ratio against generator temperature at three different absorber temperatures	60
4.11	Plot of coefficients of performance and flow ratio against condenser temperature at three different absorber temperatures	61
4.12	Plot of coefficients of performance and flow ratio against evaporator temperature at three different absorber temperatures	62
4.13	Plot of coefficients of performance and flow ratio against generator temperature at three different absorber temperatures	63

Page No.

4.14 Plot of coefficients of performance and flow ratio against condenser temperature at three different absorber temperatures 64

4.15 Plot of coefficients of performance and flow ratio against evaporator temperature at three different absorber temperatures 65

4.16 Plot of coefficients of performance and flow ratio against generator temperature at three different absorber temperatures 66

4.17 Plot of coefficients of performance and flow ratio against condenser temperature at three different absorber temperatures 67

4.18 Plot of coefficients of performance and flow ratio against evaporator temperature at three different absorber temperatures 68

4.19 Plot of coefficients of performance and flow ratio against generator temperature at three different absorber temperatures 69

4.20 Plot of coefficients of performance and flow ratio against condenser temperature at three different absorber temperatures 70

Page No.

4.21 Plot of coefficients of performance and flow ratio against evaporator temperature at three different absorber temperatures 71

4.22 Plot of coefficients of performance and flow ratio against absorber temperature at three different temperatures of the evaporator and generator 72

4.23 Plot of coefficients of performance and flow ratio against absorber temperature at three different temperatures of condenser 73

4.24 Plot of coefficients of performance and flow ratio against generator temperature at three different temperatures of the absorber 74

4.25 Plot of coefficients of performance and flow ratio against absorber temperature at three different condenser temperatures 75

4.26 Plot of coefficients of performance and flow ratio against absorber temperature at three different generator temperatures 76

		Page No.
4.27	Plot of coefficients of performance and flow ratio against generator temperature at three different absorber temperatures	77
5.1	Ammonia-water absorption refrigeration system	93
5.2	Ammonia-lithium nitrate absorption refrigeration system	94
5.3	Coefficient of performance $(COP)_{ECL}$ against generator temperature (T_{GE}) at different condenser temperatures for ammonia-water	95
5.4	Coefficient of performance $(COP)_{ECL}$ against generator temperature (T_{GE}) at different condenser temperatures (T_{CO}) for ammonia-lithium nitrate	96
5.5	Coefficient of performance $(COP)_{ECL}$ against generator temperature (T_{GE}) at different absorber temperatures (T_{AB}) for ammonia-water	97

Page No.

5.6 Coefficient of performance $(COP)_{ECL}$ against generator temperature (T_{GE}) at different absorber temperatures (T_{AB}) for ammonia-lithium nitrate 98

5.7 Coefficient of performance $(COP)_{ECL}$ against generator temperature for both ammonia-water and ammonia-lithium nitrate 99

5.8 Coefficient of performance $(COP)_{ECL}$ against condenser temperature (T_{CO}) for both ammonia-water and ammonia-lithium nitrate mixtures 100

5.9 Coefficient of performance $(COP)_{ECL}$ against absorber temperature (T_{AB}) for both ammonia-water and ammonia-lithium nitrate 101

5.10 Coefficient of performance $(COP)_{ECL}$ against evaporator temperature (T_{EV}) for both ammonia-water and ammonia-lithium nitrate mixtures 102

		Page No.
5.11	Coefficient of performance $(COP)_{ECL}$ against economiser efficiency (ETA1) for both ammonia-water and ammonia-lithium nitrate mixtures	103
5.12	Coefficient of performance $(COP)_{ECL}$ against precooler efficiency (ETA2) for both ammonia-water and ammonia-lithium nitrate mixtures	104
6.1	Flow diagram for the modified absorber with controlled reflux	112
6.2	Schematic diagram for the experimental absorber cooler	113
6.3	Actual coefficient of performance $(COP)_A$ and flow ratio (FR) against generator temperature (T_{GE})	114
6.4	Absorption ratio (η_{AB}) against flow ratio (FR)	115
6.5	Temperature rise of the solution in the absorber against absorber length	116

Page No.

6.6 Amount of water absorbed against heat load in evaporator 117

7.1 Concentration against crystallization Temperature adapted from Ohuchi; (1985) 127

7.2 Vapour pressure against concentration by weight with isotherms for aqueous solution of lithium iodide 128

7.3 Schematic diagram of absorption cooler 129

7.4 Actual coefficient of performance $(COP)_A$ and temperature levels in absorption cooler against flow ratio (FR) 130

7.5 Heat loads against flow ratio (FR) 131

7.6 Coefficient of performance $(COP)_A$ and temperature levels against flow ratio (FR) 132

7.7 Coefficient of performance $(COP)_A$ and temperature levels against mass flow rate of solution M_{AB} 133

7.8 Heat loads against mass flow rate of solution M_{AB} 134

Page No.

7.9 Coefficient of performance $(COP)_A$ and temperature levels against flow ratio (FR) 135

7.10 Heat loads against flow ratio (FR) 136

8.1 Theoretical cycle conditions for the ammonia-water system 147

8.2 Simplified block diagram of an absorption cooler 148

8.3 Schematic diagram fo experimental absorption cooler 149

8.4 Generator 150

8.5 Absorber 151

8.6 Generator heat load against generator temperature 152

8.7 Evaporator heat load against generator temperature 153

8.8 Generator temperature against flow ratio 154

8.9 Actual coefficient of performance against generator temperature 155

Page No.

8.10 Actual coefficient of performance against flow ratio 156

9.1 Schematic diagram of experimental absorption cooler 168

9.2 Schematic diagram of generator 169

9.3 Schematic diagram of absorber 170

9.4 Temperature and flow rates against time 171

9.5 Temperatures against flow ratio 172

9.6 Coefficient of performance and heat loads against generator temperature 173

9.7 Generator temperature against coefficient of performance 174

9.8 Schematic diagram of the ammonia-water absorption refrigeration system 175

9.9 Experimental ammonia-water absorption refrigeration system at the Cerro Prieto geothermal field 176

9.10 Cooling water system 177

Page No.

9.11 Actual flow ratio vs flow ratio 178

9.12 Actual flow ratio vs actual coefficient of performance 179

9.13 Actual flow ratio vs evaporator heat load 180

9.14 Actual flow ratio vs generator efficiency 181

9.15 Recuperator efficiency vs actual coefficient of performance 182

9.16 Actual flow ratio vs recuperator efficiency 183

9.17 Generator temperature vs coefficient of performance 184

ACKNOWLEDGMENTS

I wish to express my deep thanks to the Instituto de Investigaciones en Materiales, UNAM for giving me the opportunity to carry out work on heat driven cooling systems.

I also wish to thank the Instituto de Investigaciones Eléctricas for supporting my participation in the IIE/University of Salford cooperative programme and the use of experimental facilities.

I am grateful to Professor F.A. Holland for the supervision of this thesis and for his continuous valuable advice.

I am also grateful to the members of the heat pump research group at Salford, specially to Dr. M.A.R. Eisa for their stimulating companionship.

I extend my thanks to the applied thermodynamics group and the workshop staff at the Laboratorio de Energía Solar, UNAM, for their help with the experimental equipment and helpful advice.

I do wish to thank the integrated exploitation group and technical staff of the Geothermal Department at IIE for their assistance in the construction of the experimental equipment. Special thanks to Dr. Christopher Heard and Mr. Hipólito Fernández for their invaluable help and support.

I am indebted with Mrs. María Eugenia Calderón for the diligent and excellent typing of this thesis.

I also want to thank Mr. Adrián Patiño for redrawing most of the diagrams in this thesis.

ABSTRACT

The great need for cooling combined with Mexico's large availability of low enthalpy energy from non conventional energy resources such as geothermal energy, solar heat and waste heat from industrial processes, makes it very attractive to utilize these resources for cooling using heat driven absorption systems.

The main purpose of the work described in this thesis is to obtain experimental and theoretical data on heat driven absorption cooling systems for the design of large scale systems.

Thermodynamic design data have been theoretically derived for heat driven absorption heat pumps and heat transformers using the working pairs ammonia-water and ammonia-lithium nitrate for cooling, heating and simultaneous heating and cooling. The interaction between the operating parameters has been illustrated graphically.

A computer model of the steady state thermodynamics of a heat driven ammonia-water system and an ammonia-lithium nitrate system has been developed. A comparison of both systems is made by assessing the effect of operating temperatures and heat exchanger effectiveness on the coefficient of performance for cooling and the heat transfer rates within the system.

An experimental study on the performance of the absorber of an absorption cooling system operating on water-lithium bromide has been made. The experimental study of the adiabatic absorber was concerned with the determination of the effect of the evaporator heat load and the absorber reflux on the performance of the absorber.

An experimental study of the operating characteristics of an experimental absorption cooler using water-lithium bromide-lithium iodide and water-lithium bromide-zinc bromide as ternary systems has been made in order to achieve higher coefficients of performance and a lower risk of crystallization.

Experimental studies with a small heat driven absorption cooling system operating on ammonia-water using a falling film generator were made. Low generator temperatures were achieved which will enable the use of non focussing solar collectors as a heat source for the system.

An ammonia-water absorption cooler operating on low enthalpy geothermal energy was installed and operated at two geothermal fields. The system was used to cool a small cold storage facility below freezing temperatures.

The experimental and theoretical results on absorption cooling systems will provide a basis for the design of heat pump systems for industrial and commercial applications.

CHAPTER 1

INTRODUCTION AND PERSPECTIVES FOR HEAT PUMPS IN MEXICO

1.1 ENERGY RESERVES

Even though Mexico has large proven reserves of hydrocarbons, about 420 EJ, where 1EJ = 10^{18}J, the diversification of energy sources and energy conservation measures are necessary: (i) there are technical and economic limits on the volume of hydrocarbons which can be extracted from the earth, (ii) there are also restrictions on the acquisition of foreign currency needed for industrial development; the by-products of the hydrocarbons industry are of great importance, (iii) the cost per Joule for non-renewable sources may possibly increase, and (iv) an ecologically needed limit to the CO_2 emissions may be imposed.

1.2 NEED FOR HEAT PUMP TECHNOLOGY

Heat pump technology for both heating and cooling has considerable industrial and commercial potential in Mexico. Mexico has vast reserves of low grade heat in the form of geothermal energy, solar heat and waste heat from industrial processes. Heat pumps can be used to increase the temperature of this low grade heat to a more useful level, for example to produce low pressure steam. Alternatively the low grade heat can be fed to a heat driven absorption cooler or refrigeration system. It has been estimated that, in Mexico, between 35 and 50% of all the food produced is lost because of inadequate handling and cooling facilities with sea food having the highest loss [1.1]. Since Mexico is also importing large quantities of food, this is a major economic burden. Mexico's vast resources of low grade heat could be used to operate large scale heat driven absorption

refrigeration units for the storage of perishable foodstuffs.

Spauschus [1.2] has published data on the world market for refrigeration and air conditioning equipment. The study showed that North America, Japan and Europe produce and purchase almost 90% of the refrigeration equipment in the world, although they account for less than 25% of the world population. The Middle East, Africa, China, India and the USSR, with 59% of the world population, produce and purchase less than 5% of the refrigeration equipment in the world. Latin America, with 10% of the world population, produces and purchases 6% of the refrigeration equipment in the world.

The enormous potential demand for refrigeration in the less developed regions of the world, will need to be met by all the available technologies and energy sources. The low enthalpy heat from solar radiation, geothermal fluids and biomass can play an important role in meeting this demand.

1.3 SOLAR COOLING

Solar energy can be used to produce cooling in two distinct ways. The most common way is to convert solar radiation to thermal energy to drive a Rankine/Rankine vapour compression system, an absorption cooler or a desiccant system. The other approach is to convert solar radiation directly into electricity using solar cells to drive electric cooling units. This last method of cooling has been restricted to small size systems such as refrigerated boxes for vaccine conservation due to the high cost of the solar cells.

Of the various solar thermal driven systems the most common and most developed is the absorption refrigeration system. These systems have the advantage that they do not require compressors which are not always readily

available in developing countries.

Present costs of solar cooling systems are high, although an analysis made showed that solar refrigeration could be economically feasible already in certain areas of Mexico and other developing countries in regions without interconnected electricity grids.

A recent study [1.3] summarizes the main improvements needed to make solar cooling cost effective:

(i) reduction in the cost of solar collectors by using lightweight and inexpensive materials with improved optical and thermal efficiencies.

(ii) increase in the efficiency (COP) of the absorption system as a result of improvements in absorption technology.

1.4 GEOTHERMAL COOLING

It has been estimated by Mercado [1.4] that the potential reserves of high enthalpy geothermal energy, for the generation of electricity in Mexico, could be larger than 1 EJ yr^{-1}. Nevertheless, the forseen installed capacity in the year 2000 would only be generating about 91.5 PJ yr^{-1} where $1PJ = 10\ J^{15}$.

Low enthalpy resources predominate over the high enthalpy ones in a proportion of 10 to 1 [1.5]. If a range of temperatures from 140 to 200°C is considered, the proportion is reduced to 4 to 1 [1.6] and another 1 EJ yr^{-1} could be added for electricity generation using organic Rankine cycle (ORC) technology.

Mexico possesses large amounts of geothermal brine at temperatures which are too low to enable electricity to be generated efficiently and economically. Of the possible non-electric uses of low and medium enthalpy geothermal energy, the one which appears to have the greatest potential is the use of heat driven absorption systems to provide cold storage facilities for perishable food.

Most of the geothermal fields in Mexico are located near important agricultural areas. The largest geothermal field in Mexico is at Cerro Prieto which is near the growing city of Mexicali in Baja California. Mexicali is on the border with the U.S. state of California.

1.5 PROSPECTS FOR HEAT PUMPS

To date, little use has been made of Mexico's vast reserves of low grade energy, even though relatively risk free technology is available to upgrade and use it for useful and profitable purposes. Energy conservation and a more efficient use of available energy are an essential basis for future economic growth and international competitiveness. The national aims, in accordance with the National Commission for Energy Savings, should be to

(i) increase the gross national product per unit of primary energy consumed,

(ii) curtail the growth of indigenous hydrocarbon consumption,

(iii) enable Mexico to continue to benefit from an energy export income well beyond the year 2000

and

(iv) reduce environmental pollution.

Since heat pump technology can make a significant contribution to all these national aims, an investment in heat pump technology is an investment in the future.

Energy prices well below international levels and the lack of readily available equipment have inhibited indigenous developments in heat pump technology in Mexico. With the progressive opening up of international trade and development, the use of heat pumps to recycle heat energy in industrial processes should prove to be highly economic in the long term.

1.6 REFERENCES

1.1 J.C. Lague, personal communication.

1.2 H.O. Spauschus, Development in refrigeration: technical advances and opportunities for the 1990, Int. J. Refrig. 10, 263-270 (1987).

1.3 M.L. Warren and M. Wahlig, Cost and performance goals for commercial active solar absorption cooling systems, J. Solar Energy Engineering, 107 (2), 136-140 (1985).

1.4 S. Mercado, Mexico, Generando energía con el calor de la tierra, Revista de la Asociación Mexicana de Ingenieros Mecánicos y Electricistas, 22, 15-23 (1988).

1.5 S. Mercado, H. Fernández, J. Frías, A. Sánchez and F. Villaseñor, Potencial geotérmico de México en reservorios de baja entalpia y experimentación en plantas de ciclo binario de 10 kW y 50 kW, Proc. XI Conferencia IEEE Mexicon 83, Cuernavaca, Mor., pp 121-125 (1983).

1.6 C.L. Heard, H. Fernández and F.A. Holland, Developments in geothermal energy in Mexico-Part Twenty seven: The potential for geothermal organic Rankine cycle power plants in Mexico, J. Heat Recovery Systems and CHP, 10 (2), 79-86 (1990).

CHAPTER 2

HEAT PUMPS

2.1 TYPES OF HEAT PUMPS

2.1.1 VAPOUR COMPRESSION HEAT PUMPS

The most common type of heat pump is the vapour compression heat pump using a mechanical compressor, as shown schematically in Figure 2.1. It consists of a compressor, two heat exchangers an expansion valve and a working fluid. In the evaporator heat exchanger the working fluid evaporates at a temperature T_{EV} whilst extracting an amount of heat Q_{EV} from the source. The working fluid is then compressed to give up an amount of latent heat Q_{CO} at a higher temperature T_{CO} in the condenser heat exchanger. The condensed working fluid is then expanded through the expansion valve to the low evaporating pressure and is returned to the evaporator to complete the cycle. In Chapter 3 the thermodynamic basis of vapour compression heat pumps is discussed.

2.1.2 VAPOUR JET HEAT PUMPS

This system shown schematically in Figure 2.2 is analogous to a typical compression cycle with the mechanical compressor replaced by a vapour-jet ejector. In the injection nozzle, the drive vapour is expanded and a vapour jet with a velocity several times the velocity of sound is produced. This carries forward the expansion vapour and accelerates it. Because of the decreased pressure on the suction side, evaporation takes place and the vapour is cooled by extracting the evaporation enthalpy. The pressure of the vapour mixture is increased in the diffuser to the condensing pressure

P_{CO} at which condensing can take place in the condenser. Such systems are worth consideration when waste heat is available in the form of reasonably high pressure steam to act as the driving force for the jet. The system has the advantages of mechanical simplicity and low technology maintenance.

2.1.3 THERMOELECTRIC HEAT PUMPS

The principle of this type of heat pump is based on the fact that if a direct voltage is applied to a junction of two different electrical conductors so that an electric current flows, the joint is cooled or heated, depending on the direction on which the current flows. This thermoelectric effect provides the means for pumping heat without using moving parts. Heat exchangers are required at hot and cold junctions to transfer heat as needed.

2.1.4 ABSORPTION HEAT PUMPS

In the heat driven absorption heat pump the condensation, expansion and evaporation of the working fluid are the same as in the conventional compressor driven systems. However, in the absorption cycle, the compressor is replaced by a secondary circuit in which a liquid absorbent is circulated by a pump, as it is shown schematically in Figure 2.3. Details of absorption heat pumps are discussed in Chapter 3 of this Thesis.

2.1.5 COMPRESSION-ABSORPTION HEAT PUMPS

The compression-absorption heat pump shown schematically in Figure 2.4 consists of a combination of a compression heat pump and an absorption heat pump. It utilizes a binary or multicomponent mixture as the working fluid. An amount of heat Q_{DE} is transferred from the heat source to the desorber in which a small proportion of the more volatile component of the mixture

evaporates. The vapour leaving the desorber is compressed to the high pressure P_{RE} prevailing in the resorber. The strong absorbent solution from the desorber is pumped into the resorber. In the resorber the vapour is reabsorbed into the solution producing an amount of heat Q_{RE} at a relatively higher temperature T_{RE}. The weak absorbent solution is then expanded through an expansion valve before entering into the desorber to complete the cycle.

2.1.6 ABSORPTION-RESORPTION HEAT PUMPS

The absorption-resorption heat pump is shown schematically in Figure 2.5. The difference between this cycle and the conventional absorption cycle is that in the absorption-resorption cycle the condenser and the evaporator are replaced by a second solution loop called the resorption loop. This comprises a second absorber called resorber and a second generator called desorber. The absorption-resorption cycle makes it possible to operate at high temperatures and with lower pressure levels compared to those of the conventional absorption equipment.

2.1.7 HEAT OF REACTION CHEMICAL HEAT PUMPS

Chemical heat pumps utilize chemical reactions that involve formation of chemically stable products from chemically stable reactants by way of electron transfer or sharing associated with the breakage and formation of new bonds. In a typical chemical heat pump a low temperature source is used to drive an endothermic reaction and heat is liberated at a higher temperature by an exothermic reaction to deliver heat to a process stream.

2.2 HEAT PUMP IN PROCESS APPLICATIONS

Absorption heat pumps, either for heating or cooling, have enormous potential for primary energy savings in both domestic and industrial aspects. Moser and Schnitzer [2.1] described in detail a wide variety of process applications of heat pumps. Bjustrom and Raldow [2.2] gave a literature survey on the wide range of applications of the absorption process from household refrigerators to topping process in power plants. Hodgett [2.3] described the developments in absorption heat pumps in Europe since 1974 both for residential and commercial uses. Hana and Wilkinson [2.4] described the developments on absorption heat pumps for the same period in U.S.A. Bogart [2.5] presented a comprehensive book on the design of ammonia-water refrigeration plants in industrial processes. Zimmerman [2.6] presented a number of industrial applications in various nations. Zegers and Miriam [2.7z presented the most recent developments in absorption heat pumps. Holland and Heard [2.8] presented a selection of papers on energy conservation and industrial and commercial applications of heat pumps.

2.3 SOLAR ENERGY AS HEAT SOURCE FOR ABSORPTION COOLING SYSTEMS

The thermal energy produced by solar collectors can be used instead of a fuel fired heater to operate an absorption unit. The fuel fired heater provides a backup capability for periods when solar radiation is not available and the thermal storage is depleted.

Solar air conditioning systems with water-lithium bromide as the working pair are sold commercially and have proven to be efficient working with flat plate collectors [2.9, 2.10]. In order to use flat plate collectors efficiently it is necessary for the system to be water cooled. This is a

great problem for the large scale use of the solar cooling systems in hot arid zones, although a study showed that in arid areas with low wet-bulb temperatures the cooling tower coupled with the chiller could handle loads much higher than the rated capacity [2.11]. Air cooling implies condenser and absorber temperatures 15°C or more above temperatures possible with water cooling which in turn necessitates generator temperatures well in excess of 100°C. Such temperatures are in the limit of efficient flat plate collector performance.

Double effect water-lithium bromide systems with (COP) values higher than 1.0 are available but require heat source temperatures above 150°C which imposes the use of concentrating or evacuated tube solar collectors.

The use of water as a refrigerant is limited to evaporator temperatures above 0°C. The most common absorption system for below freezing applications is the ammonia-water system where ammonia is the refrigerant. Although ammonia-water systems have also been designed as direct fired air-cooled water chillers they are less efficient than the water-lithium bromide systems [2.12]. The development of commercial solar ammonia-water systems for food conservation would appear to have a great potential in the developing countries. Conventional ammonia-water systems operate with generator or heat supply temperatures in excess of 150°C. The development of efficient ammonia-water refrigeration systems operating with low enthalpy heat from solar collectors could help to meet the enormous demand for refrigeration in the less developed regions of the world.

2.4 GEOTHERMAL ENERGY AS HEAT SOURCE FOR ABSORPTION COOLING SYSTEMS

The vast bulk of geothermal energy is at too low a temperature to economically produce electricity using Rankine power cycle plants, so that currently only a tiny proportion of the world's geothermal energy is made use of.

Geothermal energy can be used to provide cooling for human comfort. Reynolds [2.13] gave a description of a geothermal energy driven commercial absorption chiller with a capacity of 445 kW (130 tons). Hot geothermal water at 150°C with a total salt content of 1786 ppm was used in a secondary heat exchanger to heat clean water to 121°C to drive the water-lithium bromide absorption chiller. Kumar [2.14] described the potential for geothermal cooling in India and the utilization of heat recovered from dry or abandoned wells and of waste natural gas. The potential for heat pump technology utilizing geothermal energy for cooling, heating and simultaneous heating and cooling has been discussed by Best et al [2.15].

2.5 REFERENCES

2.1 F. Moser and H. Schnitzer, Heat pumps for industry, Elsevier, Amsterdam, (1985).

2.2 H. Bjustrom and W. Raldow, The absorption process for heating, cooling and energy storage in a historical survey, Int. J. Energy Research, 5, 43-59 (1981).

2.3 D.L. Hodgett, Absorption heat pumps and working pair developments in Europe since 1974, New working pairs for absorption processes, Proceedings of a workshop in Berlin, Published by Swedish Building Research Association, pp 55-70, (1982).

2.4 W.T. Hana and W.H. Wilkinson, Absorption heat pumps and working pair developments in the United States since 1974, New working pairs for absorption processes, Proceedings of a workshop in Berlin, Published by Swedish Building Research Association, pp 71-81, (1982).

2.5 M. Bogart, Ammonia absorption refrigeration in industrial processes, Gulf Publishing Company, (1981).

2.6 K.H. Zimmerman, (Ed), Heat pumps, prospects in heat pump technology and marketing, Lewis Publishers, (1987).

2.7 P. Zegers and J. Miriam, (Ed), Absorption heat pumps, Proceedings of a workshop held in London, Published by the Commission of the European Communities, (1988).

2.8 F.A. Holland and C.L. Heard, (Ed), Handbook on heat pump technology, Instituto de Investigaciones Eléctricas, Cuernavaca, Mexico, (1990).

2.9 D.S. Ward, Solar absorption cooling feasibility, Solar Energy, 22, 259-268, (1969).

2.10 W.J. Biermann, An absorption machine for solar cooling, ASHRAE Transactions, No. 2, 406-412. (1979).

2.11 A.H. Uppal and T. Muneer, Cost analysis of commercial solar absorption coolers using a detailed simulation procedure, Applied Energy 26, 75-82, (1987).

2.12 ASHRAE Handbook, Fundamentals, American Society of Heating, Refrigerating and Air-conditioning Engineers, Inc., (1985).

2.13 G. Reynolds, Cooling with geothermal heat, Geothermics, Special issue, 1658-1661, (1970).

2.14 R. Kumar, Feasibility of waste recovery concepts for geothermal refrigeration and air conditioning, Heat Recovery Systems, 6 (6), 499-502, (1986).

2.15 R. Best, C.L. Heard and F.A. Holland, Developments in geothermal energy in Mexico-Part Sixteen. The potential for heat pump technology, J. Heat Recovery Systems and CHP, Vol. 8 (3), 185-202, (1988).

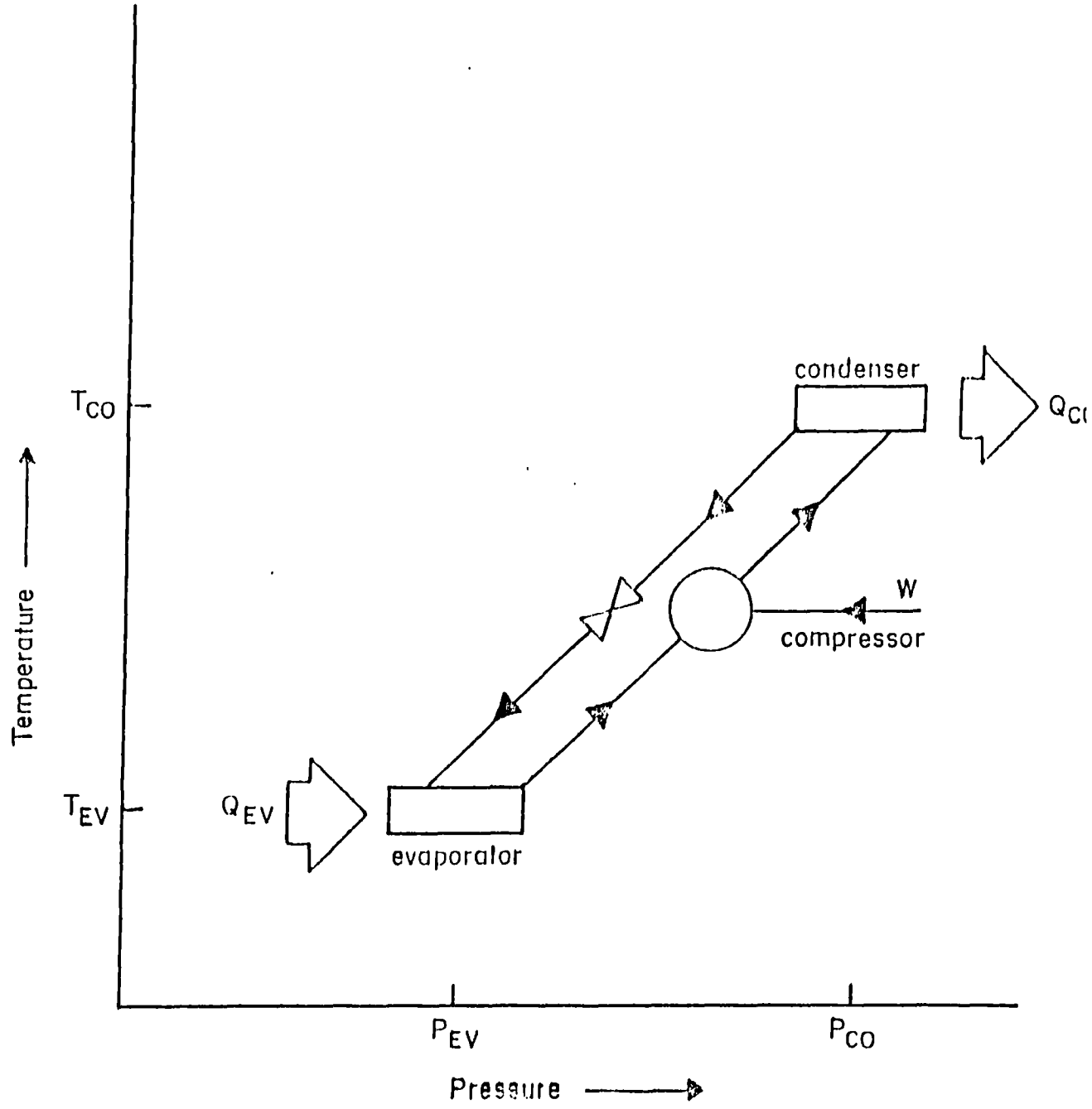

Fig. 2.1 Mechanical vapour compression heat pump.

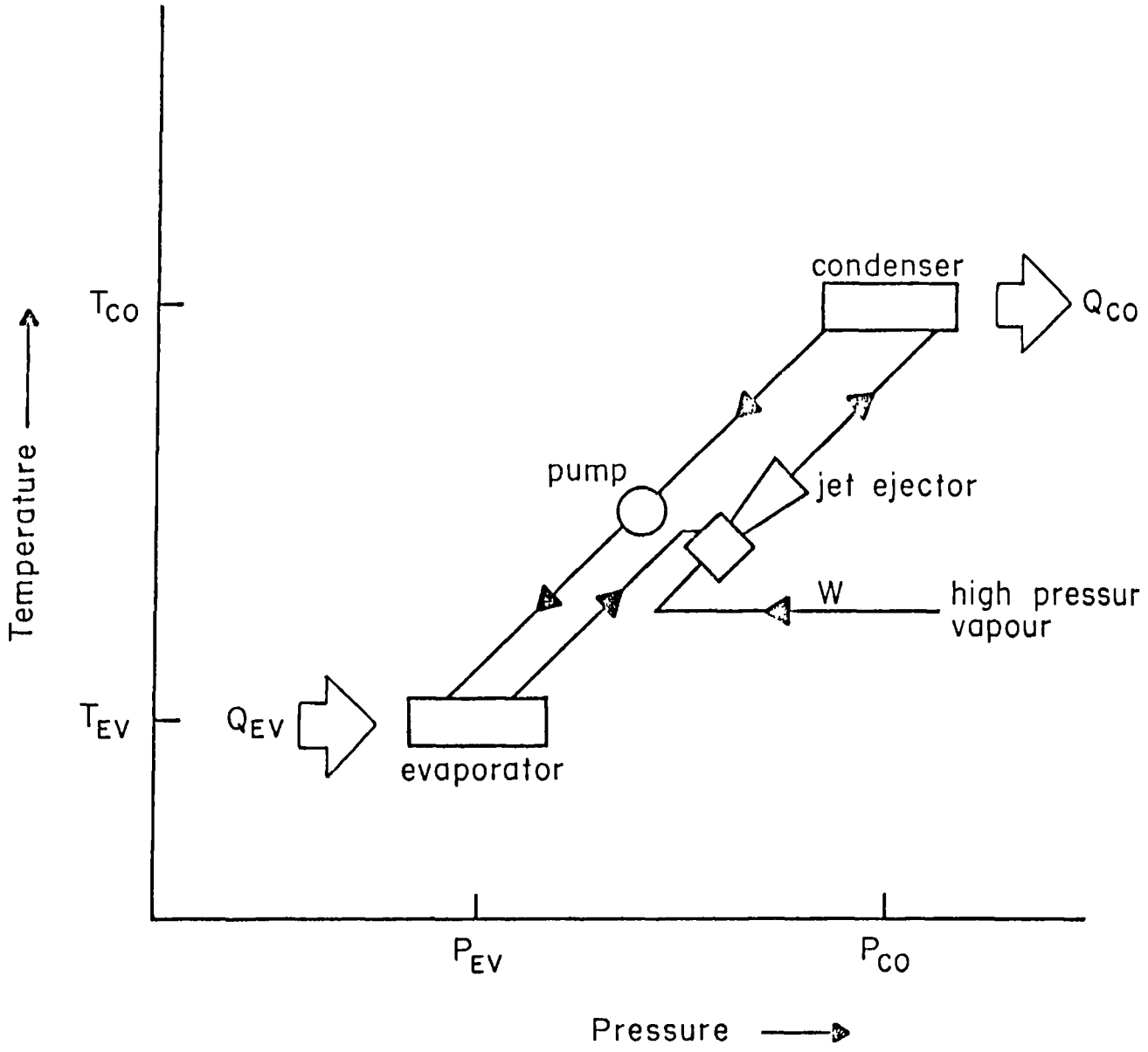

Fig. 2.2 Vapour jet heat pump

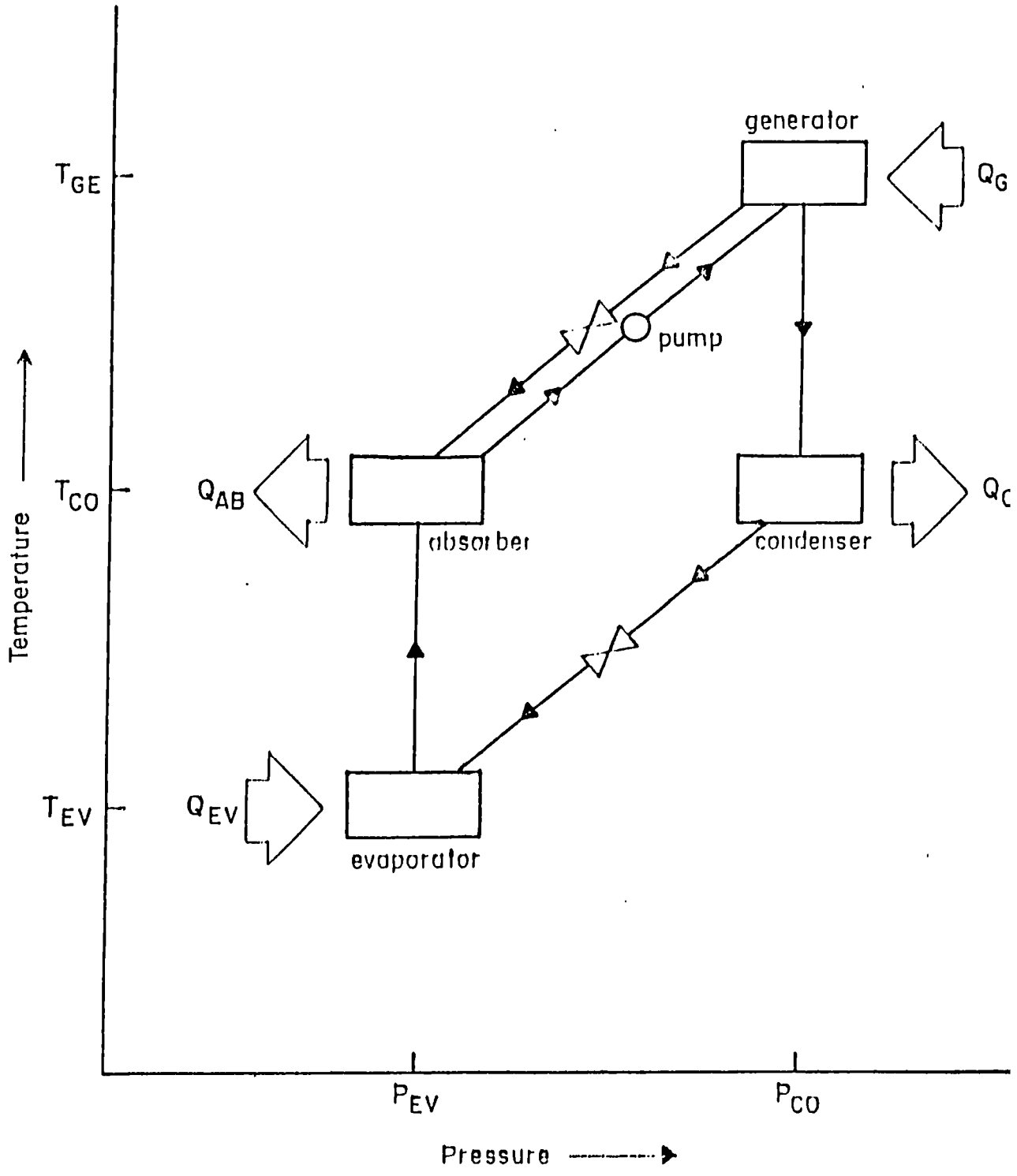

Fig. 2.3 Absorption heat pump.

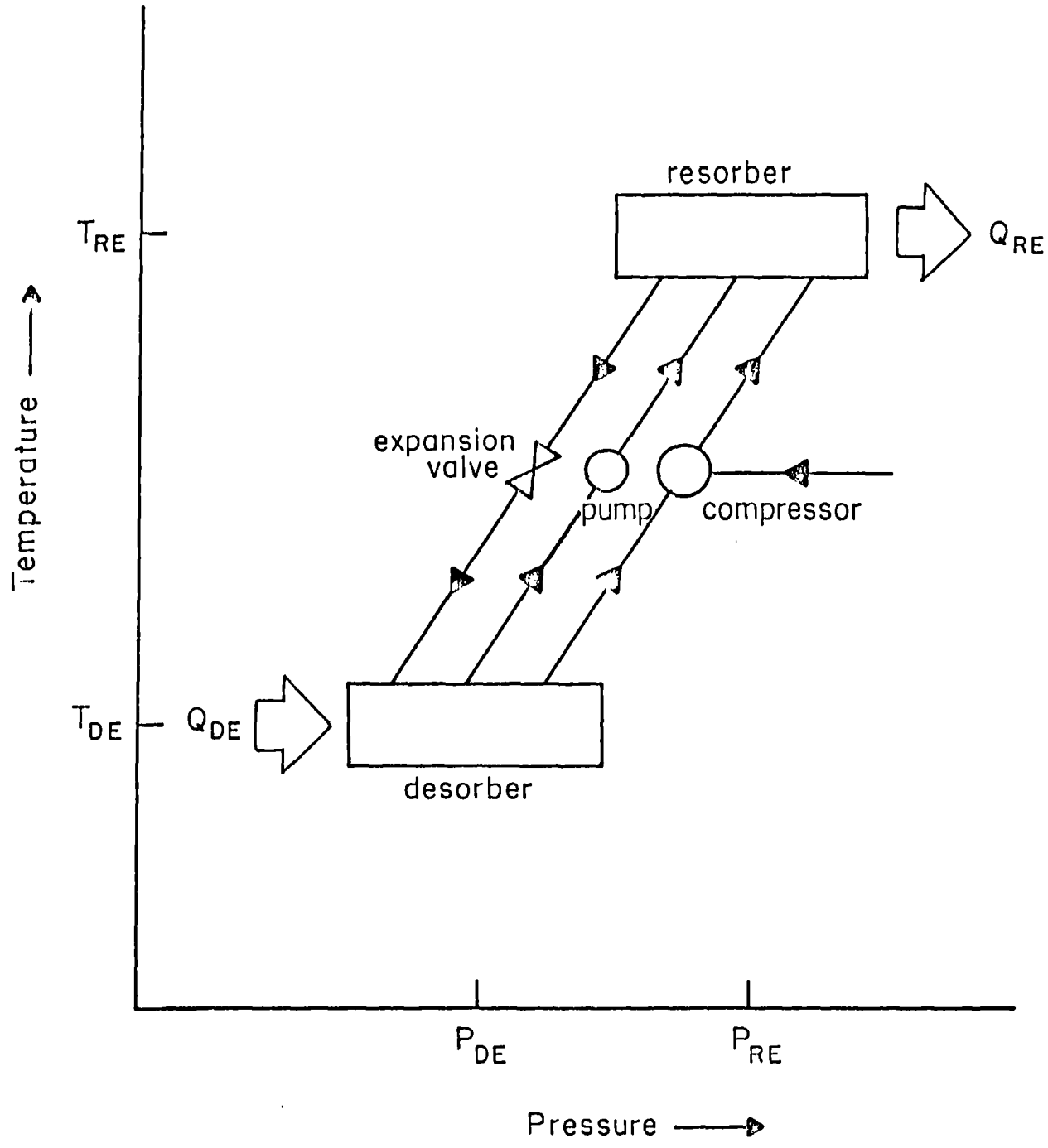

Fig. 2.4 Resorption heat pump

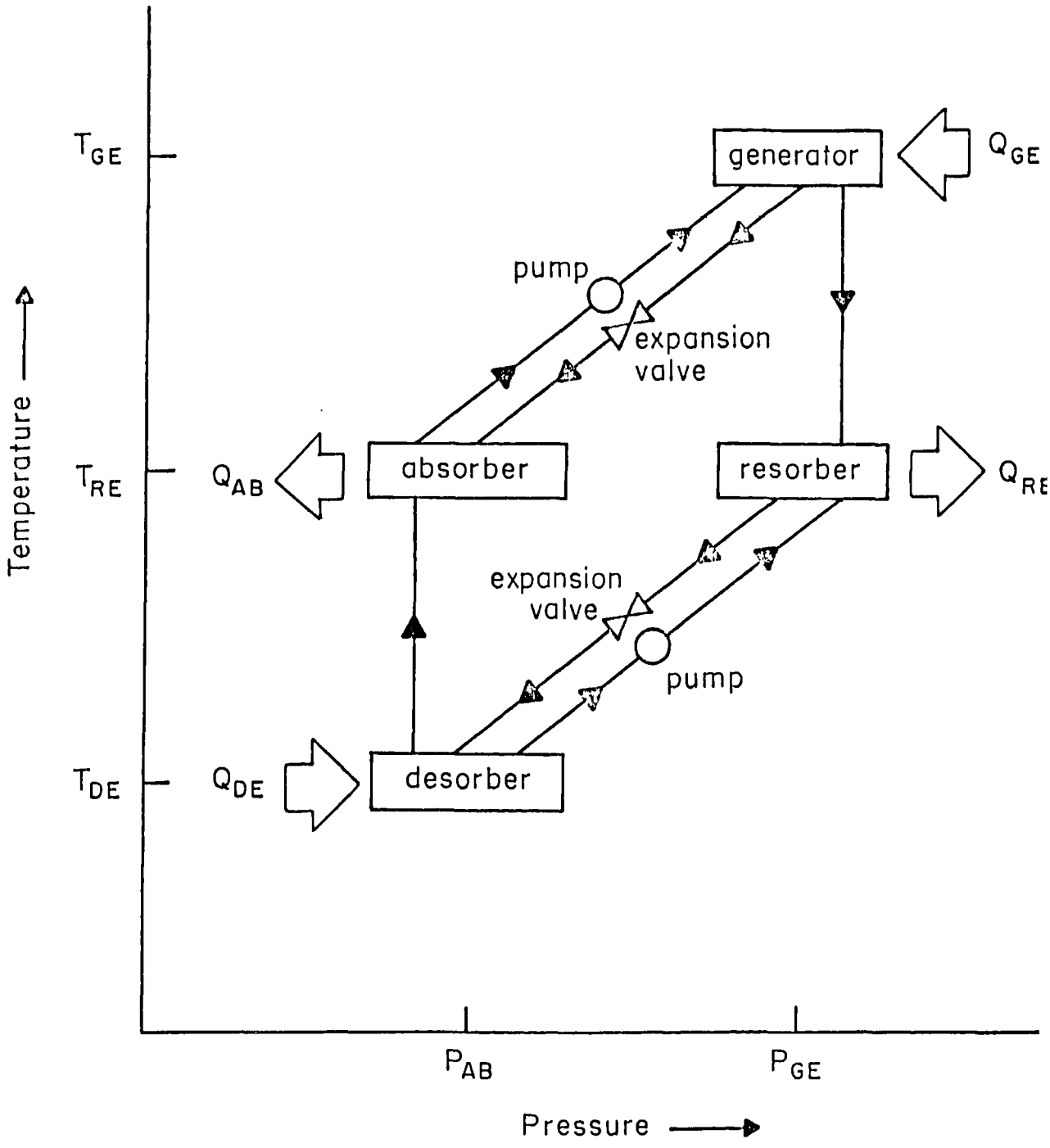

Fig. 2.5 Absorption-resorption heat pump

CHAPTER 3

THERMODYNAMIC CONSIDERATIONS FOR ABSORPTION HEAT PUMPS

3.1 HEAT PUMPS

Heat pumps are devices which are used to create temperature differences. In a heat pump cooler or refrigerator a working fluid or refrigerant extracts heat from a cooling chamber by evaporation. The evaporated working fluid is then compressed before delivering heat at a higher temperature as it is condensed. The working fluid is then expanded and returned to the evaporator to complete the cycle. A heat pump heater works on the same principle. The working fluid in a heat pump extracts heat from a source which may be at a relatively high temperature. The evaporated working fluid is then compressed before delivering heat at an even higher temperature as it is condensed. Heat pumps have been used to deliver heat at temperatures greater than 200°C. Heat pumps and coolers can be divided into two categories:

(1) mechanical vapour compression systems,

(2) heat driven absorption systems.

In the first category compressors are used to increase the pressure of the working fluid. In the second category the increase in pressure is achieved by using a secondary circuit, in which a liquid absorbent is recirculated with a pump. In the first category all the input energy is high grade mechanical energy. In the second category the bulk of the input energy is heat energy supplied to the generator in the secondary circuit since the

recirculation pump is operated on a negligible amount of mechanical energy compared with a compressor. The great advantage of absorption systems is that they do not require compressors which are expensive and not always readily available.

3.2 MECHANICAL VAPOUR COMPRESSION SYSTEMS

The most common type of heat pump is the vapour compression heat pump usin a mechanical compressor as shown schematically in Figure 3.1. It consists of two heat exchangers, a compressor, an expansion valve and a working fluid. In the evaporator heat exchanger, the working fluid evaporates at an absolute temperature T_{EV} whilst extracting an amount of heat Q_{EV} from the source which may be in the gaseous, liquid or solid state. The workin fluid is then compressed and gives up an amount of latent heat Q_{CO} at a higher absolute temperature T_{CO} in the condenser heat exchanger. The condensed working fluid is then expanded through the expansion valve and is returned to the evaporator to complete the cycle.

From the first law of thermodynamics, the amount of heat delivered Q_{CO} at higher temperature T_{CO} is related to the amount of heat extracted Q_{EV} at a lower temperature T_{EV} and the amount of high grade energy input W by equation (3.1)

$$Q_{CO} = Q_{EV} + W \tag{3.1}$$

The coefficient of performance of a compressor driven vapour compression heat pump can be the written in the forms

$$(COP)_H = \frac{Q_{CO}}{W} = \frac{Q_{CO}}{Q_{CO} - Q_{EV}} \tag{3.2}$$

and

$$(COP)_{CL} = \frac{Q_{EV}}{W} = \frac{Q_{EV}}{Q_{CO} - Q_{EV}} \qquad (3.3)$$

where $(COP)_H$ is the coefficient of performance for heating and $(COP)_{CL}$ is the coefficient of performance for cooling.

From equations (3.1 - 3.3) the coefficient of performance for a heat pump is related to the coefficient of performance of a refrigerator by equation (3.4)

$$(COP)_H = (COP)_{CL} + 1 \qquad (3.4)$$

3.3 HEAT DRIVEN ABSORPTION SYSTEMS

3.3.1 CONVENTIONAL ABSORPTION HEAT PUMPS

A conventional heat driven absorption heat pump is shown schematically in Figure 3.2. The condensation, expansion and evaporation of the working fluid are the same as in the conventional compressor driven system illustrated in Figure 3.1 however in the absorption cycle, the compressor is replaced by a secondary circuit in which a liquid absorbent is circulated by a pump. The evaporated working fluid is absorbed by the circulating liquid and the pressure increased by the pump prior to entering the generator. An amount of heat Q_{GE} is added at an absolute temperature T_{GE} in the generator to produce the high pressure working fluid vapour required to be fed to the condenser. The mechanical energy required to pump the liquid is usually negligible compared with the input of high grade heat energy Q_{GE}.

The pump in the secondary circuit of an absorption heat pump provides the compression ratio (CR) = P_{CO}/P_{EV}.

A coefficient of performance of a conventional absorption cooler can be defined as

$$(COP)_{ACL} = \frac{Q_{EV}}{Q_{GE}} \tag{3.5}$$

A coefficient of performance for an absorption heat pump can be defined as

$$(COP)_{AH} = \frac{(Q_{CO} + Q_{AB})}{Q_{GE}} \tag{3.6}$$

$$= (COP)_{ACL} + 1 \tag{3.7}$$

In a conventional absorption heat pump there are two pressure levels

$$P_{CO} = P_{GE} > P_{EV} = P_{AB}$$

and either three or four temperature levels

$$T_{GE} > T_{CO} \geq T_{AB} > T_{EV}$$

depending on whether the condenser and absorber are operated at the same temperature or not.

The flow ratio (FR) is an important design and optimising parameter. It is essentially the ratio of the mass flow rate of solution in the secondary circuit, linking the generator and the absorber, to the mass flow rate of pure working fluid or refrigerant in the primary circuit, linking the condenser and evaporator. It can be defined in terms of either the mass flow

rate of solution from the absorber to the generator, M_{AB} or the mass flow rate of solution from the generator to the absorber, M_{GE} with reference to the mass flow rate of refrigerant M_R.

Following the first definition

$$(FR) = \frac{M_{AB}}{M_R} \tag{3.8}$$

which can also be rewritten in terms of concentrations as

$$(FR) = \frac{X_{GE}}{X_{GE} - X_{AB}} \tag{3.9}$$

3.3.2 IDEAL COEFFICIENT OF PERFORMANCE OF AN ABSORPTION SYSTEM

From the overall balance

$$Q_{EV} + Q_{GE} = Q_{AB} + Q_{CO} \tag{3.10}$$

An absorption cycle may be thought of as the combination of a heat engine and a mechanical vapour compression system. The heat engine converts heat into work which, in turn, drives the mechanical vapour compression system. For a thermodynamically reversible process in the condenser and evaporator, the reduction in entropy in the condenser would equal the gain in entropy in the evaporator, i.e.

$$\frac{Q_{EV}}{T_{EV}} = \frac{Q_{CO}}{T_{CO}} \tag{3.11}$$

In this theoretically ideal situation, the change in entropy for the whole cycle would also be zero, so that

$$\frac{Q_{EV}}{T_{EV}} + \frac{Q_{GE}}{T_{GE}} = \frac{Q_{AB}}{T_{AB}} + \frac{Q_{CO}}{T_{CO}} \tag{3.12}$$

From equations (3.11) and (3.12) it can be concluded that

$$\frac{Q_{GE}}{T_{GE}} = \frac{Q_{AB}}{T_{AB}} \tag{3.13}$$

Combining equations (3.10) with equations (3.11), (3.12) and (3.13) gives

$$(COP)_{CCL} = \frac{Q_{EV}}{Q_{GE}} = \left(\frac{T_{GE} - T_{AB}}{T_{GE}}\right)\left(\frac{T_{EV}}{T_{CO} - T_{EV}}\right) \tag{3.14}$$

$$(COP)_{CH} = \frac{Q_{AB} + Q_{CO}}{Q_{GE}} = 1 + \left[\left(\frac{T_{GE} - T_{AB}}{T_{GE}}\right)\left(\frac{T_{EV}}{T_{CO} - T_{EV}}\right)\right] \tag{3.15}$$

$$= 1 + (COP)_{CCL} \tag{3.16}$$

3.3.3 ENTHALPY BASED COEFFICIENT OF PERFORMANCE

With reference to Figure 3.3, the mass and heat balances of the system using mass flow rates and enthalpies at different state points of the cycle can be expressed as follows:

$$Q_{EV} = M_4(H_4 - H_3) \tag{3.17}$$

$$Q_{CO} = M_1(H_1 - H_2) \tag{3.18}$$

$$Q_{GE} = M_1H_1 + M_5H_5 - M_{10}H_{10} \tag{3.19}$$

$$Q_{AB} = Q_{GE} + Q_{EV} - Q_{CO} \tag{3.20}$$

$$M_4 = M_1 = M_W \tag{3.21}$$

$$M_8 = M_9 = M_{10} = M_{AB} \tag{3.22}$$

$$M_{10} = M_5 + M_1 \tag{3.23}$$

$$M_8 = M_4 = M_7 \tag{3.24}$$

$$M_5 = M_7 = M_6 \tag{3.25}$$

Equations (3.8) and (3.17) - (3.25) give

$$(COP)_{ECL} = \frac{Q_{EV}}{Q_{GE}} = \frac{(H_4 - H_3)}{H_1 + [(FR) - 1]\ H_5 - (FR)\ H_{10}} \tag{3.26}$$

$$(COP)_{EH} = \frac{(Q_{CO} + Q_{AB})}{Q_{GE}} = 1 + \left[\frac{(H_4 - H_3)}{H_1 + [(FR-1)]\ H_5 - (FR)\ H_{10}}\right] \tag{3.27}$$

and

$$(COP)_{EH} = 1 + (COP)_{ECL} \tag{3.28}$$

where $(COP)_{ECL}$ and $(COP)_{EH}$ are the enthalpy based coefficients of performance for a cooler and a heat pump respectively.

3.4 HEAT TRANSFORMERS

A heat transformer which is also called a reversed absorption heat pump is shown schematically in Figure 3.4 . Heat is added at a relatively low temperature T_{GE} to the generator. The vapourized working fluid is condensed in the condenser at a temperature T_{CO}. The liquified working fluid leaving the condenser is pumped to a higher pressure region where it is evaporated by the input heat at a temperature T_{EV}. The evaporated working fluid is then absorbed in the absorber at a higher temperature T_{AB}. Thus an absorption heat transformer has the unique capability of raising the temperature of a working fluid above that of the input heat.

There are three temperature levels in an absorption heat transformer when the same input heat is used at the evaporator and generator.

The coefficient of performance of an absorption heat transformer is equal to the heat load in the absorber per unit of combined heat load in the generator and the evaporator

$$(COP)_{AT} = \frac{Q_{AB}}{Q_{GE} + Q_{EV}} \tag{3.29}$$

It can be shown that the Carnot coefficient for an absorption heat transformer shown in Figure 3.4 is

$$(COP)_{CT} = \left(1 - \frac{T_{CO}}{T_{GE}}\right)\left(\frac{T_{AB}}{T_{AB} - T_{CO}}\right) \tag{3.30}$$

Heat and mass balances can be used to theoretically derive an enthalpy based coefficient of performance for an absorption heat transformer

$$(COP)_{ET} = \frac{Q_{AB}}{Q_{GE} + Q_{EV}} = \frac{H_4+[(FR)-1]\ H_5\ (FR)\ H_{10}}{H_1 +[(FR)-1]\ H_5 - (FR)\ H_{10}+ H_4 - H_3} \quad (3.31)$$

3.5 WORKING FLUID PAIRS FOR ABSORPTION SYSTEMS

3.5.1 WORKING FLUID-ABSORBENT COMBINATIONS

The performance of an absorption system is critically dependent on the thermodynamic, physical and chemical properties of the working fluid and the absorbent. An extensive effort has been made in the evaluation of fluid combinations for absorption systems. [3.1 - 3.4].

3.5.2 PROPERTIES OF THE WORKING FLUID

Latent heat: The latent heat of vapourization of the working fluid should be as high as possible so that the mass flow rate of the working fluid within the system is reduced per unit of the heat delivered. This, in turn, will reduce the rate of circulation of the absorbent for a given change in concentration. [3.5].

Vapour pressure: The working fluid should give a reasonable pressure at the condensing temperature. Very low pressures cause inward leakage problems and cavitations in the pumps, whilst high pressures demand strong containers and expensive pumps.

Freezing point: The compounds with relatively low freezing points are preferred because the freezing point imposes a lower limit to the possibl operating temperature of the evaporator. In some cases, additives can be used to lower the freezing point of the working fluid.

Critical point: The critical point should be high relative to the top cycle temperature.

3.5.3 PROPERTIES OF THE ABSORBENT

The absorbent should have a high boiling point and a negligible vapour pressure to avoid its transference into the condenser. The absorbents with large molecular weights or high polarity will be better for absorption systems. It is generally accepted that to avoid rectification, the difference between the boiling points of the working fluid and absorbent should be greater than 200°C. The absorbent should have a high affinity towards the working fluid which is fundamental to the absorption process. Either solid or liquid absorbents can be used in absorption systems although the use of solid absorbents necessitates an intermittent cycle. A great many mineral and organic compounds simultaneously fulfil these criteria. The mineral salts such as halides and alkaline thiocyanates and organic compounds such as glycols and their derivatives are suitable absorbents.

Solubility: One of the conditions to be fulfilled by the mixture is the complete solubility of the absorbent in a working fluid, over a large range of concentrations, so that it will not crystallize during the operation. This implies that the crystallization point should be below the working temperature of the absorber and preferably below room temperature.

Negative deviations from Raoult's law: An important thermodynamic property of the working fluid-absorbent mixture is the relationship between the vapour pressure and its concentration. According to Raoult's law, the vapour pressure of an ideal solution of two components is equal to the sum of the partial pressures of the two components. The partial pressure of a component is a function of its concentration. Real solutions usually give

lower vapour pressures. This negative deviation from Raoult's law is very necessary for absorption cycles. Its importance lies in the fact that less solution is required to be circulated around the cycle for a given flow of the working fluid. Negative deviations from Raoult's law also result in a higher temperature lift between evaporator and absorber. Polar molecules generally exhibit negative deviations.

Enthalpy of mixing: The enthalpy of mixing or the heat of solution of an ideal solution is zero. The absorption working pairs, generally give a negative enthalpy of mixing. Solutions giving large negative deviations from Raoult's law, generally give high values for the enthalpy of mixing.

3.5.4 CRITERIA COMMON TO ALL FLUIDS

The other general requirements to be fulfilled by all the fluids (working fluid, absorbent and mixture) are as follows.

Chemical properties: All the fluids should be non-flammable, non-explosive non-toxic. They should be chemically stable in the operating range. Fluids which are corrosive to the material of construction should be avoided, but in certain cases, corrosive chemicals which are thermodynamically attractive may be used with inhibitors. All the fluids must be readily available, cheap and compatible with materials of construction.

Transport properties: The viscosity should be preferably low to promote the mass and heat transfer. However, the viscosity and surface tension should not be too low to inhibit dropwise condensation which improves heat transfer. The thermal conductivity of fluids should be relatively high to

maximize the heat transfer in heat exchangers. The specific heat capacity should preferably be low in order to minimize the demands on the solution heat exchanger.

3.6 REFERENCES

3.1 R.M. Buffington, Qualitative requirements for absorbent-refrigerant combinations, Refrigerating Engineering 57, 343-345, 384-386, (1949).

3.2 W. Raldow, (Ed.), New working pairs for absorption processes, Proceedings of a workshop in Berlin, Published by Swedish Building Research Association, Stockholm. Sweden, (1982).

3.3 W.J. Biermann, Candidate chemical systems for air cooled, solar powered absorption air conditioner design, Part II - Solid absorbents, high latent heat refrigerants, unpublished report prepared for Department of Energy, Contract No. EG-77-C-03-1587, Carrier Corp., June (1978).

3.4 R.A. Macriss, T.S. Zawacki, Worldwide survey of absorption fluids data, IEA-HPC Newsletter, 6 (2), 25-28 June (1988).

3.5 I.E. Smith, Absorption heat pumps, Handbook on heat pump technology, Instituto de Investigaciones Eléctricas, Cuernavaca, Mexico, pp 2.1 - 2.14, (1990).

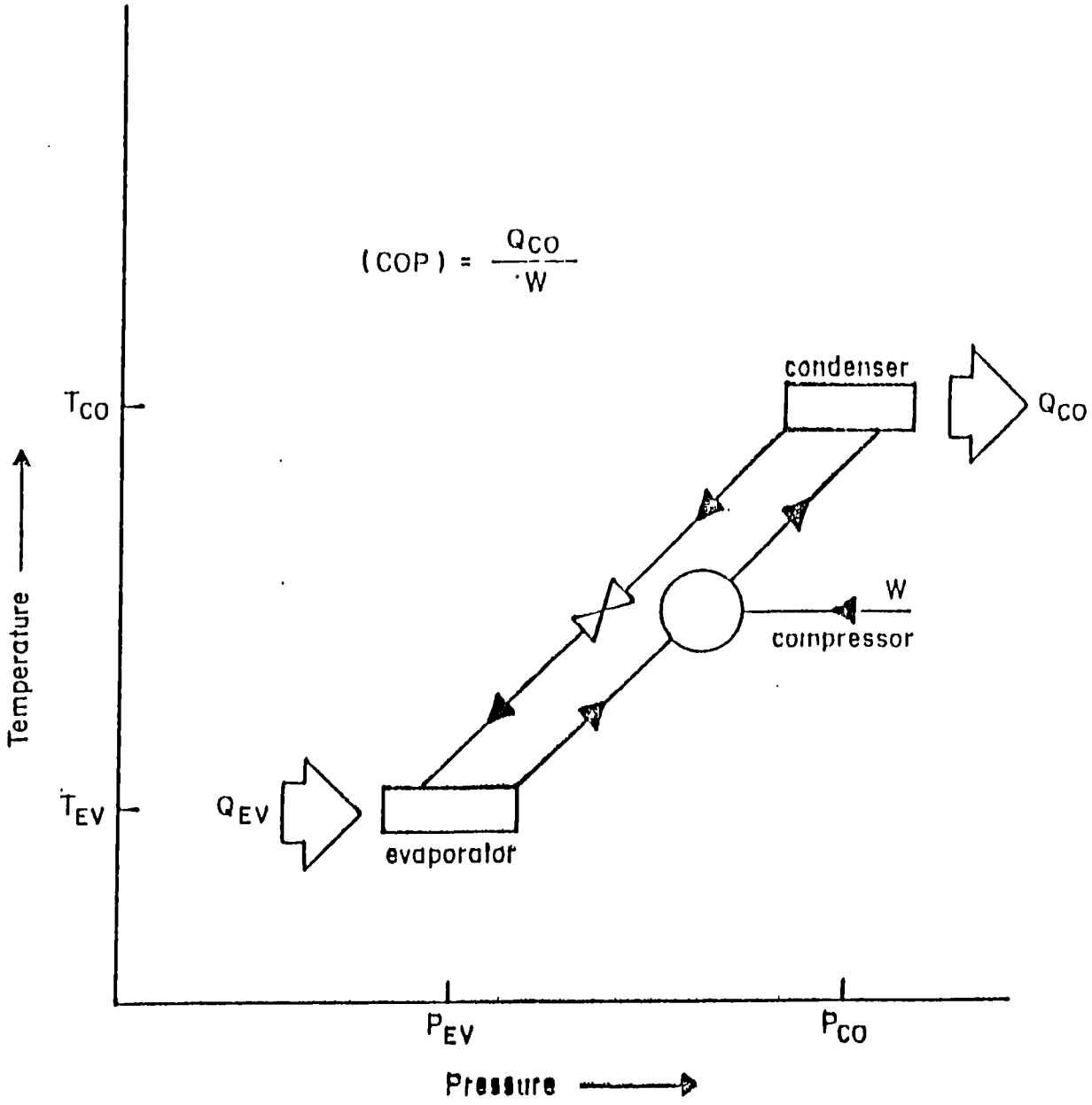

Fig. 3.1 Mechanical vapour compression heat pump.

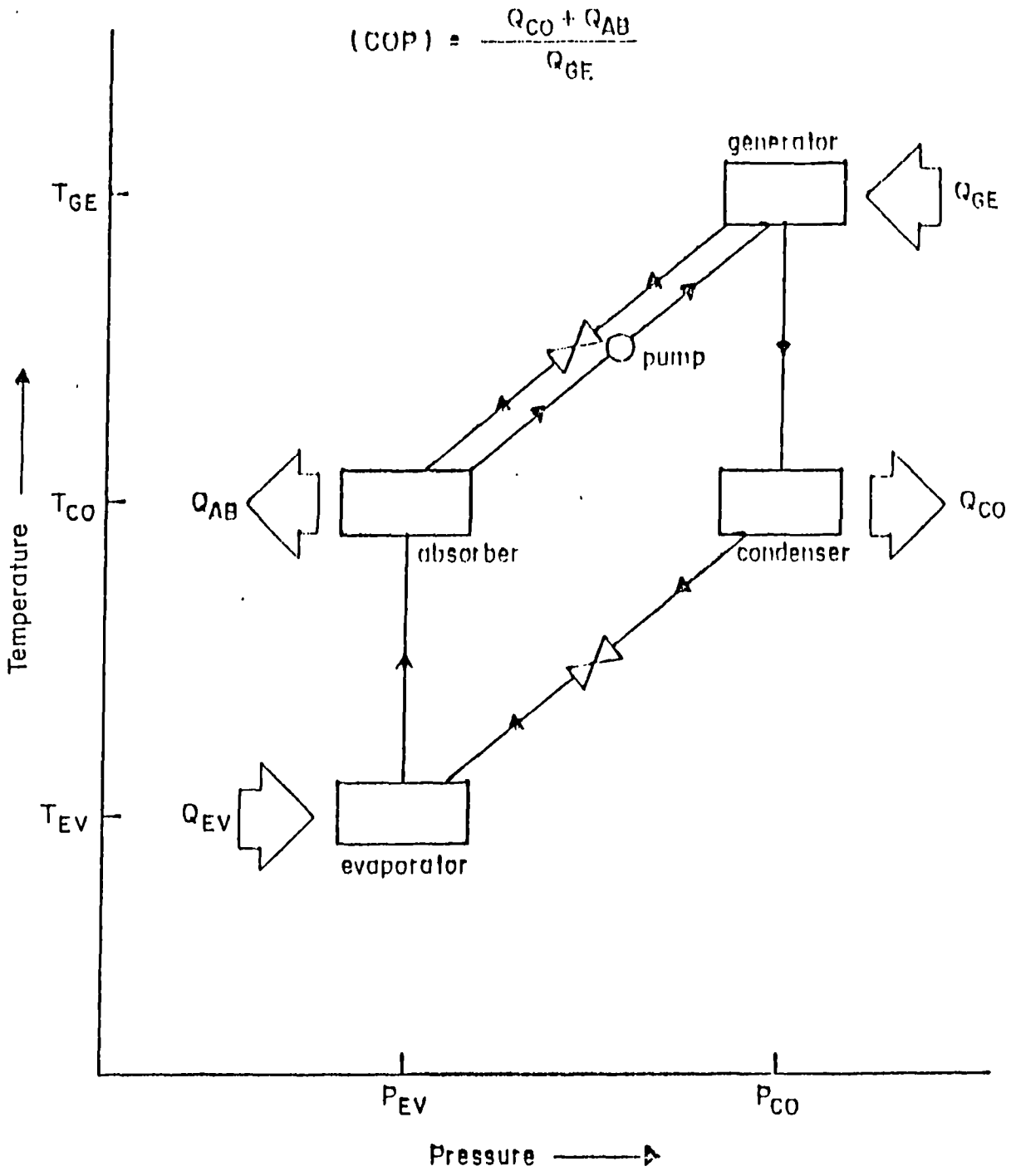

Fig. 3.2 Absorption heat pump.

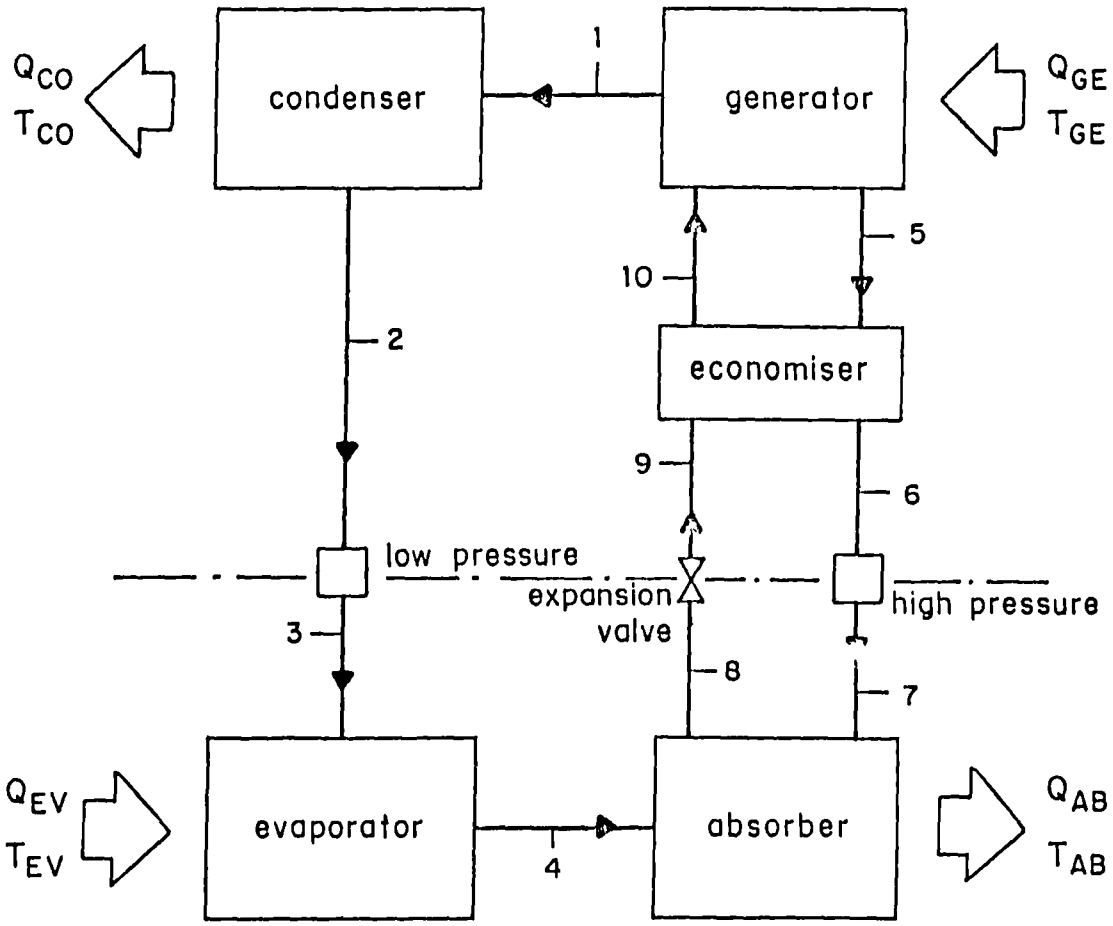

Fig. 3.3 Schematic diagram for a conventional absorption heat pump

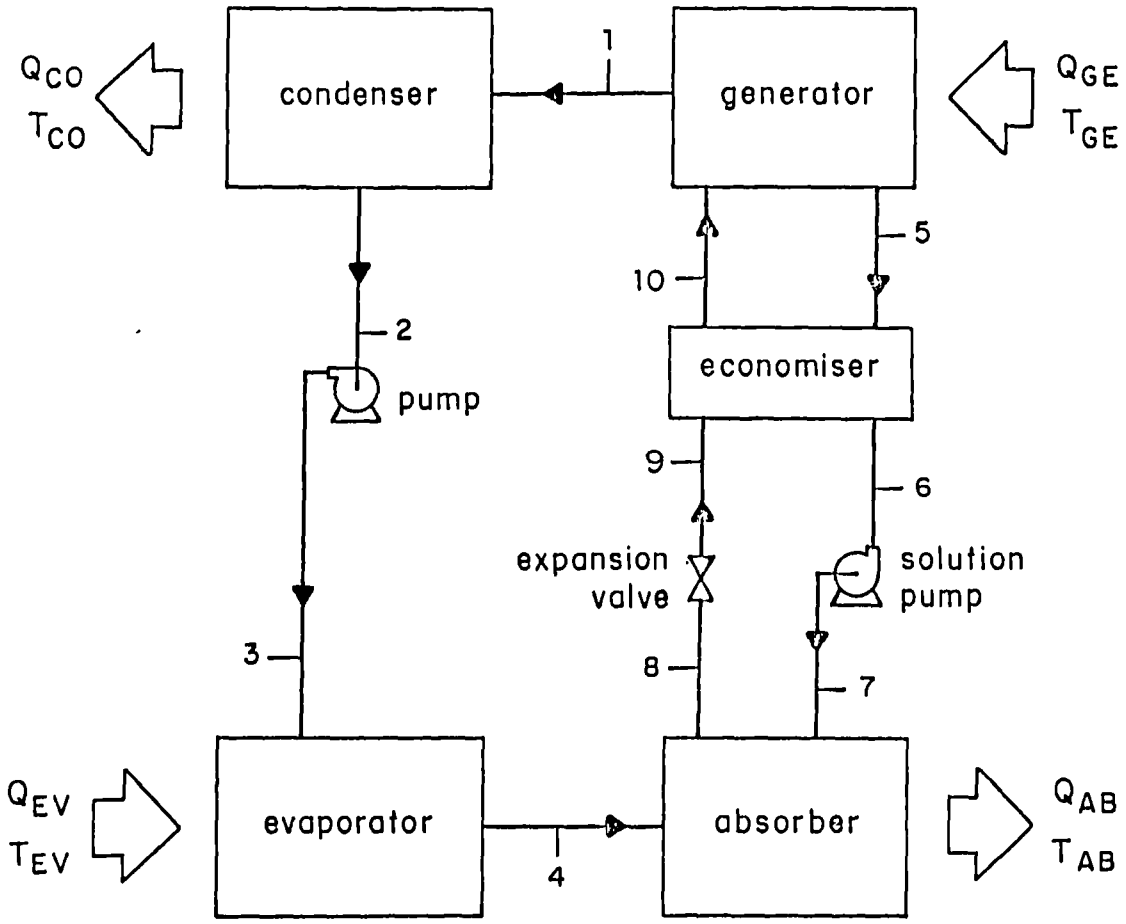

Fig. 3.4 Simplified block diagram for a basic absorption heat transformer

CHAPTER 4

THERMODYNAMIC DESIGN DATA FOR ABSORPTION HEAT PUMPS

4.1 INTRODUCTION

A conventional heat driven absorption heat pump basically consists of an evaporator, a condenser, a generator and an absorber as shown in Figure 4.1 The choice of the designer in the selection of the four basic operating temperatures T_{EV}, T_{AB}, T_{CO} and T_{GE} is limited by the Gibbs phase rule.

For an absorption system with two components and two phases, the number of degrees of freedom is two. If two of the operating variables are chosen as the free variables, then the other conditions are determined by the thermodynamic equilibrium data for the working pair.

The flow ratio (FR) is the ratio of the mass flow rate of solution to the mass flow rate of pure refrigerant in the primary circuit linking the condenser and the evaporator [4.1]. This can be written for ammonia-water as

$$(FR) = \frac{M_{AB}}{M_{AM}} \tag{4.1}$$

Alternatively, it can be rewritten in terms of concentrations as

$$(FR) = \frac{X_{AM} - X_{GE}}{X_{AB} - X_{GE}} \tag{4.2}$$

where X_{AB} is the weight per cent of ammonia in the solution entering the generator from the absorber, and X_{GE} and X_{AM} are the corresponding concentrations of ammonia in the streams leaving the generator for the absorber

and condenser respectively.

In this work, the data have been correlated using equations (1) and (2) for the ideal case of pure ammonia entering the condenser $X_{AM} = 1.0$.

Figure 4.2 illustrates the absorption cycle on an equilibrium chart for ammonia-water solutions. The points on the cycle correspond to the numbered positions in Figure 4.1. Points 3, 5, 4 and 2 represent the solution cycle.

4.2 IDEAL COEFFICIENT OF PERFORMANCE OF AN ABSORPTION COOLING SYSTEM

The coefficient of performance of an absorption cooling system is equal to the heat load in the evaporator per unit heat load in the generator

$$(COP)_{ACL} = \frac{Q_{EV}}{Q_{GE}} \tag{4.3}$$

From thermodynamic, mass and heat balance considerations and referring to Figure 4.1, it can be shown [4.2] that

$$(COP)_{CCL} = \frac{Q_{EV}}{Q_{GE}} = \left(\frac{T_{GE} - T_{AB}}{T_{GE}}\right)\left(\frac{T_{EV}}{T_{CO} - T_{EV}}\right) \tag{4.4}$$

and

$$(COP)_{ECL} = \frac{Q_{EV}}{Q_{GE}} = \frac{(H_1 - H_8)}{H_6 + [(FR) - 1] H_4 - (FR) H_5} \tag{4.5}$$

where $(COP)_{CCL}$ is the Carnot coefficient of performance for the system and is dependent only on the four basic temperatures T_{EV}, T_{AB}, T_{CO} and T_{GE}. $(COP)_{ECL}$ is the enthalpy based coefficient of performance for cooling.

4.3 IDEAL COEFFICIENT OF PERFORMANCE OF AN ABSORPTION HEATING SYSTEM

The coefficient of performance of an absorption heat pump is equal to the heat load in the absorber and condenser per unit heat load in the generator

$$(COP)_{AH} = \frac{Q_{AB} + Q_{CO}}{Q_{GE}} \tag{4.6}$$

From thermodynamic mass and heat balance considerations and with reference to Figure 4.1, it can be shown that

$$(COP)_{CH} = 1 + \left(\frac{T_{GE} - T_{AB}}{T_{GE}}\right)\left(\frac{T_{EV}}{T_{CO} - T_{EV}}\right) \tag{4.7}$$

and

$$(COP)_{EH} = \frac{H_1 + [(FR) - 1]H_4 - (FR)H_5 + H_6 - H_8}{H_6 + [(FR) - 1]H_4 - (FR)H_5} \tag{4.8}$$

where $(COP)_{CH}$ is the Carnot coefficient of performance for the system and is dependent only on the four basic temperatures T_{EV}, T_{AB}, T_{CO} and T_{GE}; $(COP)_{EH}$ is the enthalpy based coefficient of performance for heating.

In the same way it can be shown that

$$(COP)_{EH} = \frac{Q_{AB} + Q_{CO}}{Q_{GE}} = 1 + (COP)_{ECL} \tag{4.9}$$

4.4 COEFFICIENT OF PERFORMANCE OF AN ABSORPTION HEAT TRANSFORMER

The coefficient of performance of an absorption heat transformer is equal to the heat load in the absorber per unit heat load in the generator and the evaporator

$$(COP)_{AT} = \frac{Q_{AB}}{Q_{GE} + Q_{EV}} \tag{4.10}$$

From thermodynamic, mass and heat balances considerations and with reference to Figure 4.3, it was shown [4.3 - 4.5] that

$$(COP)_{CT} = \frac{(T_{EV} - T_{CO})T_{AB}}{(T_{EV} - T_{CO})T_{GE} + (T_{AB} - T_{GE})T_{EV}} \tag{4.11}$$

For $T_{EV} = T_{GE}$ equation (4.11) becomes

$$(COP)_{CT} = \left(1 - \frac{T_{CO}}{T_{GE}}\right) \left(\frac{T_{AB}}{T_{AB} - T_{CO}}\right) \tag{4.12}$$

and

$$(COP)_{ET} = \frac{H_1 + [(FR) - 1]\, H_4 - (FR)H_5}{H_6 + [(FR) - 1]\, H_4 - (FR)H_5 + H_1 - H_8} \tag{4.13}$$

where $(COP)_{CT}$ is the Carnot coefficient of performance for the system and is dependent on four basic temperatures T_{EV}, T_{AB}, T_{CO} and T_{GE}, and $(COP)_{ET}$ is the enthalpy based coefficient of performance.

4.5 THERMODYNAMIC PROCESS DESIGN DATA FOR AMMONIA-WATER FOR COOLING

The theoretical Carnot coefficient of performance $(COP)_{CCL}$, the enthalpy based coefficient of performance $(COP)_{ECL}$, the concentration of the solution in the absorber and the generator, and the flow ratio (FR) have been calculated for the ammonia-water system for the following range of temperatures:

(1) evaporator temperatures T_{EV} from -30°C to 10°C in 5°C increments at absorber temperatures T_{AB} of 30, 40 and 50°C, and

(2) generator temperatures T_{GE} from 60°C to 200°C at condenser temperatures T_{CO} from 30°C to 50°C in 10°C increments.

Equation (4.4) has been used for the calculation of the Carnot coefficient of performance. Equation (4.5) has been used for the calculation of the enthalpy based coefficient of performance. Equation (4.2) was used to calculate the flow ratio. The concentrations of ammonia in the absorber X_{AB} and the generator X_{GE} and the enthalpies at different state points were calculated using the thermodynamic data of Macriss et al [4.6]. Tables (A1.1) list the design data for each combination of the four basic operating temperatures. (Appendix 1).

4.6 THERMODYNAMIC PROCESS DESIGN DATA FOR AMMONIA-WATER FOR HEATING

The theoretical Carnot coefficient of performance $(COP)_{CH}$, the enthalpy based coefficient of performance $(COP)_{EH}$, the concentration of the solution in the absorber and generator and the flow ratio (FR) have been calculated for the ammonia-water system for the following ranges of temepratures:

(1) evaporator temperatures T_{EV} from 20°C to 50°C in 10°C increments at absorber temperatures T_{AB} from 50°C to 100°C in 10°C increments,

and

(2) generator temperatures T_{GE} from 80°C to 200°C at condenser temperatures from 50°C to 70°C in 10°C increments.

Equation (4.7) has been used for the calculation of the Carnot coefficient of performance. Equation (4.8) has been used for the calculations of the enthalpy based coefficient of performance. Equation (4.2) was used to calculate the flow ratio. The concentrations of ammonia in the absorber X_{AB} and the generator X_{GE} and the enthalpies at different state points were calculated using the thermodynamic data of Macriss et al [4.6]. Tables (A1.2) list the derived thermodynamic design data for each combination of the four basic temperatures. (Appendix 1).

4.7 THERMODYNAMIC PROCESS DESIGN DATA FOR AMMONIA-WATER FOR COOLING AND SIMULTANEOUS HEATING

The theoretical Carnot coefficient of performance $(COP)_{CL}$, the enthalpy based coefficient of performance $(COP)_{ECL}$, the concentrations of the solution in the absorber and generator, and the flow ratio (FR) have been calculated for the ammonia-water mixture for the following ranges of temperatures:

(1) evaporator temperatures T_{EV} from -10°C to 10°C in 5°C increments at absorber temperatures T_{AB} from 50°C to 100°C in 10°C increments,

and

(2) generator temperatures T_{GE} from 80°C to 200°C at condenser temperatures T_{CO} from 50°C to 70°C in 10°C increments.

Equation (4.4) has been used for the calculation of the Carnot coefficient of performance. Equation (4.5) was used for the calculation of the enthalpy based coefficient of performance. Equation (4.2) was used to calculate the flow ratio. The concentrations of ammonia in the absorber X_{AB} and in the generator X_{GE} and the enthalpies at different state points were calculated using the thermodynamic data of Macriss et al [4.6]. Tables (A1.3) list the design data for each combination of the four basic operating temperatures. (Appendix 1).

4.8 THERMODYNAMIC PROCESS DESIGN DATA FOR AMMONIA-LITHIUM NITRATE FOR COOLING

The thermodynamic design data have been calculated for the following ranges of temperatures:

(1) evaporator temperatures T_{EV} from -30°C to 0°C in 5°C increments at absorber temperatures T_{AB} of 30, 40 and 50°C,

and

(2) generator temperatures T_{EV} from 65 to 145°C at 5°C increments at condenser temperatures T_{CO} from 30 to 50°C at 10°C increments.

Tables (A1.4) list the design data for each combination of the four basic operating temperatures. (Appendix 1).

4.9 THERMODYNAMIC PROCESS DESIGN DATA FOR AMMONIA-LITHIUM NITRATE FOR HEATING

The thermodynamic design data have been calculated for the following ranges of temperatures:

(1) evaporator temperatures T_{EV} from 20 to 50°C in 10°C increments at absorber temperatures T_{AB} from 50 to 100°C in 10°C increments

and

(2) generator temperatures T_{GE} from 90 to 170°C at condenser temperatures T_{CO} from 50 to 70°C in 10°C increments.

Tables (A1.5) list the design data for each combination of the four basic operating temperatures. (Appendix 1).

4.10 THERMODYNAMIC PROCESS DESIGN DATA FOR AMMONIA-LITHIUM NITRATE FOR COOLING AND SIMULTANEOUS HEATING

The thermodynamic design data have been calculated for the following ranges of temperatures:

(1) evaporator temperatures T_{EV} from -10°C to 15°C in 5°C at absorber temperatures T_{AB} from 50°C to 100°C in 10°C increments,

and

(2) generator temperatures T_{GE} from 90°C to 170°C in 10°C increments at condenser temperatures T_{CO} from 50°C to 100°C in 10°C increments.

Tables (A1.6) list the design data for each combination of the four basic operating temperatures. (Appendix 1).

4.11 THERMODYNAMIC PROCESS DESIGN DATA FOR AMMONIA-WATER FOR HEAT TRANSFORMERS

The theoretical Carnot coefficient of performance $(COP)_{CT}$, and enthalpy based coefficient of performance $(COP)_{ET}$, the concentrations of the solution in the absorber and generator, and the flow ratio (FR) have been calculated for the ammonia-water system for the following ranges of temperatures:

(1) evaporation temperatures T_{EV} from 30°C to 70°C in 10°C increments at absorber temperatures T_{AB} from 40°C to 120°C in 10° increments,

and

(2) generator temperatures T_{GE} from 30°C to 90°C at condenser

temperatures T_{CO} from 10°C to 50°C in 10°C increments.

Equation (4.11) has been used for the calculation of the Carnot coefficient of performance. Equation (4.13) was used for the calculation of the enthalpy based coefficient of performance. Equation (4.2) was used to calculate the flow ratio. The concentrations of ammonia in the absorber X_{AB} and the generator X_{GE} and the enthalpies at different state points were calculated using the thermodynamic data of Macriss et al [4.6]. Tables (A1.7) list the design data for each combination of the four basic operating temperatures. (Appendix 1).

4.12 THERMODYNAMIC PROCESS DESIGN DATA FOR AMMONIA-LITHIUM NITRATE FOR HEAT TRANSFORMERS

The theoretical Carnot coefficient of performance $(COP)_{CT}$, and the enthalpy based coefficient of performance $(COP)_{ET}$ the concentrations of the solution in the absorber and generator, and the flow ratio (FR) have been calculated for the ammonia-lithium nitrate system for the following ranges of temperatures:

(1) evaporation temperatures T_{EV} from 30 to 90°C in 5°C increments at absorber temperatures T_{AB} from 70 to 140°C in 10°C increments,

and

(2) generator temperatures T_{GE} from 50 to 90°C in 5°C increments at condenser temperatures T_{CO} from 10 to 50°C in 10°C increments.

Equation (4.11) has been used for the calculation of the Carnot coefficient of performance. Equation (4.13) was used for the calculation of the

enthalpy based coefficient of performance. Equation (4.2) was used to calculate the flow ratio. The concentrations of ammonia in the absorber X_{AB} and the generator X_{GE} and the enthalpies at different state points wer calculated using the thermodynamic data of Infante Ferreira [4.7].

Tables (A1.8) list the derived thermodynamic design data for each combination of the four basic operating temperatures. (Appendix 1).

4.13 DISCUSSION OF THERMODYNAMIC PROCESS DESIGN DATA

For the two working systems ammonia-water and ammonia-lithium nitrate the interactions of the operating temperatures have been illustrated graphically in Figures (4.4 - 4.28) for different operating modes.

4.14 THE IMPORTANCE OF DERIVED THERMODYNAMIC DATA

In absorption systems, the coefficient of performance is a measure of the system efficiency. The flow ratio determines the size of the various item of equipment. An increase in the flow ratio affects the performance in th following ways:

(i) the concentration difference between the absorber and generator is decreased,

(ii) the load on the economiser, normally placed between the absorber and generator is increased [4.8], [4.9],

(iii) the heat losses from the system could be higher,

and

(iv) the power required for the solution pump will increase.

For the same value of the coefficient of performance, the flow ratio will be different from one working pair to another.

For working pairs for which the thermodynamic and thermophysical data are available, the correlation between the operating temperatures together wit the theoretical coefficients of performance and the flow ratios presented in this work will also help the process design engineer in the choice of items of equipment and their sizing, especially for the economiser heat exchanger. The data presented will provide information on the effect on efficiency due to changes in operating conditions and information on possible combinations and operational limits of temperatures for the ammonia-water and ammonia-lithium nitrate systems.

4.15 CONCLUSIONS

Thermodynamic design data for absorption heat pumps and heat transformers operating on ammonia-water and ammonia-lithium nitrate have been presented in tabulated form together with the possible combinations of operating temperatures and the corresponding concentrations in the absorber and generator. The interactions of these parameters have also been graphicall illustrated for different operating modes.

4.16 REFERENCES

4.1 M.A.R. Eisa, M.G. Sane, S. Devotta and F.A. Holland, Experimental studies to determine the optimum flow ratio in a water-lithium bromide absorption cooler for high absorber temperatures , Chem. Eng. Res. Des., 63 (4), 267-270 (1985).

4.2 M.A.R. Eisa, S. Devotta and F.A. Holland, Thermodynamic design data for absorption heat pump systems operating on water-lithium bromide, part 1: cooling, Applied Energy 24, 287-301 (1986).

4.3 M.A.R. Eisa, R. Best and F.A. Holland, Thermodynamic design data for absorption heat transformers, Part 1: Operating on water-lithium bromide, J. Heat Recovery Systems 6 (5), 421-432 (1986).

4.4 R.E. Siddig Mohammed, F.A. Watson and F.A. Holland, Study of the operating characteristics of a reversed absorption heat pump system (heat transformer), Chem. Eng. Res. Des. 61(6), 283-289 (1983).

4.5 M.A.R. Eisa, R. Best and F.A. Holland, Thermodynamic design data for absorption heat transformers, Part II: Operating on water-calcium chloride, J. Heat Recovery Systems 6(6), 443-450 (1986).

4.6 R.A. Macriss, B.E. Eakin, R.T. Ellington and J. Huebler, Physical and Thermodynamic Properties of Ammonia-Water Mixtures, Research Bulletin No. 34, Chicago: Institute of Gas Technology (1964).

4.7 Infante Ferreira, Thermodynamic and physical property equations for ammonia-lithium nitrate and ammonia-sodium thiocyanate solutions, Solar Energy, 32 (2), 231--236 (1984).

4.8 I.E. Smith, C.O.B. Carey and C.F. Smith, Absorption heat pump research, Proceedings of a Workshop in Berlin. Published by Swedish Building Research Association, Stockholm Sweden, pp 149-151 (1982).

4.9 M.A.R. Eisa, S. Devotta and F.A. Holland, A study of the economiser performance in a water-lithium bromide absorption cooler, Int. J. Heat and Mass Transfer 28 (12), 2323-2329 (1985).

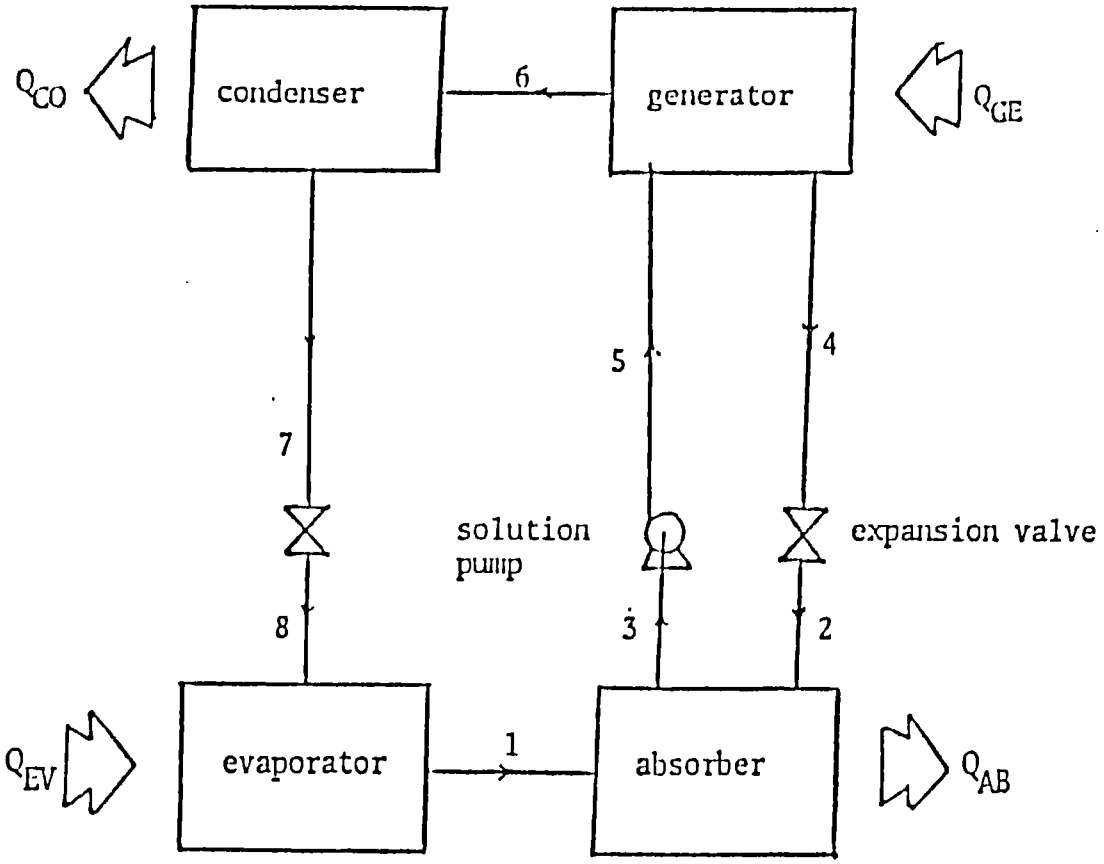

Fig.4.1 Simplified block diagram for a basic absorption heat pump.

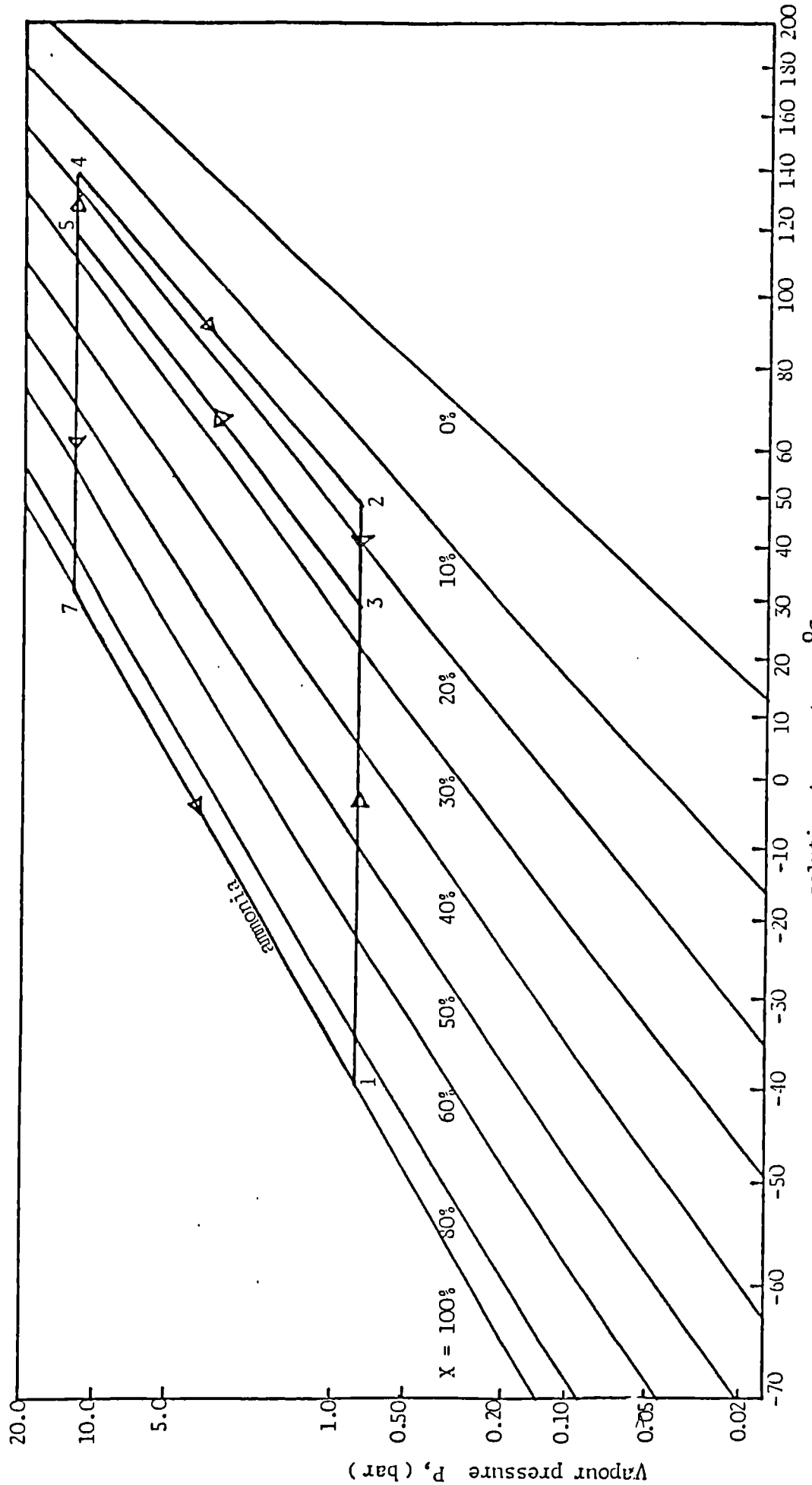

Fig. 4.2 Absorption cycle on an equilibrium chart for the ammonia-water system

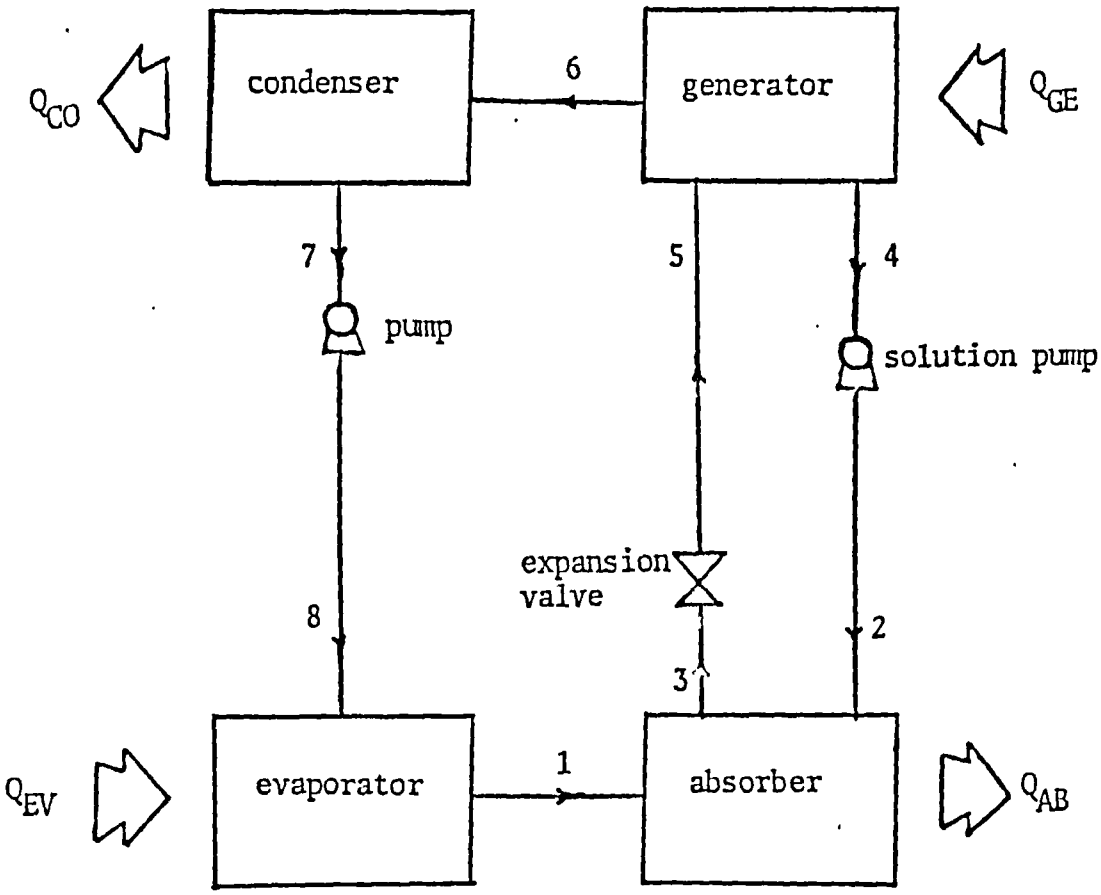

Fig. 4.3 Simplified block diagram for a basic absorption heat transformer.

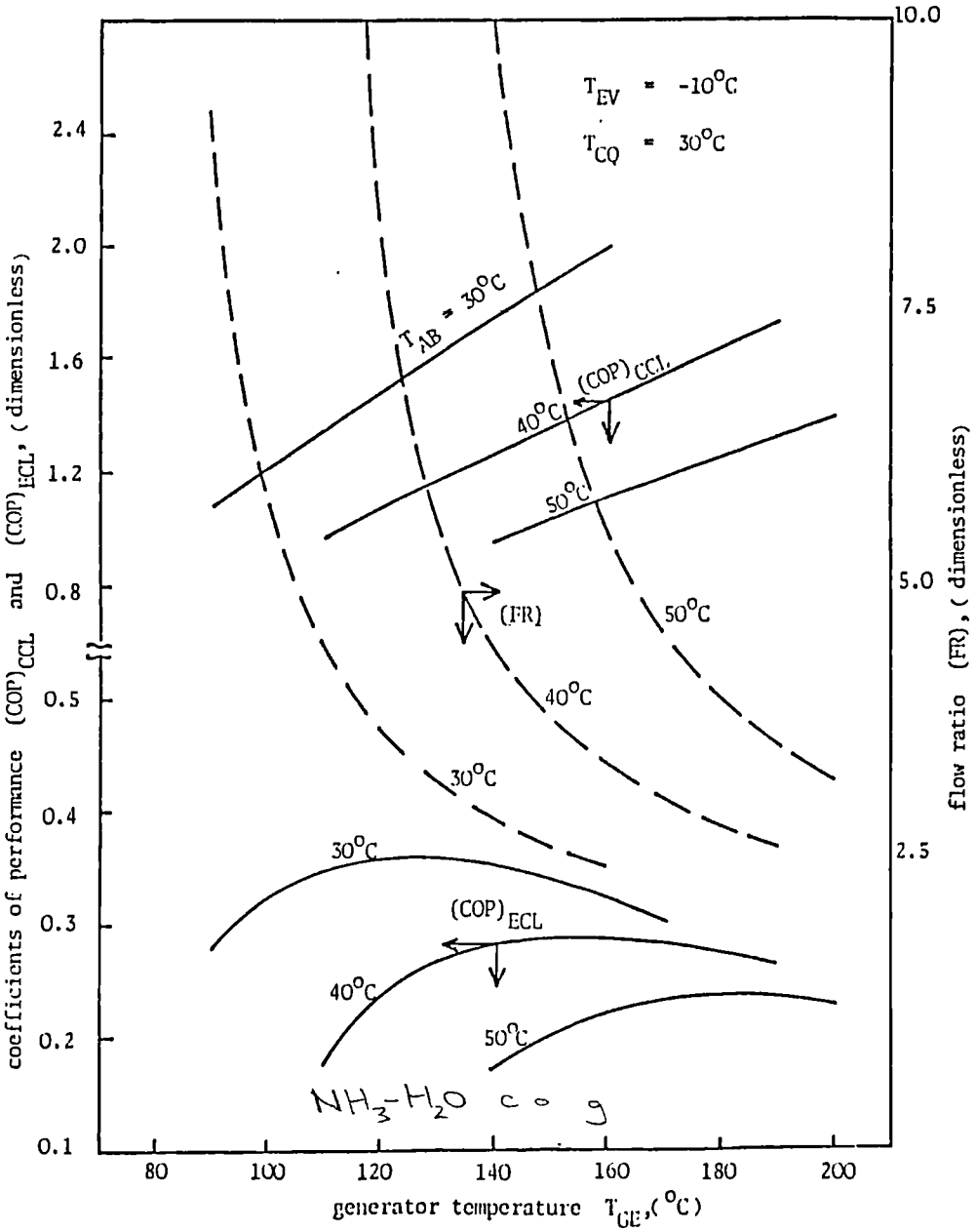

Fig. 4.4 Plot of coefficients of performance and flow ratio against generator temperature at three different absorber temperatures

Pages 54-56

ammonia-water for cooling.

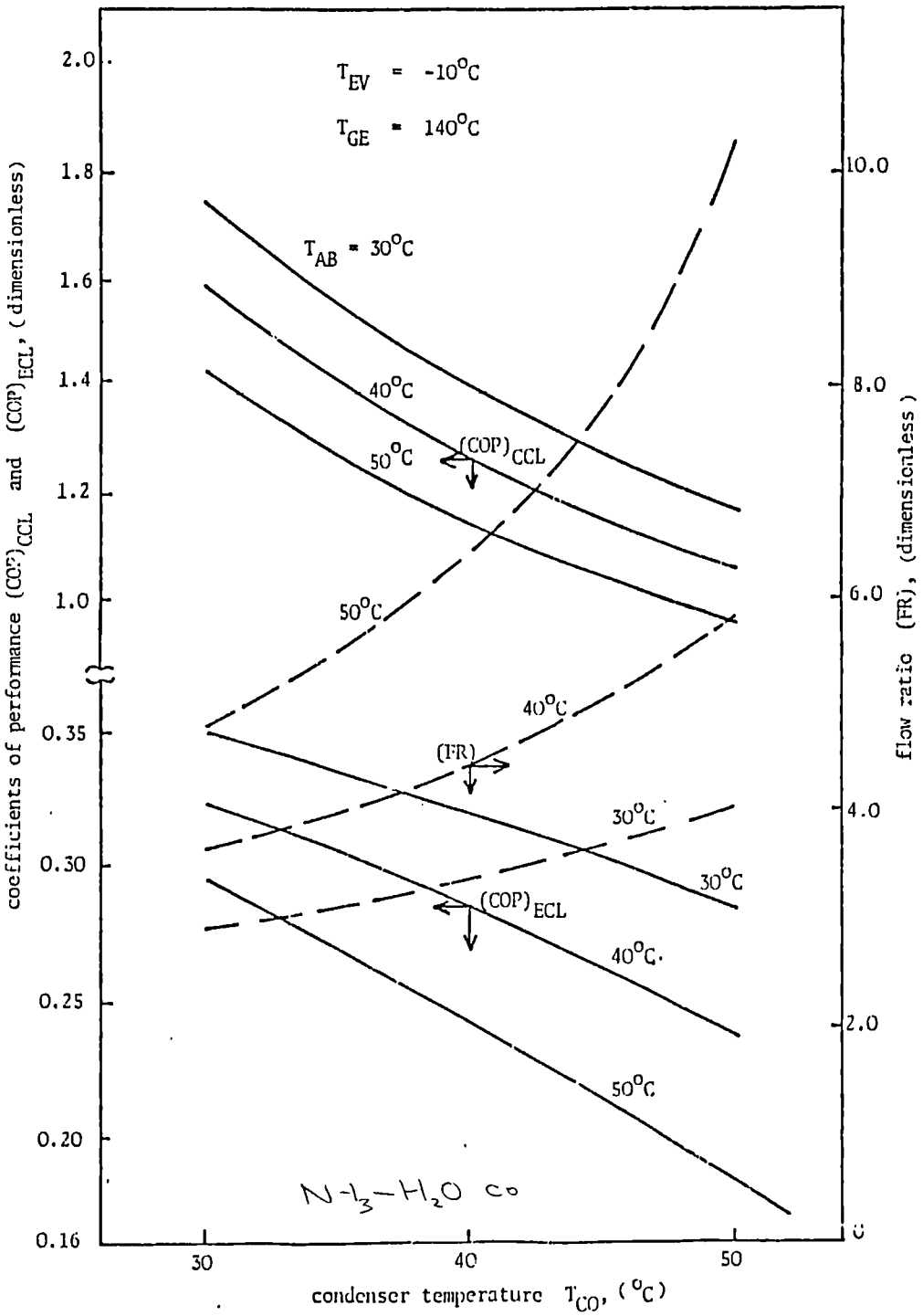

Fig. 4.5 Plot of coefficients of performance and flow ratio against condenser temperature at three different absorber temperatures

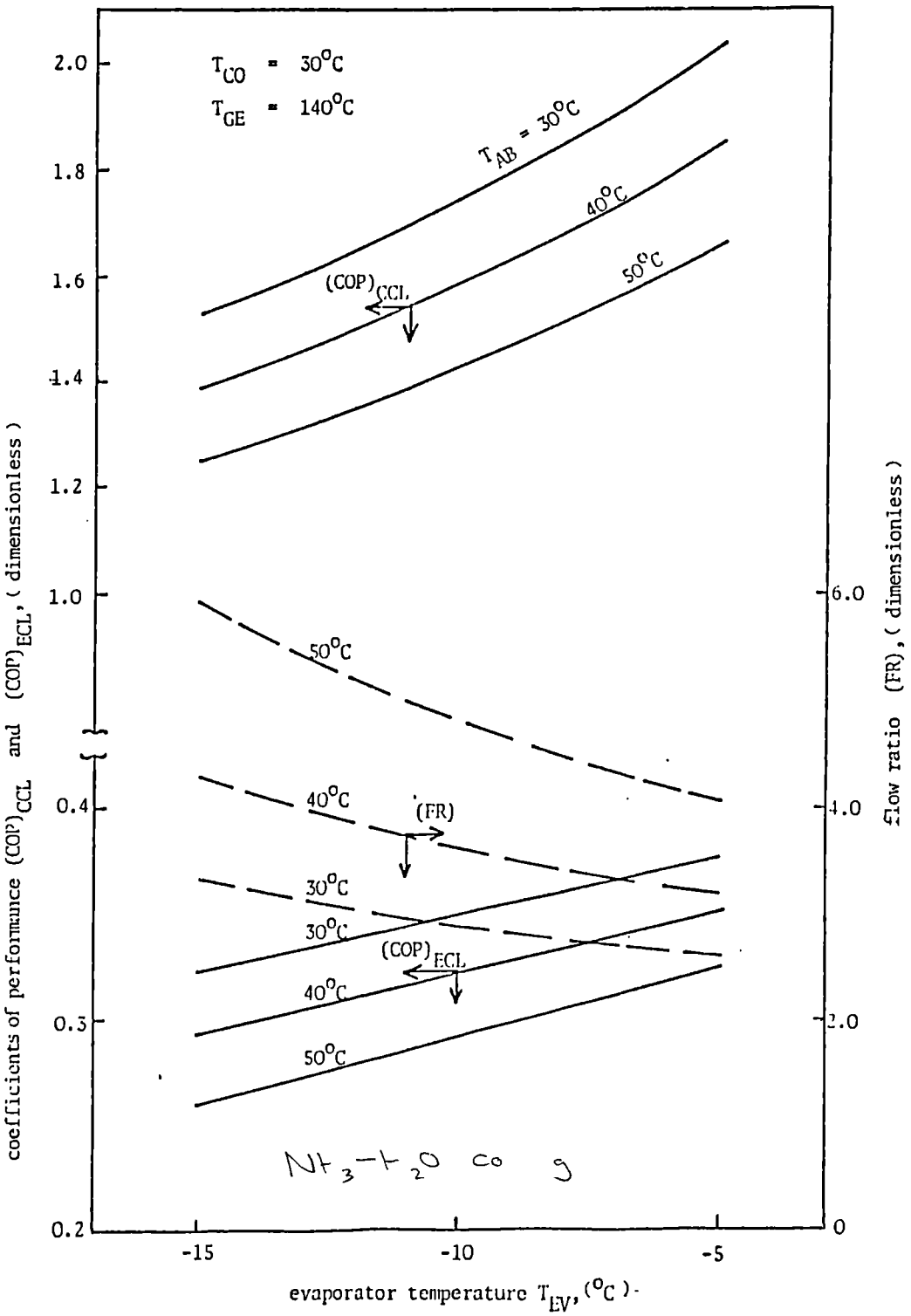

Fig.4.6 Plot of coefficients of performance and flow ratio against evaporator temperature at three different absorber temperatures.

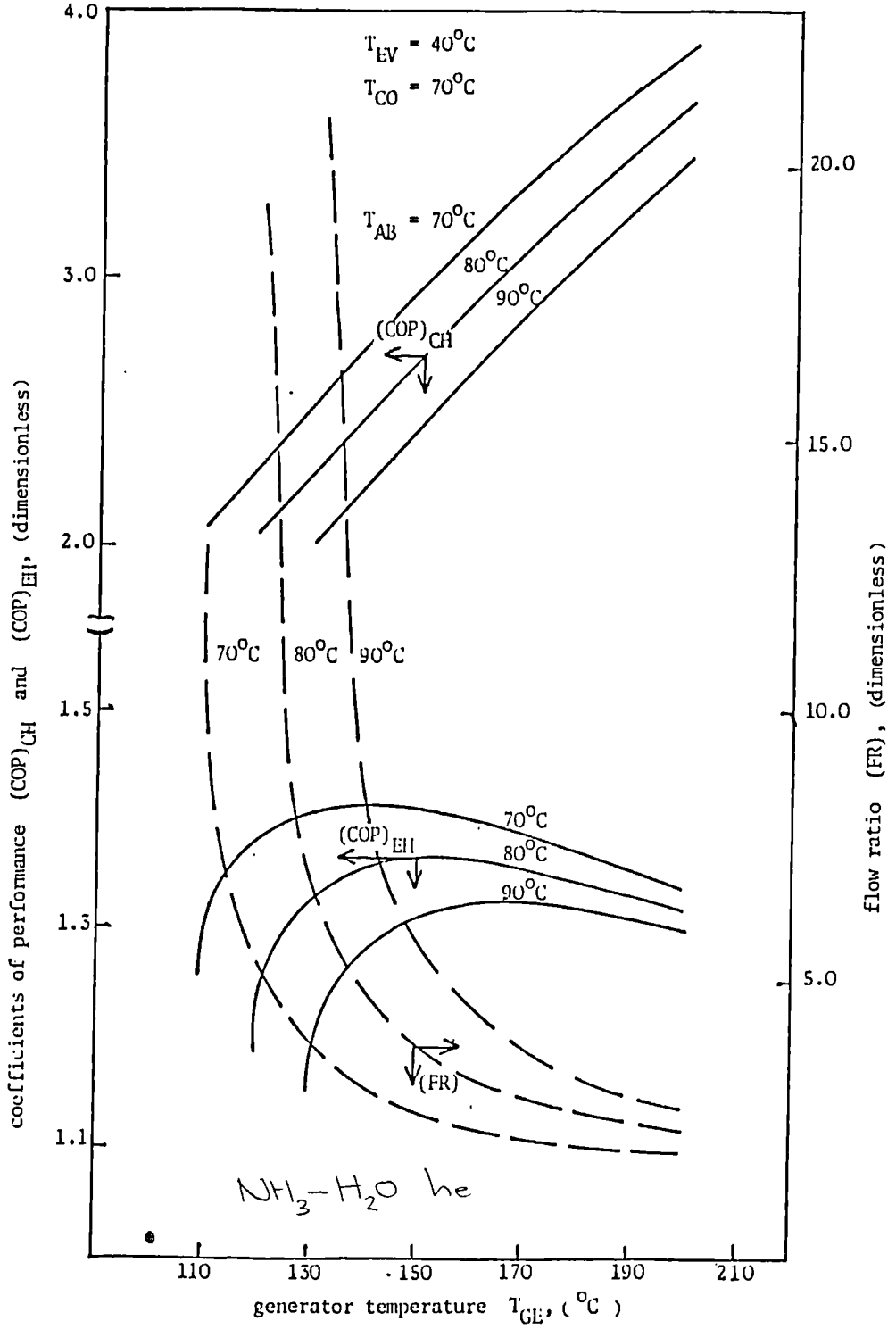

Fig. 4.7 Plot of coefficients of performance and flow ratio against generator temperature at three different absorber temperatures

Pages 57-59

ammonia-water for heating.

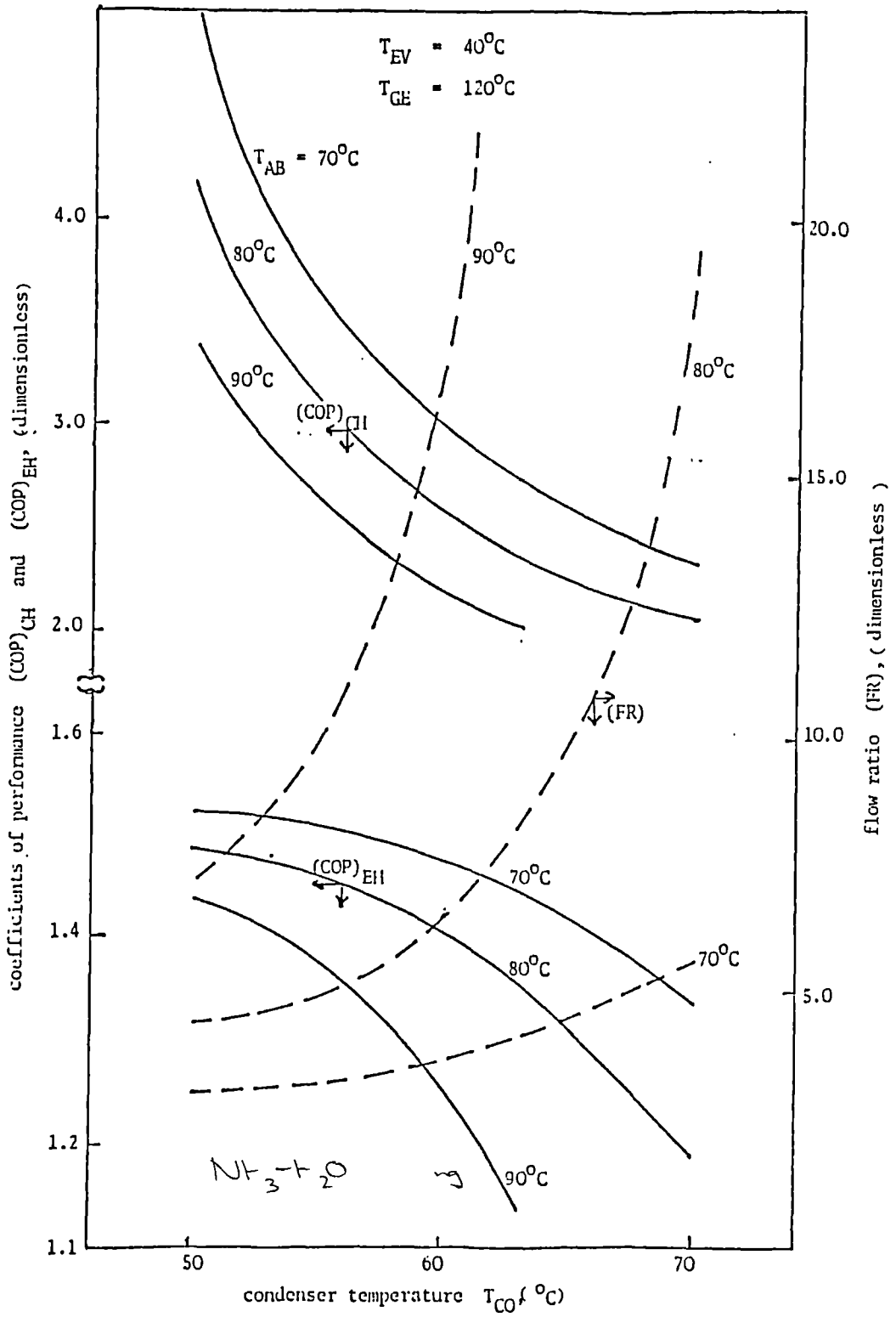

Fig.4.8 Plot of coefficients of performance and flow ratio against condenser temperature at three different absorber temperatures.

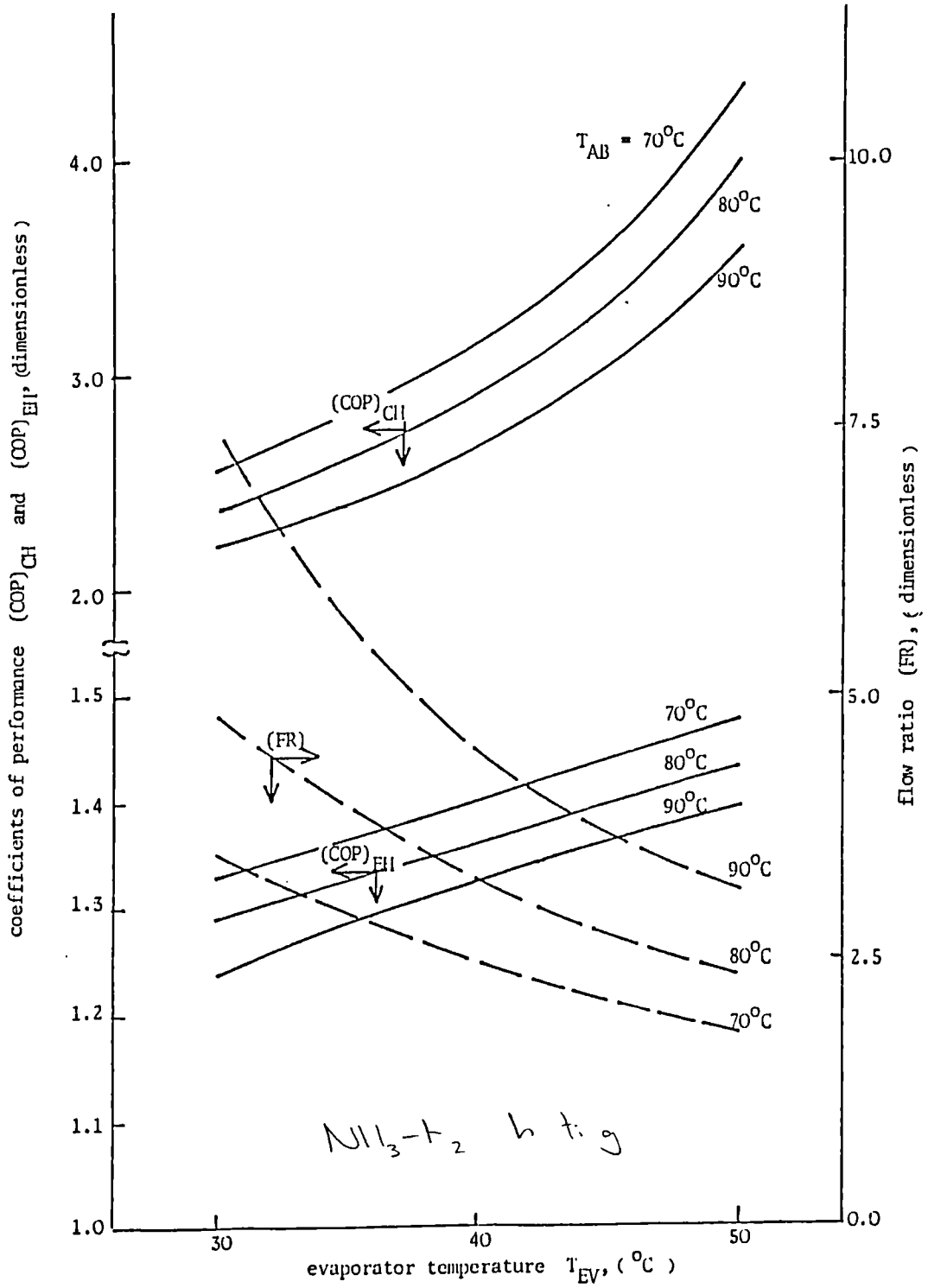

Fig.4.9 Plot of coefficients of performance and flow ratio against evaporator temperature at three different absorber temperatures.

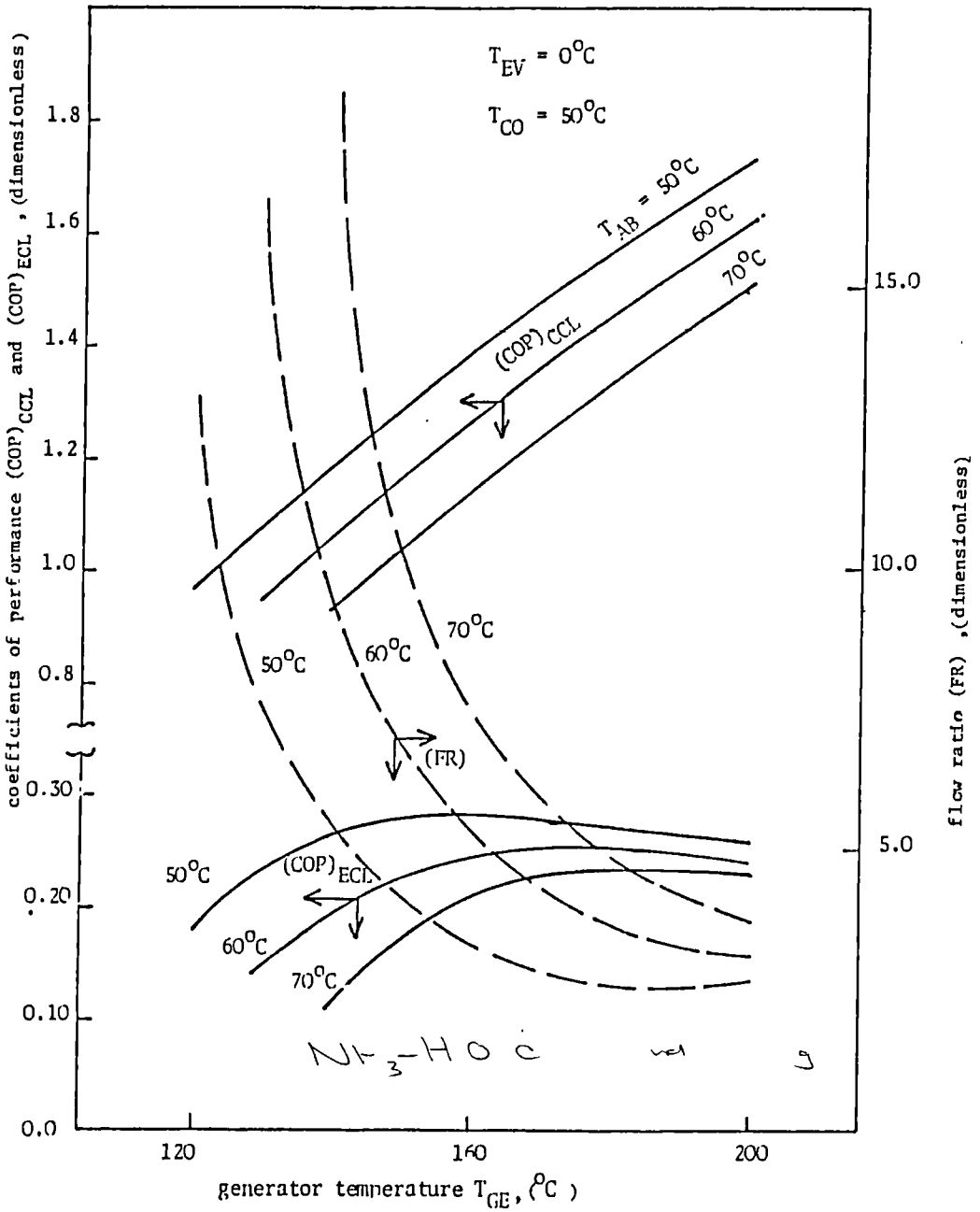

Fig. 4.10 Plot of coefficients of performance and flow ratio against generator temperature at three different absorber temperatures.

Pages 60-62

ammonia-water for cooling and simultaneous heating.

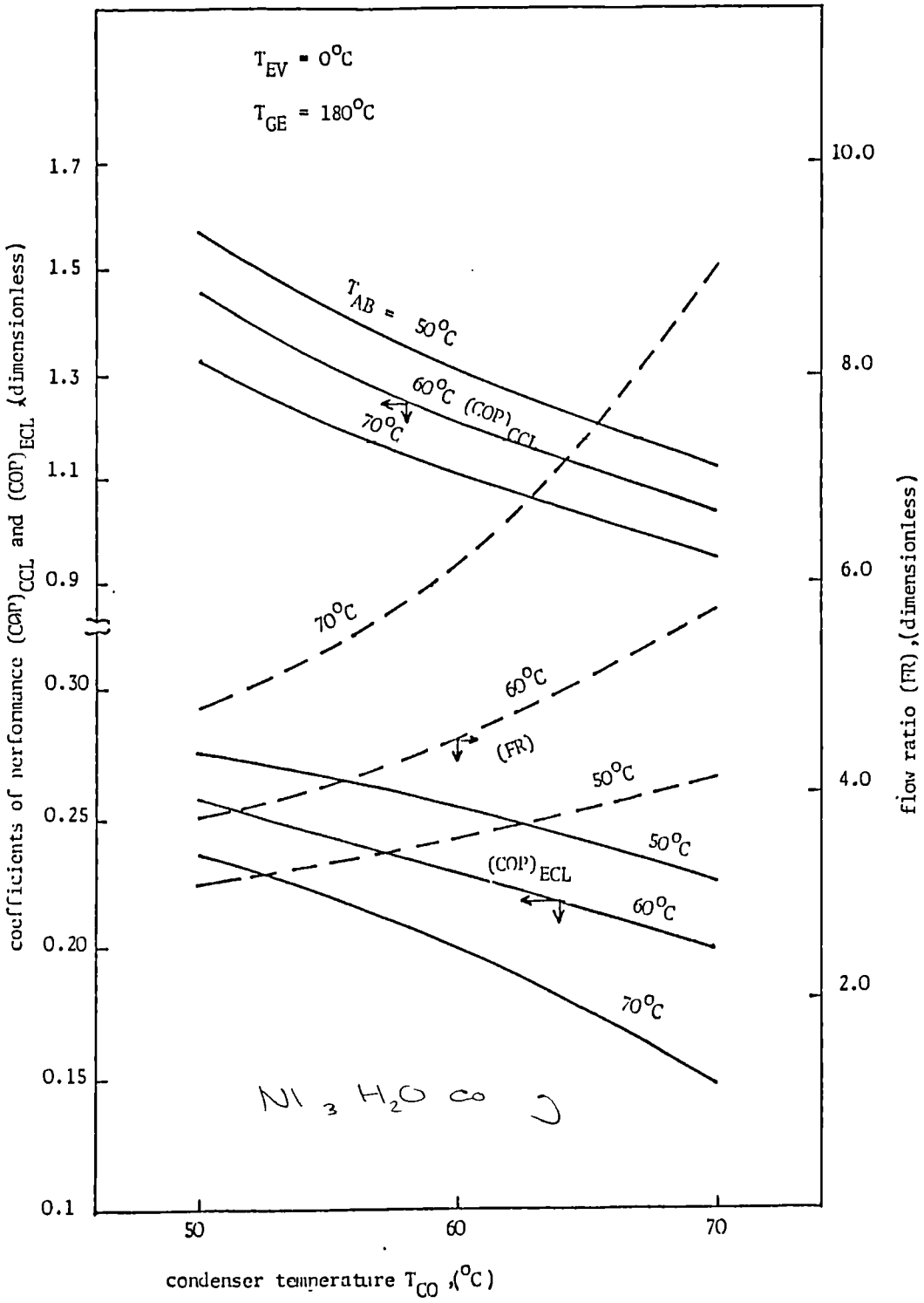

Fig. 4.11. Plot of coefficients of performance and flow ratio against condenser temperature at three different absorber temperatures.

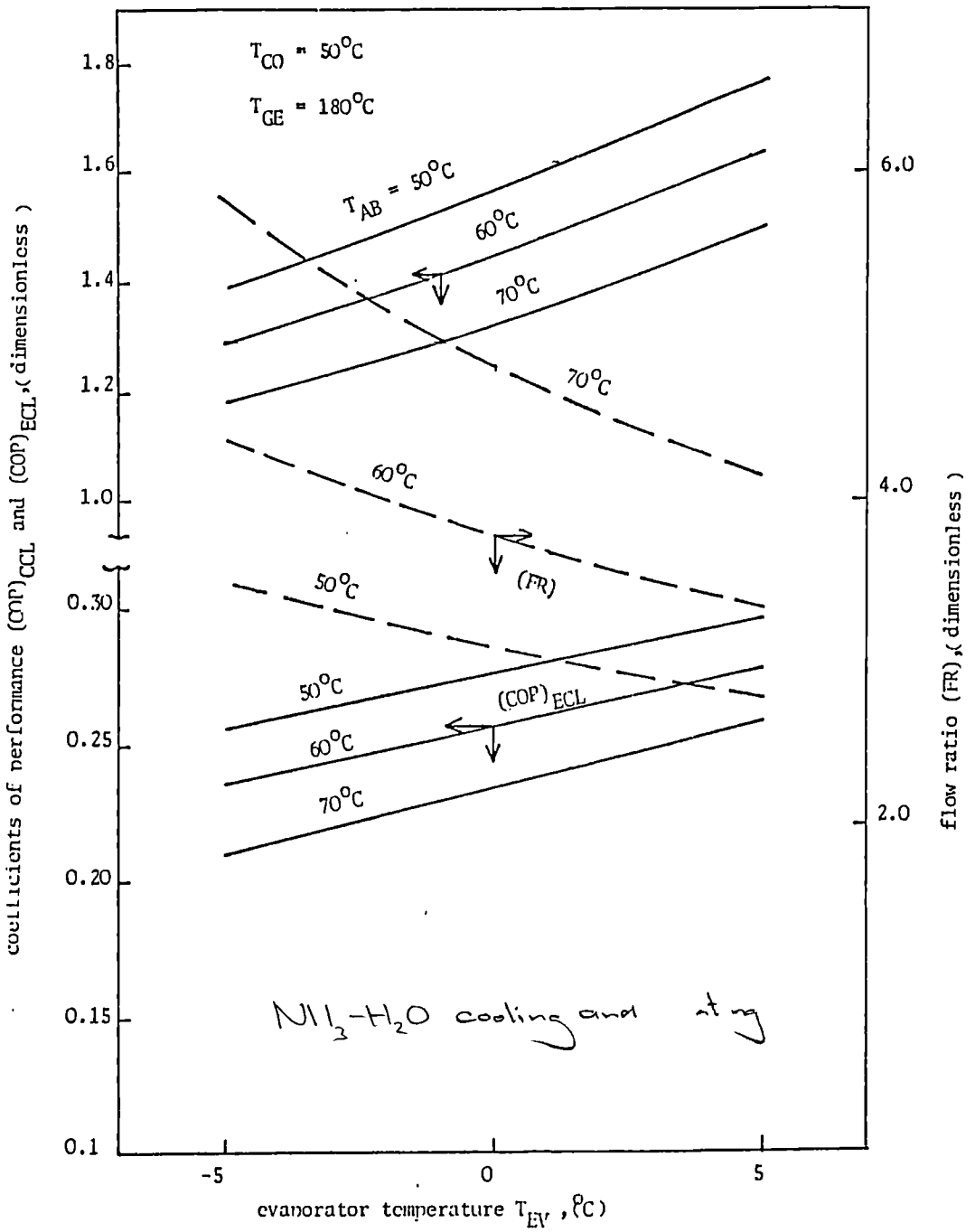

Fig. 4.12 Plot of coefficients of performance and flow ratio against evaporator temperature at three different absorber temperatures.

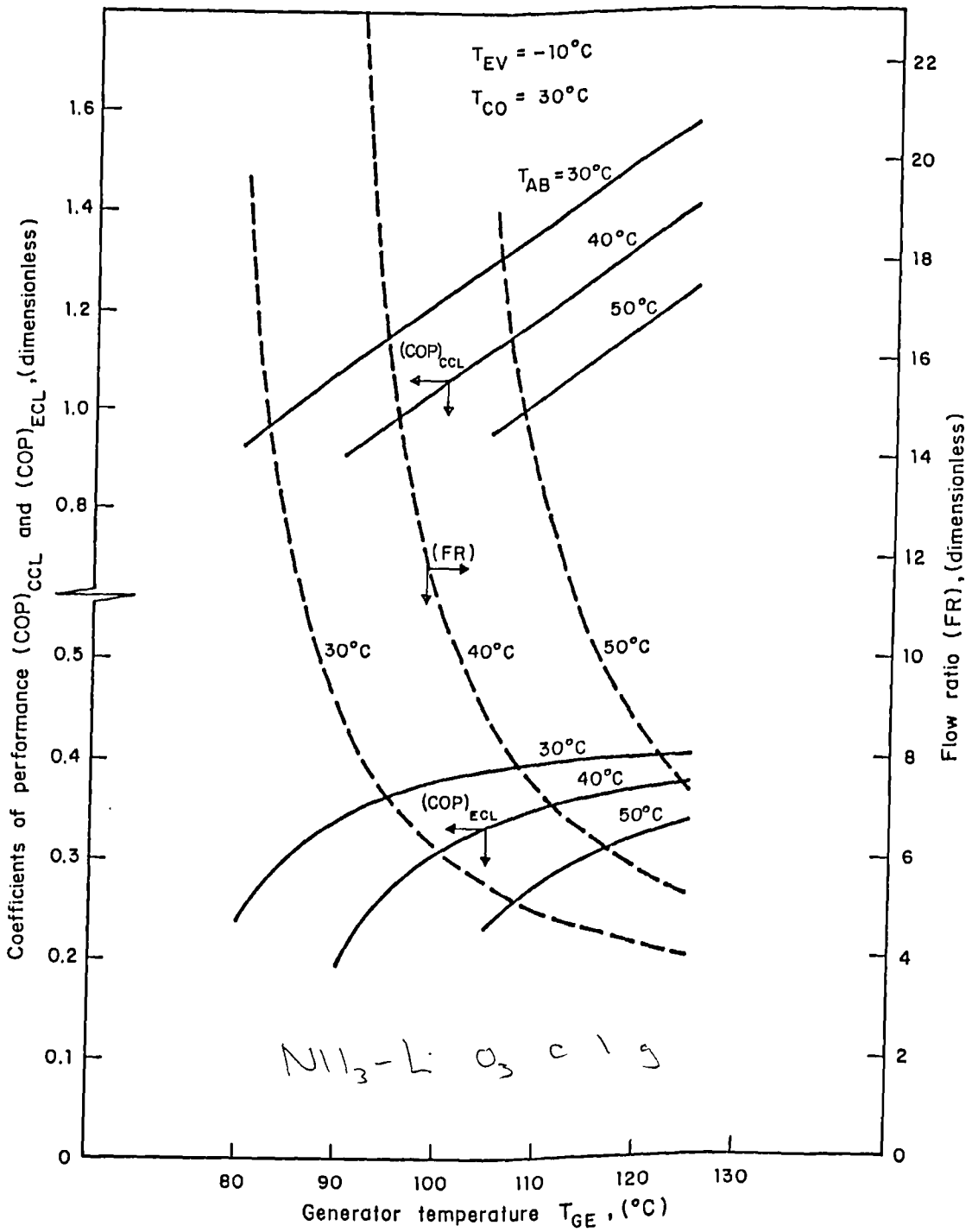

Fig. 4.13 Plot of coefficients of performance, flow ratio, against generator temperature at three different absorber temperatures.

Pages 63-65

ammonia-lithium nitrate for cooling.

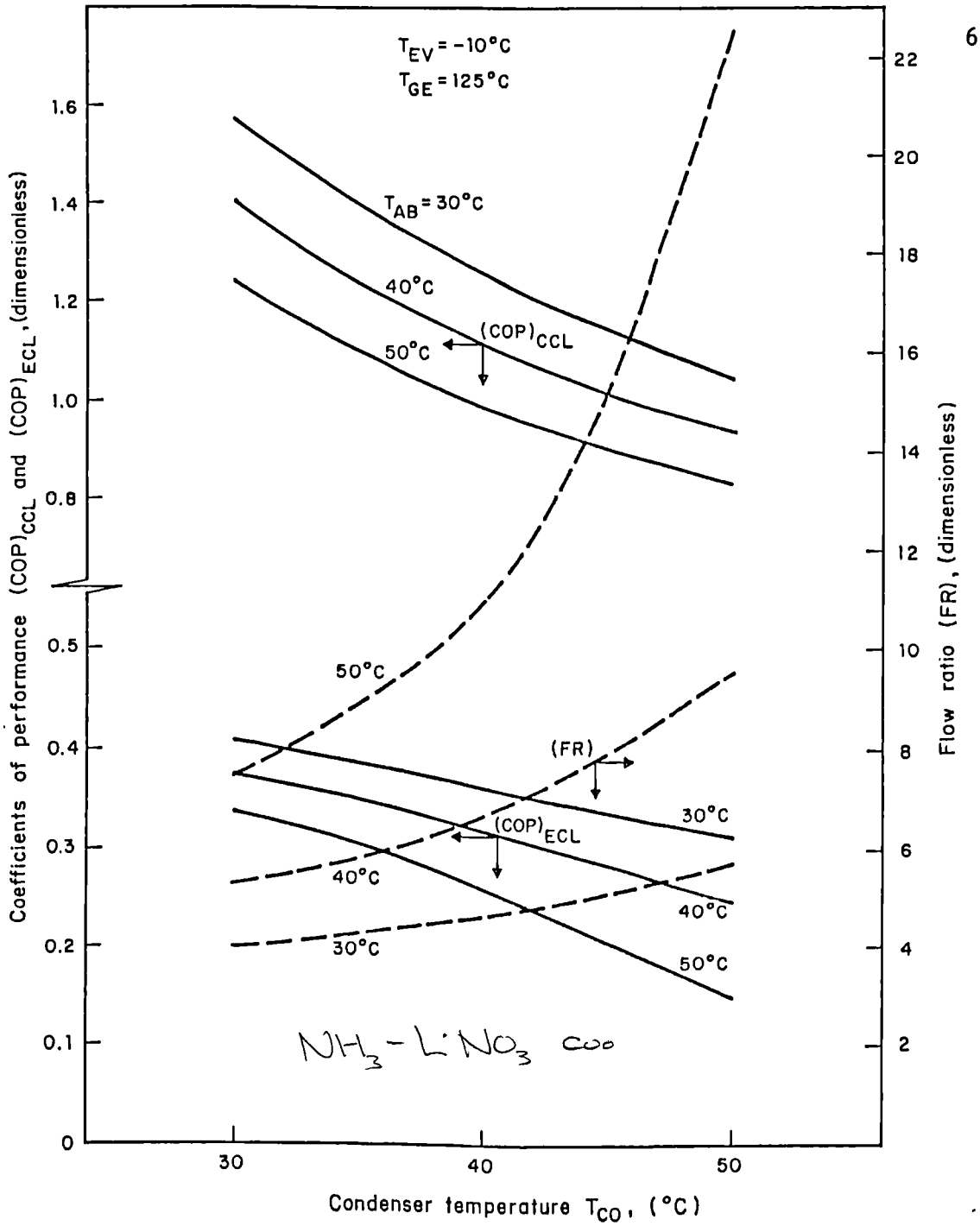

Fig. 4.14 Plots of coefficients of performance and flow ratio against condenser temperature at three different absorber temperatures

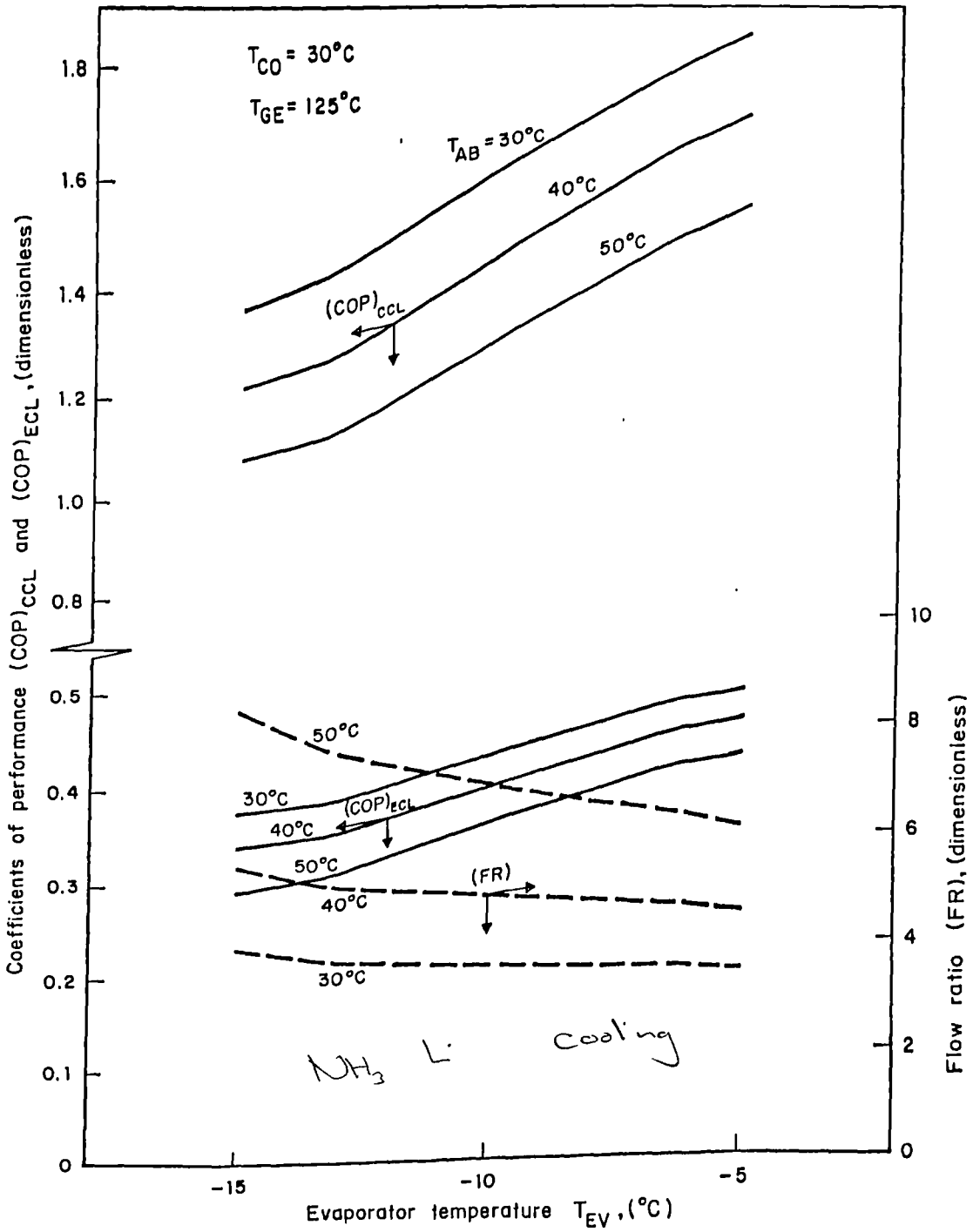

Fig. 4.15 Plot of coefficients of performance and flow ratio against evaporator temperature at three different absorber temperatures.

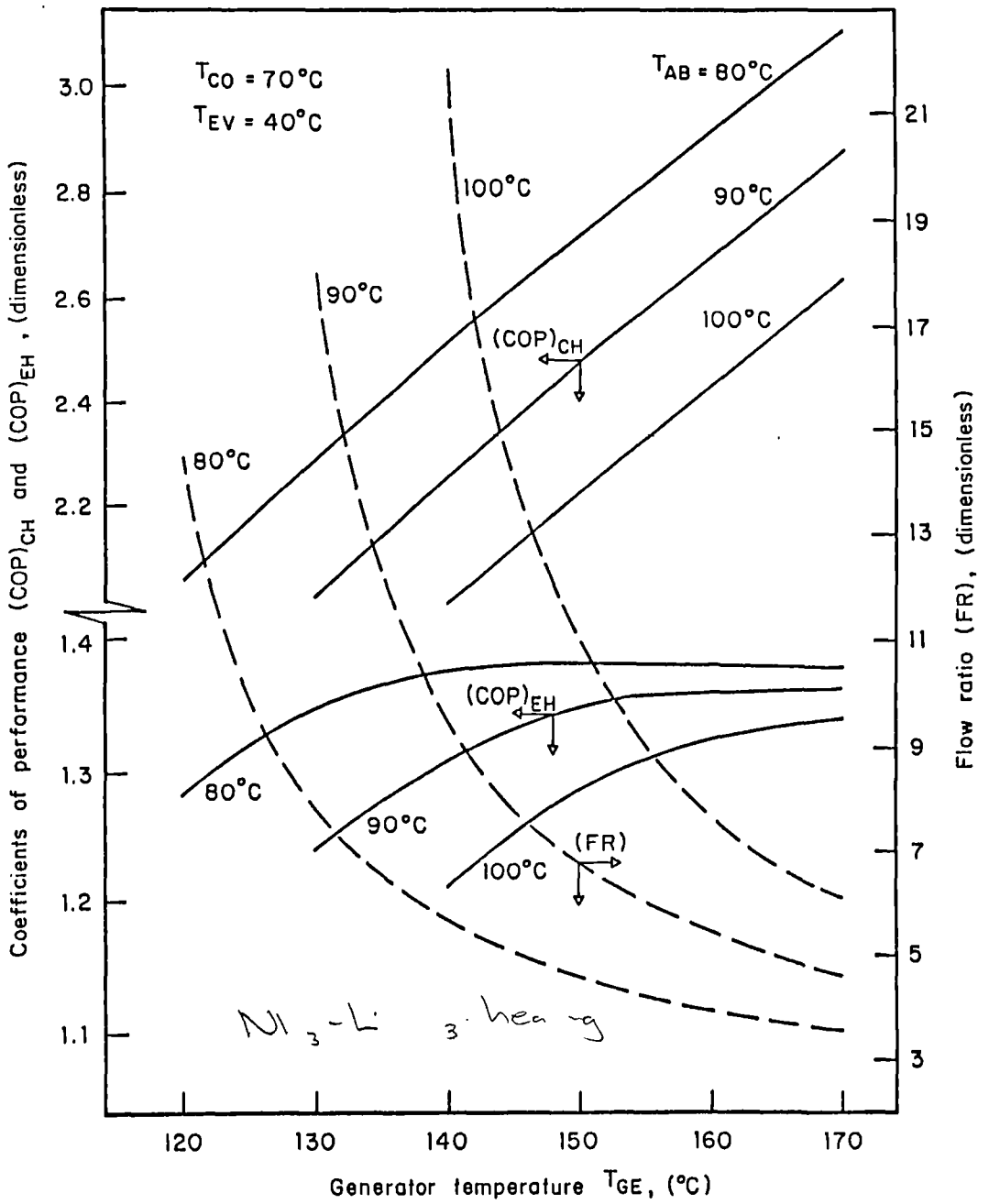

Fig. 4.16 Plots of coefficients of performance and flow ratio, against generator temperature at three different absorber temperatures.

Pages 66-68

ammonia-lithium nitrate for heating.

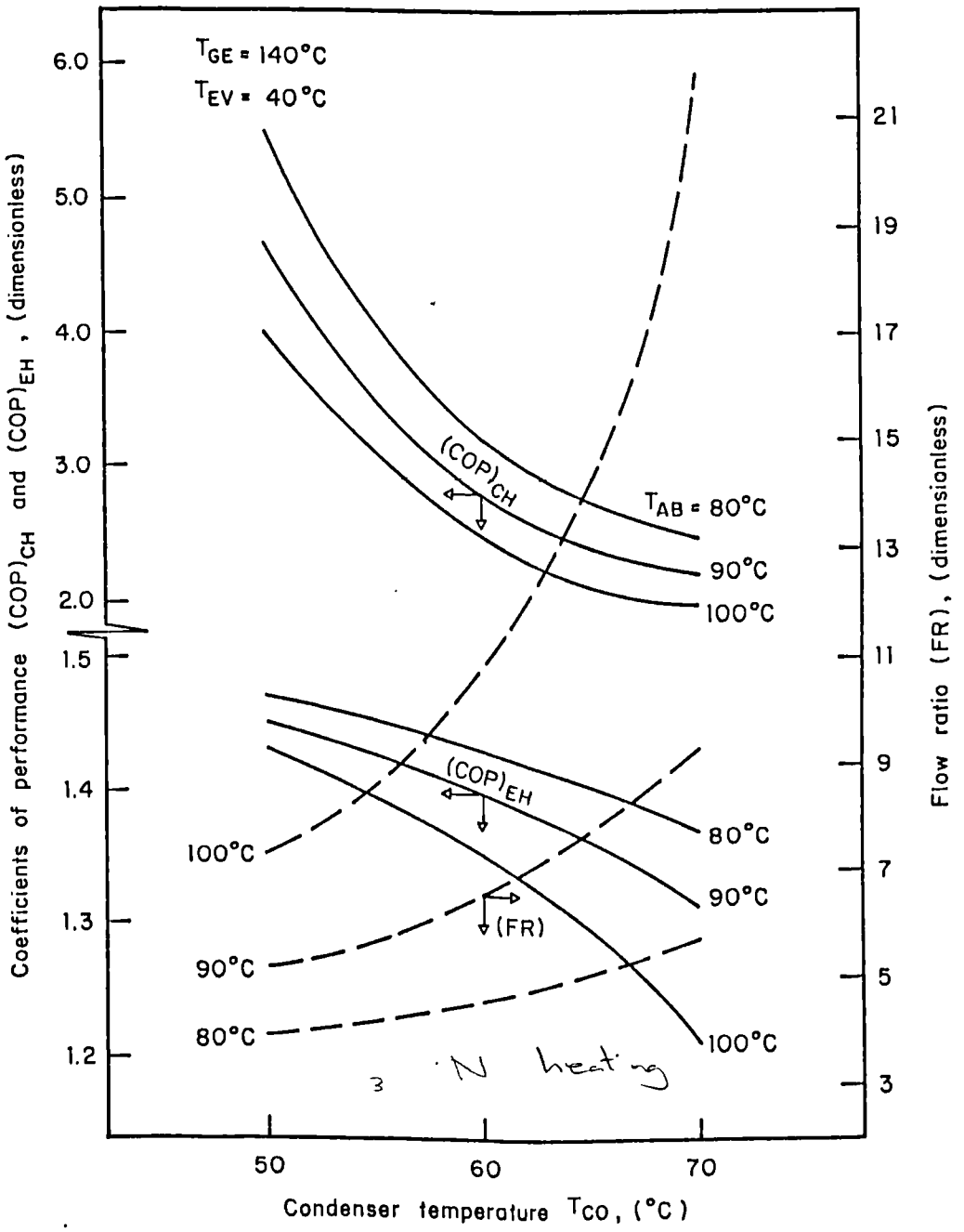

Fig. 4.17 Plots of coefficients of performance and flow ratio against condenser temperature at three different absorber temperatures.

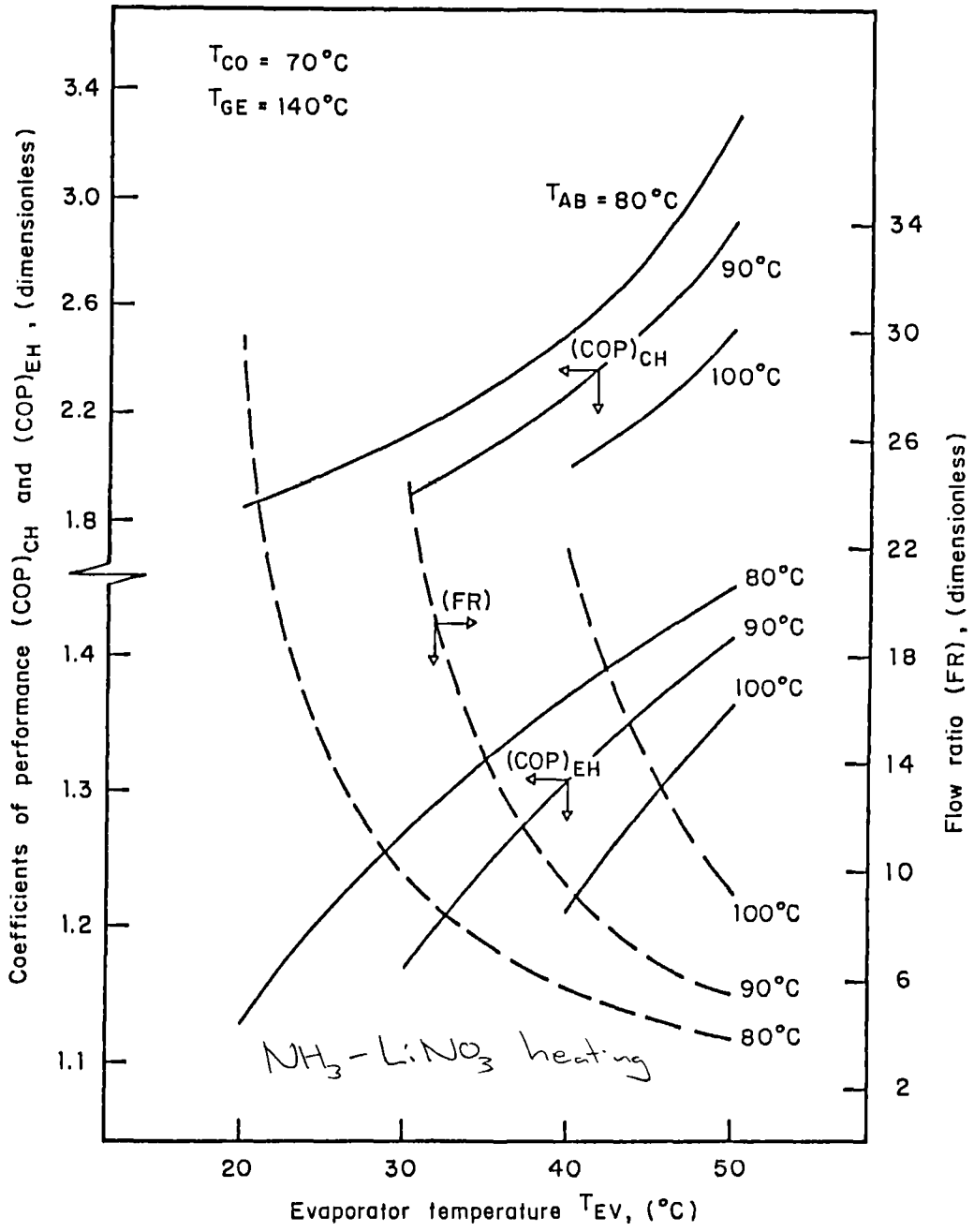

Fig.4.18 Plots of coefficients of performance, and flow ratio against evaporator temperature at three different absorber temperatures.

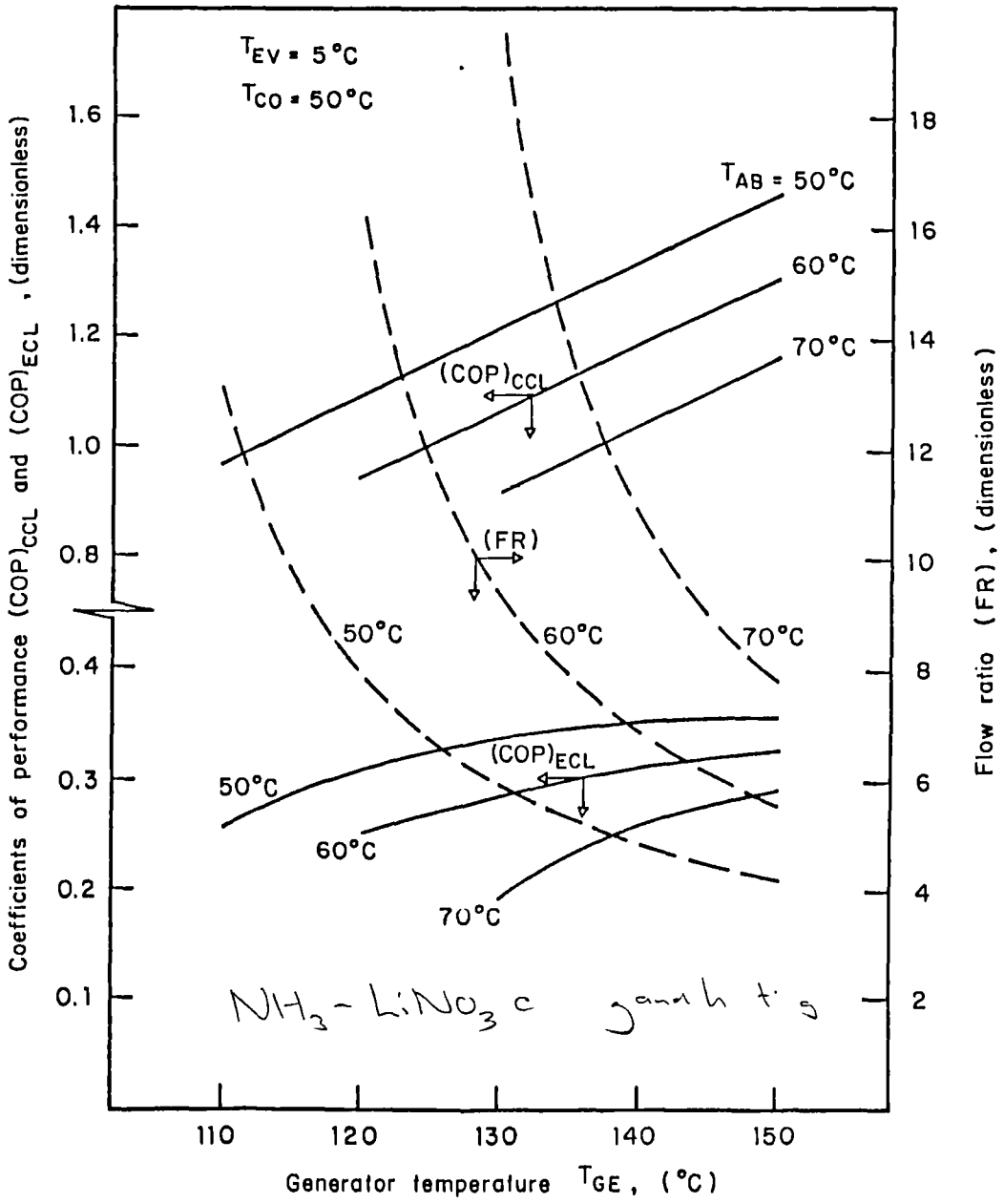

Fig. 4.19 Plots of coefficients of performance and flow ratio against generator temperature at three different absorber temperatures.

Pages 69-71

ammonia-lithium nitrate for cooling and simultaneous heating.

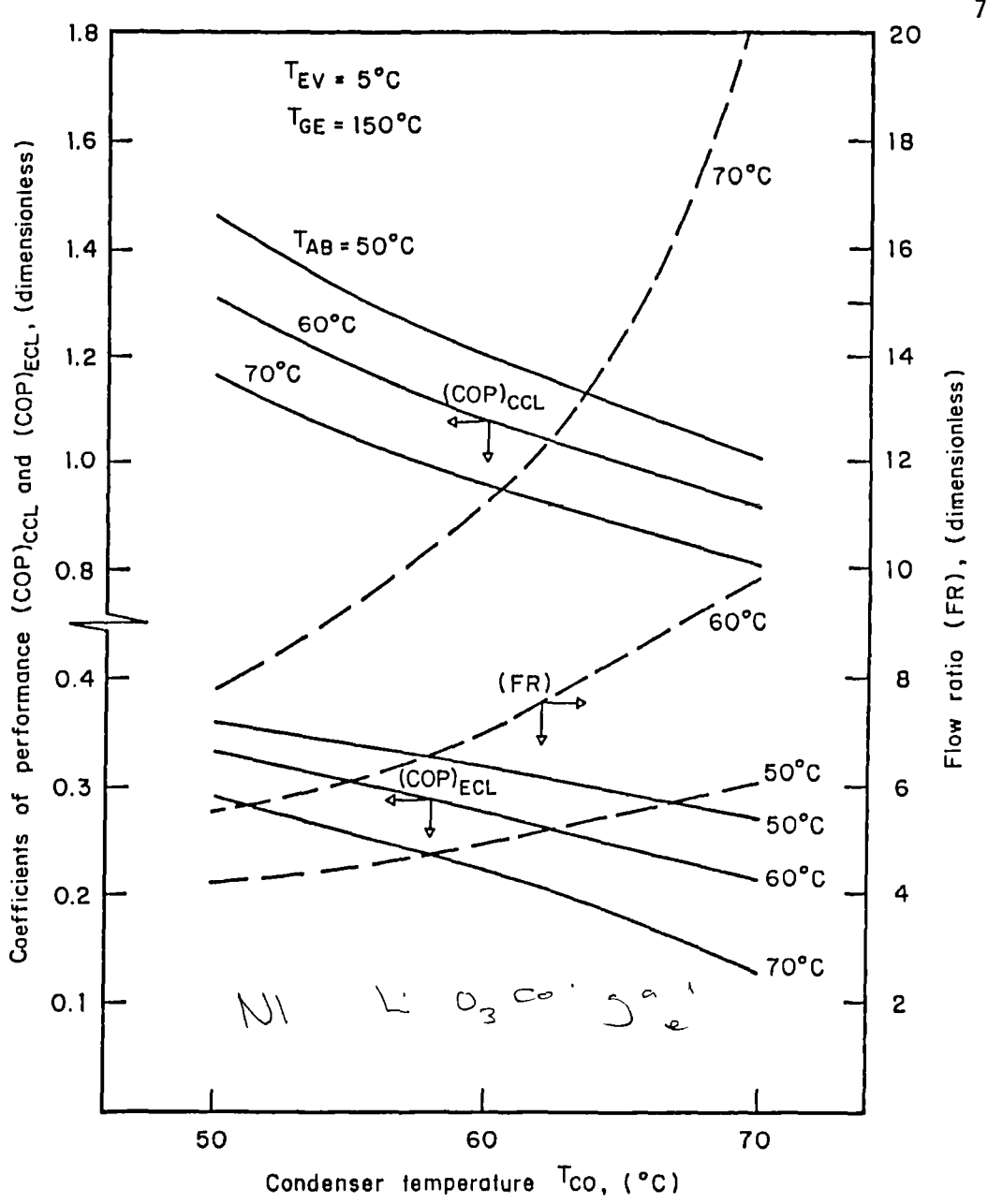

Fig. 4.20 Plots of coefficients of performance and flow ratio against condenser temperature at three different absorber temperatures.

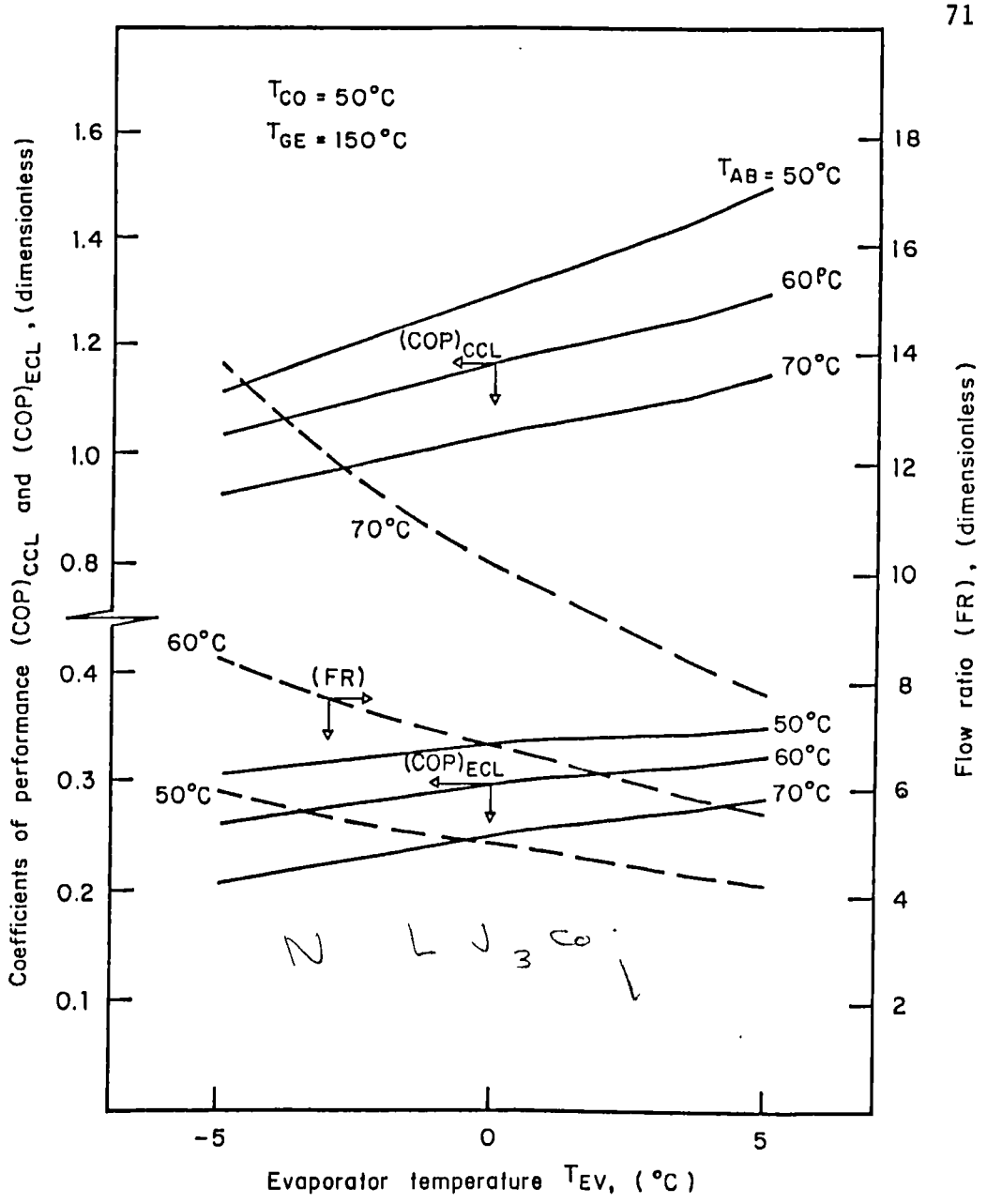

Fig. 4.21 Plots of coefficients of performance and flow ratio against evaporator temperature at three different absorber temperatures.

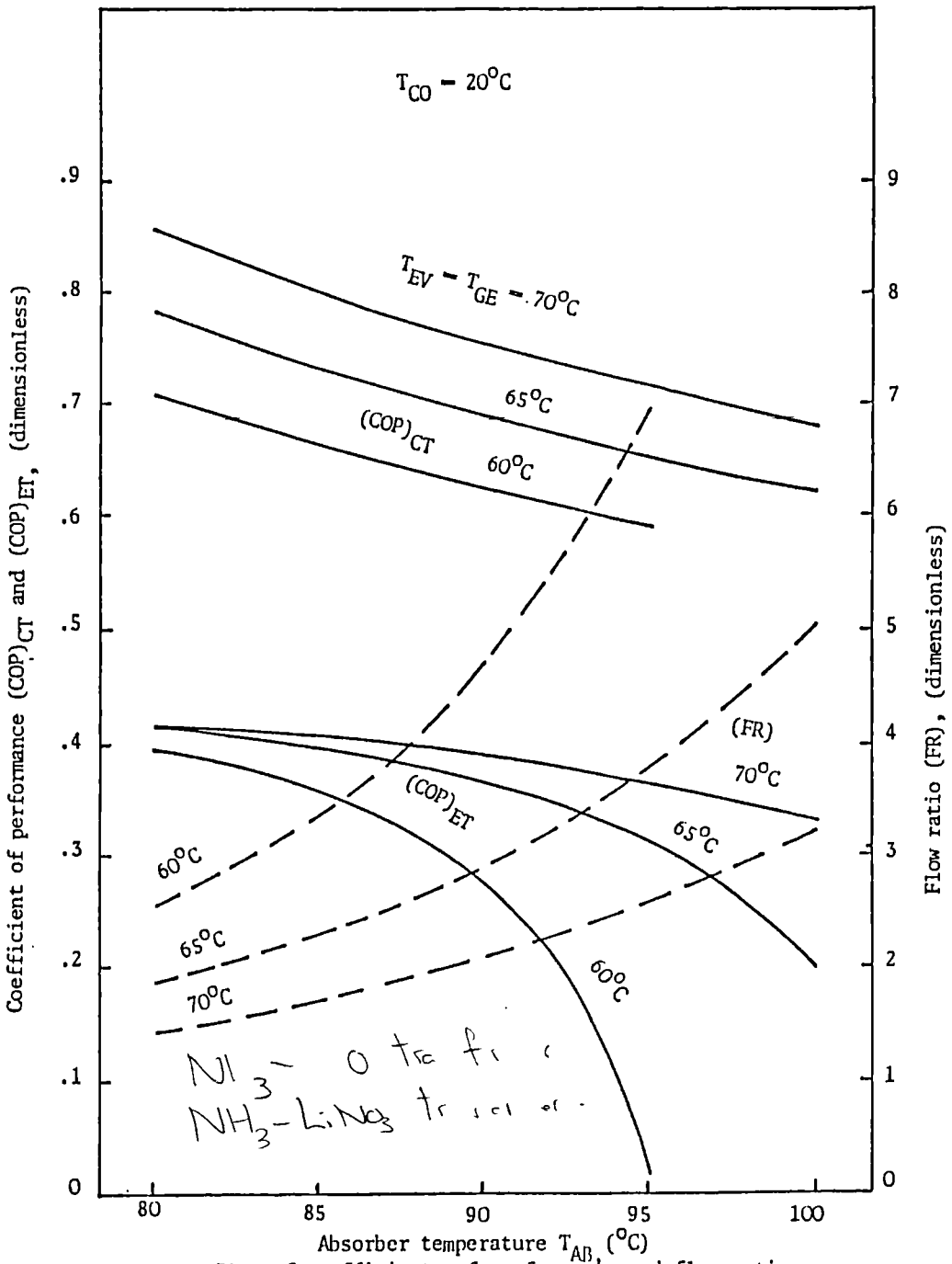

Fig. 4.22 Plot of coefficients of performance and flow ratio against absorber temperature at three different temperatures of the evaporator and generator.

Pages 72-74

ammonia-water for heat transformer.

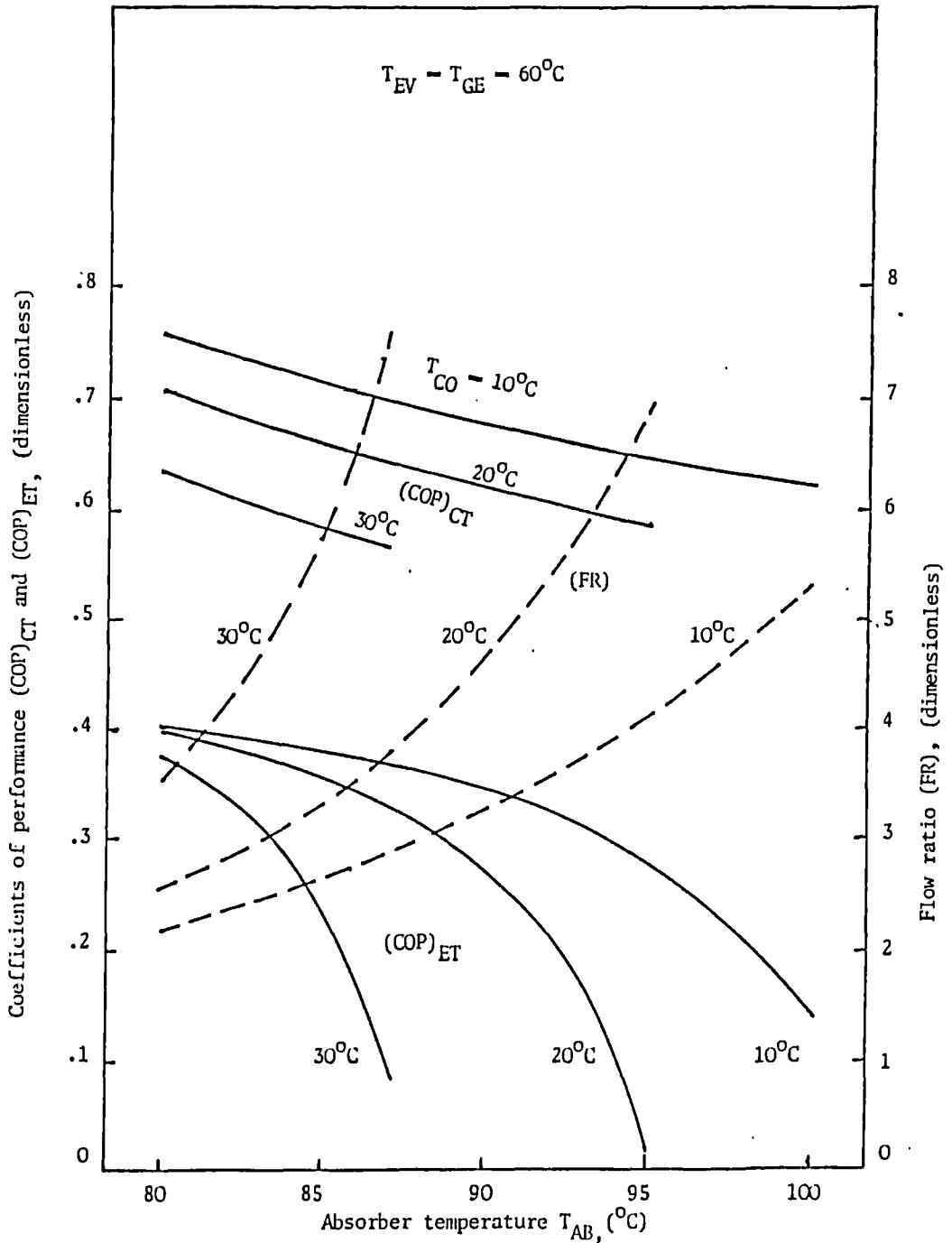

Fig. 4.23 Plot of coefficients of performance and flow ratio against absorber temperature at three different temperatures of condenser

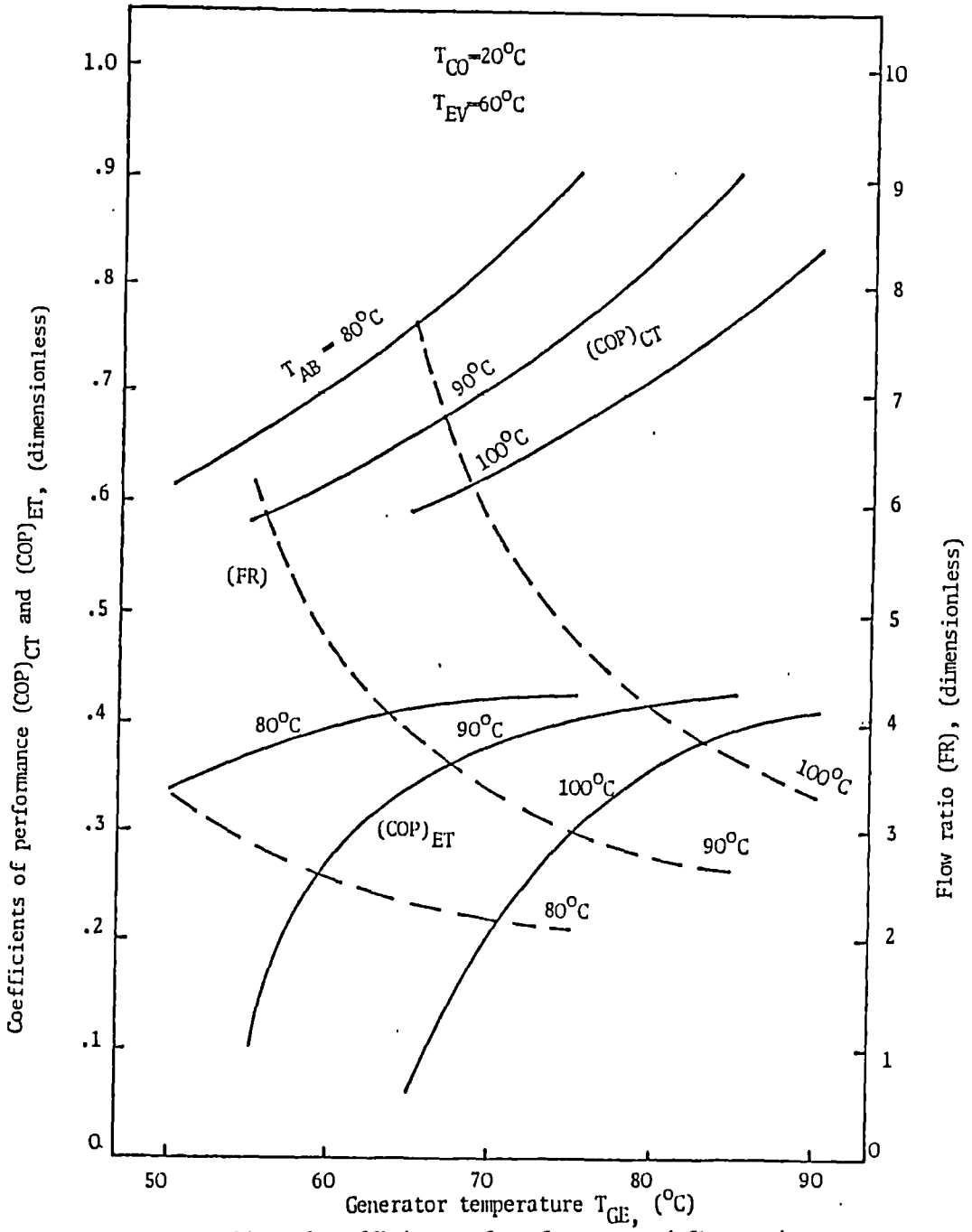

Fig. 4.24 Plot of coefficients of performance and flow ratio against generator temperature at three different temperatures of the absorber.

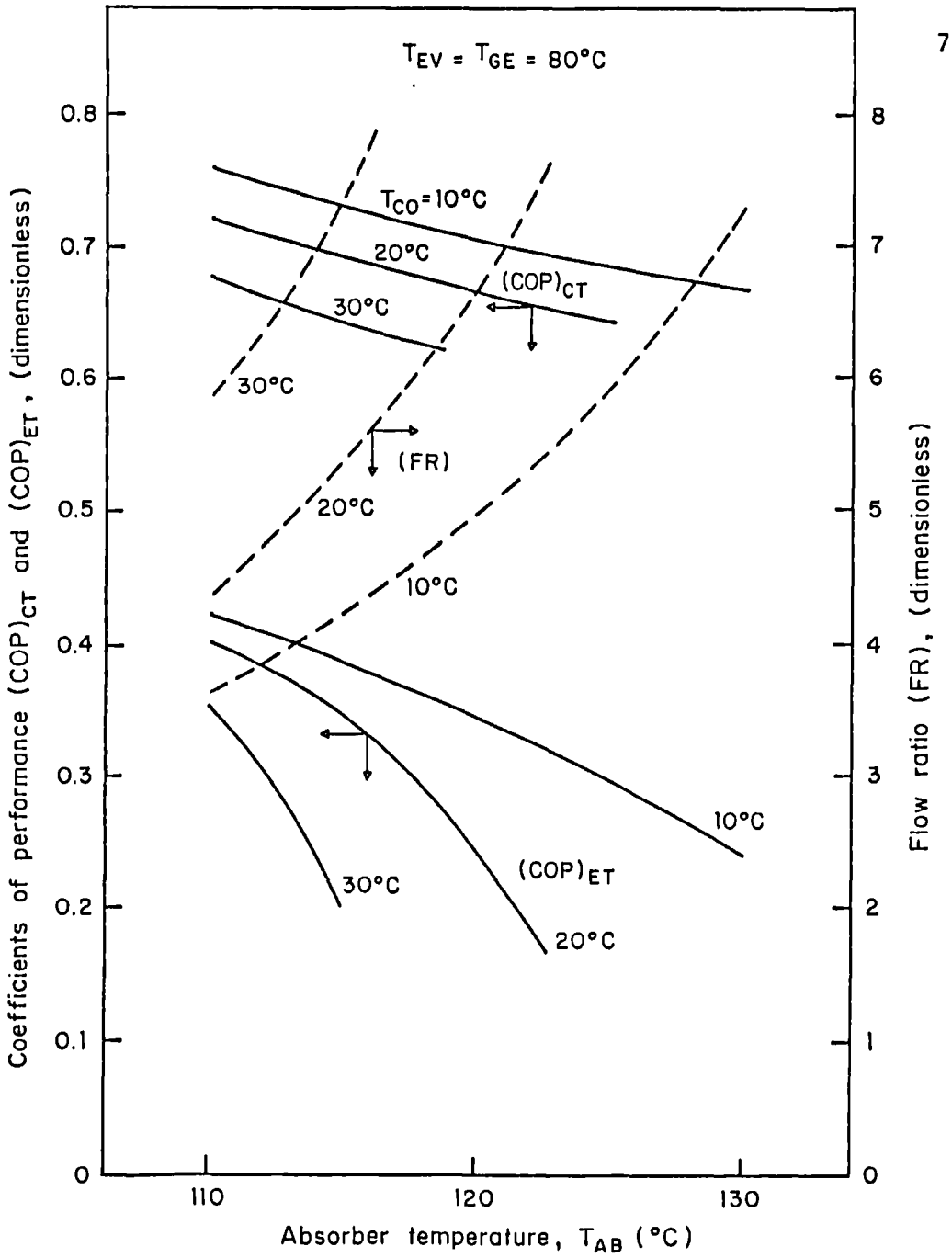

Fig. 4.25 Plot of coefficients of performance and flow ratio against absorber temperature at three different condenser temperatures

Pages 75-77

ammonia-lithium nitrate for heat transformer.

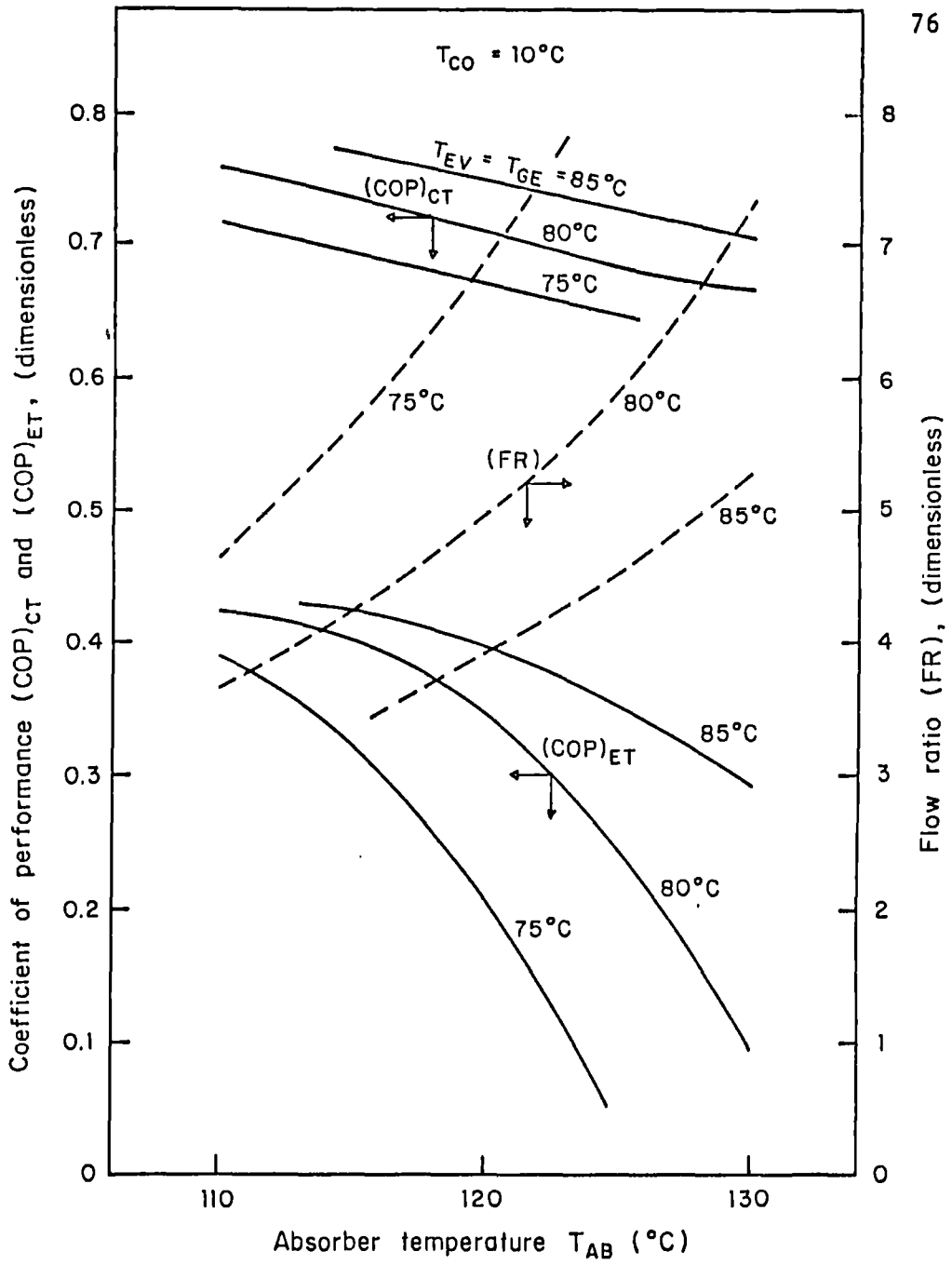

Fig. 4.26 Plot of coefficients of performance and flow ratio against absorber temperature at three different generator temperatures

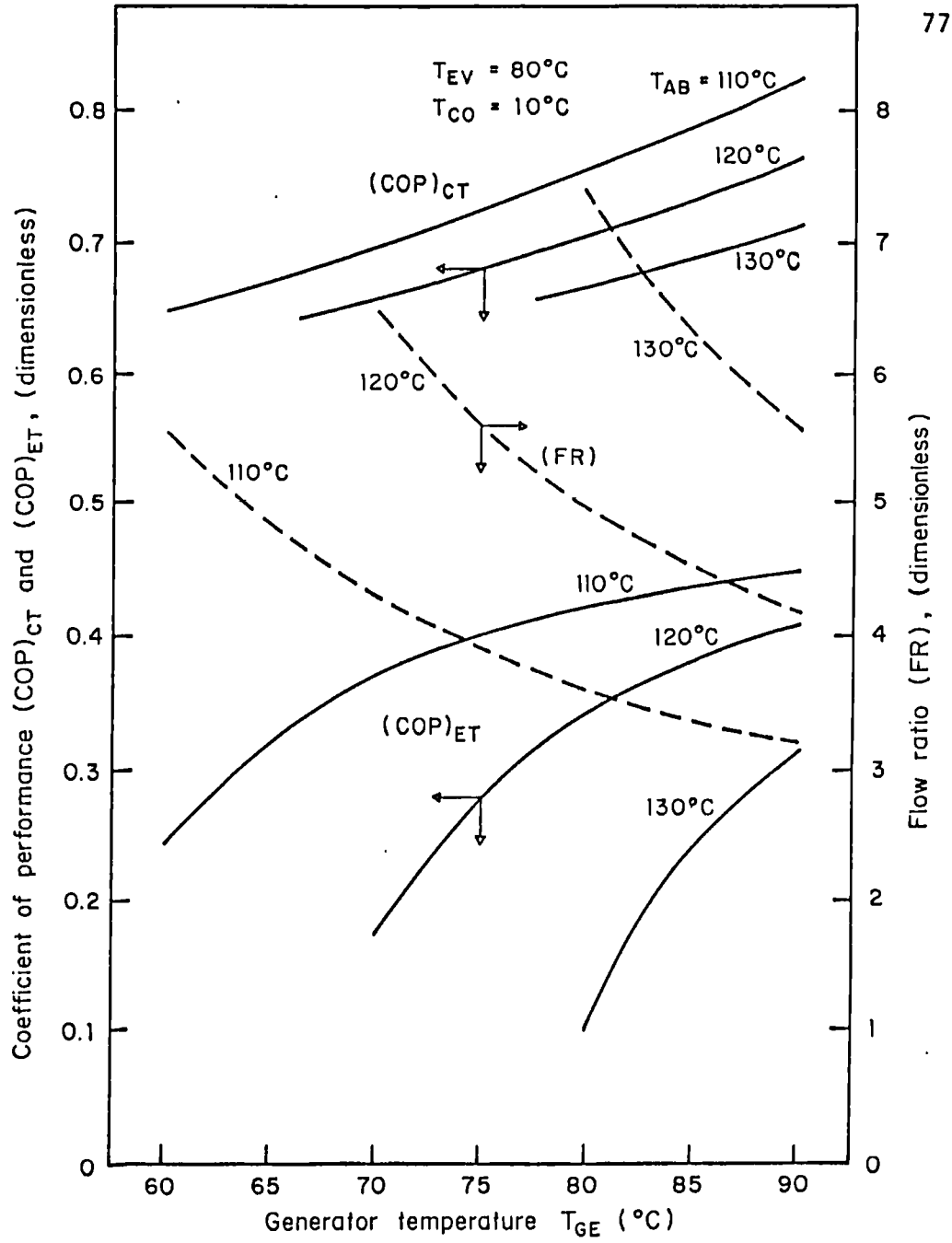

Fig. 4.27 Plot of coefficient of performance and flow ratio against generator temperature at three different absorber temperatures

CHAPTER 5

MODELLING OF CONTINUOUS ABSORPTION COOLING SYSTEMS

5.1 INTRODUCTION

Mass and energy balances for the computer modelling of continuous absorption systems for refrigeration using ammonia-water and ammonia-lithium nitrate as working pairs have been made. The performance of the systems was studied by considering the effect on the enthalpy based coefficient of performance $(COP)_{ECL}$ of varying the most important parameters which would be very difficult to achieve experimentally.

5.2 THERMODYNAMIC CONSIDERATIONS

In order to simplify the model, the following thermodynamic conditions were specified.

(1) The absorption refrigeration system operates at steady state.

(2) The high pressure in the system is the equilibrium pressure corresponding to the temperature and concentration of the refrigerant at the condenser outlet $P_{CO} = P(X_R, T_{CO})$ and is equal to the pressure in the generator and in the rectifier i.e. $P_{CO} = P_{GE} = P_{RE}$.

(3) The low pressure in the system is the equilibrium pressure corresponding to the temperature and concentration of the refrigerant at the evaporator outlet $P_{EV} = P(X_R, T_{EV})$ and is equal to the pressure in the absorber $P_{EV} = P_{AB}$.

(4) The pressure drops due to friction in the system are considered to be negligible.

(5) The temperatures in the generator, rectifier, condenser, evaporator and absorber are considered constant during the modelling.

Also following the numeration of Figures 5.1 and 5.2

$$T_{GE} = T_4 = T_7 \tag{5.1}$$

$$T_{REC} = T_8 = T_9 \tag{5.2}$$

$$T_{CO} = T_{10} \tag{5.3}$$

$$T_{EV} = T_{13} \tag{5.4}$$

$$T_{AB} = T_1 = T_2 \tag{5.5}$$

(6) The passage of the fluids through valves and pumps is considered to be an isenthalpic process

$$H_1 = H_2 \tag{5.6}$$

$$H_5 = H_6 \tag{5.7}$$

$$H_{11} = H_{12} \tag{5.8}$$

(7) There is no heat exchange between the piping, valves and pump and the ambient.

(8) The generation, rectification, condensation, evaporation and absorption processes occur at saturation conditions.

(9) The mass flow rate and concentration of the refrigerant remain constant from the rectifier outlet to the absorber inlet

$$M_R = M_9 = M_{10} = M_{11} = M_{12} = M_{13} = M_{14} \tag{5.9}$$

$$X_R = X_9 = X_{10} = X_{11} = X_{12} = X_{13} = X_{14} \tag{5.10}$$

(10) The effectiveness of the heat exchangers are defined as

$$ETA1 = (H_4 - H_5) / (H_4 - H_{52}) \tag{5.11}$$

$$ETA2 = (H_{13} - H_{14}) / (H_{13} - H_{1410}) \tag{5.12}$$

where

H_{52} is the enthalpy of the ammonia-water solution at the concentration of state 5 and at the temperature of state 2.

and

H_{1014} is the enthalpy of the refrigerant at the concentration of state 10 and at the temperature of state 14.

The same considerations were made for the ammonia-lithium nitrate mixture with the only difference that the ammonia vapour at the generator outlet was considered pure, so that no rectification was needed ($X_{REC} = X_{12} = 1$).

5.3 THERMODYNAMIC PROPERTIES OF THE AMMONIA-WATER MIXTURES

An important factor in the modelling of the absorption system is the availability of thermodynamic properties of the working pair. In this work the equations developed by Dao [5.1] based on the data published by Macriss et al [5.2] were used for ammonia-water. For ammonia-lithium nitrate the equations developed by Infante-Ferreira [5.3] were used.

5.4 MASS AND ENERGY BALANCES FOR THE AMMONIA-WATER ABSORPTION SYSTEM

In order to determine the heat and mass transfer as well as the thermodynamic properties of some components, it is necessary to make energy and mass balances on each of the components of the system as follows.

Generator:

$$M_3 + M_8 = M_4 + M_7 \tag{5.13}$$

$$M_3X_3 + M_8X_8 = M_4X_4 + M_7X_7 \tag{5.14}$$

$$M_3H_3 + M_8H_8 + Q_{GE} = M_4H_4 + M_7H_7 \tag{5.15}$$

Rectifier:

$$M_7 = M_8 + M_9 \tag{5.16}$$

$$M_7X_7 = M_8X_8 + M_9X_9 \tag{5.17}$$

$$M_7H_7 + M_8H_8 + M_9H_9 + Q_{REC} \tag{5.18}$$

Condenser:

$$M_9 = M_{10} \tag{5.19}$$

$$M_9X_9 = M_{10}X_{10} \tag{5.20}$$

$$M_9H_9 = M_{10}X_{10} + Q_{CO} \tag{5.21}$$

Absorber:

$$M_{14} + M_6 = M_1 \tag{5.22}$$

$$M_{14}X_{14} + M_6X_6 = M_1X_1 \tag{5.23}$$

$$M_{14}H_{14} + M_6H_6 = M_1H_1 + Q_{AB} \tag{5.24}$$

Evaporator:

$$M_{12} = M_{13} \tag{5.26}$$

$$M_{12}X_{12} = M_{13}H_{13} \tag{5.26}$$

$$M_{12}H_{12} + Q_{EV} = M_{13}H_{13} \tag{5.27}$$

Economiser:

$$M_2 = M_3 \tag{5.28}$$

$$M_2X_2 = M_3X_3 \tag{5.29}$$

$$M_4 = M_5 \tag{5.30}$$

$$M_4X_4 = M_5X_5 \tag{5.31}$$

$$M_2X_2 + M_4H_4 = M_3H_3 + M_5H_5 \tag{5.32}$$

$$ETA1 = (H_4 - H_5) / (H_4 - H_{52}) \tag{5.33}$$

$$Q1 = M_4 (H_4 - H_5) \tag{5.34}$$

Precooler:

$$M_{13} = M_{14} \tag{5.35}$$

$$M_{10}X_{10} = M_{11}X_{11} \tag{5.36}$$

$$M_{13}X_{13} = M_{14}X_{14} \tag{5.37}$$

$$M_{10}H_{10} + M_{13}H_{13} = M_{11}H_{11} + M_{14}H_{14} \tag{5.38}$$

$$ETA2 = (H_{13} - H_{14}) / (H_{13} - H_{1410}) \tag{5.39}$$

$$Q11 = M_{10} (H_{10} - H_{11}) \tag{5.40}$$

Pump:

$$M_1 = M_2 \tag{5.41}$$

$$M_1X_1 = M_2X_2 \tag{5.42}$$

$$M_1H_1 + W_P = M_1H_2 \tag{5.43}$$

Valves:

$$M_5 = M_6 \tag{5.44}$$

$$M_5X_5 = M_6H_6 \tag{5.45}$$

$$M_5H_5 = M_6H_6 \tag{5.46}$$

$$M_{11} = M_{12} \tag{5.47}$$

$$M_{11}X_{11} = M_{12}X_{12} \tag{5.48}$$

$$M_{11}H_{11} = M_{12}H_{12} \tag{5.49}$$

5.5 MASS AND ENERGY BALANCES FOR THE AMMONIA-LITHIUM NITRATE ABSORPTION SYSTEM

The energy and mass balances for the components of the system are as follows.

Generator:

$$M_3 = M_4 + M_7 \tag{5.50}$$

$$M_3X_3 = M_4X_4 + M_7X_7 \tag{5.51}$$

$$M_3H_3 + Q_{GE} = M_4H_4 + M_7H_7 \tag{5.52}$$

Condenser:

$$M_7 = M_8 \tag{5.53}$$

$$M_7X_7 = M_8X_8 \tag{5.54}$$

$$M_7H_7 = M_8H_8 + Q_{CO} \tag{5.55}$$

Absorber:

$$M_6 + M_{12} = M_1 \tag{5.56}$$

$$M_6X_6 + M_{12}X_{12} = M_1X_1 \tag{5.57}$$

$$M_6H_6 + M_{12}H_{12} = M_1H_1 + Q_{AB} \tag{5.58}$$

Evaporator:

$$M_{10} = M_{11} \tag{5.59}$$

$$M_{10}X_{10} = M_{11}X_{11} \tag{5.60}$$

$$Q_{EV} + M_{10}H_{10} = M_{11}H_{11} \tag{5.61}$$

Economiser:

$$M_2 = M_3 \tag{5.62}$$

$$M_2X_2 = M_3X_3 \tag{5.63}$$

$$M_4 = M_5 \tag{5.64}$$

$$M_4X_4 = M_5X_5 \tag{5.65}$$

$$M_2H_2 + M_4H_4 = M_3H_3 + M_5H_5 \tag{5.66}$$

$$ETA1 = (H_4 - H_5) / (H_4 - H_{52}) \tag{5.67}$$

$$Q_1 = M_4 (H_4 - H_5) \tag{5.68}$$

Precooler:

$$M_{11} = M_{12} \tag{5.69}$$

$$M_{11}X_{11} = M_{12}X_{12} \tag{5.70}$$

$$M_8 = M_9 \tag{5.71}$$

$$M_8X_8 = M_9X_9 \tag{5.72}$$

$$M_8H_8 + M_{11}H_{11} = M_9H_9 + M_{12}H_{12} \tag{5.73}$$

$$ETA2 = (H_{11} - H_{12}) / (H_{11} - H_{128}) \tag{5.74}$$

$$Q_{11} = M_8 (H_8 - H_9) \tag{5.75}$$

Pump:

$$M_1 = M_2 \tag{5.76}$$

$$M_1X_1 = M_2X_2 \tag{5.77}$$

$$M_1H_1 + W_P = M_2H_2 \tag{5.78}$$

Valves:

$$M_5 = M_6 \tag{5.79}$$

$$M_5X_5 = M_6X_6 \tag{5.80}$$

$$M_5H_5 = M_6H_6 \tag{5.81}$$

$$M_9 = M_{10} \tag{5.82}$$

$$M_9X_9 = M_{10}X_{10} \tag{5.83}$$

$$M_9H_{10} = M_{10}H_{10} \tag{5.84}$$

5.6 RESULTS AND DISCUSSION

A base case was selected which does not change unless specified in the simulation. The values of the parameters were as follows:

concentration of ammonia vapour for ammonia-water entering condenser,	X_R = 0.99 weight fraction ammonia
concentration of ammonia vapour for ammonia-lithium nitrate,	X_R = 1.00 weight fraction ammonia
evaporator temperature,	T_{EV} = -4.0°C

absorber temperature, $T_{AB} = 23°C$

generator temperature, $T_{GE} = 100°C$

condenser temperature, $T_{CO} = 25°C$

economiser efficiency, ETA1 = 0.7

precooler efficiency, ETA2 = 0.6

Figure 5.3 shows the effect of the generator temperature T_{GE} on the coefficient of performance $(COP)_{ECL}$ at different condensation temperatures for the ammonia-water system. It can be seen that high values of the enthalpy based coefficient of performance $(COP)_{ECL}$ are obtained at low generator and condenser temperatures. As the generator temperature increases the value of the $(COP)_{ECL}$ decreases. The rate of decrease is higher for the lower condensing temperatures. This coincides with results from other works [5.4].

Figure 5.4 shows the effect of the generator temperature T_{GE} on the coefficient of performance $(COP)_{ECL}$ at different condensation temperatures for the ammonia-lithium nitrate system. It can be seen that the $(COP)_{ECL}$ increases rapidly at low generator temperatures to a maximum value and then decreases slowly at higher values of T_{GE}. The highest $(COP)_{ECL}$ values are for the lower condensation temperatures.

Figure 5.5 shows the effect of the generator temperature T_{GE} on the coefficient of performance $(COP)_{ECL}$ at different absorption temperatures T_{AB}.

for the ammonia-water system. It can be seen that the $(COP)_{ECL}$ values ar high at low generator temperatures and absorber temperatures. As the generator temperature increases, the $(COP)_{ECL}$ decreases and the lowest values correspond to the higher absorption temperatures.

Figure 5.6 shows the effect of the generator temperature T_{GE} on the coefficient of performance $(COP)_{ECL}$ at different absorption temperatures T_{AB} for the ammonia-lithium nitrate system. It can be seen that the $(COP)_{ECL}$ increases at low generator temperatures until a maximum is reached and the decreases slowly at higher generator temperatures. The highest $(COP)_{ECL}$ values for all generator temperatures correspond to the lowest absorber temperatures.

Figure 5.7 shows the effect of the generator temperature T_{GE} on the enthalpy based coefficient of performance $(COP)_{ECL}$ for the ammonia-water and the ammonia-lithium nitrate mixtures. It can be seen that higher values o $(COP)_{ECL}$ are obtained for ammonia-water at low generator temperatures. Near 90°C both $(COP)_{ECL}$ values are equal and for higher values of T_{GE} the ammonia-lithium nitrate is more efficient.

Figure 5.8 shows the effect of the condenser temperature T_{CO} on the coefficient of performance $(COP)_{ECL}$ for both mixtures. It can be seen that th ammonia-water system has a maximum $(COP)_{ECL}$ at condenser temperatures between 30 and 33°C. For the ammonia-lithium nitrate system, the $(COP)_{ECL}$ always decreases with higher condenser temperatures and the values are always higher than for ammonia-water.

Figure 5.9 shows the effect of the absorber temperature T_{AB} on the enthalpy based coefficient of performance $(COP)_{ECL}$ for both mixtures. It can be seen that both mixtures have lower values of $(COP)_{ECL}$ as the absorber temperature increases. The ammonia-lithium nitrate mixture has higher values of $(COP)_{ECL}$ for all values of the absorber temperature.

Figure 5.10 shows the effect of the evaporator temperature T_{EV} on the enthalpy based coefficient of performance $(COP)_{ECL}$. It can be seen that higher values of the $(COP)_{ECL}$ are obtained for the ammonia-lithium nitrate system than for the ammonia-water system. Both systems show an increase in performance as the evaporator temperature increases.

Figure 5.11 shows the effect of the economiser effectiveness (ETA1) on the enthalpy based coefficient of performance $(COP)_{ECL}$ for both systems. As the effectiveness increases, the value of $(COP)_{ECL}$ increases significantly for both systems, with higher values for the ammonia-lithium nitrate system.

Figure 5.12 shows the effect of the precooler effectiveness (ETA2) on the enthalpy based coefficient of performance $(COP)_{ECL}$. It can be seen that there is only a slight increase in the $(COP)_{ECL}$ values as the effectiveness increases for both systems, with higher values for the ammonia-lithium nitrate system.

5.7 CONCLUSIONS

The computer modelling of an absorption refrigeration system using ammonia-water and ammonia-lithium nitrate has been carried out. The model results show that the ammonia-lithium nitrate system has a higher enthalpy based

coefficient of performance $(COP)_{ECL}$ at higher generator temperatures than the ammonia-water system.

A detailed parametric study for the continuous absorption refrigeration system using ammonia-water and ammonia-lithium nitrate as working fluids has been carried out for different operating temperatures of each component of the system.

The model was based on steady state operation and was used to assess the effect of operating temperatures and heat exchanger effectiveness on the coefficient of performance for cooling and the heat transfer rates within the system.

Lithium nitrate is a promising alternative absorbent for ammonia since no rectification is required. However, experimental data are needed in order to evaluate the problems which may arise from higher viscosities, possible crystallization and risk of explosion.

5.8 REFERENCES

5.1 K. Dao, Private communication.

5.2 M.A. Macriss, B.E. Eakin, R.T. Ellington and J. Huebler, Physical and thermodynamic properties of ammonia-water mixtures, Research Bulletin No. 34, Chicago; Institute of Gas TEchnology (1964).

5.3 C.A. Infante Ferreira, Thermodynamic and physical property equations for ammonia-lithium nitrate and ammonia-sodium thiocyanate solutions, Solar Energy, 32 (2), 231-236 (1984).

5.4 S.C. Kaushik and S.C. Bhardwaj, Theoretical analysis of NH_3 - H_2O absorption cycles for solar refrigeration and space conditioning systems, Int. J. Energy Research,6, 205-225 (1982).

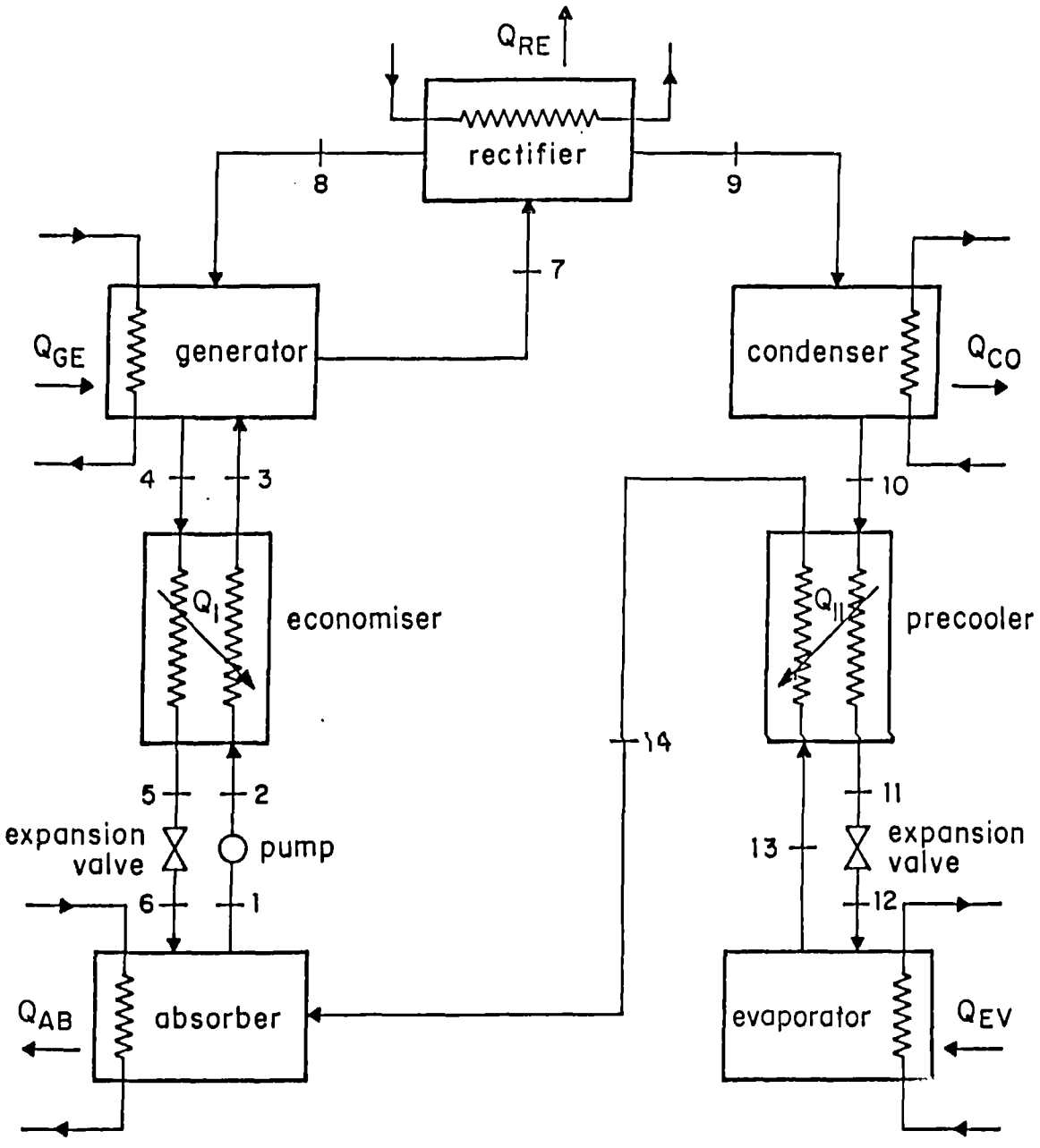

Fig. 5.1 Ammonia-water absorption refrigeration system

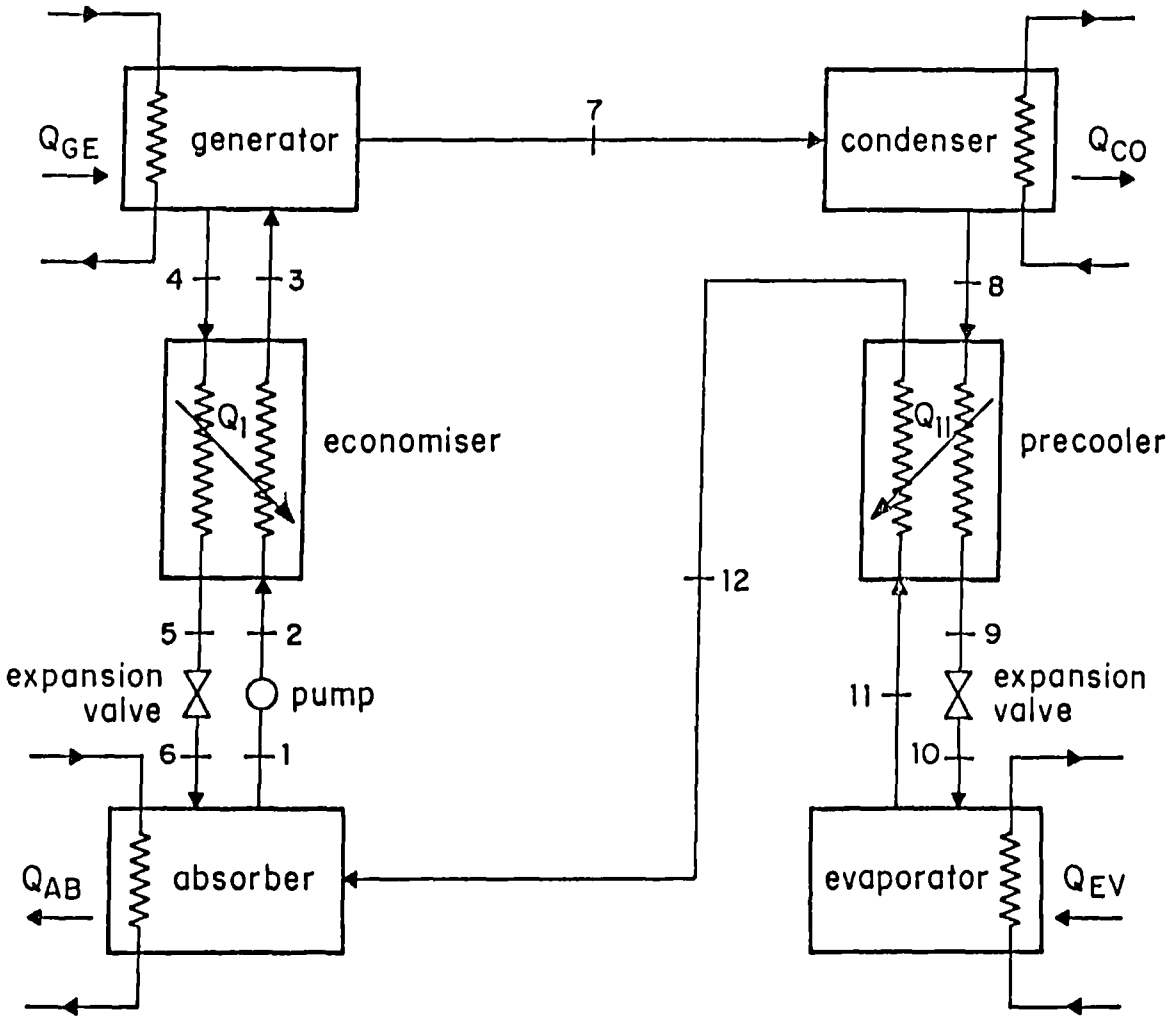

Fig. 5.2 Ammonia-lithium nitrate absorption refrigeration system

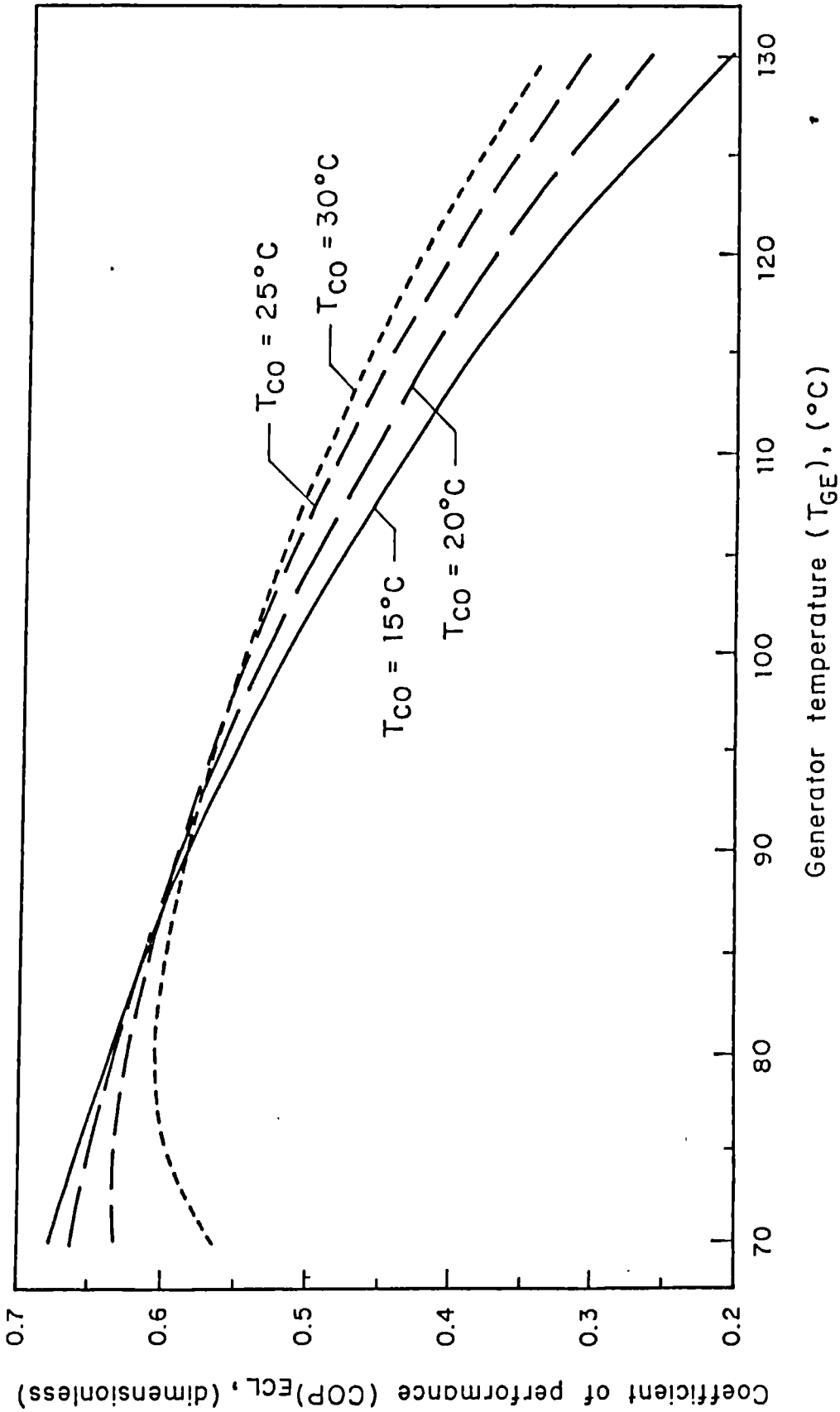

Fig. 5.3 Coefficient of performance $(COP)_{ECL}$ against generator temperature (T_{GE}) at different condenser temperatures for amonia–water

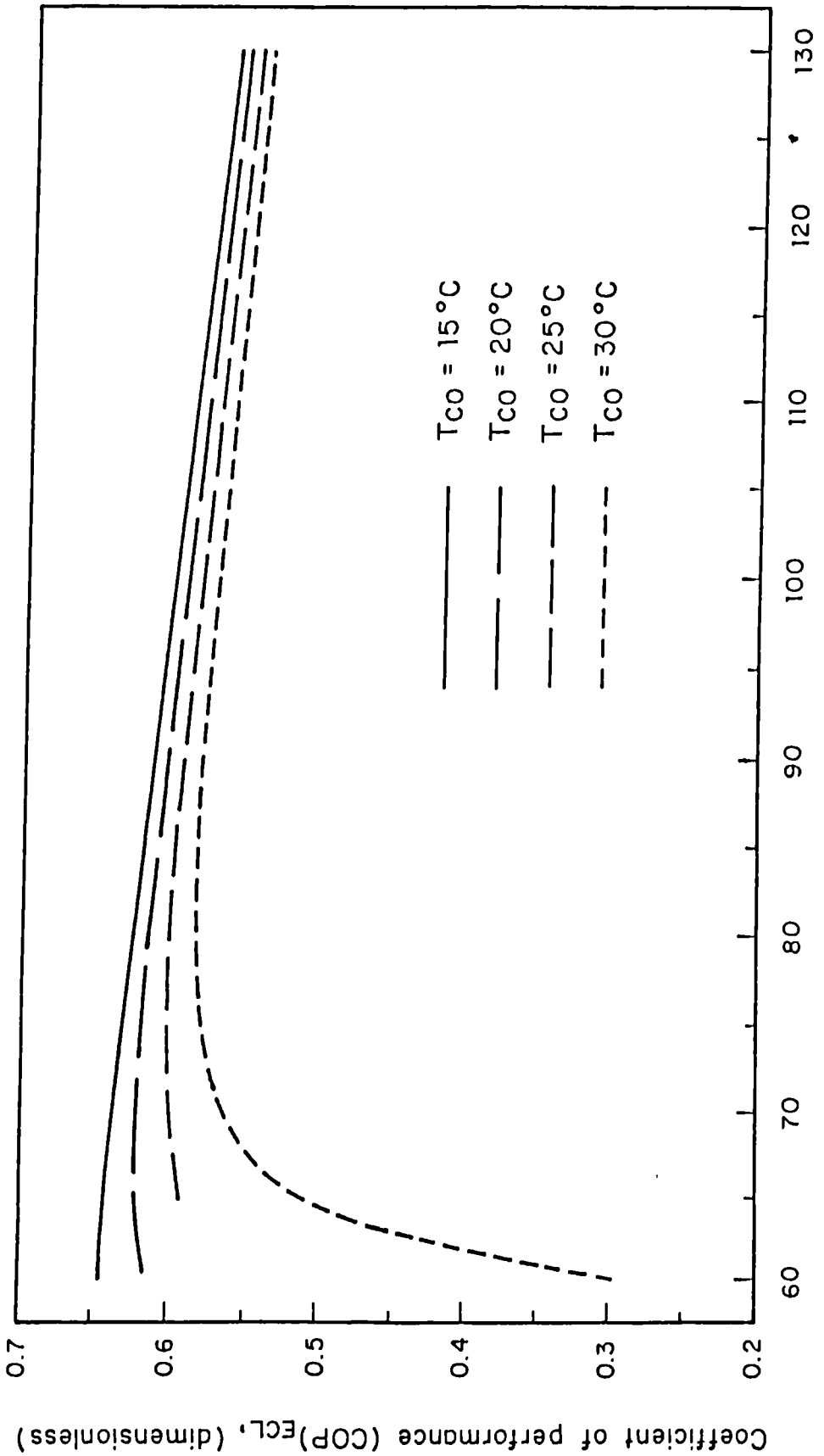

Fig. 5.4 Coefficient of performance $(COP)_{ECL}$ against generator temperature (T_{GE}) at different condenser temperatures (T_{CO}) for ammonia lithium nitrate

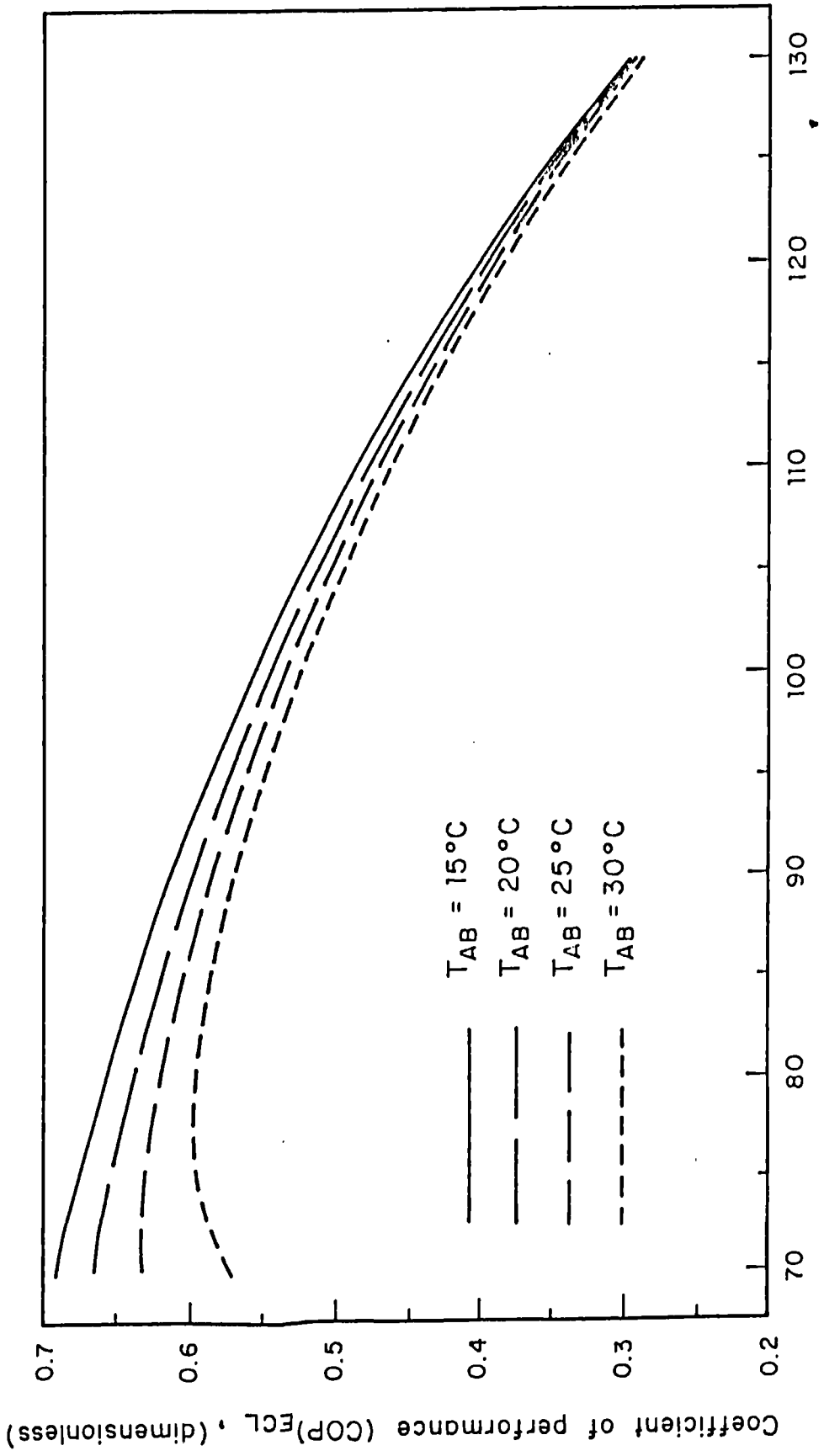

Fig. 5.5 Coefficient of performance $(COP)_{ECL}$ against generator temperature (T_{GE}) at different absorber temperatures (T_{AB}) for ammonia-water

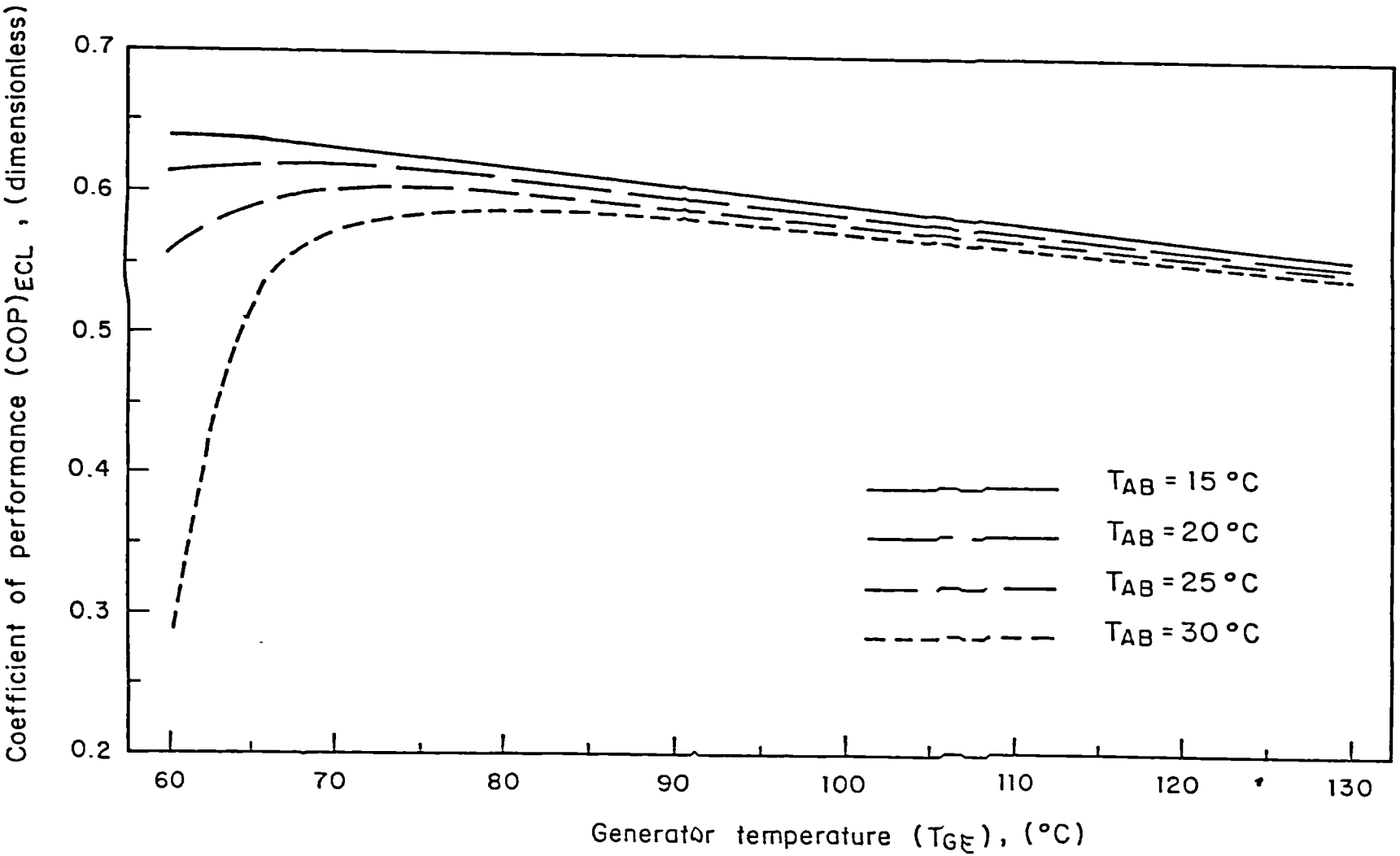

Fig. 5.6 Coefficient of performance $(COP)_{ECL}$ against generator temperature (T_{GE}) at different absorber temperatures (T_{AB}) for ammonia-lithium nitrate

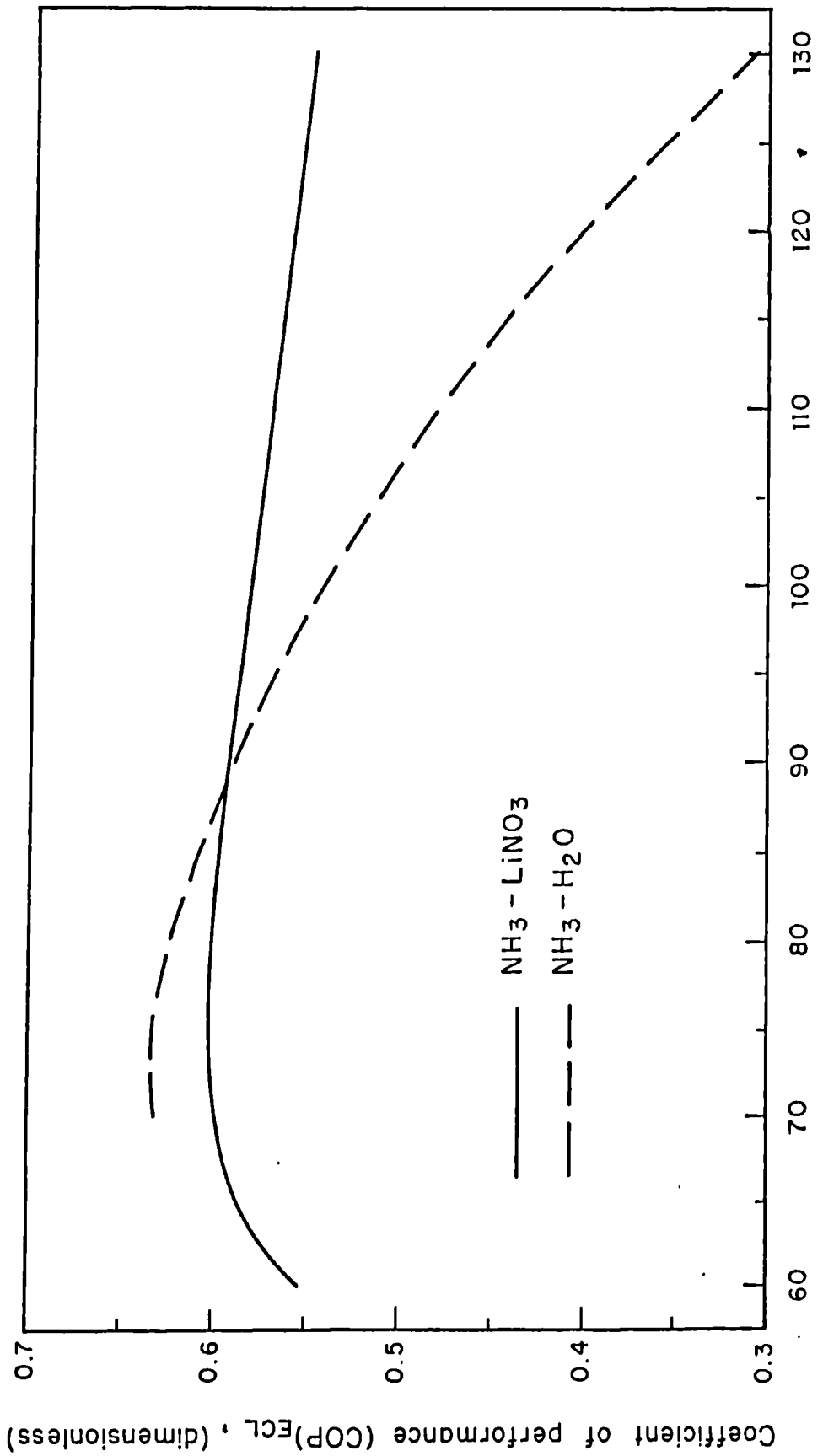

Fig. 5.7 Coefficient of performance $(COP)_{ECL}$ against generator temperature (T_{GE}) for both ammonia-water and ammonia-lithium nitrate

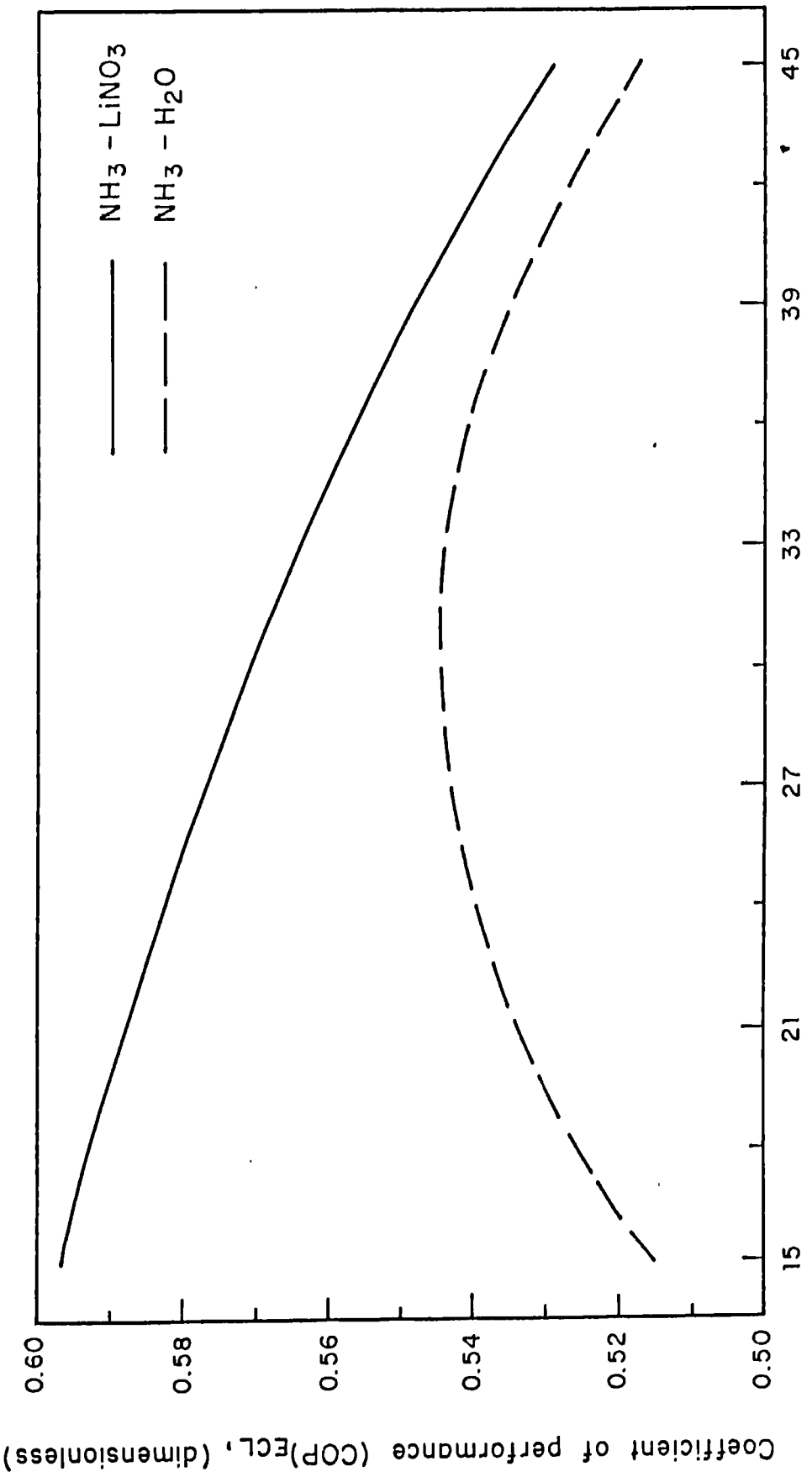

Fig. 5.8 Coefficient of performance $(COP)_{ECL}$ against condenser temperature (T_{CO}) for both ammonia-water and ammonia-lithium nitrate mixtures

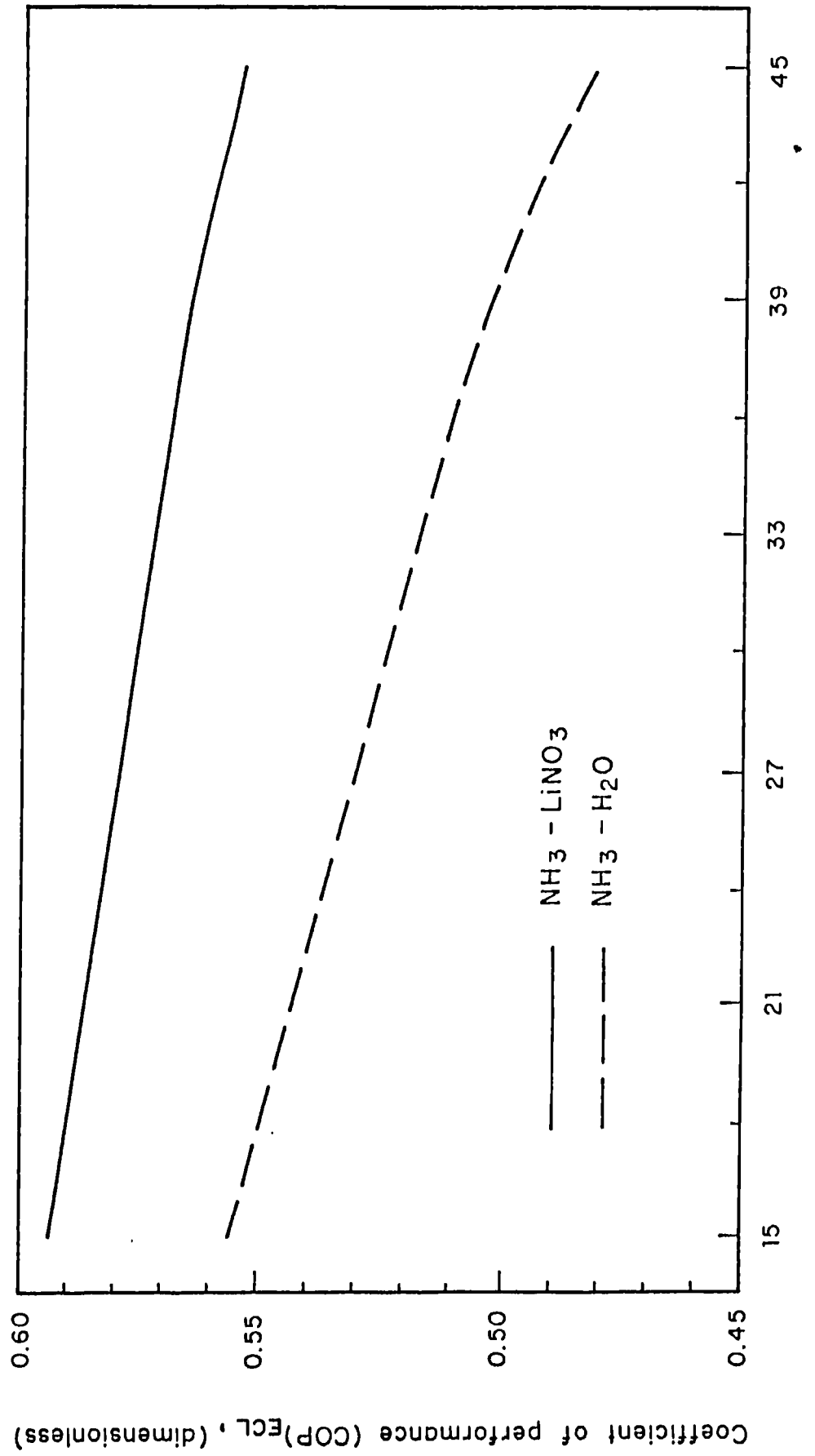

Fig. 5.9 Coefficient of performance $(COP)_{ECL}$ against absorber temperature (T_{AB}) for both ammonia-water and ammonia-lithium nitrate mixtures

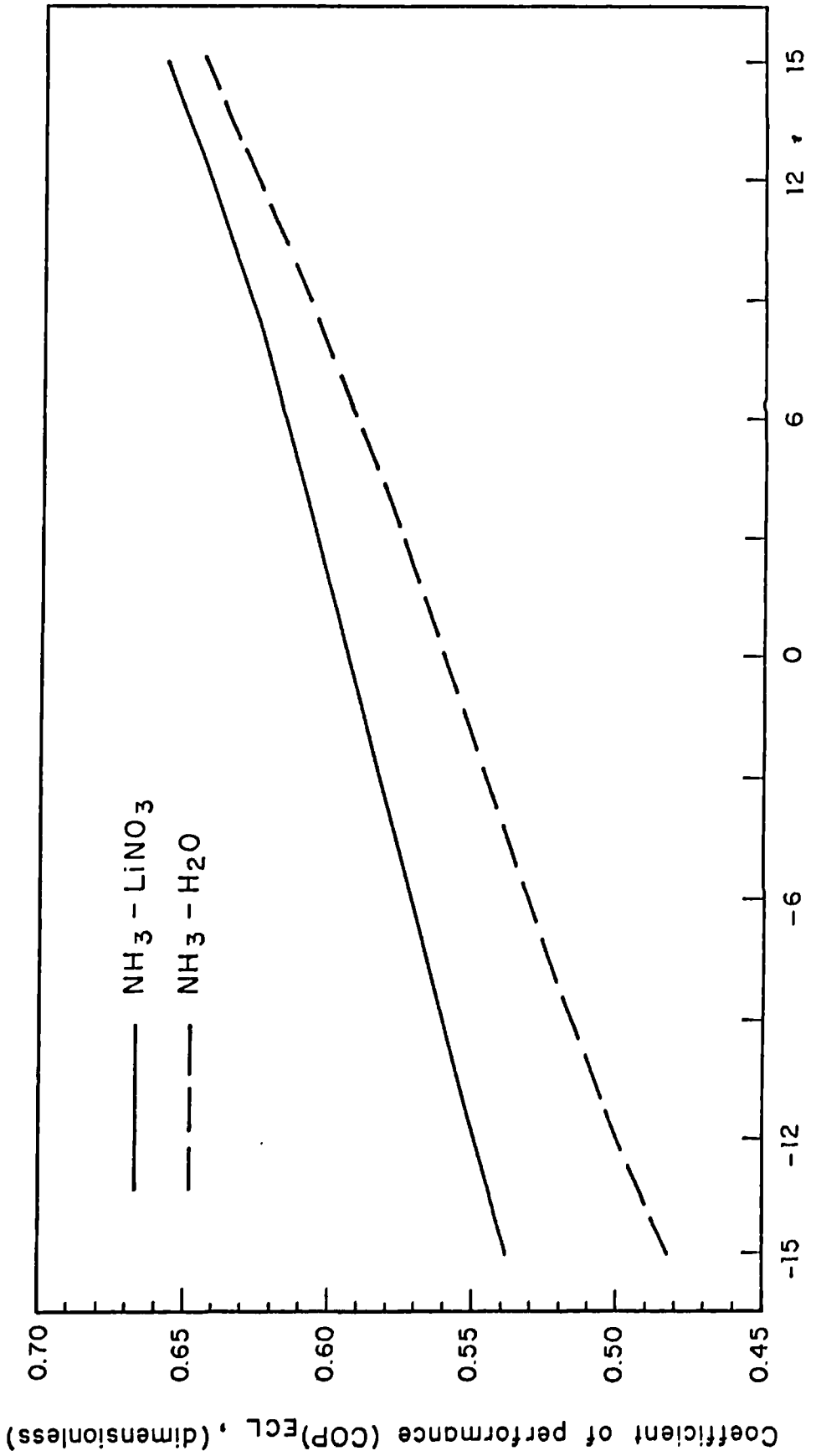

Fig. 5.10 Coefficient of performance $(COP)_{ECL}$ against evaporator temperature (T_{EV}) for both ammonia-water and ammonia-lithium nitrate mixtures

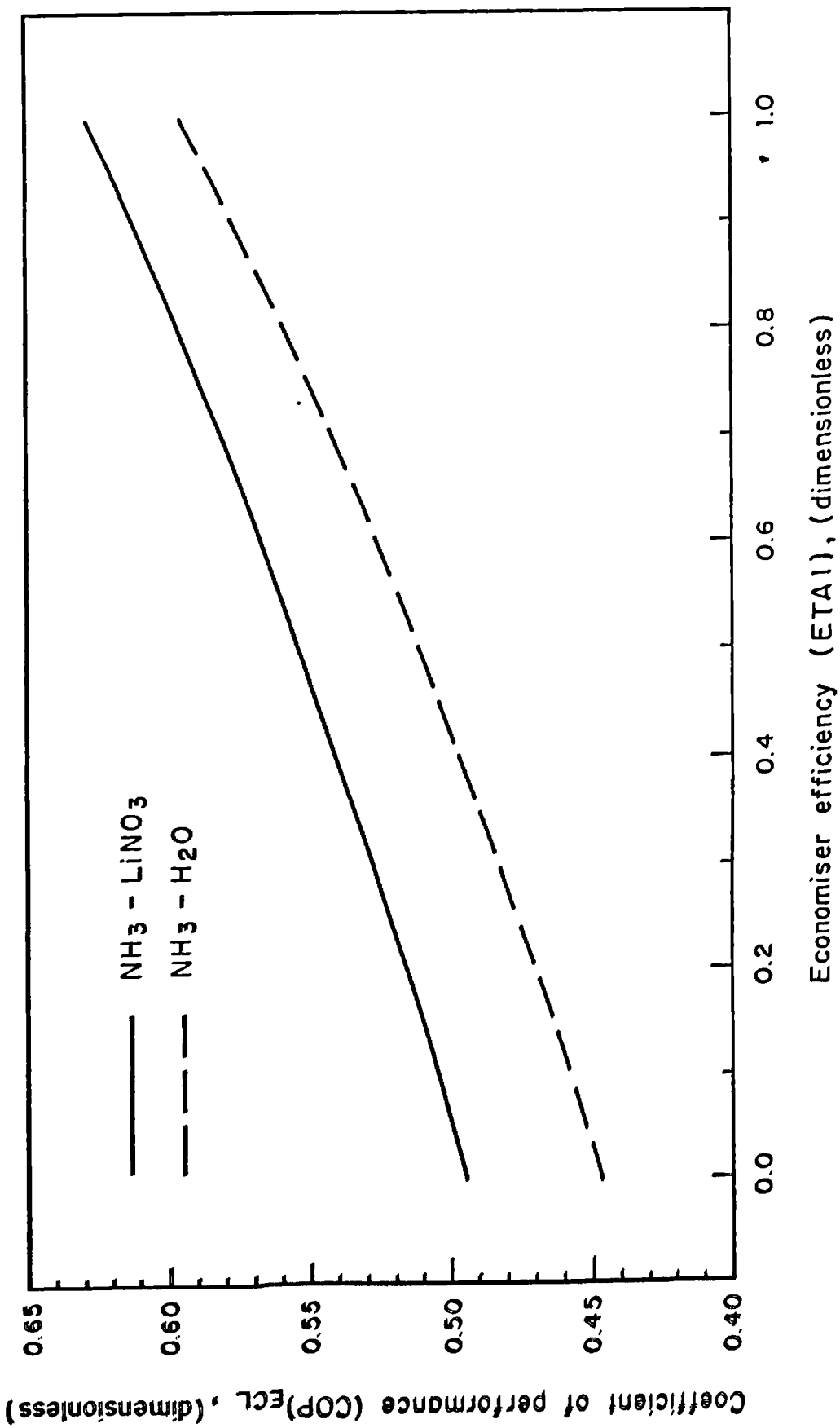

Fig. 5.11 Coefficient of performance $(COP)_{ECL}$ against economiser efficiency (ETA1) for both ammonia-water and ammonia-lithium nitrate mixtures

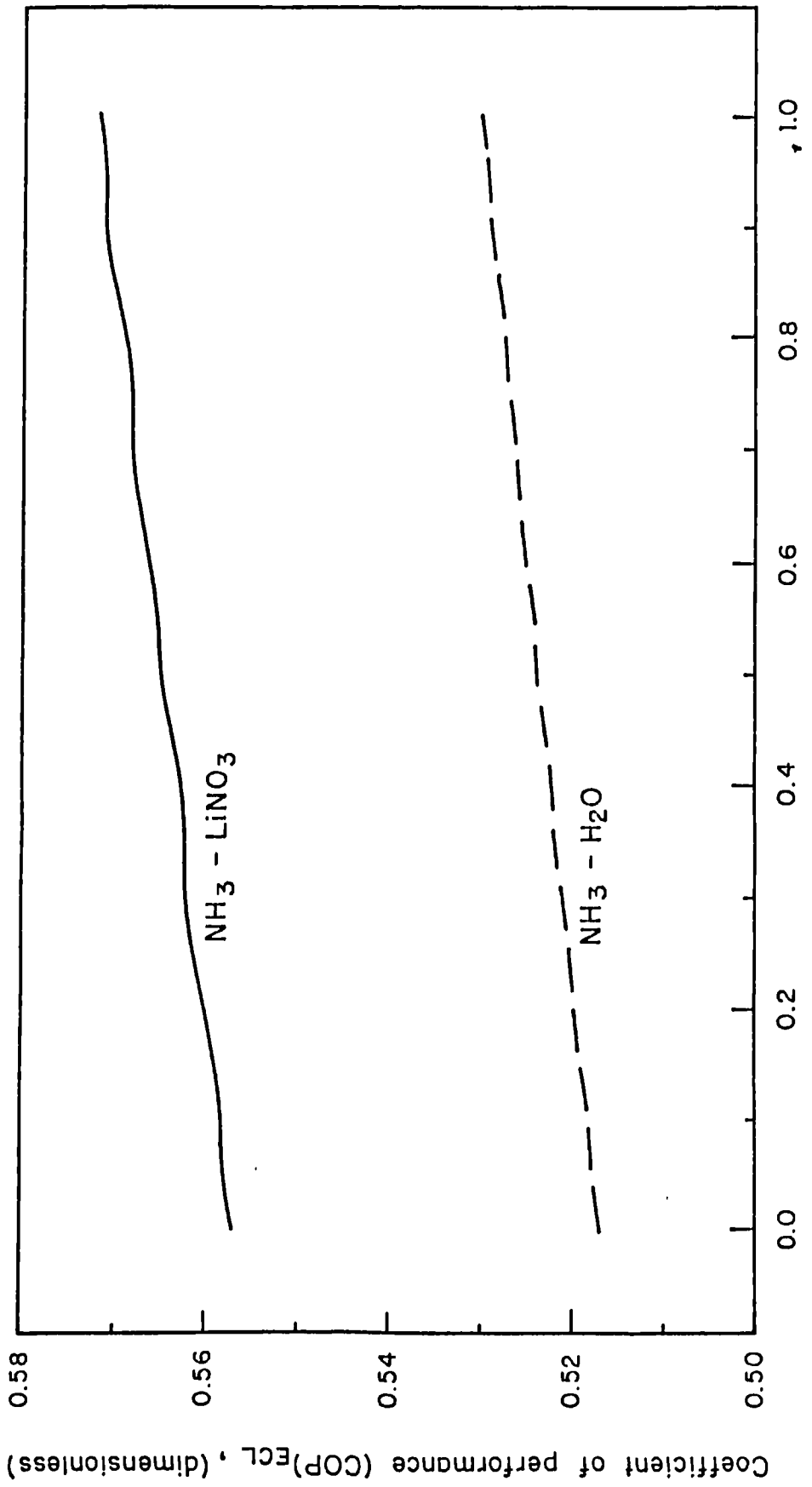

Fig. 5.12 Coefficient of performance $(COP)_{ECL}$ against precooler efficiency (ETA2), for both ammonia-water and ammonia-lithium nitrate mixtures

CHAPTER 6

EXPERIMENTAL STUDIES ON THE PERFORMANCE OF THE ABSORBER OF AN ABSORPTION COOLING SYSTEM

6.1 INTRODUCTION

In a heat driven absorption cooling system, the refrigerant vapour produced in the evaporator is absorbed by the circulating liquid in the absorber. The pressure is increased by the pump prior to entering the generator. An amount of heat Q_{GE} is added at an absolute temperature T_{GE} in the generator to produce the high pressure refrigerant vapour required to be fed to the condenser. The condensation, expansion and evaporation of the refrigerant are the same as in the conventional compressor driven system.

The absorbent liquid consists in the water-lithium bromide system of a concentrated solution of the salt.

The absorption of water vapour into salt-water solutions involves the release of a large quantity of heat due to the high value of the heat of absorption. This includes both the latent heat of condensation of water vapour and the heat of dilution of the aqueous solution. The heat is generally removed by indirect heat exchange to a coolant such as air or cooling water.

In an adiabatic absorber the release of the heat of absorption will cause an increase in the bulk temperature of the circulating liquid. Concentrations and temperature gradients are established and the gas-liquid interface must be necessarily hotter [6.1]. Due to the high value of the heat of absorption only a small amount of vapour will be absorbed in the

adiabatic process before the solution reaches equilibrium and hence the change in concentration will be small, resulting in a high value of the flow ratio.

Earlier studies showed the importance of the flow ratio and reflux ratio in the coefficient of performance of the absorption system [6.2], [6.3]. The present work deals in more detail with the absorption process and analyses the performance of an adiabatic absorber.

6.2 THERMODYNAMIC CONSIDERATIONS

The amount of heat that is transferred in a differential section of an adiabatic absorber as shown in Figure 6.1 is given by

$$dq = -M_L\, C_L\, dT_L + H dM_L = 0 \qquad (6.1)$$

The mass transfer is governed by a relation of the form

$$dM_L = KA\ \rho\ (X^* - X_B) \qquad (6.2)$$

Combining equations (6.1) and (6.2) we can obtain an expression for the increase of the solution temperature in the absorber

$$dT_L = \frac{AHK}{M_L\, C_L}\ \rho\ (X^* - X_B) \qquad (6.3)$$

Equation (6.3) shows in a simplified form that the temperature rise in the absorber is dependant for fixed absorber dimensions and operating temperatures on the flow rate of solution circulating in the absorber.

An important parameter in the evaluation of the absorber [6.4] is the

absorption ratio η_{AB} , and is defined as the actual difference between the inlet and outlet concentrations of the solution in the absorber X_{FD} and X_{AB} respectively and the maximum possible change in concentration with respect to the equilibrium concentration corresponding to the pressure and temperature in the absorber outlet.

$$\eta_{AB} = \frac{X_{FD} - X_{AB}}{X_{FD} - X^*} \tag{6.4}$$

Also with reference to Figure 6.1 the mass of solution entering the absorber M_{FD} is given by

$$M_{FD} = M_{GE} + M_{RF} \tag{6.5}$$

and the concentration of the solution entering the absorber is given by

$$X_{FD} = X_{AB} + \frac{M_{GE}}{M_{FD}} \left(X_{GE} - X_{AB} \right) \tag{6.6}$$

The amount of water absorbed in the absorber is given by

$$M_W = M_{FD} \left(\frac{X_{FD}}{X_{AB}} - 1 \right) \tag{6.7}$$

The flow ratio (FR) which is defined as the mass flow rate of solution in the secondary circuit linking the generator and absorber to the mass flow rate of refrigerant in the primary circuit linking the condenser and the evaporator is given by

$$(FR) = \frac{M_{AB}}{M_W} \tag{6.8}$$

or

$$(FR) = \frac{X_{GE}}{X_{GE} - X_{AB}} \qquad (6.9)$$

The equilibrium concentrations were calculated through an iterative process from the expressions by McNeely [6.5].

$$T' = \frac{-2E}{D + D^2 - 4E\ (C - \log P)} \qquad (6.10)$$

and

$$T_L = \Sigma_{o}^{3}\ B_n\ x^{n} + T'\ \Sigma_{o}^{3}\ A_n\ X_n \qquad (6.11)$$

where

A_o	= 2.00755	B_o	= 124.937	C =	7.05
A_1	= 0.16976	B_1	= 7.7165	D =	-1596.49
A_2	= 3.133336E-3	B_2	= 0.152286	E =	-1040955

6.3 EXPERIMENTAL

The experiments were carried out in a glass absorption cooler shown schematically in Figure 6.2.

The system consisted of a generator, an evaporator, a condenser, a condenser-receiver, an absorber, an external absorber heat exchanger, an absorber-receiver and an economiser heat exchanger.

The generator contained a sparge pipe extending longitudinally over the heater and a sump which provided a constant level of solution in the generator.

The evaporator was of a similar shape to the generator with the exemption

of the sump. The evaporator was joined to the absorber column by a glass tube and flanges; 1 kW bayonet heaters in a horizontal alignement were used as the heat source in the generator and in the evaporator.

The absorber was a spray column type. A 200 ml spherical flask, wide neck and a glass tube 0.80 m long and 0.1 m diameter were connected by flanges to form the absorber with a total height of 1.0 m.

The condenser was constructed by using two multicoil condensers. Both condensers were welded into a compact unit. The economiser heat exchanger was a standard multicoil condenser as well as the external absorber cooler.

Details of the equipment have already been published [6.6].

In the absorber, there were 9 thermocouples in the absorption section spaced 7 cm from the bottom and a thermocouple in the spray section at 0.28 m from the spray.

6.4 RESULTS

A series of experiments using a solution of H_2O-LiBr were carried out with $T_{CO} = 50°C$, $T_{EV} \leq 15°C$ and the absorber temepratures T_{AB} of 35°C or higher. The generator temperature T_{GE} was varied from 85°C up to 105°C. Figure 6.3 shows the variation of the actual value of the coefficient of performance $(COP)_A$ and flow ratio (FR) with respect to the generator temperature T_{GE} for constant condenser absorber and evaporator temperatures. The coefficient of performance increases and the flow ratio decreases as expected with an increase in generator temperature.

Figure 6.4 shows the variation of the absorption ratio η_{AB} with respect to the flow ratio (FR) at absorber temperatures T_{AB} of 35 to 40°C and generator temperatures T_{GE} of 100°C. It can be seen that the absorption increases as the flow ratio decreases.

Figure 6.5 shows the temperature rise of the solution inside the absorber for three different values of M_{FD}. It can be seen as expected from equation (6.3) that the temperature increase is higher at lower flow rates. Figure 6.5 also shows the temperature rise of the solution with respect to levels of evaporator heat load for a constant flow rate of solution in the absorber. It can be seen that at higher values of Q_{EV} there is a greater increase of solution temperature due to a higher driving force.

Figure 6.6 is a plot of the amount of water absorbed in the absorber M_W with respect to the evaporator load Q_{EV}. It can be seen that the amount of water absorbed increases as the load increases. In order to maintain an adequate evaporator temperature the temperature in the absorber must be lowered with an increase of circulating solution.

6.5 CONCLUSIONS

It has been shown that the temperature in an adiabatic absorber can increase very rapidly to values 8°C above the entering temperature. In order to reduce this temperature and in consequence the temperature in the evaporator, higher flow rates of circulating solution are required. It has also been shown that saturation conditions in the adiabatic absorber are reached very rapidly and hence higher flow rates are required than in absorbers where the heat released is simultaneously removed.

6.6 REFERENCES

6.1 M.L. King, Absorption of water vapour into aqueous salt solutions, Ph.D Thesis University of Delaware (1981).

6.2 M.A.R. Eisa, M.G. Sane, S. Devotta and F.A. Holland, Experimental studies to determine the optimum flow ratio in a lithium bromide absorption cooler for high absorber temperatures, Chem. Eng. Res. Des., 63 (4), 267-270 (1985).

6.3 M.A.R. Eisa, P.J. Diggory and F.A. Holland, Experimental studies to determine the effect of absorber reflux on the performance of a water-lithium bromide absorption cooler, Int. J. Energy Research, 10, 333-341 (1986).

6.4 J.W. Audberg, D.C. Vilet, Design guidelines for water-lithium bromide absorbers, paper AC-83-05 No. 2, ASHRAE Transactions 89 (1983).

6.5 L.A. McNeely, Thermodynamic properties of aqueous solutions of lithium bromide, ASHRAE Transactions, 85, 413-434 (1979).

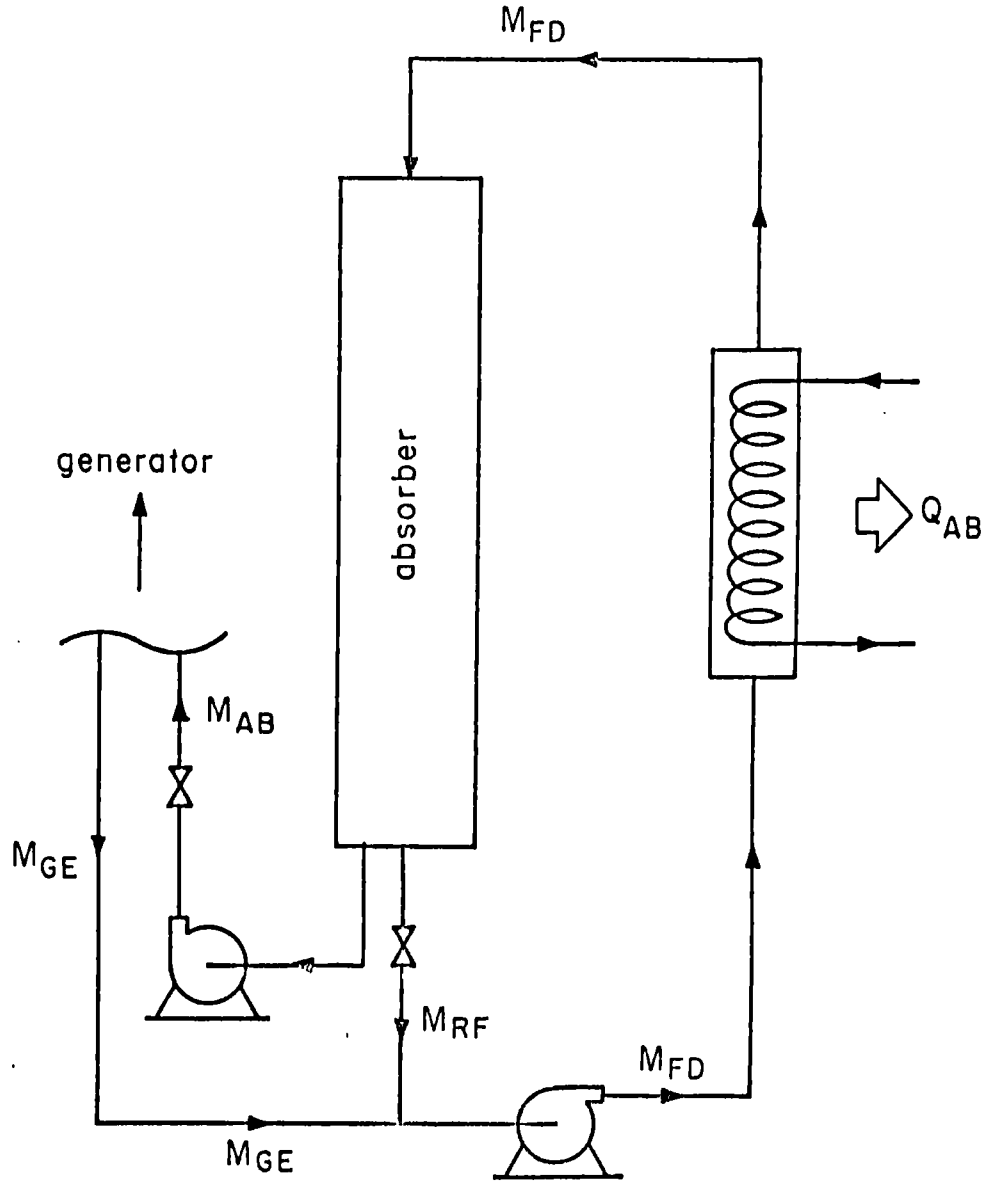

Fig. 6.1 Flow diagram for the modified absorber with controlled reflux

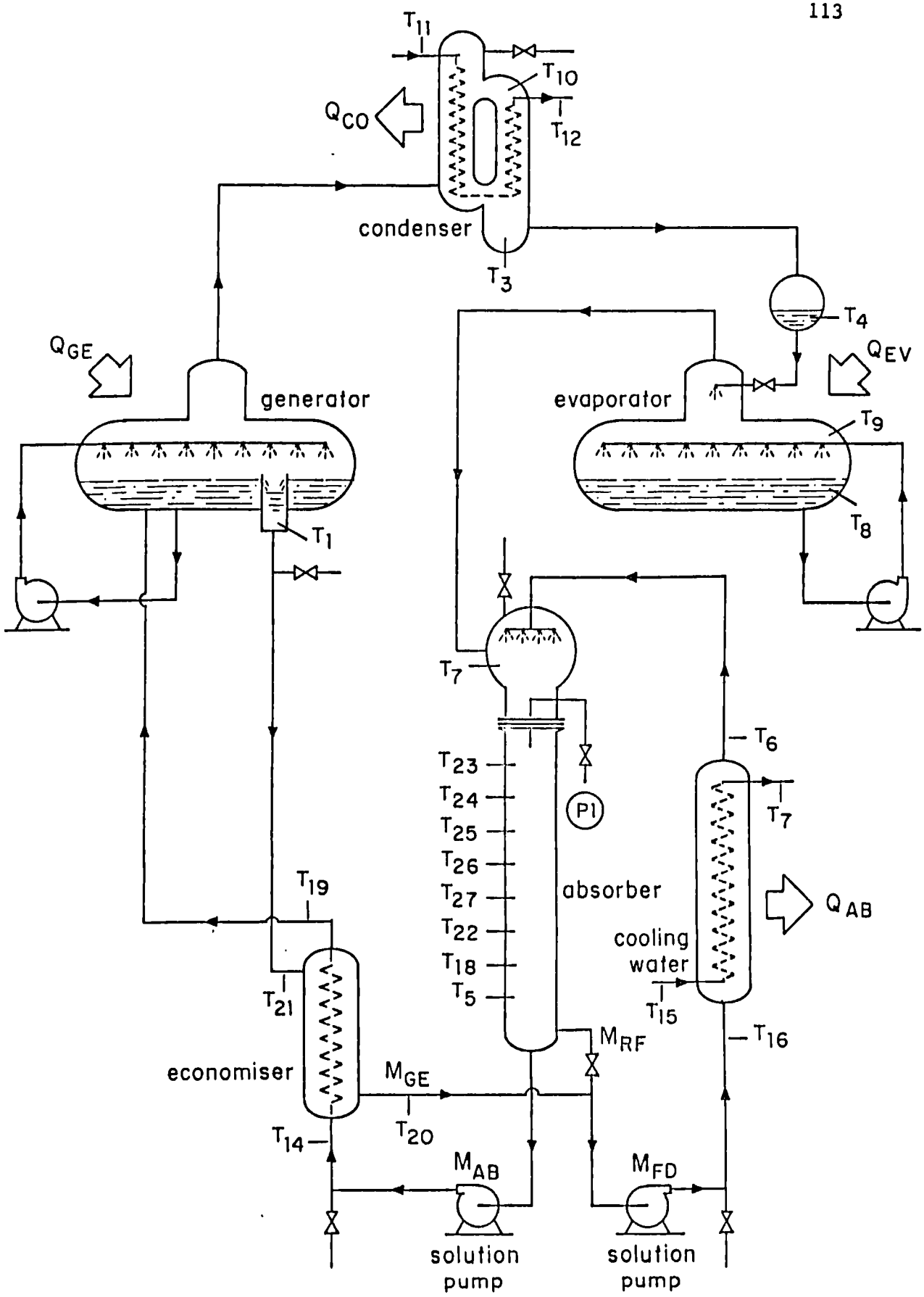

Fig. 6.2 Schematic diagram for the experimental absorber cooler

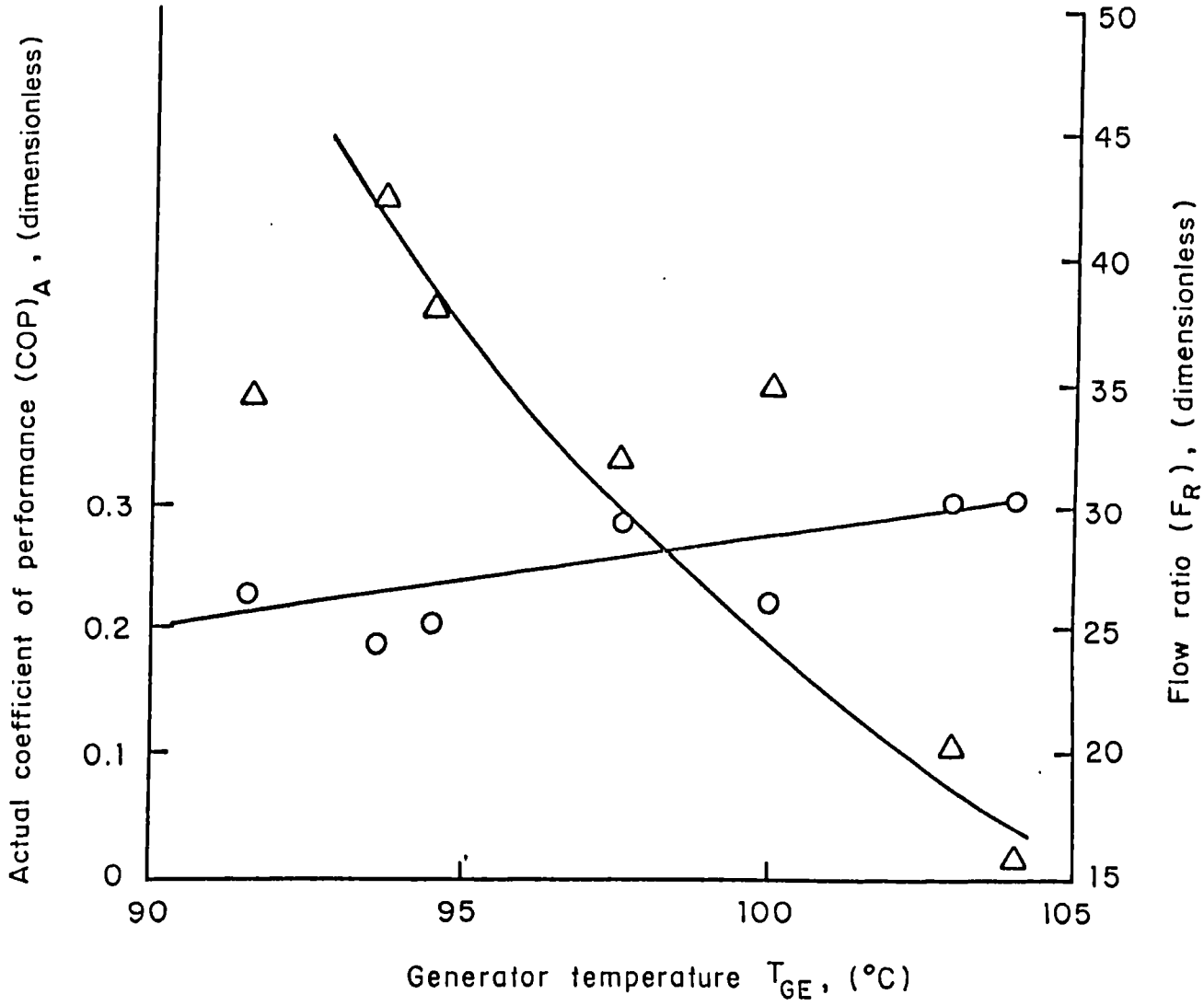

Fig. 6.3 Actual coefficient of performance $(COP)_A$ and flow ratio (F_R) against generator T_{GE}

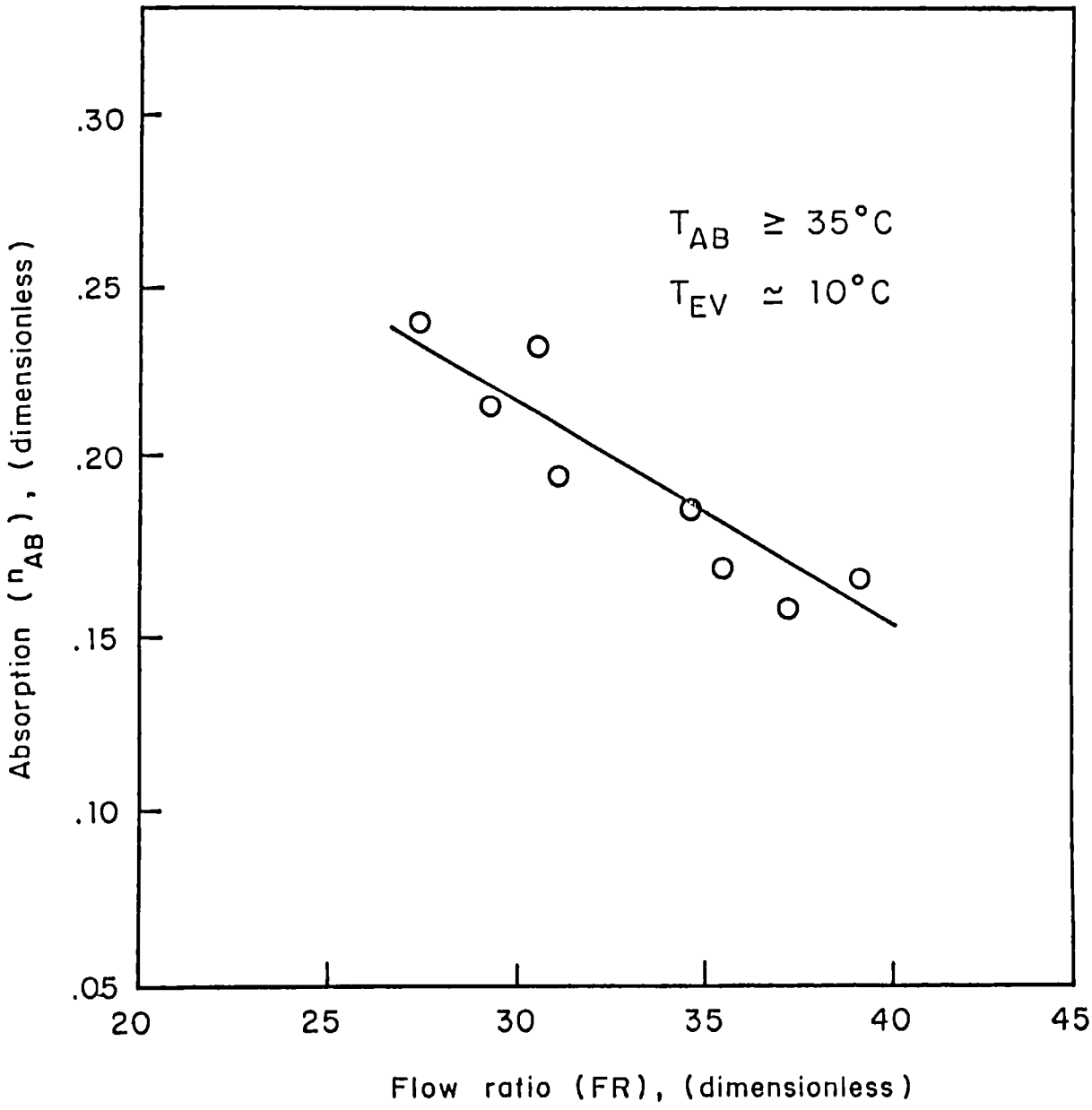

Fig. 6.4 Absorption ratio (η_{AB}) against flow ratio (FR)

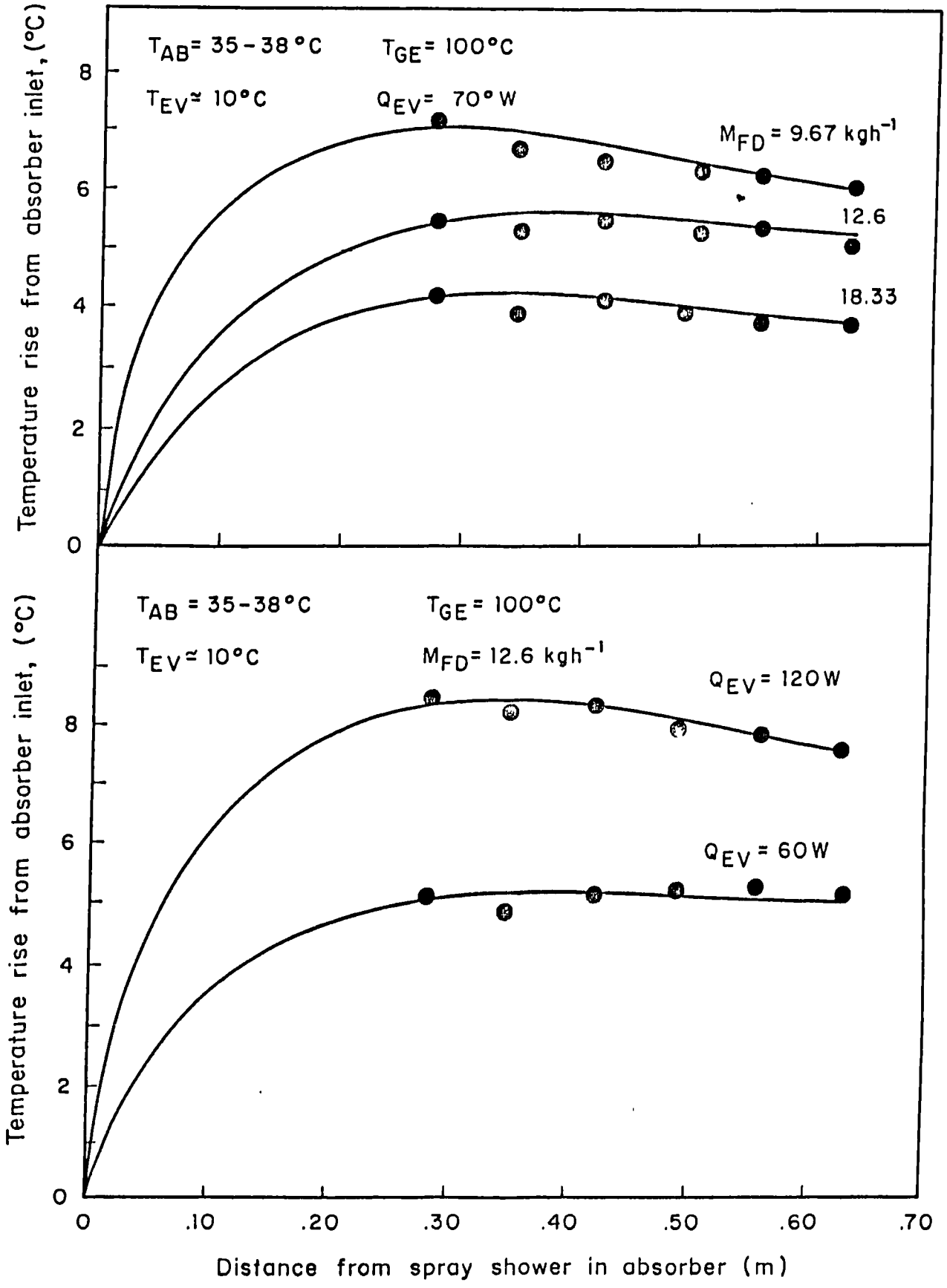

Fig. 6.5 Temperature rise of the solution in the absorber against absorber length

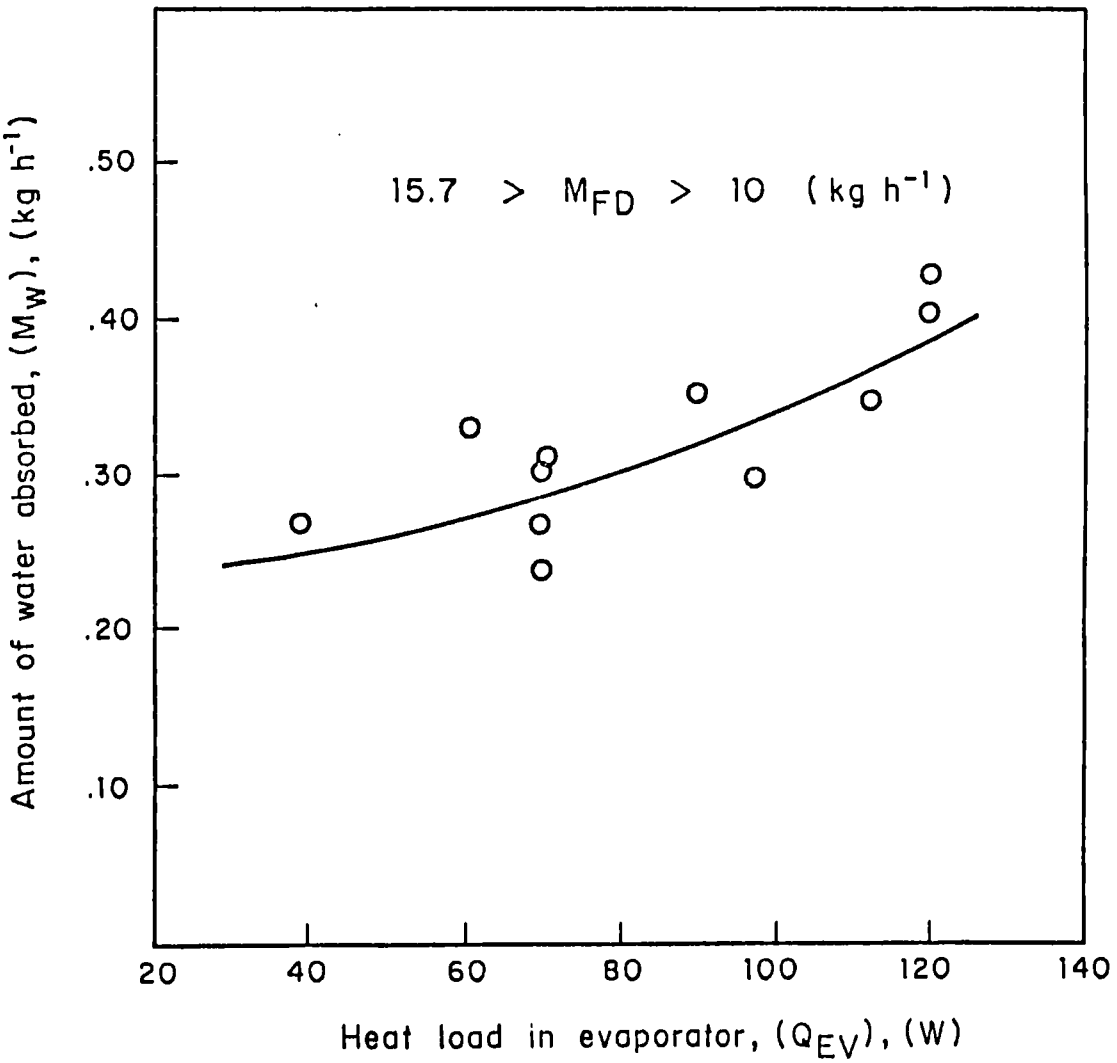

Fig. 6.6 Amount of water absorbed against heat load in evaporator

CHAPTER 7

A STUDY ON THE OPERATING CHARACTERISTICS OF AN EXPERIMENTAL ABSORPTION COOLER USING TERNARY SYSTEMS

7.1 INTRODUCTION

Absorption refrigeration systems are based on the fact that the vapour pressure of the refrigerant can be reduced by the formation of a solution between the volatile refrigerant and a much less volatile absorbent. The solution should have a lower partial pressure of refrigerant over the absorbent-refrigerant solution than would be predicted by Raoult's Law [7.1].

The most successful system for absorption refrigeration has been the use of water as a refrigerant and a strong aqueous solution of lithium bromide as the absorbent. The solution presents the risk of crystallization when high generator temperatures are used. On the other hand with lower generator temperatures, the absorber solution must be relatively cool in order that the vapour pressure of the refrigerant over the solution is low enough to permit practical operation.

Previous researchers have attempted to overcome the problem of crystallization by using high flow ratios [7.2] or by using an antifreeze additive [7.3].

The present work is concerned with the use of salt mixtures. The mixtures were selected with the following criteria:

(i) higher solubilities than lithium bromide

and

(ii) lower vapour pressures than lithium bromide

Zinc bromide is a salt with a high solubility, 82% by weight at 25°C [7.4] and with a vapour pressure of 0.67 kPa at 43°C compared with values of 62.4% by weight and 0.61 kPa for lithium bromide at the same conditions. When zinc bromide is used alone very high viscosities occur. Aronson [7.5] was the first one to propose the use of the mixture of lithium bromide and zinc bromide, together with other salts. The patent includes data on solubility and vapour pressure for ternary and quaternary systems. Ohuchi [7.6] presented a study on the development of a heat pump for heating and cooling utilizing a mixture of lithium bromide and zinc chloride. The work included studies on corrosion and corrosion inhibitors. Figure 7.1 has been adapted from Ohuchi [7.6]. It shows the crystallization curve for a lithium bromide-water solution and for a lithium bromide-zinc bromide-water solution with a composition by weight of (0.39/1.0) $(\frac{\text{zinc bromide}}{\text{total salt}})$. It clearly shows the extended use of the ternary mixture at salt concentrations higher than 80% by weight and at higher temperatures.

Lithium iodide is a salt with a high solubility and a low vapour pressure at elevated temperatures [7.7]. Theoretical research on the properties of various lithium salts showed that lithium iodide has some advantages over lithium bromide [7.8]. Unfortunately, the solubility of lithium iodide is significantly reduced at the concentrations and lower temperatures required in an absorption cooler by the formation of a series of hydrates in the solid phase. Figure 7.2 is a plot of vapour pressure against weight percentage with isotherms for aqueous solutions of lithium iodide adapted from Bach et al [7.7]. It can be seen that the crystallization curve increases rapidly from the value of X = 65% to a value of X = 70% and then decreases sharply, down to a value of X = 82%. The range of concentrations of

interest for an absorption cooler operating at absorber temperatures T_{AB} between 30 and 50°C and with corresponding vapour pressures low enough for evaporating temperatures T_{EV} for cooling (10°C) fall precisely in the 65 to 70% by weight lithium iodide region. Three solutions of 65, 67 and 70% by weight lithium iodide were made and used to verify the crystallization point. The results coincided within 1°C with those of Bach et al [7.7] despite the simplicity of the experiments.

Hensel et al [7.9] showed that a mixture of lithium bromide and lithium iodide of 10 to 50% lithium iodide in the solids had a lower crystallization temperature than each of the salts alone with a minimum at about 30% lithium iodide by weight in the solids. A mixture with this concentration was made and used to form solutions of 60, 65 and 70% weight percent of total salt. The salt of 60% did not crystallize even at -10°C. The 65% solution crystallized at 12°C and the 70% solution crystallized at 32°C. The crystallization temperatures obtained were slightly lower than the values reported by Hansel et al [7.9]. It was decided that a maximum salt concentration of 66% by weight would be a safe value to work with.

7.2 EXPERIMENTAL

The experiments were carried out in a glass absorption cooler described in chapter 6 and shown on Figure 7.3. The unit was constructed for the most part from standard items supplied by Quickfit Ltd., U.K. Landauro Paredes et al [7.10] have given a detailed description of the equipment and operating techniques.

Lithium bromide-zinc bromide-water. The absorbent solution was made from distilled water, anhydrous lithium bromide and zinc bromide hydrate

supplied by Foote Mineral Company Ltd. and John Ross Chemicals Ltd. U.K. respectively. A mixture with a concentration of (0.42)/(1.0) (lithium bromide/zinc bromide) by weight was prepared as absorbent. The concentrations of the ternary solutions were determined from refractive index measurements using a high quality Abbe refractometer supplied by Bellingham and Stanley Ltd. U.K. This was equipped with a constant temperature bath. The experimental relationship between the percentage concentration of the mixture X and the refractive index at 40°C, N_D, was determined to be

$$X = -918.85\ (N_D)^2 + 2995.29\ N_D - 2352.53 \qquad (1)$$

with a maximum error of 0.16%.

Lithium bromide-lithium iodide-water. The absorbent solution was made from distilled water, anhydrous lithium bromide and lithium iodide hydrate supplies by Foote Mineral Company Ltd. U.K. A mixture of lithium iodide-lithium bromide with a (0.30/1.0) by weight ratio was used as the absorbent. The concentrations of the ternary solutions were determined from refractive index measurements. The experimental relationship between the percentage concentration of the salt mixture, X, and the refractive index at 40°C, N_D, was determined to be

$$X = 25.70\ (N_D)^2 + 147.97\ N_D - 212.47 \qquad (2)$$

with a maximum error of 0.72%.

7.3 RESULTS AND DISCUSSION

Lithium bromide-zinc bromide-water. Performance data were obtained on the experimental absorption cooler which was charged with approximately 5

litres of a solution of 75% by weight total salt. A maximum generator temperature T_{GE} of about 110°C was used in order to avoid any damage to the glass and rubber components. The condensing temperature T_{CO} was fixed at 50°C. Figure 7.4 shows the typical performance of the system for an absorber concentration X_{AB} of 80% by weight total salt. The value of the actual coefficient of performance $(COP)_A$ against flow ratio (FR) varied from a value of 0.36 to a value of 0.286 for flow ratios of 39 to 56.45 respectively. The temperature level in the absorber T_{AB} varied between 40.3 to 42.5°C and the evaporator temperature T_{EV} showed a small increase from 11.7 to 13.7°C. The generator temperature decreased from 112 to 105.6°C.

Figure 7.5 shows the variations of the heat loads against flow ratio. The generator and absorber heat loads increased with increasing flow ratio whilst the evaporator and condenser loads remained almost constant.

Figure 7.6 shows the actual coefficient of performance $(COP)_A$ and temperature levels for a series of experiments with an absorber concentration of 79% by weight. It can be seen that lower values of $(COP)_A$ are obtained for the same temperature levels of Figure 5 although the flow ratio values are lower. A lower cooling load was required in order to maintain an evaporator temperature T_{EV} in the range of 10°C. This can be explained by the combined effect of the high viscosity of the strong solution and the lower flow rate of solution entering the absorber which caused restricted spraying. A visual inspection confirmed that the solution distribution in the absorber wall was poor.

Figures 7.7 and 7.8 show the results of a series of experiments where the temperature of the absorber T_{AB} was maintained constant as much as the practical limitations of the system would permit. The heat loads Q_{EV} and

Q_{GE} had to be manipulated to obtain this condition. Figure 7.7 shows the values of the coefficient of performance $(COP)_A$ and the temperature levels in the equipment as a function of the mass flow rate of solution M_{AB}. It can be seen that the values of $(COP)_A$ increased as the mass flow rate of solution increased. Figure 7.8 is a plot of the heat loads against mass flow rate of solution M_{AB}. It can be seen that the loads constantly increased as the flow ratio increased. The rate of increase of Q_{AB} is higher than the other loads.

Lithium bromide-lithium iodide-water. Figure 7.9 shows the typical performance of the system for an absorber concentration X_{AB} of 63% by weight. The value of the actual coefficient of performance $(COP)_A$ against flow ratio varied from a maximum value of 0.27 to a value of 0.22 for flow ratios of 30 to 68 respectively. The temperature level in the absorber T_{AB} was maintained constant as much as practical limitations of the system would permit at 36°C. The condensing temperature T_{CO} was fixed at 50°C. The generator temperature T_{GE} was maintained at around 100°C with a maximum value of 103°C corresponding to a strong solution concentration X_{GE} = 65% by weight. The evaporator temperature T_{EV} varied from 10.5 to 13°C.

Figure 7.10 shows the values of the heat loads in the system. It can be seen that generator and absorber heat loads increased with increasing flow ratio whilst the evaporator and condenser loads remained almost constant.

7.4 CONCLUSIONS

Ternary systems consisting of a mixture of lithium bromide-zinc bromide-water and lithium bromide-lithium iodide-water have been used in an absorption cooler at high absorber temperatures. For the ternary system using zinc bromide the experimental data showed a good coefficient of performance

$(COP)_A$. The flow ratio values were higher than in a lithium bromide system due to the higher level of concentrations employed. The system had a significantly higher viscosity than the lithium bromide solutions. This resulted in reduced values of the coefficient of performance $(COP)_A$ and cooling capacity Q_{EV} at low flow ratio values. It is apparent that there is no significant disadvantage with respect to heat and mass transfer rates. Further studies on this area and in viscocity and corrosiveness should be carried out.

For the lithium iodide ternary system the coefficient of performance values obtained were comparable with values of lithium bromide-water systems [7.11]. The advantage of a higher solubility should be analysed in more detail in order to fix the limiting values of the generator temperature. At present it seems that there is a slight advantage using the ternary system.

It has been shown that salt mixtures are a viable solution to overcome the problem of crystallisation in absorption systems. Higher solubilities and lower vapour pressures than lithium bromide are achieved with ternary systems.

Further studies on heat and mass transfer rates, transport properties and corrosiveness should be carried out.

7.5 REFERENCES

7.1 R.M. Buffington, Qualitative requirements for absorbent-refrigerant combinations, Refrigeration Engineering, 57, 344-345 (1949).

7.2 M.A.R. Eisa, M.G. Sons, S. Devotta and F.A. Holland, Experimental studies to determine the optimum flow ratio in a water-lithium bromide absorption cooler for high absorber temperatures, Chem. Eng. Res. Des., 63 (4), 267-270 (1985).

7.3 M.A.R. Eisa, P.J. Diggory and F.A. Holland, A study of the operating characteristics of an experimental absorption cooler using water-lithium bromide- ethylene glycol as a ternary system, Int. J. Energy Research, 12, 459-472 (1988).

7.4 International Critical Tables, Vol. 4, p. 221.

7.5 D. Aronson, Absorption refrigeration systems, U.S. Patent 3478, 530 (1969).

7.6 Y. Ohuchi, Development of a gas-fired absorption heat pump, ASHRAE Transactions, Part 2A, 292-302 (1985).

7.7 R.O. Bach and J.R.W. Boardman, Vapor pressure of aqueous lithium iodide solutions, ASHRAE Journal, 33-36, Nov. (1967).

7.8 M.A.R. Eisa, and F.A. Holland, A study on the optimum interaction between the working fluid and the absorbents in absorption heat pumps, J. Heat Recovery Systems and CHP, 7 (2), 107-117 (1987).

7.9 W.E. Jr. Hensel, W.H. Jr. Harlowe, Lithium bromide-lithium iodide compositions for absorption refrigeration systems, U.S. Patent 3, 524-815 (1970).

7.10 J.M. Landauro-Paredes, F.A. Watson and F.A. Holland, Experimental study of the operating characteristics of a water-lithium bromide absorption cooler, Chem. Eng. Res. Des. 61 (6), 362-369 (1983).

7.11 M.A.R. Eisa and F.A. Holland, A study of the operating parameters in a water-lithium bromide absorption cooler, Int. J. Energy Research, 10, 137-144 (1986).

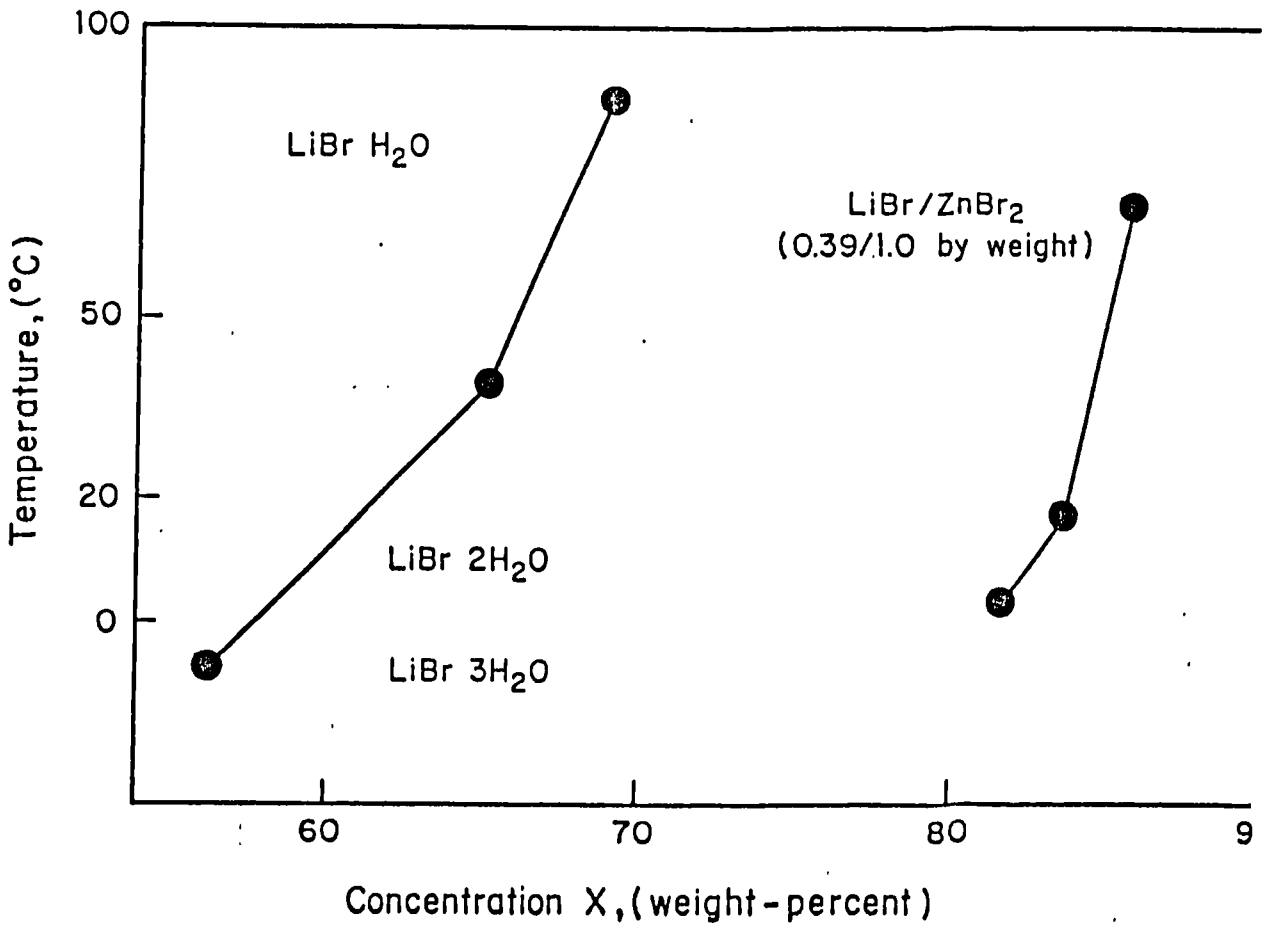

Fig. 7.1 Concentration X against crystallization temperature adapted fr
Ohuchi (1985)

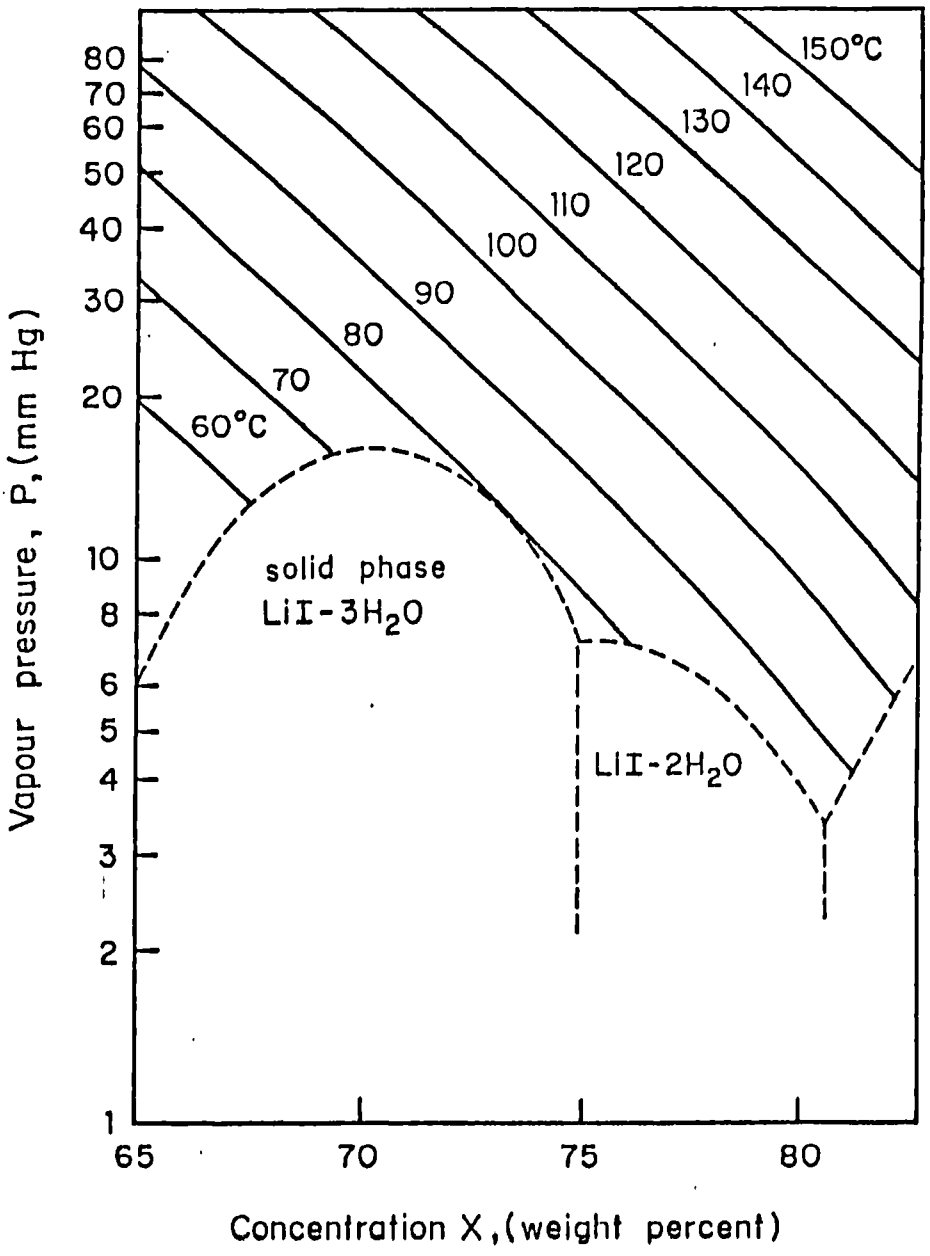

Fig. 7.2 Vapour pressure against concentration by weight with isotherms for aqueous solution of lithium iodide

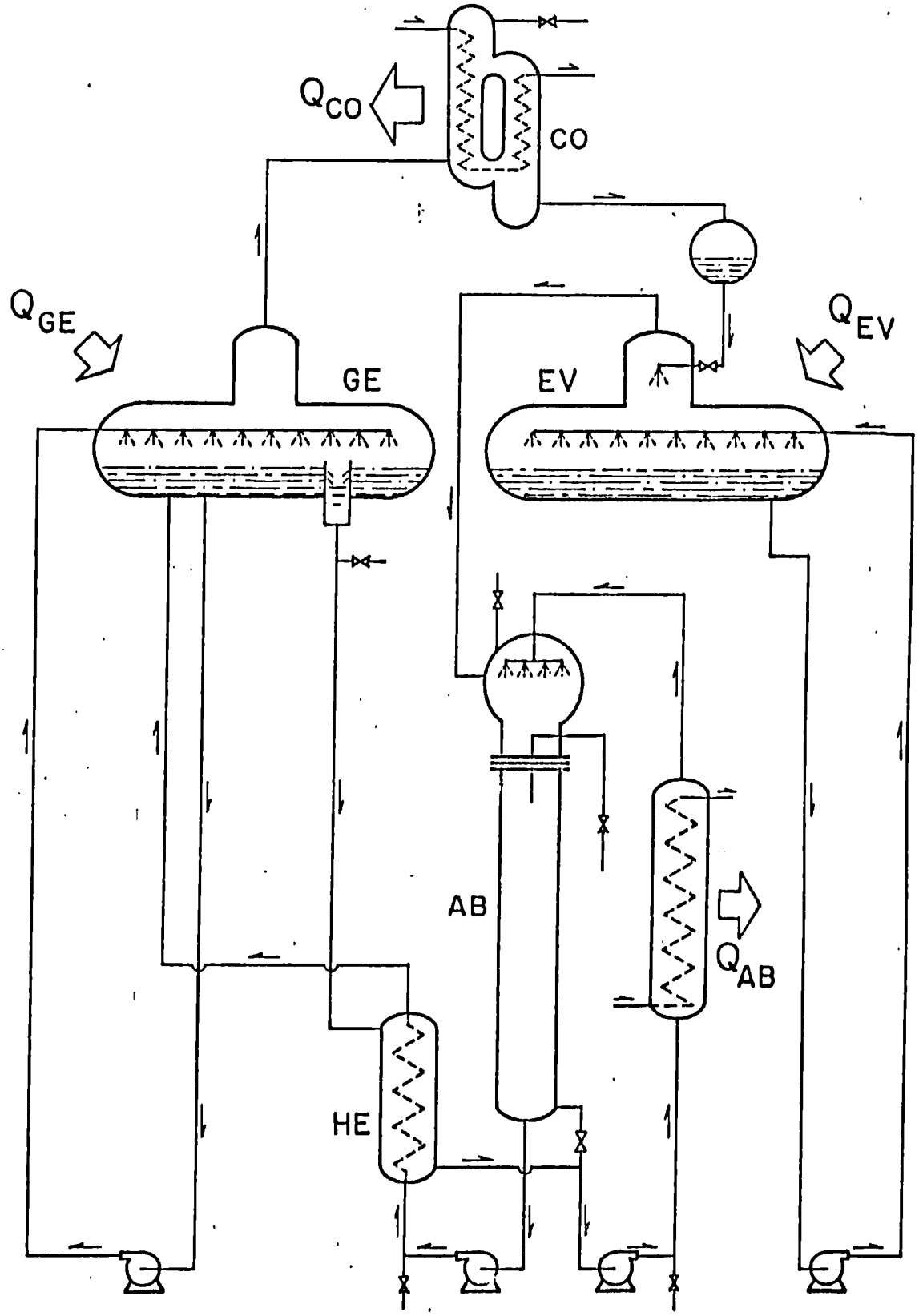

Fig. 7.3 Schematic diagram of absorption cooler

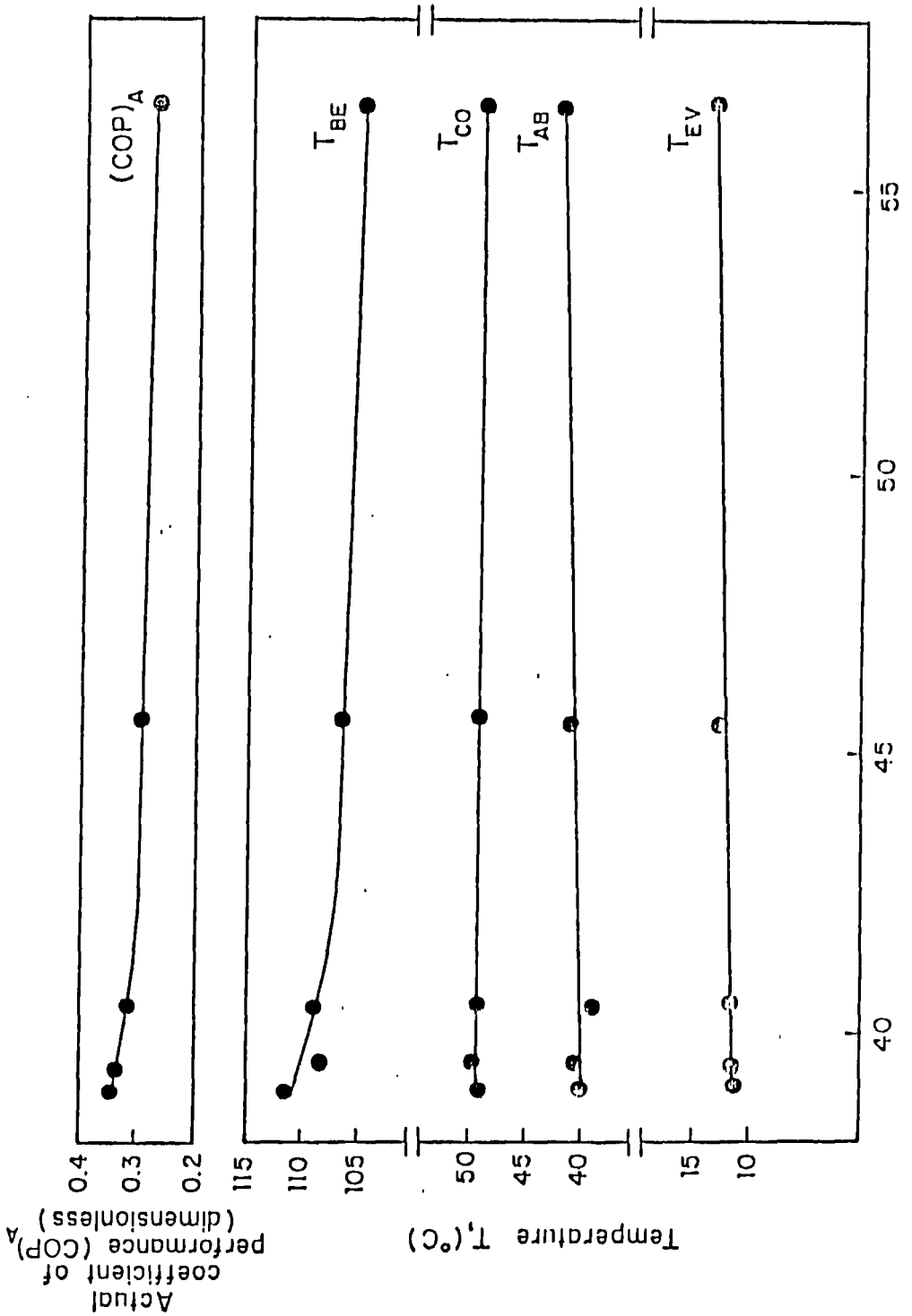

Fig. 7.4 Actual coefficient of performance $(COP)_A$ and temperature levels in absorption cooler against flow ratio (FR)

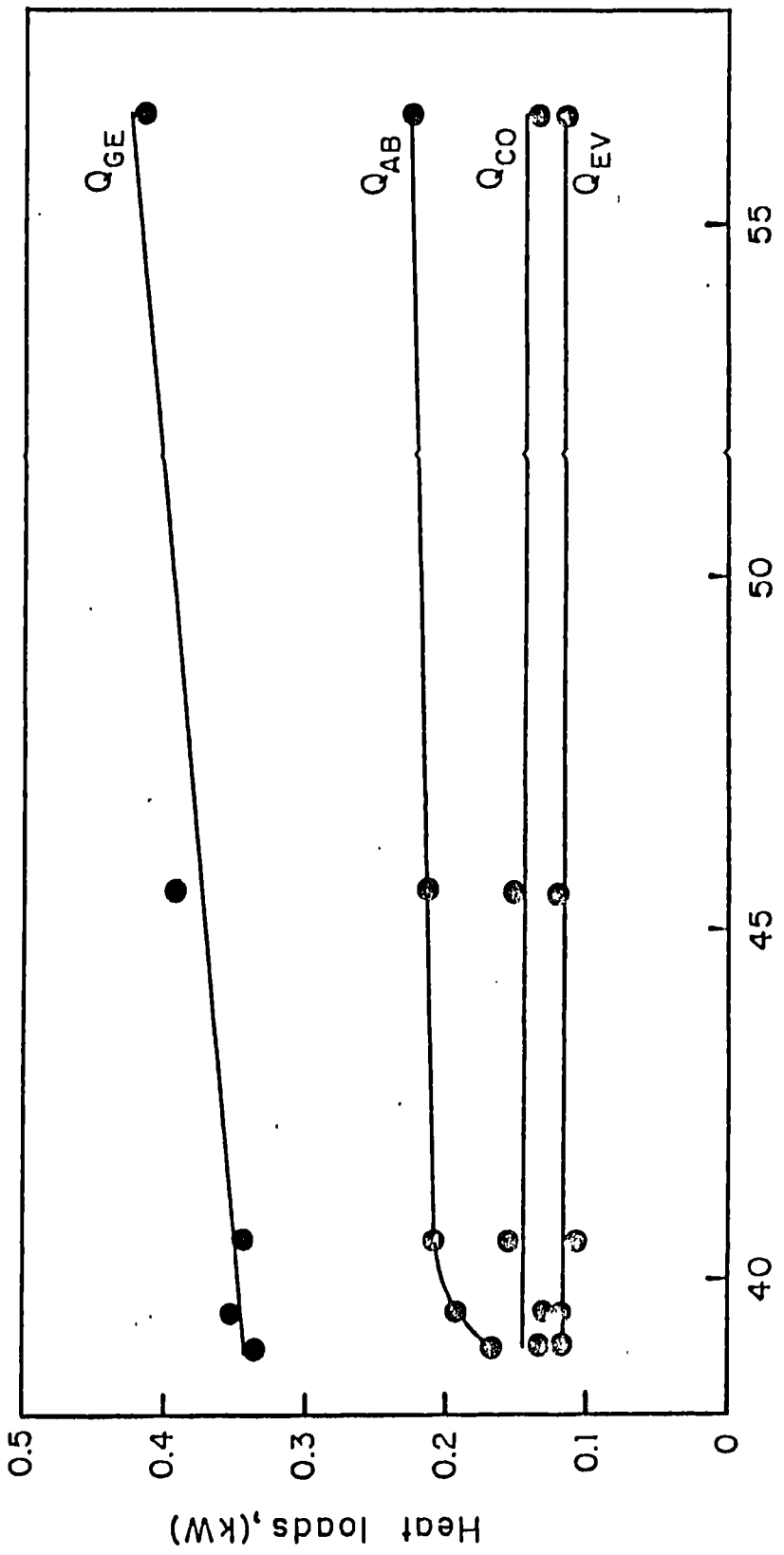

Fig. 7.5 Heat loads against flow ratio (FR)

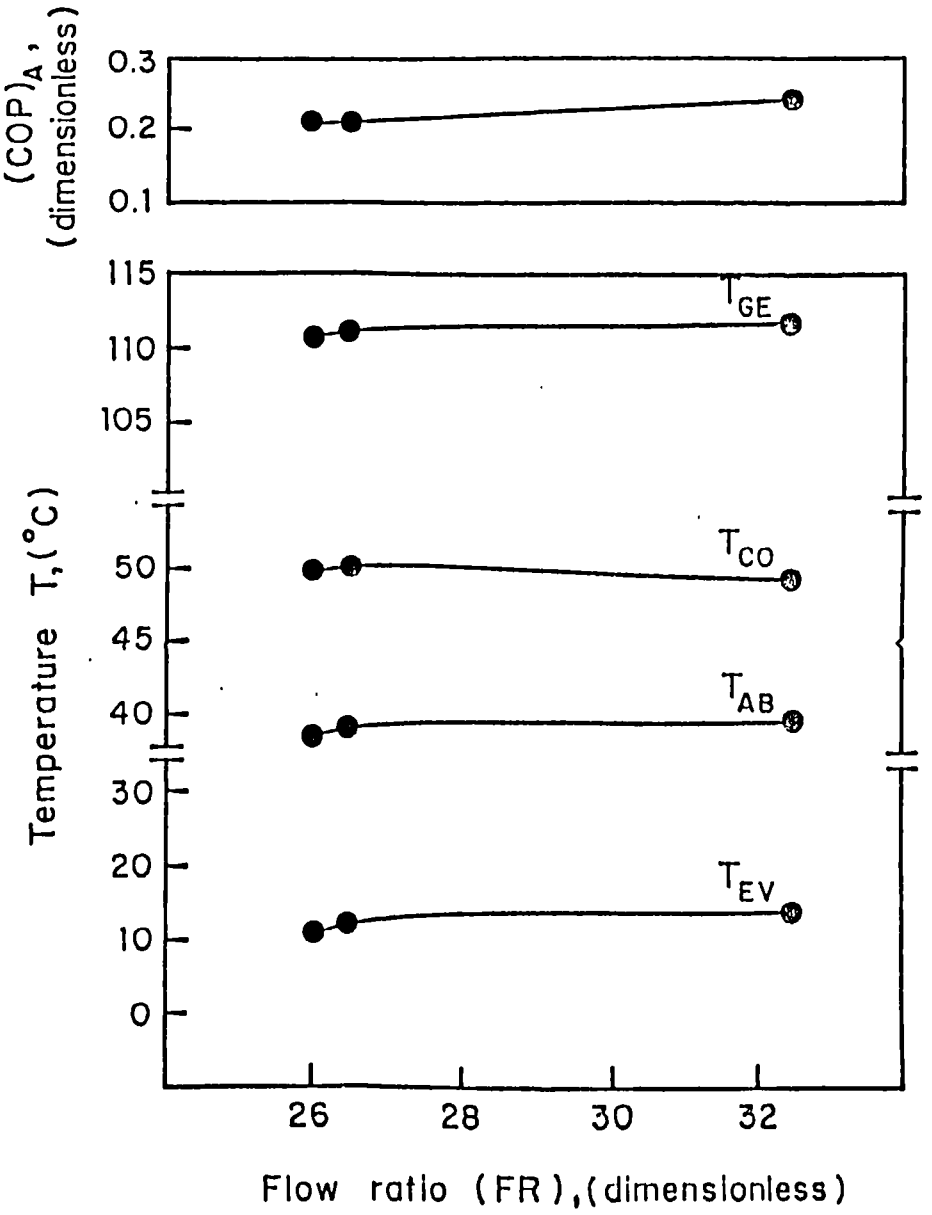

Fig. 7.6 Coefficient of performance $(COP)_A$ and temperature levels against flow ratio (FR)

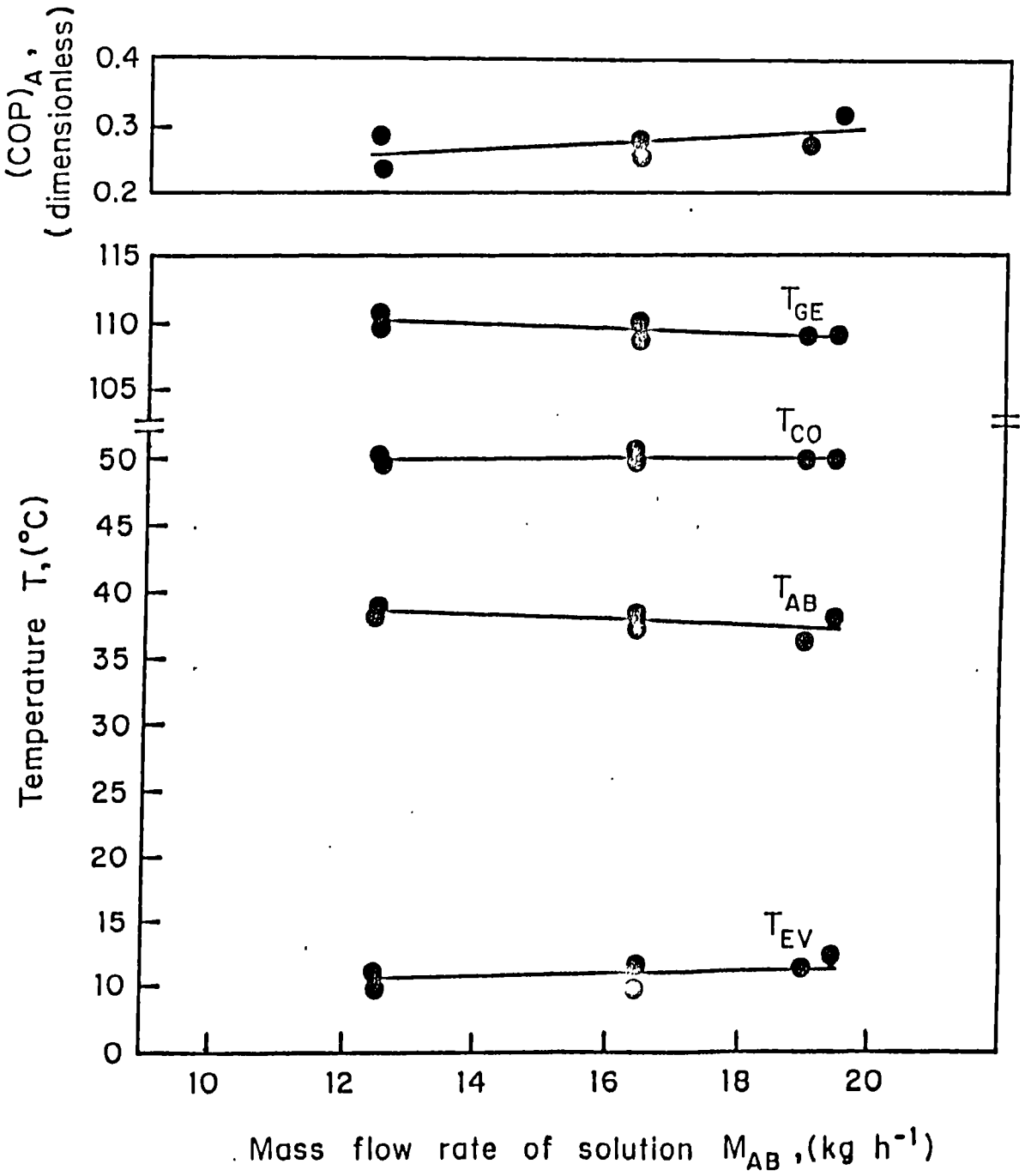

Fig. 7.7 Coefficient of performance $(COP)_A$ and temperature levels against mass flow rate of solution M_{AB}

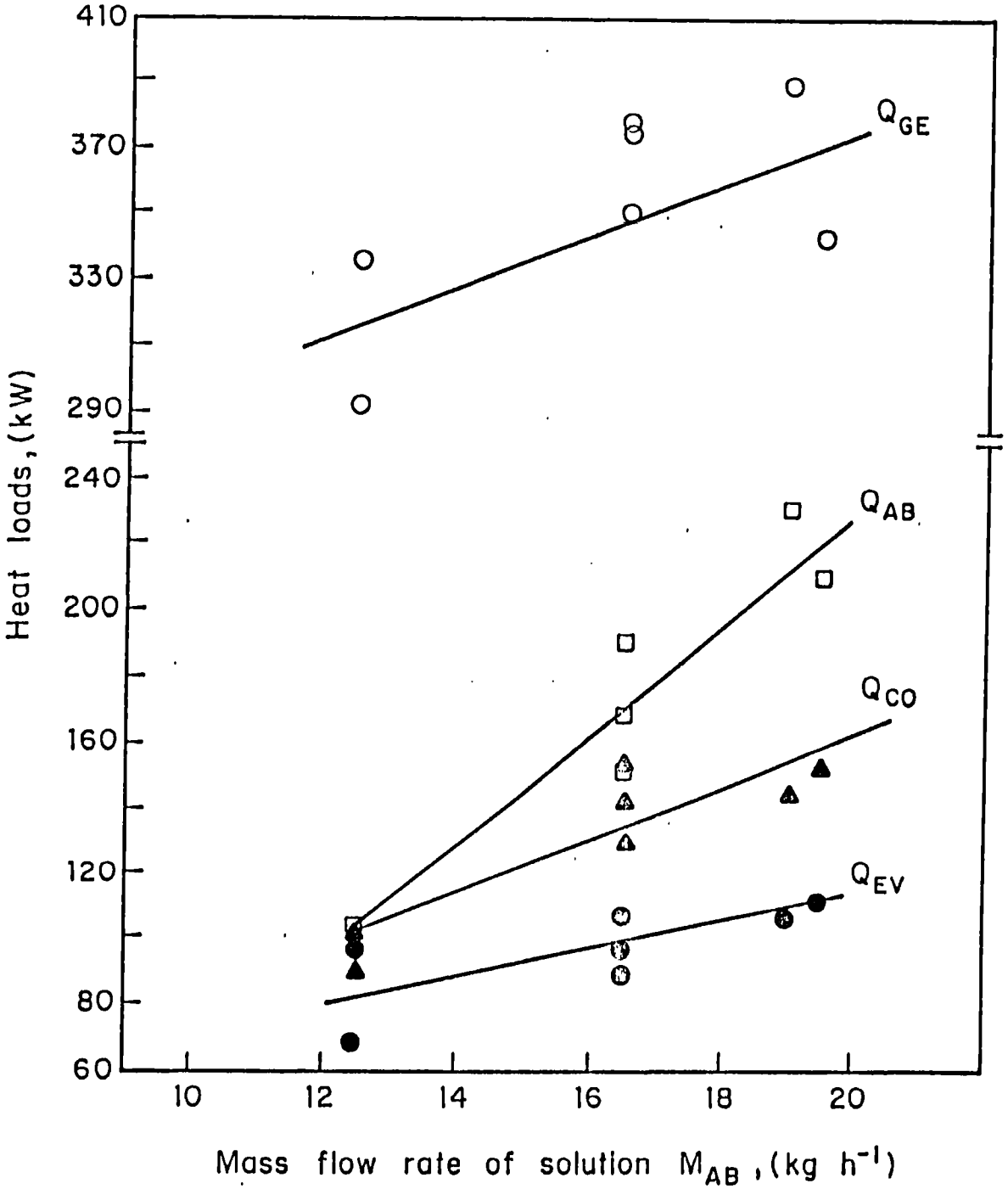

Fig. 7.8 Heat loads against mass flow rate of solution M_{AB}

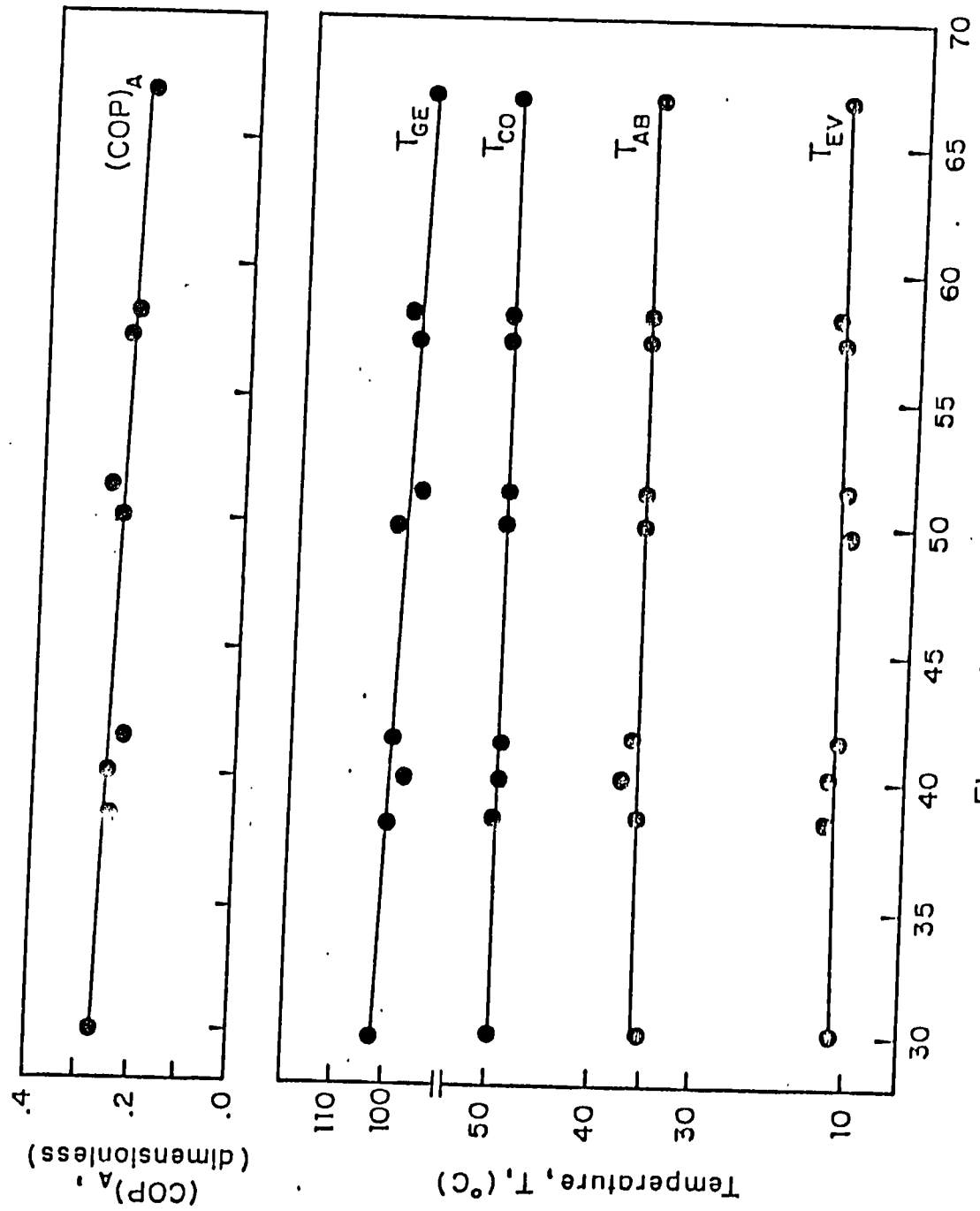

Fig. 7.9 Coefficient of performance $(COP)_A$ and temperature levels against flow ratio (FR).

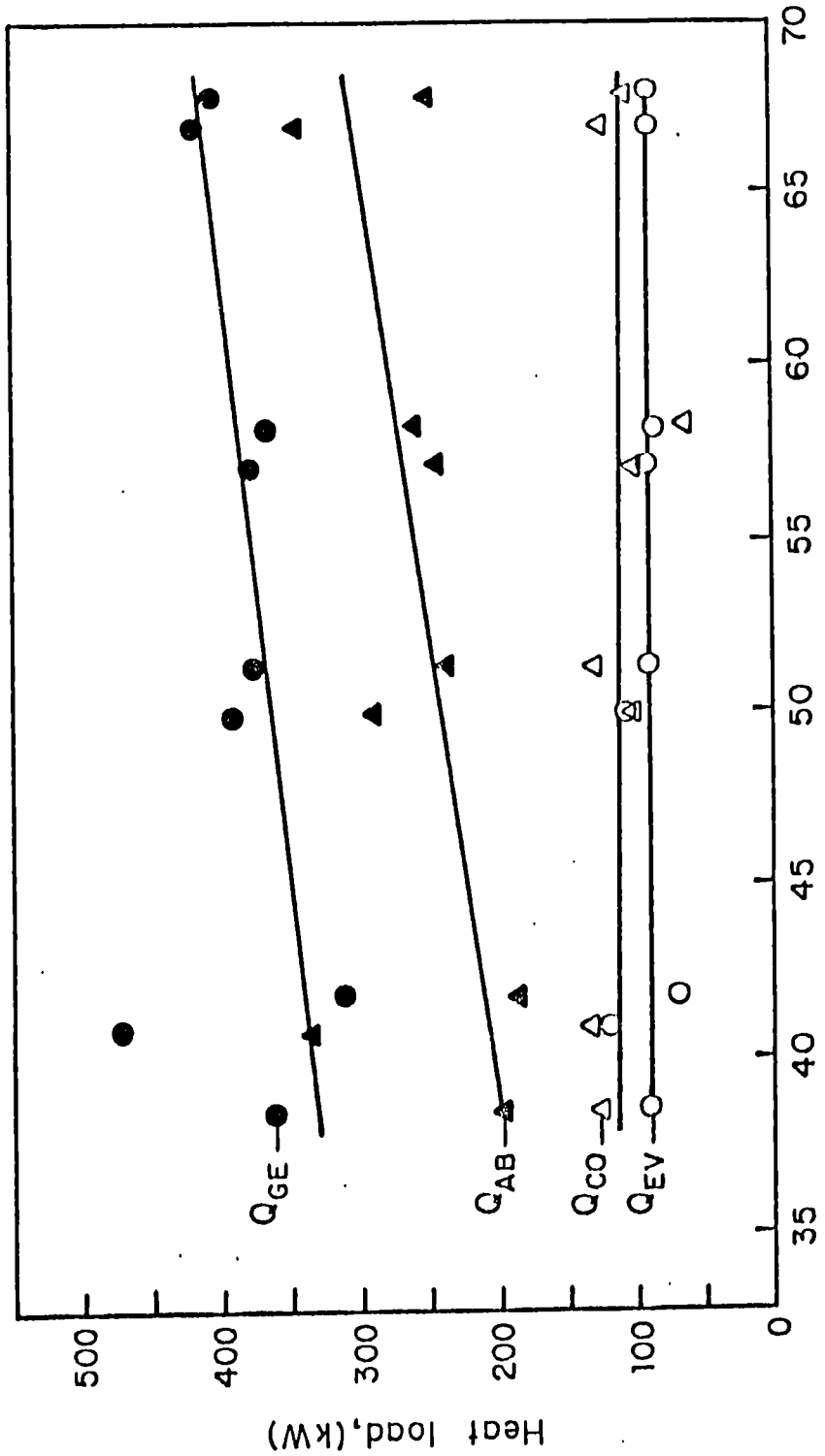

Fig. 7.10 Heat loads against flow ratio (FR)

CHAPTER 8

EXPERIMENTAL STUDIES WITH AN AMMONIA-WATER ABSORPTION SYSTEM USING A FALLING FILM GENERATOR FOR SOLAR COOLING

8.1 INTRODUCTION

Mexico, in common with most other developing countries, suffers from a deficit in cooling facilities both for food preservation and human comfort. This great need for cooling, combined with the high insolation levels in most of these countries, makes solar cooling with absorption refrigeration systems very attractive, especially where electricity from central power stations is not available.

Absorption systems have a number of advantages compared with mechanical vapour compression systems. They do not require compressors (which are not readily available in developing countries) and they can be driven with relatively low-grade heat energy.

Solar driven air conditioning systems using water-lithium bromide solutions as the working pair are sold commercially and have proved to be efficient when working with flat plate collectors [8.1]. Unfortunately, the use of water as a refrigerant is limited to applications above freezing temperatures. The ammonia-water system, which is not subject to these freezing limitations, is still at the stage of the design and testing of components and experimental prototypes. The main reason for the delay in the development of commercial solar ammonia-water systems is that conventional systems operate with generator or heat supply temperatures in excess of 150°C.

Theoretical investigations on solar cooling systems have been reported by

Wilbur and Mancini [8.2] and Clerx and Trezek [8.3]. Nakahara et al [8.4] presented experimental data for air conditioning using a lithium bromide-water absorption cooling system.

8.2 DESIGN CONSIDERATIONS

The system was designed to have a cooling capacity of 2.4 kW, when the average cooling water temperature was 22°C and the evaporator and generator temperatures were -10 and 85°C respectively. These conditions resulted in condensation and absorption temperatures of 25°C, condensation and evaporation pressures of 11 and 3 bar respectively, and strong and weak ammonia solution weight per cent concentrations of 0.48 and 0.40 respectively. The theoretical cycle is illustrated in Figure 8.1.

To improve the efficiency of the system, two heat exchangers were added. Figure 8.2 shows a block diagram of the ammonia-water absorption system.

8.3 EQUIPMENT DETAILS

The experimental absorption cooler shown schematically in Figure 8.3 consisted of a generator, a condenser with a condensate tank, an evaporator, an absorber and two heat exchangers. All the components were made of carbon steel and followed the minimum requirements specified by the standards of the Tubular Exchangers Manufacturers Association (TEMA), U.S.A.

A falling film generator was selected as the means of transferring heat efficiently from the heat source to the solution. Falling film heat exchangers have been used for heating water and also in ammonia condensers [8.5], [8.6]. Heat transfer through falling film evaporators has been used in heat exchanger equipment for the concentration of different kinds of solutions in the chemical, refrigeration, petroleum refining and food in-

dustries [8.7].

The main advantages of vertical and horizontal falling film evaporators are high heat transfer rates at small temperature differences and small liquid inventories as compared with flooded-bundle evaporators [8.8], [8.9].

The generator shown in Figure 8.4 consisted of two parts. The upper section was a rectifier. The strong ammonia solution was fed by a spray through a packed region where it was contacted with the vapour generated from the lower section. This was done in order to reduce the water content of the vapour before leaving the generator. The resultant solution passed to the lower section which was a falling film heat exchanger.

There, the solution fell to a distributor which had the function of feeding a film of solution by overflow to the inside of 25, 0.50 in. (1.27 mm) 16 BWG tubes, 1.5 m long. Liquid solution entered the tubes at such a rate that the liquid descended by gravity along the inner wall as a film. It was essential, in order to have a good liquid distribution in the tubes, that the generator was always in a completely vertical position. There, the solution was heated inside the tubes producing vapour. The vapour flowed to the upper section, whilst the weak ammonia solution was extracted from the bottom. Hot oil flowed countercurrent through the shell of the exchanger to provide the heat of generation.

The condenser was a U bend 1-2 heat exchanger in which ammonia vapour was condensed in the shell side by cooling water flowing through the tubes. The condensate was stored in a tank below the condenser.

The evaporator consisted of a coil where liquid ammonia was evaporated at a

low pressure and temperature. The coil was partially heated by an electric resistance that was controlled by a variac.

The ammonia recuperator was a coil inside a shell. The liquid ammonia coming from the condensate tank went through the coil whilst the ammonia vapour coming from the evaporator flowed countercurrently through the shell.

The absorber consisted of a jacketed vessel as shown in Figure 8.5. Weak ammonia solution was fed to the upper part of the absorber to a circumferential distributer where the solution ran in a film down the vessel wall, absorbing ammonia vapour that was fed to the lower part of the absorber. The heat of absorption was transferred through the wall to cooling water flowing countercurrently in the jacket.

The solution recuperator also consisted of a U bend 1-2 heat exchanger. The strong ammonia solution was pumped through the shell from the absorber to the generator absorbing heat from the weak solution flowing inside the tubes. The weak ammonia solution was throttled from the generator to the absorber.

Temperatures in the absorption system were measured using iron-constantan thermocouples installed in the inlet and outlet of each component. In the heating oil and cooling water lines, copper-constantan thermocouples were used. Pressure gauges were installed in the generator, condenser, absorber and evaporator. Flow rates were measured using rotameters. A controlled volume diaphragm pump was used to meter the strong ammonia solution.

8.4 EXPERIMENTAL PROCEDURE

A series of experiments was carried out in order to study the effect of changes in the generator temperature, at different strong solution flow rates with constant condenser, absorber and evaporator temperatures. A manual expansion valve helped to keep the refrigerant flow to the evaporator approximately constant, although fluctuations in the flow rate were inevitable.

Generator temperatures were varied from 80 to 100°C in approximately 5°C increments. This range of temperatures was selected as the operating range appropriate to non focussing solar collectors. The high pressure was maintained at about 11 bar in order to assure a high purity of the condensing ammonia vapour. The low pressure side was maintained below 3 bar to obtain evaporator temperatures below 0°C. Three strong solution flow rates were used: 0.012, 0.015 and 0.0175 kgs^{-1}. The absorber and condenser temperatures were kept below 30°C and the outlet evaporator temperature was maintained at 0°C or lower.

8.5 RESULTS AND DISCUSSION

Fifteen different experimental runs were carried out based on the combination of generator temperatures and strong solution flow rates previously described. Each experimental run lasted from two and a half to three hours after reaching steady state. The temperatures, pressures and flow rates were recorded every 15 minutes, in such a way that there were 11 to 13 data groups in every run. Because the temperatures of the evaporator, condenser and absorber were kept almost constant, the analysis considered the variations in generation temperature and flow ratio. Table 8.1 shows the operating conditions of the ammonia-water refrigeration prototype.

Figure 8.6 is a plot of the heat load in the generator Q_{GE} against the generator temperature T_{GE} for the three values of the strong solution flow rate M_{AB}. It can be seen that the generator heat load increased as the generator temperature increased. The highest value of Q_{GE} was about 5.7 kW at a generator temperature of 370 K and a strong solution flow rate of 0.0178 kgs^{-1}. The rate of increase of the generator heat load with temperature was higher for the highest value of the solution flow rate.

The effect of the variation of the generator temperature T_{GE} on the evaporator heat load Q_{EV}, for the three values of the solution flow rate M_{AB}, is shown in Figure 8.7. It can be seen that the cooling capacity increased with generator temperature to a value of 2.26 kW at 370 K and was independent of the solution flow rate used. This is due to the heat transfer characteristics of the falling film generator. As the solution flow rate increases from the design value of 0.012 kgs^{-1} to the highest value of 0.018 kgs^{-1}, the thickness of the falling film solution flowing in the generator also increases and less heat is effectively used for vapourising the refrigerant.

Operation with low temperature energy sources such as solar energy introduces limitations to the operating level of generator temperatures. Figure 8.8 is a plot of the generator temperature T_{GE} against the flow ratio (FR) for three values of the solution flow rate. It can be seen that the system operated at lower generator temperatures when the flow ratio was increased. An increase in the refrigerant mass flow rate will correspond to a decrease in the flow ratio (FR). As the generator temperature T_{GE} increases the refrigerant mass flow rate M_R also increases.

Figure 8.9 is a plot of the actual coefficient of performance $(COP)_A$ of the system against the generator temperature T_{GE} for three values of the solution flow rate. It can be seen that the actual coefficient of performance increases with generator temperature and is significantly higher for the lower flow rate of strong solution M_{AB} flowing in the system.

Figure 8.10 is a plot of the value of the actual coefficient of performance $(COP)_A$ against flow ratio (FR) for the three values of the solution flow rate M_{AB}. It can be seen that the value of the coefficient of performance is reduced significantly as the value of the flow ratio increases.

8.6 CONCLUSIONS

It has been shown experimentally that an ammonia-water absorption system can be operated successfully at relatively low generator temperatures of 80 to 100°C whilst providing cooling below the freezing temperature of water.

A novel type of generator using the falling film principle was used and proved to be an efficient way to extract heat from a low temperature energy source.

It was demonstrated that the performance of an absorption system with a falling film generator is very sensitive to variations of the solution flow rate. When the system was operated at the designed flow rate, less heat was required in the generator per unit mass of refrigerant generated than when higher flow rates were used.

The highest coefficient of performance $(COP)_A$ of 0.48 was achieved with the lowest value of the solution flow rate of 0.013 kgs^{-1}, a flow ratio (FR) value of 8 and a generator temperature T_{GE} of 370 K (97°C).

Lower generator temperatures can be used at higher flow ratio values and at reduced efficiencies. A generator temperature of 360 K could be used with a flow ratio of 20 and a reduced coefficient of performance of 0.27.

8.7 REFERENCES

8.1 A.H. Uppal and T. Muneer, Cost analysis of commercial solar absorption coolers using a detailed simulation procedure, Applied Energy 72, 75-82 (1987).

8.2 P.J. Wilbur and T.R. Mancini, A comparison of solar absorption air conditioning systems, Solar Energy, 18 (6), 569-576 (1976).

8.3 M. Clerx and G.J. Trezek, Performance of an aqua-ammonia absorption solar refrigerator at subfreezing evaporator conditions, Solar Energy 39 (5), 379-389 (1987).

8.4 N. Nakahara, Y. Miyakawa and M. Yamamoto, Experimental study of house cooling and heating with solar energy using flat plate collectors, Solar Energy 19 (6), 557-662 (1977).

8.5 ASHRAE Handbook and Product Directory, Equipment, American Society of Heating Refrigeration and Air Conditioning Engineering, New York, U.S.A. pp 16.7 (1979).

8.6 D.Q. Kern, Process heat transfer, pp 746 McGraw Hill International Book Company (1950).

8.7 R.H. Perry and D. Green, Perry's Chemical Engineers Handbook, Sixth Edition, International Student Edition, McGraw Hill Book Company (1984).

8.8 T. Fujita and T. Ueda, Heat transfer to falling film liquid films and film breakdown. II: Saturated liquid films with nucleate boiling, Int. J. Heat Mass Transfer, 21, 109-118 (1978).

8.9 M. Cerza and V. Sernas, Nucleate boiling in thermally developing and fully developed laminar falling water films, J. of Heat Transfer, Transactions of the ASME, 110 (1), 221-228 (1988).

GENERATOR	
working pressure	1.072 MPa
heating medium inlet/outlet temperature	102.7/98.0°C
ammonia-water solution inlet/outlet temperature	54.5/96.1°C
refrigerant vapour leaving generator	67.2°C
mass flow rates-strong solution	$1.49X10^{-2}$ kgs^{-1}
weak solution	$1.37X10^{-2}$ kgs^{-1}
ammonia	$0.12X10^{-2}$ kgs^{-1}
hot oil	0.38 kgs^{-1}
heat load solution	4.6 kW
heat load hot oil	3.9 kW
RECTIFIER	
working pressure	1.072 MPa
temperature inlet/outlet	67.2/62.1°C
mass flow rate	$0.12X10^{-2}$ kgs^{-1}
*concentration inlet/outlet	0.987/0.991
*heat load	$3.3X10^{-2}$ kW
CONDENSER	
condensing pressure	1.072 MPa
condensing temperature	28.1°C
*heat load ammonia	1.53 kW
heat load water	1.16 kW
cooling water inlet/outlet temperature	11.6/14.5
cooling water consumption	$9.5X10^{-2}$ kgs^{-1}

PRECOOLER	
liquid ammonia pressure	1.072 MPa
liquid ammonia inlet/outlet temperature	28/8.4
ammonia vapour pressure	0.155 MPa
ammonia vapour inlet/outlet temperature	-12/-10.8
heat exchange rate	0.22 kW
ECONOMISER	
working pressure	0.993 MPa
inlet/outlet temperature	
-weak solution	96.1/68.4
-strong solution	31.0/57.0
heat exchange rate	1.83 kW
EVAPORATOR	
evaporating temperature	-13.0°C
evaporating pressure	0.155 MPa
refrigeration heat load	1.62 kW
ABSORBER	
absorption pressure	0.141 MPa
final absorption temperature	33.2
ammonia vapour temperature	-10.8°C
cooling water inlet/outlet temperature	11.7/14.7
cooling water consumption	0.18 kgs^{-1}
heat load water	2.26 kW
heat load solution	3.9 kW

*calculated

Table 8.1 Operating conditions of the ammonia-water refrigeration prototype

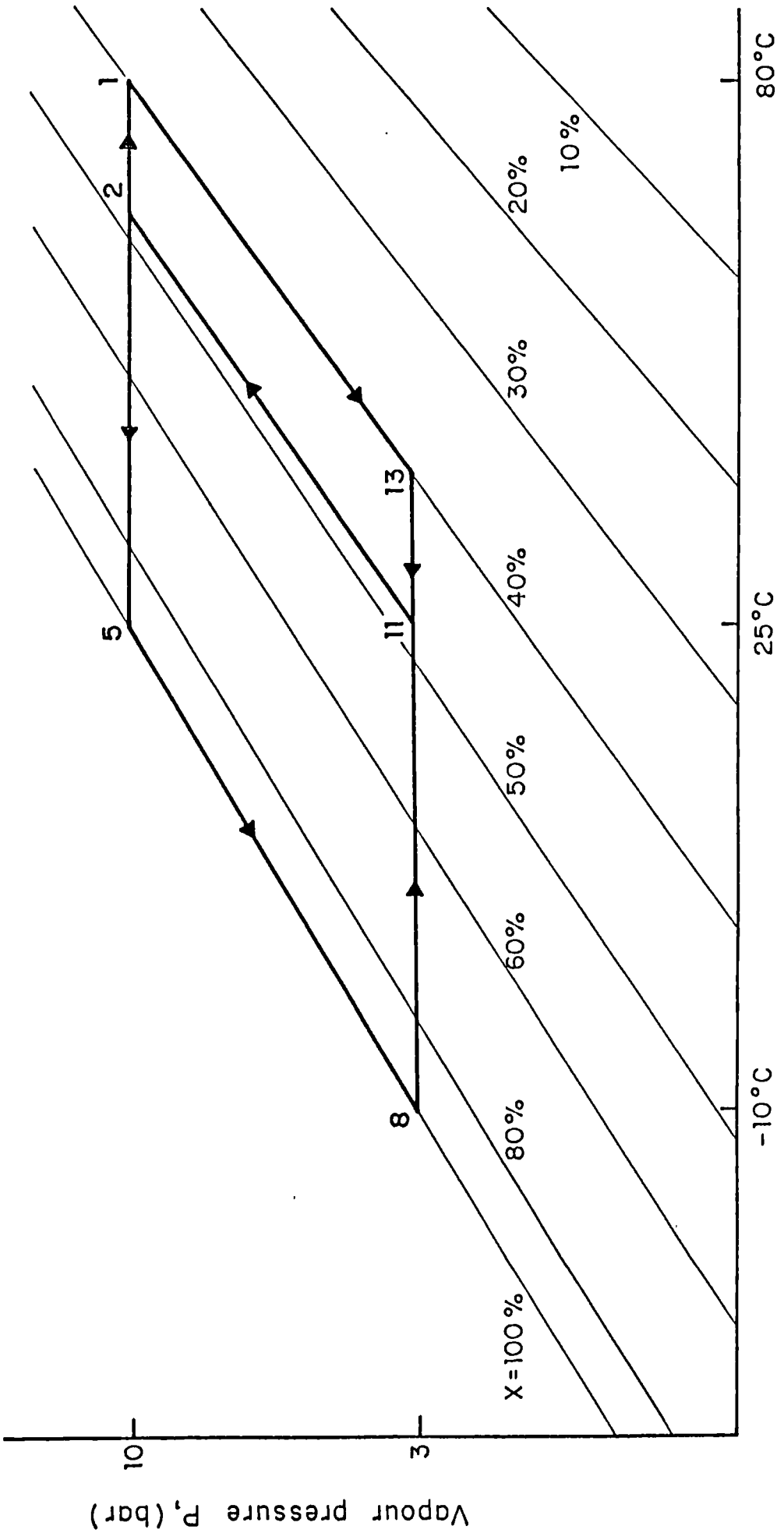

Fig. 8.1 Theoretical cycle conditions for the ammonia – water system

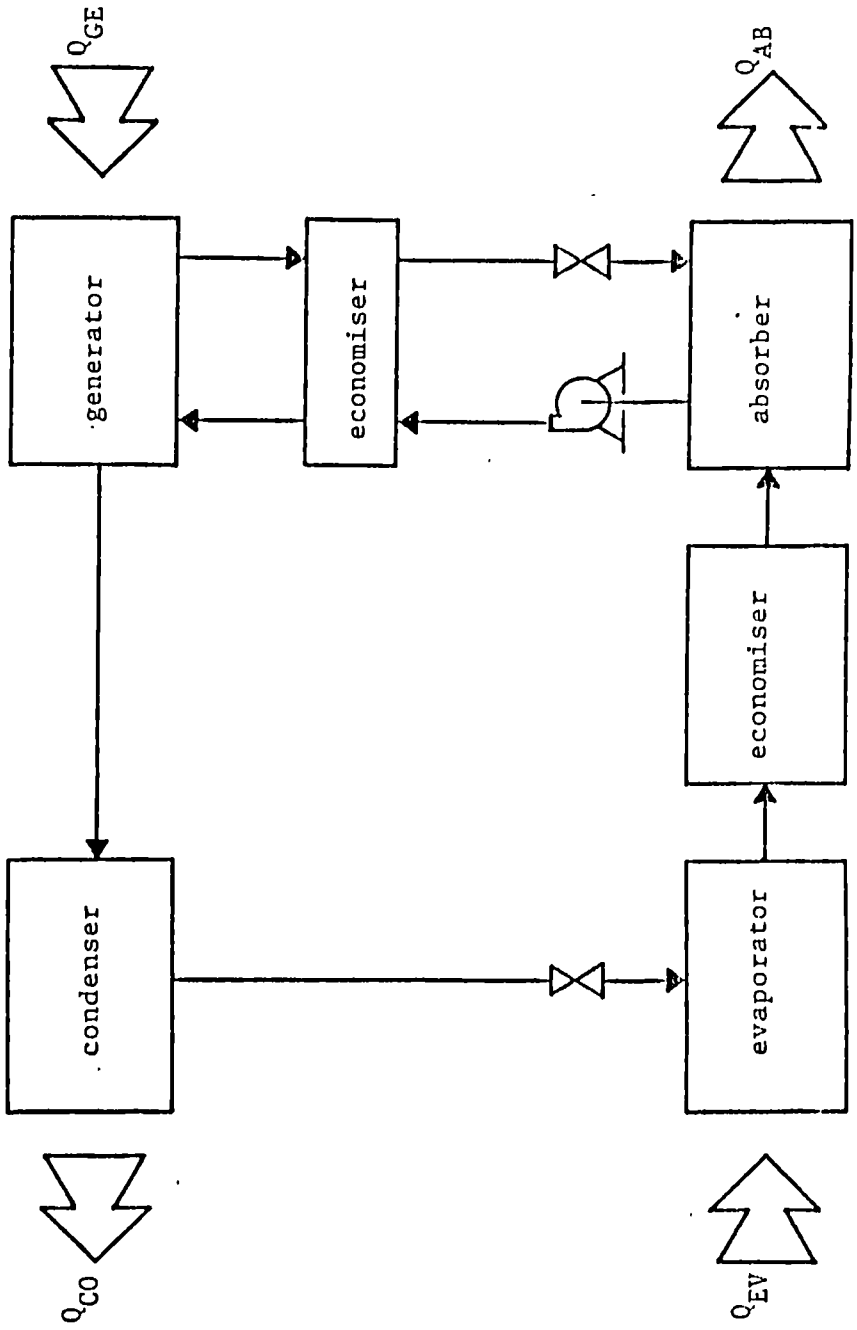

Fig. 8,2 Simplified block diagram of an absorption cooler

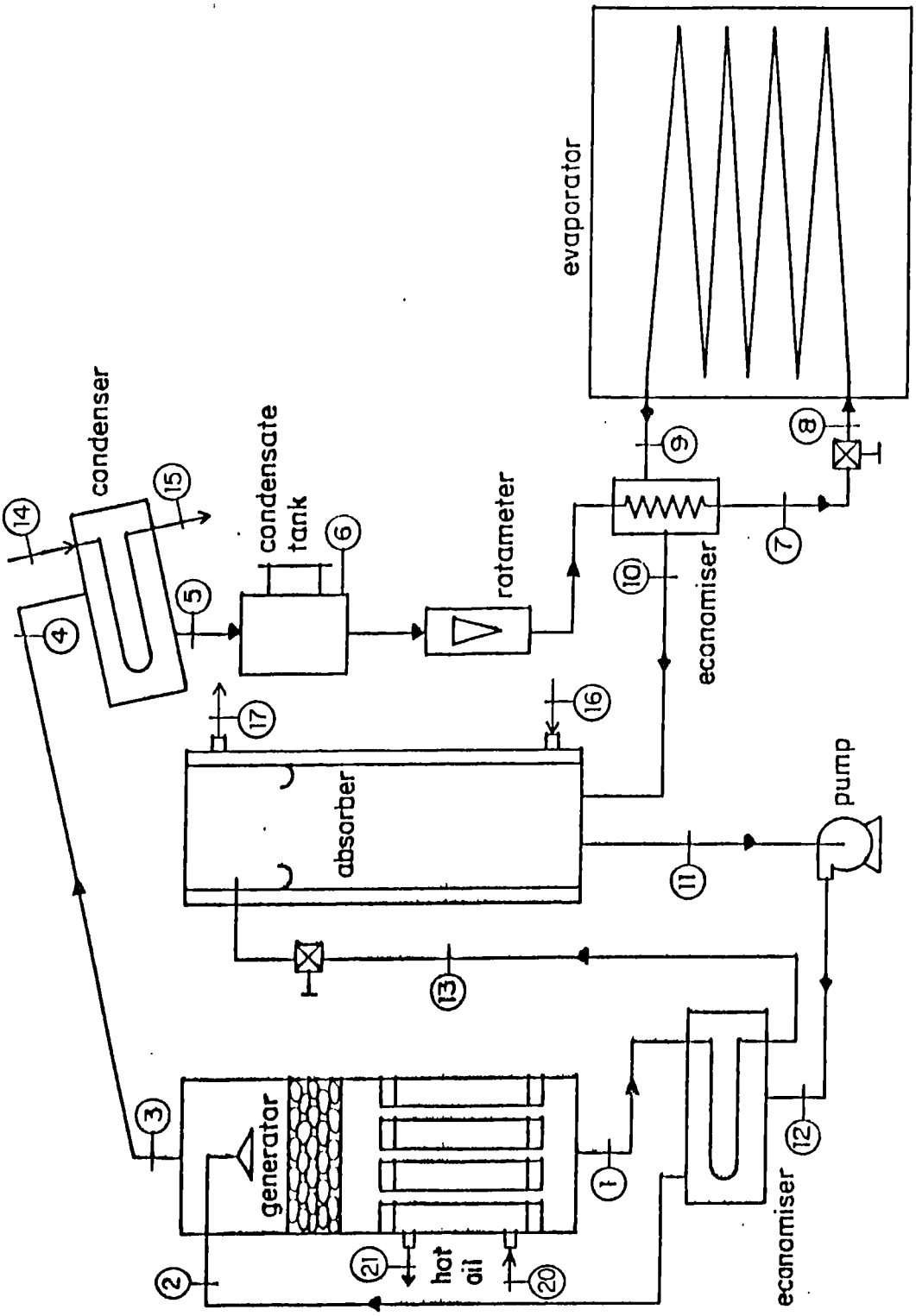

Fig. 8.3 Schematic diagram of experimental absorption cooler

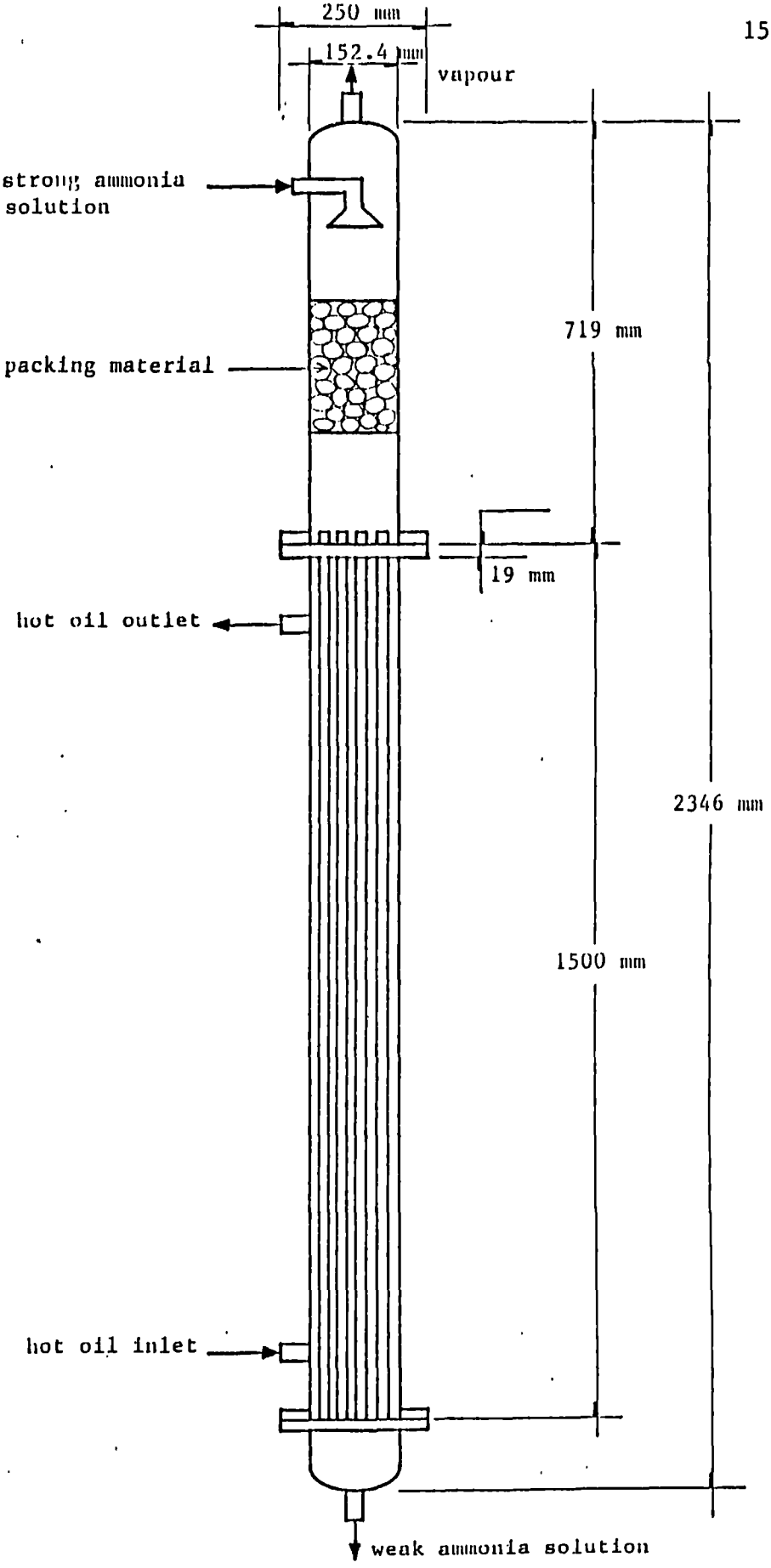

Fig. 8.4 Generator

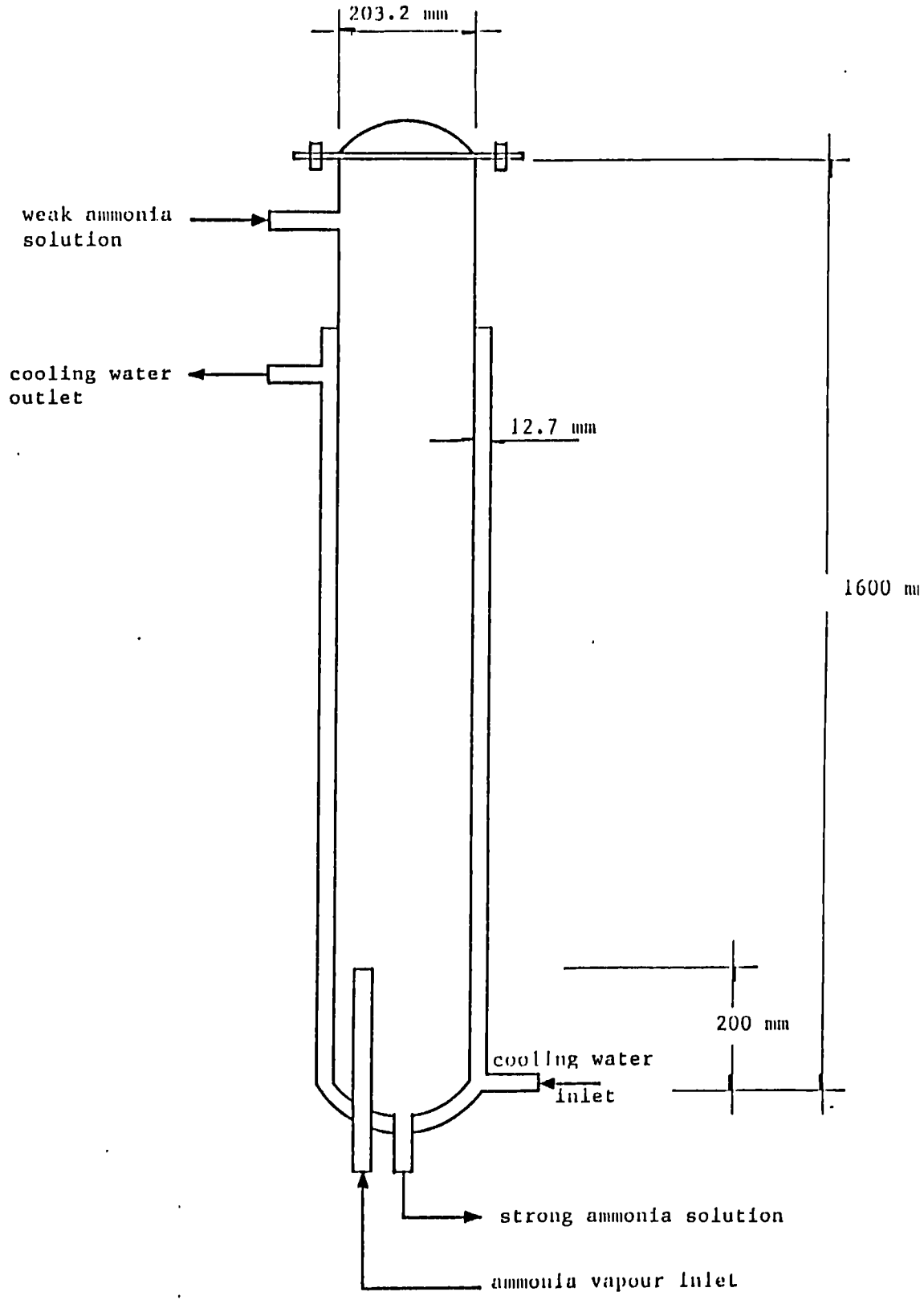

Fig. 8.5 Absorber

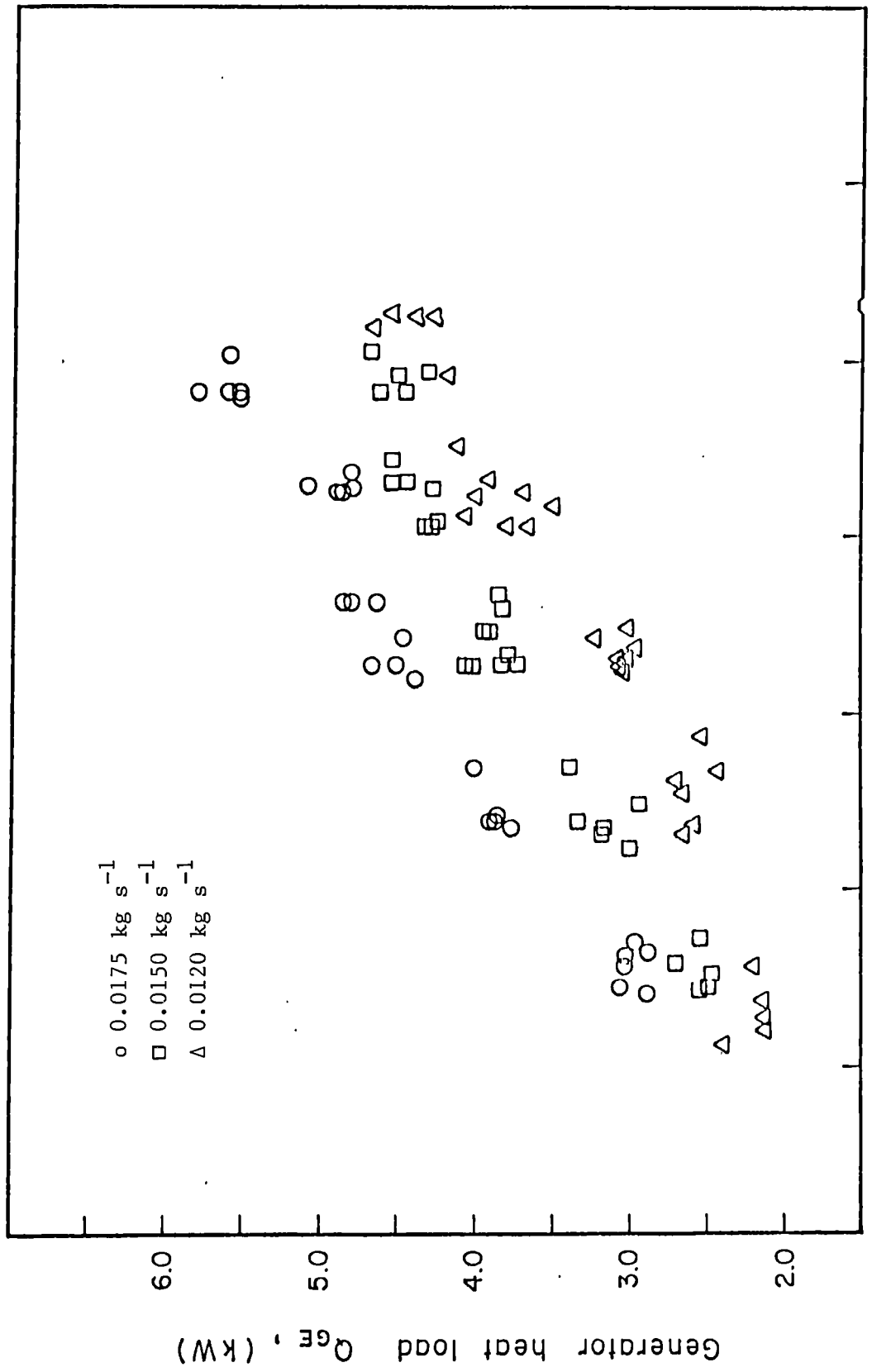

Fig. 8.6 Generator heat load against generator temperature.

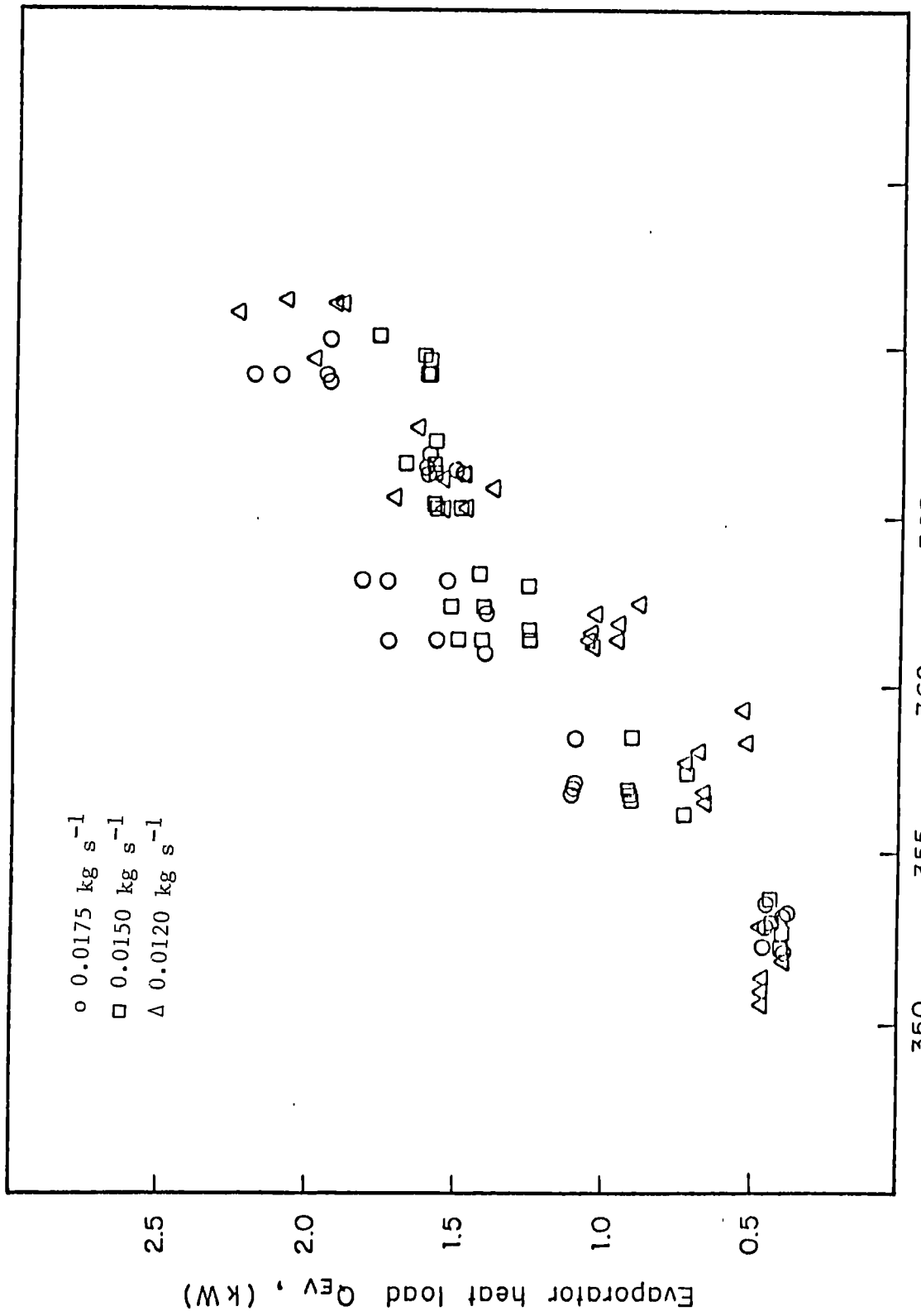

Fig. 8.7 Evaporator heat load against generator temperature

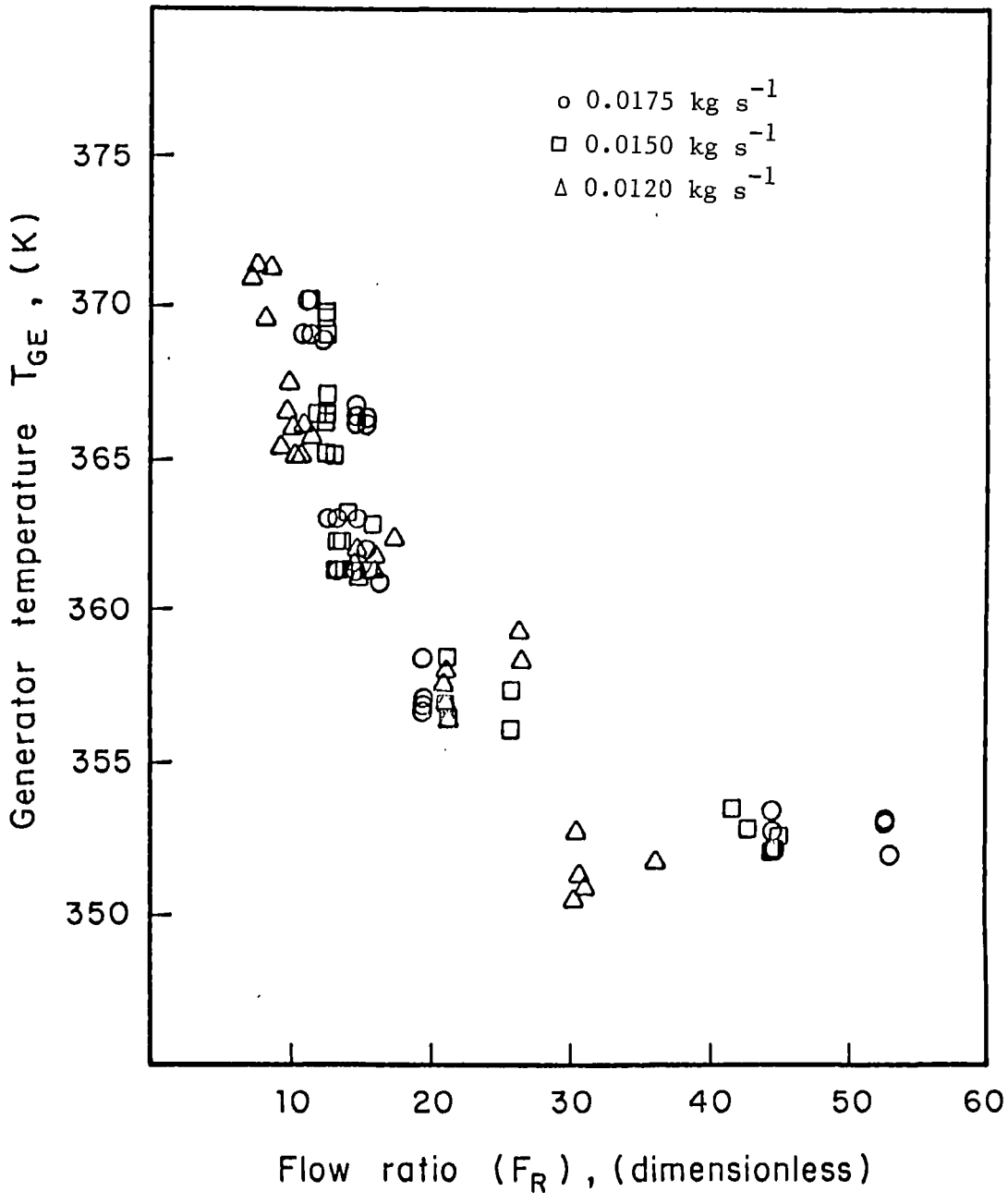

Fig. 8.8 Generator temperature against flow ratio.

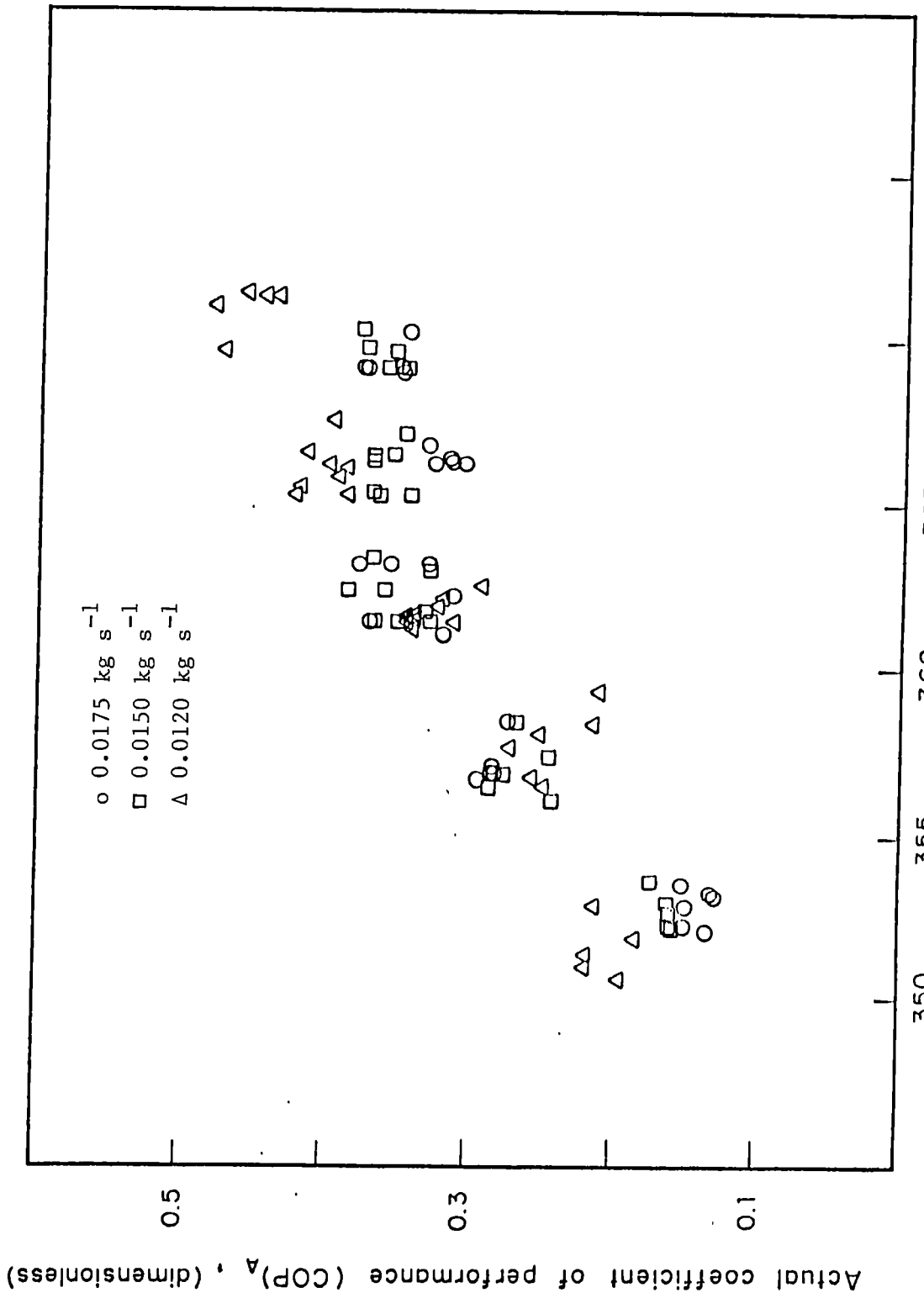

Fig. 8.9 Actual coefficient of performance against generator temperature.

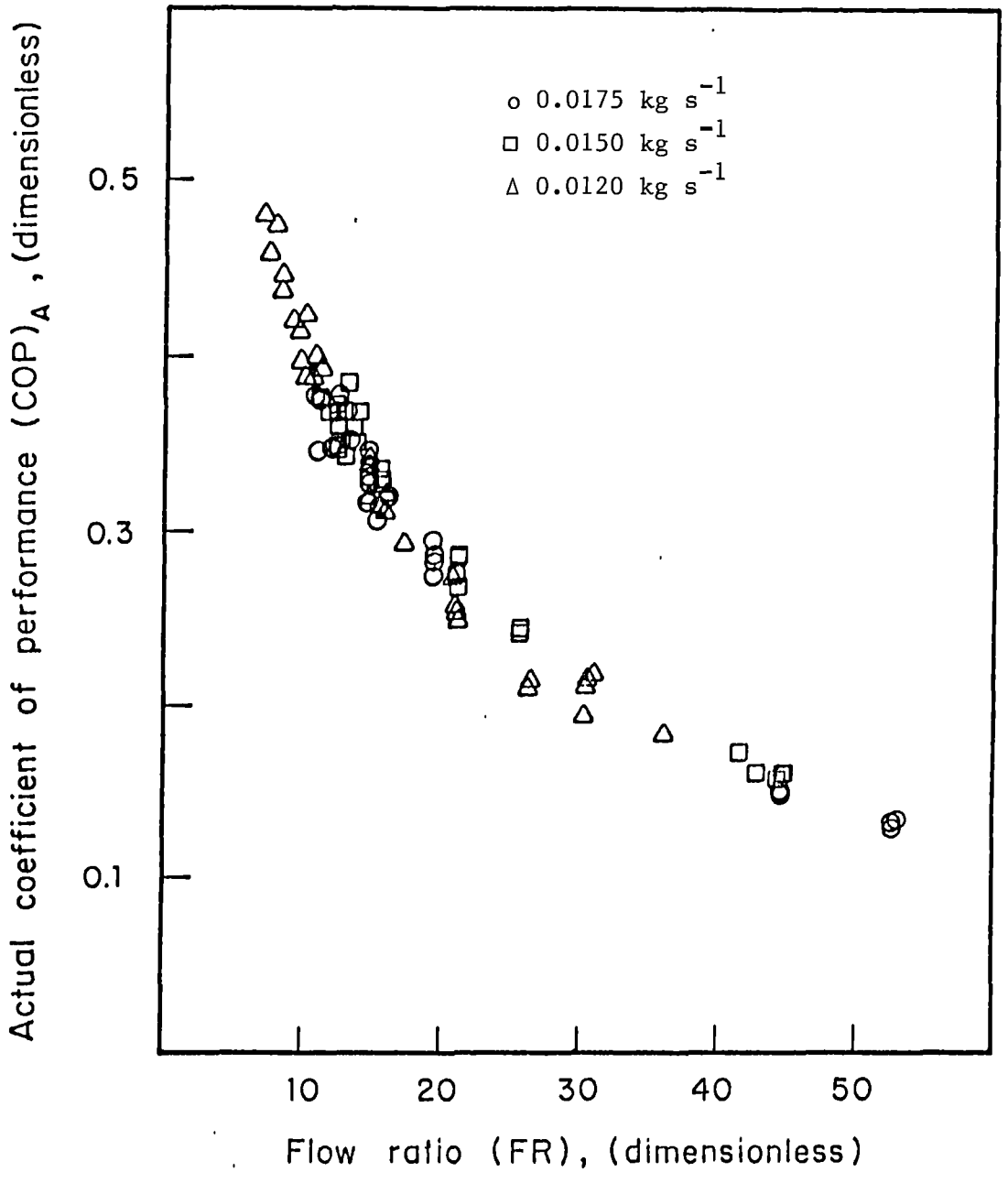

Fig. 8.10 Actual coefficient of performance against flow ratio.

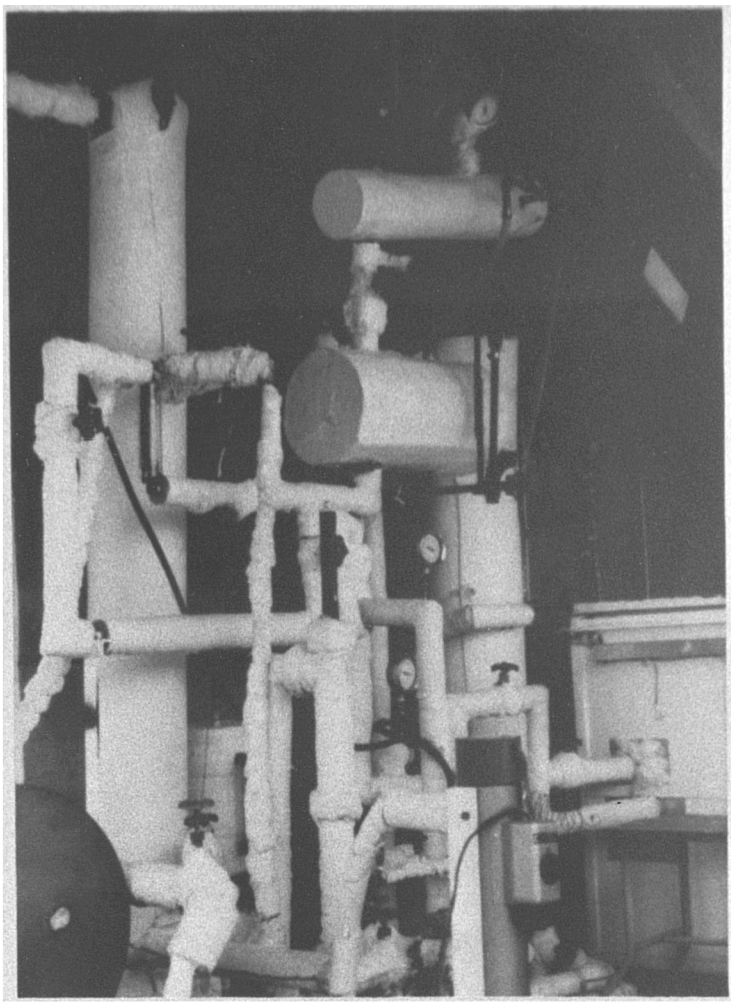

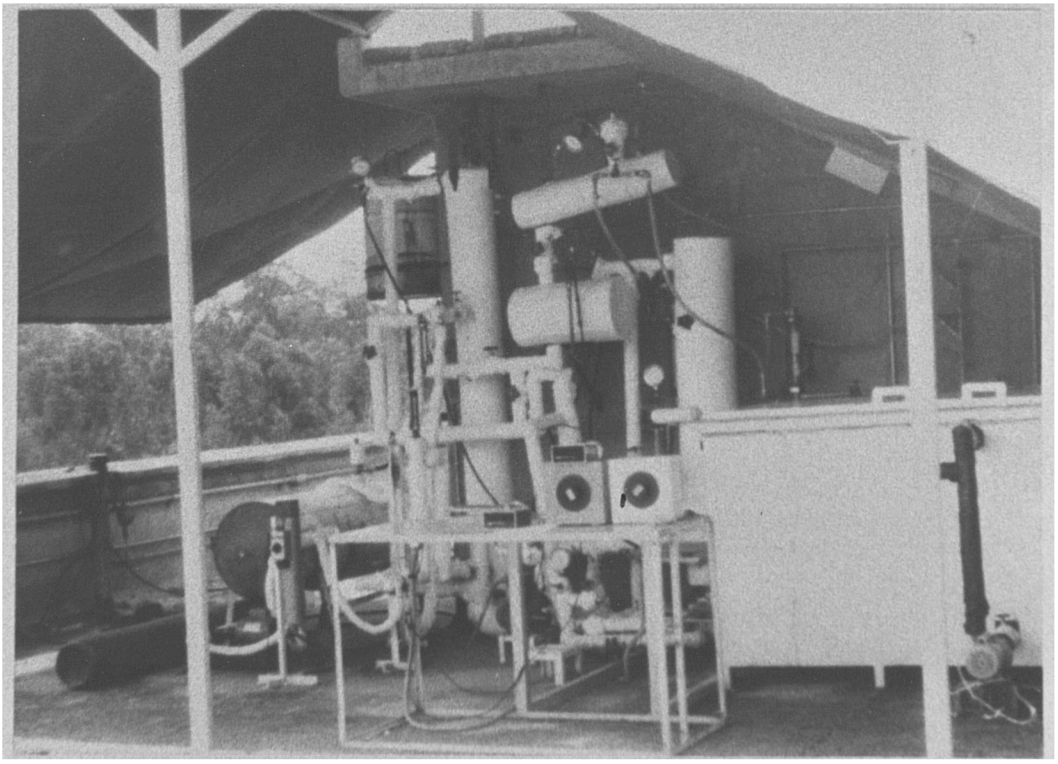

Experimental ammonia-water absorption refrigeration system, at the Solar Energy Laboratory, UNAM.

CHAPTER 9

EXPERIMENTAL STUDIES WITH AN AMMONIA-WATER ABSORPTION SYSTEM OPERATING ON LOW ENTHALPY GEOTHERMAL ENERGY

9.1 INTRODUCTION

Mexico possesses large amounts of geothermal brine at temperatures which are too low to enable electricity to be generated efficiently and economically. Of the possible nonelectric uses of low and medium enthalpy geothermal energy, the one which appears to have the greatest potential is the use of heat driven absorption systems to provide cold storage facilities for perishable food. It has been estimated that perishable food losses in Mexico, resulting from inadequate handling and cooling facilities, vary from 35 to 50% with sea food having the highest loss [9.1]. Spauschus [9.2] has published data on the world market for refrigeration and air conditioning equipment. The study showed that North America, Japan and Europe produce and purchase almost 90% of the refrigeration equipment in the world, although they account for less than 25% of the world population. The Middle East, Africa, China, India and the USSR, with 59% of the world population, produce and purchase less than 5% of the refrigeration equipment in the world. Latin America, with 10% of the world population, produces and purchases 6% of the refrigeration equipment in the world.

The enormous potential demand for refrigeration in the less developed regions of the world, will need to be met by all the available technologies and energy sources. The low enthalpy heat from solar radiation, geothermal fluids and biomass can play an important role in meeting this demand.

Most of the geothermal fields in Mexico are located near important agricultural areas. The largest geothermal field in Mexico is at Cerro prieto which is near the growing city of Mexicali in Baja California. Mexicali is on the border with the U.S. state of California.

In order to prove the technical feasibility of operating heat driven absorption cooling systems on low enthalpy geothermal energy, a prototype ammonia-water absorption cooler was installed in the Cerro Prieto geothermal field, where the ambient temperatures exceed 40°C and the cooling water temperatures reach 30°C. This prototype ammonia-water cooler was originally designed for and installed in the Los Azufres geothermal field where the ambient conditions are much less demanding than at Cerro Prieto.

9.2 EXPERIMENTAL FOR INSTALLATION AT LOS AZUFRES

9.2.1 EQUIPMENT

Figure 9.1 is a schematic diagram of the experimental absorption cooler which was installed at the Los Azufres geothermal field. The unit was designed for fabrication at minimum expense. The helical coil in the generator was the only component made of stainless steel. This was necessary to minimize corrosion and scaling during its contact with geothermal fluid. The other components in the system were made of carbon steel. The size of the components were determined by the availability of materials.

The condenser and evaporator were standard commercially available units. The condenser was a model CAH-06 shell and tube heat exchanger with a nominal capacity of 17.6 kW supplied by the Herdel Co., Mexico. It consisted of a 0.27 m internal diameter shell and thirty 2.5 m long tubes with an internal diameter of 0.016 m in a pass arrangement. The evaporator was a model 1500 XRWA shell and tube heat exchanger supplied by the Recold Co.,

Mexico, with a nominal capacity of 10.6 kW at a 5.6°C difference in temperature between the air entering the evaporator and the saturation temperature of the working fluid at the evaporator.

The generator, rectifier and precooler were all shell and tube heat exchangers. The generator is illustrated schematically in Figure 9.2. The 1 m long shell was made of available tube with an internal diameter of 0.318 m. Geothermal steam entered at the bottom of the shell and was distributed through a perforated vertical pipe (not shown) with an internal diameter of 0.027 m in the centre of the surrounding coil. The ammonia-water solution circulated through the 17.3 m long stainless steel helical coil which had an internal diameter of 0.0158 m.

The shells of the rectifier and precooler were constructed of available tube with an internal diameter of 0.15 m. The rectifier was filled with glass packing. The helical coils were constructed of piping with an internal diameter of 0.0097 m. The coils in the rectifier and cooler were 5.1 and 10.0 m long respectively.

The recuperator was a double pipe heat exchanger fabricated from carbon steel pipes with internal diameters of 0.016 and 0.04 m respectively. The recuperator was 12 m long.

The absorber is illustrated schematically in Figure 9.3. It consisted of a vertical one pass shell and tube heat exchanger. The internal diameter of the shell was 0.20 m and the tube bundle contained thirty six tubes with an internal diameter of 0.02 m. Dilute ammonia solution was mixed with ammonia vapour before entering the absorber in order to enhance heat and mass transfer. The absorber was 1.8 m long.

The evaporator was enclosed in a 17.5 m^3 cold storage chamber which was fitted with an insulated door. The chamber was constructed from expanded multipanel 0.064 m thick polyurethane modules and covered by a thin sheet of galvanized steel.

The unit also included a separator for the two phase mixture produced by the generator and three accumulators to reduce the effect of flow fluctuations. A 0.56 kW model 2607AF rotary vane pump supplied by the Procon Pump Co., U.S.A. was used to pump the ammonia-water solution in the secondary circuit.

Temperatures were measured to an accuracy of $\pm$ 1°C using iron constantan thermocouples. The wires were soldered to the external surface of the pipes and covered with thermal insulation. Temperatures were read directly from a digital temperature indicator supplied by the Transmation Co., U.S.A. Pressures were measured to an accuracy of $\pm$ 1 psi using Bourdon gauges supplied by the Wika Co., W. Germany. The flow rates of the dilute ammonia solution and the liquid ammonia were measured using No. 5HCFB and No. 3HCFB Safeguard rotameters respectively. Separate cooling water lines were installed for the absorber, condenser and rectifier. The water was obtained from a nearby stream and the flow rates were measured by weighing amounts of water collected in a given time using a stop watch.

9.2.2 EXPERIMENTAL PROCEDURE

Initially the system was put under vacuum before charging with 49.3 kg of water, 35.7 kg of ammonia and 0.74 kg of sodium chromate as a corrosion inhibitor. Geothermal steam was fed to the generator and the pressure and temperature were controlled until the required steam temperature was

reached. When the pressure of the ammonia solution in the generator increased to the operating value, the solution pump and the evaporator fans were turned on. The various temperatures, pressures and flows were continuously recorded during each run. For a particular geothermal steam temperature, steady state conditions were achieved when the flow readings in the rotameters and the liquid levels in the accumulators were constant. Steam temperatures were varied from 90°C to a maximum temperature of 104°C. The cold storage temperature was maintained at -5°C or lower.

9.2.3 RESULTS AND DISCUSSION FOR INSTALLATION AT LOS AZUFRES

A number of experimental runs were carried out on the absorption cooler. On average, steady state conditions were reached in about thirty minutes. Temperatures, pressures and flow rates were all recorded. Manually operated expansion valves were used to maintain the refrigerant and dilute ammonia solution flow rates constant.

Figure 9.4 is a plot of the temperature levels and flow rates for a typical run. The operation of the unit was very stable. The absorber temperature was always higher than the condenser temperature as a result of the relatively high inlet temperature of the dilute ammonia solution and the small size of the recuperator used. The cold storage temperature decreased rapidly from ambient (17 to 24°C) to -5°C or lower.

Figure 9.5 is a plot of the temperature levels in the system against flow ratio for the various runs. The generator temperatures ranged from 81 to 95°C and the flow ratios from 10.6 to 25.4. The flow ratios were calculated from the actual flow rates measured by the rotameters. These were somewhat higher than the equilibrium values obtained using equations (6)

and (7). Generator pressures ranged from 9.0 to 10.0 bar and evaporator pressures from 2.4 to 2.8 bar. The pressure drops between the generator and condenser and the evaporator and absorber were 0.50 and 0.36 bar respectively. Absorber temperatures varied from 30.0 to 35.0°C and condensing temperatures from 22.0 to 25.7°C. The evaporator was maintained at a temperature between -10.3 and -15.1°C. The unit could operate at even lower generator temperatures with increasing flow ratios. This trend was previously observed by Kumar et al [9.3].

Fig. 9.6 is a plot of the generator and evaporator heat loads and the actual coefficient of performance $(COP)_A$ against generator temperature. Generator temperatures as low as 81°C can be used to give a reduced $(COP)_A$ value of 0.30 and a reduced cooling capacity Q_{EV} of 6 kW. As the generator temperature is increased the cooling capacity increases significantly. The actual coefficient of performance $(COP)_A$ also increases but at a lower rate.

A comparison of the Carnot coefficient of performance $(COP)_C$, the enthalpy based coefficient of performance $(COP)_{ECL}$ and the actual coefficient of performance $(COP)_A$ plotted against the generator temperature is shown in Figure 9.7. The comparison was made for a constant evaporator temperature $T_{EV} = -13°C$ and a constant condenser and absorber temperature $T_{CO} = T_{AB} = 25°C$. The generator temperatures T_{GE} were varied between 80 and 96°C. The effectiveness of the precooler was fixed at 0.40 and that of the recuperator at 0.80. The experimental values of the actual coefficient of performance $(COP)_A$ were between 50 to 70% of the calculated coefficients of performance based on enthalpy values.

9.3 EXPERIMENTAL FOR INSTALLATION AT CERRO PRIETO

9.3.1 EQUIPMENT

The prototype ammonia-water absorption refrigerator used in the experiments, which were carried out in the Cerro Prieto geothermal field, was a modified version of the unit already described. The layout of the unit is shown schematically in Figure 9.8. A more detailed diagram is shown in Figure 9.9 and Figure 9.10 shows the cooling water system used.

The following modifications were made to the original unit. A new separator/rectifier was installed. This consisted of a single vessel with a larger inside volume for vapour-liquid separation than the one originally used. This enabled the system to be operated over a wider range of strong solution flow rates M_{AB}. An extra heat exchanger using water from the cooling tower was installed between the recuperator and the mixer. This was used to provide further cooling for the weak ammonia solution before entering the absorber when the cooling water temperature was high. The original rotary vane solution pump suffered from cavitation problems. This was replaced by a piston pump. The modified unit shown in Figures 9.8 to 9.10 was fully instrumented. A data acquisition system was also installed to record flow rates, temperatures and pressures. The evaporator was located inside a strong chamber with a volume of 19.2 m^3. It was equipped with three low energy consumption fans to increase the air circulation rate and to make the temperature uniform. The storage chamber was constructed with 0.05 m thick polyethane and covered by a 0.06 m thick wood sheet.

The system was operated manually. It was controlled by fixing the flow rates of the solution and the refrigerant. This was accomplished by manipulating the liquid refrigerant expansion valve between the precooler and

the evaporator and the ammonia-water solution expansion valve between the recuperator and the mixer. Geothermal steam was fed to the generator from a small separator adjacent to the unit and the pressure and temperature were controlled until the required steam temperature was reached. When the pressure of the ammonia solution in the generator increased to the operating value, the solution pump and evaporator fans were turned on. Separate water lines from the cooling tower were installed to the absorber, condenser and rectifier.

9.3.2 RESULTS AND DISCUSSION FOR INSTALLATION AT CERRO PRIETO

The system was operated at fixed generator temperatures and the solution flow rate was varied for each of the generator temperatures selected. Steady state conditions were achieved when the flow readings in the rotameters and the liquid levels in the accumulators were constant. In order to check that the latter was true, the actual flow ratio $(FR)_A$ was compared with the thermodynamic flow ratio (FR) as given by equation (5). The experimental values which were more than 10% below the thermodynamic values were rejected. Figure 9.11 is a plot of the ratio of the thermodynamic flow ratio (FR) against the actual flow ratio $(FR)_A$ for all the data that met the preceeding criteria. All the data points above the 45° line are the experimental values where $(FR)_A < (FR)$ but that fell in the 10% error range.

Figure 9.12 is a plot of the actual coefficient of performance $(COP)_A$ against actual flow ratio $(FR)_A$. It can be seen that at lower values of the flow ratio the system operated at higher efficiencies and values of $(COP)_A$ of 0.50 were obtained.

Figure 9.13 is a plot of the evaporation cooling load Q_{EV} against the actual flow ratio $(FR)_A$ for four different values of the strong solution flow rate FS. It can be seen that values of Q_{EV} of 18 kW were obtained which were 1.8 times higher than the design value of 10 kW. As higher values of the solution rate FS were used, higher values of $(FR)_A$ were obtained and hence lower values of Q_{EV}.

Figure 9.14 is a plot of the efficiency of the generator against flow ratio. It can be seen that the efficiency of transferring heat from the geothermal steam to the ammonia-water solution in the generator varied from 0.65 to 0.90 with no evident effect of changes in the flow ratio. Such differences in efficiency show the necessity of controlling the steam flow rate and temperature in a better way in order to maintain the high efficiency values.

Figure 9.15 is a plot of the value of the actual coefficient of performance against the efficiency of the recuperator heat exchanger. It can be seen that as the efficiency of the heat exchanger increases, the coefficient of performance also increases. The values of N_{REC} varied between 0.4 and 0.7.

Figure 9.16 is a plot of the efficiency of the recuperator N_{REC} against values of the actual flow ratio $(FR)_A$. It can be seen that as the flow ratio increases the efficiency of the recuperator heat exchanger decreases.

Figure 9.17 is a plot of Carnot coefficient of performance $(COP)_{CCL}$, the enthalpy coefficient of performance $(COP)_{ECL}$ and the actual coefficient of performance $(COP)_A$ against generator temperature for a fixed value of solution flow rate of 6.3×10^{-5} m^3 s^{-1} (1.0 gpm). It can be seen that the

actual coefficient of performance $(COP)_A$ is always less than the enthalpy based coefficient of performance and both are much lower than the maximum limit given by the Carnot coefficient of performance $(COP)_{CCL}$. The values of $(COP)_A$ are within 60% of $(COP)_{ECL}$. All (COP) values increase as the generator temperature increases.

9.4 CONCLUSIONS

It has been shown that an ammonia-water absorption refrigeration system can be operated successfully using low enthalpy geothermal steam in Los Azufres and the Cerro Prieto geothermal field, with extreme hot weather conditions and high cooling water temperatures. The experimental data obtained, will be used to improve the design and operation of the system and will provide an excellent basis for the design of large scale heat driven absorption refrigeration systems which can operate on various kinds of low enthalpy heat available throughout the world.

The actual coefficient of performance $(COP)_A$ was higher at lower flow ratio values where a $(COP)_A$ value of 0.5 was obtained.

The heat load in the evaporator was increased to 1.8 times the design value of 10 kW. As higher values of the solution flow rate were used higher values of the flow ratio $(FR)_A$ were obtained and hence lower values of Q_{EV}.

The actual coefficient of performance $(COP)_A$ values obtained were within 60% of the enthalpy based coefficient of performance $(COP)_{ECL}$.

9.5 REFERENCES

9.1 J.C. Lague, personal communication.

9.2 H.O. Spauschus, Development in refrigeration: technical advances and opportunities for the 1990, Int. J. Refrig. 10 (5), 263-270 (1987).

9.3 P. Kumar, S. Devotta and F.A. Holland, Effect of flow ratio on the performance of an experimental absorption cooling system, Chem. Eng. Res. Des. 62 (3), 194-196 (1984).

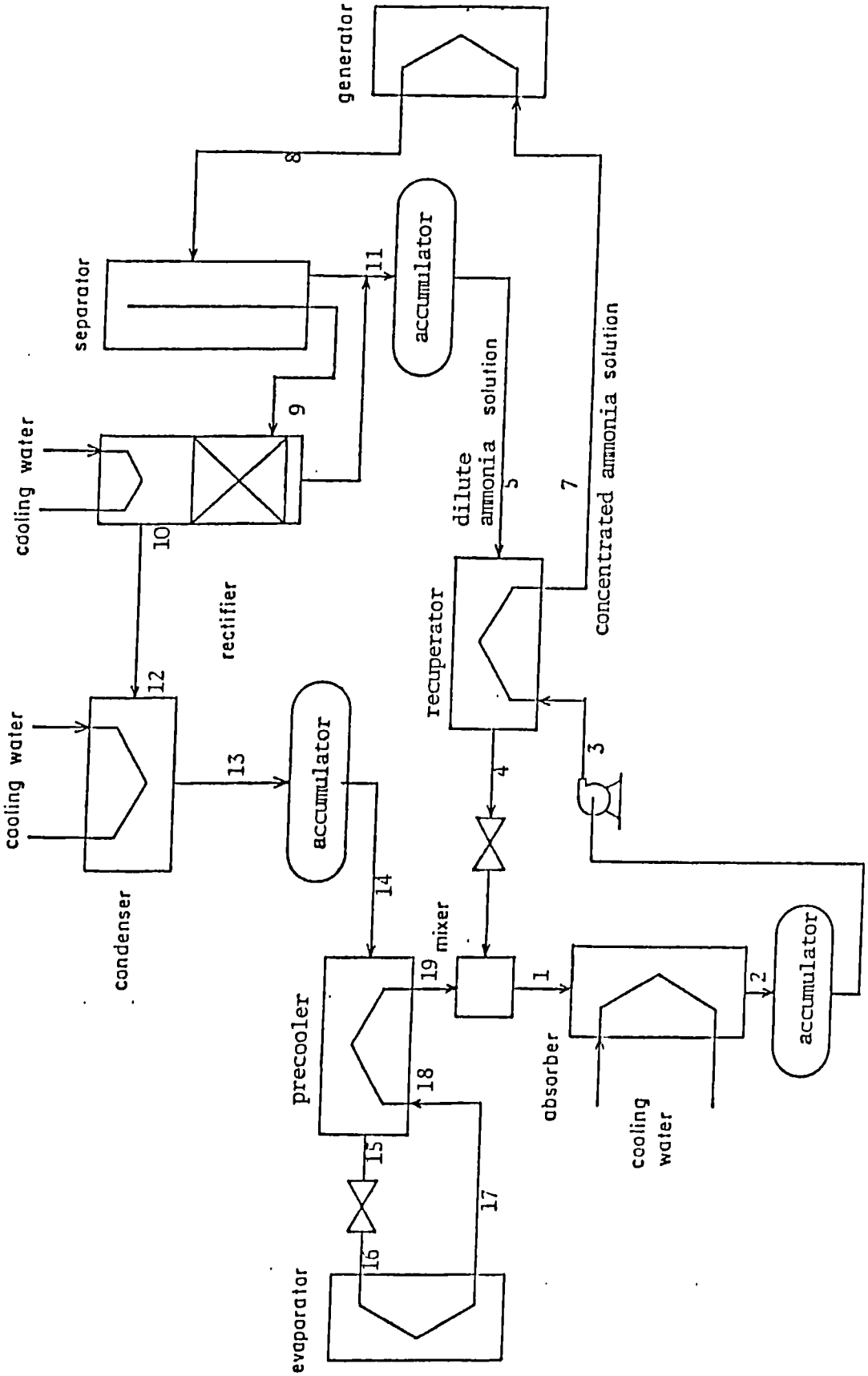

Fig. 9.1 Schematic diagram of experimental absorption cooler.

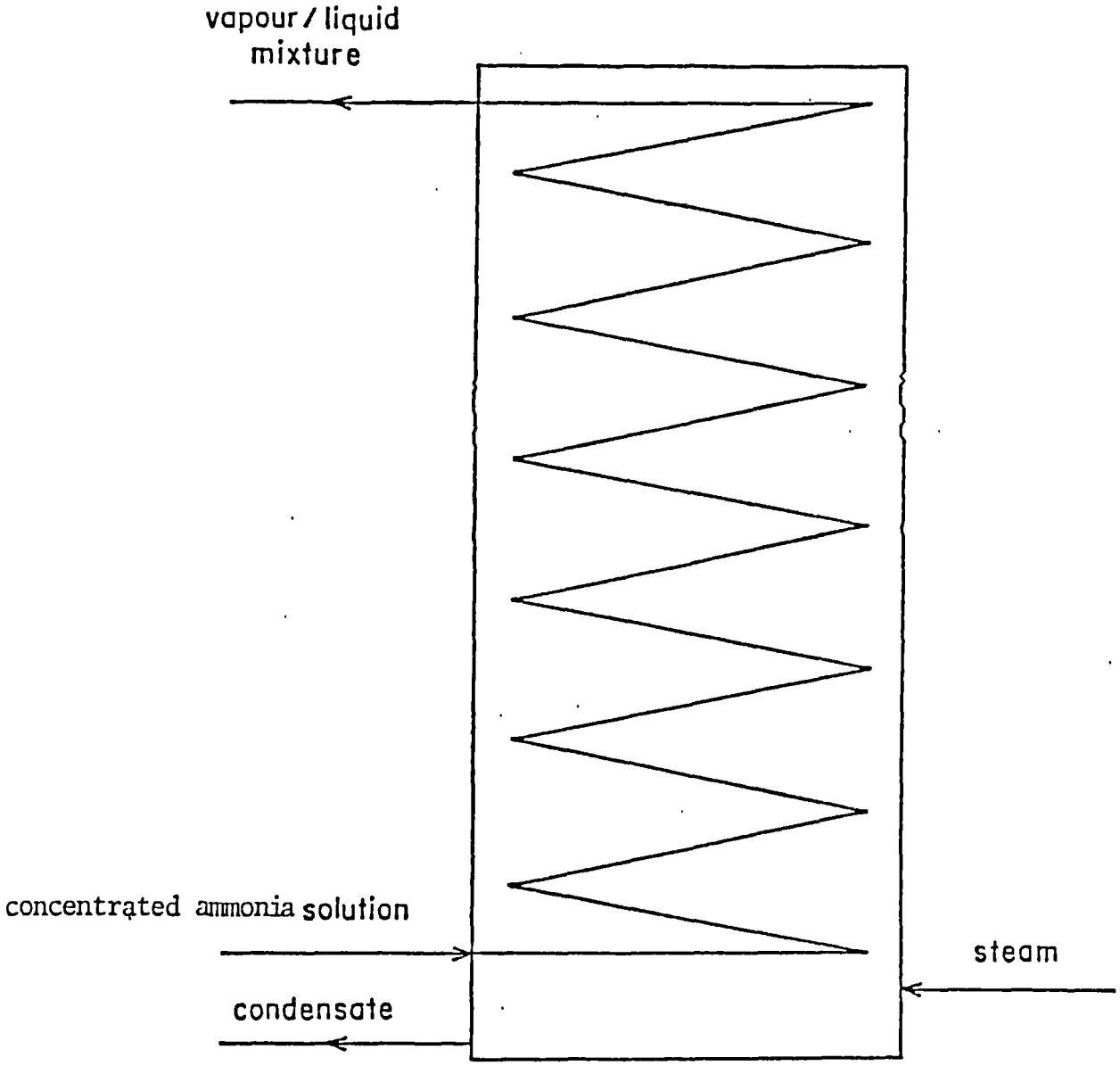

Fig. 9.2 Schematic diagram of generator

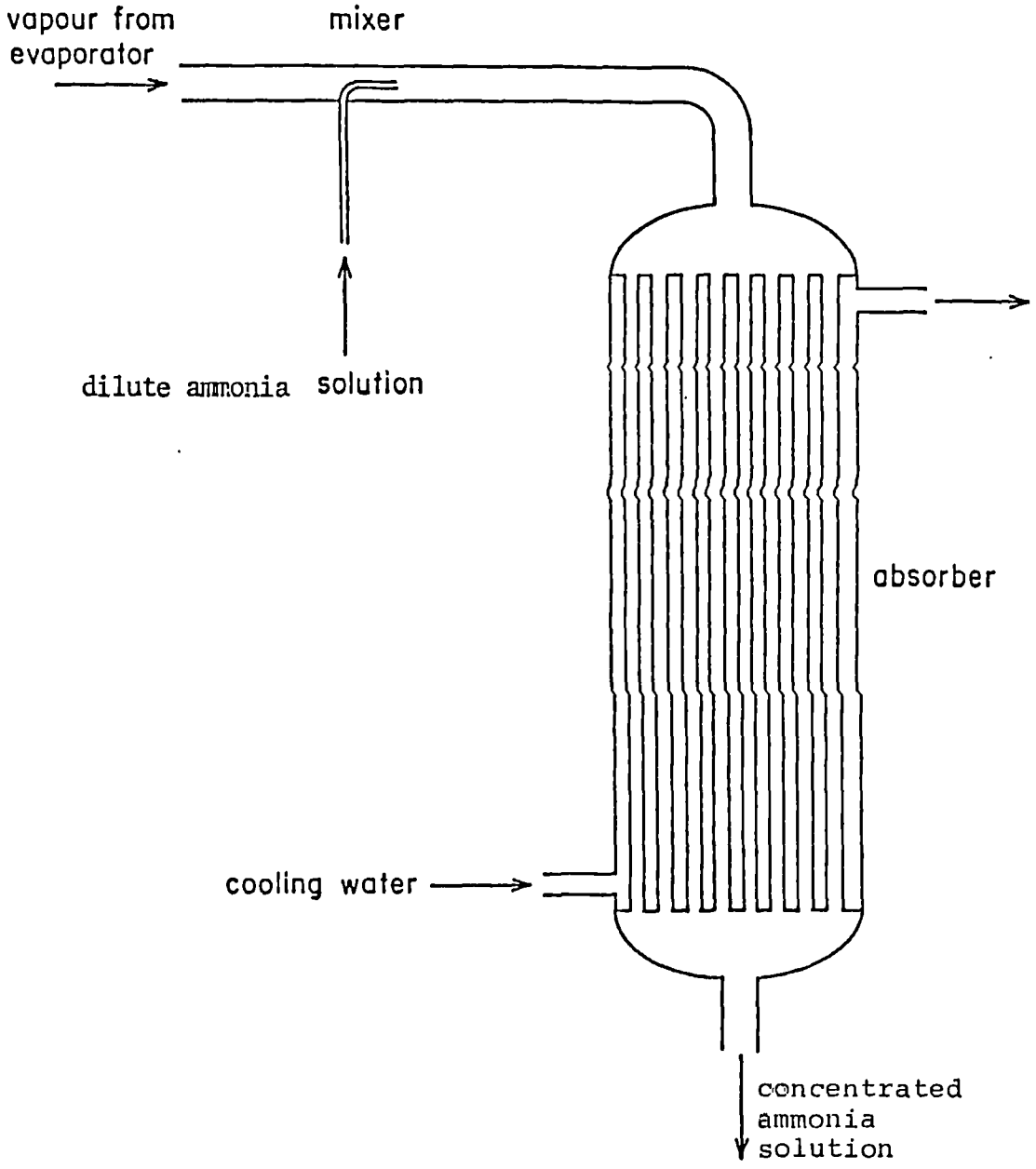

Fig. 9.3 Schematic diagram of absorber

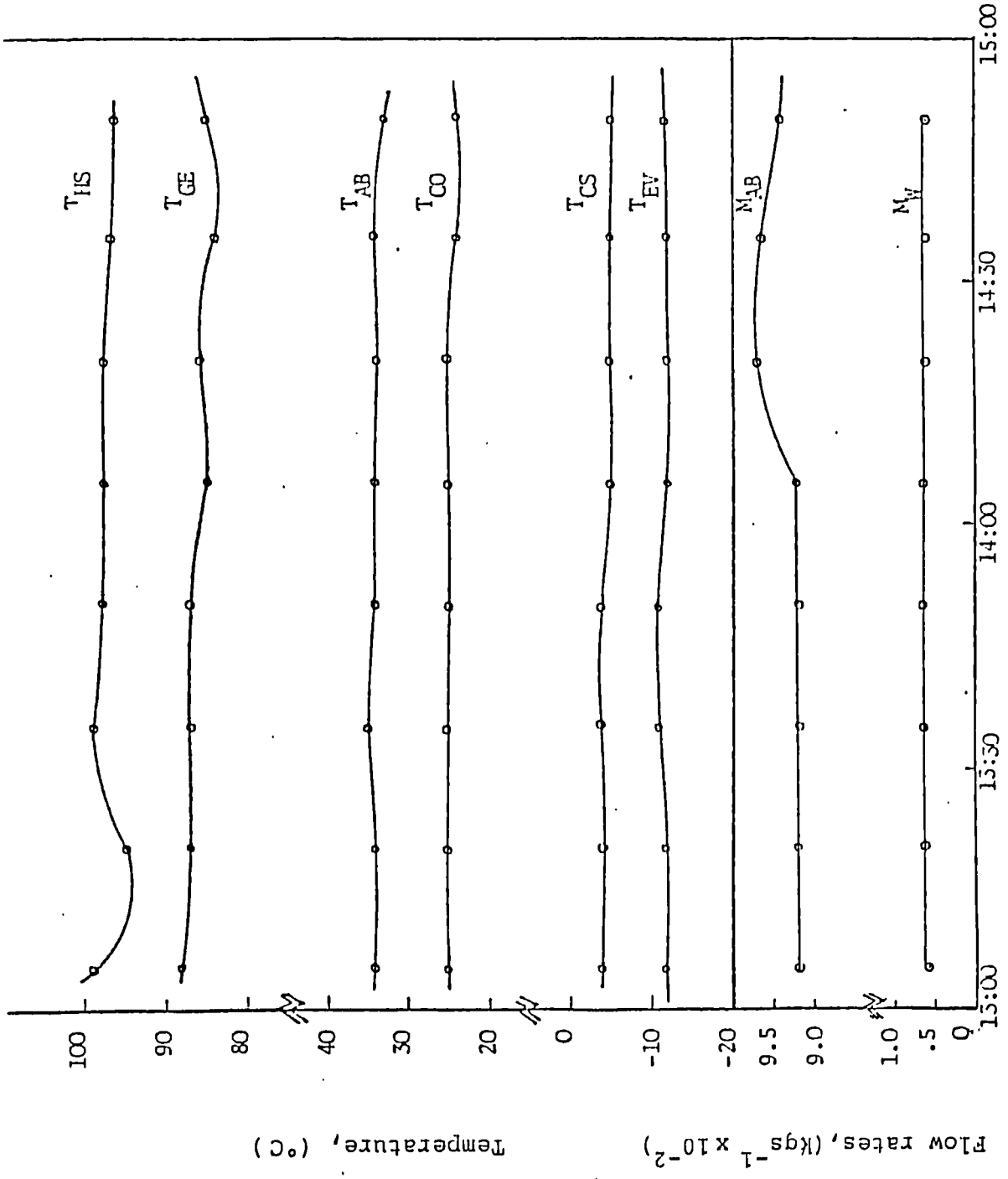

Fig. 9.4 Temperature and flow rates against time

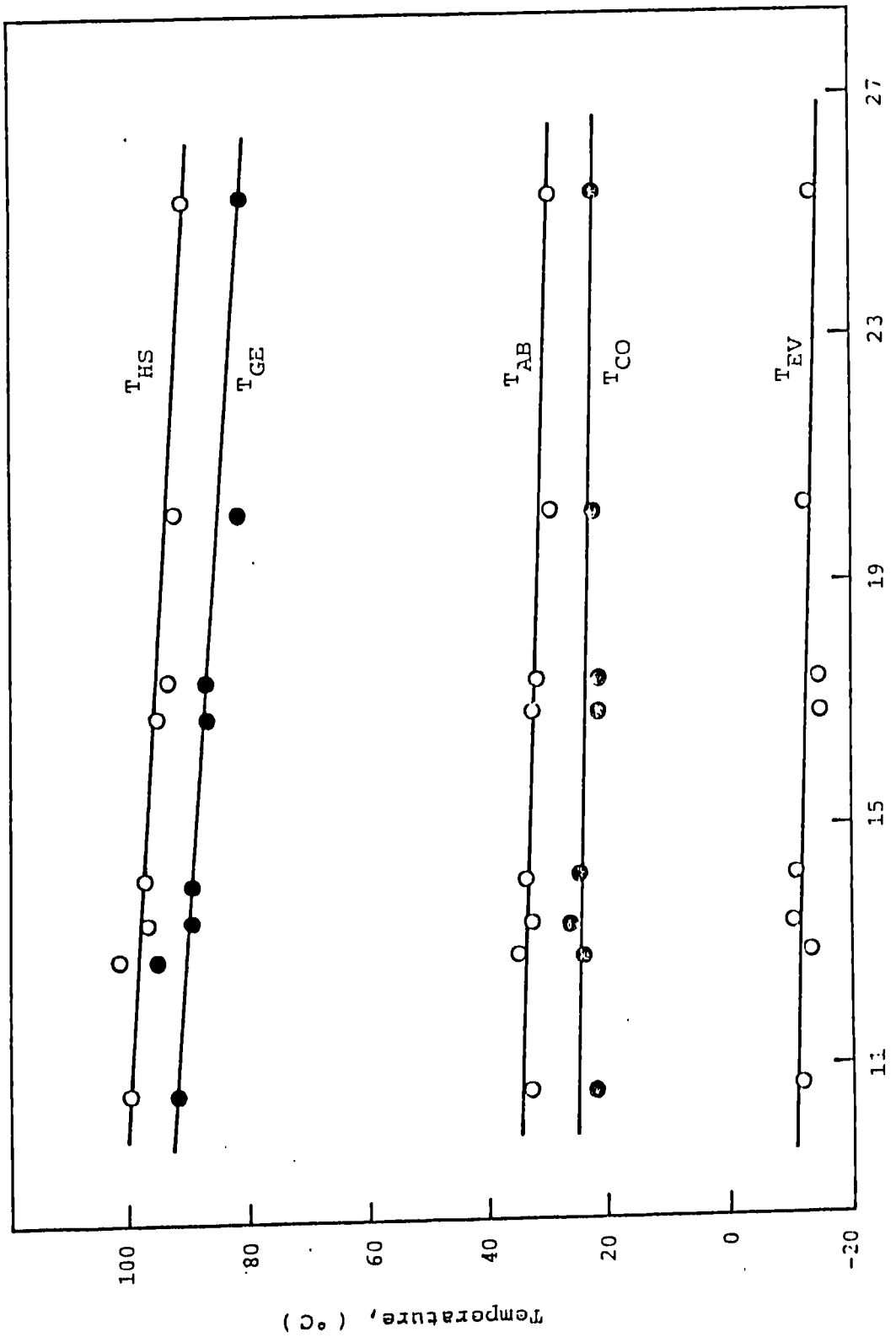

Fig. 9.5 Temperatures against flow ratio

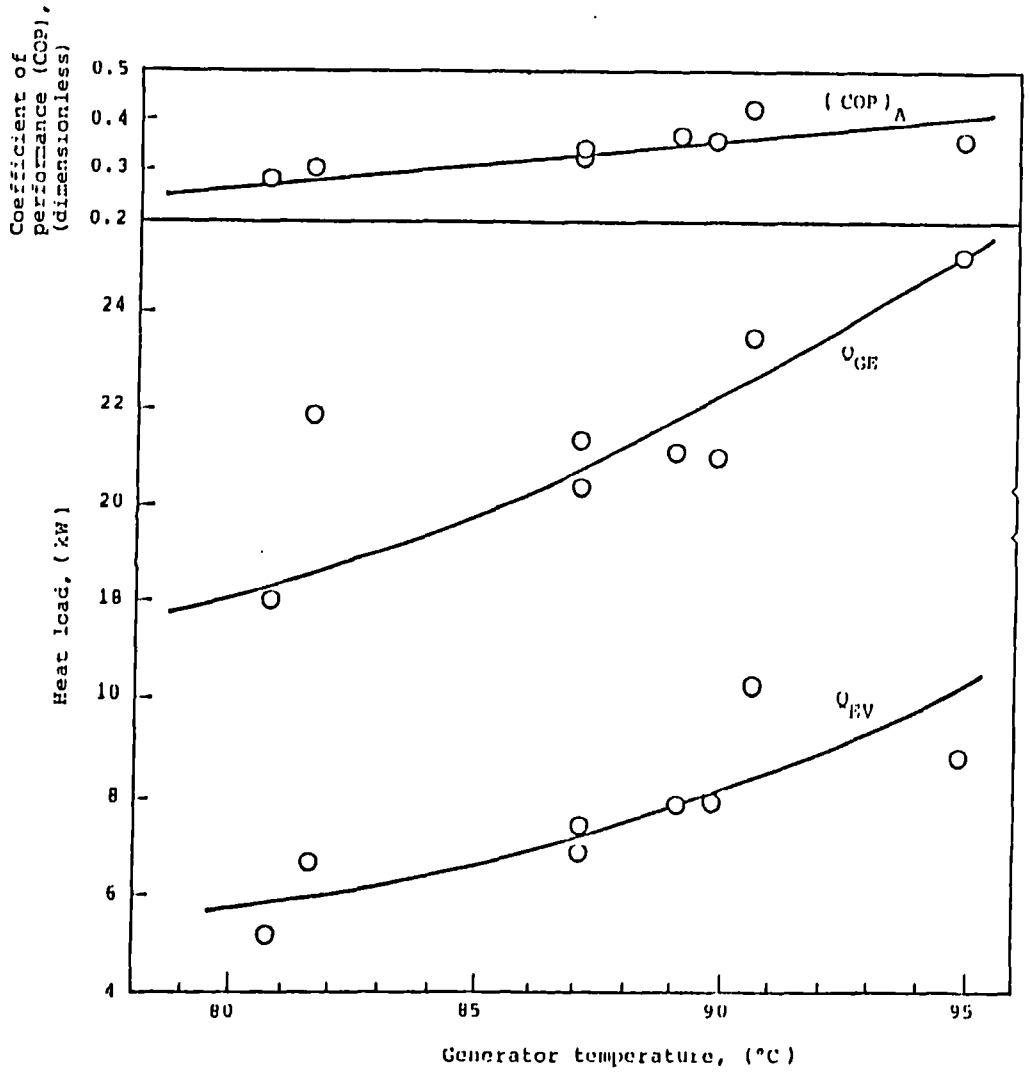

Fig. 9.6 Coefficient of performance and heat loads against generator temperature

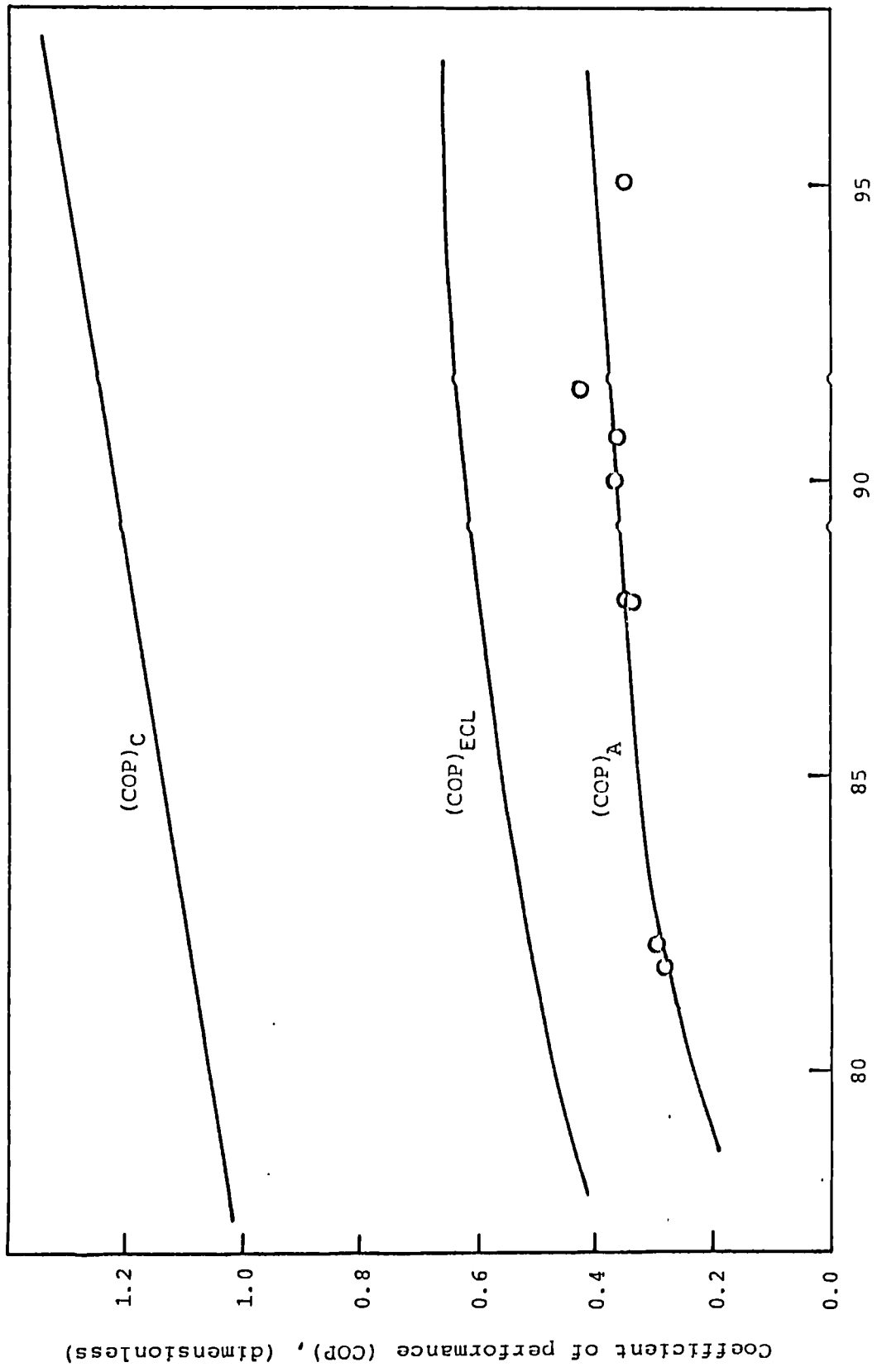

Fig. 9.7 Generator temperature against coeficient of perfo[illegible]nance

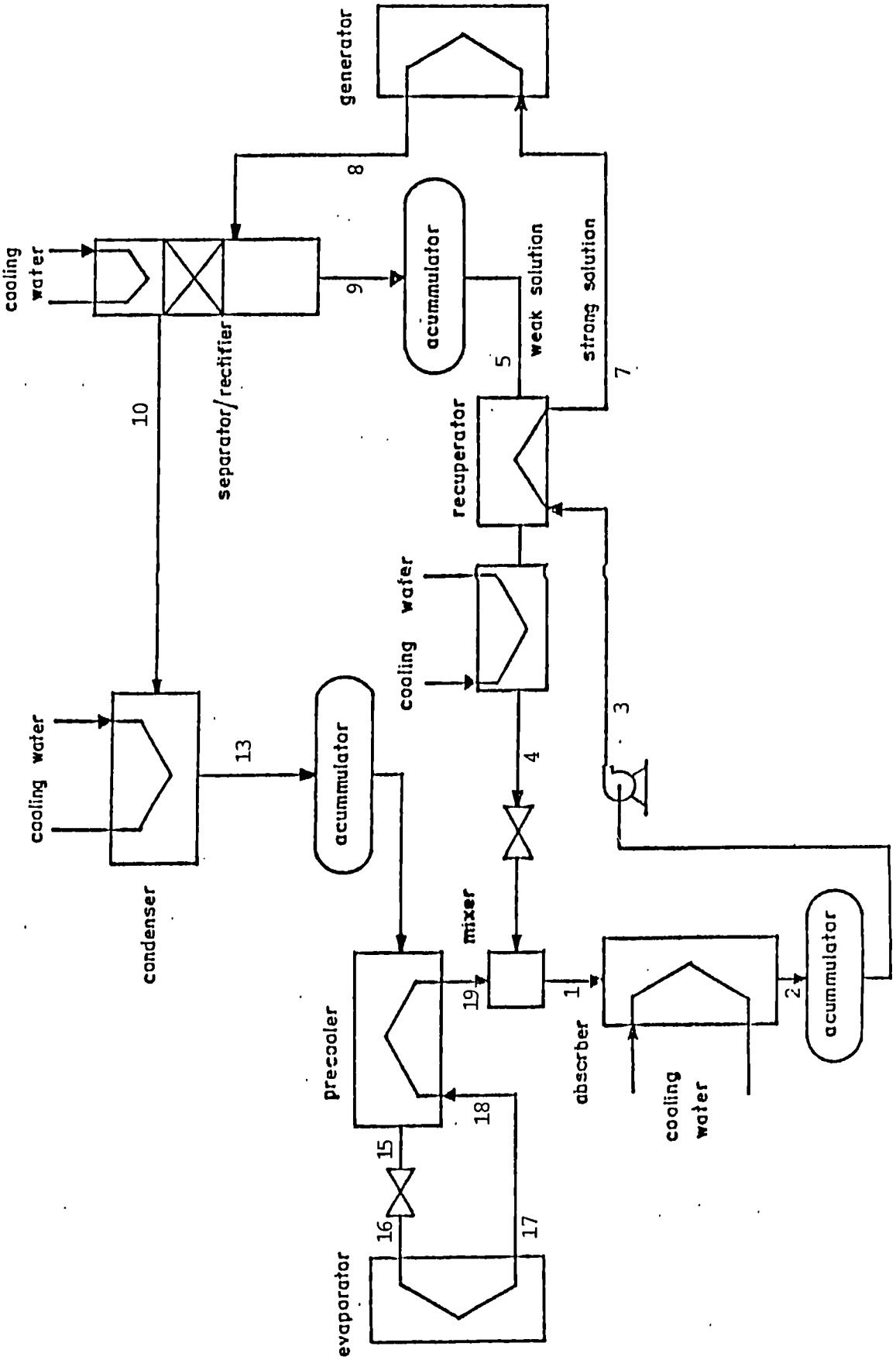

Fig. 9.8 Schematic diagram of the ammonia-water absorption refrigeration system

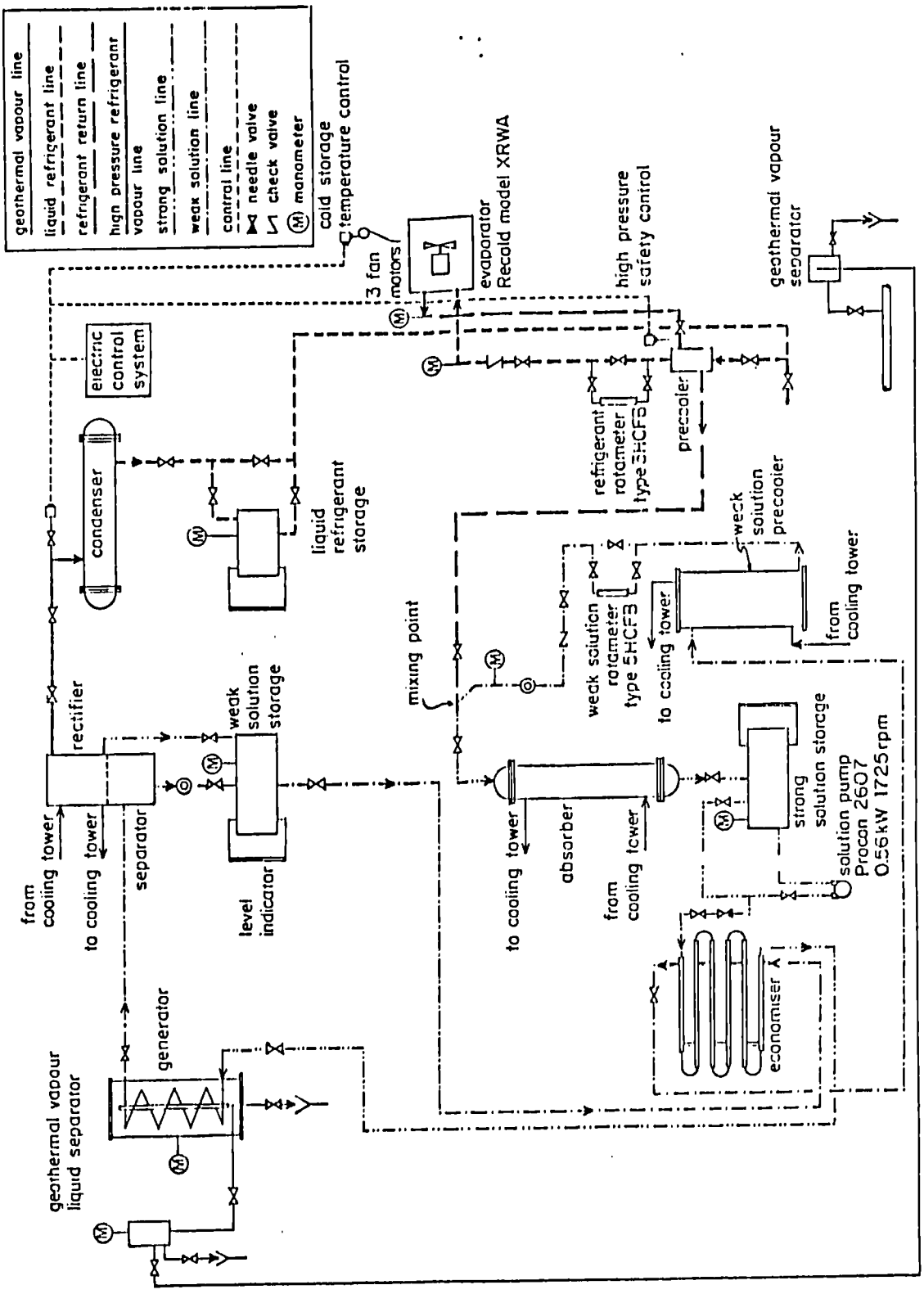

Fig. 9.9 Experimental ammonia-water absorption refrigeration system at the Cerro Prieto geothermal field

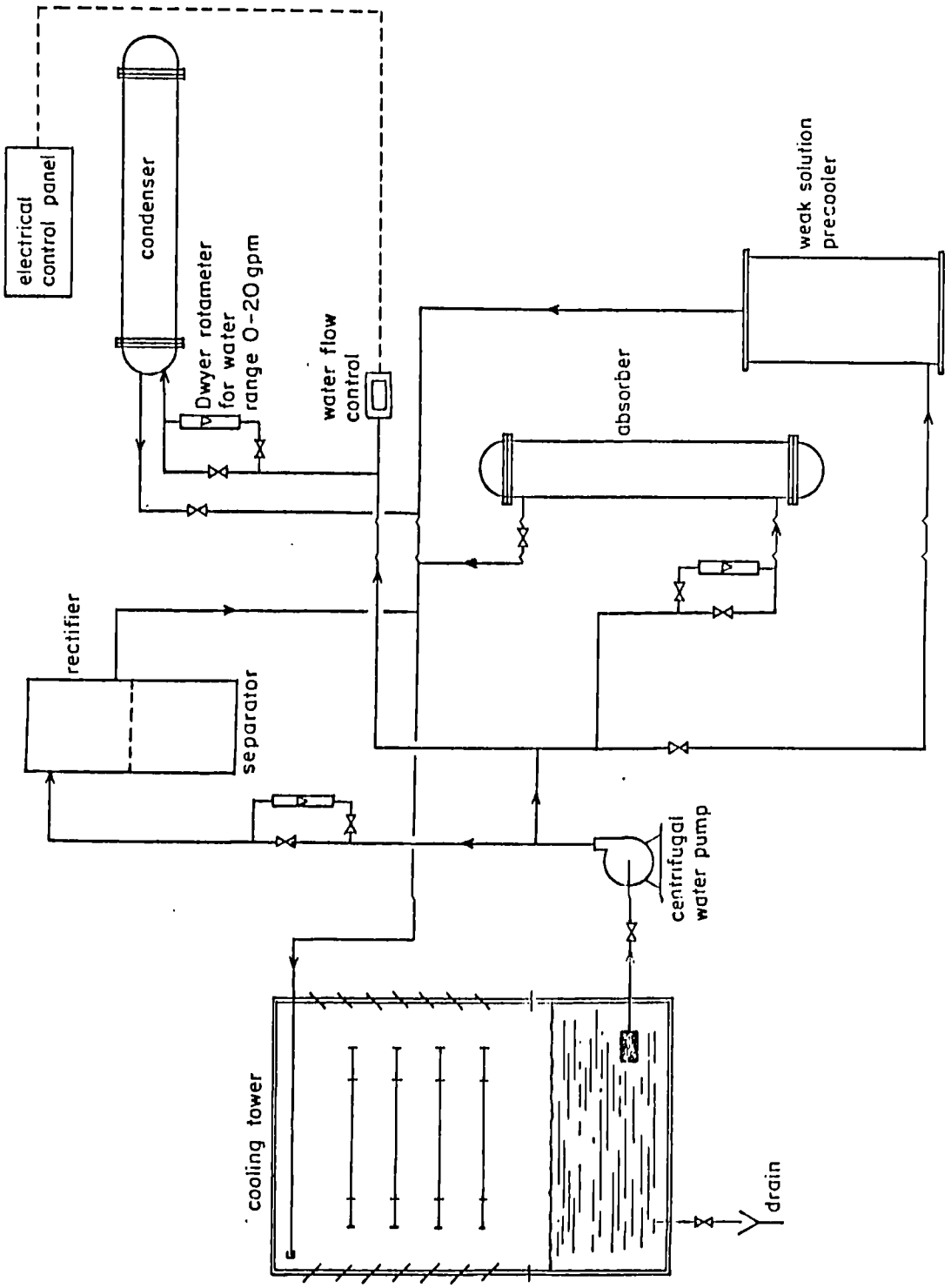

Fig. 9.10 Cooling water system

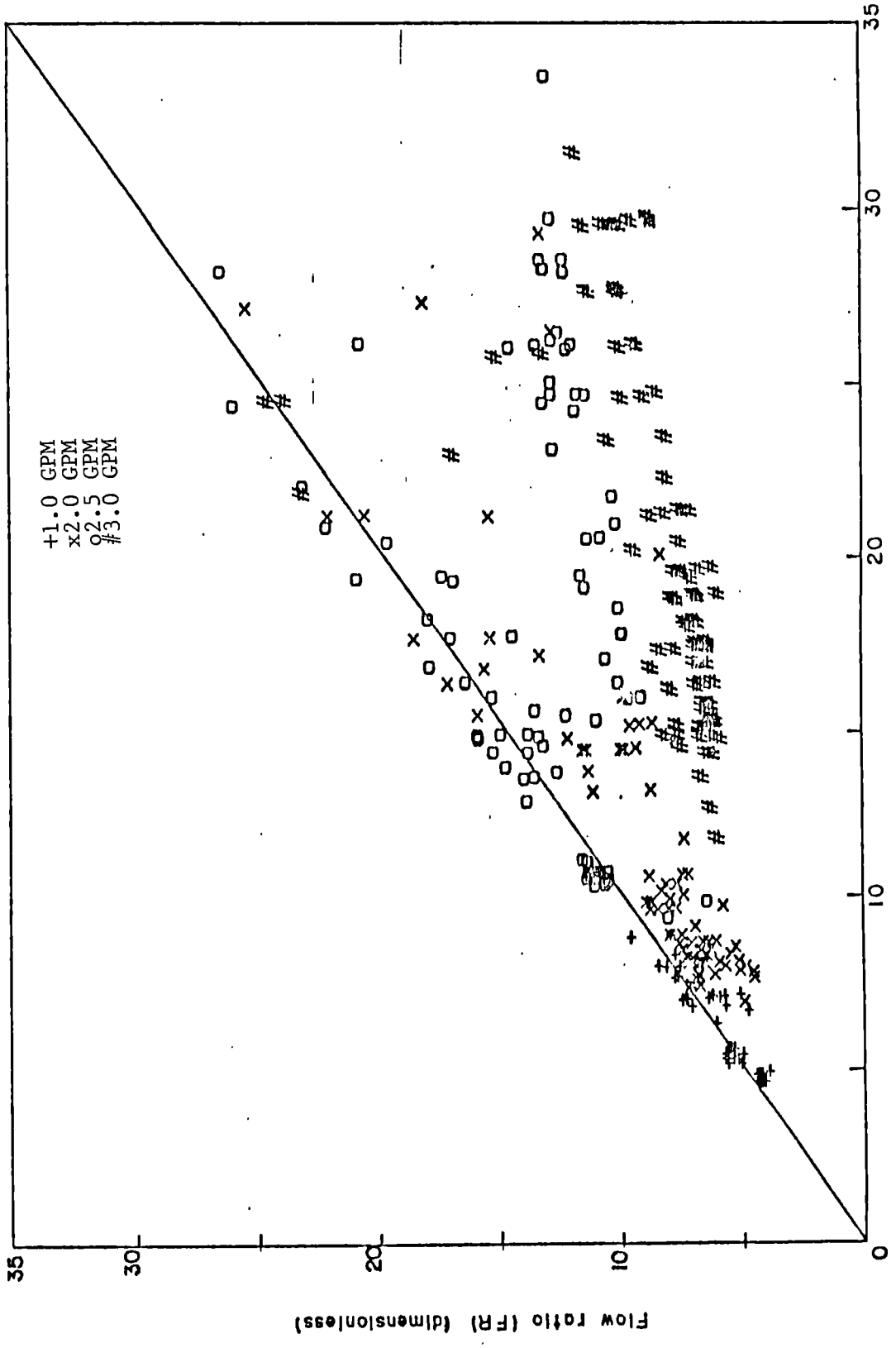

Fig. 9.11 Actual flow ratio vs flow ratio

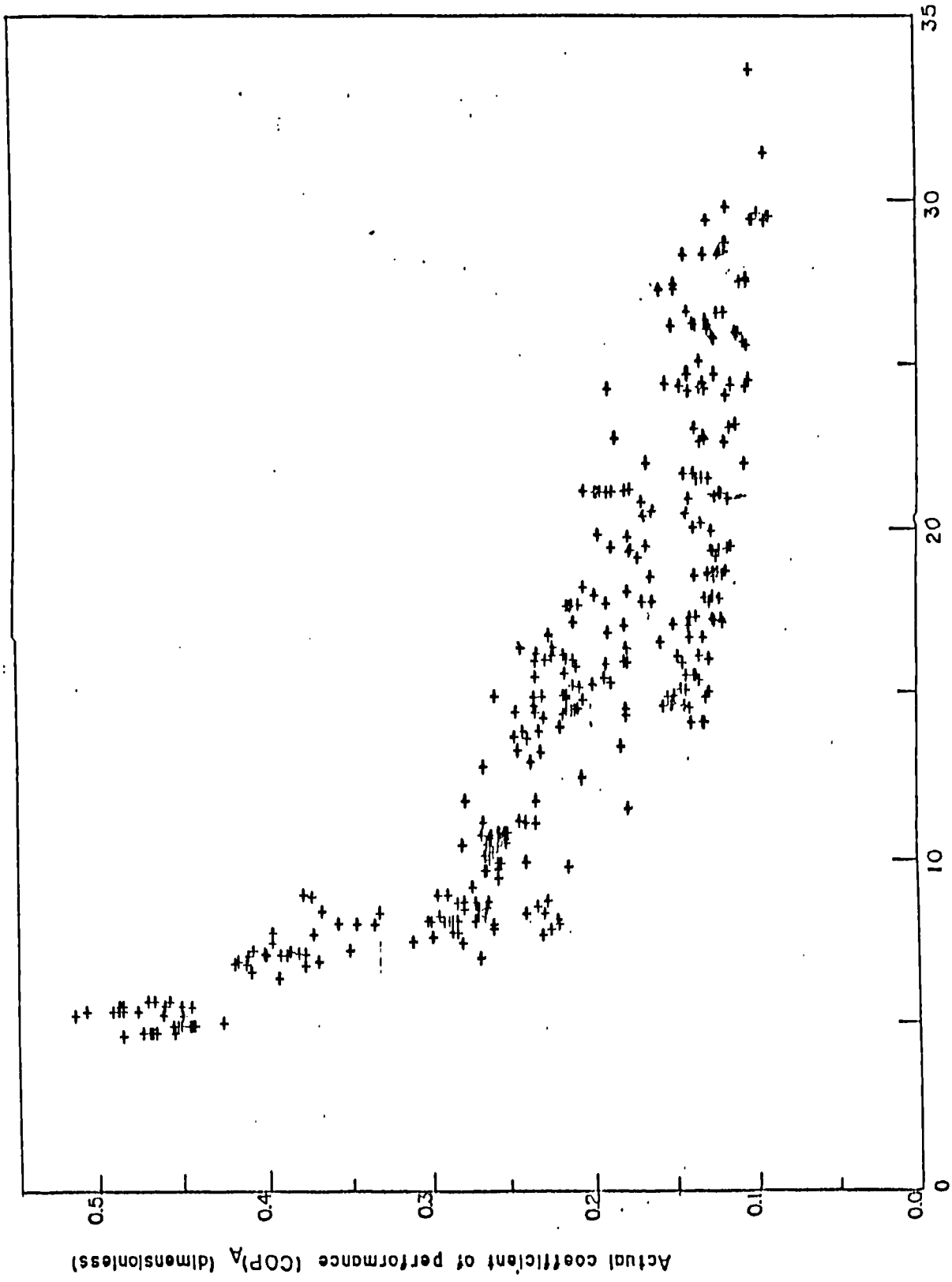

Fig. 9.12 Actual flow ratio vs actual coefficient of performance

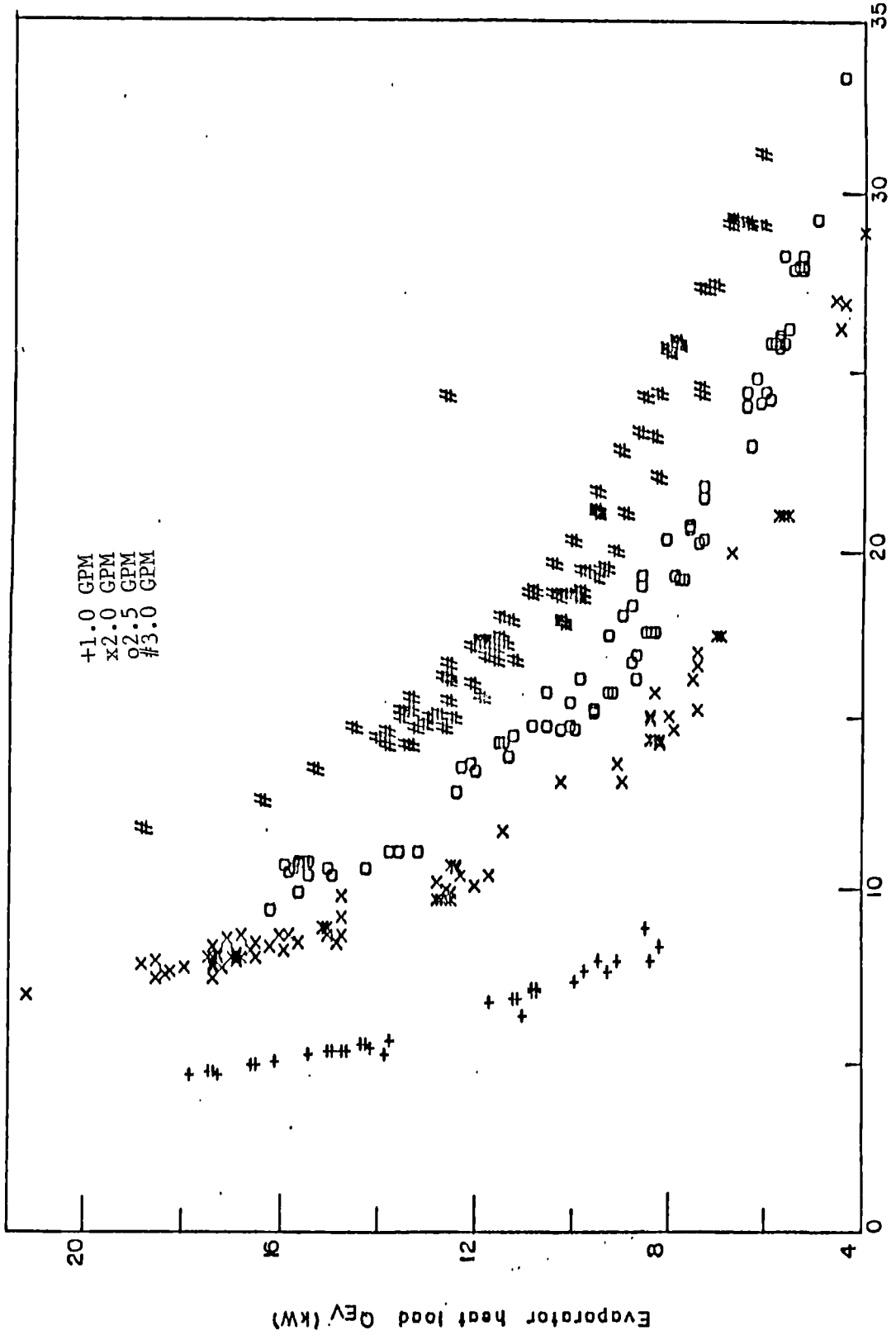

Fig. 9.13 Actual flow ratio vs evaporator heat load

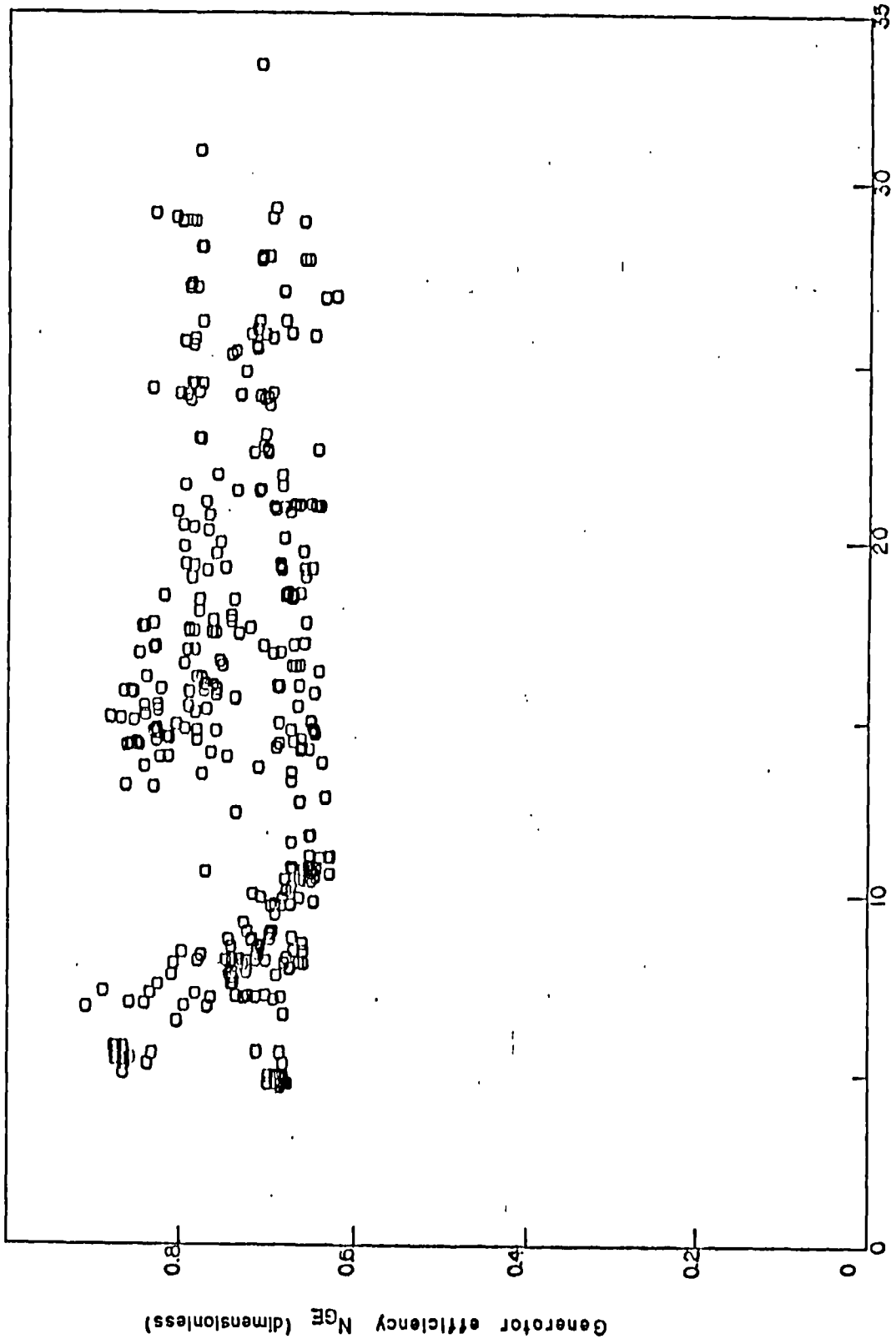

Fig. 9.14 Actual flow ratio vs generator efficiency

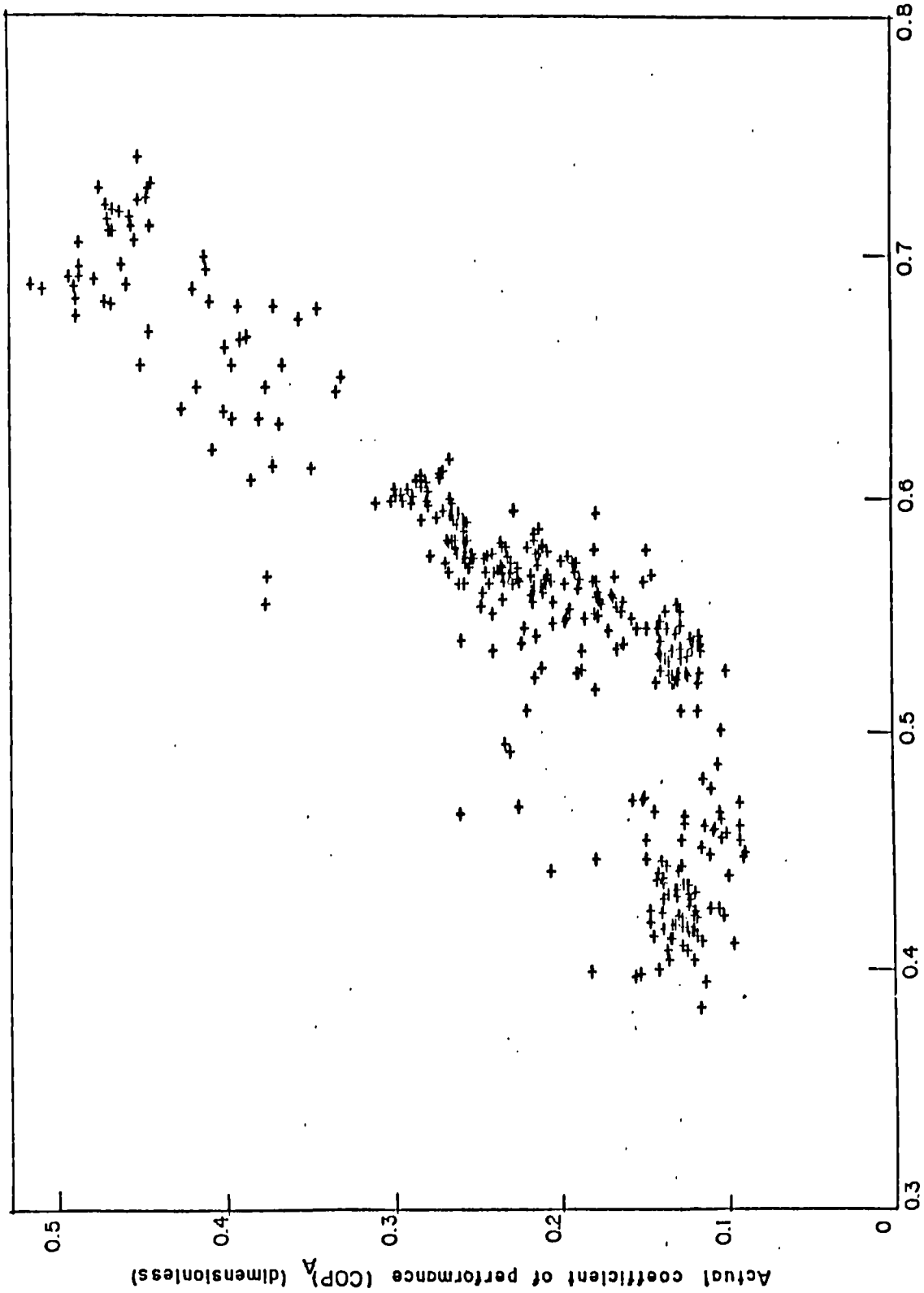

Fig. 9.15 Recuperator efficiency vs actual coefficient of performance

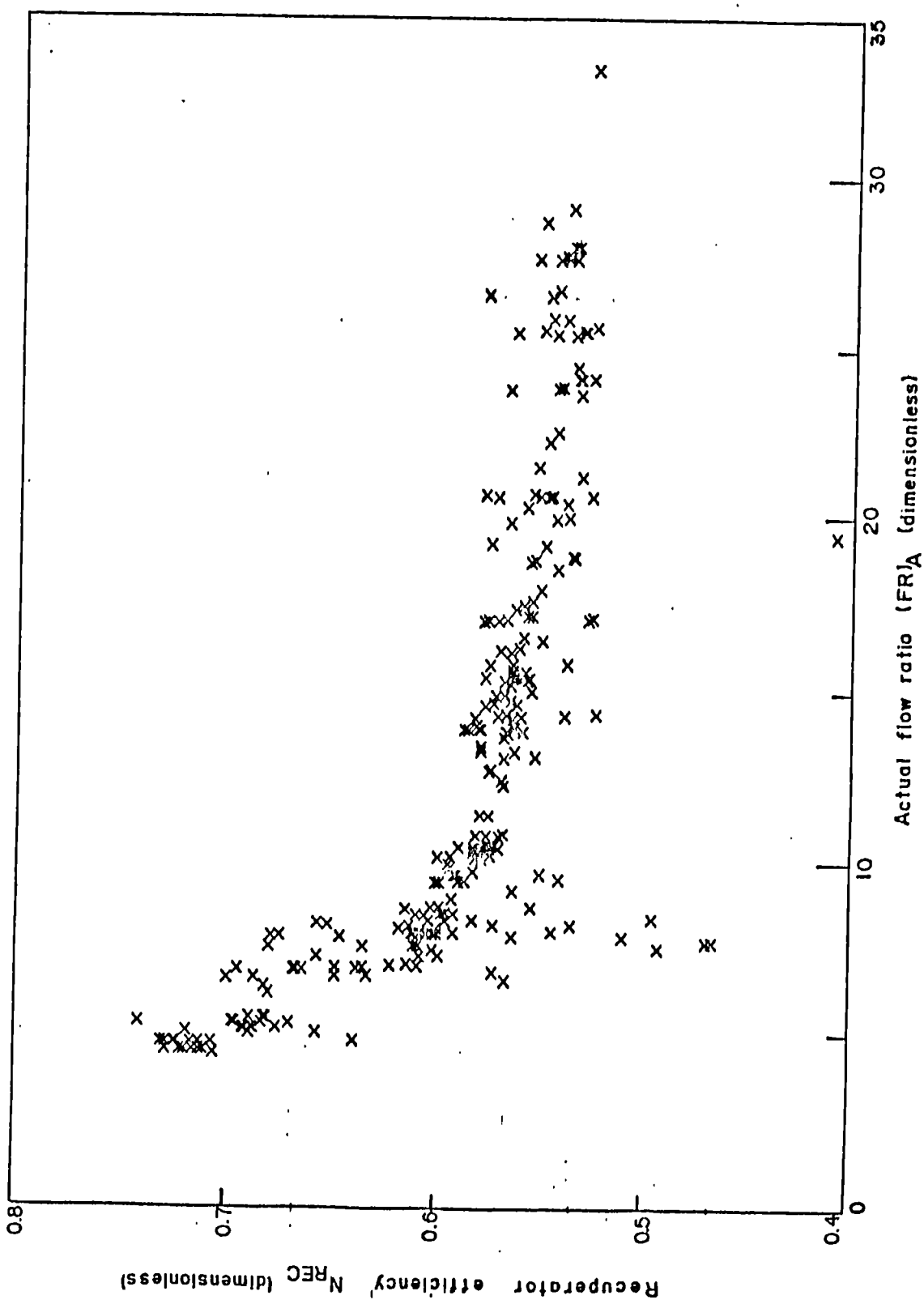

Fig. 9.16 Actual flow ratio vs recuperator efficiency

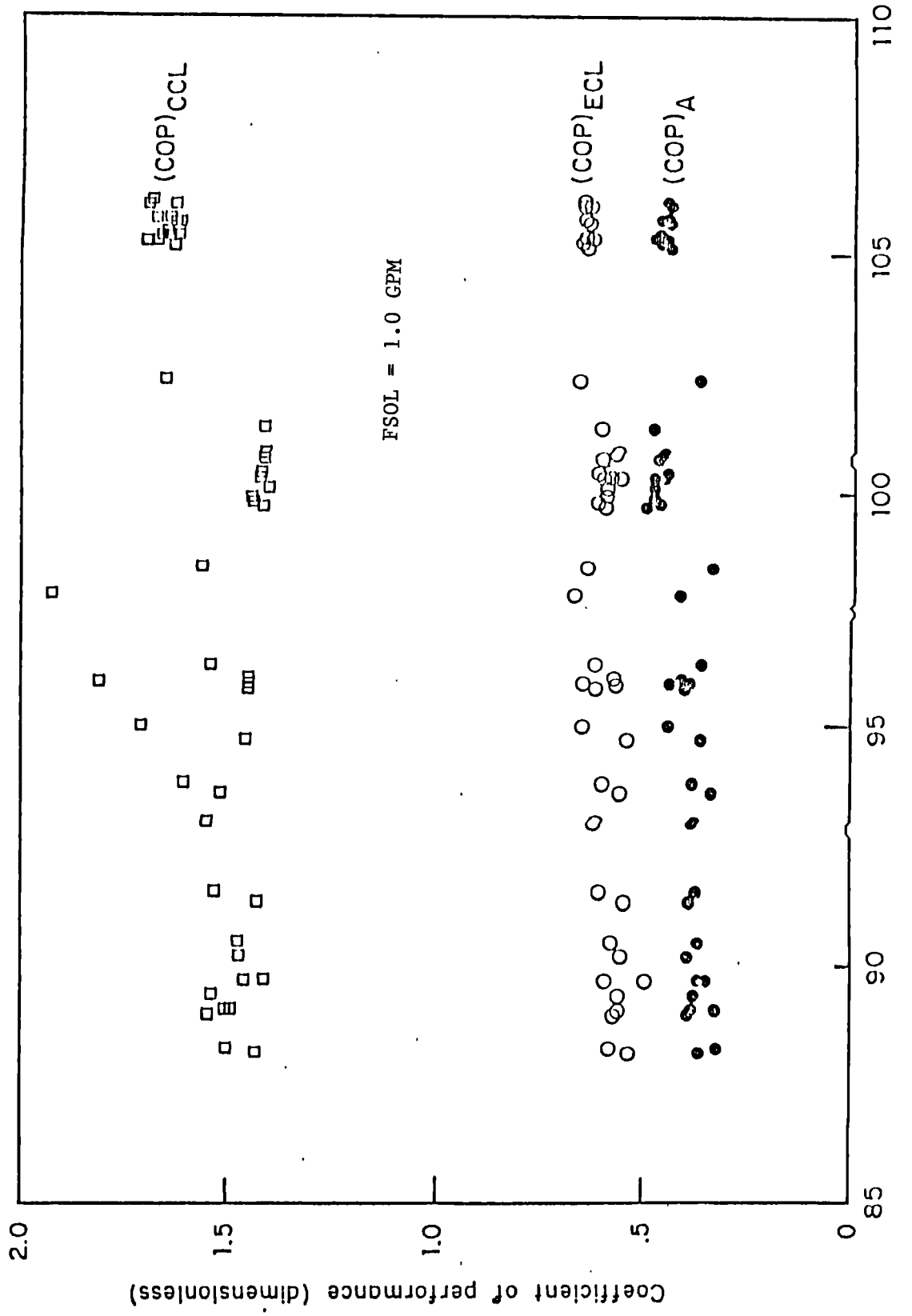

Fig. 9.17 Generator temperature vs. coefficient of performance

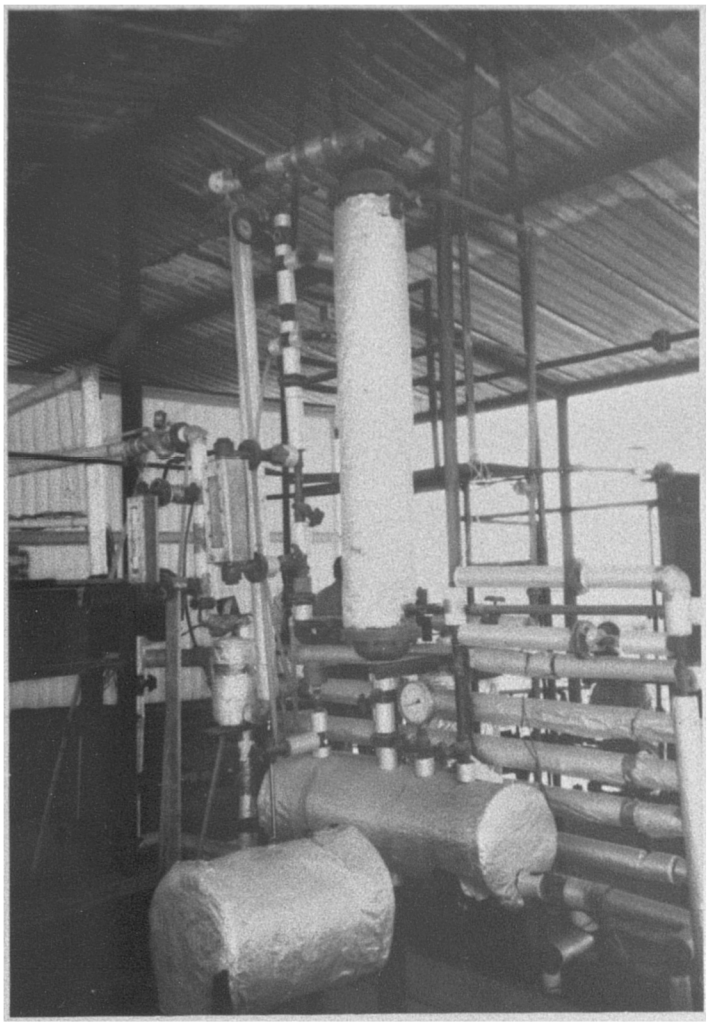

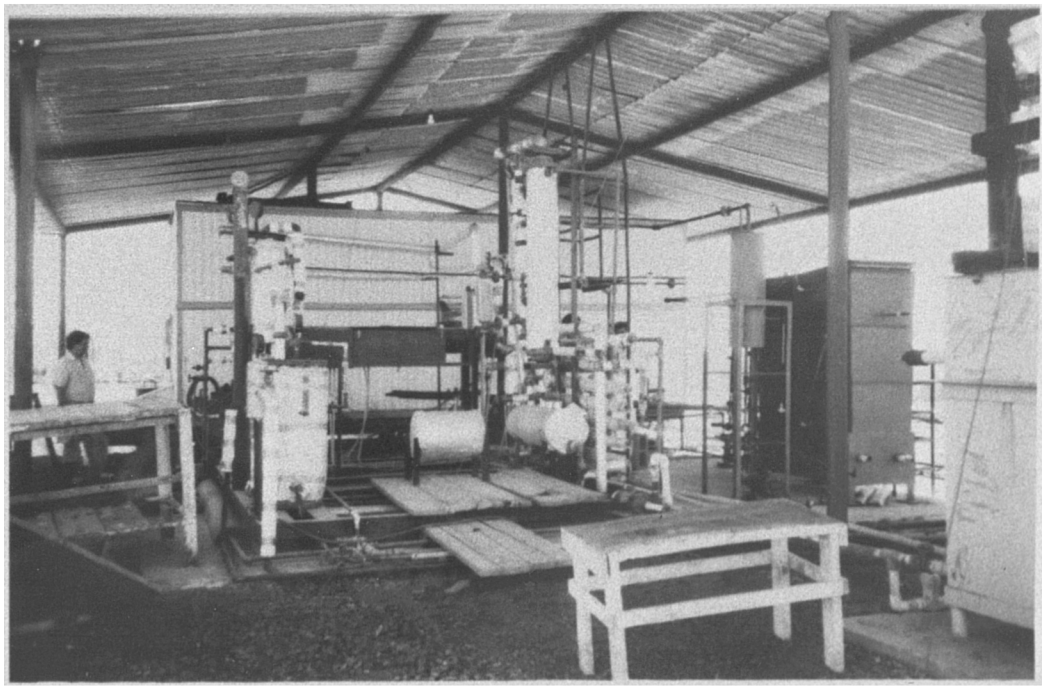

Experimental ammonia-water absorption refrigeration system, at the Cerro Prieto, geothermal field.

CHAPTER 10

CONCLUSIONS AND RECOMMENDATIONS

10.1 CONCLUSIONS

Thermodynamic design data have been theoretically derived for coolers, heat pumps and heat transformers operating on ammonia-water and ammonia-lithium nitrate for different conditions. The data provide the process design engineer with the operating efficiencies of possible combinations of conditions for each system and the mode of operation.

A computer model of the steady state thermodynamics of a heat driven absorption cooler operating on ammonia-water and ammonia-lithium nitrate has been carried out. The model results showed that the ammonia-lithium nitrate system has a higher enthalpy based coefficient of performance than ammonia-water at temperatures above 90°C at the fixed operating conditions considered.

The model was based on steady state operation and was used to assess the effect of operating temperatures and heat exchanger effectiveness on the coefficient of performance for cooling and the heat transfer rates within the system.

A glass absorption cooler was utilized in order to do experimental work in the following areas:

A) A study was carried out in order to evaluate the performance of an adiabatic absorber in a lithium bromide-water absorption cooler.

The performance of the absorber was quantified at various cooling loads, flow rates and solution temperatures. It was shown that the amount of solution circulated in the absorber is the critical parameter in the design of an adiabatic absorber.

B) An alternative to the use of the traditional lithium bromide-water system for absorption cooling was investigated. A study was completed on the use of salt mixtures of lithium bromide-zinc bromide and lithium bromide-lithium iodide as absorbents for water.

For the ternary system using zinc bromide the experimental data showed a good coefficient of performance $(COP)_A$. The flow ratio values were higher than in a lithium bromide system due to the higher level of concentrations employed. The system has a significantly higher viscosity than the lithium bromide solutions. This resulted in a reduced $(COP)_A$ and cooling capacity Q_{EV} at low flow ratio values.

For the lithium iodide ternary system the coefficient of performance values obtained were comparable with values for lithium bromide-water systems. The advantage of higher solubility should be analyzed in more detail in order to fix the limiting values of the generator temperature T_{GE}. At present it seems that there is a slight advantage using the ternary system.

An ammonia-water absorption cooling system using a falling film generator was designed and constructed using hot oil as a heat source at temperatures compatible with non-focussing solar collectors.

A series of experiments was carried out in order to study the effect of changes in generator temperature, at different strong solution flow rates with constant condenser, absorber and evaporator temperatures. It was demonstrated that the performance of an absorption system with a falling film generator is very sensitive to variations of the solution flow rate. When the system was operated at the design flow rate, less heat was required in the generator per unit mass of refrigerant generated than when higher flow rates were used.

An ammonia-water absorption cooling system was designed and constructed to operate on low enthalpy geothermal heat at the Cerro Prieto geothermal field. The system was operated with low pressure steam and cooling water from a small cooling tower at high ambient temperatures. Initially the ammonia-water absorption cooler was successfully operated in the geothermal field of Los Azufres which has a cold to mild climate. It was subsequently modified in order to operate in Cerro Prieto's extreme conditions.

The objective of the experimental work, which was done with the prototype ammonia-water absorption cooler at Cerro Prieto, was to operate with evaporator temperatures in the region of 0°C or lower at the existing high ambient temperatures. This objective has been achieved.

The experimental data obtained from the prototype heat driven absorption coolers will provide a basis for the design of large scale commercial systems.

10.2 RECOMMENDATIONS

Further studies on the operation of adiabatic absorbers and ways to increase its efficiency should be carried out due to their simplicity of construction and maintenance.

The large temperature increase at the adiabatic absorber inlet could be used in advantage in an absorption heat pump system designed for cooling and simultaneous heating or in a heat transformer.

Salt mixtures are a viable solution to overcome the problem of crystallization in absorption systems. Higher solubilities and lower vapour pressures than lithium bromide are achieved with ternary systems. Further studies on heat and mass transfer rates, transport properties and corrosiveness should be carried out.

Absorption cooling systems operating on solar energy from non-focussing solar collectors for food conservation would appear to have a great potential in the developing countries. In order to be economically feasible the actual coefficient of performance of the absorption system should be increased.

At present, it seems that ammonia-water would be selected as the working fluid for below freezing applications. The use of other non-volatile absorbents such as lithium nitrate should be evaluated experimentally.

Geothermal energy is an excellent and abundant resource in Mexico. The potential for the large scale use of absorption cooling systems for cold

storage should be analyzed extensivelly. The experimental evaluation of new heat exchange technologies such as fluidized bed heat exchangers in order to minimize scaling of the generator heat transfer surface should be carried out.

Concern on environmental aspects in the use of energy such as the green house effect, the depletion of the ozone layer by the CFC refrigerants together with the need in energy conservation measures are motivating an increased interest in absorption heat pump technology and in traditional fluids such as ammonia.

Nevertheless, thermodynamic data on environmentally safe new working fluid mixtures is necessary in order to evaluate their potential use in advanced heat pump systems.

The use of low grade heat as a heat source limits the use of absorption systems to one stage systems. Two stage systems could be used when resources above 130°C are available.

Research in systems capable of cooling and simultaneous heating would enhance the industrial use of absorption heat pumps. Double effect coolers combining the best working fluids for the particular range of each effect should be investigated.

Research in double effect heat transformers, compression-absorption and resorption heat pumps should be carried out as systems for the future as energy saving and environmentally safe large scale industrial systems.

T_{EV}	T_{AB}	T_{CO}	T_{GE}	X_{AB}	X_{GE}	(FR)	$(COP)_{CCL}$	$(COP)_{ECL}$
-30	30	30	110	31.18	29.94	56.50	0.85	0.080
-30	30	30	160	31.18	9.26	4.14	1.22	0.240
-30	30	30	180	31.18	2.33	3.39	1.34	0.230
-30	30	40	120	31.18	30.00	59.32	0.80	0.039
-30	30	40	170	31.18	10.50	4.33	1.10	0.217
-30	30	40	190	31.18	3.51	3.49	1.20	0.214
-30	30	50	140	31.18	26.80	16.74	0.81	0.096
-30	30	50	190	31.18	8.20	4.00	1.05	0.197
-30	30	50	200	31.18	4.67	3.60	1.09	0.197
-30	40	30	120	25.76	24.63	66.70	0.82	0.041
-30	40	30	170	25.76	5.80	4.72	1.19	0.216
-30	40	30	180	25.76	2.33	4.17	1.25	0.214
-30	40	40	140	25.76	21.79	19.70	0.84	0.095
-30	40	40	190	25.76	3.51	4.33	1.13	0.196
-30	40	50	150	25.76	22.90	26.96	0.79	0.063
-30	40	50	200	25.76	4.67	4.52	1.03	0.179
-30	50	30	140	20.58	16.54	20.64	0.88	0.105
-30	50	30	180	20.58	2.33	5.35	1.16	0.196
-30	50	40	150	20.58	17,88	30.41	0.82	0.066
-30	50	40	190	20.58	3.51	5.65	1.05	0.176
-30	50	50	160	20.58	19.19	58.14	0.77	0.032

TABLE A1.1 Derived thermodynamic design data for absorption systems operating on ammonia-water for cooling.

...continued

T_{EV}	T_{AB}	T_{CO}	T_{GE}	X_{AB}	X_{GE}	(FR)	$(COP)_{CCL}$	$(COP)_{ECL}$
-30	50	50	200	20.58	4.67	6.00	0.96	0.157
-25	30	30	100	34.68	33.52	57.31	0.85	0.054
-25	30	30	150	34.68	12.81	3.99	1.28	0.267
-25	30	30	180	34.68	2.33	3.02	1.49	0.246
-25	30	40	110	34.68	34.52	409.25	0.80	0.006
-25	30	40	160	34.68	14.11	4.18	1.15	0.240
-25	30	50	130	34.68	31.00	18.78	0.82	0.096
-25	30	50	180	34.68	11.75	3.85	1.09	0.217
-25	30	50	200	34.68	4.67	3.18	1.19	0.213
-25	40	30	110	29.20	28.94	273.31	0.82	0.012
-25	40	30	160	29.20	9.27	4.55	1.25	0.240
-25	40	30	180	29.20	2.33	3.63	1.39	0.232
-25	40	40	130	29.20	25.76	21.58	0.85	0.097
-25	40	40	180	29.20	7.00	4.19	1.18	0.216
-25	40	40	190	29.20	3.51	3.76	1.24	0.214
-25	40	50	140	29.20	26.80	30.50	0.80	0.062
-25	40	50	200	29.20	4.67	3.89	1.12	0.197
-25	50	30	130	23.97	20.59	23.47	0.90	0.105
-25	50	30	180	23.97	2.33	4.51	1.29	0.216
-25	50	40	140	23.97	21.79	35.88	0.83	0.063
-25	50	40	190	23.97	3.51	4.72	1.15	0.197

TABLE A1.1 (continued) Derived thermodynamic design data for absorption systems operating on ammonia-water for cooling.

T_{EV}	T_{AB}	T_{CO}	T_{GE}	X_{AB}	X_{GE}	(FR)	$(COP)_{CCL}$	$(COP)_{ECL}$
-25	50	50	150	23.97	22.90	72.06	0.78	0.028
-25	50	50	200	23.97	4.67	4.94	1.05	0.178
-20	30	30	100	38.15	33.52	14.36	0.95	0.176
-20	30	30	140	38.15	16.54	3.86	1.35	0.295
-20	30	30	180	38.15	2.33	2.37	1.68	0.260
-20	30	40	110	38.15	34.52	18.04	0.88	0.127
-20	30	40	160	38.15	14.11	3.57	1.27	0.265
-20	30	40	190	38.15	3.51	2.79	1.46	0.245
-20	30	50	120	38.15	35.48	24.14	0.83	0.086
-20	30	50	170	38.15	15,38	3.72	1.14	0.239
-20	30	50	200	38.15	4.67	2.85	1.30	0.228
-20	40	30	110	32.60	28.95	19.47	0.93	0.138
-20	40	30	150	32.60	12.81	4.40	1.32	0.266
-20	40	30	180	32.60	2.33	3.22	1.56	0.248
-20	40	40	120	32.60	30.00	26.92	0.86	0.090
-20	40	40	170	32.60	10.52	4.05	1.24	0.239
-20	40	40	190	32.60	3.51	3.32	1.37	0.231
-20	40	50	130	32.60	31.00	43.13	0.81	0.050
-20	40	50	190	32.60	8.20	3.76	1.17	0.216
-20	40	50	200	32.60	4.67	3.41	1.22	0.213
-20	50	30	120	27.32	24.63	27.99	0.90	0.101

TABLE AA1.1 (continued) Derived thermodynamic design data for absorption systems operating on ammonia-water for cooling.

T_{EV}	T_{AB}	T_{CO}	T_{GE}	X_{AB}	X_{GE}	(FR)	$(COP)_{CCL}$	$(COP)_{ECL}$
-20	50	30	160	27.32	9.27	5.03	1.29	0.240
-20	50	30	200	27.32	2.33	3.91	1.45	0.234
-20	50	40	130	27.32	25.76	47.59	0.84	0.054
-20	50	40	180	27.32	7.00	4.58	1.21	0.216
-20	50	40	190	27.32	3.51	4.05	1.27	0.215
-20	50	50	140	27.32	26.80	140.77	0.79	0.016
-20	50	50	200	27.32	4.67	4.21	1.15	0.197
-15	30	30	90	41.56	38.32	19.04	0.95	0.163
-15	30	30	130	41.56	20.59	3.79	1.42	0.323
-15	30	30	180	41.56	2.33	2.49	1.90	0.274
-15	30	40	100	41.56	39.28	26.63	0.88	0.104
-15	30	40	150	41.56	17.88	3.47	1.33	0.292
-15	30	40	190	41.56	3.51	2.54	1.62	0.259
-15	30	50	110	41.56	40.23	44.91	0.83	0.055
-15	30	50	170	41.56	15.38	3.23	1.25	0.263
-15	30	50	200	41.56	4.67	2.58	1.43	0.243
-15	40	30	100	35.98	33.52	27.02	0.92	0.121
-15	40	30	140	35.98	16.54	4.29	1.39	0.294
-15	40	30	180	35.98	2.33	2.90	1.77	0.262
-15	40	40	120	35.98	30.00	11.73	0.96	0.177
-15	40	40	160	35.98	14.11	3.93	1.30	0.264

TABLE A1.1 (continued) Derived thermodynamic design data for absorption systems operating on ammonia-water for cooling.

T_{EV}	T_{AB}	T_{CO}	T_{GE}	X_{AB}	X_{GE}	(FR)	$(COP)_{CCL}$	$(COP)_{ECL}$
-15	40	40	190	35.98	3.51	2.97	1.52	0.246
-15	40	50	120	35.98	35.48	129.04	0.81	0.020
-15	40	50	180	35.98	11.75	3.64	1.23	0.237
-15	40	50	200	35.98	4.67	3.05	1.34	0.228
-15	50	30	110	30.63	28.95	42.06	0.90	0.082
-15	50	30	150	30.63	12.81	4.89	1.36	0.266
-15	50	30	180	30.63	2.33	3.45	1.65	0.250
-15	50	40	120	30.63	30.00	111.11	0.84	0.028
-15	50	40	170	30.63	10.52	4.45	1.27	0.239
-15	50	40	190	30.63	3.51	3.56	1.42	0.232
-15	50	50	140	30.63	26.80	19.11	0.87	0.104
-15	50	50	200	30.63	4.67	3.67	1.26	0.214
-10	30	30	80	45.00	43.51	37.91	0.93	0.110
-10	30	30	120	45.00	24.63	3.70	1.51	0.358
-10	30	30	180	45.00	2.33	2.29	2.18	0.288
-10	30	40	90	45.00	44.53	118.02	0.87	0.031
-10	30	40	140	45.00	21.79	3.37	1.40	0.321
-10	30	40	190	45.00	3.51	2.33	1.82	0.273
-10	30	50	110	45.00	40.23	12.50	0.92	0.169
-10	30	50	150	45.00	22.90	3.49	1.24	0.289
-10	30	50	200	45.00	4.67	2.36	1.58	0.257

TABLE A1.1 (continued) Derived thermodynamic design data for absorption systems operating on ammonia-water for cooling.

T_{EV}	T_{AB}	T_{CO}	T_{GE}	X_{AB}	X_{GE}	(FR)	$(COP)_{CCL}$	$(COP)_{ECL}$
-10	40	30	90	39.32	38.32	61.68	0.91	0.070
-10	40	30	140	39.32	16.54	3.66	1.59	0.323
-10	40	30	180	39.32	2.33	2.64	2.03	0.276
-10	40	40	110	39.32	34.52	13.64	0.96	0.178
-10	40	40	150	39.32	17.88	3.83	1.37	0.290
-10	40	40	190	39.32	3.51	2.69	1.70	0.260
-10	40	50	120	39.32	35.48	16.80	0.89	0.130
10	40	50	170	39.32	15.38	3.53	1.29	0.261
-10	40	50	200	39.32	4.67	2.75	1 48	0.243
-10	50	30	110	33.92	28.95	14.29	1.03	0.198
-10	50	30	140	33.92	16.54	4.80	1.43	0.294
-10	50	30	180	33.92	2.33	3.09	1.89	0.265
-10	50	40	120	33.92	30.00	17.91	0.94	0.143
-10	50	40	160	33.92	14.11	4.34	1.34	0.264
-10	50	40	190	33.92	3.51	3.17	1.59	0.247
-10	50	50	130	33.92	31.00	23.63	0.87	0.097
-10	50	50	180	33.92	11.75	3.98	1.26	0.237
-10	50	50	200	33.92	4.68	3.26	1.39	0.229
- 5	30	30	80	48.66	43.51	10.98	1.08	0.287
- 5	30	30	110	48.66	28.94	3.60	1.60	0.399
- 5	30	30	180	48.66	2.33	2.11	2.54	0.302

TABLE A1.1 (continued) Derived thermodynamic design data for absorption systems operating on ammonia-water for cooling.

T_{EV}	T_{AB}	T_{CO}	T_{GE}	X_{AB}	X_{GE}	(FR)	$(COP)_{CCL}$	$(COP)_{ECL}$
- 5	30	40	90	48.66	44.53	13.45	0.98	0.211
- 5	30	40	130	48.66	25.76	3.24	1.48	0.357
- 5	30	40	190	48.66	3.51	2.14	2.06	0.287
- 5	30	50	100	48.66	45.56	17.56	0.91	0.145
- 5	30	50	140	48.66	26.80	3.35	1.30	0.321
- 5	30	50	200	48.66	4.67	2.17	1.75	0.271
- 5	40	30	90	42.63	38.32	14.30	1.06	0.235
- 5	40	30	120	42.63	24.63	4.19	1.56	0.356
- 5	40	30	180	42.63	2.33	2.42	2.37	0.290
- 5	40	40	100	42.63	39.28	18.10	0.96	0.167
- 5	40	40	*140*	*42.63*	*21.79*	*3.75*	*1.44*	*0.318*
- 5	40	40	190	42.63	3.51	2.47	1.93	0.274
- 5	40	50	110	42.63	40.22	24.81	0.89	0.108
- 5	40	50	160	42.63	19.19	3.45	1.35	0.286
- 5	40	50	200	42.63	4.67	2.51	1.65	0.257
- 5	50	30	100	37.17	33.52	18.18	1.03	0.193
- 5	50	30	140	37.17	16.54	4.04	1.67	0.325
- 5	50	30	180	37.17	2.33	2.80	2.20	0.279
- 5	50	40	110	37.17	34.52	24.71	0.93	0.126
- 5	50	40	150	37.17	17.88	4.26	1.41	0.289
- 5	50	40	190	37.17	3.51	2.87	1.80	0.262

TABLE A1.1 (continued) Derived thermodynamic design data for absorption systems operating on ammonia-water for cooling.

T_{EV}	T_{AB}	T_{CO}	T_{GE}	X_{AB}	X_{GE}	(FR)	$(COP)_{CCL}$	$(COP)_{ECL}$
- 5	50	50	120	37.17	35.48	38.18	0.87	0.073
- 5	50	50	170	37.17	15.34	3.88	1.32	0.260
- 5	50	50	200	37.17	4.67	2.93	1.55	0.244
0	30	30	70	52.59	49.25	15.19	1.06	0.272
0	30	30	100	52.59	33.52	3.49	1.71	0.447
0	30	30	180	52.59	2.33	1.94	3.01	0.317
0	30	40	80	52.59	50.31	21.79	0.97	0.169
0	30	40	120	52.59	30.00	3.10	1.56	0.399
0	30	40	190	52.59	3.51	1.97	2.36	0.321
0	30	50	90	52.59	51.36	39.49	0.90	0.083
0	30	50	130	52.59	31.00	3.20	1.35	0.359
0	30	50	200	52.59	4.67	1.99	1.96	0.286
0	40	30	80	46.08	43.51	21.98	1.03	0.206
0	40	30	110	46.08	28.95	4.15	1.66	0.396
0	40	30	180	46.08	2.33	2.23	2.81	0.304
0	40	40	90	46.08	44.53	35.79	0.94	0.111
0	40	40	130	46.08	25.76	3.65	1.52	0.353
0	40	40	190	46.08	3.51	2.27	2.21	0.288
0	40	50	100	46.08	45.56	104.69	0.88	0.033
0	40	50	150	46.08	22.90	3.33	1.42	0.316
0	40	50	200	46.08	4.67	2.30	1.85	0.271

TABLE A1.1 (continued) Derived thermodynamic design data for absorption systems operating on ammonia-water for cooling.

T_{EV}	T_{AB}	T_{CO}	T_{GE}	X_{AB}	X_{GE}	(FR)	$(COP)_{CCL}$	$(COP)_{ECL}$
0	50	30	90	40.41	38.32	29.54	1.00	0.161
0	50	30	130	40.41	20.59	4.00	1.81	0.355
0	50	30	200	40.41	2.33	2.57	2.61	0.292
0	50	40	100	40.41	39.28	53.74	0.92	0.076
0	50	40	150	40.41	17.88	3.65	1.61	0.317
0	50	40	190	40.41	3.51	2.62	2.06	0.275
0	50	50	110	40.41	35.48	13.09	0.97	0.178
0	50	50	160	40.41	19.19	3.81	1.39	0.283
0	50	50	200	40.41	4.67	2.67	1.73	0.258
5	30	30	60	56.96	55.91	41.99	1.00	0.157
5	30	30	90	56.96	38.32	3.31	1.84	0.506
5	30	30	180	56.96	2.33	1.79	3.68	0.332
5	30	40	80	56.96	50.31	7.46	1.13	0.362
5	30	40	100	56.96	39.28	3.43	1.49	0.451
5	30	40	190	56.96	3.51	1.81	2.74	0.318
5	30	50	90	56.96	51.36	8.68	1.02	0.282
5	30	50	120	56.96	35.48	3.00	1.41	0.406
5	30	50	200	56.96	4.67	1.82	2.22	0.302
5	40	30	80	49.74	43.51	9.07	1.26	0.374
5	40	30	100	49.74	33.52	4.10	1.79	0.443
5	40	30	180	49.74	2.33	2.06	3.44	0.317

TABLE A1.1 (continued) Derived thermodynamic design data for absorption systems operating on ammonia-water for cooling.

T_{EV}	T_{AB}	T_{CO}	T_{GE}	X_{AB}	X_{GE}	(FR)	$(COP)_{CCL}$	$(COP)_{ECL}$
5	40	40	90	49.74	44.53	10.65	1.09	0.285
5	40	40	120	49.74	30.00	3.55	1.62	0.394
5	40	40	190	49.74	3.51	2.09	2.57	0.302
5	40	50	100	49.74	45.56	13.06	0.99	0.209
5	40	50	130	49.74	31.00	3.68	1.38	0.352
5	40	50	200	49.74	4.67	2.11	2.09	0.286
5	50	30	90	43.69	38.32	11.48	1.23	0.318
5	50	30	120	43.69	24.63	3.95	1.98	0.395
5	50	30	180	43.69	2.33	2.36	3.19	0.305
5	50	40	100	43.70	39.28	13.76	1.06	0.235
5	50	40	130	43.70	25.76	4.14	1.58	0.350
5	50	40	190	43.70	3.51	2.40	2.40	0.289
5	50	50	110	43.69	40.23	17.27	0.97	0.167
5	50	50	150	43.69	22.90	3.71	1.46	0.313
5	50	50	200	43.69	4.67	2.44	1.96	0.272
10	30	30	60	62.13	55.91	7.09	1.27	0.510
10	30	30	80	62.13	43.51	3.03	2.00	0.578
10	30	30	180	62.13	2.33	1.63	4.69	0.350
10	30	40	70	62.13	57.02	8.41	1.10	0.391
10	30	40	90	62.13	44.53	3.15	1.56	0.516
10	30	40	190	62.13	3.51	1.65	3.26	0.336

TABLE A1.1 (continued) Derived thermodynamic design data for absorption systems operating on ammonia-water for cooling

T_{EV}	T_{AB}	T_{CO}	T_{GE}	X_{AB}	X_{GE}	(FR)	$(COP)_{CCL}$	$(COP)_{ECL}$
10	30	50	80	62.13	58.12	10.43	1.00	0.286
10	30	50	110	62.13	40.23	2.73	1.48	0.465
10	30	50	200	62.13	4.67	1.66	2.54	0.320
10	40	30	70	53.70	49.25	11.42	1.24	0.392
10	40	30	90	53.70	38.32	4.01	1.95	0.500
10	40	30	180	53.70	2.33	1.90	4.37	0.332
10	40	40	80	53.70	50.31	14.66	1.07	0.271
10	40	40	110	53.70	34.52	3.41	1.72	0.443
10	40	40	190	53.70	3.51	1.92	3.06	0.317
10	40	50	90	53.70	51.36	20.79	0.98	0.169
10	40	50	120	53,70	35.48	3.54	1.44	0.394
10	40	50	200	53.70	4.67	1.94	2.39	0.301
10	50	30	80	47.14	43.51	15.56	1.20	0.322
10	50	30	100	47.14	33.52	4.88	1.90	0.442
10	50	30	180	47.14	2.33	2.18	4.06	0.319
10	50	40	90	47.14	44.53	21.25	1.04	0.205
10	50	40	120	47.14	30.00	4.08	1.68	0.390
10	50	40	190	47.14	3.51	2.21	2.85	0.303
10	50	50	100	47.14	45.56	34.46	0.95	0.110
10	50	50	140	47.14	26.80	3.60	1.54	0.347
10	50	50	200	47.14	4.67	2.24	2.24	0.286

TABLE A1.1 (continued) Derived thermodynamic design data for absorption systems operating on ammonia-water for cooling.

T_{EV}	T_{AB}	T_{CO}	T_{GE}	X_{AB}	X_{GE}	(FR)	$(COP)_{CCL}$	$(COP)_{ECL}$
20	50	50	90	54.81	51.36	14.10	2.08	1.269
20	50	50	120	54.81	35.48	3.34	2.74	1.437
20	50	50	200	54.81	4.67	1.90	4.10	1.315
20	50	60	100	54.81	52.41	19.83	1.98	1.168
20	50	60	140	54.81	31.94	2.98	2.60	1.388
20	50	60	200	54.81	9.37	1.99	3.32	1.313
20	50	70	110	54.81	53.46	34.47	1.92	1.085
20	50	70	150	54.81	27.78	3.06	2.39	1.347
20	50	70	200	54.81	14.13	2.11	2.86	1.305
20	60	50	100	48.20	45.56	20.62	2.05	1.200
20	60	50	130	48.20	31.00	4.01	2.70	1.384
20	60	50	200	48.20	4.67	2.19	3.89	1.301
20	60	60	110	48.20	46.58	32.98	1.96	1.109
20	60	60	150	48.20	27.78	3.54	2.56	1.341
20	60	60	200	48.20	9.37	2.33	3.17	1.30
20	60	70	120	48.20	47.61	88.80	1.89	1.035
20	60	70	160	48.20	28.70	3.66	2.35	1.303
20	60	70	200	48.20	14.13	2.52	2.73	1.284
20	70	50	110	42.49	40.23	26.45	2.02	1.165
20	70	50	140	42.49	26.80	4.67	2.66	1.342
20	70	50	200	42.49	4.67	2.52	3.68	1.288
20	70	60	120	42.49	41.21	45.93	1.93	1.081
20	70	60	160	42.49	23.93	4.10	2.52	1.303
20	70	60	200	42.49	9.37	2.74	3.01	1.280

TABLE A1.2 Derived thermodynamic design data for absorption systems operating on ammonia-water for heating.

continued

T_{EV}	T_{AB}	T_{CO}	T_{GE}	X_{AB}	X_{GE}	(FR)	$(COP)_{CCL}$	$(CCP)_{ECL}$
20	70	70	130	42.49	42.21	206.40	1.87	1.015
20	70	70	180	42.49	21.40	3.73	2.42	1.269
20	70	70	200	42.49	14.13	3.03	2.61	1.264
20	80	50	120	37.32	35.48	35.12	1.99	1.128
20	80	50	160	37.32	19.19	4.46	2.80	1.312
20	80	50	200	37.32	4.67	2.92	3.48	1.278
20	80	60	130	37.32	36.40	69.17	1.91	1.056
20	80	60	180	37.32	16.61	4.03	2.62	1.276
20	80	60	200	37.32	9.37	3.24	2.86	1.266
20	80	70	150	37.32	32.84	14.99	1.97	1.146
20	80	70	200	37.32	14.13	3.70	2.49	1.245
20	90	50	130	32.45	31.00	47.73	1.97	1.098
20	90	50	170	32.45	15.38	4.96	2.76	1.288
20	90	50	200	32.45	4.67	3.43	3.27	1.268
20	90	60	140	32.45	31.94	134.56	1.897	1.030
20	90	60	190	32.45	12.95	4.46	2.58	1.254
20	90	60	200	32.45	9.37	3.93	2.70	1.252
20	90	70	160	32.45	28.70	19.03	1.95	1.120
20	90	70	200	32.45	14.13	4.69	2.36	1.225
20	100	50	150	27.81	22.90	15.71	2.15	1.195
20	100	50	200	27.81	4.67	4.12	3.06	1.260

TABLE A1.2 (continued) Derived thermodynamic design data for absorption systems operating on ammonia-water for heating.

T_{EV}	T_{AB}	T_{CO}	T_{GE}	X_{AB}	X_{GE}	(FR)	$(COP)_{CCL}$	$(COP)_{ECL}$
20	100	60	160	27.81	23.93	19.63	2.02	1.138
20	100	60	200	27.81	9.37	4.92	2.55	1.235
20	100	70	170	27.81	24.89	25.76	1.93	1.093
20	100	70	200	27.81	14.13	6.28	2.24	1.200
30	50	50	80	64.62	58.12	6.44	2.29	1.514
30	50	50	100	64.62	45.56	2.86	3.03	1.573
30	50	50	200	64.62	4.67	1.59	5.80	1.350
30	50	60	90	64.62	59.19	7.52	2.11	1.397
30	50	60	110	64.62	46.58	2.96	2.58	1.509
30	50	60	200	64.62	9.37	1.64	4.20	1.353
30	50	70	100	64.62	60.28	9.15	2.02	1.292
30	50	70	130	64.62	42.21	2.58	2.50	1.454
30	50	70	200	64.62	14.13	1.70	3.40	1.350
30	60	50	90	55.91	51.36	10.68	2.25	1.386
30	60	50	110	55.91	40.23	3.81	2.98	1.492
30	60	50	200	55.91	4.67	1.86	5.48	1.329
30	60	60	100	55.91	52.41	13.59	2.08	1.266
30	60	60	130	55.91	36.40	3.26	2.75	1.431
30	60	60	200	55.91	9.37	1.95	3.99	1.329
30	60	70	110	55.91	53.46	18.94	1.99	1.167
30	60	70	140	55.91	37.29	3.37	2.47	1.382
30	60	70	200	55.91	14.31	2.06	3.24	1.320

TABLE A1.2 (continued) Derived thermodynamic design data for absorption systems operating on ammonia-water for heating.

T_{EV}	T_{AB}	T_{CO}	T_{GE}	X_{AB}	X_{GE}	(FR)	$(COP)_{CCL}$	$(COP)_{ECL}$
30	70	50	100	49.25	45.56	14.73	2.22	1.314
30	70	50	120	49.25	35.48	4.68	2.93	1.431
30	70	50	200	49.25	4.67	2.14	5.16	1.315
30	70	60	110	49.25	46.58	20.01	2.05	1.199
30	70	60	140	49.25	27.78	3.36	2.91	1.374
30	70	60	200	49.25	9.37	2.27	3.78	1.312
30	70	70	110	49.25	47.61	31.95	1.96	1.107
30	70	70	160	49.25	28.70	3.47	2.57	1.333
30	70	70	200	49.25	14.13	2.44	3.08	1.301
30	80	50	110	43.51	40.23	18.20	2.19	1.269
30	80	50	140	43.51	26.80	4.38	3.20	1.384
30	80	50	200	43.51	4.67	2.45	4.84	1.304
30	80	60	120	43.51	41.21	25.61	2.03	1.162
30	80	60	150	43.51	23.93	3.89	2.87	1.334
30	80	60	200	43.51	9.37	2.65	3.56	1.297
30	80	70	130	43.51	42.21	43.45	1.94	1.080
30	80	70	170	43.51	24.89	4.03	2.54	1.295
30	80	70	200	43.51	14.13	2.92	2.92	1.283
30	90	50	120	38.32	35.48	22.72	2.16	1.223
30	90	50	150	38.32	22.90	5.00	3.15	1.347
30	90	50	200	38.32	4.67	2.83	4.52	1.294

TABLE A1.2 (continued) Derived thermodynamic design data for absorption systems operating on ammonia-water for heating.

T_{EV}	T_{AB}	T_{CO}	T_{GE}	X_{AB}	X_{GE}	(FR)	$(COP)_{CCL}$	$(COP)_{ECL}$
30	90	60	130	38.32	36.40	33.08	2.00	1.129
30	90	60	170	38.32	20.39	4.44	2.82	1.302
30	90	60	200	38.32	9.37	3.13	3.35	1.284
30	90	70	140	38.32	37.29	59.88	1.92	1.060
30	90	70	190	38.32	17.82	4.01	2.64	1.267
30	90	70	200	38.32	14.13	3.55	2.76	1.265
30	100	50	130	33.52	31.00	27.45	2.13	1.193
30	100	50	160	33.52	19.19	5.64	3.10	1.320
30	100	50	200	33.52	4.67	3.30	4.20	1.286
30	100	60	140	33.52	31.94	43.25	1.98	1.102
30	100	60	180	33.52	16.61	4.93	2.78	1.280
30	100	60	200	33.52	9.37	3.75	3.14	1.272
30	100	70	150	33.52	32.84	*97.76*	*1.90*	*1.038*
30	100	70	200	33.52	14.13	4.43	2.60	1.247
40	50	50	70	78.48	67.12	2.89	2.83	*1.769*
40	50	50	200	78.48	4.67	1.29	10.92	1.394
40	50	60	80	78.48	68.40	3.13	2.33	1.665
40	50	60	90	78.48	59.19	2.16	2.72	1.693
40	50	60	200	78.48	9.37	1.31	5.96	1.404
40	50	70	90	78.48	69.70	3.45	2.15	1.566
40	50	70	100	78.48	60.28	2.18	2.40	1.624
40	50	70	200	78.48	14.13	1.33	4.31	1.407

TABLE A1.2 (continued) Derived thermodynamic design data for absorption systems operating on ammonia-water for heating.

T_{EV}	T_{AB}	T_{CO}	T_{GE}	X_{AB}	X_{GE}	(FR)	$(COP)_{CCL}$	$(COP)_{ECL}$
40	60	50	80	65.86	58.12	5.41	2.77	1.648
40	60	50	90	65.86	51.36	3.35	3.59	1.660
40	60	50	200	65.86	4.67	1.56	10.26	1.364
40	60	60	90	65.86	59.20	6.12	2.29	1.515
40	60	60	100	65.86	46.58	2.77	3.04	1.567
40	60	60	200	65.86	9.37	1.60	5.63	1.370
40	60	70	100	65.68	60.28	7.12	2.19	1.396
40	60	70	120	65.86	47.61	2.87	2.59	1.503
40	60	70	200	65.86	14.13	1.66	4.09	1.368
40	70	50	90	57.02	51.36	8.59	2.72	1.530
40	70	50	100	57.02	45.56	4.75	3.52	1.561
40	70	50	200	57.02	4.67	1.82	9.60	1.344
40	70	60	100	57.02	52.41	10.32	2.26	1.381
40	70	60	120	57.02	41.21	3.72	2.99	1.483
40	70	60	200	57.02	9.37	1.90	5.30	1.345
40	70	70	110	57.02	53.46	13.06	2.09	1.262
40	70	70	140	57.02	37.29	3.18	2.77	1.422
40	70	70	200	57.02	14.13	2.00	3.87	1.340
40	80	50	100	50.31	45.56	11.46	2.68	1.452
40	80	50	110	50.31	40.23	5.93	3.45	1.500
40	80	50	200	50.31	4.67	2.09	8.94	1.330

TABEL A1.2 (continued) Derived thermodynamic design data for absorption systems operating on ammonia-water for cooling.

T_{EV}	T_{AB}	T_{CO}	T_{GE}	X_{AB}	X_{GE}	(FR)	$(COP)_{CCL}$	$(COP)_{ECL}$
40	80	60	110	50.31	46.58	14.35	2.23	1.308
40	80	60	130	50.31	36.38	4.57	2.94	1.424
40	80	60	200	50.31	9.37	2.21	4.97	1.329
40	80	70	120	50.31	47.61	19.45	2.06	1.194
40	80	70	150	50.31	32.84	3.65	2.73	1.369
40	80	70	200	50.31	14.13	2.73	3.65	1.319
40	90	50	110	44.53	40.22	13.88	2.63	1.402
40	90	50	120	44.53	35.48	7.13	3.39	1.441
40	90	50	200	44.53	4.67	2.39	8.28	1.319
40	90	60	120	44.53	41.21	17.72	2.19	1.264
40	90	60	150	44.53	27.78	4.31	3.22	1.375
40	90	60	200	44.53	9.37	2.58	4.64	1.315
40	90	70	130	44.53	42.21	24.90	2.04	1.158
40	90	70	160	44.53	28.70	4.50	2.69	1.327
40	90	70	200	44.53	14.13	2.82	3.43	1.302
40	100	50	120	39.28	35.48	16.98	2.59	1.342
40	100	50	140	39.28	26.80	5.87	4.03	1.397
40	100	50	200	39.28	4.67	2.75	7.62	1.310
40	100	60	130	39.28	36.40	22.06	2.17	1.218
40	100	60	160	39.28	23.93	4.96	3.17	1.337

TABLE A1.2 (continued) Derived thermodynamic design data for absorption systems operating on ammonia-water for heating.

T_{EV}	T_{AB}	T_{CO}	T_{GE}	X_{AB}	X_{GE}	(FR)	$(COP)_{CCL}$	$(COP)_{ECL}$
40	100	60	200	39.28	9,37	3.03	4.31	1.302
40	100	70	140	39.28	37.29	31.45	2.01	1.128
40	100	70	180	39.28	21.40	4.40	2.84	1.292
40	100	70	200	39.28	14.13	3.41	3.21	1.284
50	60	60	80	79.83	68.40	2.76	2.83	1.758
50	60	60	200	78.93	9.37	1.28	10.56	1.419
50	60	70	90	79.83	69.71	2.99	2.33	1.656
50	60	70	100	79.83	60.28	2.03	2.73	1.683
50	60	70	200	79.83	14.13	1.31	5.78	1.424
50	70	60	90	67.12	59.19	5.15	2.78	1.648
50	70	60	100	67.12	52.41	3.24	3.60	1.652
50	70	60	200	67.12	9.37	1.57	9.88	1.386
50	70	70	100	67.12	60.28	5.81	2.30	1.513
50	70	70	110	67.12	47.61	2.69	3.05	1.560
50	70	70	200	67.12	14.13	1.62	5.44	1.386
50	80	60	100	58.12	52.41	8.34	2.73	1.519
50	80	60	110	58.12	46.58	4.63	3.53	1.552
50	80	60	200	58.12	9.37	1.86	9.19	1.361
50	80	70	110	58.12	53.46	9.99	2.27	1.375
50	80	70	130	58.12	42.21	3.63	3.00	1.473

TABLE A1.2 (continued) Derived thermodynamic design data for absorption systems operating on ammonia-water for heating.

T_{EV}	T_{AB}	T_{CO}	T_{GE}	X_{AB}	X_{GE}	(FR)	$(COP)_{CCL}$	$(COP)_{ECL}$
50	80	70	200	58.12	14.13	1.95	5.10	1.357
50	90	60	110	51.36	46.58	11.18	2.69	1.444
50	90	60	120	51.36	41.21	5.79	3.47	1.490
50	90	60	200	51.36	9.37	2.16	8.51	1.345
50	90	70	120	51.36	47.61	13.98	2.23	1.300
50	90	70	140	51.36	37.29	4.46	2.96	1.415
50	90	70	200	51.36	14.13	2.31	4.76	1.338
50	100	60	120	45.56	41.21	13.54	2.64	1.394
50	100	60	130	45.56	36.40	6.94	3.40	1.434
50	100	60	200	45.56	9.37	2.50	7.83	1.332
50	100	70	130	45.56	42.21	17.28	2.20	1.257
50	100	70	150	45.56	28.70	4.23	3.24	1.366
50	100	70	200	45.56	14.13	2.73	4.41	1.321

TABLE A1.2 (continued) Derived thermodynamic design data for absorption systems operating on ammonia-water for heating.

T_{EV}	T_{AB}	T_{CO}	T_{GE}	X_{AB}	X_{GE}	(FR)	$(COP)_{CCL}$	$(COP)_{ECL}$
-10	50	50	130	33.92	31.00	23.67	0.87	0.097
-10	50	50	180	33.92	11.75	3.98	1.26	0.237
-10	50	50	200	33.92	4.67	3.26	1.39	0.229
-10	50	60	140	33.92	31.94	34.37	0.82	0.060
-10	50	60	200	33.92	9.37	3.69	1.19	0.210
-10	50	70	150	33.92	32.84	62.15	0.78	0.029
-10	50	70	200	33.92	14.13	4.34	1.04	0.189
-10	60	50	140	28.76	26.80	37.35	0.85	0.065
-10	60	50	200	28.76	4.67	3.96	1.30	0.215
-10	60	60	150	28.76	27,78	73.69	0.80	0.029
-10	60	60	200	28.76	9.37	4.67	1.11	0.193
-10	60	70	170	28.76	24.89	19.43	0.82	0.078
-10	60	70	200	28.76	14.13	5.87	0.97	0.162
-10	70	50	150	23.83	22.90	82.90	0.83	0.031
-10	70	50	200	23.83	4.67	4.98	1.20	0.197
-10	70	60	170	23.83	20.39	23.16	0.85	0.077
-10	70	60	200	23.83	9.37	6.27	1.03	0.168
-10	70	70	180	23.83	21.40	32.40	0.80	0.050
-10	70	70	200	23.83	14.13	8.85	0.90	0.128
-10	80	50	170	18.98	15.38	23.52	0.89	0.088
-10	80	50	200	18.98	4.67	6.66	1.11	0.175
-10	80	60	180	18.98	16.61	35.32	0.83	0.054
-10	80	60	200	18.98	9.37	9.43	0.95	0.135

$(COP)_{CH} = (COP)_{CCL} + 1$ $(COP)_{EH} = (COP)_{ECL} + 1$

TABLE A1.3 Derived thermodynamic design data for absorption systems operating on ammonia - water for cooling and simultaneou heating.

...continued

T_{EV}	T_{AB}	T_{CO}	T_{GE}	X_{AB}	X_{GE}	(FR)	$(COP)_{CCL}$	$(COP)_{ECL}$
-10	80	70	190	18.98	17.82	71.14	0.78	0.024
-10	80	70	200	18.98	14.13	17.71	0.83	0.079
-10	90	50	180	14.51	11.75	31.93	0.87	0.068
-10	90	50	200	14.51	4.67	9.69	1.02	0.146
-10	90	60	190	14.51	12.95	55.74	0.81	0.036
-10	90	60	200	14.51	9.37	17.62	0.87	0.090
-10	100	50	190	10.80	8.20	35.35	0.85	0.062
-10	100	50	200	10.80	4.67	15.56	0.93	0.112
-10	100	60	200	10.80	9.37	63.41	0.79	0.032
- 5	50	50	120	37.17	35.48	38.12	0.87	0.073
- 5	50	50	170	37.17	15.38	3.88	1.32	0.260
- 5	50	50	200	37.17	4.67	2.93	1.55	0.244
- 5	50	60	130	37.17	36.40	82.03	0.82	0.030
- 5	50	60	190	37.17	12.95	3.59	1.25	0.233
- 5	50	60	200	37.17	9.37	3.26	1.31	0.231
- 5	50	70	150	37.17	32.84	15.49	0.84	0.104
- 5	50	70	200	37.17	14.13	3.73	1.13	0.210
- 5	60	50	140	31.95	26.80	14.21	0.94	0.147
- 5	60	50	180	31.95	11.75	4.37	1.29	0.236
- 5	60	50	200	31.95	4.67	3.49	1.44	0.231
- 5	60	60	150	31.95	27.78	17.31	0.88	0.109
- 5	60	60	200	31.95	9.37	4.01	1.22	0.213
- 5	60	70	160	31.95	28.70	21.92	0.83	0.077
- 5	60	70	200	31.95	14.13	4.82	1.06	0.186
- 5	70	50	160	26.97	19.19	10.39	1.01	0.168

$(COP)_{CH} = (COP)_{CCL} + 1$ $\qquad$ $(COP)_{EH} = (COP)_{ECL} + 1$

TABLE A1.3 Derived thermodynamic design data for absorption systems (continued) operating on ammonia - water for cooling and simultaneous

T_{EV}	T_{AB}	T_{CO}	T_{GE}	X_{AB}	X_{GE}	(FR)	$(COP)_{CCL}$	$(COP)_{ECL}$
- 5	70	50	200	26.97	4.67	4.28	1.34	0.216
- 5	70	60	160	26.97	23.93	25.07	0.86	0.079
- 5	70	60	200	26.97	9.37	5.15	1.13	0.192
- 5	70	70	170	26.97	24.89	36.21	0.81	0.049
- 5	70	70	200	26.97	14.13	6.69	0.98	0.157
- 5	80	50	160	22.20	19.19	26.80	0.90	0.087
- 5	80	50	200	22.20	4.67	5.44	1.24	0.198
- 5	80	60	170	22.20	20.39	43.78	0.84	0.048
- 5	80	60	200	22.20	9.37	7.06	1.04	0.166
- 5	80	70	180	22.20	21.40	97.47	0.79	0.019
- 5	80	70	200	22.20	14.13	10.63	0.91	0.119
- 5	90	50	170	17.45	15.38	40.78	0.88	0.061
- 5	90	50	200	17.45	4.67	7.46	1.13	0.174
- 5	90	60	180	17.45	16.61	99.46	0.82	0.023
- 5	90	60	200	17.45	9.37	11.21	0.96	0.128
- 5	90	70	200	17.45	14.13	25.83	0.83	0.062
- 5	100	50	180	13.37	11.75	54.57	0.86	0.047
- 5	100	50	200	13.37	4.67	10.96	1.03	0.144
- 5	100	60	190	13.37	12.95	209.94	0.80	0.011
- 5	100	60	200	13.37	9.37	22.67	0.87	0.080
0	50	50	120	40.41	35.48	13.09	0.97	0.178
0	50	50	160	40.41	19.19	3.38	1.39	0.283
0	50	50	200	40.41	4.67	2.67	1.73	0.258
0	50	60	130	40.41	36.40	15.86	0.90	0.132

$(COP)_{CH} = (COP)_{CCL} + 1$ $\qquad$ $(COP)_{EH} = (COP)_{ECL} + 1$

TABLE A1.3 Derived thermodynamic design data for absorption systems (continued) operating on ammonia - water for cooling and simultaneous heating.

T_{EV}	T_{AB}	T_{CO}	T_{GE}	X_{AB}	X_{GE}	(FR)	$(COP)_{CCL}$	$(COP)_{ECL}$
0	50	60	180	40.41	16.61	3.50	1.31	0.255
0	50	60	200	40.41	9.37	2.92	1.44	0.247
0	50	70	140	40.41	37.29	20.09	0.85	0.093
0	50	70	200	40.41	14.13	3.27	1.24	0.229
0	60	50	130	35.13	31.00	16.72	0.95	0.145
0	60	50	170	35.13	15.38	4.28	1.36	0.259
0	60	50	200	35.13	4.67	3.13	1.62	0.246
0	60	60	140	35.13	31.94	21.36	0.88	0.102
0	60	60	190	35.13	12.95	3.93	1.28	0.232
0	60	60	200	35.13	9.37	3.52	1.35	0.231
0	60	70	150	35.13	32.84	29.28	0.83	0.066
0	60	70	200	35.13	14.13	4.09	1.15	0.208
0	70	50	140	30.08	26.80	22.34	0.93	0.115
0	70	50	190	30.08	8.20	4.20	1.42	0.236
0	70	50	200	30.08	4.67	3.75	1.50	0.232
0	70	60	150	30.08	27.78	31.43	0.86	0.073
0	70	60	200	30.08	9.37	4.38	1.25	0.212
0	70	70	160	30.08	28.70	51.68	0.81	0.039
0	70	70	200	30.08	14.13	5.38	1.07	0.183
0	80	50	150	25.26	22.90	32.68	0.90	0.083
0	80	50	200	25.26	4.67	4.63	1.39	0.217

$(COP)_{CH} = (COP)_{CCL} + 1$ $\qquad$ $(COP)_{EH} = (COP)_{ECL} + 1$

TABLE A1.3 (continued) Derived thermodynamic design data for absorption systems operating on ammonia - water for cooling and simultaneous heating.

T_{EV}	T_{AB}	T_{CO}	T_{GE}	X_{AB}	X_{GE}	(FR)	$(COP)_{CCL}$	$(COP)_{ECL}$
0	80	60	160	25.26	23.93	57.30	0.84	0.042
0	80	60	200	25.26	9.37	5.70	1.15	0.190
0	80	70	180	25.26	21.40	20.37	0.86	0.082
0	80	70	200	25.26	14.13	7.71	0.99	0.151
0	90	50	160	20.67	19.19	54.49	0.88	0.053
0	90	50	200	20.67	4.67	5.96	1.27	0.199
0	90	60	180	20.67	16.61	20.54	0.90	0.095
0	90	60	200	20.67	9.37	8.02	1.06	0.163
0	90	70	190	20.67	17.82	28.79	0.84	0.061
0	90	70	200	20.67	14.13	13.12	0.91	0.109
0	100	50	170	16.12	15.38	114.74	0.86	0.027
0	100	50	200	16.12	4.67	8.33	1.15	0.173
0	100	60	190	16.12	12.95	27.52	0.88	0.074
0	100	60	200	16.12	9.37	13.43	0.96	0.121
0	100	70	200	16.12	14.13	43.21	0.82	0.043
5	50	50	110	43.69	40.23	17.23	0.97	0.167
5	50	50	150	43.69	22.90	3.71	1.46	0.313
5	50	50	200	43.69	4.67	2.44	1.96	0.272
5	50	60	120	43.69	41.21	23.71	0.90	0.107
5	50	60	170	43.69	20.39	3.42	1.37	0.279
5	50	60	200	43.69	9.37	2.64	1.60	0.263
5	50	70	130	43.69	42.21	38.98	0.85	0.058
5	50	70	190	43.69	17.82	3.18	1.29	0.250
5	50	70	200	43.69	14.13	2.90	1.36	0.248

$(COP)_{CH} = (COP)_{CCL} + 1$ $(COP)_{EH} = (COP)_{ECL} + 1$

TABLE A1.3 (continued) Derived thermodynamic design data for absorption systems operating on ammonia - water for cooling and simultaneous heating

T_{EV}	T_{AB}	T_{CO}	T_{GE}	X_{AB}	X_{GE}	(FR)	$(COP)_{CCL}$	$(COP)_{ECL}$
5	60	50	120	38.29	35.48	23.00	0.94	0.129
5	60	50	170	38.29	15.38	3.69	1.53	0.283
5	60	50	200	38.29	4.67	2.84	2.83	0.259
5	60	60	130	38.29	36.40	33.68	0.88	0.078
5	60	60	180	38.29	16.61	3.85	1.34	0.253
5	60	60	200	38.29	9.37	3.13	1.50	0.247
5	60	70	140	38.29	37.29	62.73	0.83	0.037
5	60	70	200	38.29	14.13	3.55	1.27	0.227
5	70	50	130	33.18	31.00	31.74	0.92	0.098
5	70	50	180	33.18	11.75	4.19	1.50	0.259
5	70	50	200	33.18	4.67	3.34	1.70	0.248
5	70	60	140	33.18	31.94	55.15	0.86	0.049
5	70	60	190	33.18	12.95	4.30	1.31	0.232
5	70	60	200	33.18	9.37	3.81	1.39	0.231
5	70	70	160	33.18	28.70	15.93	0.89	0.112
5	70	70	200	33.18	14.13	4.51	1.18	0.206
5	80	50	140	28.29	26.80	49.23	0.90	0.066
5	80	50	190	28.29	8.20	4.57	1.47	0.237
5	80	50	200	28.29	4.67	4.04	1.57	0.234
5	80	60	160	28.29	23.93	17.45	0.93	0.120
5	80	60	200	28.29	9.37	4.79	1.28	0.210

$(COP)_{CH} = (COP)_{CCL} + 1$ $\qquad$ $(COP)_{EH} = (COP)_{ECL} + 1$

TABLE A1.3 (continued) Derived thermodynamic design data for absorption systems operating on ammonia - water for cooling and simultaneous heating

T_{EV}	T_{AB}	T_{CO}	T_{GE}	X_{AB}	X_{GE}	(FR)	$(COP)_{CCL}$	$(COP)_{ECL}$
5	80	70	170	28.29	24.89	22.10	0.87	0.085
5	80	70	200	28.29	14.13	6.06	1.09	0.179
5	90	50	160	23.64	19.19	18.18	0.99	0.135
5	90	50	200	23.64	4.67	5.03	1.47	0.219
5	90	60	170	23.64	20.39	24.51	0.91	0.090
5	90	60	200	23.64	9.37	6.35	1.18	0.189
5	90	70	180	23.64	21.40	35.15	0.85	0.056
5	90	70	200	23.64	14.13	9.03	0.99	0.145
5	100	50	170	19.13	15.38	22.55	0.98	0.114
5	100	50	200	19.13	4.67	6.59	1.31	0.200
5	100	60	180	19.13	16.61	33.14	0.89	0.070
5	100	60	200	19.13	9.37	9.28	1.07	0.158
5	100	70	190	19.13	17.82	62.73	0.83	0.033
5	100	70	200	19.13	14.13	17.16	0.90	0.096
10	50	50	100	47.14	45.56	34.35	0.95	0.110
10	50	50	140	47.14	22.90	3.18	1.67	0.344
10	50	50	200	47.14	4.67	2.24	2.24	0.286
10	50	60	120	47.14	41.21	9.92	1.01	0.217
10	50	60	160	47.14	23.93	3.28	1.44	0.310
10	50	60	200	47.14	9.37	2.40	1.79	0.280
10	50	70	130	47.14	42.21	11.72	0.94	0.164

$(COP)_{CH} = (COP)_{CCL} + 1$ $(COP)_{EH} = (COP)_{ECL} + 1$

TABLE A1.3 Derived thermodynamic design data for absorption systems (continued) operating on ammonia - water for cooling and simultaneous heating.

T_{EV}	T_{AB}	T_{CO}	T_{GE}	X_{AB}	X_{GE}	(FR)	$(COP)_{CCL}$	$(COP)_{ECL}$
10	50	70	170	47.14	24.89	3.38	1.28	0.278
10	50	70	200	47.14	14.13	2.60	1.50	0.266
10	60	50	120	41.45	35.48	10,80	1.08	0.231
10	60	50	150	41.45	22.90	4.16	1.51	0.310
10	60	50	200	41.45	4.67	2.59	2.09	0.273
10	60	60	130	41.45	36.40	12.58	0.98	0.177
10	60	60	170	41.45	20.39	3.78	1.41	0.276
10	60	60	200	41.45	9.37	2.82	1.68	0.263
10	60	70	140	41.45	37.29	15.05	0.91	0.132
10	60	70	190	41.45	17.82	3.48	1.32	0.248
10	60	70	200	41.45	14.13	3.14	1.40	0.246
10	70	50	130	36.26	31.00	13.13	1.05	0.198
10	70	50	170	36.26	15.38	4.05	1.60	0.284
10	70	50	200	36.26	4.67	3.02	1.94	0.262
10	70	60	140	36.26	31.94	15.77	0.96	0.146
10	70	60	180	36.26	16.61	4.24	1.37	0.252
10	70	60	200	36.26	9.37	3.37	1.56	0.248
10	70	70	150	36.26	32.84	19.62	0.89	0.105
10	70	70	200	36.26	14.13	3.88	0.29	0.226
10	80	50	140	31.31	26.80	16.25	1.03	0.167
10	80	50	180	31.31	11.75	4.51	0.56	0.260

$(COP)_{CH} = (COP)_{CCL} + 1$ $(COP)_{EH} = (COP)_{ECL} + 1$

TABLE A1.3 Derived thermodynamic design data for absorption systems (continued)operating on ammonia - water for cooling and simultaneous heating

T_{EV}	T_{AB}	T_{CO}	T_{GE}	X_{AB}	X_{GE}	(FR)	$(COP)_{CCL}$	$(COP)_{ECL}$
10	80	50	200	31.31	4.67	3.58	1.79	0.250
10	80	60	150	31.31	27.78	20.49	0.94	0.118
10	80	60	200	31.31	9.37	4.13	1.44	0.232
10	80	70	160	31.31	28.70	27.36	0.81	0.078
10	80	70	200	31.31	14.13	5.00	1.20	0.204
10	90	50	150	26.58	22.90	20.94	1.00	0.137
10	90	50	190	26.58	8.20	4.99	1.53	0.239
10	90	50	200	26.58	4.67	4.35	1.65	0.237
10	90	60	160	26.58	23.93	28.70	0.92	0.089
10	90	60	200	26.58	9,37	5.27	1.32	0.213
10	90	70	170	26.58	24.89	44.43	0.85	0.051
10	90	70	200	26.58	14.13	6.89	1.10	0.175
10	100	50	160	22.10	19.19	27.79	0.98	0.109
10	100	50	200	22.10	4.67	5.47	1.50	0.222
10	100	60	170	22.10	20.39	46.52	0.89	0.058
10	100	60	200	22.10	9.37	7.12	1.20	0.188
10	100	70	190	22.10	17.82	19.20	0.92	0.096
10	100	70	200	22.10	14.13	10.77	1.00	0.138

$(COP)_{CH} = (COP)_{CCL} + 1$ $\qquad$ $(COP)_{EH} = (COP)_{ECL} + 1$

TABLE A1.3 (continued) Derived thermodynamic design data for absorption systems operating on ammonia water for cooling and simultaneous heating.

T_{EV}	T_{AB}	T_{CC}	T_{GE}	X_{AB}	X_{GE}	(FR)	$(COP)_{CCL}$	$(COP)_{ECL}$
-30	30	30	100	38.99	38.46	123	0.76	0.043
-30	30	30	105	38.99	36.87	29.75	0.80	0.133
-30	30	30	110	38.99	35.34	17.68	0.85	0.189
-30	30	30	115	38.99	33.85	12.86	0.89	0.226
-30	30	40	115	38.99	37.17	34.47	0.76	0.101
-30	30	40	120	38.99	35.64	19.22	0.80	0.154
-30	30	40	125	38.99	34.17	13.65	0.83	0.191
-30	30	40	130	38.99	32.73	10.75	0.86	0.218
-30	30	50	125	38.99	37.42	39.77	0.73	0.076
-30	30	50	130	38.99	35.90	20.75	0.75	0.126
-30	30	50	135	38.99	34.43	14.39	0.78	0.162
-30	30	50	140	38.99	33.01	11.20	0.81	0.188
-30	40	30	115	35.48	33.85	40.58	0.78	0.104
-30	40	30	120	35.48	32.41	22.00	0.82	0.162
-30	40	30	125	35.48	31.01	15.42	0.87	0.201
-30	40	40	125	35.48	34.17	50.16	0.74	0.073
-30	40	40	130	35.48	32.73	24.50	0.78	0.129
-30	40	40	135	35.48	31.34	16.58	0.81	0.167
-30	40	50	135	35.48	34.43	62.70	0.71	0.051
-30	40	50	140	35.48	33.01	27.11	0.74	0.102
-30	40	50	145	35.48	31.62	17.72	0.76	0.139

Table A1.4 Derived thermodynamic design data for absorption systems operating on ammonia-lithium nitrate for cooling.

... continued

T_{EV}	T_{AB}	T_{CO}	T_{GE}	X_{AB}	X_{GE}	(FR)	$(COP)_{CCL}$	$(COP)_{ECL}$
-25	30	30	95	41.20	40.11	55.20	0.80	0.089
-25	30	30	100	41.20	38.46	22.48	0.85	0.174
-25	30	30	105	41.20	36.87	14.59	0.90	0.225
-25	30	30	110	41.20	35.34	11.03	0.94	0.259
-25	30	30	115	41.20	33.85	9.00	1.00	0.282
-25	30	30	120	41.20	32.41	7.69	1.03	0.298
-25	30	30	125	41.20	31.01	6.77	1.08	0.311
-25	30	40	110	41.20	38.75	25.02	0.80	0.137
-25	30	40	115	41.20	37.20	15.60	0.84	0.187
-25	30	40	120	41.20	35.64	11.59	0.87	0.221
-25	30	40	125	41.20	34.17	9.37	0.91	0.246
-25	30	40	130	41.20	32.73	7.95	0.95	0.264
-25	30	40	135	41.20	31.34	6.97	0.98	0.277
-25	30	50	120	41.20	38.99	27.62	0.76	0.108
-25	30	50	125	41.20	37.42	16.56	0.79	0.156
-25	30	50	130	41.20	35.90	12.11	0.82	0.190
-25	30	50	135	41.20	34.43	9.70	0.85	0.214
-25	30	50	140	41.20	33.01	8.18	0.88	0.232
-25	30	50	145	41.20	31.62	7.14	0.91	0.246
-25	40	30	110	37.53	35.34	29.41	0.82	0.143
-25	40	30	115	37.53	33.85	17.96	0.87	0.196

Table A1.4 (continued) Derived thermodynamic design data for absorption systems operating on ammonia-lithium nitrate for cooling.

T_{EV}	T_{AB}	T_{CO}	T_{GE}	X_{AB}	X_{GE}	(FR)	$(COP)_{CCL}$	$(COP)_{ECL}$
-25	40	30	120	37.53	32.41	13.19	0.92	0.232
-25	40	30	125	37.53	31.01	10.57	0.96	0.257
-25	40	40	120	37.53	35.64	34.06	0.78	0.107
-25	40	40	125	37.53	34.17	19.56	0.82	0.160
-25	40	40	130	37.53	32.73	14.01	0.85	0.196
-25	40	40	135	37.53	31.34	11.08	0.89	0.221
-25	40	50	130	37.53	35.90	39.29	0.74	0.081
-25	40	50	135	37.53	34.43	21.15	0.77	0.130
-25	40	50	140	37.53	33.01	14.80	0.80	0.165
-25	40	50	145	37.53	31.62	11.57	0.83	0.190
-25	50	30	125	34.17	31.01	27.77	0.85	0.172
-20	30	30	90	43.47	41.84	35.55	0.84	0.136
-20	30	30	95	43.47	40.11	17.82	0.89	0.216
-20	30	30	100	43.47	38.46	12.28	0.95	0.263
-20	30	30	105	43.47	36.87	9.56	1.00	0.293
-20	30	30	110	43.47	35.34	7.95	1.06	0.313
-20	30	30	115	43.47	33.85	6.87	1.11	0.328
-20	30	30	120	43.47	32.41	6.11	1.16	0.338
-20	30	30	125	43.47	31.01	5.53	1.21	0.346
-20	30	40	100	43.47	42.10	42.26	0.79	0.098
-20	30	40	105	43.47	40.39	19.34	0.84	0.174

Table A1.4 (continued) Derived thermodynamic design data for absorption systems operating on ammonia-lithium nitrate for cooling.

T_{EV}	T_{AB}	T_{CU}	T_{GE}	X_{AB}	X_{GE}	(FR)	$(COP)_{CCL}$	$(COP)_{ECL}$
-20	30	40	110	43.47	38.75	12.97	0.88	0.222
-20	30	40	115	43.47	37.17	9.97	0.92	0.253
-20	30	40	120	43.47	35.64	8.22	0.97	0.275
-20	30	40	125	43.47	34.17	7.08	1.01	0.291
-20	30	40	130	43.47	32.73	6.26	1.05	0.302
-20	30	40	135	43.47	31.34	5.66	1.09	0.311
-20	30	50	110	43.47	42.32	49.96	0.76	0.071
-20	30	50	115	43.47	40.62	20.80	0.79	0.142
-20	30	50	120	43.47	38.99	13.60	0.83	0.187
-20	30	50	125	43.47	37.42	10.34	0.86	0.219
-20	30	50	130	43.47	35.90	8.47	0.90	0.241
-20	30	50	135	43.47	34.43	7.25	0.93	0.258
-20	30	60	140	43.47	33.01	6.40	0.96	0.270
-20	30	50	145	43.47	31.62	5.77	0.99	0.280
-20	40	30	100	39.63	38.46	52.45	0.81	0.100
-20	40	30	105	39.63	36.87	22.85	0.87	0.182
-20	40	30	110	39.63	35.34	15.05	0.93	0.232
-20	40	30	115	39.63	33.85	11.44	0.98	0.264
-20	40	30	120	39.63	32.41	9.36	1.03	0.287
-20	40	30	125	39.63	31.01	8.00	1.08	0.303

Table A1.4 (continued) Derived thermodynamic design data for absorption systems operating on ammonia-lithium nitrate for cooling.

T_{EV}	T_{AB}	T_{CO}	T_{GE}	X_{AB}	X_{GE}	(FR)	$(COP)_{CCL}$	$(COP)_{ECL}$
-20	40	40	110	39.63	38.75	69.30	0.77	0.064
-20	40	40	115	39.63	37.17	25.50	0.82	0.142
-20	40	40	120	39.63	35.64	16.13	0.86	0.191
-20	40	40	125	39.63	34.17	12.05	0.90	0.225
-20	40	40	130	39.63	32.73	9.75	0.94	0.250
-20	40	40	135	39.63	31.34	8.28	0.98	0.266
-20	40	50	120	39.63	38.99	94.56	0.74	0.039
-20	40	50	125	39.63	37.42	28.26	0.77	0.111
-20	40	50	130	39.63	35.90	17.18	0.81	0.159
-20	40	50	135	39.63	34.43	12.61	0.84	0.192
-20	40	50	140	39.63	33.01	10.11	0.88	0.216
-20	40	50	145	39.63	31.62	8.54	0.91	0.234
-20	50	30	110	36.14	35.34	79.99	0.79	0.069
-20	50	30	115	36.14	33.85	28.84	0.85	0.154
-20	50	30	120	36.14	32.41	18.09	0.90	0.206
-20	50	30	125	36.14	31.01	13.43	0.95	0.240
-20	50	40	120	36.14	35.64	128.87	0.75	0.036
-20	50	40	125	36.14	34.17	33.31	0.80	0.115
-20	50	40	130	36.14	32.73	19.73	0.84	0.166
-20	50	40	135	36.14	31.34	14.29	0.88	0.201
-20	50	50	130	36.14	35.90	265.72	0.72	0.015

Table A1.4 (continued) Derived thermodynamic design data for absorption systems operating on ammonia-lithium nitrate for cooling.

T_{EV}	T_{AB}	T_{CO}	T_{GE}	X_{AB}	X_{GE}	(FR)	$(COP)_{CCL}$	$(COP)_{ECL}$
-20	50	50	135	36.14	34.43	38.36	0.75	0.087
-20	50	50	140	36.14	33.00	21.37	0.79	0.135
-20	50	50	145	36.14	31.62	15.12	0.82	0.169
-15	30	30	80	45.84	45.55	187.58	0.81	0.036
-15	30	30	85	45.84	43.64	25.69	0.88	0.186
-15	30	30	90	45.84	41.84	14.54	0.95	0.260
-15	30	30	95	45.84	40.11	10.46	1.01	0.302
-15	30	30	100	45.84	38.46	8.34	1.08	0.329
-15	30	30	105	45.84	36.87	7.04	1.14	0.346
-15	30	30	110	45.84	35.33	6.16	1.20	0.358
-15	30	30	115	45.84	33.85	5.52	1.26	0.366
-15	30	30	120	45.84	32.41	5.03	1.31	0.372
-15	30	30	125	45.84	31.01	4.65	1.37	0.376
-15	30	40	95	45.84	43.90	28.91	0.83	0.142
-15	30	40	100	45.84	42.10	15.50	0.88	0.214
-15	30	40	105	45.84	40.39	10.94	0.93	0.258
-15	30	40	110	45.84	38.75	8.64	0.98	0.286
-15	30	40	115	45.84	37.17	7.25	1.03	0.306
-15	30	40	120	45.84	35.64	6.31	1.07	0.319
-15	30	40	125	45.84	34.17	5.64	1.12	0.330
-15	30	40	130	45.84	32.73	5.13	1.16	0.337

Table A1.4 (continued) Derived thermodynamic design data for absorption systems operating on ammonia-lithium nitrate for cooling.

T_{EV}	T_{AB}	T_{CO}	T_{GE}	X_{AB}	X_{GE}	(FR)	$(COP)_{CCL}$	$(COP)_{ECL}$
-15	30	40	135	45.84	31.34	4.74	1.21	0.342
-15	30	50	105	45.84	44.10	32.14	0.79	0.109
-15	30	50	110	45.84	42.32	16.39	0.83	0.177
-15	30	50	115	45.84	40.62	11.38	0.87	0.220
-15	30	50	120	45.84	38.99	8.91	0.91	0.249
-15	30	50	125	45.84	37.42	7.43	0.95	0.270
-15	30	50	130	45.84	35.90	6.45	0.99	0.284
-15	30	50	135	45.84	34.43	5.75	1.02	0.295
-15	30	50	140	45.84	33.01	5.22	1.06	0.304
-15	30	50	145	45.84	31.62	4.81	1.09	0.310
-15	40	30	95	41.79	40.11	35.71	0.86	0.146
-15	40	30	100	41.79	38.46	18.48	0.92	0.223
-15	40	30	105	41.79	36.87	12.83	0.99	0.268
-15	40	30	110	41.79	35.34	10.02	1.05	0.298
-15	40	30	115	41.79	33.85	8.33	1.11	0.317
-15	40	30	120	41.79	32.41	7.21	1.17	0.331
-15	40	30	125	41.79	31.01	6.40	1.22	0.341
-15	40	40	105	41.79	40.39	42.62	0.81	0.104
-15	40	40	110	41.79	38.75	20.15	0.86	0.179
-15	40	40	115	41.79	37.17	13.60	0.91	0.225
-15	40	40	120	41.79	35.64	10.47	0.96	0.256

Table A1.4 (continued) Derived thermodynamic design data for absorption systems operating on ammonia-lithium nitrate for cooling.

T_{EV}	T_{AB}	T_{CO}	T_{GE}	X_{AB}	X_{GE}	(FR)	$(COP)_{CCL}$	$(COP)_{ECL}$
-15	40	40	125	41.79	34.17	8.64	1.00	0.277
-15	40	40	130	41.79	32.73	7.43	1.05	0.293
-15	40	40	135	41.79	31.39	6.57	1.09	0.304
-15	40	50	115	41.79	40.62	50.71	0.77	0.074
-15	40	50	120	41.79	38.99	21.78	0.81	0.144
-15	40	50	125	41.79	37.42	14.32	0.85	0.189
-15	40	50	130	41.79	35.90	10.89	0.89	0.220
-15	40	50	135	41.79	34.43	8.92	0.92	0.242
-15	40	50	140	41.79	33.01	7.63	0.96	0.258
-15	40	50	145	41.79	31.62	6.73	1.00	0.271
-15	50	30	105	38.15	36.87	49.34	0.83	0.113
-15	50	30	110	38.15	35.34	22.98	0.90	0.193
-15	50	30	115	38.15	33.85	15.39	0.96	0.240
-15	50	30	120	38.15	32.41	11.77	1.02	0.272
-15	50	30	125	38.15	31.01	9.66	1.08	0.293
-15	50	40	115	38.15	37.17	64.13	0.79	0.074
-15	50	40	120	38.15	35.64	25.69	0.84	0.149
-15	50	40	125	38.15	34.17	16.53	0.88	0.198
-15	50	40	130	38.15	32.73	12.42	0.93	0.230
-15	50	40	135	38.15	31.34	10.08	0.98	0.253

Table A1.4 (continued) Derived thermodynamic design data for absorption systems operating on ammonia-lithium nitrate for cooling.

T_{EV}	T_{AB}	T_{CO}	T_{GE}	X_{AB}	X_{GE}	(FR)	$(COP)_{CCL}$	$(COP)_{ECL}$
-15	50	50	125	38.15	37.42	85.59	0.75	0.047
-15	50	50	130	38.15	35.90	28.53	0.79	0.117
-15	50	50	135	38.15	34.43	17.65	0.83	0.163
-15	50	50	140	38.15	33.01	13.03	0.87	0.195
-15	50	50	145	38.15	31.62	10.47	0.90	0.219
-10	30	30	75	48.31	47.57	69.96	0.85	0.096
-10	30	30	80	48.31	45.55	19.67	0.93	0.239
-10	30	30	85	48.31	43.64	12.06	1.01	0.306
-10	30	30	90	48.31	41.84	8.98	1.09	0.343
-10	30	30	95	48.31	40.11	7.30	1.16	0.366
-10	30	30	100	48.31	38.46	6.25	1.23	0.380
-10	30	30	105	48.31	36.87	5.52	1.31	0.390
-10	30	30	110	48.31	35.34	4.98	1.37	0.396
-10	30	30	115	48.31	33.85	4.57	1.44	0.400
-10	30	30	120	48.31	32.41	4.25	1.51	0.403
-10	30	30	125	48.31	31.01	3.99	1.57	0.404
-10	30	40	85	48.31	47.79	98.95	0.81	0.056
-10	30	40	90	48.31	45.79	21.43	0.87	0.188
-10	30	40	95	48.31	43.90	12.70	0.93	0.256
-10	30	40	100	48.31	42.10	9.32	0.99	0.296
-10	30	40	105	48.31	40.39	7.52	1.04	0.321

Table A1.4 (continued) Derived thermodynamic design data for absorption systems operating on ammonia-lithium nitrate for cooling.

T_{EV}	T_{AB}	T_{CO}	T_{GE}	X_{AB}	X_{GE}	(FR)	$(COP)_{CCL}$	$(COP)_{ECL}$
-10	30	40	110	48.31	38.75	6.40	1.10	0.338
-10	30	40	115	48.31	37.17	5.64	1.15	0.350
-10	30	40	120	48.31	35.64	5.08	1.21	0.358
-10	30	40	125	48.31	34.17	4.65	1.26	0.363
-10	30	40	130	48.31	32.73	4.32	1.31	0.367
-10	30	40	135	48.31	31.34	4.05	1.35	0.370
-10	30	50	95	48.31	47.96	145.19	0.77	0.031
-10	30	50	100	48.31	45.97	23.06	0.82	0.150
-10	30	50	115	48.31	40.62	7.62	0.96	0.282
-10	30	50	120	48.31	38.99	6.54	1.00	0.300
-10	30	50	125	48.31	37.42	5.74	1.05	0.313
-10	30	50	130	48.31	35.90	5.16	1.09	0.322
-10	30	50	135	48.31	34.43	4.72	1.13	0.329
-10	30	50	140	48.31	33.01	4.38	1.17	0.334
-10	30	50	145	48.31	31.62	4.10	1.21	0.338
-10	40	30	85	44.02	43.64	151.03	0.83	0.049
-10	40	30	90	44.02	41.84	26.68	0.91	0.195
-10	40	30	95	44.02	40.11	15.34	0.98	0.266
-10	40	30	100	44.02	38.46	11.08	1.06	0.307
-10	40	30	105	44.02	36.87	8.83	1.13	0.332
-10	40	30	110	44.02	35.34	7.45	1.20	0.350

Table A1.4 (continued) Derived thermodynamic design data for absorption systems operating on ammonia-lithium nitrate for cooling.

T_{EV}	T_{AB}	T_{CO}	T_{GE}	X_{AB}	X_{GE}	(FR)	$(COP)_{CCL}$	$(COP)_{ECL}$
-10	40	30	115	44.02	33.85	6.51	1.27	0.361
-10	40	30	120	44.02	32.41	5.82	1.34	0.369
-10	40	30	125	44.02	31.01	5.30	1.40	0.374
-10	40	40	95	44.02	43.90	467.20	0.79	0.013
-10	40	40	100	44.02	42.10	30.25	0.85	0.146
-10	40	40	105	44.02	40.39	16.44	0.90	0.217
-10	40	40	110	44.02	38.75	11.63	0.96	0.260
-10	40	40	115	44.02	37.17	9.18	1.02	0.288
-10	40	40	120	44.02	35.64	7.69	1.07	0.307
-10	40	40	125	44.02	34.17	6.70	1.12	0.320
-10	40	40	130	44.02	32.73	5.96	1.18	0.330
-10	40	40	135	44.02	31.34	5.42	1.23	0.337
-10	40	50	110	44.02	42.32	33.96	0.80	0.111
-10	40	50	115	44.02	40.62	17.47	0.85	0.178
-10	40	50	120	44.02	38.99	12.13	0.89	0.220
-10	40	50	125	44.02	37.42	9.49	0.94	0.249
-10	40	50	130	44.02	35.90	7.90	0.98	0.270
-10	40	50	135	44.02	34.43	6.84	1.02	0.284
-10	40	50	140	44.02	33.01	6.09	1.06	0.295
-10	40	50	145	44.02	31.62	5.52	1.10	0.304

Table A1.4 (continued) Derived thermodynamic design data for absorption systems operating on ammonia-lithium nitrate for cooling.

T_{EV}	T_{AB}	T_{CO}	T_{GE}	X_{AB}	X_{GE}	(FR)	$(COP)_{CCL}$	$(COP)_{ECL}$
-10	50	30	95	40.20	40.11	670.01	0.80	0.012
-10	50	30	100	40.20	38.46	35.33	0.88	0.159
-10	50	30	105	40.20	36.87	18.95	0.96	0.233
-10	50	30	110	40.20	35.33	13.29	1.03	0.277
-10	50	30	115	40.20	33.85	10.42	1.10	0.304
-10	50	30	120	40.20	32.41	8.67	1.17	0.323
-10	50	30	125	40.20	31.01	7.50	1.24	0.336
-10	50	40	110	40.20	38.75	42.17	0.82	0.112
-10	50	40	115	40.20	37.17	20.72	0.88	0.185
-10	50	40	120	40.20	35.64	14.12	0.94	0.230
-10	50	40	125	40.20	34.17	10.91	0.99	0.260
-10	50	40	130	40.20	32.73	9.01	1.04	0.281
-10	50	40	135	40.20	31.34	7.75	1.10	0.296
-10	50	50	120	40.20	38.99	50.27	0.78	0.080
-10	50	50	125	40.20	37.42	22.49	0.83	0.148
-10	50	50	130	40.20	35.90	14.91	0.87	0.192
-10	50	50	135	40.20	34.43	11.37	0.91	0.222
-10	50	50	140	40.20	33.01	9.31	0.96	0.244
-10	50	50	145	40.20	31.62	7.97	1.00	0.260

Table A1.4 (continued) Derived thermodynamic design data for absorption systems operating on ammonia-lithium nitrate for cooling.

T_{EV}	T_{AB}	T_{CO}	T_{GE}	X_{AB}	X_{GE}	(FR)	$(COP)_{CCL}$	$(COP)_{ECL}$
-5	30	30	70	50.94	49.72	41.36	0.89	0.162
-5	30	30	75	50.94	47.56	15.55	0.99	0.296
-5	30	30	80	50.94	45.55	10.10	1.09	0.356
-5	30	30	85	50.94	43.64	7.73	1.18	0.388
-5	30	30	90	50.94	41.84	6.39	1.27	0.406
-5	30	30	95	50.94	40.11	5.53	1.35	0.417
-5	30	30	100	50.94	38.46	4.93	1.44	0.424
-5	30	30	105	50.94	36.87	4.50	1.52	0.428
-5	30	30	110	50.94	35.33	4.15	1.60	0.430
-5	30	30	115	50.94	33.85	3.87	1.68	0.431
-5	30	30	120	50.94	32.41	3.65	1.75	0.431
-5	30	30	125	50.94	31.01	3.46	1.83	0.431
-5	30	40	80	50.94	49.92	49.46	0.84	0.111
-5	30	40	85	50.94	47.79	16.58	0.92	0.239
-5	30	40	90	50.94	45.79	10.52	0.98	0.302
-5	30	40	95	50.94	43.90	7.97	1.05	0.337
-5	30	40	100	50.94	42.10	6.55	1.12	0.359
-5	30	40	105	50.94	40.39	5.65	1.18	0.373
-5	30	40	110	50.94	38.75	5.03	1.24	0.382
-5	30	40	115	50.94	37.17	4.56	1.31	0.388
-5	30	40	120	50.94	35.64	4.21	1.36	0.392

Table A1.4 (continued) Derived thermodynamic design data for absorption systems operating on ammonia-lithium nitrate for cooling.

T_{EV}	T_{AB}	T_{CO}	T_{GE}	X_{AB}	X_{GE}	(FR)	$(COP)_{CCL}$	$(COP)_{ECL}$
-5	30	40	125	50.94	35.64	4.21	1.36	0.392
-5	30	40	130	50.94	32.73	3.70	1.48	0.396
-5	30	40	135	50.94	31.34	3.50	1.53	0.397
-5	30	50	90	50.94	50.07	57.85	0.81	0.078
-5	30	50	95	50.94	47.96	17.46	0.86	0.195
-5	30	50	100	50.94	45.97	10.88	0.91	0.257
-5	30	50	105	50.94	44.10	8.17	0.97	0.293
-5	30	50	110	50.94	42.32	6.69	1.02	0.317
-5	30	50	115	50.94	40.62	5.76	1.07	0.333
-5	30	50	120	50.94	38.99	5.11	1.12	0.343
-5	30	50	125	50.94	37.42	4.63	1.16	0.351
-5	30	50	130	50.94	35.90	4.26	1.21	0.356
-5	30	50	135	50.94	34.43	3.97	1.25	0.360
-5	30	50	140	50.94	33.10	3.74	1.30	0.363
-5	30	50	145	50.94	31.62	3.54	1.34	0.364
-5	40	30	80	46.33	45.55	69.28	0.87	0.108
-5	40	30	85	46.33	43.64	20.95	0.96	0.247
-5	40	30	90	46.33	41.84	12.94	1.06	0.318
-5	40	30	95	46.33	40.11	9.63	1.14	0.348
-5	40	30	100	46.33	38.46	7.82	1.23	0.369
-5	40	30	105	46.33	36.87	6.67	1.32	0.383

Table A1.4 (continued) Derived thermodynamic design data for absorption systems operating on ammonia-lithium nitrate for cooling.

T_{EV}	T_{AB}	T_{CO}	T_{GE}	X_{AB}	X_{GE}	(FR)	$(COP)_{CCL}$	$(COP)_{ECL}$
-5	40	30	110	46.33	35.34	5.88	1.40	0.392
-5	40	30	115	46.33	33.85	5.30	1.48	0.398
-5	40	30	120	46.33	32.41	4.85	1.56	0.402
-5	40	30	125	46.33	31.01	4.50	1.64	0.404
-5	40	40	90	46.33	45.76	99.00	0.82	0.061
-5	40	40	95	46.33	43.90	23.03	0.89	0.191
-5	40	40	100	46.33	42.10	13.69	0.96	0.258
-5	40	40	105	46.33	40.39	10.03	1.02	0.297
-5	40	40	110	46.33	38.75	8.08	1.09	0.322
-5	40	40	115	46.33	37.17	6.86	1.15	0.338
-5	40	40	120	46.33	35.64	6.02	1.21	0.350
-5	40	40	125	46.33	34.17	5.41	1.27	0.358
-5	40	40	130	46.33	32.73	4.95	1.33	0.363
-5	40	40	135	46.33	31.34	4.58	1.39	0.367
-5	40	50	100	46.33	45.97	149.59	0.78	0.033
-5	40	50	105	46.33	44.10	25.01	0.84	0.150
-5	40	50	110	46.33	42.32	14.37	0.89	0.214
-5	40	50	115	46.33	40.62	10.39	0.94	0.254
-5	40	50	120	46.33	38.99	8.31	0.99	0.281
-5	40	50	125	46.33	37.42	7.02	1.04	0.299
-5	40	50	130	46.33	35.90	6.15	1.09	0.312

Table A1.4 (continued) Derived thermodynamic design data for absorption systems operating on ammonia-lithium nitrate for cooling.

T_{EV}	T_{AB}	T_{CO}	T_{GE}	X_{AB}	X_{GE}	(FR)	$(COP)_{CCL}$	$(COP)_{ECL}$
-5	40	50	135	46.33	34.43	5.51	1.14	0.321
-5	40	50	140	46.33	33.01	5.03	1.18	0.328
-5	40	50	145	46.33	31.62	4.65	1.22	0.333
-5	50	30	90	42.31	41.84	122.51	0.84	0.066
-5	50	30	95	42.31	40.11	27.24	0.94	0.208
-5	50	30	100	42.31	38.46	15.98	1.03	0.276
-5	50	30	105	42.31	36.87	11.60	1.11	0.315
-5	50	30	110	42.31	35.34	9.27	1.20	0.339
-5	50	30	115	42.31	33.85	7.82	1.28	0.355
-5	50	30	120	42.31	32.41	6.83	1.36	0.366
-5	50	30	125	42.31	31.01	6.10	1.44	0.373
-5	50	40	100	42.31	42.10	277.82	0.80	0.023
-5	50	40	105	42.31	40.39	31.04	0.87	0.154
-5	50	40	110	42.31	38.75	17.20	0.93	0.223
-5	50	40	115	42.31	37.17	12.22	1.00	0.265
-5	50	40	120	42.31	35.64	9.65	1.06	0.292
-5	50	40	125	42.31	34.17	8.08	1.12	0.310
-5	50	40	130	42.31	32.73	7.02	1.18	0.323
-5	50	40	135	42.31	31.34	6.26	1.24	0.333
-5	50	50	115	42.31	40.62	35.08	0.82	0.115
-5	50	50	120	42.31	38.99	18.36	0.87	0.181

Table A1.4 (continued) Derived thermodynamic design data for absorption systems operating on ammonia-lithium nitrate for cooling.

T_{EV}	T_{AB}	T_{CO}	T_{GE}	X_{AB}	X_{GE}	(FR)	$(COP)_{CCL}$	$(COP)_{ECL}$
-5	50	50	125	42.31	37.42	12.79	0.92	0.223
-5	50	50	130	42.31	35.90	10.00	0.97	0.251
-5	50	50	135	42.31	34.43	8.32	1.02	0.271
-5	50	50	140	42.31	33.01	7.20	1.06	0.286
-5	50	50	145	42.31	31.62	6.40	1.11	0.297
0	30	30	65	53.75	52.05	28.19	0.94	0.236
0	30	30	70	53.75	49.72	12.49	1.06	0.358
0	30	30	75	53.75	47.57	8.48	1.18	0.409
0	30	30	80	53.75	45.55	6.64	1.29	0.435
0	30	30	85	53.75	43.64	5.58	1.40	0.448
0	30	30	90	53.75	41.84	4.88	1.50	0.456
0	30	30	95	53.75	40.11	4.39	1.61	0.460
0	30	30	100	53.75	38.46	4.03	1.71	0.462
0	30	30	105	53.75	36.87	3.74	1.81	0.462
0	30	30	110	53.75	35.34	3.51	1.90	0.461
0	30	30	115	53.75	33.85	3.32	1.99	0.460
0	30	30	120	53.75	32.41	3.17	2.08	0.458
0	30	30	125	53.75	31.01	3.03	2.17	0.456
0	30	40	75	53.75	52.23	31.43	0.88	0.173
0	30	40	80	53.75	49.92	13.10	0.97	0.295
0	30	40	85	53.75	47.79	8.76	1.05	0.351

Table A1.4 (continued) Derived thermodynamic design data for absorption systems operating on ammonia-lithium nitrate for cooling.

T_{EV}	T_{AB}	T_{CO}	T_{GE}	X_{AB}	X_{GE}	(FR)	$(COP)_{CCL}$	$(COP)_{ECL}$
0	30	40	90	53.75	45.79	6.81	1.13	0.381
0	30	40	95	53.75	43.90	5.70	1.21	0.399
0	30	40	100	53.75	42.10	4.97	1.28	0.410
0	30	40	105	53.75	40.39	4.46	1,35	0.416
0	30	40	110	53.75	38.75	4.08	1.43	0.420
0	30	40	115	53.75	37.17	3.79	1.50	0.423
0	30	40	120	53.75	35.64	3.56	1.56	0.424
0	30	40	125	53.75	34.17	3.36	1.63	0.424
0	30	40	130	53.75	32.73	3.20	1.70	0.423
0	30	40	135	53.75	31.34	3.06	1.76	0.422
0	30	50	85	53.75	52.36	34.19	0.84	0.130
0	30	50	90	53.75	50.07	13.59	0.90	0.245
0	30	50	95	53.75	47.96	8.99	0.96	0.302
0	30	50	100	53.75	45.79	6.95	1.03	0.334
0	30	50	105	53.75	44.10	5.79	1.08	0.355
0	30	50	110	53.75	42.32	5.05	1.14	0.368
0	30	50	115	53.75	40.62	4.52	1.20	0.376
0	30	50	120	53.75	38.99	4.13	1.25	0.382
0	30	50	125	53.75	37.42	3.83	1.30	0.386
0	30	50	130	53.75	35.90	3.59	1.36	0.388
0	30	50	135	53.75	34.43	3.40	1.41	0.389

Table A1.4 (continued) Derived thermodynamic design data for absorption systems operating on ammonia-lithium nitrate for cooling.

T_{EV}	T_{AB}	T_{CO}	T_{GE}	X_{AB}	X_{GE}	(FR)	$(COP)_{CCL}$	$(COP)_{ECL}$
0	30	50	140	53.75	33.01	3.23	1.45	0.390
0	30	50	145	53.75	31.62	3.09	1.50	0.390
0	40	30	75	48.76	47.57	43.82	0.92	0.173
0	40	30	80	48.76	45.55	16.94	1.03	0.303
0	40	30	85	48.76	43.64	11.01	1.14	0.360
0	40	30	90	48.76	41.84	8.40	1.25	0.391
0	40	30	95	48.76	40.11	6.92	1.36	0.408
0	40	30	100	48.76	38.46	5.97	1.46	0.419
0	40	30	105	48.76	36.87	5.31	1.57	0.425
0	40	30	110	48.76	35.34	4.82	1.66	0.429
0	40	30	115	48.76	33.85	4.44	1.76	0.431
0	40	30	120	48.76	32.41	4.13	1.85	0.432
0	40	30	125	48.76	31.01	3.89	1.94	0.431
0	40	40	85	48.76	47.79	53.57	0.86	0.114
0	40	40	90	48.76	45.79	18.22	0.94	0.240
0	40	40	95	48.76	43.90	11.53	1.02	0.302
0	40	40	100	48.76	42.10	8.90	1.10	0.337
0	40	40	105	48.76	40.39	7.12	1.17	0.358
0	40	40	110	48.76	38.75	6.12	1.25	0.372
0	40	40	115	48.76	37.17	5.42	1.32	0.381
0	40	40	120	48.76	35.64	4.91	1.39	0.387

Table A1.4 (continued) Derived thermodynamic design data for absorption systems operating on ammonia-lithium nitrate for cooling.

T_{EV}	T_{AB}	T_{CO}	T_{GE}	X_{AB}	X_{GE}	(FR)	$(COP)_{CCL}$	$(COP)_{ECL}$
0	40	40	125	48.76	34.17	4.51	1.46	0.391
0	40	40	130	48.76	32.73	4.20	1.52	0.394
0	40	40	135	48.76	31.34	3.94	1.59	0.395
0	40	50	95	48.76	47.96	64.61	0.82	0.077
0	40	50	100	48.76	45.97	19.37	0.88	0.192
0	40	50	105	48.76	44.10	11.99	0.94	0.254
0	40	50	110	48.76	42.32	8.95	1.00	0.290
0	40	50	115	48.76	40.62	7.29	1.06	0.314
0	40	50	120	48.76	38.99	6.24	1.11	0.330
0	40	50	125	48.76	37.42	5.52	1.17	0.341
0	40	50	130	48.76	35.90	4.99	1.22	0.349
0	40	50	135	48.76	34.43	4.58	1.27	0.354
0	40	50	140	48.76	33.01	4.25	1.32	0.358
0	40	50	145	48.76	31.62	3.99	1.37	0.361
0	50	30	85	44.49	43.64	66.40	0.89	0.126
0	50	30	90	44.49	41.84	21.90	1.00	0.260
0	50	30	95	44.49	40.11	13.67	1.11	0.321
0	50	30	100	44.49	38.46	10.20	1.22	0.355
0	50	30	105	44.49	36.87	8.28	1.32	0.375
0	50	30	110	44.49	35.34	7.06	1.43	0.388
0	50	30	115	44.49	33.85	6.22	1.52	0.396

Table A1.4 (continued) Derived thermodynamic design data for absorption systems operating on ammonia-lithium nitrate for cooling.

T_{EV}	T_{AB}	T_{CO}	T_{GE}	X_{AB}	X_{GE}	(FR)	$(COP)_{CCL}$	$(COP)_{ECL}$
0	50	30	120	44.49	32.41	5.59	1.62	0.402
0	50	30	125	44.49	31.01	5.12	1.72	0.405
0	50	40	95	44.49	43.90	94.19	0.84	0.070
0	50	40	100	44.49	42.10	24.23	0.92	0.198
0	50	40	105	44.49	40.39	14.53	0.99	0.263
0	50	40	110	44.49	38.75	10.67	1.07	0.301
0	50	40	115	44.49	37.17	8.58	1.14	0.325
0	50	40	120	44.49	35.64	7.27	1.22	0.341
0	50	40	125	44.49	34.17	6.38	1.29	0.352
0	50	40	130	44.49	32.73	5.72	1.36	0.360
0	50	40	135	44.49	31.34	5.22	1.42	0.365
0	50	50	105	44.49	44.10	141.88	0.79	0.038
0	50	50	110	44.49	42.32	26.53	0.86	0.153
0	50	50	115	44.49	40.62	15.33	0.92	0.216
0	50	50	120	44.49	38.99	11.09	0.97	0.256
0	50	50	125	44.49	37.42	8.85	1.03	0.282
0	50	50	130	44.49	35.90	7.46	1.08	0.300
0	50	50	135	44.49	34.43	6.52	1.14	0.312
0	50	50	140	44.49	33.01	5.83	1.19	0.322
0	50	50	145	44.49	31.62	5.31	1.24	0.329

Table A1.4 (continued) Derived thermodynamic design data for absorption systems operating on ammonia-lithium nitrate for cooling.

T_{EV}	T_{AB}	T_{CO}	T_{GE}	X_{AB}	X_{GE}	(FR)	$(COP)_{CH}$	$(COP)_{EH}$
20	50	50	90	54.37	50.07	11.62	2.076	1.346
20	50	50	100	54.37	45.97	6.43	2.309	1.415
20	50	50	110	54.37	42.32	4.79	2.530	1.435
20	50	50	120	54.37	38.99	3.97	2.740	1.441
20	50	50	130	54.37	35.90	3.47	2.939	1.441
20	50	50	140	54.37	33.01	3.14	3.128	1.438
20	50	50	150	54.37	30.27	2.89	3.309	1.434
20	50	60	100	54.37	50.17	11.87	1.982	1.286
20	50	60	110	54.37	46.11	6.52	2.148	1.363
20	50	60	120	54.37	42.48	4.84	2.305	1.389
20	50	60	130	54.37	39.18	4.00	2.454	1.399
20	50	60	140	54.37	36.11	3.50	2.596	1.403
20	50	60	150	54.37	33.23	3.16	2.732	1.402
20	50	60	160	54.37	30.51	2.91	2.861	1.400
20	50	70	110	54.37	50.22	12.00	1.918	1.240
20	50	70	120	54.37	46.20	6.58	2.044	1.318
20	50	70	130	54.37	42.60	4.88	2.163	1.348
20	50	70	140	54.37	39.32	4.03	2.277	1.361
20	50	70	150	54.37	36.28	3.52	2.385	1.367
20	50	70	160	54.37	33.41	3.18	2.489	1.369
20	50	70	170	54.37	30.70	2.93	2.587	1.368
20	60	50	100	49.46	45.97	15.48	2.047	1.294
20	60	50	110	49.46	42.32	8.07	2.275	1.372
20	60	50	120	49.46	38.99	5.83	2.491	1.399
20	60	50	130	49.46	35.90	4.73	2.696	1.408
20	60	50	140	49.46	33.01	4.07	2.892	1.411

Table A1.5 Derived thermodynamic design data for absorption systems operating on ammonia-lithium nitrate for heating.

... continued

T_{EV}	T_{AB}	T_{CO}	T_{GE}	X_{AB}	X_{GE}	(FR)	$(COP)_{CH}$	$(COP)_{EH}$
20	60	50	150	49.46	30.27	3.63	3.078	1.411
20	60	60	110	49.46	46.11	16.07	1.956	1.237
20	60	60	120	49.46	42.48	8.24	2.118	1.320
20	60	60	130	49.46	39.18	5.91	2.272	1.352
20	60	60	140	49.46	36.11	4.79	2.419	1.367
20	60	60	150	49.46	33.23	4.11	2.559	1.373
20	60	60	160	49.46	30.51	3.67	2.692	1.375
20	60	70	120	49.46	46.20	16.49	1.895	1.194
20	60	70	130	49.46	42.60	8.37	2.018	1.276
20	60	70	140	49.46	39.32	5.98	2.135	1.312
20	60	70	150	49.46	36.28	4.83	2.247	1.329
20	60	70	160	49.46	33.41	4.15	2.353	1.338
20	60	70	170	49.46	30.70	3.69	2.455	1.342
20	70	50	110	45.25	42.32	19.65	2.020	1.254
20	70	50	120	45.25	38.99	9.74	2.243	1.338
20	70	50	130	45.25	35.90	6.85	2.454	1.369
20	70	50	140	45.25	33.01	5.47	2.655	1.382
20	70	50	150	45.25	30.27	4.65	2.847	1.387
20	70	60	120	45.25	42.48	20.77	1.932	1.199
20	70	60	130	45.25	39.18	10.01	2.091	1.287
20	70	60	140	45.25	36.11	6.99	2.242	1.323
20	70	60	150	45.25	33.23	5.55	2.385	1.341
20	70	60	160	45.25	30.51	4.71	2.523	1.349
20	70	70	130	45.25	42.60	21.66	1.872	1.159
20	70	70	140	45.25	39.32	10.23	1.993	1.244
20	70	70	150	45.25	36.28	7.10	2.108	1.283

Table A1.5 (continued) Derived thermodynamic design data for absorption systems operating on ammonia-lithium nitrate for heating.

T_{EV}	T_{AB}	T_{CO}	T_{GE}	X_{AB}	X_{GE}	(FR)	$(COP)_{CH}$	$(COP)_{EH}$
20	70	70	160	45.25	33.41	5.62	2.218	1.303
20	70	70	170	45.25	30.70	4.76	2.323	1.315
20	80	50	120	41.52	38.99	24.13	1.994	1.222
20	80	50	130	41.52	35.90	11.42	2.212	1.310
20	80	50	140	41.52	33.01	7.87	2.419	1.344
20	80	50	150	41.52	30.27	6.20	2.616	1.360
20	80	60	130	41.52	39.18	26.01	1.909	1.169
20	80	60	140	41.52	36.11	11.82	2.064	1.260
20	80	60	150	41.52	33.23	8.06	2.212	1.299
20	80	60	160	41.52	30.51	6.31	2.353	1.319
20	80	70	140	41.52	39.32	27.66	1.851	1.131
20	80	70	150	41.52	36.28	12.16	1.970	1.218
20	80	70	160	41.52	33.41	8.22	2.083	1.260
20	80	70	170	41.52	30.70	6.41	2.191	1.282
20	90	50	130	38.12	35.90	28.95	1.969	1.196
20	90	50	140	38.12	33.01	13.11	2.182	1.287
20	90	50	150	38.12	30.27	8.88	2.385	1.324
20	90	60	140	38.12	36.11	31.87	1.887	1.145
20	90	60	150	38.12	33.23	13.68	2.039	1.237
20	90	60	160	38.12	30.51	9.13	2.184	1.279
20	90	70	150	38.12	36.28	34.62	1.831	1.110
20	90	70	160	38.12	33.41	14.16	1.947	1.197
20	90	70	170	38.12	30.70	9.35	2.058	1.241
20	100	50	140	34.97	33.01	34.11	1.946	1.174
20	100	50	150	34.97	30.27	14.82	2.154	1.268
20	100	60	150	34.97	33.23	38.41	1.866	1.125

Table A1.5 (continued) Derived thermodynamic design data for absorption systems operating on ammonia-lithium nitrate for heating.

T_{EV}	T_{AB}	T_{CO}	T_{GE}	X_{AB}	X_{GE}	(FR)	$(COP)_{CH}$	$(COP)_{EH}$
20	100	60	160	34.97	30.51	15.56	2.015	1.219
20	100	70	160	34.97	33.41	42.73	1.812	1.092
20	100	70	170	34.97	30.70	16.22	1.926	1.180
30	60	50	90	54.59	50.07	11.06	2.252	1.412
30	60	50	100	54.59	45.97	6.27	2.625	1.464
30	60	50	110	54.59	42.32	4.70	2.978	1.476
30	60	50	120	54.59	38.99	3.91	3.313	1.476
30	60	50	130	54.59	35.90	3.43	3.632	1.471
30	60	50	140	54.59	33.01	3.10	3.935	1.465
30	60	50	150	54.59	30.27	2.87	4.223	1.459
30	60	60	100	54.59	50.17	11.29	2.083	1.337
30	60	60	110	54.59	46.11	6.36	2.319	1.404
30	60	60	120	54.59	42.48	4.75	2.542	1.424
30	60	60	130	54.59	39.18	3.95	2.754	1.430
30	60	60	140	54.59	36.11	3.46	2.956	1.430
30	60	60	150	54.59	33.23	3.13	3.149	1.427
30	60	60	160	54.59	30.51	2.89	3.333	1.423
30	60	70	110	54.59	50.22	11.40	1.989	1.280
30	60	70	120	54.59	46.20	6.41	2.156	1.352
30	60	70	130	54.59	42.60	4.79	2.316	1.378
30	60	70	140	54.59	39.32	3.98	2.467	1.388
30	60	70	150	54.59	36.28	3.48	2.612	1.391
30	60	70	160	54.59	33.41	3.14	2.749	1.391
30	60	70	170	54.59	30.70	2.90	2.881	1.389
30	70	50	100	49.72	45.97	14.41	2.218	1.361
30	70	50	110	49.72	42.32	7.79	2.582	1.423

Table A1.5 (continued) Derived thermodynamic design data for absorption systems operating on ammonia-lithium nitrate for heating.

T_{EV}	T_{AB}	T_{CO}	T_{GE}	X_{AB}	X_{GE}	(FR)	$(COP)_{CH}$	$(COP)_{EH}$
30	70	50	120	49.72	38.99	5.68	2.927	1.440
30	70	50	130	49.72	35.90	4.64	3.256	1.443
30	70	50	140	49.72	33.01	4.01	3.568	1.442
30	70	50	150	49.72	30.27	3.58	3.865	1.438
30	70	60	110	49.72	46.11	14.92	2.055	1.287
30	70	60	120	49.72	42.48	7.95	2.285	1.362
30	70	60	130	49.72	39.18	5.77	2.504	1.388
30	70	60	140	49.72	36.11	4.69	2.712	1.398
30	70	60	150	49.72	33.23	4.05	2.910	1.401
30	70	60	160	49.72	30.51	3.62	3.099	1.400
30	70	70	120	49.72	46.20	15.27	1.964	1.233
30	70	70	130	49.72	42.60	8.07	2.128	1.311
30	70	70	140	49.72	39.32	5.83	2.284	1.342
30	70	70	150	49.72	36.28	4.74	2.433	1.356
30	70	70	160	49.72	33.41	4.08	2.574	1.362
30	70	70	170	49.72	30.70	3.64	2.710	1.365
30	80	50	110	45.55	42.32	17.86	2.187	1.321
30	80	50	120	45.55	38.99	9.30	2.542	1.390
30	80	50	130	45.55	35.90	6.65	2.880	1.411
30	80	50	140	45.55	33.01	5.34	3.201	1.418
30	80	50	150	45.55	30.27	4.56	3.507	1.419
30	80	60	120	45.55	42.48	18.78	2.028	1.249
30	80	60	130	45.55	39.18	9.55	2.253	1.329
30	80	60	140	45.55	36.11	6.77	2.467	1.359
30	80	60	150	45.55	33.23	5.42	2.671	1.372
30	80	60	160	45.55	30.51	4.62	2.866	1.377

Table A1.5 (continued) Derived thermodynamic design data for absorption systems operating on ammonia-lithium nitrate for heating.

T_{EV}	T_{AB}	T_{CO}	T_{GE}	X_{AB}	X_{GE}	(FR)	$(COP)_{CH}$	$(COP)_{EH}$
30	80	70	130	45.55	42.60	19.51	1.940	1.197
30	80	70	140	45.55	39.32	9.75	2.100	1.278
30	80	70	150	45.55	36.28	6.87	2.254	1.313
30	80	70	160	45.55	33.41	5.49	2.400	1.330
30	80	70	170	45.55	30.70	4.67	2.539	1.339
30	90	50	120	41.84	38.99	21.42	2.156	1.290
30	90	50	130	41.84	35.90	10.80	2.504	1.362
30	90	50	140	41.84	33.01	7.59	2.834	1.387
30	90	50	150	41.84	30.27	6.03	3.149	1.396
30	90	60	130	41.84	39.18	22.88	2.002	1.218
30	90	60	140	41.84	36.11	11.16	2.223	1.302
30	90	60	150	41.84	33.23	7.76	2.433	1.335
30	90	60	160	41.84	30.51	6.13	2.633	1.350
30	90	70	140	41.84	39.32	24.13	1.917	1.169
30	90	70	150	41.84	36.28	11.46	2.074	1.252
30	90	70	160	41.84	33.41	7.91	2.225	1.290
30	90	70	170	41.84	30.70	6.22	2.368	1.309
30	100	50	130	38.46	35.90	25.07	2.128	1.263
30	100	50	140	38.46	33.01	12.29	2.467	1.340
30	100	50	150	38.46	30.27	8.51	2.791	1.367
30	100	60	140	38.46	36.11	27.22	1.978	1.194
30	100	60	150	38.46	33.23	12.78	2.194	1.279
30	100	60	160	38.46	30.51	8.74	2.400	1.315
30	100	70	150	38.46	36.28	29.18	1.895	1.146
30	100	70	160	38.46	33.41	13.20	2.050	1.231
30	100	70	170	38.46	30.70	8.93	2.197	1.271

Table A1.5 (continued) Derived thermodynamic design data for absorption systems operating on ammonia-lithium nitrate for heating.

T_{EV}	T_{AB}	T_{CO}	T_{GE}	X_{AB}	X_{GE}	(FR)	$(COP)_{CH}$	$(COP)_{EH}$
40	70	50	90	54.74	50.07	10.69	2.725	1.499
40	70	50	100	54.74	45.97	6.16	3.517	1.524
40	70	50	110	54.74	42.32	4.64	4.269	1.522
40	70	50	120	54.74	38.99	3.87	4.982	1.515
40	70	50	130	54.74	35.90	3.40	5.660	1.505
40	70	50	140	54.74	33.01	3.08	6.305	1.496
40	70	50	150	54.74	30.27	2.85	6.920	1.487
40	70	60	100	54.74	50.17	10.90	2.259	1.401
40	70	60	110	54.74	46.11	6.24	2.634	1.453
40	70	60	120	54.74	42.48	4.69	2.991	1.464
40	70	60	130	54.74	39.18	3.91	3.330	1.464
40	70	60	140	54.74	36.11	3.43	3.653	1.460
40	70	60	150	54.74	33.23	3.10	3.960	1.455
40	70	60	160	54.74	30.51	2.87	4.253	1.448
40	70	70	110	54.74	50.22	11.01	2.090	1.328
40	70	70	120	54.74	46.20	6.30	2.327	1.392
40	70	70	130	54.74	42.60	4.73	2.553	1.412
40	70	70	140	54.74	39.32	3.93	2.768	1.418
40	70	70	150	54.74	36.28	3.45	2.973	1.418
40	70	70	160	54.74	33.41	3.12	3.169	1.416
40	70	70	170	54.74	30.70	2.88	3.355	1.412
40	80	50	100	49.92	45.97	13.67	2.678	1.451
40	80	50	110	49.92	42.32	7.58	3.452	1.485
40	80	50	120	49.92	38.99	5.58	4.186	1.488
40	80	50	130	49.92	35.90	4.57	4.883	1.483
40	80	50	140	49.92	33.01	3.96	5.547	1.477

Table A1.5 (continued) Derived thermodynamic design data for absorption systems operating on ammonia-lithium nitrate for heating.

T_{EV}	T_{AB}	T_{CO}	T_{GE}	X_{AB}	X_{GE}	(FR)	$(COP)_{CH}$	$(COP)_{EH}$
40	80	50	150	49.92	30.27	3.55	6.180	1.469
40	80	60	110	49.92	46.11	14.12	2.226	1.351
40	80	60	120	49.92	42.48	7.73	2.593	1.412
40	80	60	130	49.92	39.18	5.66	2.942	1.428
40	80	60	140	49.92	36.11	4.63	3.274	1.432
40	80	60	150	49.92	33.23	4.00	3.590	1.431
40	80	60	160	49.92	30.51	3.58	3.891	1.428
40	80	70	120	49.92	46.20	14.44	2.062	1.280
40	80	70	130	49.92	42.60	7.84	2.294	1.351
40	80	70	140	49.92	39.32	5.72	2.516	1.376
40	80	70	150	49.92	36.28	4.67	2.727	1.386
40	80	70	160	49.92	33.41	4.03	2.928	1.389
40	80	70	170	49.92	30.70	3.60	3.120	1.389
40	90	50	110	45.79	42.32	16.64	2.634	1.414
40	90	50	120	45.79	38.99	8.98	3.389	1.453
40	90	50	130	45.79	35.90	6.49	4.107	1.460
40	90	50	140	45.79	33.01	5.24	4.789	1.458
40	90	50	150	45.79	30.27	4.49	5.440	1.454
40	90	60	120	45.79	42.48	17.42	2.195	1.313
40	90	60	130	45.79	39.18	9.21	2.553	1.379
40	90	60	140	45.79	36.11	6.60	2.895	1.400
40	90	60	150	45.79	33.23	5.32	3.220	1.407
40	90	60	160	45.79	30.51	4.55	3.530	1.408
40	90	70	130	45.79	42.60	18.04	2.036	1.243
40	90	70	140	45.79	39.32	9.39	2.263	1.319
40	90	70	150	45.79	36.28	6.70	2.480	1.348

Table A1.5 (continued) Derived thermodynamic design data for absorption systems operating on ammonia-lithium nitrate for heating.

T_{EV}	T_{AB}	T_{CO}	T_{GE}	X_{AB}	X_{GE}	(FR)	$(COP)_{CH}$	$(COP)_{EH}$
40	90	70	160	45.79	33.41	5.38	2.687	1.361
40	90	70	170	45.79	30.70	4.59	2.884	1.366
40	100	50	120	42.10	38.99	19.59	2.593	1.383
40	100	50	130	42.10	35.90	10.34	3.330	1.427
40	100	50	140	42.10	33.01	7.37	4.031	1.437
40	100	50	150	42.10	30.27	5.89	4.700	1.438
40	100	60	130	42.10	39.18	20.80	2.165	1.282
40	100	60	140	42.10	36.11	10.66	2.516	1.352
40	100	60	150	42.10	33.23	7.53	2.850	1.376
40	100	60	160	42.10	30.51	5.99	3.169	1.386
40	100	70	140	42.10	39.32	21.82	2.010	1.214
40	100	70	150	42.10	36.28	10.94	2.233	1.292
40	100	70	160	42.10	33.41	7.66	2.446	1.325
40	100	70	170	42.10	30.70	6.08	2.649	1.340
50	80	60	100	54.84	50.17	10.67	2.732	1.486
50	80	60	110	54.84	46.11	6.17	3.530	1.512
50	80	60	120	54.84	42.48	4.65	4.288	1.511
50	80	60	130	54.84	39.18	3.88	5.007	1.504
50	80	60	140	54.84	36.11	3.41	5.692	1.495
50	80	60	150	54.84	33.23	3.09	6.345	1.485
50	80	60	160	54.84	30.51	2.86	6.968	1.476
50	80	70	110	54.84	50.22	10.78	2.265	1.389
50	80	70	120	54.84	46.20	6.22	2.644	1.440
50	80	70	130	54.84	42.60	4.69	3.004	1.452
50	80	70	140	54.84	39.32	3.91	3.346	1.453

Table A1.5 (continued) Derived thermodynamic design data for absorption systems operating on ammonia-lithium nitrate for heating.

T_{EV}	T_{AB}	T_{CO}	T_{GE}	X_{AB}	X_{GE}	(FR)	$(COP)_{CH}$	$(COP)_{EH}$
50	80	70	150	54.84	36.28	3.43	3.673	1.449
50	80	70	160	54.84	33.41	3.11	3.984	1.444
50	80	70	170	54.84	30.70	2.87	4.281	1.438
50	90	60	110	50.07	46.11	13.59	2.687	1.439
50	90	60	120	50.07	42.48	7.58	3.466	1.473
50	90	60	130	50.07	39.18	5.58	4.206	1.477
50	90	60	140	50.07	36.11	4.58	4.910	1.473
50	90	60	150	50.07	33.23	3.96	5.582	1.466
50	90	60	160	50.07	30.51	3.55	6.222	1.459
50	90	70	120	50.07	46.20	13.88	2.233	1.341
50	90	70	130	50.07	42.60	7.68	2.603	1.400
50	90	70	140	50.07	39.32	5.64	2.955	1.417
50	90	70	150	50.07	36.28	4.62	3.291	1.421
50	90	70	160	50.07	33.41	4.00	3.611	1.420
50	90	70	170	50.07	30.70	3.58	3.916	1.417
50	100	60	120	45.97	42.48	16.49	2.644	1.402
50	100	60	130	45.97	39.18	8.95	3.404	1.442
50	100	60	140	45.97	36.11	6.48	4.128	1.449
50	100	60	150	45.97	33.23	5.24	4.818	1.448
50	100	60	160	45.97	30.51	4.49	5.476	1.444
50	100	70	130	45.97	42.60	17.05	2.202	1.304
50	100	70	140	45.97	39.32	9.13	2.564	1.368
50	100	70	150	45.97	36.28	6.57	2.909	1.389
50	100	70	160	45.97	33.41	5.30	3.238	1.396
50	100	70	170	45.97	30.70	4.54	3.552	1.397

Table A1.5 (continued) Derived thermodynamic design data for absorption systems operating on ammonia-lithium nitrate for heating.

T_{EV}	T_{AB}	T_{CO}	T_{GE}	X_{AB}	X_{GE}	(FR)	$(COP)_{CCL}$	$(COP)_{ECL}$
-10	50	50	120	40.20	38.99	50.27	0.781	0.080
-10	50	50	130	40.20	35.90	14.91	0.870	0.192
-10	50	50	140	40.20	33.01	9.31	0.955	0.244
-10	50	50	150	40.20	30.27	7.02	1.036	0.273
-10	50	60	130	40.20	39.18	59.43	0.746	0.057
-10	50	60	140	40.20	36.11	15.62	0.819	0.161
-10	50	60	150	40.20	33.23	9.58	0.888	0.212
-10	50	60	160	40.20	30.51	7.17	0.954	0.242
-10	50	70	140	40.20	39.32	69.01	0.716	0.042
-10	50	70	150	40.20	36.28	16.23	0.777	0.135
-10	50	70	160	40.20	33.41	9.81	0.835	0.185
-10	50	70	170	40.20	30.70	7.29	0.891	0.214
-10	50	80	150	40.20	39.42	77.74	0.691	0.031
-10	50	80	160	40.20	36.40	16.71	0.742	0.115
-10	50	80	170	40.20	33.55	9.99	0.792	0.161
-10	50	90	160	40.20	39.48	83.88	0.668	0.025
-10	50	90	170	40.20	36.47	17.04	0.712	0.098
-10	50	100	170	40.20	39.50	85.90	0.648	0.020
-10	60	50	130	36.73	35.90	77.02	0.761	0.055
-10	60	50	140	36.73	33.01	17.98	0.849	0.168
-10	60	50	150	36.73	30.27	10.78	0.933	0.223
-10	60	60	150	36.73	33.23	19.08	0.799	0.139
-10	60	60	160	36.73	30.51	11.16	0.868	0.192
-10	60	70	160	36.73	33.41	20.06	0.759	0.115
-10	60	70	170	36.73	30.70	11.49	0.816	0.166

Table A1.6 Derived thermodynamic design data for absorption systems operating on ammonia-lithium nitrate for cooling and simultaneous heating.

... continued

T_{EV}	T_{AB}	T_{CO}	T_{GE}	X_{AB}	X_{GE}	(FR)	$(COP)_{CCL}$	$(COP)_{ECL}$
-10	60	80	170	36.73	33.55	20.87	0.726	0.096
-10	70	50	150	33.53	30.27	21.37	0.829	0.149
-10	70	60	160	33.53	30.51	22.99	0.781	0.120
-10	70	70	170	33.53	30.70	24.49	0.742	0.098
-5	50	50	120	42.31	38.99	18.36	0.868	0.181
-5	50	50	130	42.31	35.90	10.00	0.967	0.251
-5	50	50	140	42.31	33.01	7.20	1.062	0.286
-5	50	50	150	42.31	30.27	5.79	1.152	0.305
-5	50	60	130	42.31	39.18	19.41	0.818	0.148
-5	50	60	140	42.31	36.11	10.31	0.898	0.216
-5	50	60	150	42.31	33.23	7.36	0.975	0.252
-5	50	60	160	42.31	30.51	5.89	1.047	0.273
-5	50	70	140	42.31	39.32	20.30	0.779	0.122
-5	50	70	150	42.31	36.28	10.56	0.845	0.187
-5	50	70	160	42.31	33.41	7.48	0.908	0.223
-5	50	70	170	42.31	30.70	5.97	0.968	0.244
-5	50	80	150	42.31	39.42	20.97	0.745	0.102
-5	50	80	160	42.31	36.40	10.75	0.801	0.162
-5	50	80	170	42.31	33.55	7.58	0.854	0.197
-5	50	90	160	42.31	39.48	21.38	0.717	0.087
-5	50	90	170	42.31	36.47	10.88	0.764	0.141
-5	50	100	170	42.31	39.50	21.50	0.691	0.074
-5	60	50	130	38.69	35.90	22.95	0.846	0.154
-5	60	50	140	38.69	33.01	11.78	0.944	0.227
-5	60	50	150	38.69	30.27	8.27	1.037	0.264

Table A1.6 (continued) Derived thermodynamic design data for absorption systems operating on ammonia-lithium nitrate for cooling and simultaneous heating.

T_{EV}	T_{AB}	T_{CO}	T_{GE}	X_{AB}	X_{GE}	(FR)	$(COP)_{CCL}$	$(COP)_{ECL}$
-5	60	60	140	38.69	36.11	24.74	0.799	0.123
-5	60	60	150	38.69	33.23	12.23	0.877	0.193
-5	60	60	160	38.69	30.51	8.49	0.952	0.231
-5	60	70	150	38.69	36.28	26.34	0.760	0.099
-5	60	70	160	38.69	33.41	12.61	0.825	0.165
-5	60	70	170	38.69	30.70	8.67	0.887	0.203
-5	60	80	160	38.69	36.40	27.66	0.728	0.081
-5	60	80	170	38.69	33.55	12.92	0.783	0.142
-5	60	90	170	38.69	36.47	28.59	0.700	0.068
-5	70	50	140	35.38	33.01	28.26	0.826	0.131
-5	70	50	150	35.38	30.27	13.64	0.922	0.206
-5	70	60	150	35.38	33.23	31.14	0.780	0.102
-5	70	60	160	35.38	30.51	14.27	0.857	0.174
-5	70	70	160	35.38	33.41	33.90	0.743	0.080
-5	70	70	170	35.38	30.70	14.81	0.807	0.147
-5	70	80	170	35.38	33.55	36.33	0.712	0.064
-5	80	50	150	32.29	30.27	34.42	0.806	0.113
-5	80	60	160	32.29	30.51	38.91	0.762	0.085
-5	80	70	170	32.29	30.70	43.51	0.726	0.065
0	50	50	110	44.49	42.32	26.53	0.855	0.153
0	50	50	120	44.49	38.99	11.08	0.973	0.256
0	50	50	130	44.49	35.90	7.46	1.084	0.300
0	50	50	140	44.49	33.01	5.83	1.190	0.322
0	50	50	150	44.49	30.27	4.90	1.291	0.334
0	50	60	120	44.49	42.48	28.65	0.810	0.120

Table A1.6 (continued) Derived thermodynamic design data for absorption systems operating on ammonia-lithium nitrate for cooling and simultaneous heating.

T_{EV}	T_{AB}	T_{CO}	T_{GE}	X_{AB}	X_{GE}	(FR)	$(COP)_{CCL}$	$(COP)_{ECL}$
0	50	60	130	44.49	39.18	11.45	0.903	0.218
0	50	60	140	44.49	36.11	7.62	0.992	0.263
0	50	60	150	44.49	33.23	5.93	1.076	0.287
0	50	60	160	44.49	30.51	4.97	1.156	0.301
0	50	70	130	44.49	42.60	30.41	0.774	0.095
0	50	70	140	44.49	39.32	11.74	0.850	0.186
0	50	70	150	44.49	36.28	7.76	0.922	0.231
0	50	70	160	44.49	33.41	6.01	0.991	0.256
0	50	70	170	44.49	30.70	5.02	1.056	0.272
0	50	80	140	44.49	42.68	31.64	0.744	0.078
0	50	80	150	44.49	39.42	11.95	0.807	0.160
0	50	80	160	44.49	36.40	7.86	0.867	0.203
0	50	80	170	44.49	33.55	6.07	0.924	0.229
0	50	90	150	44.49	42.71	32.21	0.717	0.065
0	50	90	160	44.49	39.48	12.07	0.771	0.139
0	50	90	170	44.49	36.47	7.92	0.822	0.179
0	50	100	160	44.49	42.71	32.08	0.694	0.056
0	50	100	170	44.49	39.50	12.11	0.740	0.121
0	60	50	120	40.70	38.99	35.59	0.834	0.121
0	60	50	130	40.70	35.90	13.35	0.948	0.227
0	60	50	140	40.70	33.01	8.71	1.058	0.275
0	60	50	150	40.70	30.27	6.68	1.162	0.299
0	60	60	130	40.70	39.18	39.91	0.790	0.091
0	60	60	140	40.70	36.11	13.92	0.881	0.191
0	60	60	150	40.70	33.23	8.94	0.968	0.239

Table A1.6 (continued) Derived thermodynamic design data for absorption systems operating on ammonia-lithium nitrate for cooling and simultaneous heating.

T_{EV}	T_{AB}	T_{CO}	T_{GE}	X_{AB}	X_{GE}	(FR)	$(COP)_{CCL}$	$(COP)_{ECL}$
0	60	60	160	40.70	30.51	6.82	1.051	0.266
0	60	70	140	40.70	39.32	43.97	0.755	0.070
0	60	70	150	40.70	36.28	14.40	0.830	0.161
0	60	70	160	40.70	33.41	9.14	0.901	0.208
0	60	70	170	40.70	30.70	6.93	0.968	0.235
0	60	80	150	40.70	39.42	47.33	0.726	0.055
0	60	80	160	40.70	36.40	14.77	0.788	0.137
0	60	80	170	40.70	33.55	9.29	0.847	0.182
0	60	90	160	40.70	39.48	49.52	0.701	0.044
0	60	90	170	40.70	36.47	15.02	0.753	0.117
0	60	100	170	40.70	39.50	50.21	0.678	0.037
0	70	50	130	37.26	35.90	47.30	0.813	0.096
0	70	50	140	37.26	33.01	15.77	0.925	0.204
0	70	50	150	37.26	30.27	9.98	1.033	0.254
0	70	60	140	37.26	36.11	55.78	0.771	0.068
0	70	60	150	37.26	33.23	16.60	0.861	0.169
0	70	60	160	37.26	30.51	10.30	0.946	0.219
0	70	70	150	37.26	36.28	64.91	0.738	0.049
0	70	70	160	37.26	33.41	17.33	0.811	0.140
0	70	70	170	37.26	30.70	10.57	0.880	0.189
0	70	80	160	37.26	36.40	73.77	0.709	0.036
0	70	80	170	37.26	33.55	17.92	0.770	0.118
0	70	90	170	37.26	36.47	80.94	0.685	0.028
0	80	50	140	34.07	33.01	62.86	0.793	0.076
0	80	50	150	34.07	30.27	18.32	0.904	0.184

Table A1.6 (continued) Derived thermodynamic design data for absorption systems operating on ammonia-lithium nitrate for cooling and simultaneous heating.

T_{EV}	T_{AB}	T_{CO}	T_{GE}	X_{AB}	X_{GE}	(FR)	$(COP)_{CCL}$	$(COP)_{ECL}$
0	80	60	150	34.07	33.23	79.53	0.753	0.050
0	80	60	160	34.07	30.51	19.49	0.841	0.150
0	80	70	170	34.07	30.70	20.54	0.792	0.123
0	90	50	150	31.09	30.27	84.34	0.774	0.059
5	50	50	100	46.76	45.97	68.38	0.828	0.079
5	50	50	110	46.76	42.32	12.98	0.968	0.254
5	50	50	120	46.76	38.99	7.85	1.100	0.314
5	50	50	130	46.76	35.90	5.90	1.226	0.341
5	50	50	140	46.76	33.01	4.87	1.346	0.354
5	50	50	150	46.76	30.27	4.23	1.460	0.360
5	50	60	110	46.76	46.11	82.51	0.792	0.053
5	50	60	120	46.76	42.48	13.45	0.900	0.213
5	50	60	130	46.76	39.18	8.02	1.003	0.274
5	50	60	140	46.76	36.11	6.00	1.101	0.303
5	50	60	150	46.76	33.23	4.94	1.195	0.319
5	50	60	160	46.76	30.51	4.28	1.284	0.328
5	50	70	120	46.76	46.20	95.49	0.762	0.038
5	50	70	130	46.76	42.60	13.81	0.849	0.180
5	50	70	140	46.76	39.32	8.16	0.932	0.239
5	50	70	150	46.76	36.28	6.08	1.011	0.270
5	50	70	160	46.76	33.41	4.99	1.087	0.287
5	50	70	170	46.76	30.70	4.31	1.159	0.297
5	50	80	140	46.76	42.68	14.04	0.808	0.153
5	50	80	150	46.76	39.42	8.25	0.876	0.209
5	50	80	160	46.76	36.40	6.14	0.942	0.240

Table A1.6 (continued) Derived thermodynamic design data for absorption systems operating on ammonia-lithium nitrate for cooling and simultaneous heating.

T_{EV}	T_{AB}	T_{CO}	T_{GE}	X_{AB}	X_{GE}	(FR)	$(COP)_{CCL}$	$(COP)_{ECL}$
5	50	80	170	46.76	33.55	5.03	1.004	0.258
5	50	90	150	46.76	42.71	14.15	0.773	0.131
5	50	90	160	46.76	39.48	8.31	0.831	0.184
5	50	90	170	46.76	36.47	6.17	0.886	0.213
5	50	100	150	46.76	46.20	96.57	0.692	0.021
5	50	100	160	46.76	42.71	14.13	0.743	0.113
5	50	100	170	46.76	39.50	8.33	0.793	0.161
5	60	50	120	42.77	38.99	16.14	0.943	0.221
5	60	50	130	42.77	35.90	9.34	1.073	0.285
5	60	50	140	42.77	33.01	6.86	1.197	0.315
5	60	50	150	42.77	30.27	5.58	1.314	0.331
5	60	60	130	42.77	39.18	16.95	0.878	0.181
5	60	60	140	42.77	36.11	9.60	0.979	0.246
5	60	60	150	42.77	33.23	7.00	1.075	0.278
5	60	60	160	42.77	30.51	5.67	1.167	0.296
5	60	70	140	42.77	39.32	17.61	0.828	0.150
5	60	70	150	42.77	36.28	9.82	0.910	0.212
5	60	70	160	42.77	33.41	7.12	0.988	0.245
5	60	70	170	42.77	30.70	5.74	1.062	0.265
5	60	80	150	42.77	39.42	18.11	0.789	0.126
5	60	80	160	42.77	36.40	9.98	0.856	0.184
5	60	80	170	42.77	33.55	7.21	0.920	0.217
5	60	90	160	42.77	39.48	18.41	0.755	0.106
5	60	90	170	42.77	36.47	10.09	0.812	0.160
5	60	100	170	42.77	39.50	18.50	0.727	0.091

Table A1.6 (continued) Derived thermodynamic design data for absorption systems operating on ammonia-lithium nitrate for cooling and simultaneous heating.

T_{EV}	T_{AB}	T_{CO}	T_{GE}	X_{AB}	X_{GE}	(FR)	$(COP)_{CCL}$	$(COP)_{ECL}$
5	70	50	130	39.17	35.90	19.59	0.920	0.194
5	70	50	140	39.17	33.01	10.86	1.047	0.261
5	70	50	150	39.17	30.27	7.83	1.168	0.294
5	70	60	140	39.17	36.11	20.86	0.857	0.156
5	70	60	150	39.17	33.23	11.24	0.956	0.222
5	70	60	160	39.17	30.51	8.02	1.051	0.257
5	70	70	150	39.17	36.28	21.98	0.809	0.127
5	70	70	160	39.17	33.41	11.56	0.889	0.190
5	70	70	170	39.17	30.70	8.18	0.965	0.225
5	70	80	160	39.17	36.40	22.88	0.770	0.104
5	70	80	170	39.17	33.55	11.81	0.837	0.163
5	70	90	170	39.17	36.47	23.51	0.738	0.087
5	80	50	140	35.88	33.01	23.33	0.897	0.171
5	80	50	150	35.88	30.27	12.43	1.022	0.241
5	80	60	150	35.88	33.23	25.24	0.836	0.135
5	80	60	160	35.88	30.51	12.94	0.934	0.203
5	80	70	160	35.88	33.41	27.01	0.790	0.108
5	80	70	170	35.88	30.70	13.38	0.869	0.172
5	80	80	170	35.88	33.55	28.52	0.753	0.087
5	90	50	150	32.81	30.27	27.39	0.876	0.153
5	90	60	160	32.81	30.51	30.14	0.817	0.118
5	90	70	170	32.81	30.70	32.80	0.772	0.092
10	50	50	100	49.14	45.97	17.04	0.948	0.239
10	50	50	110	49.14	42.32	8.45	1.108	0.329
10	50	50	120	49.14	38.99	6.01	1.260	0.362

Table A1.6 (continued) Derived thermodynamic design data for absorption systems operating on ammonia-lithium nitrate for cooling and simultaneous heating.

T_{EV}	T_{AB}	T_{CO}	T_{GE}	X_{AB}	X_{GE}	(FR)	$(COP)_{CCL}$	$(COP)_{ECL}$
10	50	50	130	49.14	35.90	4.84	1.404	0.377
10	50	50	140	49.14	33.01	4.15	1.542	0.384
10	50	50	150	49.14	30.27	3.69	1.673	0.386
10	50	60	110	49.14	46.11	17.76	0.887	0.194
10	50	60	120	49.14	42.48	8.64	1.008	0.284
10	50	60	130	49.14	39.18	6.10	1.124	0.321
10	50	60	140	49.14	36.11	4.90	1.233	0.339
10	50	60	150	49.14	33.23	4.20	1.338	0.348
10	50	60	160	49.14	30.51	3.73	1.438	0.352
10	50	70	120	49.14	46.20	18.27	0.840	0.160
10	50	70	130	49.14	42.60	8.78	0.936	0.246
10	50	70	140	49.14	39.32	6.18	1.028	0.284
10	50	70	150	49.14	36.28	4.95	1.115	0.304
10	50	70	160	49.14	33.41	4.23	1.198	0.315
10	50	70	170	49.14	30.70	3.76	1.278	0.321
10	50	80	130	49.14	46.24	18.54	0.803	0.134
10	50	80	140	49.14	42.68	8.87	0.881	0.214
10	50	80	150	49.14	39.42	6.23	0.956	0.252
10	50	80	160	49.14	36.40	4.99	1.027	0.273
10	50	80	170	49.14	33.55	4.26	1.095	0.285
10	50	90	140	49.14	46.24	18.55	0.771	0.114
10	50	90	150	49.14	42.71	8.91	0.836	0.186
10	50	90	160	49.14	39.48	6.26	0.899	0.224
10	50	90	170	49.14	36.47	5.01	0.958	0.245
10	50	100	150	49.14	46.20	18.31	0.743	0.098

Table A1.6 (continued) Derived thermodynamic design data for absorption systems operating on ammonia-lithium nitrate for cooling and simultaneous heating.

T_{EV}	T_{AB}	T_{CO}	T_{GE}	$X_{AB.}$	X_{GE}	(FR)	$(COP)_{CCL}$	$(COP)_{ECL}$
10	50	100	160	49.14	42.71	8.90	0.799	0.163
10	50	100	170	49.14	39.50	6.27	0.852	0.198
10	60	50	110	44.90	42.32	22.31	0.924	0.199
10	60	50	120	44.90	38.99	10.31	1.080	0.294
10	60	50	130	44.90	35.90	7.12	1.229	0.332
10	60	50	140	44.90	33.01	5.63	1.370	0.350
10	60	50	150	44.90	30.27	4.76	1.505	0.359
10	60	60	120	44.90	42.48	23.78	0.864	0.157
10	60	60	130	44.90	39.18	10.62	0.983	0.250
10	60	60	140	44.90	36.11	7.27	1.096	0.292
10	60	60	150	44.90	33.23	5.72	1.204	0.313
10	60	60	160	44.90	30.51	4.83	1.307	0.324
10	60	70	130	44.90	42.60	24.97	0.819	0.125
10	60	70	140	44.90	39.32	10.87	0.914	0.214
10	60	70	150	44.90	36.28	7.39	1.004	0.256
10	60	70	160	44.90	33.41	5.80	1.089	0.279
10	60	70	170	44.90	30.70	4.88	1.171	0.292
10	60	80	140	44.90	42.68	25.78	0.783	0.102
10	60	80	150	44.90	39.42	11.05	0.860	0.184
10	60	80	160	44.90	36.40	7.48	0.934	0.225
10	60	80	170	44.90	33.55	5.85	1.004	0.249
10	60	90	150	44.90	42.71	26.16	0.753	0.085
10	60	90	160	44.90	39.48	11.16	0.817	0.159
10	60	90	170	44.90	36.47	7.54	0.878	0.198
10	60	100	160	44.90	42.71	26.07	0.726	0.073

Table A1.6 (continued) Derived thermodynamic design data for absorption systems operating on ammonia-lithium nitrate for cooling and simultaneous heating.

T_{EV}	T_{AB}	T_{CO}	T_{GE}	X_{AB}	X_{GE}	(FR)	$(COP')_{CCL}$	$(COP')_{ECL}$
10	60	100	170	44.90	39.50	11.19	0.781	0.138
10	70	50	120	41.14	38.99	28.36	0.900	0.168
10	70	50	130	41.14	35.90	12.24	1.053	0.266
10	70	50	140	41.14	33.01	8.24	1.199	0.308
10	70	50	150	41.14	30.27	6.41	1.338	0.328
10	70	60	130	41.14	39.18	31.01	0.843	0.128
10	70	60	140	41.14	36.11	12.71	0.959	0.223
10	70	60	150	41.14	33.23	8.45	1.070	0.267
10	70	60	160	41.14	30.51	6.54	1.176	0.291
10	70	70	140	41.14	39.32	33.40	0.799	0.099
10	70	70	150	41.14	36.28	13.10	0.892	0.188
10	70	70	160	41.14	33.41	8.62	0.980	0.233
10	70	70	170	41.14	30.70	6.64	1.065	0.258
10	70	80	150	41.14	39.42	35.28	0.765	0.079
10	70	80	160	41.14	36.40	13.41	0.840	0.160
10	70	80	170	41.14	33.55	8.76	0.913	0.203
10	70	90	160	41.14	39.48	36.48	0.735	0.064
10	70	90	170	41.14	36.47	13.61	0.799	0.137
10	70	100	170	41.14	39.50	36.85	0.710	0.054
10	80	50	130	37.72	35.90	35.32	0.878	0.142
10	80	50	140	37.72	33.01	14.23	1.028	0.243
10	80	50	150	37.72	30.27	9.36	1.171	0.287
10	80	60	140	37.72	36.11	39.81	0.822	0.104
10	80	60	150	37.72	33.23	14.90	0.937	0.201
10	80	60	160	37.72	30.51	9.64	1.046	0.247

Table A1.6 (continued) Derived thermodynamic design data for absorption systems operating on ammonia-lithium nitrate for cooling and simultaneous heating.

T_{EV}	T_{AB}	T_{CO}	T_{GE}	X_{AB}	X_{GE}	(FR)	$(COP)_{CCL}$	$(COP)_{ECL}$
10	80	70	150	37.72	36.28	44.22	0.781	0.078
10	80	70	160	37.72	33.41	15.48	0.871	0.168
10	80	70	170	37.72	30.70	9.88	0.958	0.214
10	80	80	160	37.72	36.40	48.13	0.747	0.060
10	80	80	170	37.72	33.55	15.95	0.821	0.141
10	80	90	170	37.72	36.47	51.05	0.719	0.047
10	90	50	140	34.55	33.01	43.36	0.857	0.121
10	90	50	150	34.55	30.27	16.27	1.004	0.223
10	90	60	150	34.55	33.23	50.63	0.803	0.085
10	90	60	160	34.55	30.51	17.18	0.915	0.182
10	90	70	160	34.55	33.41	58.46	0.763	0.061
10	90	70	170	34.55	30.70	17.99	0.852	0.150
10	90	80	170	34.55	33.55	66.22	0.730	0.045
10	100	50	150	31.59	30.27	52.67	0.836	0.104
10	100	60	160	31.59	30.51	64.11	0.784	0.070
10	100	70	170	31.59	30.70	77.79	0.745	0.048
15	50	50	90	51.67	50.07	31.37	0.907	0.180
15	50	50	100	51.67	45.97	9.49	1.103	0.341
15	50	50	110	51.67	42.32	6.17	1.289	0.387
15	50	50	120	51.67	38.99	4.81	1.466	0.404
15	50	50	130	51.67	35.90	4.07	1.633	0.410
15	50	50	140	51.67	33.01	3.59	1.793	0.411
15	50	50	150	51.67	30.27	3.26	1.945	0.410
15	50	60	100	51.67	50.17	33.37	0.858	0.136
15	50	60	110	51.67	46.11	9.70	1.003	0.290

Table A1.6 (continued) Derived thermodynamic design data for absorption systems operating on ammonia-lithium nitrate for cooling and simultaneous heating.

T_{EV}	T_{AB}	T_{CO}	T_{GE}	X_{AB}	X_{GE}	(FR)	$(COP)_{CCL}$	$(COP)_{ECL}$
15	50	60	120	51.67	42.48	6.26	1.140	0.341
15	50	60	130	51.67	39.18	4.87	1.270	0.362
15	50	60	140	51.67	36.11	4.11	1.395	0.372
15	50	60	150	51.67	33.23	3.62	1.513	0.376
15	50	60	160	51.67	30.51	3.28	1.626	0.377
15	50	70	110	51.67	50.22	34.48	0.820	0.107
15	50	70	120	51.67	46.20	9.84	0.933	0.248
15	50	70	130	51.67	42.60	6.33	1.039	0.301
15	50	70	140	51.67	39.32	4.92	1.141	0.325
15	50	70	150	51.67	36.28	4.14	1.238	0.337
15	50	70	160	51.67	33.41	3.65	1.330	0.342
15	50	70	170	51.67	30.70	3.31	1.418	0.345
15	50	80	120	51.67	50.23	34.56	0.789	0.088
15	50	80	130	51.67	46.24	9.91	0.880	0.214
15	50	80	140	51.67	42.68	6.38	0.966	0.265
15	50	80	150	51.67	39.42	4.95	1.047	0.291
15	50	80	160	51.67	36.40	4.17	1.126	0.304
15	50	80	170	51.67	33.55	3.67	1.200	0.312
15	50	90	130	51.67	50.18	33.63	0.762	0.074
15	50	90	140	51.67	46.24	9.92	0.837	0.185
15	50	90	150	51.67	42.71	6.40	0.908	0.234
15	50	90	160	51.67	39.48	4.97	0.976	0.260
15	50	90	170	51.67	36.47	4.18	1.040	0.274
15	50	100	140	51.67	50.10	31.89	0.738	0.065
15	50	100	150	51.67	46.20	9.85	0.801	0.162

Table A1.6 (continued) Derived thermodynamic design data for absorption systems operating on ammonia-lithium nitrate for cooling and simultaneous heating.

T_{EV}	T_{AB}	T_{CO}	T_{GE}	X_{AB}	X_{GE}	(FR)	$(COP)_{CCL}$	$(COP)_{ECL}$
15	50	100	160	51.67	42.71	6.39	0.861	0.207
15	50	100	170	51.67	39.50	4.97	0.918	0.232
15	60	50	100	47.13	45.97	46.74	0.882	0.133
15	60	50	110	47.13	42.32	11.99	1.074	0.300
15	60	50	120	47.13	38.99	7.50	1.256	0.351
15	60	50	130	47.13	35.90	5.71	1.429	0.373
15	60	50	140	47.13	33.01	4.74	1.594	0.382
15	60	50	150	47.13	30.27	4.14	1.751	0.386
15	60	60	110	47.13	46.11	52.89	0.836	0.093
15	60	60	120	47.13	42.48	12.39	0.977	0.250
15	60	60	130	47.13	39.18	7.65	1.112	0.306
15	60	60	140	47.13	36.11	5.80	1.240	0.331
15	60	60	150	47.13	33.23	4.81	1.362	0.344
15	60	60	160	47.13	30.51	4.18	1.478	0.350
15	60	70	120	47.13	46.20	57.90	0.799	0.069
15	60	70	130	47.13	42.60	12.69	0.910	0.210
15	60	70	140	47.13	39.32	7.77	1.014	0.267
15	60	70	150	47.13	36.28	5.87	1.114	0.294
15	60	70	160	47.13	33.41	4.86	1.209	0.309
15	60	70	170	47.13	30.70	4.22	1.300	0.318
15	60	80	130	47.13	46.24	60.77	0.770	0.053
15	60	80	140	47.13	42.68	12.89	0.858	0.178
15	60	80	150	47.13	39.42	7.86	0.943	0.233
15	60	80	160	47.13	36.40	5.93	1.023	0.261
15	60	80	170	47.13	33.55	4.89	1.100	0.278

Table A1.6 (continued) Derived thermodynamic design data for absorption systems operating on ammonia-lithium nitrate for cooling and simultaneous heating.

T_{EV}	T_{AB}	T_{CO}	T_{GE}	X_{AB}	X_{GE}	(FR)	$(COP)_{CCL}$	$(COP)_{ECL}$
15	60	90	140	47.13	46.24	60.87	0.744	0.044
15	60	90	150	47.13	42.71	12.98	0.817	0.152
15	60	90	160	47.13	39.48	7.91	0.887	0.204
15	60	90	170	47.13	36.47	5.96	0.953	0.232
15	60	100	150	47.13	46.20	58.29	0.721	0.038
15	60	100	160	47.13	42.71	12.96	0.783	0.131
15	60	100	170	47.13	39.50	7.93	0.841	0.179
15	70	50	110	43.16	42.32	68.40	0.859	0.097
15	70	50	120	43.16	38.99	14.62	1.047	0.266
15	70	50	130	43.16	35.90	8.83	1.225	0.323
15	70	50	140	43.16	33.01	6.60	1.395	0.347
15	70	50	150	43.16	30.27	5.41	1.556	0.359
15	70	60	120	43.16	42.48	84.99	0.814	0.062
15	70	60	130	43.16	39.18	15.27	0.953	0.218
15	70	60	140	43.16	36.11	9.06	1.085	0.278
15	70	60	150	43.16	33.23	6.73	1.210	0.306
15	70	60	160	43.16	30.51	5.49	1.330	0.321
15	70	70	140	43.16	39.32	15.81	0.888	0.180
15	70	70	150	43.16	36.28	9.26	0.990	0.239
15	70	70	160	43.16	33.41	6.83	1.088	0.270
15	70	70	170	43.16	30.70	5.56	1.182	0.287
15	70	80	150	43.16	39.42	16.20	0.838	0.150
15	70	80	160	43.16	36.40	9.40	0.921	0.207
15	70	80	170	43.16	33.55	6.91	1.000	0.238
15	70	90	160	43.16	39.48	16.44	0.798	0.127

Table A1.6 (continued) Derived thermodynamic design data for absorption systems operating on ammonia-lithium nitrate for cooling and simultaneous heating.

T_{EV}	T_{AB}	T_{CO}	T_{GE}	X_{AB}	X_{GE}	(FR)	$(COP)_{CCL}$	$(COP)_{ECL}$
15	70	90	170	43.16	36.47	9.50	0.867	0.180
15	70	100	170	43.16	39.50	16.51	0.765	0.108
15	80	50	130	39.59	35.90	17.37	1.021	0.239
15	80	50	140	39.59	33.01	10.17	1.195	0.299
15	80	50	150	39.59	30.27	7.48	1.362	0.326
15	80	60	140	39.59	36.11	18.35	0.930	0.192
15	80	60	150	39.59	33.23	10.50	1.059	0.254
15	80	60	160	39.59	30.51	7.65	1.182	0.285
15	80	70	150	39.59	36.28	19.21	0.867	0.156
15	80	70	160	39.59	33.41	10.78	0.967	0.217
15	80	70	170	39.59	30.70	7.79	1.064	0.250
15	80	80	160	39.59	36.40	19.89	0.819	0.129
15	80	80	170	39.59	33.55	11.00	0.900	0.186
15	80	90	170	39.59	36.47	20.36	0.780	0.107
15	90	50	140	36.32	33.01	20.24	0.996	0.217
15	90	50	150	36.32	30.27	11.52	1.167	0.279
15	90	60	150	36.32	33.23	21.65	0.908	0.171
15	90	60	160	36.32	30.51	11.96	1.035	0.235
15	90	70	160	36.32	33.41	22.92	0.847	0.137
15	90	70	170	36.32	30.70	12.34	0.946	0.199
15	90	80	170	36.32	33.55	24.00	0.800	0.111
15	100	50	150	33.27	30.27	23.22	0.973	0.198
15	100	60	160	33.27	30.51	25.14	0.887	0.154
15	100	70	170	33.27	30.70	26.96	0.827	0.121

Table A1.6 (continued) Derived thermodynamic design data for absorption systems operating on ammonia-lithium nitrate for cooling and simultaneous heating.

T_{EV}	T_{AB}	T_{CO}	T_{GE}	X_{AB}	X_{GE}	(FR)	$(COP)_{CT}$	$(COP)_{ET}$
30	40	10	30	77.15	62.13	2.52	.689	.457
30	40	20	30	77.15	75.85	18.60	.517	.200
30	50	10	40	64.62	53.70	4.24	.695	.437
30	60	10	50	55.91	47.14	6.02	.702	.419
30	70	10	60	49.25	41.45	7.51	.708	.399
30	80	10	70	43.51	36.26	8.79	.714	.392
30	90	10	80	38.32	31.31	9.80	.716	.387
30	100	10	90	33.52	26.59	10.59	.725	.369
40	50	10	30	78.48	62.13	2.32	.631	.434
40	50	10	40	78.48	53.70	1.87	.774	.453
40	50	20	40	78.48	63.38	2.43	.688	.454
40	50	30	40	78.48	77.15	17.18	.516	.222
40	60	10	40	65.86	53.70	3.81	.638	.393
40	60	10	50	65.86	47.14	2.82	.779	.440
40	60	20	50	65.86	54.81	4.09	.694	.430
40	70	10	50	57.02	47.14	5.35	.645	.355
40	70	10	60	57.02	41.45	3.76	.784	.432
40	70	20	60	57.02	48.20	5.87	.701	.411
40	80	10	60	50.31	41.45	6.61	.652	.316
40	80	10	70	50.31	36.26	4.54	.789	.425
40	80	20	70	50.31	42.49	7.35	.707	.390
40	90	10	70	44.53	36.26	7.70	.658	.293
40	90	10	80	44.53	31.31	5.19	.794	.421

Table A1.7 Derived thermodynamic design data for absorption heat

T_{EV}	T_{AB}	T_{CO}	T_{GE}	X_{AB}	X_{GE}	(FR)	$(COP)_{CT}$	$(COP)_{ET}$
40	90	20	80	44.53	37.32	8.69	.712	.378
40	100	10	80	39.28	31.31	8.62	.664	.280
40	100	10	90	39.28	26.58	5.78	.798	.416
40	100	20	90	39.28	32.45	9.89	.718	.375
50	60	10	30	79.83	62.13	2.14	.611	.412
50	60	10	40	79.83	53.70	1.77	.702	.434
50	60	10	50	79.83	47.14	1.62	.825	.442
50	60	20	30	79.83	75.85	6.07	.532	.218
50	60	20	40	79.83	63.38	2.23	.630	.431
50	60	20	50	79.83	54.81	1.81	.773	.449
50	60	30	40	79.83	77.15	8.53	.524	.230
50	60	30	50	79.83	64.62	2.33	.687	.452
50	70	10	30	67.18	62.13	7.59	.548	.234
50	70	10	40	67.18	53.70	3.45	.618	.351
50	70	10	50	67.18	47.14	2.65	.708	.409
50	70	10	60	67.18	41.45	2.28	.829	.431
50	70	20	50	67.18	54.81	3.67	.637	.384
50	70	20	60	67.18	48.20	2.74	.778	.432
50	70	30	60	67.18	55.91	3.94	.694	.422
50	80	10	50	58.12	47.14	4.82	.625	.292
50	80	10	60	58.12	41.45	3.51	.714	.390
50	80	10	70	58.12	36.26	2.92	.833	.429

Table A1.7 Derived thermodynamic design data for absorption heat transformers operating on ammonia-water. (continued)

T_{EV}	T_{AB}	T_{CO}	T_{GE}	X_{AB}	X_{GE}	(FR)	$(COP)_{CT}$	$(COP)_{ET}$
50	80	20	60	58.12	48.20	5.22	.644	.344
50	80	20	70	58.12	42.49	3.68	.783	.423
50	80	30	70	58.12	49.25	5.72	.700	.402
50	90	10	60	51.36	41.45	5.91	.631	.231
50	90	10	70	51.36	36.26	4.22	.720	.375
50	90	10	80	51.36	31.31	3.43	.837	.424
50	90	20	70	51.36	42.49	6.48	.650	.302
50	90	20	80	51.36	37.32	4.46	.788	.414
50	90	30	80	51.36	43.51	7.20	.706	.379
50	100	10	70	45.56	36.26	6.86	.637	.188
50	100	10	80	45.56	31.31	4.82	.725	.365
50	100	10	90	45.56	26.58	3.87	.841	.418
50	100	20	80	45.56	37.32	7.61	.656	.272
50	100	20	90	45.56	32.45	5.15	.792	.410
50	100	30	90	45.56	38.32	8.52	.711	.363
60	70	10	30	81.14	62.13	1.99	.602	.390
60	70	10	40	81.14	53.70	1.69	.669	.414
60	70	10	50	81.14	47.14	1.55	.752	.423
60	70	10	60	81.14	41.45	1.48	.858	.427
60	70	20	30	81.14	75.85	4.56	.539	.210
60	70	20	40	81.14	63.38	2.06	.610	.407
60	70	20	50	81.14	54.81	1.72	.701	.428

Table A1.7. Derived thermodynamic design data for absorption heat transformers operating on ammonia-water. (continued)

T_{EV}	T_{AB}	T_{CO}	T_{GE}	X_{AB}	X_{GE}	(FR)	$(COP)_{CT}$	$(COP)_{ET}$
60	70	20	60	81.14	48.20	1.57	.824	.435
60	70	30	40	81.14	77.15	5.72	.531	.219
60	70	30	50	81.14	64.62	2.14	.630	.426
60	70	30	60	81.14	55.91	1.75	.773	.443
60	70	40	50	81.14	78.48	8.08	.523	.224
60	70	40	60	81.14	65.86	2.23	.687	.448
60	80	10	40	68.40	53.70	3.15	.609	.310
60	80	10	50	68.40	47.14	2.49	.675	.377
60	80	10	60	68.40	41.45	2.17	.757	.404
60	80	10	70	68.40	36.26	1.98	.862	.419
60	80	20	50	68.40	54.81	3.32	.616	.340
60	80	20	60	68.40	48.20	2.56	.707	.399
60	80	20	70	68.40	42.49	2.22	.828	.422
60	80	30	50	68.40	64.62	9.37	.538	.042
60	80	30	60	68.40	55.91	3.53	.636	.375
60	80	30	70	68.40	49.25	2.65	.778	.423
60	80	40	70	68.40	57.02	3.78	.693	.413
60	90	10	50	59.19	47.14	4.39	.616	.226
60	90	10	60	59.19	41.45	3.30	.681	.347
60	90	10	70	59.19	36.26	2.78	.762	.395
60	90	10	80	59.19	31.31	2.46	.865	.418
60	90	20	60	59.19	48.20	4.71	.623	.276

Table A1.7 Derived thermodynamic design data for absorption heat transformers operating on ammonia-water. (continued)

T_{EV}	T_{AB}	T_{CO}	T_{GE}	X_{AB}	X_{GE}	(FR)	$(COP)_{CT}$	$(COP)_{ET}$
60	90	20	70	59.19	42.49	3.44	.712	.379
60	90	20	80	59.19	37.32	2.87	.832	.418
60	90	30	70	59.19	49.25	5.10	.642	.331
60	90	30	80	59.19	43.51	3.60	.782	.413
60	90	40	80	59.19	50.30	5.59	.699	.392
60	100	10	60	52.41	41.45	5.34	.622	.141
60	100	10	70	52.41	36.26	3.95	.687	.323
60	100	10	80	52.41	31.31	3.25	.767	.385
60	100	10	90	52.41	26.58	2.84	.868	.412
60	100	20	70	52.41	42.49	5.79	.629	.211
60	100	20	80	52.41	37.32	4.15	.718	.361
60	100	20	90	52.41	32.45	3.38	.836	.413
60	100	30	80	52.41	43.51	6.35	.649	.286
60	100	30	90	52.41	38.32	4.38	.787	.402
60	100	40	90	52.41	44.53	7.04	.704	.367
60	110	10	70	46.58	36.26	6.17	.628	.074
60	110	10	80	46.58	31.31	4.50	.693	.305
60	110	10	90	46.58	26.58	3.67	.772	.375
60	110	20	80	46.58	37.32	6.77	.635	.158
60	110	20	90	46.58	32.45	4.78	.723	.349
60	110	30	90	46.58	38.32	7.47	.655	.250
60	120	10	80	41.21	31.31	6.93	.634	.024

Table A1.7 Derived thermodynamic design data for absorption heat transformers operating on ammonia-water. (continued)

T_{EV}	T_{AB}	T_{CO}	T_{GE}	X_{AB}	X_{GE}	(FR)	$(COP)_{CT}$	$(COP)_{ET}$
60	120	10	90	41.21	26.58	5.02	.698	.288
60	120	20	90	41.21	32.45	7.71	.641	.120
70	80	10	30	82.43	62.13	1.87	.599	.367
70	80	10	40	82.43	53.70	1.61	.652	.393
70	80	10	50	82.43	47.14	1.50	.714	.403
70	80	10	60	82.43	41.45	1.43	.789	.407
70	80	10	70	82.43	36.26	1.38	.882	.409
70	80	20	30	82.43	75.85	3.67	.546	.198
70	80	20	40	82.43	63.38	1.92	.601	.382
70	80	20	50	82.43	54.81	1.64	.668	.406
70	80	20	60	82.43	48.20	1.51	.751	.414
70	80	20	70	82.43	42.49	1.44	.858	.417
70	80	30	40	82.43	77.15	4.33	.538	.203
70	80	30	50	82.43	64.62	1.99	.608	.400
70	80	30	60	82.43	55.91	1.66	.700	.419
70	80	30	70	82.43	49.25	1.53	.823	.426
70	80	40	50	82.43	78.48	5.45	.530	.205
70	80	40	60	82.43	65.86	2.06	.628	.420
70	80	40	70	82.43	57.02	1.69	.772	.435
70	80	50	60	82.43	79.83	7.76	.522	.195
70	80	50	70	82.43	67.12	2.15	.686	.442
70	90	10	40	69.71	53.70	2.89	.606	.270

Table A1.7 Derived thermodynamic design data for absorption heat transformers operating on ammonia-water.(continued)

T_{EV}	T_{AB}	T_{CO}	T_{GE}	X_{AB}	X_{GE}	(FR)	$(COP)_{CT}$	$(COP)_{E}$
70	90	10	50	69.71	47.14	2.34	.658	.345
70	90	10	60	69.71	41.45	2.07	.720	.375
70	90	10	70	69.71	36.26	1.91	.794	.393
70	90	10	80	69.71	31.31	1.79	.885	.402
70	90	20	50	69.71	54.81	3.03	.608	.298
70	90	20	60	69.71	48.20	2.41	.674	.366
70	90	20	70	69.71	42.49	2.11	.756	.393
70	90	20	80	69.71	37.32	1.94	.861	.408
70	90	30	60	69.71	55.91	3.20	.615	.330
70	90	30	70	69.71	49.25	2.48	.706	.389
70	90	30	80	69.71	43.51	2.16	.827	.411
70	90	40	70	69.71	57.02	3.39	.635	.365
70	90	40	80	69.71	50.31	2.56	.777	.414
70	90	50	80	69.71	58.12	3.61	.692	.405
70	100	10	50	60.28	47.14	4.02	.613	.157
70	100	10	60	60.28	41.45	3.11	.664	.301
70	100	10	70	60.28	36.26	2.65	.725	.358
70	100	10	80	60.28	31.31	2.37	.798	.387
70	100	10	90	60.28	26.58	2.18	.888	.401
70	100	20	60	60.28	48.20	4.29	.614	.204
70	100	20	70	60.28	42.49	3.23	.680	.332
70	100	20	80	60.28	37.32	2.73	.761	.381

Table A1.7 Derived thermodynamic design data for absorption heat transformers operating on ammonia-water. (continued)

T_{EV}	T_{AB}	T_{CO}	T_{GE}	X_{AB}	X_{GE}	(FR)	$(COP)_{CT}$	$(COP)_{ET}$
70	100	20	90	60.28	32.45	2.43	.864	.406
70	100	30	70	60.28	49.25	4.60	.621	.256
70	100	30	80	60.28	43.51	3.37	.711	.366
70	100	30	90	60.28	38.32	2.81	.831	.406
70	100	40	80	60.28	50.31	4.98	.611	.315
70	100	40	90	60.28	44.53	3.52	.781	.401
70	100	50	90	60.28	51.36	5.45	.698	.379
70	110	10	60	53.46	41.45	4.88	.619	.045
70	110	10	70	53.46	36.26	3.71	.670	.267
70	110	10	80	53.46	31.31	3.10	.730	.343
70	110	10	90	53.46	26.58	2.73	.802	.378
70	110	20	70	53.46	42.49	5.24	.620	.113
70	110	20	80	53.46	37.32	3.88	.685	.305
70	110	20	90	53.46	32.45	3.22	.766	.371
70	110	30	80	53.46	43.51	5.68	.628	.187
70	110	30	90	53.46	38.32	4.07	.717	.346
70	110	40	90	53.46	44.53	6.21	.647	.268
70	120	10	80	47.61	31.31	4.21	.676	.240
70	120	10	90	47.61	26.58	3.49	.735	.329
70	120	20	80	47.61	37.32	6.09	.626	.033
70	120	20	90	47.61	32.45	4.45	.691	.284
70	120	30	90	47.61	38.32	6.64	.634	.126

Table A1.7 Derived thermodynamic design data for absorption heat transformers operating on ammonia-water. (continued)

T_{EV}	T_{AB}	T_{CO}	T_{GE}	X_{AB}	X_{GE}	(FR)	$(COP)_{CT}$	$(COP)_{ET}$
30	70	10	55	49.72	46.95	19.16	0.618	0.299
30	70	10	60	49.72	44.90	11.44	0.708	0.463
30	70	10	65	49.72	42.97	8.45	0.829	0.507
30	80	10	65	45.55	42.97	22.15	0.625	0.250
30	80	10	70	45.55	41.14	13.35	0.714	0.450
30	80	10	75	45.55	39.39	9.85	0.833	0.503
30	90	10	75	41.84	39.39	24.79	0.631	0.199
30	90	10	80	41.84	37.72	15.12	0.720	0.438
30	90	10	85	41.84	36.11	11.15	0.837	0.499
30	100	10	85	38.46	36.11	27.16	0.637	0.148
30	100	10	90	38.46	34.55	16.76	0.725	0.425
35	70	10	50	52.14	49.14	16.94	0.602	0.212
35	70	10	55	52.14	46.95	10.22	0.669	0.429
35	70	10	60	52.14	44.90	7.61	0.752	0.484
35	70	10	65	52.14	42.97	6.22	0.858	0.509
35	80	10	60	47.68	44.90	19.82	0.609	0.128
35	80	10	65	47.68	42.97	12.11	0.675	0.408
35	80	10	70	47.68	41.14	9.00	0.757	0.476
35	80	10	75	47.68	39.39	7.31	0.862	0.506
35	90	10	70	43.78	41.14	22.32	0.616	0.041
35	90	10	75	43.78	39.39	13.82	0.681	0.387
35	90	10	80	43.78	37.72	10.28	0.762	0.467
35	90	10	85	43.78	36.11	8.33	0.865	0.503
35	100	10	85	40.26	36.11	15.39	0.687	0.366
35	100	10	90	40.26	34.55	11.47	0.767	0.458
35	100	20	90	40.26	38.12	28.90	0.656	0.288

Table A1.8 Derived thermodynamic design data for absorption heat transformers operating on ammonia-lithium nitrate.

... continued

T_{EV}	T_{AB}	T_{CO}	T_{GE}	X_{AB}	X_{GE}	(FR)	$(COP)_{CT}$	$(COP)_{ET}$
40	70	10	50	54.74	49.14	9.08	0.645	0.398
40	70	10	55	54.74	46.95	6.81	0.708	0.463
40	70	10	60	54.74	44.90	5.60	0.784	0.492
40	70	10	65	54.74	42.97	4.84	0.879	0.508
40	80	10	60	49.92	44.90	10.97	0.652	0.367
40	80	10	65	49.92	42.97	8.20	0.714	0.450
40	80	10	70	49.92	41.14	6.70	0.789	0.486
40	80	10	75	49.92	39.39	5.75	0.882	0.506
40	90	10	70	45.79	41.14	12.67	0.658	0.335
40	90	10	75	45.79	39.39	9.48	0.720	0.436
40	90	10	80	45.79	37.72	7.72	0.794	0.479
40	90	10	85	45.79	36.11	6.60	0.885	0.503
40	100	10	80	42.10	37.72	14.20	0.664	0.304
40	100	10	85	42.10	36.11	10.66	0.725	0.422
40	100	10	90	42.10	34.55	8.67	0.798	0.472
40	100	20	85	42.10	39.78	25.93	0.629	0.112
40	100	20	90	42.10	38.12	15.53	0.718	0.422
45	80	10	55	52.30	46.95	9.92	0.636	0.328
45	80	10	60	52.30	44.90	7.45	0.686	0.425
45	80	10	65	52.30	42.97	6.11	0.744	0.467
45	80	10	70	52.30	41.14	5.27	0.814	0.490
45	80	10	75	52.30	39.39	4.70	0.897	0.504
45	90	10	65	47.88	42.97	11.62	0.642	0.283
45	90	10	70	47.88	41.14	8.73	0.692	0.406
45	90	10	75	47.88	39.39	7.14	0.750	0.457
45	90	10	80	47.88	37.72	6.13	0.818	0.485

Table A1.8 (continued) Derived thermodynamic design data for absorption heat transformers operating on ammonia-lithium nitrate.

T_{EV}	T_{AB}	T_{CO}	T_{GE}	X_{AB}	X_{GE}	(FR)	$(COP)_{CT}$	$(COP)_{ET}$
45	90	10	85	47.88	36.11	5.43	0.900	0.502
45	100	10	75	44.00	39.39	13.14	0.649	0.236
45	100	10	80	44.00	37.72	9.91	0.698	0.386
45	100	10	85	44.00	36.11	8.09	0.755	0.446
45	100	10	90	44.00	34.55	6.93	0.822	0.479
45	100	20	85	44.00	39.78	14.26	0.680	0.362
45	100	20	90	44.00	38.12	10.51	0.761	0.457
45	100	30	90	44.00	41.84	26.84	0.649	0.279
50	80	10	50	54.84	49.14	8.92	0.625	0.294
50	80	10	55	54.84	46.95	6.72	0.666	0.404
50	80	10	60	54.84	44.90	5.54	0.714	0.450
50	80	10	65	54.84	42.97	4.80	0.769	0.475
50	80	10	70	54.84	41.14	4.30	0.833	0.491
50	80	10	75	54.84	39.39	3.92	0.909	0.502
50	90	10	60	50.07	44.90	10.66	0.631	0.231
50	90	10	65	50.07	42.97	8.03	0.672	0.377
50	90	10	70	50.07	41.14	6.59	0.720	0.435
50	90	10	75	50.07	39.39	5.67	0.774	0.467
50	90	10	80	50.07	37.72	5.04	0.837	0.487
50	90	10	85	50.07	36.11	4.57	0.911	0.500
50	100	10	70	45.97	41.14	12.18	0.637	0.165
50	100	10	75	45.97	39.39	9.21	0.678	0.349
50	100	10	80	45.97	37.72	7.55	0.725	0.420
50	100	10	85	45.97	36.11	6.48	0.779	0.458
50	100	10	90	45.97	34.55	5.73	0.841	0.481
50	100	20	80	45.97	41.52	13.13	0.656	0.298

Table A1.8 (continued) Derived thermodynamic design data for absorption heat transformers operating on ammonia-lithium nitrate.

T_{EV}	T_{AB}	T_{CO}	T_{GE}	X_{AB}	X_{GE}	(FR)	$(COP)_{CT}$	$(COP)_{ET}$
50	100	20	85	45.97	39.78	9.73	0.718	0.421
50	100	20	90	45.97	38.12	7.88	0.792	0.471
50	100	30	85	45.97	43.64	24.20	0.621	0.090
50	100	30	90	45.97	41.84	14.06	0.711	0.422
55	90	10	55	52.40	46.95	9.74	0.623	0.181
55	90	10	60	52.40	44.90	7.35	0.658	0.350
55	90	10	65	52.40	42.97	6.05	0.698	0.416
55	90	10	70	52.40	41.14	5.23	0.743	0.450
55	90	10	75	52.40	39.39	4.66	0.794	0.472
55	90	10	80	52.40	37.72	4.24	0.852	0.487
55	90	10	85	52.40	36.11	3.92	0.920	0.497
55	100	10	65	48.02	42.97	11.29	0.629	0.090
55	100	10	70	48.02	41.14	8.55	0.664	0.313
55	100	10	75	48.02	39.39	7.02	0.703	0.396
55	100	10	80	48.02	37.72	6.04	0.748	0.438
55	100	10	85	48.02	36.11	5.36	0.798	0.465
55	100	10	90	48.02	34.55	4.86	0.856	0.482
55	100	20	75	48.02	43.34	12.09	0.641	0.230
55	100	20	80	48.02	41.52	8.99	0.690	0.386
55	100	20	85	48.02	39.78	7.31	0.748	0.446
55	100	20	90	48.02	38.12	6.25	0.817	0.478
55	100	30	85	48.02	43.64	12.87	0.672	0.363
55	100	30	90	48.02	41.84	9.40	0.755	0.457
55	100	40	90	48.02	45.79	24.24	0.641	0.281
55	110	10	80	44.18	37.72	9.64	0.670	0.275
55	110	10	85	44.18	36.11	7.91	0.709	0.375

Table A1.8 (continued) Derived thermodynamic design data for absorption heat transformers operating on ammonia-lithium nitrate.

T_{EV}	T_{AB}	T_{CO}	T_{GE}	X_{AB}	X_{GE}	(FR)	$(COP)_{CT}$	$(COP)_{ET}$
55	110	10	90	44.18	34.55	6.80	0.753	0.426
55	110	20	85	44.18	39.78	13.69	0.647	0.167
55	110	20	90	44.18	38.12	10.21	0.696	0.360
55	120	10	90	40.71	34.55	10.62	0.676	0.235
60	90	10	50	54.89	49.14	8.86	0.616	0.138
60	90	10	55	54.89	46.95	6.69	0.647	0.327
60	90	10	60	54.89	44.90	5.52	0.681	0.398
60	90	10	65	54.89	42.97	4.79	0.720	0.436
60	90	10	70	54.89	41.14	4.28	0.762	0.459
60	90	10	75	54.89	39.39	3.91	0.810	0.474
60	90	10	80	54.89	37.72	3.63	0.865	0.485
60	90	10	85	54.89	36.11	3.40	0.928	0.493
60	100	10	60	50.17	44.90	10.46	0.622	0.013
60	100	10	65	50.17	42.97	7.92	0.653	0.279
60	100	10	70	50.17	41.14	6.52	0.687	0.372
60	100	10	75	50.17	39.39	5.62	0.725	0.420
60	100	10	80	50.17	37.72	5.00	0.767	0.449
60	100	10	85	50.17	36.11	4.54	0.815	0.468
60	100	10	90	50.17	34.55	4.19	0.868	0.481
60	100	20	70	50.17	45.25	11.13	0.629	0.161
60	100	20	75	50.17	43.34	8.29	0.671	0.351
60	100	20	80	50.17	41.52	6.76	0.718	0.421
60	100	20	85	50.17	39.78	5.79	0.772	0.458
60	100	20	90	50.17	38.12	5.13	0.836	0.481
60	100	30	80	50.17	45.55	11.77	0.649	0.302
60	100	30	85	50.17	43.64	8.63	0.711	0.423

Table A1.8 (continued) Derived thermodynamic design data for absorption heat transformers operating on ammonia-lithium nitrate.

T_{EV}	T_{AB}	T_{CO}	T_{GE}	X_{AB}	X_{GE}	(FR)	$(COP)_{CT}$	$(COP)_{ET}$
60	100	30	90	50.17	41.84	6.98	0.787	0.472
60	100	40	85	50.17	47.79	21.89	0.614	0.092
60	100	40	90	50.17	45.79	12.36	0.704	0.425
60	110	10	75	46.11	39.39	9.02	0.659	0.228
60	110	10	80	46.11	37.72	7.42	0.693	0.345
60	110	10	85	46.11	36.11	6.39	0.730	0.403
60	110	10	90	46.11	34.55	5.66	0.772	0.438
60	110	20	80	46.11	41.52	12.73	0.635	0.067
60	110	20	85	46.11	39.78	9.52	0.677	0.316
60	110	20	90	46.11	38.12	7.74	0.723	0.403
60	110	30	90	46.11	41.84	13.61	0.655	0.249
60	120	10	85	42.48	36.11	10.02	0.665	0.175
60	120	10	90	42.48	34.55	8.25	0.698	0.317
65	100	10	60	52.45	44.90	7.30	0.644	0.247
65	100	10	65	52.45	42.97	6.02	0.674	0.351
65	100	10	70	52.45	41.14	5.21	0.707	0.403
65	100	10	75	52.45	39.39	4.64	0.744	0.434
65	100	10	80	52.45	37.72	4.23	0.784	0.454
65	100	10	85	52.45	36.11	3.91	0.829	0.469
65	100	10	90	52.45	34.55	3.66	0.879	0.480
65	100	20	65	52.45	47.29	10.22	0.621	0.092
65	100	20	70	52.45	45.25	7.61	0.656	0.319
65	100	20	75	52.45	43.34	6.22	0.696	0.399
65	100	20	80	52.45	41.52	5.35	0.741	0.440
65	100	20	85	52.45	39.78	4.75	0.792	0.464
65	100	20	90	52.45	38.12	4.32	0.851	0.481

Table A1.8 (continued) Derived thermodynamic design data for absorption heat transformers operating on ammonia-lithium nitrate.

T_{EV}	T_{AB}	T_{CO}	T_{GE}	X_{AB}	X_{GE}	(FR)	$(COP)_{CT}$	$(COP)_{ET}$
65	100	30	75	52.45	47.57	10.74	0.633	0.240
65	100	30	80	52.45	45.55	7.89	0.683	0.391
65	100	30	85	52.45	43.64	6.40	0.742	0.448
65	100	30	90	52.45	41.84	5.48	0.812	0.478
65	100	40	85	52.45	47.79	11.20	0.665	0.371
65	100	40	90	52.45	45.79	8.14	0.749	0.460
65	100	50	90	52.45	50.07	21.04	0.634	0.296
65	110	10	70	48.12	41.14	8.44	0.650	0.182
65	110	10	75	48.12	39.39	6.95	0.680	0.316
65	110	10	80	48.12	37.72	5.99	0.713	0.382
65	110	10	85	48.12	36.11	5.32	0.749	0.420
65	110	10	90	48.12	34.55	4.83	0.788	0.445
65	110	20	80	48.12	41.52	8.86	0.662	0.271
65	110	20	85	48.12	39.78	7.22	0.702	0.374
65	110	20	90	48.12	38.12	6.19	0.746	0.425
65	110	30	85	48.12	43.64	12.60	0.639	0.159
65	110	30	90	48.12	41.84	9.26	0.689	0.361
65	120	10	80	44.31	37.72	9.45	0.656	0.112
65	120	10	85	44.31	36.11	7.79	0.686	0.281
65	120	10	90	44.31	34.55	6.71	0.718	0.360
65	120	20	90	44.31	38.12	9.99	0.668	0.220
65	130	10	90	40.87	34.55	10.36	0.662	0.036
70	100	10	55	54.88	46.95	6.69	0.637	0.221
70	100	10	60	54.88	44.90	5.52	0.664	0.333
70	100	10	65	54.88	42.97	4.79	0.693	0.388
70	100	10	70	54.88	41.14	4.28	0.725	0.420

Table A1.8 (continued) Derived thermodynamic design data for absorption heat transformers operating on ammonia-lithium nitrate.

T_{EV}	T_{AB}	T_{CO}	T_{GE}	X_{AB}	X_{GE}	(FR)	$(COP)_{CT}$	$(COP)_{ET}$
70	100	10	75	54.88	39.39	3.91	0.760	0.442
70	100	10	80	54.88	37.72	3.63	0.798	0.457
70	100	10	85	54.88	36.11	3.40	0.841	0.468
70	100	10	90	54.88	34.55	3.22	0.888	0.477
70	100	20	60	54.88	49.46	9.33	0.614	0.029
70	100	20	65	54.88	47.29	6.94	0.645	0.290
70	100	20	70	54.88	45.25	5.69	0.680	0.379
70	100	20	75	54.88	43.34	4.91	0.718	0.423
70	100	20	80	54.88	41.52	4.38	0.761	0.450
70	100	20	85	54.88	39.78	3.99	0.809	0.467
70	100	20	90	54.88	38.12	3.69	0.864	0.480
70	100	30	70	54.88	49.72	9.75	0.621	0.182
70	100	30	75	54.88	47.57	7.17	0.663	0.361
70	100	30	80	54.88	45.55	5.83	0.711	0.426
70	100	30	85	54.88	43.64	5.02	0.767	0.460
70	100	30	90	54.88	41.84	4.46	0.831	0.480
70	100	40	80	54.88	49.92	10.11	0.641	0.318
70	100	40	85	54.88	47.79	7.36	0.704	0.429
70	100	40	90	54.88	45.79	5.96	0.781	0.473
70	100	50	85	54.88	52.35	18.87	0.606	0.128
70	100	50	90	54.88	50.07	10.39	0.698	0.433
70	110	10	65	50.22	42.97	7.87	0.643	0.137
70	110	10	70	50.22	41.14	6.48	0.670	0.289
70	110	10	75	50.22	39.39	5.60	0.699	0.361
70	110	10	80	50.22	37.72	4.98	0.730	0.403
70	110	10	85	50.22	36.11	4.53	0.765	0.430

Table A1.8 (continued) Derived thermodynamic design data for absorption heat transformers operating on ammonia-lithium nitrate.

T_{EV}	T_{AB}	T_{CO}	T_{GE}	X_{AB}	X_{GE}	(FR)	$(COP)_{CT}$	$(COP)_{ET}$
70	110	10	90	50.22	34.55	4.18	0.802	0.449
70	110	20	75	50.22	43.34	8.23	0.651	0.227
70	110	20	80	50.22	41.52	6.72	0.685	0.346
70	110	20	85	50.22	39.78	5.77	0.723	0.404
70	110	20	90	50.22	38.12	5.11	0.766	0.437
70	110	30	80	50.22	45.55	11.65	0.628	0.062
70	110	30	85	50.22	43.64	8.57	0.669	0.318
70	110	30	90	50.22	41.84	6.94	0.717	0.404
70	110	40	90	50.22	45.79	12.22	0.647	0.254
70	120	10	75	46.20	39.39	8.90	0.649	0.045
70	120	10	80	46.20	37.72	7.34	0.676	0.244
70	120	10	85	46.20	36.11	6.33	0.704	0.334
70	120	10	90	46.20	34.55	5.62	0.735	0.384
70	120	20	85	46.20	39.78	9.38	0.657	0.159
70	120	20	90	46.20	38.12	7.66	0.691	0.312
70	130	10	90	42.60	34.55	8.13	0.681	0.196
75	110	10	60	52.45	44.90	7.30	0.638	0.096
75	110	10	65	52.45	42.97	6.02	0.662	0.265
75	110	10	70	52.45	41.14	5.21	0.687	0.342
75	110	10	75	52.45	39.39	4.64	0.715	0.387
75	110	10	80	52.45	37.72	4.23	0.746	0.416
75	110	10	85	52.45	36.11	3.91	0.779	0.436
75	110	10	90	52.45	34.55	3.66	0.815	0.451
75	110	20	70	52.45	45.25	7.61	0.643	0.186
75	110	20	75	52.45	43.34	6.22	0.673	0.320
75	110	20	80	52.45	41.52	5.35	0.706	0.384

Table A1.8 (continued) Derived thermodynamic design data for absorption heat transformers operating on ammonia-lithium nitrate.

T_{EV}	T_{AB}	T_{CO}	T_{GE}	X_{AB}	X_{GE}	(FR)	$(COP)_{CT}$	$(COP)_{ET}$
75	110	20	85	52.45	39.78	4.75	0.742	0.420
75	110	20	90	52.45	38.12	4.32	0.782	0.444
75	110	30	80	52.45	45.55	7.89	0.655	0.278
75	110	30	85	52.45	43.64	6.40	0.695	0.378
75	110	30	90	52.45	41.84	5.48	0.740	0.427
75	110	40	85	52.45	47.79	11.20	0.631	0.172
75	110	40	90	52.45	45.79	8.14	0.682	0.367
75	120	10	75	48.16	39.39	6.91	0.667	0.208
75	120	10	80	48.16	37.72	5.96	0.693	0.308
75	120	10	85	48.16	36.11	5.30	0.721	0.364
75	120	10	90	48.16	34.55	4.81	0.751	0.400
75	120	20	80	48.16	41.52	8.80	0.648	0.095
75	120	20	85	48.16	39.78	7.18	0.678	0.276
75	120	20	90	48.16	38.12	6.16	0.711	0.357
75	120	30	90	48.16	41.84	9.19	0.661	0.215
75	130	10	85	44.39	36.11	7.71	0.673	0.147
75	130	10	90	44.39	34.55	6.65	0.698	0.273
80	110	10	55	54.82	46.95	6.74	0.633	0.063
80	110	10	60	54.82	44.90	5.55	0.655	0.245
80	110	10	65	54.82	42.97	4.81	0.678	0.327
80	110	10	70	54.82	41.14	4.30	0.703	0.373
80	110	10	75	54.82	39.39	3.93	0.730	0.403
80	110	10	80	54.82	37.72	3.64	0.759	0.424
80	110	10	85	54.82	36.11	3.41	0.791	0.440
80	110	10	90	54.82	34.55	3.23	0.826	0.451
80	110	20	65	54.82	47.29	7.00	0.635	0.151

Table A1.8 (continued) Derived thermodynamic design data for absorption heat transformers operating on ammonia-lithium nitrate.

T_{EV}	T_{AB}	T_{CO}	T_{GE}	X_{AB}	X_{GE}	(FR)	$(COP)_{CT}$	$(COP)_{ET}$
80	110	20	70	54.82	45.25	5.72	0.662	0.298
80	110	20	75	54.82	43.34	4.93	0.691	0.366
80	110	20	80	54.82	41.52	4.39	0.723	0.405
80	110	20	85	54.82	39.78	4.00	0.758	0.431
80	110	20	90	54.82	38.12	3.70	0.797	0.448
80	110	30	75	54.82	47.57	7.22	0.644	0.242
80	110	30	80	54.82	45.55	5.87	0.678	0.354
80	110	30	85	54.82	43.64	5.04	0.717	0.407
80	110	30	90	54.82	41.84	4.48	0.760	0.439
80	110	40	80	54.82	49.92	10.22	0.620	0.089
80	110	40	85	54.82	47.79	7.42	0.662	0.330
80	110	40	90	54.82	45.79	6.00	0.710	0.410
80	110	50	90	54.82	50.07	10.51	0.640	0.274
80	120	10	70	50.23	41.14	6.48	0.660	0.174
80	120	10	75	50.23	39.39	5.59	0.684	0.285
80	120	10	80	50.23	37.72	4.98	0.708	0.346
80	120	10	85	50.23	36.11	4.53	0.735	0.384
80	120	10	90	50.23	34.55	4.18	0.764	0.410
80	120	20	75	50.23	43.34	8.23	0.641	0.031
80	120	20	80	50.23	41.52	6.72	0.668	0.242
80	120	20	85	50.23	39.78	5.77	0.697	0.333
80	120	20	90	50.23	38.12	5.11	0.728	0.384
80	120	30	85	50.23	43.64	8.56	0.649	0.157
80	120	30	90	50.23	41.84	6.93	0.684	0.313
80	130	10	80	46.24	37.72	7.31	0.666	0.097
80	130	10	85	46.24	36.11	6.30	0.689	0.241

Table A1.8 (continued) Derived thermodynamic design data for absorption heat transformers operating on ammonia-lithium nitrate.

T_{EV}	T_{AB}	T_{CO}	T_{GE}	X_{AB}	X_{GE}	(FR)	$(COP)_{CT}$	$(COP)_{ET}$
80	130	10	90	46.24	34.55	5.60	0.714	0.317
80	130	20	90	46.24	38.12	7.62	0.674	0.181
80	140	10	90	42.68	34.55	8.05	0.671	0.013
85	120	10	65	52.40	42.97	6.05	0.654	0.144
85	120	10	70	52.40	41.14	5.23	0.676	0.264
85	120	10	75	52.40	39.39	4.66	0.698	0.329
85	120	10	80	52.40	37.72	4.24	0.723	0.369
85	120	10	85	52.40	36.11	3.92	0.748	0.397
85	120	10	90	52.40	34.55	3.67	0.776	0.417
85	120	20	75	52.40	43.34	6.25	0.660	0.211
85	120	20	80	52.40	41.52	5.37	0.685	0.311
85	120	20	85	52.40	39.78	4.77	0.714	0.365
85	120	20	90	52.40	38.12	4.33	0.744	0.400
85	120	30	80	52.40	45.55	7.94	0.641	0.100
85	120	30	85	52.40	43.64	6.44	0.671	0.281
85	120	30	90	52.40	41.84	5.51	0.704	0.360
85	120	40	90	52.40	45.79	8.20	0.653	0.224
85	130	10	75	48.17	39.39	6.91	0.660	0.047
85	130	10	80	48.17	37.72	5.96	0.681	0.210
85	130	10	85	48.17	36.11	5.30	0.704	0.293
85	130	10	90	48.17	34.55	4.81	0.728	0.344
85	130	20	85	48.17	39.78	7.18	0.665	0.133
85	130	20	90	48.17	38.12	6.16	0.691	0.267
85	140	10	90	44.43	34.55	6.63	0.686	0.152
90	120	10	60	54.72	44.90	5.61	0.649	0.119
90	120	10	65	54.72	42.97	4.85	0.669	0.246

Table A1.8 (continued) Derived thermodynamic design data for absorption heat transformers operating on ammonia-lithium nitrate.

T_{EV}	T_{AB}	T_{CO}	T_{GE}	X_{AB}	X_{GE}	(FR)	$(COP)_{CT}$	$(COP)_{ET}$
90	120	10	70	54.72	41.14	4.33	0.690	0.314
90	120	10	75	54.72	39.39	3.95	0.712	0.356
90	120	10	80	54.72	37.72	3.66	0.735	0.385
90	120	10	85	54.72	36.11	3.43	0.760	0.405
90	120	10	90	54.72	34.55	3.25	0.787	0.421
90	120	20	70	54.72	45.25	5.78	0.653	0.184
90	120	20	75	54.72	43.34	4.98	0.676	0.291
90	120	20	80	54.72	41.52	4.43	0.701	0.349
90	120	20	85	54.72	39.78	4.03	0.728	0.386
90	120	20	90	54.72	38.12	3.73	0.758	0.410
90	120	30	75	54.72	47.57	7.33	0.634	0.050
90	120	30	80	54.72	45.55	5.94	0.661	0.253
90	120	30	85	54.72	43.64	5.09	0.690	0.339
90	120	30	90	54.72	41.84	4.51	0.722	0.387
90	120	40	85	54.72	47.79	7.53	0.642	0.176
90	120	40	90	54.72	45.79	6.07	0.677	0.323
90	130	10	70	50.18	41.14	6.51	0.655	0.000
90	130	10	75	50.18	39.39	5.62	0.674	0.181
90	130	10	80	50.18	37.72	5.00	0.695	0.272
90	130	10	85	50.18	36.11	4.54	0.717	0.327
90	130	10	90	50.18	34.55	4.19	0.740	0.363
90	130	20	80	50.18	41.52	6.75	0.658	0.087
90	130	20	85	50.18	39.78	5.79	0.681	0.237
90	130	20	90	50.18	38.12	5.13	0.706	0.315
90	130	30	90	50.18	41.84	6.97	0.666	0.179
90	140	10	85	46.24	36.11	6.30	0.680	0.109
90	140	10	90	46.24	34.55	5.60	0.700	0.227

Table A1.8 (continued) Derived thermodynamic design data for absorption heat transformers operating on ammonia-lithium nitrate.

R. No.	1	2	3	4	5	6
T_1	93.7	92.8	91.6	91.3	95.2	94.7
T_2	29.2	29.9	29.3	29.4	29.8	30.3
T_3	49.8	50.0	49.9	49.9	50.1	49.9
T_4	39.4	40.2	42.2	38.8	40.1	39.4
T_5	32.3	34.9	35.2	35.2	35.5	36.4
T_6	28.6	30.0	30.9	30.3	29.9	30.4
T_7	32.9	35.7	36.6	35.9	36.0	37.0
T_8	19.9	20.3	18.8	13.6	14.8	15.6
T_9	29.4	17.5	32.8	13.7	13.4	16.6
T_{10}	26.9	27.5	27.7	27.6	28.3	28.5
T_{11}	25.1	25.7	25.7	25.8	26.2	26.4
T_{12}	30.0	31.5	31.5	29.1	29.9	30.9
T_{13}	-	-	-	-	-	-
T_{14}	30.7	32.8	33.8	34.0	33.6	34.1
T_{15}	25.0	25.3	25.5	25.7	26.1	26.5
T_{16}	32.9	35.5	36.5	36.3	35.3	46.7
T_{17}	28.6	30.2	31.0	30.2	30.0	30.3
T_{18}	29.7	30.3	29.9	29.5	29.9	29.9
T_{19}	72.1	75.2	75.9	68.2	71.9	60.0
T_{20}	46.5	54.3	49.3	60.3	58.7	35.6
T_{21}	77.0	78.3	86.8	88.3	82.4	77.4
T_{22}	32.6	35.0	35.7	35.1	35.3	36.2
T_{23}	31.9	35.3	36.1	34.2	35.5	34.7
T_{24}	32.9	35.7	36.4	35.4	35.9	37.0
T_{25}	32.7	35.6	36.2	35.4	35.8	36.7
T_{26}	32.6	35.4	36.0	35.4	35.7	36.7
T_{27}	32.6	35.3	36.0	35.3	35.5	36.5
T_{28}	29.3	30.0	29.4	29.2	29.8	30.0
M_{WAB}†	42.5	41.0	41.5	40.5	46.5	46.5
M_{WCO}†	23.5	23.5	23.5	23.5	23.5	23.5
Q_{GE}+	371.0	358.8	393.0	364.0	344.3	364.0
Q_{EV}+	70.0	97.5	90.0	65.0	70.0	111.6
X_{GE}*	59.2	60.5	60.2	60.0	60.8	61.6
X_{AB}*	57.8	58.4	58.5	58.0	59.2	59.9

T in °C † kg h^{-1} + W * dimensionless

Table A2.1 Raw experimental performance data for the operating characteristics of the water-lithium bromide absorption cooler.

...continued

R. No.	7	8	9	10	11	12
T_1	94.5	84.9	84.6	97.6	97.5	103.2
T_2	30.4	29.3	29.4	30.2	30.9	26.6
T_3	50.0	50.3	50.0	50.2	50.1	50.1
T_4	38.6	37.5	39.0	40.4	40.7	37.9
T_5	34.6	33.3	35.2	37.9	39.2	37.7
T_6	30.0	31.1	32.5	31.2	31.9	34.3
T_7	35.1	34.2	36.3	38.6	40.4	39.5
T_8	13.7	10.9	24.5	12.3	14.8	16.5
T_9	25.1	11.8	27.7	20.2	30.5	30.2
T_{10}	28.3	29.2	30.3	29.1	29.5	31.9
T_{11}	26.3	28.4	29.7	27.4	28.0	31.3
T_{12}	32.1	30.8	32.2	32.8	34.3	37.3
T_{13}	-	30.4	31.0	-	-	-
T_{14}	33.5	32.1	33.9	34.7	35.4	32.4
T_{15}	26.2	28.4	29.8	27.6	27.9	32.3
T_{16}	35.3	36.4	36.0	38.5	38.8	37.9
T_{17}	30.0	31.3	32.6	31.7	32.1	34.7
T_{18}	30.2	29.0	29.6	29.9	30.0	27.1
T_{19}	73.3	69.8	68.7	77.6	76.9	81.1
T_{20}	47.0	48.1	43.9	53.7	48.8	43.3
T_{21}	81.1	72.1	70.7	84.8	84.5	80.1
T_{22}	34.8	33.6	35.6	37.5	38.9	37.5
T_{23}	34.5	34.1	35.2	39.8	39.8	37.9
T_{24}	35.1	34.4	36.3	38.6	40.2	39.5
T_{25}	35.1	34.2	36.0	38.2	39.8	39.2
T_{26}	35.2	34.0	35.8	38.2	39.7	39.1
T_{27}	35.1	33.9	35.6	38.2	39.4	38.6
T_{28}	29.9	29.4	29.8	29.3	29.4	26.5
M_{WAB}†	46.5	48.5	46.5	48.5	48.5	48.5
M_{WCO}†	23.5	24.0	25.5	23.5	23.5	23.5
Q_{GE}+	293.8	247.8	247.8	420.0	420.0	391.5
Q_{EV}+	60.3	38.5	70.0	120.0	120.0	120.0
X_{GE}*	61.5	56.1	56.1	63.5	63.5	64.6
X_{AB}*	59.8	54.3	54.1	60.6	61.5	61.5

T in °C † kg h^{-1} + W * dimensionless

Table A2.1 (continued) Raw experimental performance data for the operating characteristics of the water-lithium bromide absorption cooler.

R. No.	13	14	15	16	17	18
T_1	104.0	100.1	99.4	99.7	99.4	97.9
T_2	26.7	23.2	24.0	24.1	24.2	24.2
T_3	50.1	50.0	50.0	50.1	50.1	50.1
T_4	38.4	34.4	36.1	35.6	35.8	33.7
T_5	39.0	33.2	35.2	35.5	33.3	31.9
T_6	34.6	29.7	30.8	30.4	30.6	28.3
T_7	40.5	34.7	36.3	37.6	34.8	33.5
T_8	17.5	9.2	9.7	11.1	8.4	8.2
T_9	37.7	9.7	14.9	23.5	10.7	23.4
T_{10}	32.1	26.8	27.3	27.4	27.7	24.2
T_{11}	31.4	27.1	27.5	27.6	27.2	22.8
T_{12}	37.4	30.0	32.4	30.4	30.3	25.9
T_{13}	-	-	30.1	30.2	29.7	-
T_{14}	33.1	28.8	30.3	30.3	31.3	29.2
T_{15}	32.5	27.5	27.9	27.9	27.6	22.8
T_{16}	38.6	33.4	35.7	35.6	33.7	33.9
T_{17}	34.7	30.1	31.1	30.7	30.9	27.8
T_{18}	27.1	24.5	24.6	24.6	24.9	25.1
T_{19}	79.1	68.2	78.9	73.8	67.9	82.7
T_{20}	41.4	40.8	46.8	48.0	48.0	54.0
T_{21}	76.0	72.8	78.3	77.4	73.4	80.0
T_{22}	39.3	33.7	35.5	35.7	33.2	32.6
T_{23}	39.2	33.7	35.8	36.7	33.9	32.5
T_{24}	40.6	34.7	36.3	36.9	34.7	33.4
T_{25}	40.3	34.5	36.1	36.6	34.5	33.1
T_{26}	40.1	34.4	36.1	36.5	34.4	33.0
T_{27}	39.8	34.2	35.8	36.2	34.2	32.7
T_{28}	25.8	23.5	23.5	23.3	24.0	23.2
M_{WAB}†	48.3	46.0	46.5	47.0	46.5	47.0
M_{WCO}†	23.5	23.5	24.0	24.5	23.0	23.0
Q_{GE}+	376.3	312.0	312.0	298.5	312.0	312.0
Q_{EV}+	120.0	70.0	70.0	70.0	70.0	70.0
X_{GE}*	65.8	63.5	64.0	63.7	63.8	62.9
X_{AB}*	61.5	61.7	62.0	61.4	61.4	61.6

T in °C † kg h^{-1} + W * dimensionless

Table A2.1 (continued) Raw experimental performance data for the operating characteristics of the water-lithium bromide absorption cooler.

R. No.	1	2	3	4	5	6
T_1	111.0	111.0	110.0	110.1	109.1	109.1
T_2	26.1	25.8	25.5	28.7	28.9	28.3
T_3	50.1	50.1	50.2	50.2	50.1	49.9
T_4	35.8	36.2	38.4	37.8	38.4	40.6
T_5	38.8	38.2	37.4	38.1	38.3	37.9
T_6	34.8	34.4	33.1	33.4	33.3	32.7
T_7	40.3	39.6	42.0	40.4	41.1	39.8
T_8	11.4	10.2	10.2	11.7	11.9	11.9
T_9	10.5	9.8	11.2	10.3	10.9	11.0
T_{10}	31.8	31.8	30.3	30.9	30.3	30.1
T_{11}	32.7	32.3	29.7	30.4	29.8	29.0
T_{12}	34.7	35.6	35.7	35.2	35.1	34.7
T_{13}	-	-	-	-	-	-
T_{14}	31.5	30.3	33.1	32.5	33.0	34.0
T_{15}	33.4	33.0	30.6	30.4	30.1	29.0
T_{16}	38.7	37.8	37.9	38.6	39.3	38.5
T_{17}	35.4	34.9	33.7	33.4	33.4	32.6
T_{18}	25.8	25.5	24.5	27.6	28.0	28.3
T_{19}	78.2	70.4	76.6	76.5	82.5	73.4
T_{20}	47.7	33.1	38.9	51.5	55.6	49.6
T_{21}	75.1	68.6	79.2	77.5	83.1	77.4
T_{22}	40.0	39.2	38.9	39.1	40.0	39.3
T_{23}	41.2	40.2	40.0	40.0	40.7	39.7
T_{24}	41.1	40.4	39.9	39.7	40.8	40.1
T_{25}	40.9	40.1	39.8	39.5	40.5	39.9
T_{26}	40.8	40.0	39.8	39.5	40.5	40.0
T_{27}	40.5	39.7	39.3	39.4	40.1	39.8
T_{28}	24.0	24.1	24.2	25.8	25.6	25.7
M_{WAB}†	43.0	43.0	42.5	49.0	50.5	50.5
M_{WCO}†	23.5	23.5	22.5	23.5	23.5	23.5
Q_{GE}+	293.8	293.8	381.3	376.3	376.3	345.0
Q_{EV}+	70.0	70.0	97.5	108.3	108.3	111.6
X_{GE}*	82.0	82.5	81.8	81.3	81.8	81.9
X_{AB}*	80.0	80.0	79.8	79.7	79.7	79.9

T in °C † kg h^{-1} + W * dimensionless

Table A2.2 Raw experimental performance data for the operating characteristics of the water-lithium bromide-zinc bromide absorption cooler.

...continued

R. No.	7	8	9	10	11	12
T_1	109.2	109.2	110.5	110.5	111.3	111.5
T_2	27.9	27.8	26.3	28.5	29.2	29.3
T_3	50.0	50.3	50.0	49.9	50.1	50.1
T_4	40.2	40.0	39.5	40.2	40.5	37.5
T_5	36.1	34.4	34.2	37.7	38.6	40.0
T_6	30.6	29.4	29.4	32.5	32.8	33.3
T_7	39.1	37.1	35.7	39.1	39.8	41.6
T_8	11.7	11.1	10.7	11.0	12.6	14.6
T_9	10.6	9.9	9.6	10.2	11.4	13.3
T_{10}	28.1	27.3	27.2	31.1	30.9	30.4
T_{11}	26.5	26.3	26.3	30.7	30.3	30.6
T_{12}	31.9	30.0	30.0	35.6	36.2	37.6
T_{13}	-	-	-	-	-	-
T_{14}	32.4	31.4	30.8	31.7	32.7	34.3
T_{15}	26.4	26.2	26.2	31.0	30.6	30.6
T_{16}	37.1	35.3	34.8	36.7	37.6	39.8
T_{17}	30.4	29.5	29.5	33.2	33.2	33.8
T_{18}	28.3	28.0	27.5	25.2	25.3	30.9
T_{19}	82.1	73.2	66.2	77.2	84.5	86.9
T_{20}	54.0	51.6	45.4	41.3	40.8	53.6
T_{21}	80.6	76.2	70.6	76.3	78.2	80.4
T_{22}	37.5	36.0	34.9	38.2	39.3	40.5
T_{23}	37.7	34.1	35.3	38.8	40.5	-
T_{24}	38.1	36.1	34.1	39.3	40.5	40.8
T_{25}	38.0	35.8	34.2	39.1	40.2	40.8
T_{26}	38.1	36.0	34.4	38.9	40.0	40.6
T_{27}	38.0	35.0	35.1	38.6	39.7	41.0
T_{28}	25.5	25.5	25.5	27.2	27.3	29.6
M_{WAB}†	50.5	50.5	50.5	40.0	43.0	43.0
M_{WCO}†	23.5	23.5	23.5	23.5	22.5	23.5
Q_{GE}+	391.5	351.9	337.5	337.5	337.5	297.0
Q_{EV}+	108.5	90.0	97.5	70.0	70.0	70.0
X_{GE}*	82.2	82.0	82.1	81.9	82.0	82.4
X_{AB}*	80.1	80.0	79.8	78.8	78.9	79.8

T in °C † kg h^{-1} + W * dimensionless

Table A2.2 (continued) Raw experimental performance data for the operating characteristics of the water-lithium bromide-zinc bromide absorption cooler.

R. No.	13	14	15	16	17	18
T_1	111.4	108.7	110.8	109.4	110.4	111.9
T_2	24.6	23.1	24.9	23.4	22.8	29.3
T_3	49.8	50.0	50.1	49.8	49.9	49.9
T_4	36.6	35.7	36.5	36.5	37.1	35.3
T_5	28.5	28.6	28.9	30.2	28.4	40.3
T_6	24.7	24.3	25.3	24.7	23.5	33.9
T_7	28.8	31.4	30.0	30.8	30.9	42.0
T_8	7.7	8.1	11.8	9.7	8.6	12.9
T_9	5.4	10.6	10.8	19.9	14.0	11.7
T_{10}	23.5	23.1	23.5	23.1	22.2	31.4
T_{11}	22.1	22.1	22.3	21.7	20.5	30.4
T_{12}	27.7	27.9	26.0	28.8	24.1	34.8
T_{13}	-	-	-	-	-	-
T_{14}	26.6	25.8	26.9	26.9	27.4	34.6
T_{15}	44.7	22.2	46.4	21.5	20.7	30.7
T_{16}	-	29.5	30.0	30.6	29.6	39.5
T_{17}	24.6	24.4	25.2	24.4	23.3	33.9
T_{18}	25.6	23.2	25.6	23.3	23.0	27.4
T_{19}	68.9	74.9	82.3	76.9	61.9	76.6
T_{20}	31.2	55.4	50.7	32.0	43.9	38.9
T_{21}	65.3	79.3	78.5	66.4	66.2	78.9
T_{22}	28.0	29.6	28.7	31.0	30.0	40.3
T_{23}	29.2	31.4	29.7	33.5	32.2	42.2
T_{24}	28.1	30.7	31.0	32.4	31.5	41.8
T_{25}	27.7	30.2	29.5	32.3	31.3	41.4
T_{26}	27.8	29.9	29.0	31.8	30.9	40.9
T_{27}	28.1	29.3	28.9	30.3	30.5	40.8
T_{28}	25.2	23.6	25.3	23.5	23.7	28.8
M_{WAB}†	58.5	58.5	57.5	58.0	58.0	45.5
M_{WCO}†	23.5	23.5	23.5	24.0	24.0	26.5
Q_{GE}+	376.3	364.0	364.0	351.9	325.9	337.5
Q_{EV}+	93.8	93.0	120.0	115.2	77.0	120.0
X_{GE}*	81.8	81.9	82.0	82.0	82.2	82.3
X_{AB}*	80.1	79.6	80.1	79.7	79.7	80.2

T in °C † kg h^{-1} + W * dimensionless

Table A2.2 (continued) Raw experimental performance data for the operating characteristics of the water-lithium bromide-zinc bromide absorption cooler.

R. No.	19	20	21			
T_1	108.8	107.2	105.6			
T_2	30.3	29.9	30.6			
T_3	50.2	49.8	50.2			
T_4	35.7	35.8	36.3			
T_5	41.0	41.4	42.5			
T_6	34.3	34.7	35.1			
T_7	42.6	43.1	44.1			
T_8	13.2	13.0	13.7			
T_9	11.9	14.9	15.1			
T_{10}	31.5	31.6	31.6			
T_{11}	30.5	30.5	30.5			
T_{12}	34.8	35.5	35.0			
T_{13}	-	-	-			
T_{14}	36.0	37.2	38.5			
T_{15}	30.7	30.7	31.0			
T_{16}	40.7	41.4	43.1			
T_{17}	34.3	34.6	35.2			
T_{18}	27.7	27.7	27.6			
T_{19}	79.9	82.0	78.9			
T_{20}	55.3	54.1	58.7			
T_{21}	80.3	85.3	86.4			
T_{22}	40.6	41.2	42.1			
T_{23}	42.7	42.9	43.5			
T_{24}	42.5	43.1	43.9			
T_{25}	41.9	42.6	43.4			
T_{26}	41.5	42.2	42.9			
T_{27}	41.3	41.9	42.7			
T_{28}	28.5	28.5	28.6			
M_{WAB}†	46.5	47.0	47.0			
M_{WCO}†	26.5	26.5	26.0			
Q_{GE}+	352.0	391.5	420.0			
Q_{EV}+	120.0	120.0	120.0			
X_{GE}*	82.0	81.6	81.3			
X_{AB}*	79.9	79.8	79.9			

T in °C † kg h^{-1} + W * dimensionless

Table A2.2 (continued) Raw experimental performance data for the operating characteristics of the water-lithium bromide-zinc bromide absorption cooler.

R. No.	1	2	3	4	5	6
T_1	97.2	95.8	100.7	103.9	102.9	101.7
T_2	28.5	28.4	29.1	28.4	29.0	28.2
T_3	50.0	50.2	50.5	49.9	50.0	50.0
T_4	38.9	38.6	36.0	37.3	36.6	37.4
T_5	36.1	36.2	36.1	33.8	36.7	36.5
T_6	31.2	31.0	32.3	30.1	32.1	32.2
T_7	36.9	37.0	37.0	34.6	37.5	37.8
T_8	12.5	13.1	12.3	16.2	11.1	11.0
T_9	11.4	11.9	11.5	15.4	13.9	17.2
T_{10}	27.8	26.9	29.7	28.4	28.4	28.3
T_{11}	25.8	25.9	28.8	26.8	27.2	27.2
T_{12}	30.3	31.1	33.4	32.3	31.0	31.0
T_{13}	-	-	-	-	-	-
T_{14}	36.6	35.9	33.5	32.3	35.0	35.2
T_{15}	25.6	25.9	28.9	26.9	27.4	27.2
T_{16}	38.7	38.8	36.8	34.9	38.7	38.7
T_{17}	30.7	30.9	32.5	30.1	32.4	32.3
T_{18}	27.1	27.2	28.4	27.7	27.6	27.6
T_{19}	70.6	70.6	75.7	75.8	83.8	82.9
T_{20}	61.1	57.5	48.2	50.8	59.1	59.4
T_{21}	83.2	83.7	77.6	78.7	87.1	87.6
T_{22}	36.3	36.4	36.3	34.2	37.2	37.4
T_{23}	36.9	36.7	35.8	34.1	-	-
T_{24}	37.2	37.1	37.2	35.1	38.0	38.1
T_{25}	37.0	36.9	36.9	34.9	37.7	37.9
T_{26}	36.8	36.7	36.8	34.7	37.6	37.6
T_{27}	36.9	36.8	36.7	34.6	37.7	37.5
T_{28}	28.7	28.8	28.8	28.2	28.6	28.1
M_{WAB}†	58.5	58.5	46.5	47.5	48.5	48.5
M_{WCO}†	23.5	22.0	23.5	23.2	24.0	23.7
Q_{GE}+	420.0	458.0	364.0	391.5	364.0	391.5
Q_{EV}+	90.0	90.0	90.0	80.0	108.5	108.5
X_{GE}*	63.45	62.75	64.36	65.88	64.85	64.83
X_{AB}*	62.39	62.14	62.69	63.85	63.78	63.53

T in °C † kg h^{-1} + W * dimensionless

Table A2.3 Raw experimental performance data for the operating characteristics of the water-lithium bromide-lithium iodide absorption cooler.

...continued

R. No.	7	8	9	10	11	12
T_1	100.2	99.0	98.7	97.8	99.3	99.8
T_2	28.6	27.4	26.9	28.3	27.2	26.8
T_3	50.0	49.7	50.0	50.1	51.0	50.3
T_4	38.5	37.1	37.4	38.3	39.4	38.6
T_5	36.8	36.4	37.1	37.6	36.4	34.7
T_6	32.5	32.9	33.2	33.6	34.3	31.9
T_7	38.0	36.7	37.7	38.6	37.0	35.0
T_8	11.7	10.5	11.1	12.0	12.7	15.5
T_9	13.9	9.6	10.1	10.8	12.3	13.9
T_{10}	28.4	28.8	28,8	29.0	30.2	30.1
T_{11}	27.3	28.1	28.3	28.0	30.0	28.8
T_{12}	32.0	32.6	32.4	32.9	31.8	34.7
T_{13}	-	-	-	-	-	-
T_{14}	35.5	35.2	35.7	36.8	34.9	33.0
T_{15}	27.4	28.5	28.7	28.1	30.5	28.2
T_{16}	38.7	38.5	37.8	40.3	40.2	35.4
T_{17}	32.5	32.9	33.0	33.8	34.9	31.5
T_{18}	27.3	26.0	26.2	26.5	26.6	26.6
T_{19}	79.4	80.3	76.1	78.2	80.7	75.5
T_{20}	55.3	57.2	44.2	58.6	55.9	43.6
T_{21}	85.6	86.2	81.7	86.6	84.9	78.5
T_{22}	37.5	36.8	37.0	37.4	37.3	34.8
T_{23}	-	37.6	38.3	38.5	37.5	34.5
T_{24}	38.4	37.6	37.7	38.5	38.0	35.3
T_{25}	38.2	37.4	37.5	38.3	37.9	35.2
T_{26}	38.0	37.4	37.5	38.3	37.8	35.1
T_{27}	38.0	37.2	37.3	38.2	37.7	35.0
T_{28}	27.7	27.2	27.0	26.7	27.5	27.7
M_{WAB}†	48.5	51.0	50.0	51.0	51.0	52.5
M_{WCO}†	23.5	23.5	23.0	23.5	23.5	24.0
Q_{GE}+	420.0	420.0	407.0	476.0	386.0	323.4
Q_{EV}+	120.0	90.0	90.0	120.0	87.0	64.7
X_{GE}*	64.28	64.14	63.78	64.10	64.05	64.65
X_{AB}*	63.18	63.39	62.83	62.83	62.96	63.16

T in °C † kg h^{-1} + W * dimensionless

Table A2.3 (continued) Raw experimental performance data for the operating characteristics of the water-lithium bromide-lithium iodide absorption cooler

R. No.	13	14	15	16		
T_1	100.2	97.0	98.3	102.8		
T_2	27.8	27.6	27.8	28.9		
T_3	49.8	49.9	50.2	50.0		
T_4	37.4	39.0	39.0	39.3		
T_5	36.9	36.1	36.5	35.4		
T_6	33.1	32.3	32.5	31.8		
T_7	38.1	37.1	37.5	36.3		
T_8	11.2	11.3	12.0	11.5		
T_9	9.8	10.4	11.7	10.4		
T_{10}	29.7	28.7	28.8	28.2		
T_{11}	29.4	27.9	28.0	26.5		
T_{12}	32.3	32.7	31.8	33.1		
T_{13}	-	-	-	-		
T_{14}	35.4	35.6	35.9	33.9		
T_{15}	29.8	28.0	28.2	26.6		
T_{16}	37.7	37.7	38.2	35.9		
T_{17}	33.3	32.4	32.7	32.2		
T_{18}	27.3	27.0	27.0	27.3		
T_{19}	76.8	71.5	72.0	79.3		
T_{20}	54.7	60.3	62.8	44.5		
T_{21}	79.4	81.8	82.5	84.4		
T_{22}	37.4	36.7	37.0	35.8		
T_{23}	37.4	37.0	37.3	-		
T_{24}	38.1	37.6	37.7	36.6		
T_{25}	37.9	37.5	37.6	36.4		
T_{26}	37.8	37.2	37.3	36.1		
T_{27}	37.7	37.2	37.3	36.1		
T_{28}	28.5	28.0	28.2	28.5		
M_{WAB}†	46.5	46.5	46.5	46.5		
M_{WCO}†	22.5	23.2	22.5	23.2		
Q_{GE}+	312.0	377.0	377.0	391.5		
Q_{EV}+	70.0	90.0	90.0	105.0		
X_{GE}*	64.38	63.87	63.78	64.85		
X_{AB}*	62.83	62.62	62.66	62.67		

T in °C † kg h^{-1} + W * dimensionless

Table A2.3 (continued) Raw experimental performance data for the operation characteristics of the water-lithium bromide-lithium iodide absorption cooler.

T1	solution vapour vapour mixture entering absorber (after mixer), °C
T2	solution leaving absorber, °C
T3	strong refrigerant solution entering economiser, °C
T4	strong refrigerant solution leaving economiser, °C
T5	weak refrigerant solution leaving economiser, °C
T6	weak refrigerant solution entering economiser, °C
T7	strong refrigerant solution entering generator, °C
T8	two-phase mixture leaving generator, °C
T9	two-phase mixture entering rectifier, °C
T10	refrigerant vapour leaving rectifier, °C
T11	strong refrigerant solution leaving rectifier, °C
T12	refrigerant vapour entering condenser, °C
T13	cooling water entering condenser, °C
T14	cooling water leaving condenser, °C
T15	cooling water entering absorber, °C
T16	cooling water leaving absorber, °C
T17	cooling water entering rectifier, °C
T18	cooling water leaving rectifier, °C
T19	geothermal fluid entering generator, °C
T20	geothermal fluid leaving generator, °C
T21	ambient temperature, °C
T22	liquid refrigerant entering precooler, °C
T23	liquid refrigerant leaving precooler, °C
T24	liquid refrigerant entering evaporator, °C
T25	refrigerant vapour leaving evaporator, °C
T26	refrigerant vapour entering precooler, °C
T27	refrigerant vapour leaving precooler, °C
T28	cold storage temperature, °C
FEV	liquid refrigerant flow rate, GPM
FAB	weak refrigerant solution flow rate, GPM
FWRE	cooling water flow rate to rectifier, LPM
FWAB	cooling water flow rate to absorber, LPM
FWCO	cooling water flow rate to condenser, LPM
FCS	geothermal steam flow rate, LPM
PCO	condenser pressure, PSIG
PAB	absorber pressure, PSIG
PREC	rectifier pressure, PSIG

Table A2.4 Raw experimental performance data for the operating characteristics of the ammonia-water absorption refrigerator operated with geothermal steam at Los Azufres, Michoacán, Mexico.

... continued

R. No.	1	2	3	4	5	6
T_1	42.6	41.33	45.7	44.0	44.1	45.9
T_2	29.6	29.4	32.8	32.1	32.5	31.4
T_3	30.8	30.7	34.4	33.1	33.7	33.2
T_4	54.0	54.1	58.3	55.4	56.6	57.3
T_5	77.6	78.7	86.2	82.4	85.0	86.2
T_6	56.6	56.9	63.1	59.7	62.9	62.9
T_7	55.8	56.1	62.4	59.0	62.5	62.5
T_8	82.2	82.5	90.8	87.1	90.0	91.6
T_9	78.6	79.1	87.8	84.3	87.8	89.6
T_{10}	57.0	60.1	67.4	63.9	68.3	71.7
T_{11}	55.0	66.7	64.6	66.3	60.1	63.8
T_{12}	46.6	48.0	61.1	56.1	63.2	68.3
T_{13}	21.2	21.3	23.4	20.4	25.9	20.6
T_{14}	23.4	23.1	25.9	22.4	28.2	24.1
T_{15}	21.8	22.6	23.5	21.4	24.7	19.8
T_{16}	25.4	25.3	26.4	24.4	27.5	23.4
T_{17}	20.6	21.6	22.0	19.3	24.6	18.8
T_{18}	25.2	36.9	30.25	28.4	31.3	27.5
T_{19}	93.2	93.1	98.7	96.1	96.7	100.1
T_{20}	86.4	84.6	94.9	91.3	93.7	95.4
T_{21}	22.4	22.1	23.7	21.5	26.3	21.8
T_{22}	22.4	22.3	23.9	21.3	26.6	22.5
T_{23}	17.8	12.1	10.3	14.9	13.7	10.6
T_{24}	-11.4	-13.3	-13.4	-14.9	-10.5	-12.7
T_{25}	- 2.8	- 5.6	- 6.1	- 1.0	- 7.0	- 4.1
T_{26}	- 0.6	- 4.6	- 5.8	0.5	- 6.7	- 3.8
T_{27}	9.4	1.9	0.1	10.3	- 4.7	- 1.4
T_{28}	- 5.4	- 6.9	- 7.2	- 4.1	- 7.1	- 4.8

T in °C

Table A2.4 (continued) Raw experimental performance data for the operating characteristics of the ammonia-water absorption refrigerator operated with geothermal steam at Los Azufres, Michoacán, Mexico.

R. No.	7	8	9			
T_1	47.8	43.9	40.7			
T_2	33.5	32.1	30.4			
T_3	34.7	32.6	31.1			
T_4	59	56.8	53.8			
T_5	88.9	83.7	77.7			
T_6	65.4	61.2	56.8			
T_7	64.6	60.6	55.9			
T_8	94.4	88.1	81.6			
T_9	92.4	85.2	78.1			
T_{10}	72.9	64.0	56.1			
T_{11}	64.5	60.9	56.1			
T_{12}	66.9	55.8	47.5			
T_{13}	23.9	22.0	22.1			
T_{14}	27.1	24.4	23.5			
T_{15}	23.8	22.4	23.2			
T_{16}	26.8	25.3	25.6			
T_{17}	22.7	21.2	21.1			
T_{18}	30.3	27.6	26.4			
T_{19}	101.6	94.8	92.1			
T_{20}	97.1	91.5	82.5			
T_{21}	24.8	22.8	22.3			
T_{22}	24.9	22.4	22.1			
T_{23}	16.1	16.2	17.1			
T_{24}	-11.9	-14.6	-14.1			
T_{25}	- 1.9	- 2.1	0.4			
T_{26}	- 1.3	- 0.6	3.2			
T_{27}	4.4	7.6	13.0			
T_{28}	- 3.6	- 4.2	- 2.5			

T in °C

Table A2.4 (continued) Raw experimental performance data for the operating characteristics of the ammonia-water absorption refrigerator operated with geothermal steam at Los Azufres, Michoacán, Mexico.

R. No.	1	2	3	4	5	6
F_{EV}*	0.14	0.13	0.16	0.16	0.17	0.21
F_{AB}*	2.11	2.02	1.68	1.75	1.56	1.64
F_{WRE}+	2.0	2.0	3.6	3.7	6.0	5.0
F_{WAB}+	35.3	35.3	75.0	66.7	66.7	66.7
F_{WCO}+	42.0	42.0	46.7	38.2	42.0	35.3
F_{GS}+	-	-	0.67	0.75	0.59	0.79
P_{CO}°	111.2	111.1	118.1	110.7	126.8	112.4
P_{AB}°	25.3	22.5	22.4	20.6	26.2	22.8
P_{RE}°	120.0	119.0	126.4	119.4	134.2	121.4

* GPM + LPM ° PSIG

Table A2.4 (continued) Raw experimental performance data for the operating characteristics of the ammonia-water absorption refrigerator operated with geothermal steam at Los Azufres, Michoacán, Mexico.

R. No.	7	8	9			
F_{EV}*	0.19	0.15	0.10			
F_{AB}*	1.64	1.80	1.85			
F_{WRE}+	6.0	5.4	5.4			
F_{WAB}+	75.0	75.0	75.0			
F_{WCO}+	35.3	33.3	31.6			
F_{GS}+	0.9	0.76	0.58			
P_{CO}°	122.5	115.0	113.4			
P_{AB}°	23.7	20.5	22.1			
P_{RE}°	130.9	123.6	121.9			

* GPM + LPM ° PSIG

Table A2.4 (continued) Raw experimental performance data for the operating characteristics of the ammonia-water absorption refrigerator operated with geothermal steam at Los Azufres, Michoacán, Mexico.

T1	weak refrigerant solution leaving generator, K
T2	strong refrigerant solution entering generator, K
T3	refrigerant vapour leaving generator, K
T4	refrigerant vapour entering condenser, K
T5	liquid refrigerant leaving condenser, K
T6	liquid refrigerant entering economiser (precooler), K
T7	liquid refrigerant leaving economiser (precooler), K
T8	liquid refrigerant entering evaporator, K
T9	refrigerant leaving evaporator (entering precooler), K
T10	refrigerant leaving economiser (precooler), K
T11	strong refrigerant solution leaving absorber, K
T12	strong refrigerant solution entering economiser, K
T13	weak refrigerant solution entering absorber, K
T14	cooling water entering condenser, K
T15	cooling water leaving condenser, K
T16	cooling water entering absorber, K
T17	cooling water leaving absorber, K
T20	hot oil entering generator, K
T21	hot oil leaving generator, K
P2	condenser pressure, MPa absolute
P3	absorber pressure, MPa absolute
P4	evaporator pressure, MPa absolute
M7	liquid refrigerant mass flow rate, kg s^{-1}
M11	strong solution flow rate, kg s^{-1}
M14	cooling water flow rate to condenser, kg s^{-1}
M16	cooling water flow rate to absorber, kg s^{-1}
M20	hot oil flow rate, kg s^{-1}

Table A2.5 Raw experimental performance data for the operating characteristics of the ammonia-water absorption system at UNAM.

... continued

T1	T2	T3	T4	T5	T6	T7
351.8	319.7	304.1	301.6	301.1	299.1	292.0
351.6	317.0	301.0	300.7	300.8	300.1	290.9
351.4	320.5	302.0	301.3	301.7	300.3	292.5
351.0	320.4	303.9	302.1	301.0	300.6	292.5
352.8	320.1	305.1	303.2	302.3	300.7	290.9
350.4	311.2	306.9	303.0	299.6	300.8	299.8
353.7	322.9	305.9	304.1	302.7	300.0	291.2
351.6	320.1	304.5	302.1	300.0	300.0	292.7
349.9	318.1	303.0	301.3	301.3	300.0	294.0
350.6	315.2	303.4	302.2	302.4	300.7	291.3

T8	T9	T10	T11	T12	T13	T14
268.0	290.7	291.6	295.5	296.0	331.1	285.5
271.0	289.5	293.1	298.9	297.4	329.9	284.9
269.5	290.0	291.8	296.1	296.8	330.8	285.4
270.5	291.9	292.5	296.0	296.4	331.4	283.4
269.7	292.5	292.3	295.5	296.5	331.9	283.0
263.2	290.1	290.1	296.7	297.8	325.2	282.8
271.2	288.7	297.5	295.2	295.6	334.8	282.5
271.5	288.5	295.1	294.5	295.5	335.9	282.6
268.5	288.1	294.3	296.7	297.4	330.9	282.8
265.9	288.3	293.2	296.7	296.9	326.8	283.5

T15	T16	T17	T20	T21	P2	P3
287.9	283.8	285.4	373.4	352.6	1.072	0.311
287.9	283.3	283.3	363.7	352.3	1.051	0.301
288.5	283.8	283.4	363.0	353.7	1.072	0.331
287.0	283.5	283.1	365.3	354.2	1.051	0.342
287.4	283.2	282.6	367.2	355.6	1.092	0.340
286.9	282.9	283.3	368.8	355.2	1.031	0.260
285.7	282.1	282.6	367.4	355.7	1.087	0.352
286.3	281.4	282.3	364.9	354.2	1.062	0.385
286.8	281.0	281.6	362.3	352.2	1.062	0.321
287.8	281.1	280.9	364.5	353.0	1.092	0.291

P4	M7	M11	M14	M16	M20
0.330	0.000333	0.011984	0.010822	0.232452	0.101663
0.386	0.000207	0.012154	0.010822	0.232452	0.125815
0.345	0.000393	0.012035	0.010822	0.232452	0.155486
0.355	0.000393	0.012159	0.010822	0.235066	0.146301
0.347	0.000393	0.011925	0.010822	0.235066	0.140774
0.276	0.000393	0.012144	0.010822	0.227224	0.132462
0.366	0.000207	0.011966	0.010822	0.229838	0.134181
0.404	0.000207	0.012136	0.010822	0.232452	0.127615
0.335	0.000269	0.012086	0.010822	0.229838	0.150054
0.299	0.000393	0.011864	0.010822	0.229838	0.147300

Table A2.5 (continued) Raw experimental performance data for the operating characteristics of the ammonia-water absorption system at UNAM.

T1	T2	T3	T4	T5	T6	T7
356.6	318.7	319.3	313.5	300.1	299.8	295.9
359.3	323.7	320.1	314.4	302.1	300.9	300.5
358.2	323.3	312.1	306.1	302.9	300.7	298.4
356.5	322.3	308.8	303.2	300.5	301.4	299.7
356.8	323.3	309.0	304.0	301.4	300.8	299.8
358.3	324.5	309.9	305.6	301.9	300.9	299.2
358.1	322.9	308.6	305.5	302.4	301.5	296.4
357.3	324.2	308.8	306.0	302.4	301.7	287.0
357.7	323.4	313.8	308.6	302.7	299.8	282.0

T8	T9	T10	T11	T12	T13	T14
279.0	295.9	299.1	297.5	298.1	335.0	284.5
267.3	292.7	293.7	294.3	300.1	337.7	283.2
267.4	291.8	298.4	298.9	299.2	335.5	283.6
269.9	292.1	299.7	302.1	301.4	335.5	283.5
270.7	291.1	299.6	299.9	299.8	336.5	283.1
270.5	285.9	299.8	299.9	299.5	336.8	283.5
272.6	285.1	302.0	302.5	302.1	335.7	283.1
270.8	283.9	285.4	303.7	302.1	336.6	283.5
269.7	283.0	282.7	301.5	302.1	335.6	283.2

T15	T16	T17	T20	T21	P2	P3
287.9	284.1	285.7	389.7	358.4	1.031	0.280
287.8	283.2	286.4	387.9	357.6	1.072	0.301
292.0	283.6	287.2	388.0	354.0	1.072	0.301
290.5	283.2	283.4	390.6	352.6	1.051	0.301
291.0	283.4	283.2	390.7	353.7	1.072	0.321
292.0	283.3	282.8	391.4	354.5	1.092	0.331
291.7	283.6	282.0	391.6	354.7	1.072	0.301
287.6	283.1	282.4	396.2	354.6	1.092	0.321
291.5	282.8	281.7	392.7	353.4	1.072	0.311

P4	M7	M11	M14	M16	M20
0.294	0.000208	0.012196	0.039026	0.159261	0.101658
0.315	0.000455	0.011937	0.039026	0.151419	0.082643
0.315	0.000455	0.012043	0.022104	0.130507	0.066071
0.345	0.000578	0.012225	0.022104	0.130507	0.071770
0.355	0.000579	0.012106	0.022104	0.130507	0.079240
0.366	0.000455	0.012016	0.022104	0.130507	0.080907
0.386	0.000578	0.012125	0.022104	0.130507	0.081383
0.366	0.000701	0.012084	0.050308	0.122665	0.071431
0.325	0.000581	0.012121	0.039026	0.122665	0.076353

Table A2.5 (continued) Raw experimental performance data for the operating characteristics of the ammonia-water absorption system at UNAM.

T1	T2	T3	T4	T5	T6	T7
360.8	314.0	321.3	317.0	300.2	298.2	268.4
367.2	317.9	327.9	323.1	301.7	299.3	273.1
366.6	326.7	329.6	324.0	301.3	301.3	271.5
366.2	329.2	331.8	325.8	300.8	301.6	269.0
367.6	324.7	329.8	323.6	300.7	300.4	267.7
364.3	329.6	328.1	323.0	300.9	301.0	269.3
365.2	330.2	330.4	325.1	302.6	301.2	270.1
365.7	327.3	331.6	325.4	302.6	301.8	270.7
365.5	323.9	331.1	325.3	303.0	302.3	269.0
365.2	328.3	327.4	325.2	302.7	302.4	268.8
365.8	329.1	324.3	322.6	301.4	302.8	270.2
365.2	324.8	332.2	325.5	300.8	301.4	268.8
366.1	323.4	331.7	326.6	301.5	301.7	268.3

T8	T9	T10	T11	T12	T13	T14
263.6	293.8	286.2	299.5	298.3	331.3	285.0
265.8	294.1	286.6	302.8	301.9	333.5	285.2
265.7	282.0	286.6	303.5	303.1	340.6	284.6
265.8	282.0	284.0	304.2	303.6	342.4	283.7
265.2	281.2	266.8	304.7	304.0	339.1	283.6
267.9	282.9	268.4	305.1	304.1	342.9	283.6
269.1	282.1	268.8	304.2	304.6	342.4	282.5
268.4	282.0	268.2	302.3	303.1	340.8	281.4
268.3	281.7	267.5	302.4	302.7	337.5	281.1
268.2	281.2	267.4	302.9	303.0	343.3	281.5
268.7	281.4	268.6	303.6	303.0	342.0	281.5
267.2	280.7	267.2	303.1	302.3	338.0	280.7
268.0	280.8	280.2	302.3	302.4	337.2	281.0

T15	T16	T17	T20	T21	P2	P3
287.2	284.8	286.4	402.7	360.7	1.031	0.260
287.4	284.5	286.5	398.0	371.0	1.092	0.260
286.9	284.4	285.8	395.1	365.9	1.072	0.260
286.5	283.8	284.7	391.7	366.5	1.031	0.260
287.1	283.7	283.3	390.1	369.3	1.051	0.250
286.9	283.3	284.5	388.2	365.4	1.062	0.280
286.3	282.4	283.1	387.7	367.8	1.072	0.280
285.6	281.7	282.5	384.6	368.9	1.072	0.280
285.3	281.0	282.3	382.0	367.8	1.082	0.280
284.9	281.2	281.1	380.1	367.3	1.072	0.280
285.0	281.4	281.2	378.8	367.4	1.072	0.285
284.3	281.0	280.8	376.3	365.5	1.072	0.270
284.9	281.4	281.9	374.8	364.9	1.072	0.260

P4	M7	M11	M14	M16	M20
0.284	0.000986	0.012204	0.151843	0.133121	0.090757
0.294	0.001083	0.011936	0.129280	0.133121	0.132334
0.294	0.001262	0.012063	0.123639	0.133121	0.118564
0.294	0.001137	0.012307	0.117998	0.133121	0.130170
0.294	0.001254	0.012186	0.072871	0.140963	0.138939
0.315	0.001326	0.012201	0.072871	0.140963	0.124604
0.335	0.001449	0.012122	0.072871	0.140963	0.133011
0.325	0.001384	0.012077	0.072871	0.143577	0.143143
0.325	0.001320	0.012025	0.084153	0.138349	0.154069
0.325	0.001196	0.012091	0.095435	0.138349	0.162706
0.335	0.001070	0.012117	0.095435	0.138349	0.183376
0.315	0.001138	0.012075	0.095435	0.138349	0.186140
0.315	0.001199	0.012039	0.095435	0.138349	0.187804

Table A2.5 (continued) Raw experimental performance data for the operating characteristics of the ammonia-water absorption system at UNAM.

T1	T2	T3	T4	T5	T6	T7
360.9	316.6	318.3	314.3	302.1	299.4	279.4
362.1	324.2	323.9	318.9	301.0	301.0	280.8
364.5	326.3	326.6	321.2	301.4	301.9	275.9
361.4	326.9	327.2	321.0	300.5	301.0	273.6
361.7	326.6	323.8	318.0	300.3	300.5	274.7
361.5	326.4	328.3	321.7	301.4	300.7	275.1
361.4	326.4	327.6	321.2	301.7	301.4	275.0
361.0	328.4	326.3	319.7	301.3	301.4	275.6
361.5	327.0	329.5	322.5	302.4	301.6	275.9
361.2	326.6	330.3	324.0	300.9	301.7	275.2
362.4	326.0	331.3	325.3	301.7	301.5	275.5
361.4	325.0	333.2	327.1	301.5	302.2	276.1
361.8	327.8	333.5	327.1	302.4	292.6	277.1

T8	T9	T10	T11	T12	T13	T14
267.6	292.7	288.9	301.6	300.6	326.6	287.5
267.8	283.2	289.2	302.8	301.9	338.2	285.6
268.1	283.3	288.0	303.8	304.5	339.2	285.6
268.6	282.6	284.7	304.7	304.2	339.3	284.7
268.4	282.4	281.4	304.3	304.4	339.3	283.7
268.7	281.5	281.9	305.7	304.9	339.3	283.5
268.9	281.4	281.2	305.2	304.9	338.8	284.0
269.5	281.2	281.5	304.8	304.2	339.9	283.1
269.5	281.7	281.6	304.0	304.2	339.3	283.0
268.9	281.2	281.0	304.5	303.6	338.4	282.9
269.1	282.1	281.0	303.3	303.2	338.2	282.1
269.3	282.2	282.0	302.9	303.7	337.7	282.3
270.7	283.0	283.6	303.1	304.3	339.2	282.1

T15	T16	T17	T20	T21	P2	P3
289.6	286.2	286.8	395.6	366.4	1.092	0.280
287.9	285.0	285.2	392.0	366.4	1.072	0.280
288.1	284.8	285.6	389.8	365.0	1.051	0.270
287.0	285.0	283.7	388.3	362.5	1.051	0.280
287.4	284.0	282.8	386.9	362.6	1.051	0.291
286.9	283.8	281.7	385.9	362.2	1.072	0.291
286.9	283.7	282.1	385.7	361.3	1.072	0.291
286.5	283.0	281.5	384.8	361.9	1.072	0.301
286.7	283.2	282.1	384.0	362.7	1.092	0.301
285.8	282.5	281.5	383.9	361.8	1.072	0.295
285.0	282.3	282.3	383.0	360.9	1.072	0.291
285.7	282.2	281.4	382.8	360.1	1.072	0.280
285.6	282.0	281.6	382.6	360.8	1.072	0.303

P4	M7	M11	M14	M16	M20
0.305	0.000957	0.011950	0.151843	0.122665	0.132170
0.315	0.000828	0.012089	0.157484	0.117437	0.135006
0.315	0.000950	0.012204	0.123639	0.122665	0.119825
0.325	0.000828	0.012247	0.081333	0.106981	0.107700
0.335	0.000705	0.012258	0.067231	0.101753	0.106374
0.335	0.000829	0.012181	0.055949	0.106981	0.102958
0.335	0.000827	0.012168	0.055949	0.106981	0.102274
0.345	**0.000951**	**0.012180**	**0.055949**	**0.127893**	**0.099194**
0.345	0.000827	0.012047	0.055949	0.133121	0.102621
0.343	0.000827	0.012159	0.055949	0.133121	0.099180
0.345	0.000703	0.012120	0.067231	0.135735	0.099967
0.345	0.000764	0.012091	0.067231	0.135735	0.100198
0.362	0.000763	0.012142	0.064410	0.133121	0.097400

Table A2.5 (continued) Raw experimental performance data for the operating characteristics of the ammonia-water absorption system at UNAM.

T1	T2	T3	T4	T5	T6	T7
370.6	323.7	335.9	331.9	299.2	300.8	285.2
371.3	330.9	340.4	335.8	299.1	301.9	274.1
371.2	332.1	341.0	335.6	299.5	300.9	266.8
371.2	330.1	341.7	336.3	300.2	300.9	264.0
371.0	329.4	342.0	336.7	301.1	300.8	264.2
369.6	332.2	340.5	335.1	301.9	301.9	264.6
368.1	329.6	339.7	335.0	302.1	302.1	265.6
369.1	330.9	341.2	335.8	302.6	302.2	265.7
368.1	328.6	339.0	332.7	301.9	301.9	266.1
368.1	327.0	337.2	332.5	301.3	301.6	266.5

T8	T9	T10	T11	T12	T13	T14
268.7	295.7	295.6	306.9	304.3	340.1	287.6
263.5	284.1	290.8	307.2	307.7	345.5	285.8
263.4	283.6	285.3	305.6	306.2	345.2	284.8
262.4	282.6	263.0	305.1	304.9	343.9	284.8
263.9	282.4	262.9	304.4	304.2	343.3	284.7
264.4	282.6	263.9	304.1	304.2	343.4	284.8
265.2	282.7	264.0	304.0	304.8	342.9	283.6
265.6	282.6	265.2	305.1	305.0	342.2	283.7
266.4	282.7	265.2	303.5	304.5	341.2	283.7
266.7	282.2	266.0	301.0	305.0	340.9	282.9

T15	T16	T17	T20	T21	P2	P3
289.2	287.2	289.5	388.9	376.0	1.072	0.331
287.5	285.8	287.1	385.9	374.8	1.062	0.260
287.6	284.7	285.2	383.4	373.0	1.051	0.250
287.6	284.7	285.2	383.4	373.0	1.051	0.250
287.7	284.3	285.1	382.2	371.9	1.072	0.260
287.6	284.6	284.8	381.1	371.4	1.072	0.270
286.5	283.8	283.7	379.4	370.1	1.082	0.275
286.4	283.6	282.9	378.5	369.1	1.072	0.280
286.0	283.3	283.5	377.2	368.2	1.072	0.280
285.8	283.0	286.6	375.9	367.1	1.072	0.291

P4	M7	M11	M14	M16	M20
0.345	0.001204	0.012303	0.208252	0.080842	0.216473
0.274	0.001637	0.012211	0.219533	0.075614	0.200007
0.264	0.001455	0.012208	0.123639	0.075614	0.192857
0.264	0.001456	0.012196	0.123639	0.075614	0.192857
0.264	0.001706	0.012085	0.095435	0.075614	0.206007
0.284	0.001512	0.012098	0.112357	0.075614	0.213647
0.284	0.001399	0.012050	0.123639	0.075614	0.215131
0.284	0.001300	0.012144	0.123639	0.075614	0.215918
0.294	0.001449	0.012104	0.123639	0.075614	0.217056
0.305	0.001450	0.012069	0.123639	0.075614	0.218197

Table A2.5 (continued) Raw experimental performance data for the operating characteristics of the ammonia-water absorption system at UNAM.

T1	T2	T3	T4	T5	T6	T7
366.8	320.3	332.1	328.9	303.0	302.7	296.5
366.5	325.6	337.5	333.2	299.1	301.8	269.2
367.2	326.6	340.0	333.8	300.1	301.3	267.6
366.5	327.4	338.5	333.2	296.9	300.8	265.8
366.3	329.4	337.2	331.3	299.6	300.3	266.5
365.3	328.0	336.9	329.9	301.8	300.9	267.7
365.2	327.5	336.7	330.1	302.7	301.7	268.4
365.2	325.8	335.9	330.8	298.9	300.6	268.4
364.7	325.3	336.4	330.9	301.5	301.1	269.2
364.3	325.6	336.3	330.8	301.6	301.4	269.4

T8	T9	T10	T11	T12	T13	T14
285.6	295.6	284.4	304.8	304.0	336.1	287.4
266.8	293.7	290.7	303.5	304.1	338.6	286.5
266.8	284.5	290.2	305.7	303.9	340.8	285.2
265.6	283.0	266.6	303.0	302.5	341.6	285.0
265.9	283.6	265.8	304.1	303.3	342.9	285.5
267.6	285.4	267.0	304.2	303.0	341.9	284.8
268.1	285.1	267.4	302.8	301.9	340.3	284.6
268.1	284.3	267.7	303.5	301.9	339.4	284.4
268.7	284.2	268.0	302.9	302.1	338.8	283.8
268.4	284.2	267.6	304.4	301.3	338.4	283.8

T15	T16	T17	T20	T21	P2	P3
289.3	286.8	288.6	388.5	371.1	1.132	0.311
288.3	286.0	290.8	384.8	372.6	1.092	0.250
286.8	285.0	286.9	382.0	370.7	1.062	0.255
287.7	285.4	285.8	380.2	370.0	1.051	0.260
289.1	285.6	288.1	379.5	369.9	1.062	0.280
289.5	285.0	287.9	378.2	369.0	1.072	0.280
287.3	284.9	287.5	376.9	367.7	1.072	0.301
287.3	284.2	285.5	376.2	366.5	1.072	0.285
287.1	283.7	286.3	375.2	365.6	1.072	0.291
287.1	283.7	286.2	374.4	364.9	1.072	0.301

P4	M7	M11	M14	M16	M20
0.305	0.000206	0.014635	0.242097	0.075614	0.150229
0.305	0.001263	0.014736	0.151843	0.159261	0.200744
0.259	0.001203	0.014986	0.140562	0.195856	0.199555
0.294	0.001205	0.014973	0.095435	0.201084	0.194794
0.305	0.001207	0.014973	0.039026	0.190628	0.201999
0.325	0.001203	0.014918	0.039026	0.190628	0.184039
0.325	0.001200	0.014908	0.039026	0.185400	0.185476
0.325	0.001143	0.014903	0.078512	0.221996	0.211582
0.305	0.001701	0.014895	0.067231	0.232452	0.212516
0.325	0.001139	0.014955	0.067231	0.232452	0.213264

Table A2.5 (continued) Raw experimental performance data for the operating characteristics of the ammonia-water absorption system at UNAM.

T1	T2	T3	T4	T5	T6	T7
364.3	327.1	331.8	330.9	302.5	302.7	268.6
364.3	328.1	335.9	330.3	300.9	302.2	265.9
363.3	329.7	336.1	329.5	300.0	301.0	266.0
362.9	326.6	316.7	309.4	298.9	300.2	268.8
360.4	326.2	307.1	305.3	298.8	299.2	268.9
362.3	327.6	318.4	311.3	299.8	299.1	267.0
362.3	324.7	313.9	307.4	302.6	300.3	268.4
361.6	324.3	328.3	322.5	302.7	300.9	267.2
361.4	326.4	334.5	329.2	298.5	300.7	267.9
361.4	324.8	335.3	330.7	299.7	300.0	266.6
361.4	324.2	335.0	330.3	300.3	300.7	267.1
361.4	324.6	335.1	330.0	298.5	300.8	266.2

T8	T9	T10	T11	T12	T13	T14
265.0	294.5	281.6	303.6	303.4	340.6	286.8
264.5	293.1	284.5	305.0	304.7	343.3	286.7
263.6	284.6	286.7	304.3	304.8	343.3	285.8
265.4	285.3	299.7	301.0	300.7	340.9	288.1
265.5	285.4	296.7	302.6	302.6	338.6	289.0
265.9	285.3	303.2	305.6	304.8	341.3	286.6
266.4	284.9	266.0	302.6	303.6	339.2	285.2
267.8	284.6	272.9	301.0	300.8	340.0	284.6
266.7	284.6	266.3	303.2	301.8	340.1	284.3
264.6	282.8	264.3	302.3	302.5	338.8	284.0
265.6	283.1	264.8	302.1	301.9	338.9	284.2
265.2	282.8	264.3	301.9	301.3	338.0	283.1

T15	T16	T17	T20	T21	P2	P3
288.3	286.2	292.4	385.9	373.7	1.132	0.280
287.8	286.3	292.4	383.7	372.7	1.092	0.275
287.2	285.4	289.7	381.2	371.2	1.051	0.270
288.3	285.6	289.0	371.8	364.0	1.051	0.291
289.0	285.5	288.9	382.9	358.6	0.971	0.280
288.4	285.1	289.2	382.4	363.8	1.051	0.280
289.3	284.8	288.5	382.8	362.0	1.122	0.291
287.1	284.8	286.1	382.2	363.5	1.112	0.311
286.3	284.3	287.5	380.6	365.1	1.072	0.301
286.9	284.1	286.9	378.9	365.8	1.072	0.280
286.9	283.9	286.9	377.6	364.8	1.072	0.280
287.4	283.7	286.7	377.1	364.5	1.072	0.280

P4	M7	M11	M14	M16	M20
0.294	0.001134	0.014548	0.208252	0.086069	0.061449
0.284	0.001012	0.014817	0.213893	0.080842	0.000000
0.284	0.001078	0.015024	0.208252	0.106981	0.000000
0.294	0.000954	0.014959	0.010822	0.133121	0.065076
0.294	0.000957	0.015457	0.010822	0.211540	0.085056
0.294	0.001145	0.015079	0.010822	0.211540	0.103700
0.305	0.001078	0.014596	0.055949	0.232452	0.091148
0.315	0.000953	0.014641	0.140562	0.195856	0.116193
0.305	0.000955	0.014917	0.078512	0.195856	0.143090
0.294	0.000958	0.014862	0.084153	0.227224	0.164126
0.294	0.001080	0.014857	0.084153	0.216768	0.165667
0.335	0.001141	0.014852	0.081333	0.227224	0.172580

Table A2.5 (continued) Raw experimental performance data for the operating characteristics of the ammonia-water absorption system at UNAM.

T1	T2	T3	T4	T5	T6	T7
357.0	319.2	323.4	317.6	300.5	300.1	271.4
358.4	322.7	329.4	324.8	301.1	301.8	274.3
357.4	325.7	328.7	321.8	299.5	300.8	283.2
357.1	322.9	329.1	322.7	299.8	300.7	273.4
356.5	323.4	330.3	323.8	300.7	300.3	271.9
357.3	323.5	331.1	325.0	301.2	300.9	271.3
356.7	323.6	329.8	323.2	300.5	301.1	271.2
356.9	321.0	331.3	325.2	301.9	301.7	268.3
356.1	323.2	331.9	325.3	300.5	300.8	278.7

T8	T9	T10	T11	T12	T13	T14
265.7	285.8	277.8	301.3	301.5	330.0	287.0
266.8	287.8	296.6	300.2	300.6	336.6	285.8
267.9	285.9	277.1	301.5	302.3	336.9	284.7
266.3	285.1	272.6	300.7	300.4	335.6	284.6
266.8	284.8	270.1	301.1	299.6	335.1	284.1
267.4	284.9	270.1	299.4	299.8	336.0	284.1
268.5	284.7	270.2	300.6	300.2	336.4	283.8
267.0	285.0	292.1	299.9	299.8	336.1	283.6
268.5	284.9	277.9	300.5	300.1	334.7	283.3

T15	T16	T17	T20	T21	*P2*	*P3*
289.0	286.8	289.5	399.7	359.1	1.031	0.280
287.8	285.9	287.4	397.6	364.4	1.072	0.301
288.4	284.8	289.0	396.6	357.1	1.072	0.321
288.1	284.5	288.3	396.0	355.5	1.062	0.301
288.4	284.1	287.7	395.2	354.5	1.072	0.301
288.4	284.2	287.8	394.7	354.8	1.072	0.321
289.1	284.2	287.4	394.0	355.6	1.072	0.331
287.3	283.5	287.0	393.3	354.4	1.092	0.321
286.6	283.7	287.1	393.0	354.0	1.072	0.331

P4	M7	M11	M14	M16	M20
0.294	0.000457	0.015070	0.084153	0.138349	0.064456
0.315	0.000702	0.014835	0.143382	0.195856	0.068636
0.325	0.000580	0.014901	0.039026	0.237680	0.085099
0.305	0.000892	0.014907	0.039026	0.237680	0.086477
0.315	0.000706	0.014860	0.039026	0.242908	0.088316
0.325	0.000953	0.014842	0.039026	0.242908	0.097002
0.345	0.000704	0.014890	0.033386	0.248136	0.094894
0.325	0.000703	0.014741	0.067231	0.232452	0.096558
0.335	0.000580	0.014888	0.061590	0.232452	0.096264

Table A2.5 (continued) Raw experimental performance data for the operating characteristics of the ammonia-water absorption system at UNAM.

T1	T2	T3	T4	T5	T6	T7
351.7	319.1	307.2	308.3	295.7	296.9	285.6
351.6	315.1	307.4	303.7	297.2	296.2	287.0
353.6	322.3	313.2	308.0	299.2	297.4	287.4
353.1	320.1	304.3	302.8	301.3	298.8	285.6
352.9	320.1	299.3	299.5	299.1	299.0	285.2
350.7	318.5	297.4	297.6	297.5	297.6	287.0
352.1	319.6	297.8	302.2	300.5	298.0	287.1
352.2	321.3	307.9	305.0	300.3	298.6	290.8
352.6	322.2	311.1	306.6	300.3	299.9	291.6

T8	T9	T10	T11	T12	T13	T14
279.8	291.7	292.5	298.0	298.3	329.9	288.2
282.6	290.7	298.1	297.7	297.7	330.1	288.6
284.5	290.9	297.5	297.6	297.6	335.5	285.6
269.5	291.5	300.8	298.1	298.8	333.2	285.7
270.7	290.8	294.7	296.6	297.3	331.9	285.8
268.9	291.1	294.4	297.2	297.2	330.0	285.8
269.5	291.2	294.3	296.4	296.9	332.4	285.4
268.9	289.8	291.6	298.7	298.6	333.8	283.8
269.5	290.3	291.5	299.4	299.8	334.1	283.3

T15	T16	T17	T20	T21	P2	P3
287.9	286.3	289.1	391.0	346.5	1.031	0.321
288.3	286.3	288.5	390.3	357.5	1.051	0.321
289.0	285.4	287.0	388.7	356.5	1.051	0.352
287.8	284.7	286.1	388.6	354.1	1.072	0.321
287.9	284.2	285.2	390.0	348.7	0.971	0.342
287.2	283.9	284.9	392.2	349.5	0.971	0.321
287.4	283.9	284.7	391.3	353.8	1.072	0.331
286.0	283.8	284.2	390.9	354.8	1.072	0.342
287.2	283.0	283.7	390.4	354.0	1.072	0.331

P4	M7	M11	M14	M16	M20
0.335	0.000335	0.015030	0.010822	0.258591	0.072644
0.325	0.000336	0.014907	0.010822	0.263819	0.114323
0.355	0.000360	0.014943	0.010822	0.258591	0.088237
0.335	0.000208	0.014804	0.010822	0.258591	0.074227
0.345	0.000358	0.015292	0.010822	0.258591	0.070457
0.335	0.000334	0.015350	0.010822	0.258591	0.082810
0.345	0.000334	0.014767	0.010822	0.263819	0.095430
0.355	0.000333	0.014850	0.010822	0.263819	0.094326
0.345	0.000332	0.014856	0.010822	0.263819	0.078525

Table A2.5 (continued) Raw experimental performance data for the operating characteristics of the ammonia-water absorption system at UNAM.

T1	T2	T3	T4	T5	T6	T7
371.1	299.1	319.3	316.2	302.1	296.8	262.7
371.0	320.9	335.0	330.2	300.0	300.2	260.7
370.3	329.8	339.6	334.4	300.3	300.8	261.6
370.5	328.2	341.7	336.1	296.1	299.3	258.5
369.7	331.7	341.8	335.2	299.9	300.4	261.4
369.6	329.8	341.7	339.9	300.8	301.4	261.4
369.1	330.0	339.1	334.7	299.7	300.1	262.4
369.1	327.5	340.2	335.1	301.1	301.0	262.2
368.1	330.7	338.2	332.4	301.7	301.5	271.3
368.1	326.4	336.3	329.2	300.4	300.3	287.2

T8	T9	T10	T11	T12	T13	T14
253.8	297.0	285.8	296.4	295.8	314.0	292.0
259.0	294.4	281.5	303.8	303.5	336.0	290.1
261.5	282.1	282.9	304.8	304.2	344.0	289.0
258.2	282.6	258.6	304.1	304.5	343.7	288.8
261.1	283.4	261.1	305.9	305.5	345.3	287.7
260.8	282.4	260.0	304.9	304.1	343.6	285.9
261.6	282.2	260.8	306.5	304.0	343.1	285.1
261.0	281.3	260.0	306.2	304.0	341.4	284.6
261.6	289.6	300.6	300.5	301.1	342.4	284.0
268.4	283.8	275.1	306.2	304.9	337.7	283.5

T15	T16	T17	T20	T21	P2	P3
291.7	289.9	294.9	400.7	378.9	1.172	0.178
290.2	288.0	292.4	394.3	379.1	1.122	0.229
289.7	288.9	294.4	391.7	378.2	1.092	0.260
290.0	288.4	292.8	388.1	376.3	1.072	0.219
290.3	288.6	291.9	384.8	374.9	1.072	0.209
288.7	286.2	290.6	382.0	372.7	1.072	0.240
288.2	285.2	289.3	379.1	371.0	1.072	0.250
287.5	284.7	287.7	375.7	369.5	1.072	0.240
286.3	284.4	286.3	372.8	369.4	1.051	0.260
286.4	283.6	286.3	371.6	366.5	1.072	0.301

P4	M7	M11	M14	M16	M20
0.193	0.001469	0.014025	0.213893	0.080842	0.198516
0.243	0.001456	0.014542	0.185688	0.127893	0.247764
0.264	0.001330	0.014789	0.185688	0.122665	0.243113
0.233	0.001464	0.014838	0.151843	0.164488	0.233648
0.254	0.001208	0.014885	0.067231	0.174944	0.214437
0.243	0.001206	0.014883	0.095435	0.169717	0.233086
0.264	0.001209	0.014944	0.078512	0.174944	0.268244
0.254	0.001205	0.014922	0.095435	0.180172	0.378063
0.264	0.001451	0.014907	0.163125	0.174944	0.401659
0.335	0.001156	0.015012	0.089794	0.227224	0.398040

Table A2.5 (continued) Raw experimental performance data for the operating characteristics of the ammonia-water absorption system at UNAM.

T1	T2	T3	T4	T5	T6	T7
362.1	326.6	336.1	330.9	300.5	299.8	282.9
363.1	326.9	336.4	330.5	299.5	300.0	273.4
363.1	328.0	336.3	330.2	299.7	299.6	269.7
363.1	326.0	335.2	329.9	299.9	299.6	267.6
361.4	325.9	334.9	329.7	300.2	300.3	268.0
361.4	325.4	334.8	328.8	301.1	300.8	268.0
361.0	324.4	332.5	326.9	299.6	300.3	268.1
360.4	323.8	332.6	328.0	300.0	300.9	269.0
358.4	322.9	331.4	326.4	299.5	300.0	268.9
358.4	323.7	331.8	327.3	299.5	299.5	268.7
357.5	323.4	331.2	326.2	298.9	299.7	270.4
356.5	322.0	330.3	325.4	299.9	300.4	273.4

T8	T9	T10	T11	T12	T13	T14
264.2	280.8	285.4	300.0	300.9	340.2	288.8
263.9	280.0	271.4	303.3	303.0	340.4	289.6
265.4	281.0	268.4	302.9	303.3	340.9	289.9
264.8	280.7	265.7	302.2	302.3	338.9	289.8
266.3	281.8	267.2	300.6	301.8	339.7	290.8
267.0	282.4	267.0	301.5	302.3	338.2	290.8
267.4	282.3	266.9	301.5	300.2	337.4	290.5
267.5	283.3	267.3	302.5	302.1	335.9	291.9
268.2	283.4	268.2	300.9	299.9	335.8	291.5
268.9	284.2	281.7	298.6	299.7	335.8	290.8
269.4	284.7	268.9	299.6	300.4	335.3	291.3
269.0	285.3	269.1	298.9	300.3	335.5	288.8

T15	T16	T17	T20	T21	P2	P3
292.2	288.4	290.2	384.3	373.1	1.072	0.280
292.3	289.0	291.2	382.5	372.2	1.072	0.280
292.8	289.5	292.1	380.9	371.1	1.072	0.291
293.0	289.0	292.1	379.4	369.7	1.072	0.291
294.2	290.1	292.9	378.6	369.5	1.072	0.311
294.2	290.5	293.9	377.8	369.4	1.092	0.321
294.0	290.4	293.9	376.4	368.2	1.092	0.342
294.2	291.4	295.5	376.7	367.5	1.072	0.337
293.2	290.5	295.6	375.3	366.7	1.072	0.337
292.2	289.3	294.9	372.8	365.0	1.072	0.352
292.8	290.2	296.1	373.3	365.2	1.072	0.362
288.2	285.5	292.3	369.2	359.5	1.072	0.352

P4	M7	M11	M14	M16	M20
0.294	0.001146	0.017484	0.067231	0.159261	0.218364
0.294	0.001207	0.017587	0.067231	0.159261	0.212428
0.305	0.001409	0.017581	0.055949	0.211540	0.217138
0.305	0.001334	0.017556	0.055949	0.227224	0.221682
0.325	0.001206	0.017514	0.055949	0.232452	0.183597
0.325	0.001328	0.017437	0.055949	0.232452	0.184481
0.355	0.001080	0.017449	0.055949	0.227224	0.186030
0.345	0.000954	0.017593	0.078512	0.211540	0.185697
0.355	0.000832	0.017536	0.078512	0.216768	0.187249
0.366	0.000958	0.017463	0.078512	0.211540	0.190027
0.376	0.000957	0.017504	0.055949	0.227224	0.189471
0.366	0.000207	0.017474	0.055949	0.227224	0.194046

Table A2.5 (continued) Raw experimental performance data for the operating characteristics of the ammonia-water absorption system at UNAM.

T1	T2	T3	T4	T5	T6	T7
357.5	320.3	307.3	305.2	300.0	296.6	272.2
356.1	326.6	300.1	300.0	296.8	297.6	275.5
356.6	320.7	301.4	301.3	296.0	296.9	277.8
356.7	322.7	306.3	304.0	300.7	297.8	283.2
356.2	321.3	305.5	302.4	298.8	298.9	287.1
356.7	323.8	308.8	304.8	299.0	299.6	284.6
356.9	322.0	302.8	301.4	300.7	299.6	284.5
357.1	323.1	303.1	301.7	301.3	300.7	285.4
355.7	321.9	301.5	300.1	300.2	300.5	285.7
358.4	322.5	305.0	302.2	302.2	300.1	285.8
356.9	322.7	310.6	305.2	298.7	300.5	285.8

T8	T9	T10	T11	T12	T13	T14
265.9	282.8	283.4	310.2	308.3	333.9	285.6
269.5	283.7	274.2	301.5	301.8	337.3	284.8
271.2	285.1	295.6	301.8	301.1	338.8	284.9
268.6	285.7	300.8	298.8	299.0	336.0	283.9
267.8	285.8	299.3	299.5	299.2	335.8	284.2
266.8	282.7	300.8	299.5	299.7	337.3	284.2
267.6	281.8	301.9	299.2	299.1	335.3	284.3
267.3	282.7	303.1	300.8	299.5	335.8	285.7
267.7	283.4	303.7	299.0	298.4	334.9	285.9
268.5	284.1	304.2	298.6	299.8	336.9	284.4
266.8	284.8	300.7	299.5	298.4	337.5	284.6

T15	T16	T17	T20	T21	P2	P3
287.6	285.8	282.9	408.3	364.5	1.092	0.311
287.2	284.7	284.2	406.8	354.8	0.971	0.331
286.0	284.4	284.3	406.4	357.8	1.031	0.331
289.2	284.4	284.0	404.3	355.6	1.072	0.321
288.3	284.2	283.9	402.8	355.5	1.031	0.321
290.2	284.2	284.1	399.8	357.2	1.072	0.311
287.1	284.0	283.8	398.5	357.7	1.072	0.321
288.2	284.3	285.0	397.8	356.7	1.072	0.321
288.4	284.2	284.7	398.5	357.5	1.072	0.321
291.1	284.2	285.5	396.6	360.6	1.072	0.331
289.6	284.4	285.7	396.0	360.9	1.072	0.321

P4	M7	M11	M14	M16	M20
0.305	0.000210	0.017749	0.123639	0.195856	0.052939
0.345	0.000209	0.018104	0.010822	0.263819	0.050435
0.345	0.000209	0.017784	0.010822	0.258591	0.062792
0.345	0.000459	0.017458	0.039026	0.248136	0.067541
0.335	0.000458	0.017702	0.039026	0.248136	0.070943
0.325	0.000906	0.017478	0.039026	0.253363	0.084615
0.335	0.000905	0.017471	0.010822	0.258591	0.087763
0.325	0.000902	0.017525	0.010822	0.263819	0.089460
0.325	0.000903	0.017465	0.010822	0.263819	0.094825
0.345	0.000904	0.017455	0.010822	0.263819	0.099680
0.325	0.000903	0.017482	0.039026	0.263819	0.101216

Table A2.5 (continued) Raw experimental performance data for the operating characteristics of the ammonia-water absorption system at UNAM.

T1	T2	T3	T4	T5	T6	T7
351.1	314.0	302.1	301.6	298.7	298.1	285.8
353.0	320.7	308.4	304.7	299.7	298.8	291.2
353.1	320.3	306.7	302.3	300.1	299.6	293.6
352.2	320.1	302.0	299.9	298.8	299.7	294.5
352.0	321.0	301.2	300.2	299.1	300.2	295.3
352.8	321.2	302.1	301.1	298.9	299.5	299.9
353.5	320.3	303.2	302.2	300.9	300.1	301.4
353.2	321.5	302.2	301.2	300.6	299.8	299.6
353.5	322.0	302.1	301.2	301.3	300.2	300.0
352.8	320.6	301.6	301.7	301.2	300.5	299.3

T8	T9	T10	T11	T12	T13	T14
282.5	297.0	299.9	299.3	298.9	327.8	291.3
267.2	295.9	299.2	299.9	300.1	334.5	288.5
267.0	295.3	298.3	298.6	298.6	333.3	287.2
267.7	295.8	296.9	298.2	298.4	334.1	287.4
268.3	294.9	297.4	298.3	298.2	334.0	286.8
269.1	295.0	303.4	298.9	298.7	333.8	286.6
272.7	294.8	301.3	298.4	298.8	334.1	285.8
272.1	293.9	305.4	297.8	297.8	334.3	285.1
270.2	293.6	302.6	298.4	298.3	333.8	284.9
269.3	293.6	302.1	299.3	298.9	333.6	284.7

T15	T16	T17	T20	T21	P2	P3
290.4	288.7	289.9	388.5	357.1	1.072	0.301
289.8	286.6	288.9	387.2	358.0	1.072	0.321
293.1	286.4	288.5	387.0	356.7	1.072	0.316
290.6	285.8	288.0	387.0	355.5	1.051	0.321
288.7	284.8	286.9	386.2	354.8	1.051	0.321
288.3	283.9	286.4	386.1	354.4	1.072	0.342
287.9	283.6	286.2	385.9	353.7	1.072	0.337
287.5	283.0	285.4	385.6	353.2	1.072	0.352
287.8	282.9	285.3	385.4	353.2	1.072	0.342
287.8	282.6	285.4	385.7	352.2	1.072	0.342

P4	M7	M11	M14	M16	M20
0.305	0.000459	0.017468	0.010822	0.263819	0.108364
0.325	0.000583	0.017495	0.010822	0.263819	0.097365
0.315	0.000332	0.017450	0.033386	0.253363	0.083516
0.325	0.000394	0.017548	0.010822	0.263819	0.083516
0.335	0.000331	0.017551	0.010822	0.263819	0.081289
0.355	0.000208	0.017469	0.010822	0.263819	0.081011
0.345	0.000207	0.017450	0.010822	0.263819	0.086847
0.355	0.000332	0.017434	0.010822	0.263819	0.085955
0.355	0.000394	0.017452	0.010822	0.263819	0.079059
0.345	0.000393	0.017483	0.010822	0.263819	0.079896

Table A2.5 (continued) Raw experimental performance data for the operating characteristics of the ammonia-water absorption system at UNAM.

T1	T2	T3	T4	T5	T6	T7
374.0	322.8	338.0	333.6	299.5	297.9	291.6
371.0	326.9	337.5	333.3	294.8	298.0	294.1
370.2	329.6	336.5	330.3	294.7	298.2	291.2
370.1	324.2	331.7	323.5	293.9	296.4	269.4
371.0	323.0	334.2	326.4	297.4	297.3	275.1
369.1	328.8	335.4	329.1	297.2	298.1	266.3
369.1	327.8	332.2	325.0	297.0	298.2	265.2
369.1	325.6	330.3	323.0	299.1	298.0	263.5
368.9	326.7	329.7	323.4	301.0	300.1	265.5

T8	T9	T10	T11	T12	T13	T14
258.0	294.1	292.3	298.4	297.9	341.1	288.2
256.5	291.4	294.1	305.3	305.5	342.4	288.7
258.3	282.5	295.4	306.3	307.2	342.9	289.9
256.0	279.9	278.6	304.2	303.4	341.0	291.4
259.3	281.4	278.3	305.1	304.9	341.6	292.0
261.3	283.4	280.3	300.9	301.3	343.2	292.3
261.7	282.8	263.6	305.1	304.9	342.3	289.9
261.2	282.2	262.1	302.4	303.1	341.2	288.4
263.8	*283.8*	*263.8*	*303.9*	*304.2*	*341.2*	*287.3*

T15	T16	T17	T20	T21	P2	P3
290.1	287.9	297.0	400.1	383.6	1.172	0.219
289.5	288.2	299.6	394.7	381.7	1.072	0.209
291.8	289.4	293.9	392.4	380.8	1.072	0.229
292.8	291.0	294.1	391.0	382.0	1.031	0.219
293.9	291.4	295.1	389.4	378.9	1.072	0.240
294.0	292.0	296.4	387.0	378.5	1.051	0.260
292.5	289.7	292.5	382.4	377.6	1.051	0.260
290.0	287.3	289.1	377.9	370.3	1.092	0.270
288.5	285.6	287.3	377.0	366.8	1.072	0.280

P4	M7	M11	M14	M16	M20
0.233	0.000965	0.016870	0.213893	0.075614	0.240086
0.223	0.001216	0.017656	0.213893	0.070386	0.258087
0.233	0.001617	0.017684	0.106716	0.211540	0.258511
0.223	0.001473	0.017839	0.089794	0.242908	0.257951
0.254	0.001721	0.017641	0.106716	0.211540	0.292986
0.274	0.001592	0.017620	0.134921	0.201084	0.288539
0.264	0.001464	0.017758	0.039026	0.242908	0.430318
0.284	0.001640	0.017445	0.055949	0.237680	0.275143
0.284	0.001455	0.017609	0.055949	0.237680	0.268796

Table A2.5 (continued) Raw experimental performance data for the operating characteristics of the ammonia-water absorption system at UNAM.

T1	T2	T3	T4	T5	T6	T7
365.7	312.1	325.8	321.8	300.9	294.5	278.3
367.1	320.8	334.8	330.4	300.3	299.3	265.4
366.4	325.4	335.5	332.0	299.1	298.5	262.3
366.2	327.6	334.9	327.2	299.1	299.5	264.1
366.8	328.5	327.7	318.1	306.4	299.4	266.0
366.3	328.5	329.9	320.4	299.2	300.0	268.6
366.2	327.0	329.6	322.1	300.7	300.6	272.2
366.2	328.2	332.4	324.8	300.3	300.8	274.1
365.2	326.0	332.7	326.0	300.7	300.2	275.0

T8	T9	T10	T11	T12	T13	T14
259.2	285.2	276.8	297.2	296.8	330.9	289.6
262.5	284.4	280.1	301.4	300.7	337.1	290.5
261.6	280.2	282.6	302.3	301.4	341.7	291.5
263.1	280.9	284.4	303.9	303.3	342.3	291.5
265.7	282.3	264.8	303.3	303.9	343.0	290.0
268.8	283.6	267.8	301.9	301.8	341.9	290.3
272.0	285.2	271.5	304.4	302.2	341.1	289.1
274.4	286.5	273.2	302.8	303.0	341.6	287.4
274.4	286.7	273.6	301.5	301.3	341.0	287.8

T15	T16	T17	T20	T21	P2	P3
292.0	289.2	292.5	397.9	374.1	1.092	0.219
292.8	290.2	293.9	393.0	378.4	1.092	0.229
294.5	291.1	294.3	388.9	377.0	1.072	0.260
295.0	290.8	294.1	386.4	376.5	1.072	0.260
293.5	289.6	292.3	384.0	374.7	1.092	0.260
293.0	290.6	292.3	383.0	373.1	1.051	0.270
292.4	288.0	290.8	380.4	371.9	1.072	0.270
290.2	286.9	289.7	377.3	370.1	1.072	0.291
290.3	287.2	289.4	375.9	368.6	1.092	0.301

P4	M7	M11	M14	M16	M20
0.233	0.000720	0.017290	0.163125	0.154033	0.177481
0.274	0.001210	0.017408	0.168766	0.154033	0.258110
0.274	0.001214	0.017552	0.055949	0.195856	0.234642
0.284	0.001208	0.017602	0.039026	0.195856	0.220247
0.305	0.001207	0.017468	0.010822	0.216768	0.216580
0.355	0.001155	0.017652	0.039026	0.237680	0.211993
0.396	0.001153	0.017623	0.039026	0.242908	0.230835
0.427	0.001028	0.017577	0.039026	0.237680	0.314654
0.447	0.001018	0.017427	0.055949	0.237680	0.313921

Table A2.5 (continued) Raw experimental performance data for the operating characteristics of the ammonia-water absorption system at UNAM.

T1	geothermal fluid leaving generator, °C
T2	geothermal fluid entering generator, °C
T3	refrigerant vapour entering condenser, °C
T4	solution-vapour mixture entering absorber (after mixer), °C
T5	solution leaving absorber, °C
T6	refrigerant leaving condenser, °C
T7	two-phase mixture leaving generator, °C
T8	refrigerant entering evaporator, °C
T9	refrigerant leaving evaporator, °C
T10	cold storage temperature, °C
T11	ambient air temperature, °C
T12	refrigerant vapour entering mixer, °C
T13	weak refrigerant solution entering mixer, °C
T14	weak refrigerant solution leaving economiser, °C
T15	weak refrigerant solution entering economiser, °C
T16	cooling water entering absorber, °C
T17	cooling water leaving absorber, °C
T18	strong refrigerant solution entering generator, °C
T19	strong refrigerant solution leaving economiser, °C
T20	strong refrigerant solution entering economiser, °C
T21	liquid refrigerant leaving precooler, °C
T22	liquid refrigerant entering precooler, °C
T23	refrigerant vapour leaving precooler, °C
T24	refrigerant vapour entering precooler, °C
T25	cooling water entering rectifier, °C
T26	cooling water entering condenser, °C
T27	cooling water leaving condenser, °C
T28	two-phase mixture entering separator-rectifier, °C
T29	refrigerant vapour leaving separator-rectifier, °C
T30	weak refrigerant solution leaving separator-rectifier, °C
T31	cooling water leaving rectifier, °C
PEV	evaporator pressure, bar absolute
PCO	condenser pressure, bar absolute
FSOL	weak refrigerant solution flow rate, $m^3\ s^{-1}\ (10^{-3})$
FREF	liquid refrigerant flow rate, $m^3\ s^{-1}\ (10^{-3})$
FWRE	cooling water flow rate to rectifier, $m^3\ s^{-1}\ (10^{-3})$
FWCO	cooling water flow rate to condenser, $m^3\ s^{-1}\ (10^{-3})$
FWAB	cooling water flow rate to absorber, $m^3\ s^{-1}\ (10^{-3})$
FGS	geothermal steam flow rate to generator, $kg\ h^{-1}$

Table A.2.6 Raw experimental performance data for the operating characteristics of the ammonia-water absorption refrigerator at the Cerro Prieto geothermal field.

... continued

date 6/10/88

time	T1	T2	T3	T4	T5	T6	T7	T8	T9	T10	T11	T12
12:04:07	100.3	114.2	72.5	45.0	39.1	34.1	105.5	-1.0	-0.8	0.8	32.1	-0.8
12:17:21	98.2	118.7	72.8	43.8	38.2	33.6	104.3	-1.3	-0.9	1.3	32.6	-0.9
12:33:57	99.0	116.2	72.3	44.8	38.1	33.7	104.6	-1.4	-1.0	0.4	32.5	-1.0
12:47:02	99.1	118.0	71.9	44.2	38.0	33.4	104.7	-1.3	-1.1	0.3	32.3	-0.9
13:00:45	96.3	116.4	71.8	42.2	38.1	33.3	103.5	-1.2	-1.0	0.2	----	-1.0
13:15:10	96.8	117.4	72.5	43.4	38.1	33.5	103.8	-1.4	-1.0	0.1	----	-0.9
13:32:01	97.2	117.7	71.8	44.8	38.1	33.5	104.0	-1.6	-1.2	0.2	33.5	-1.2
13:46:10	97.3	118.5	72.2	43.8	38.4	33.6	104.1	-1.1	-1.1	0.7	33.2	-0.7
14:04:38	96.8	118.6	72.0	44.9	38.3	33.5	103.9	-1.4	-1.2	0.2	34.1	-1.2
14:32:21	99.8	121.5	74.4	45.4	38.1	34.7	105.7	-1.0	-0.6	0.6	34.5	-0.6
15:02:03	101.4	120.9	75.6	46.9	39.0	35.5	106.9	-0.7	-0.5	0.7	35.0	-0.3
15:18:14	102.0	122.1	76.1	46.7	39.1	35.6	107.0	-0.6	-0.4	0.8	35.2	-0.4
15:31:53	100.4	118.6	74.6	45.8	39.1	35.3	105.4	-0.6	-0.4	1.0	35.3	-0.2
15:47:57	98.4	118.8	74.5	45.9	39.5	35.1	104.7	-0.5	-0.1	1.4	35.1	-0.1
16:02:32	99.6	118.8	74.8	44.5	38.7	35.3	105.2	-0.8	-0.6	0.8	35.5	-0.4

date 7/10/88

10:00:35	103.1	124.2	80.8	44.4	38.5	34.2	110.7	-0.4	-0.4	1.1	26.5	0.0
10:30:15	103.1	123.3	80.0	46.5	38.1	34.3	110.5	-0.8	-0.6	0.8	27.5	-0.4
10:47:17	103.4	123.5	80.5	46.1	38.5	34.6	110.8	-1.0	-0.8	0.5	28.3	-0.5
11:01:01	105.8	124.8	82.2	45.5	38.1	34.8	112.3	-0.6	-0.6	0.7	28.6	-0.3
11:31:03	104.0	124.2	82.0	46.7	38.4	35.2	110.8	-0.5	-0.5	0.7	29.8	-0.1
11:45:28	104.1	124.3	81.2	46.4	39.7	35.3	110.7	-0.2	0.0	1.0	30.2	0.2
12:00:13	103.8	124.2	81.4	47.6	39.7	35.7	111.0	-0.1	0.1	1.3	30.7	0.3
12:16:01	105.0	125.9	82.5	47.1	39.8	36.2	111.8	0.4	0.4	1.6	31.4	0.8
12:30:32	104.6	123.2	80.8	45.6	39.1	35.7	110.5	0.0	0.4	1.6	31.6	0.6
12:46:11	103.8	123.3	80.2	47.3	40.9	36.3	110.1	0.5	0.7	1.9	----	0.9
13:00:04	104.6	122.6	80.6	47.7	40.0	36.6	110.8	0.8	0.8	1.9	32.5	1.1
13:31:54	106.4	124.6	80.9	46.7	40.0	35.8	111.4	0.5	0.7	2.1	33.3	0.9
13:46:25	104.0	123.4	80.2	46.7	41.6	36.6	110.1	1.0	1.0	2.4	----	1.2
14:00:10	102.9	122.1	80.6	47.3	41.0	36.6	110.0	1.2	1.4	2.4	33.5	1.6

date 10/10/88

10:46:19	108.9	127.8	88.1	48.7	41.4	37.0	116.0	0.2	0.4	2.2	30.8	0.6
11:00:16	108.7	127.3	85.5	46.8	40.7	36.5	115.3	0.4	0.8	2.4	31.1	1.4
11:29:34	111.4	129.4	87.7	48.4	41.9	37.1	117.5	0.9	0.9	2.5	31.5	1.3
11:47:10	109.3	125.1	87.6	49.1	41.9	36.9	116.3	1.5	1.7	2.9	32.3	2.3
12:03:20	110.5	128.5	86.6	48.7	42.2	37.6	116.8	1.2	1.4	2.8	32.9	2.0
12:15:21	105.4	123.3	84.4	47.0	40.9	36.5	113.4	2.1	2.3	3.0	33.4	2.9
12:32:03	106.3	125.6	85.5	48.5	41.8	36.8	114.0	1.8	1.8	3.0	33.3	2.2
12:45:57	107.5	126.4	86.1	48.6	41.3	36.7	114.8	1.5	1.7	2.9	34.0	2.3
13:00:53	107.8	127.4	85.8	47.7	41.4	36.8	115.1	1.4	1.6	2.8	33.5	2.2
13:18:05	109.0	129.1	87.1	46.5	40.9	36.9	115.9	1.5	1.5	2.9	33.6	2.1
13:31:39	108.8	127.7	86.7	48.8	41.6	37.1	115.8	1.5	1.5	2.9	33.9	1.9
13:51:45	109.9	128.0	87.2	49.7	42.1	37.7	116.3	1.9	1.9	3.3	34.6	2.3
14:00:52	108.1	125.0	86.7	49.0	41.9	37.3	115.4	1.9	1.9	3.3	34.8	2.5

Table A2.6 (continued) Raw experimental performance data for the operating characteristics of the ammonia-water absorption system at Cerro Prieto.

date
6/10/88

T13	T14	T15	T16	T17	T18	T19	T20	T21	T22	T23	T24	T25
38.9	62.5	95.1	26.7	28.9	70.6	71.2	38.3	5.3	35.2	0.4	-0.8	27.5
39.0	61.9	95.1	27.0	29.0	69.0	69.4	38.2	30.5	34.7	0.1	-0.9	27.8
39.1	62.3	95.0	26.9	29.1	70.1	70.3	38.5	19.5	34.6	0.2	-0.8	27.5
38.8	62.1	94.7	26.7	28.8	69.8	70.2	38.6	28.4	34.5	0.5	-0.9	27.4
38.7	60.8	94.0	27.0	28.9	67.1	67.3	38.3	24.6	34.4	0.0	-1.0	27.7
38.8	61.1	94.5	26.7	28.8	67.8	67.8	38.3	25.5	34.6	-0.1	-1.1	27.5
39.3	61.6	94.6	26.9	28.9	68.2	68.6	38.2	30.5	34.5	0.0	-1.1	27.8
39.2	61.5	94.7	26.6	28.8	68.3	68.3	38.3	15.6	34.6	-0.2	-0.8	27.3
39.5	61.4	94.2	27.2	29.1	68.0	68.0	38.3	29.8	34.8	0.1	-1.1	27.9
40.4	63.5	96.6	27.5	29.9	71.4	71.4	38.9	6.5	35.6	0.6	-0.4	28.3
41.3	64.7	98.8	28.8	30.7	73.2	73.2	39.7	3.0	36.9	0.5	-0.3	29.4
41.0	64.4	98.7	28.7	30.8	72.9	73.1	40.0	5.5	36.7	0.7	-0.4	29.4
41.0	63.9	98.0	28.9	31.0	72.5	72.5	40.0	19.0	36.4	0.6	-0.2	29.6
40.9	63.2	97.2	28.9	30.9	70.5	70.3	39.9	7.5	36.4	0.8	-0.2	29.5
41.0	63.7	97.8	28.9	31.0	71.6	72.0	39.8	21.5	36.4	0.4	-0.4	29.6

date
7/10/88

37.5	63.1	99.6	24.4	26.9	71.2	71.2	38.3	8.4	35.8	1.1	-0.2	25.4
37.3	62.9	99.8	24.4	26.7	70.8	71.2	38.2	7.4	35.7	1.1	-0.7	25.3
37.9	63.0	100.3	25.2	27.5	71.2	71.5	38.2	5.3	36.2	0.2	-0.8	26.0
38.7	64.7	101.4	25.5	27.9	74.2	74.4	38.9	8.1	36.6	0.6	-0.4	26.4
39.4	64.3	100.8	26.1	28.6	72.4	72.8	39.0	20.9	36.9	1.5	-0.3	27.1
39.3	64.2	100.5	26.4	28.7	72.5	72.7	39.5	13.9	37.0	1.2	0.0	27.1
39.7	64.5	101.0	26.6	29.0	71.9	72.4	39.5	12.0	37.2	1.6	0.1	27.6
40.4	65.3	101.8	27.3	29.6	73.3	73.5	40.2	9.6	37.7	1.9	0.5	28.1
40.5	65.4	100.8	27.6	29.9	74.1	74.6	40.4	27.5	37.2	1.8	0.4	28.3
40.9	64.9	100.5	28.2	30.6	73.2	73.2	40.5	15.0	37.8	1.7	0.9	29.0
41.2	65.9	101.4	28.1	30.6	74.6	74.4	40.9	13.3	38.1	2.1	0.9	29.0
40.8	66.5	101.2	27.7	30.0	76.1	76.4	40.9	32.7	37.3	1.9	0.9	28.6
41.0	65.0	100.3	28.5	30.8	73.1	73.5	41.2	13.7	38.1	2.5	0.9	29.2
41.4	65.0	100.7	28.7	31.0	72.5	72.5	41.2	22.8	38.3	2.5	1.5	29.6

date
10/10/88

40.4	67.6	105.5	26.0	28.7	76.9	76.9	41.6	16.5	38.9	2.8	0.4	27.2
39.7	66.2	104.5	26.4	28.9	76.0	76.3	40.8	33.5	38.1	3.0	1.0	27.7
40.4	67.6	106.4	26.7	29.2	78.1	78.7	41.3	13.0	39.0	3.2	0.8	27.8
40.3	66.4	105.1	27.0	29.6	75.6	76.0	41.4	12.2	38.9	2.7	1.8	27.9
40.8	67.3	105.5	27.3	29.9	76.7	77.4	41.5	6.0	39.4	3.2	1.3	28.8
40.3	65.3	102.7	27.6	29.9	72.8	73.0	41.6	24.6	38.5	3.7	2.4	28.7
40.6	65.9	103.3	27.2	29.7	73.7	74.1	41.5	8.6	38.6	3.3	1.9	28.2
40.4	66.2	104.2	26.5	29.2	74.5	74.9	41.6	20.7	38.5	3.2	2.0	27.5
40.4	66.3	104.4	26.6	29.3	75.0	75.4	41.3	21.0	38.6	3.8	1.7	27.8
40.5	66.8	105.4	26.7	29.2	76.2	76.0	41.4	12.8	38.9	2.7	1.8	27.9
41.0	66.8	105.1	27.3	29.8	75.9	76.3	41.8	22.9	39.1	3.8	1.6	28.3
41.3	67.5	106.0	27.6	30.1	77.1	77.5	42.1	13.7	39.6	3.5	2.0	28.7
41.0	67.0	105.1	27.3	29.8	75.7	76.2	42.2	16.1	39.3	3.8	2.0	28.3

Table A2.6 (continued) Raw experimental performance data for the operating characteristics of the ammonia-water absorption system at Cerro Prieto.

date
6/10/88

T26	T27	T28	T29	T30	T31	PEV	PCO	FSOL	FREF	FWRE	FWCO	FWAB
27.0	34.1	100.2	73.8	93.8	28.1	4.15	13.48	0.123	0.017	0.442	0.631	1.140
27.2	33.8	98.0	74.1	93.7	28.4	4.16	13.34	0.123	0.019	0.442	0.631	1.140
27.1	33.7	98.8	73.4	94.2	28.3	4.12	13.34	0.123	0.018	0.442	0.631	1.140
26.8	33.6	98.9	73.0	94.5	28.2	4.11	13.26	0.123	0.019	0.442	0.631	1.140
27.1	33.5	95.9	73.2	92.1	28.3	4.13	13.24	0.123	0.019	0.442	0.631	1.140
26.9	33.6	96.6	73.4	92.9	28.2	4.13	13.30	0.123	0.019	0.442	0.631	1.140
27.0	33.8	97.0	73.3	92.6	28.3	4.08	13.30	0.126	0.019	0.442	0.631	1.140
26.9	33.7	97.0	73.2	93.4	28.3	4.14	13.29	0.126	0.018	0.442	0.631	1.140
27.3	33.8	96.6	73.4	93.0	28.6	4.12	13.38	0.126	0.019	0.442	0.631	1.140
27.7	34.6	99.4	74.8	96.2	29.2	4.16	13.72	0.126	0.016	0.442	0.631	1.140
29.0	35.9	101.2	76.2	98.2	30.1	4.20	14.16	0.123	0.017	0.442	0.631	1.140
28.8	35.8	101.6	76.8	98.5	30.4	4.23	14.11	0.123	0.017	0.442	0.631	1.140
29.3	35.4	100.0	76.3	96.6	30.4	4.26	13.96	0.120	0.017	0.435	0.624	1.120
29.1	35.4	98.1	75.9	95.9	30.2	4.29	13.98	0.120	0.017	0.429	0.618	1.120
29.0	35.4	99.4	76.3	96.6	30.4	4.26	13.92	0.120	0.018	0.429	0.618	1.120

date
7/10/88

24.8	34.4	102.7	77.6	98.5	26.5	4.17	13.51	0.126	0.024	0.442	0.631	1.140
24.7	34.4	103.0	78.1	97.8	26.5	4.11	13.51	0.126	0.024	0.442	0.631	1.140
25.4	34.9	103.3	78.7	98.0	27.2	4.08	13.71	0.126	0.024	0.442	0.631	1.140
25.8	35.1	105.5	79.3	100.9	27.5	4.18	13.79	0.126	0.024	0.442	0.631	1.140
26.5	35.4	103.6	79.2	99.0	28.0	4.17	13.90	0.126	0.023	0.442	0.631	1.140
26.8	35.6	103.9	79.8	99.6	28.3	4.21	13.97	0.126	0.024	0.442	0.631	1.140
27.0	35.9	103.5	80.7	99.1	28.6	4.22	14.08	0.126	0.023	0.442	0.631	1.140
27.7	36.4	104.7	81.3	101.0	29.2	4.30	14.30	0.126	0.022	0.442	0.631	1.140
27.7	36.0	104.6	80.2	100.4	29.3	4.30	14.13	0.126	0.022	0.442	0.631	1.140
28.6	36.7	103.6	80.3	99.9	29.9	4.35	14.39	0.126	0.021	0.442	0.631	1.140
28.4	36.7	104.4	80.7	100.3	30.0	4.34	14.43	0.126	0.021	0.442	0.631	1.140
27.8	36.1	106.2	80.3	101.2	29.6	4.39	14.18	0.126	0.023	0.442	0.631	1.140
28.6	36.7	103.8	80.6	99.6	30.2	4.38	14.48	0.126	0.021	0.442	0.631	1.140
29.0	36.9	102.7	81.3	98.8	30.4	4.46	14.46	0.126	0.022	0.442	0.631	1.140

date
10/10/88

26.2	37.2	108.5	85.5	103.0	28.3	4.26	14.60	0.126	0.027	0.505	0.694	1.200
26.8	36.6	108.5	84.9	101.5	28.7	4.34	14.36	0.126	0.027	0.505	0.694	1.200
26.8	37.4	111.1	85.1	103.7	28.9	4.34	14.64	0.126	0.026	0.505	0.694	1.200
27.1	37.2	109.0	85.5	103.5	29.1	4.48	14.60	0.123	0.023	0.505	0.694	1.200
27.6	37.6	110.4	84.8	102.3	29.6	4.42	14.89	0.126	0.023	0.505	0.694	1.200
27.9	37.0	105.1	84.5	99.4	29.5	4.52	14.49	0.126	0.023	0.505	0.694	1.200
27.4	37.1	106.0	85.0	100.8	29.2	4.52	14.56	0.126	0.022	0.505	0.694	1.200
26.8	37.0	107.2	84.3	102.0	28.7	4.46	14.51	0.126	0.024	0.505	0.694	1.200
26.8	37.1	107.5	84.4	101.4	28.8	4.48	14.51	0.126	0.025	0.505	0.694	1.200
26.9	37.2	108.3	85.5	103.1	28.9	4.49	14.58	0.126	0.025	0.505	0.694	1.200
27.6	37.6	108.5	85.5	102.2	29.5	4.48	14.76	0.126	0.025	0.505	0.694	1.200
27.9	37.9	109.4	86.2	104.0	29.8	4.48	14.94	0.126	0.024	0.505	0.694	1.200
27.6	37.8	107.8	85.9	102.4	29.5	4.52	14.84	0.126	0.024	0.505	0.694	1.200

Table A2.6 (continued) Raw experimental performance data for the operating characteristics of the ammonia-water absorption system at Cerro Prieto.

time	T1	T2	T3	T4	T5	T6	T7	T8	T9	T10	T11	T12
						date 24/10/88						
11:01:41	95.8	104.3	66.6	44.5	38.0	33.8	100.2	-2.3	-1.3	-0.1	22.2	0.1
11:16:41	95.2	104.4	66.7	44.7	37.2	34.1	100.2	-2.4	-2.0	-0.6	22.1	-0.2
11:31:14	96.8	105.1	67.4	46.7	37.1	34.4	101.4	-3.2	-2.2	-1.0	22.4	15.2
11:46:20	96.7	105.1	66.0	43.2	38.6	33.4	100.3	-2.5	-2.3	-0.9	22.4	-0.7
12:01:25	97.6	105.6	65.8	44.9	38.0	34.0	101.4	-2.7	-2.3	-0.9	22.8	-0.5
12:15:43	95.8	104.7	64.9	44.0	38.8	33.8	99.9	-2.7	-2.3	-0.9	23.6	-0.9
12:30:27	95.6	104.7	65.3	44.6	37.7	34.2	100.6	-2.7	-2.3	-0.9	24.0	-0.7
12:46:02	96.2	104.9	65.1	43.8	38.7	34.1	100.5	-2.8	-2.4	-1.0	23.4	0.4
13:00:53	95.0	104.4	65.0	43.3	38.7	33.9	100.2	-2.6	-2.2	-0.8	24.8	-0.2
13:15:22	96.5	105.4	65.0	44.7	37.4	34.3	101.3	-2.1	-1.9	-0.8	22.5	1.0
13:30:46	96.2	105.0	67.3	45.3	37.8	34.6	101.0	-2.3	-2.1	-0.7	24.7	-0.5
13:45:31	96.7	105.1	69.2	45.3	38.0	34.8	101.7	-2.3	-2.1	-0.7	26.1	-0.1
14:01:48	95.0	104.1	67.3	44.9	39.3	34.5	100.4	-1.9	-1.5	-0.4	24.3	0.4
						date 25/10/88						
12:30:17	92.2	102.6	62.6	45.3	39.5	33.2	97.1	-1.1	6.7	6.6	31.1	23.3
12:46:45	92.4	102.3	63.2	45.1	39.9	32.8	97.1	-1.9	4.8	4.6	31.3	22.2
13:00:15	91.4	101.5	61.4	44.1	39.5	32.7	95.9	-2.6	1.6	1.6	30.0	20.2
13:15:09	90.8	101.4	61.5	44.0	39.2	----	95.4	-2.3	-1.3	0.5	31.5	9.0
13:30:07	88.8	101.1	59.7	42.6	38.5	32.0	94.1	-2.9	-1.8	-0.2	32.2	5.7
13:45:50	90.1	101.4	60.0	42.1	38.5	32.5	95.3	-3.0	-2.2	-0.6	32.7	6.8
14:00:38	89.8	101.5	60.3	42.4	38.3	32.6	95.2	-2.9	-2.4	-0.8	33.2	3.0
14:15:29	90.2	101.5	60.9	42.0	38.2	32.6	95.4	-3.3	-2.5	-0.9	33.0	3.6
14:30:07	90.1	101.6	60.8	42.0	37.7	32.5	95.9	-3.2	-2.6	-1.0	34.1	0.6
						date 26/10/88						
10:01:40	84.0	100.5	52.7	40.0	35.8	29.7	89.9	-3.8	3.7	4.1	26.2	24.2
10:30:56	84.8	100.6	54.4	40.1	36.7	30.7	90.8	-3.7	2.0	1.7	27.4	27.4
10:46:29	84.2	100.2	54.1	40.3	36.7	30.5	90.0	-3.7	0.5	0.1	26.3	27.4
11:32:12	83.2	100.1	52.0	38.5	35.0	29.6	89.0	-5.6	-0.6	-0.4	27.5	24.8
11:46:10	86.6	100.4	57.5	39.0	34.3	30.9	91.5	-5.9	0.3	0.3	28.6	25.7
12:00:38	84.7	100.0	59.9	39.8	36.0	30.0	90.1	-5.2	0.2	-0.4	28.5	27.1
12:15:42	85.4	100.1	63.2	39.8	35.8	30.4	90.8	-5.0	-0.7	-0.9	29.2	28.0
12:31:45	85.4	100.1	63.8	40.2	36.1	30.2	90.4	-4.6	-1.1	-1.3	24.5	24.9
12:45:42	84.9	100.0	63.1	39.5	35.7	30.1	90.2	-4.9	-1.1	-1.1	29.5	27.4
13:00:36	84.9	100.0	62.5	39.6	35.8	30.2	89.9	-4.8	-1.0	-1.0	31.0	23.1
13:15:46	86.3	100.1	64.1	40.0	35.9	31.3	91.3	-5.0	-0.1	-0.1	30.9	25.9
13:31:04	85.8	99.6	64.0	41.4	35.6	30.2	90.5	-4.0	-1.0	-0.8	31.0	20.2
13:45:27	84.6	99.7	61.6	41.1	34.3	29.9	90.0	-3.7	-0.3	-0.3	31.8	28.4
14:00:19	84.4	99.7	59.0	39.8	33.8	29.6	89.3	-4.4	0.1	0.5	32.5	30.0

Table A2.6 (continued) Raw experimental performance data for the operating characteristics of the ammonia-water absorption system at Cerro Prieto.

date 24/10/88

T13	T14	T15	T16	T17	T18	T19	T20	T21	T22	T23	T24	T25
40.7	61.6	92.6	29.9	31.6	69.6	69.2	38.7	30.8	34.5	0.4	-1.2	30.4
41.0	61.6	92.6	30.0	31.6	68.0	68.2	38.4	15.4	34.8	-0.5	-1.7	30.5
41.7	63.0	93.8	30.0	----	70.6	70.6	38.6	14.2	34.3	-1.1	-2.3	30.5
40.5	61.7	92.5	30.0	31.5	69.8	70.4	38.5	33.9	34.5	-1.0	-1.9	30.5
41.1	62.8	93.7	29.9	31.7	71.7	71.5	38.3	31.2	35.1	-0.4	-1.8	30.4
40.7	61.1	92.4	29.9	31.5	68.3	69.0	38.2	29.5	34.7	-0.6	-1.9	30.5
41.1	61.5	93.0	30.2	31.9	68.3	68.5	38.2	27.4	34.9	-0.5	-1.9	30.7
40.8	61.2	92.1	30.0	31.5	68.0	69.1	38.2	21.1	34.6	-0.7	-2.1	30.5
40.8	61.0	92.7	30.2	31.8	67.6	67.8	38.3	32.9	34.6	-0.8	-1.8	30.6
41.6	62.0	93.3	30.3	32.2	69.0	69.2	38.3	0.6	34.9	-0.8	-1.6	30.8
41.5	61.8	93.0	30.5	32.2	68.7	69.0	38.6	2.0	35.5	-1.1	-1.9	31.0
42.6	63.4	95.2	30.7	32.6	70.9	70.9	39.1	27.8	35.7	-1.0	-1.7	31.2
42.0	61.8	93.3	30.9	32.6	68.1	68.6	39.0	34.1	35.2	0.0	-1.2	31.4

date 25/10/88

40.1	61.4	88.3	28.2	30.3	67.5	67.5	39.9	23.3	33.9	20.7	12.2	28.9
40.3	61.7	90.0	28.8	30.7	67.3	67.5	39.9	21.4	33.2	18.3	8.7	29.3
40.2	61.0	89.2	29.1	31.0	66.7	66.9	39.8	18.7	32.9	16.2	5.8	29.8
40.5	61.1	88.6	29.2	31.1	66.6	66.8	39.9	32.0	33.2	5.4	-1.0	29.7
40.1	59.3	86.4	29.1	30.8	63.9	64.1	39.2	30.0	32.7	2.5	-1.1	29.6
40.0	59.8	87.7	29.0	30.8	64.9	65.1	38.9	22.2	33.2	2.0	-1.3	29.5
39.9	59.7	87.4	28.9	30.6	64.6	64.8	39.0	22.8	33.2	0.3	-1.9	29.6
40.1	59.9	87.6	28.9	30.7	65.4	65.4	38.8	21.6	33.2	-0.5	-2.1	29.4
40.0	60.1	87.7	28.7	30.4	65.2	65.4	38.5	15.9	33.2	-1.2	-2.1	29.1

date 26/10/88

37.5	56.1	81.7	26.9	28.5	59.9	59.9	37.0	26.0	30.1	19.2	9.7	27.4
38.2	56.3	82.4	27.8	29.3	60.3	60.5	36.8	27.7	31.2	20.2	9.7	28.3
38.6	56.7	82.2	28.2	29.8	61.1	61.3	37.4	28.0	31.0	18.3	4.8	28.7
37.9	55.3	81.5	28.3	29.4	58.3	58.5	35.8	26.1	30.2	9.6	3.1	45.6
38.8	57.5	83.5	28.2	29.5	62.4	62.6	35.3	15.4	30.7	11.6	6.6	62.0
38.7	57.4	82.8	28.3	29.4	61.8	61.9	36.0	27.1	30.6	14.3	8.4	66.9
38.6	57.3	82.8	28.2	29.4	61.9	62.1	36.3	22.6	31.3	15.6	4.3	69.5
39.0	57.9	83.3	28.2	29.6	62.6	62.6	36.5	28.4	31.1	15.4	2.1	70.6
38.8	57.5	82.7	28.4	29.7	61.6	61.8	36.3	23.9	30.9	15.2	2.8	70.5
38.9	57.4	82.5	28.5	29.8	61.8	61.9	36.4	24.8	31.2	14.9	2.0	70.8
39.4	58.1	84.1	28.6	29.8	62.8	63.0	36.1	19.3	31.7	14.6	3.6	71.9
39.5	58.9	83.2	28.5	30.0	65.2	65.2	36.8	29.6	31.4	12.1	1.7	72.1
39.1	57.5	82.9	28.6	29.7	62.8	63.0	36.0	21.7	30.6	13.4	3.0	71.8
38.6	56.4	82.0	28.4	29.8	62.3	62.4	35.1	24.5	30.3	15.6	5.4	70.7

Table A2.6 (continued) Raw experimental performance data for the operating characteristics of the ammonia-water absorption system at Cerro Prieto.

date
24/10/88

T26	T27	T28	T29	T30	T31	PEV	PCO	FSOL	FREF	FWRE	FWCO	FWAB
30.0	33.5	----	68.7	92.2	31.0	4.00	13.36	0.126	0.013	0.397	0.568	1.060
30.0	33.8	----	68.9	92.1	31.1	3.97	13.46	0.126	0.012	0.397	0.574	1.060
30.1	34.3	----	69.4	93.9	31.1	3.90	13.66	0.126	0.012	0.397	0.574	1.070
30.1	33.4	----	68.4	91.6	31.0	3.95	13.23	0.126	0.014	0.397	0.574	1.070
30.1	33.9	----	67.8	93.7	31.0	3.96	13.46	0.126	0.013	0.397	0.574	1.060
30.1	33.7	----	67.1	91.5	31.0	3.94	13.37	0.123	0.012	0.397	0.568	1.060
30.3	34.1	----	67.5	92.8	31.3	3.93	13.53	0.126	0.013	0.397	0.574	1.060
30.1	34.2	95.3	67.5	92.3	30.9	3.94	13.44	0.126	0.013	0.397	0.574	1.070
30.4	34.0	----	67.6	91.9	31.2	3.96	13.43	0.126	0.013	0.397	0.574	1.060
30.6	34.5	----	68.2	93.8	31.4	4.01	13.64	0.126	0.014	0.397	0.574	1.060
30.9	34.7	95.7	69.9	93.3	31.6	3.96	13.70	0.126	0.011	0.397	0.574	1.060
31.0	34.9	96.5	71.1	95.2	31.8	4.00	13.73	0.126	0.012	0.397	0.574	1.060
31.2	34.8	----	70.4	92.5	31.7	4.02	13.61	0.126	0.013	0.397	0.574	1.060

date
25/10/88

28.7	33.3	----	63.3	89.4	29.5	4.07	13.09	0.129	0.011	0.410	0.574	1.040
29.1	33.2	----	64.8	89.4	29.9	3.97	13.06	0.126	0.011	0.410	0.574	1.040
29.4	32.9	----	64.2	88.6	30.2	3.89	12.95	0.123	0.011	0.410	0.574	1.040
29.7	32.8	90.3	63.5	87.7	30.3	3.96	12.82	0.123	0.011	0.410	0.568	1.030
29.4	32.5	88.4	62.6	86.0	30.0	3.84	12.67	0.126	0.010	0.410	0.568	1.030
29.5	32.8	----	62.4	87.0	30.1	3.81	12.83	0.126	0.010	0.410	0.568	1.030
29.6	32.8	----	62.4	86.7	29.9	3.84	12.88	0.126	0.010	0.410	0.568	1.030
29.4	32.8	----	62.6	87.0	29.9	3.82	12.89	0.126	0.010	0.397	0.568	1.020
28.9	32.8	----	63.3	87.7	29.7	3.83	12.90	0.126	0.010	0.397	0.568	1.020

date
26/10/88

27.2	29.7	----	56.3	81.6	27.7	3.67	11.80	0.126	0.008	0.423	0.574	1.050
27.9	30.6	----	57.4	82.7	29.3	3.71	12.12	0.126	0.009	0.442	0.309	1.100
28.5	30.8	----	57.6	81.4	29.7	3.75	12.18	0.126	0.008	0.442	0.315	1.100
28.4	29.8	----	58.9	80.7	45.6	3.47	11.79	0.126	0.006	0.467	0.000	1.170
28.4	30.9	----	65.6	84.0	60.3	3.44	12.17	0.126	0.006	0.473	0.000	1.170
28.5	30.2	----	70.4	82.3	65.2	3.54	11.96	0.126	0.008	0.473	0.000	1.170
28.4	30.6	----	73.2	83.2	68.1	3.53	12.04	0.126	0.008	0.467	0.000	1.160
28.4	30.6	----	74.5	83.0	69.1	3.56	12.00	0.126	0.008	0.467	0.000	1.160
28.6	30.5	----	74.7	82.3	69.2	3.51	11.98	0.126	0.008	0.467	0.000	1.160
28.7	30.6	----	74.8	82.5	69.5	3.53	12.00	0.126	0.006	0.467	0.000	1.160
28.8	30.9	----	75.8	84.1	70.4	3.48	12.19	0.126	0.008	0.467	0.000	1.160
28.7	30.6	----	76.1	83.4	70.6	3.69	11.99	0.126	0.008	0.467	0.000	1.160
28.7	30.3	----	75.9	82.5	70.5	3.72	11.85	0.123	0.006	0.467	0.000	1.160
28.6	29.9	----	74.7	82.0	69.6	3.66	11.79	0.123	0.006	0.467	0.000	1.160

Table A2.6 (continued) Raw experimental performance data for the operating characteristics of the ammonia-water absorption system at Cerro Prieto.

date
28/10/88

time	T1	T2	T3	T4	T5	T6	T7	T8	T9	T10	T11	T12
10:16:15	96.5	121.8	71.9	45.9	40.9	35.2	105.4	0.3	0.3	2.1	26.7	0.7
10:30:33	97.0	122.1	72.3	45.4	40.6	35.2	105.7	0.0	0.0	1.8	27.1	0.0
10:47:12	97.2	121.8	71.5	44.7	40.7	35.3	105.6	-0.5	-0.3	1.4	27.6	0.1
11:01:19	96.5	120.7	71.3	43.9	40.3	35.1	105.6	-0.2	0.0	1.4	28.2	0.4
11:15:43	96.1	120.4	70.6	43.3	39.5	34.5	105.3	-0.4	-0.4	1.2	29.1	0.0
11:30:12	96.4	121.7	70.6	44.0	39.6	34.5	106.1	-0.4	-0.4	1.0	29.4	-0.2
11:47:47	95.7	119.5	70.1	42.9	39.5	34.3	105.4	-0.8	-0.6	0.8	30.3	-0.4
12:00:55	95.5	121.7	70.3	43.1	39.5	34.3	105.6	-0.8	-0.8	0.8	30.7	-0.6
12:15:16	95.8	121.4	70.3	42.8	39.0	34.2	105.6	-0.9	-0.9	0.5	30.1	-0.7
12:30:33	96.1	121.7	70.6	43.3	39.3	34.3	105.9	-1.0	-0.8	0.6	31.2	-0.6
12:46:07	95.2	119.4	69.6	43.8	39.2	34.0	105.0	-0.9	-0.9	0.7	31.9	-0.7
13:00:15	94.7	121.0	69.1	43.5	38.9	33.9	104.9	-1.0	-1.0	0.6	31.9	-0.6
13:16:19	95.0	121.8	69.4	42.2	38.4	34.2	105.2	-1.1	-0.9	0.5	32.1	-0.7
13:31:36	94.2	120.4	68.9	42.9	39.1	34.1	104.6	-0.6	-0.6	0.9	31.7	-0.2
13:46:22	94.8	121.6	69.7	43.0	39.7	34.1	105.2	-0.4	-0.2	1.2	31.8	0.2
14:00:54	94.5	121.6	69.2	43.6	39.1	34.0	105.0	-0.3	-0.1	1.2	31.4	0.1

date
31/10/88

12:00:13	104.7	124.2	79.7	47.6	42.6	36.8	110.9	1.6	1.8	3.2	31.3	1.8
12:16:50	106.6	124.4	82.2	49.2	41.1	36.9	111.9	1.3	1.5	2.9	----	1.5
12:32:47	95.4	105.6	70.5	47.2	39.7	33.2	101.5	-0.1	0.7	2.2	29.0	1.5
12:45:59	92.1	103.7	66.0	46.1	37.8	32.2	99.3	-1.7	-0.7	0.9	32.2	1.5
13:00:14	91.8	104.3	65.2	44.3	39.3	31.8	99.1	-2.3	-1.7	-0.2	32.6	-0.4
13:16:28	93.7	105.0	66.1	45.2	38.2	32.2	100.2	-2.2	-1.6	0.0	32.4	-0.6
13:30:27	93.0	104.7	65.5	44.4	38.4	31.3	99.9	-2.9	-2.5	-0.7	33.8	-1.3
13:45:22	91.6	103.8	65.2	42.5	39.6	31.9	98.8	-2.2	-2.0	-0.8	33.7	-0.8
14:00:39	94.6	105.0	66.3	44.8	38.9	32.9	100.2	-2.6	-2.0	-0.6	33.1	0.0
14:17:51	93.9	104.8	65.4	45.6	39.5	33.0	100.0	-2.5	-1.8	0.0	33.7	-0.6
14:30:25	95.7	105.5	67.4	46.0	39.6	33.5	101.3	-2.2	-1.6	-0.2	34.8	-0.4
14:45:28	93.4	104.8	65.1	45.4	38.1	32.9	100.1	-2.0	-1.4	0.0	33.9	-0.2
15:00:21	93.3	104.6	65.3	44.0	38.1	32.5	99.8	-2.0	-1.8	-0.4	31.9	-0.8

date
1/11/88

10:33:24	94.1	116.2	65.2	45.2	40.1	29.1	101.9	-2.5	5.5	4.8	22.7	20.2
10:45:43	93.8	114.7	65.7	44.9	40.2	30.3	101.4	-2.3	-1.7	1.1	22.4	2.1
11:00:22	91.7	114.4	65.8	43.5	38.7	32.6	100.0	-0.7	-0.5	1.2	22.7	-0.2
11:16:03	93.3	116.6	67.2	43.3	40.0	33.9	101.6	-0.8	-0.8	1.0	23.5	-0.4
11:30:54	92.3	112.5	65.5	44.8	40.4	33.8	100.3	-0.9	-0.7	0.9	23.0	0.1
11:45:35	92.4	113.5	66.5	42.9	39.9	34.1	100.4	-0.8	-0.6	0.8	22.7	-0.2
12:01:00	93.2	114.3	66.3	43.8	40.2	34.4	100.8	-0.5	-0.5	0.9	23.2	-0.3
12:15:34	93.3	114.4	66.7	44.5	40.3	34.9	101.1	-0.3	-0.3	0.8	23.7	-0.1
12:30:59	94.2	111.6	67.8	45.4	40.8	34.8	101.4	-0.6	-0.2	1.0	23.4	-0.2
12:45:32	93.5	113.9	67.9	45.7	40.9	34.7	101.0	-0.7	-0.5	0.7	23.5	-0.1
13:01:11	93.7	113.6	67.3	43.3	40.6	34.7	101.1	-0.4	-0.4	0.8	22.9	0.4
13:15:36	94.1	113.4	68.5	45.5	40.9	35.0	101.6	-0.5	-0.1	1.1	22.2	0.3
13:30:26	94.4	111.8	67.6	45.6	40.8	34.7	101.3	-1.0	-0.6	0.6	23.5	0.0

Table A2.6 (continued) Raw experimental performance data for the operating characteristics of the ammonia-water absorption system at Cerro Prieto.

date
28/10/88

T13	T14	T15	T16	T17	T18	T19	T20	T21	T22	T23	T24	T25
41.7	63.8	93.9	27.6	29.8	69.2	68.9	41.2	26.9	36.4	2.9	0.3	27.9
41.6	63.3	93.5	27.5	29.8	69.5	68.6	40.6	27.7	36.4	1.6	0.0	27.9
41.8	63.3	93.9	27.6	29.9	69.2	69.2	40.9	7.1	36.4	1.6	-0.2	28.0
41.6	63.1	93.3	27.6	29.7	68.8	68.2	40.4	13.8	36.0	1.8	0.2	27.9
40.6	62.3	92.7	26.8	29.1	68.2	67.6	40.0	16.2	35.6	1.3	-0.2	27.1
41.0	62.7	92.7	26.3	28.7	68.4	68.0	40.0	7.0	35.6	0.9	-0.5	26.7
40.6	62.2	91.5	25.8	28.1	67.7	67.5	39.9	5.7	35.3	0.6	-0.4	26.2
40.5	62.2	92.2	25.6	28.1	67.7	67.3	39.5	4.5	35.3	0.6	-0.6	26.0
40.3	62.0	92.2	25.5	27.8	67.5	67.3	39.4	4.0	35.1	0.1	-0.9	25.9
40.8	62.3	92.5	25.6	28.1	67.6	67.4	39.5	4.7	35.4	0.6	-0.8	26.2
40.5	62.0	92.1	25.5	28.0	67.3	67.1	39.4	5.0	35.2	0.7	-0.7	25.9
40.2	61.5	91.4	25.4	27.9	66.7	66.3	39.3	4.1	34.8	0.6	-0.8	25.8
39.9	61.3	91.7	25.5	27.8	66.6	66.2	39.0	2.7	35.2	0.3	-0.9	25.9
39.8	61.2	90.8	25.4	27.9	66.3	65.7	39.1	7.3	35.0	1.4	-0.2	25.8
40.7	61.8	91.1	25.4	28.1	67.1	66.7	39.3	6.9	35.3	1.6	-0.2	25.8
40.3	61.6	91.1	25.3	28.0	66.7	66.6	39.3	8.3	35.1	1.8	-0.2	25.6

date
31/10/88

45.7	68.1	99.5	28.6	----	76.2	76.7	43.2	35.3	38.4	3.2	1.8	29.1
46.9	70.4	102.5	29.0	----	79.8	80.2	43.6	33.6	38.6	2.6	1.7	29.7
44.0	64.3	93.0	28.2	30.9	71.5	72.0	41.8	30.0	34.5	3.1	0.8	28.9
43.4	62.4	90.6	27.6	30.1	67.1	67.5	39.6	31.7	32.9	3.3	-0.5	28.3
42.6	60.9	89.8	27.8	29.9	65.8	66.2	38.8	31.7	32.6	1.3	-1.5	28.4
43.1	62.5	91.3	27.4	29.9	68.8	69.3	39.1	30.5	33.0	0.2	-1.6	27.9
42.1	61.5	90.4	27.0	29.0	67.5	68.1	38.8	30.9	32.3	-0.1	-2.3	27.6
42.7	60.2	89.9	28.5	30.4	64.8	65.0	38.5	1.3	32.7	-0.7	-1.6	29.0
43.5	62.3	91.4	28.9	31.2	68.9	69.7	39.0	24.2	33.8	-0.1	-2.0	29.6
43.7	62.7	91.3	28.5	30.7	68.6	69.2	39.4	17.4	33.7	0.4	-1.6	29.0
44.6	64.0	93.1	29.3	31.6	71.2	71.6	39.8	32.6	34.4	0.3	-1.5	29.9
43.8	62.5	90.8	28.3	30.8	68.3	68.0	39.6	25.3	34.0	0.1	-1.1	29.0
42.9	61.9	90.8	28.1	30.4	67.8	68.0	39.2	30.7	33.2	-0.5	-1.5	28.6

date
1/11/88

40.1	60.7	89.4	25.2	27.6	66.3	65.8	39.3	23.1	28.9	18.9	10.7	25.7
40.7	61.7	90.0	26.3	28.2	67.0	66.4	40.4	5.9	29.8	3.5	-1.4	26.5
41.2	61.4	89.4	26.8	28.7	65.8	65.4	39.7	32.8	33.4	1.1	-0.3	27.0
42.3	61.8	89.9	27.5	29.5	66.5	65.9	40.1	13.6	34.9	1.4	-0.6	27.7
42.6	61.9	89.7	----	30.0	66.2	66.2	40.4	6.0	34.6	1.1	-0.5	28.2
42.8	61.8	89.6	28.1	30.1	66.1	66.3	40.1	23.7	35.1	0.8	-0.4	28.3
43.1	61.9	89.5	----	30.4	66.8	66.8	40.2	30.2	35.4	1.3	-0.2	29.0
43.6	62.4	90.4	----	30.9	67.1	67.3	40.7	14.4	35.9	0.7	-0.1	29.3
44.6	63.6	91.6	28.9	31.0	68.2	68.5	41.6	1.9	35.6	0.2	-0.2	29.4
44.1	63.0	91.1	29.1	31.1	67.5	67.7	41.1	9.5	35.5	1.1	-0.3	29.5
44.1	63.1	91.1	29.1	31.2	67.8	68.0	41.4	4.9	35.4	0.6	0.0	29.5
44.6	63.8	90.6	29.4	31.3	68.3	68.3	41.7	6.8	35.7	1.3	-0.1	29.8
44.7	63.5	90.7	29.1	31.2	68.4	68.4	41.6	3.0	35.5	0.4	-0.4	29.5

Table A2.6 (continued) Raw experimental performance data for the operating characteristics of the ammonia-water absorption system at Cerro Prieto.

date
28/10/88

T26	T27	T28	T29	T30	T31	PEV	PCO	FSOL	FREF	FWRE	FWCO	FWAB
27.9	35.2	----	69.3	93.2	29.2	4.24	13.83	0.155	0.021	0.423	0.580	1.070
27.7	35.1	----	70.7	93.3	29.1	4.21	13.88	0.158	0.021	0.423	0.580	1.070
27.8	35.3	----	69.9	93.3	29.1	4.15	13.92	0.158	0.021	0.416	0.599	1.080
27.7	35.1	----	69.1	93.1	29.1	4.20	13.79	0.155	0.021	0.410	0.587	1.070
26.9	34.4	----	68.3	92.3	28.3	4.16	13.61	0.151	0.021	0.410	0.587	1.070
26.5	34.4	----	67.8	92.3	27.9	4.14	13.62	0.158	0.021	0.410	0.593	1.070
26.0	34.1	----	67.4	92.0	27.5	4.13	13.54	0.158	0.021	0.410	0.593	1.070
25.8	34.1	----	67.5	91.8	27.4	4.11	13.51	0.158	0.021	0.416	0.587	1.070
25.7	34.0	----	67.5	91.9	27.2	4.10	13.44	0.158	0.021	0.416	0.599	1.070
26.0	34.1	----	67.8	92.3	27.3	4.11	13.51	0.158	0.021	0.416	0.599	1.070
25.7	33.8	----	67.2	91.5	27.2	4.09	13.43	0.158	0.021	0.423	0.587	1.070
25.4	33.7	----	66.5	90.9	26.9	4.09	13.38	0.156	0.021	0.423	0.587	1.070
25.5	34.0	----	66.4	91.3	27.1	4.10	13.47	0.155	0.021	0.423	0.587	1.070
25.6	34.1	----	66.1	91.0	27.1	4.14	13.45	0.151	0.021	0.423	0.587	1.070
25.6	33.9	----	66.2	91.5	27.2	4.21	13.48	0.161	0.022	0.423	0.587	1.070
25.4	33.9	----	66.3	90.9	27.0	4.22	13.41	0.158	0.022	0.423	0.587	1.070

date
31/10/88

28.8	37.0	----	77.3	99.8	30.3	4.49	14.50	0.158	0.025	0.429	0.599	1.140
29.2	37.2	106.3	80.7	102.6	30.7	4.44	14.50	0.158	0.024	0.429	0.599	1.140
28.3	33.7	----	74.8	91.8	29.4	4.27	13.06	0.155	0.014	0.429	0.599	1.140
27.9	32.5	----	70.0	89.7	28.8	4.03	12.69	0.155	0.014	0.429	0.599	1.140
28.0	32.1	----	68.3	89.3	29.0	3.95	12.55	0.156	0.015	0.429	0.599	1.140
27.6	32.4	----	67.5	90.5	28.5	3.97	12.70	0.158	0.013	0.429	0.599	1.140
27.2	31.7	----	67.3	89.7	28.2	3.88	12.44	0.155	0.015	0.429	0.599	1.140
28.6	32.3	----	67.6	89.3	29.4	3.93	12.59	0.153	0.015	0.429	0.599	1.140
29.0	33.3	----	68.3	89.9	30.2	3.90	13.02	0.156	0.015	0.429	0.599	1.140
28.7	33.1	----	67.8	90.7	29.6	3.89	13.01	0.158	0.015	0.429	0.599	1.140
29.6	33.6	----	69.0	92.8	30.5	4.00	13.17	0.158	0.013	0.429	0.599	1.140
28.6	33.2	----	67.9	91.1	29.6	4.00	13.00	0.158	0.013	0.429	0.599	1.140
28.2	32.7	----	67.2	90.6	29.2	3.97	12.82	0.151	0.013	0.429	0.599	1.140

date
1/11/88

25.5	31.8	----	62.6	90.6	26.6	3.79	12.67	0.158	0.016	0.442	0.631	1.200
26.5	32.3	----	64.0	89.9	27.5	3.87	12.79	0.158	0.020	0.442	0.631	1.200
27.0	32.6	----	64.9	88.3	28.0	4.12	12.78	0.155	0.020	0.442	0.631	1.200
27.7	33.9	----	66.5	90.0	28.7	4.12	13.33	0.158	0.018	0.442	0.631	1.200
28.2	33.8	----	65.5	88.8	29.2	4.10	13.39	0.156	0.018	0.442	0.631	1.200
28.3	33.9	----	66.2	89.0	29.3	4.14	13.50	0.158	0.016	0.442	0.631	1.200
28.7	34.4	----	66.3	89.5	29.8	4.19	13.68	0.156	0.015	0.442	0.631	1.200
29.1	34.7	----	65.8	90.4	30.3	4.22	13.87	0.158	0.015	0.442	0.631	1.200
29.1	34.8	----	69.1	91.0	30.2	4.15	13.22	0.156	0.016	0.442	0.631	1.200
29.3	34.7	----	68.5	90.6	30.3	4.15	13.64	0.157	0.015	0.442	0.631	1.200
29.3	34.9	----	67.8	90.7	30.2	4.21	13.60	0.158	0.016	0.442	0.631	1.200
29.6	35.2	----	68.3	91.5	30.5	4.20	13.69	0.161	0.017	0.442	0.631	1.200
29.3	34.9	----	69.2	91.3	30.3	4.12	13.72	0.158	0.016	0.442	0.631	1.200

Table A2.6 (continued) Raw experimental performance data for the operating characteristics of the ammonia-water absorption system at Cerro Prieto.

date
2/11/88

time	T1	T2	T3	T4	T5	T6	T7	T8	T9	T10	T11	T12
11:01:38	88.7	102.6	63.7	42.0	37.6	30.3	96.1	-4.9	-4.7	-2.9	23.3	-4.5
11:15:47	86.3	102.3	57.9	40.9	36.9	29.4	94.3	-4.6	-4.4	-2.8	23.6	-3.4
11:31:06	86.8	102.6	58.0	40.4	36.4	30.1	94.6	-4.3	-4.1	-2.8	23.9	-3.9
11:45:32	88.7	103.5	60.7	41.8	37.4	30.7	96.5	-3.9	-3.7	-2.3	24.5	-3.1
12:15:27	88.3	102.4	59.4	41.8	37.8	30.5	95.6	-4.7	-4.1	-2.7	25.3	-1.9
12:33:55	89.9	103.6	60.0	42.1	37.9	31.1	96.9	-4.6	-4.2	-2.8	25.5	-3.0
12:45:22	88.0	102.5	60.4	39.8	37.3	30.7	95.8	-4.3	-4.1	-2.9	25.5	-3.1
13:00:35	88.2	102.8	59.6	41.1	37.3	30.7	95.4	-4.1	-3.9	-2.7	26.3	-3.5
13:15:12	88.5	103.0	60.3	40.5	37.6	30.9	96.0	-3.9	-3.7	-2.5	26.3	-2.5
13:30:12	90.0	102.8	62.8	42.6	38.2	31.5	96.9	-4.1	-4.3	-2.5	26.8	-2.3
13:45:32	87.9	102.4	59.0	42.0	37.6	30.5	95.6	-4.7	-4.3	-2.7	27.4	-2.5
14:01:12	86.6	102.2	57.8	39.9	36.8	29.9	94.8	-4.3	-4.3	-2.9	27.2	-2.7
14:32:37	89.3	103.6	59.5	40.6	37.3	31.0	96.6	-4.8	-4.4	-3.0	27.9	-3.0

date
3/11/88

10:46:16	87.8	103.0	59.6	41.9	36.9	27.8	95.8	-5.1	-4.7	-2.5	24.1	-4.1
11:02:06	87.5	103.5	59.1	40.3	36.0	28.5	95.9	-5.7	-5.1	-3.3	24.3	-3.7
11:17:17	86.1	102.8	59.1	40.3	36.0	28.1	95.0	-5.1	-4.9	-3.3	24.7	-4.3
11:30:34	88.2	103.4	59.4	40.5	36.7	29.7	96.2	-5.3	-4.9	-3.5	25.3	-4.1
11:46:37	87.3	103.3	60.4	41.1	37.3	29.8	95.8	-4.4	-4.2	-2.8	25.7	-3.6
12:00:50	90.0	102.7	61.9	41.1	37.6	30.5	96.7	-3.7	-3.3	-2.3	25.9	-3.3
12:16:03	90.7	102.4	62.0	43.1	38.4	30.7	96.7	-3.9	-3.5	-2.3	26.2	-2.9
12:30:50	88.7	102.1	60.7	41.9	38.0	30.3	95.6	-4.2	-3.8	-2.5	26.7	-2.9
12:46:09	87.3	102.4	58.5	40.6	37.5	30.0	94.6	-4.8	-4.2	-3.0	26.8	-2.4
13:00:43	87.7	102.4	58.6	41.0	37.2	30.3	95.2	-4.7	-4.3	-3.1	27.2	-2.3
13:15:32	90.6	104.1	61.3	42.2	38.0	31.5	97.6	-4.5	-4.1	-2.7	27.6	-3.1
13:30:55	89.8	102.8	60.5	41.5	37.6	30.9	96.5	-4.1	-3.9	-2.7	27.6	-2.9
13:45:40	89.5	102.8	62.0	42.6	38.2	31.3	96.5	-3.5	-3.3	-2.1	28.0	-2.7
14:00:46	88.3	102.6	60.9	41.5	37.8	31.3	96.0	-3.5	-3.3	-2.1	27.8	-2.5
14:15:56	90.4	102.8	61.2	42.6	38.6	31.6	97.0	-3.3	-2.9	-1.7	29.1	-1.7
14:30:54	89.7	102.0	61.4	42.2	38.7	31.4	96.3	-3.2	-3.0	-1.6	29.1	-2.6

Table A2.6 (continued) Raw experimental performance data for the operating characteristics of the ammonia-water absorption system at Cerro Prieto.

date 2/11/88

T13	T14	T15	T16	T17	T18	T19	T20	T21	T22	T23	T24	T25
40.7	59.9	87.5	25.4	27.4	63.7	63.9	38.2	-3.3	29.9	-3.9	-4.5	26.0
39.8	57.9	84.3	25.5	27.3	61.3	61.5	37.3	26.9	30.0	-1.9	-4.0	26.1
39.7	57.8	83.8	25.6	27.4	61.4	61.6	37.0	27.5	30.6	-2.4	-4.0	26.2
40.5	58.8	85.1	25.8	27.8	63.0	63.1	37.6	-0.2	31.4	-1.8	-3.6	26.4
40.9	59.0	85.3	26.6	28.4	63.0	63.2	38.1	26.4	31.2	-0.6	-4.0	27.1
41.1	59.4	86.0	26.5	28.4	63.8	64.0	38.0	11.3	31.8	-1.7	-4.1	27.0
40.9	59.2	86.1	26.5	28.4	62.8	62.8	38.0	-2.3	31.4	-3.3	-3.9	27.0
40.9	58.8	84.8	26.3	28.2	63.0	63.2	37.6	21.0	31.4	-2.3	-3.7	27.0
40.9	59.2	85.9	26.5	28.4	63.4	63.6	38.2	0.6	31.6	-2.3	-3.3	27.0
42.2	61.3	87.0	26.4	28.6	65.8	66.0	38.9	2.0	32.4	-2.6	-4.0	27.0
41.1	59.2	84.8	26.0	28.2	63.0	63.0	38.1	7.6	31.2	-2.2	-4.0	26.7
40.8	58.6	84.6	26.2	27.9	61.8	61.8	37.9	29.8	30.4	-3.0	-4.0	26.7
41.0	58.9	84.3	26.3	28.3	63.2	63.4	37.6	13.0	31.7	-2.5	-4.3	27.0

date 3/11/88

39.2	58.1	85.4	23.0	25.1	62.4	62.6	36.9	4.7	28.4	-2.2	-4.4	23.6
38.7	57.2	84.2	23.3	25.2	60.6	61.0	36.4	6.3	29.3	-2.4	-4.5	23.9
39.3	57.4	84.4	23.7	25.6	60.7	60.9	36.6	26.0	28.9	-2.8	-4.6	24.4
40.1	58.1	85.0	24.5	26.5	62.0	62.0	36.8	-2.2	30.4	-3.4	-4.8	25.2
40.6	58.1	85.0	25.2	27.1	61.3	61.5	37.6	1.8	30.6	-2.4	-4.0	25.8
42.4	61.5	86.9	25.7	27.8	66.8	67.0	38.1	28.4	31.1	-2.5	-3.2	26.3
42.8	62.0	87.4	26.4	28.5	67.5	67.5	38.7	28.3	31.4	-1.4	-3.3	27.0
42.1	59.8	86.3	26.7	28.6	64.3	64.7	38.2	25.7	31.1	-1.7	-3.7	27.2
41.2	58.5	84.9	26.6	28.3	61.6	61.8	38.1	19.9	30.8	-2.2	-3.8	27.1
41.2	58.6	84.9	26.4	28.1	61.8	61.8	37.9	-1.8	31.0	-2.8	-3.8	26.9
41.8	59.7	86.3	26.2	28.2	64.3	64.5	38.1	-2.4	32.0	-3.3	-4.1	27.0
41.7	60.3	85.7	26.5	28.4	64.9	64.9	38.2	-1.4	31.6	-2.5	-3.5	27.0
42.2	60.3	86.9	26.8	28.8	64.9	64.9	38.7	-0.6	32.0	-1.9	-3.1	27.6
42.0	59.4	86.1	27.0	29.0	63.7	63.7	38.5	20.0	32.0	-2.0	-3.2	27.5
42.8	61.2	85.7	27.2	29.1	66.2	66.2	39.0	2.9	32.3	-1.6	-2.8	27.7
42.9	61.6	87.1	27.1	29.1	66.7	66.9	39.0	17.7	32.1	-1.9	-2.9	27.6

Table A2.6 (continued) Raw experimental performance data for the operating characteristics of the ammonia-water absorption system at Cerro Prieto.

date
2/11/88

T26	T27	T28	T29	T30	T31	PEV	PCO	FSOL	FREF	FWRE	FWCO	FWAB
25.6	30.5	----	64.7	86.3	26.6	3.52	11.94	0.158	0.014	0.442	0.631	1.200
25.7	29.6	----	61.7	83.3	26.5	3.58	11.74	0.155	0.014	0.442	0.631	1.200
25.8	30.0	----	60.2	83.4	26.7	3.62	11.91	0.155	0.012	0.442	0.631	1.200
26.0	30.8	----	60.8	85.3	27.0	3.68	12.11	0.158	0.014	0.442	0.631	1.200
26.8	30.6	87.9	62.9	85.3	27.5	3.56	12.03	0.156	0.014	0.442	0.631	1.200
26.8	31.1	89.1	61.8	86.1	27.6	3.60	12.38	0.161	0.011	0.442	0.631	1.200
26.6	30.9	87.4	62.0	85.1	27.6	3.65	12.13	0.156	0.014	0.442	0.631	1.200
26.6	30.8	87.2	61.0	84.6	27.6	3.65	12.17	0.158	0.011	0.442	0.631	1.200
26.6	31.0	88.1	61.4	85.3	27.6	3.72	12.24	0.158	0.014	0.442	0.631	1.200
26.6	31.4	----	65.0	86.8	27.5	3.60	12.38	0.164	0.016	0.442	0.631	1.200
26.3	30.6	----	62.3	84.9	27.1	3.59	12.12	0.161	0.010	0.442	0.631	1.200
26.3	30.0	----	61.2	84.1	27.1	3.63	11.87	0.158	0.013	0.442	0.631	1.200
26.6	30.9	88.9	60.9	85.7	27.6	3.58	12.35	0.161	0.011	0.442	0.631	1.200

date
3/11/88

23.2	27.8	----	59.8	84.5	24.2	3.54	11.15	0.155	0.016	0.442	0.631	1.250
23.5	28.5	----	59.5	83.6	24.4	3.40	11.36	0.156	0.016	0.442	0.631	1.250
24.0	28.3	----	59.9	83.0	25.0	3.50	11.35	0.155	0.014	0.442	0.631	1.250
24.8	29.6	----	60.0	84.7	25.8	3.47	11.80	0.161	0.013	0.442	0.631	1.250
25.4	29.8	87.0	60.8	84.3	26.4	3.61	11.92	0.158	0.015	0.442	0.631	1.250
25.9	30.5	89.7	62.6	86.7	26.9	3.72	12.03	0.158	0.015	0.442	0.631	1.250
26.8	30.8	90.3	63.5	87.5	27.6	3.71	12.10	0.158	0.013	0.442	0.631	1.250
26.8	30.5	88.2	63.0	86.1	27.6	3.65	11.97	0.156	0.011	0.442	0.631	1.250
26.7	30.0	86.7	61.2	83.9	27.5	3.56	11.93	0.156	0.009	0.442	0.631	1.250
26.6	30.4	87.1	60.8	84.7	27.5	3.57	12.07	0.156	0.013	0.442	0.631	1.250
26.6	31.4	90.0	61.8	86.6	27.5	3.56	12.49	0.164	0.011	0.442	0.631	1.250
26.8	30.8	----	61.6	86.2	27.6	3.70	12.22	0.153	0.013	0.442	0.631	1.250
27.2	31.4	----	62.9	86.2	27.9	3.75	12.36	0.155	0.012	0.442	0.631	1.250
27.1	31.2	----	62.7	85.3	28.1	3.76	12.41	0.158	0.011	0.442	0.631	1.250
27.3	31.7	----	61.9	87.3	28.3	3.79	12.56	0.158	0.013	0.442	0.631	1.250
27.2	31.5	----	62.8	86.9	28.2	3.80	12.47	0.158	0.011	0.442	0.631	1.250

Table A2.6 (continued) Raw experimental performance data for the operating characteristics of the ammonia-water absorption system at Cerro Prieto.

date 4/11/88

time	T1	T2	T3	T4	T5	T6	T7	T8	T9	T10	T11	T12
10:45:27	88.8	103.0	58.6	43.3	34.7	28.5	96.1	-4.9	-3.7	-2.0	25.0	0.2
11:00:33	88.9	102.8	59.0	42.6	34.9	28.3	96.3	-5.1	-4.5	-2.7	25.3	-1.7
11:15:36	88.6	102.5	58.5	41.2	34.7	28.3	95.9	-5.4	-5.0	-3.2	26.0	-2.4
11:30:43	87.9	102.4	58.0	41.0	34.5	28.1	95.4	-5.1	-4.9	-3.3	26.4	-3.5
11:46:46	88.1	102.2	58.2	41.8	34.7	28.5	95.4	-5.3	-4.7	-3.3	26.6	-2.3
12:00:44	88.7	102.3	58.1	42.4	34.8	28.8	95.2	-5.4	-5.0	-3.5	27.4	-2.7
12:17:06	88.4	102.0	58.0	42.5	34.9	28.9	95.0	-5.2	-4.8	-3.4	27.7	-2.4
12:31:06	89.2	102.2	58.3	41.5	35.0	----	95.9	-5.2	-4.4	-3.4	27.9	-2.0
12:47:16	88.8	102.0	58.9	42.5	36.0	29.4	95.3	-4.8	-4.2	-3.0	28.8	-2.6
13:00:29	89.6	102.0	58.7	43.3	36.2	30.2	95.9	-4.8	-4.2	-2.8	29.3	0.2
13:15:48	89.0	101.9	59.2	43.3	36.4	30.1	95.2	-4.1	-3.7	-2.3	29.5	-0.7
13:30:12	88.9	101.7	58.0	42.8	36.7	30.1	95.2	-3.9	-3.1	-2.1	29.5	0.1
13:45:58	89.7	102.0	58.1	43.4	36.1	30.4	95.6	-4.2	-3.0	-2.0	30.4	9.4
14:00:13	89.2	101.8	57.8	43.3	36.4	30.2	95.5	-4.0	-3.6	-2.2	30.0	2.9
14:15:56	88.7	101.5	57.9	43.2	36.5	29.9	95.0	-4.1	-3.1	-2.1	30.5	1.7
14:30:33	88.6	101.6	56.8	42.7	35.4	29.4	95.3	-4.8	-3.2	-2.4	31.0	4.7

date 7/11/88

11:46:06	85.5	101.1	52.7	42.4	35.5	28.6	92.4	-3.3	8.7	7.3	29.3	24.5
12:00:27	83.2	100.5	52.9	41.2	34.7	28.3	90.5	-3.6	5.9	5.3	29.5	26.2
12:15:12	85.0	100.7	54.9	41.3	34.6	28.8	91.6	-4.2	5.1	4.7	30.2	27.9
12:31:10	83.5	100.6	59.0	40.9	34.2	28.4	90.8	-4.1	4.0	3.6	30.5	26.7
12:45:18	83.8	100.5	61.2	41.0	34.1	28.5	91.0	-4.4	3.3	3.1	30.6	28.1
13:00:29	84.0	100.6	62.0	40.7	33.8	28.2	91.1	-4.7	2.8	2.4	31.2	27.6
13:15:53	84.1	100.6	62.1	41.1	33.8	28.4	91.5	-4.6	1.9	1.5	31.9	27.3
13:30:14	84.1	100.6	62.5	40.9	34.2	28.2	91.2	-4.8	1.5	1.1	30.6	27.1
13:46:11	84.7	100.7	62.5	41.2	34.4	28.5	91.6	-4.6	0.5	0.3	31.5	21.3
14:01:26	83.2	100.8	60.6	39.6	35.0	27.9	90.6	-5.2	0.3	-0.1	31.3	23.8
14:15:57	81.6	100.3	60.5	38.8	35.2	27.8	89.5	-5.8	-0.1	-0.3	32.7	24.3
14:30:54	82.7	100.6	61.1	38.9	35.5	28.6	90.4	-5.3	0.2	0.1	32.2	25.8
14:48:04	82.9	101.1	62.6	39.3	35.7	28.5	90.5	-5.1	-0.2	-0.8	31.8	17.5
15:00:36	84.5	101.2	64.2	39.4	35.6	29.2	92.3	-5.8	-1.0	-1.0	32.3	22.9

Table A2.6 (continued) Raw experimental performance data for the operating characteristics of the ammonia-water absorption system at Cerro Prieto.

date
4/11/88

T13	T14	T15	T16	T17	T18	T19	T20	T21	T22	T23	T24	T25
40.1	59.3	85.9	23.3	25.8	63.9	64.3	35.6	10.1	29.4	-0.5	-3.8	24.0
39.9	59.0	86.2	23.7	----	63.7	63.9	35.2	12.9	29.2	-1.7	-4.2	24.3
40.0	58.7	85.8	24.2	26.4	63.3	63.5	34.9	-3.6	28.9	-3.8	-4.6	24.8
39.9	58.0	85.1	24.5	26.6	62.7	63.1	34.9	25.4	29.1	-3.6	-4.8	25.0
40.1	58.2	85.5	24.7	26.8	62.6	62.9	34.8	-2.6	29.0	-3.2	-4.4	25.2
40.5	58.8	85.7	24.9	27.0	64.3	65.1	35.0	3.3	29.4	-3.6	-4.8	25.6
40.8	59.1	85.8	25.6	27.7	64.4	64.6	35.3	24.7	29.7	-2.5	-4.5	26.2
41.2	59.3	86.7	26.0	28.1	64.2	64.2	35.2	-1.6	30.2	-3.0	-4.0	26.6
41.5	59.1	86.2	26.7	28.6	64.4	64.7	36.0	27.7	30.2	-2.6	-4.0	27.3
42.3	60.1	86.9	27.1	29.3	65.7	65.9	36.2	6.7	30.8	-2.2	-3.8	27.7
42.4	59.7	86.6	27.6	29.5	65.2	65.4	36.4	24.4	30.8	-1.8	-3.4	28.1
42.4	59.8	86.7	27.8	29.7	64.9	65.1	36.6	27.6	30.8	-1.4	-2.7	28.3
42.9	60.6	86.7	27.7	29.8	66.4	66.6	36.7	8.0	31.1	-1.5	-2.9	28.4
42.5	60.2	86.9	27.7	29.6	65.7	66.1	36.7	18.9	31.0	-0.6	-2.8	28.3
42.0	59.8	86.1	27.2	29.3	65.2	65.6	36.6	18.9	30.7	-0.5	-2.7	27.8
41.7	59.8	86.2	26.5	28.6	65.3	65.7	36.3	6.8	30.2	-1.3	-2.9	27.1

date
7/11/88

40.5	57.8	83.3	26.0	28.0	62.6	62.6	35.4	22.6	28.4	21.5	17.6	26.5
40.1	56.5	81.2	26.4	28.3	59.9	60.5	35.5	24.9	28.9	21.6	15.5	27.0
40.2	57.7	82.6	26.3	28.3	63.4	63.4	35.0	24.0	29.6	21.5	14.1	54.5
40.0	56.6	81.8	26.1	28.0	60.9	61.1	34.8	24.9	29.4	21.1	12.5	64.1
40.0	56.6	82.1	26.4	28.1	61.2	61.2	34.5	20.0	29.3	19.4	10.2	67.4
40.1	56.7	82.1	26.0	28.0	61.6	61.6	34.3	18.4	29.3	17.9	8.9	69.0
40.7	57.1	82.4	26.3	28.0	61.5	61.7	34.6	18.7	29.5	16.4	5.8	70.0
40.7	57.0	81.8	26.1	28.0	61.3	61.5	34.6	15.8	29.2	15.4	5.4	70.3
40.8	57.6	82.4	26.3	28.1	62.3	62.5	34.8	22.0	29.6	14.2	3.6	55.2
40.2	55.8	81.3	25.9	27.5	59.8	60.0	34.7	25.5	28.8	14.6	4.2	67.3
40.0	55.0	80.0	26.3	27.8	57.5	57.5	35.5	18.3	28.7	14.4	3.4	69.4
40.7	56.5	80.8	26.4	28.0	59.2	59.2	35.8	17.2	29.8	14.9	4.1	69.5
40.1	56.1	80.3	25.8	27.8	59.0	59.1	36.3	25.4	29.4	13.3	2.3	68.5
40.4	57.0	81.7	25.6	27.3	60.2	60.2	35.9	18.3	30.1	11.9	2.5	69.8

Table A2.6 (continued) Raw experimental performance data for the operating characteristics of the ammonia-water absorption system at Cerro Prieto.

date
4/11/88

T26	T27	T28	T29	T30	T31	PEV	PCO	FSOL	FREF	FWRE	FWCO	FWAB
23.6	28.4	----	59.8	85.0	24.6	3.59	11.34	0.158	0.010	0.442	0.631	1.250
24.2	28.4	----	60.0	85.6	24.9	3.57	11.32	0.161	0.011	0.442	0.631	1.250
24.4	28.7	----	60.3	84.7	25.2	3.49	11.36	0.158	0.011	0.442	0.631	1.250
24.6	28.3	----	60.2	84.5	25.4	3.52	11.35	0.158	0.011	0.442	0.631	1.250
25.0	28.7	----	60.4	84.9	25.8	3.50	11.37	0.155	0.011	0.442	0.631	1.250
25.2	28.9	----	60.6	84.7	26.0	3.50	11.49	0.158	0.008	0.442	0.631	1.250
25.8	29.1	----	60.5	85.1	26.6	3.54	11.49	0.158	0.009	0.442	0.631	1.250
26.2	29.7	----	60.8	86.4	27.1	3.58	11.74	0.158	0.011	0.442	0.631	1.250
26.9	29.8	----	62.1	85.8	27.7	3.60	11.78	0.158	0.009	0.442	0.631	1.250
27.3	30.4	----	61.9	86.7	28.1	3.63	12.08	0.158	0.009	0.442	0.631	1.250
27.7	30.2	----	62.0	85.8	28.5	3.72	11.95	0.158	0.008	0.442	0.631	1.250
27.9	30.5	----	61.6	85.7	28.7	3.73	11.97	0.156	0.009	0.442	0.631	1.250
28.0	30.7	----	61.5	86.7	28.8	3.69	12.01	0.158	0.009	0.442	0.631	1.250
27.9	30.6	----	61.7	86.5	28.6	3.72	12.08	0.155	0.008	0.442	0.631	1.250
27.6	30.1	----	60.9	85.5	28.2	3.68	11.85	0.158	0.008	0.442	0.631	1.250
26.7	29.6	----	60.2	85.8	27.5	3.60	11.77	0.155	0.009	0.442	0.631	1.250

date
7/11/88

26.1	29.0	----	55.1	83.0	28.6	3.73	11.53	0.161	0.009	0.429	0.126	1.060
26.6	28.7	----	55.7	80.6	28.9	3.72	11.42	0.156	0.008	0.429	0.126	1.060
26.5	29.1	----	59.7	82.4	52.6	3.67	11.57	0.158	0.006	0.442	0.000	1.080
26.3	28.6	----	66.2	81.3	62.1	3.65	11.36	0.158	0.008	0.442	0.000	1.080
26.6	28.9	----	69.5	81.5	65.4	3.62	11.37	0.158	0.008	0.435	0.000	1.080
26.2	28.5	----	71.6	81.9	66.5	3.56	11.29	0.157	0.008	0.435	0.000	1.080
26.3	28.8	----	72.0	82.2	67.5	3.60	11.39	0.157	0.008	0.435	0.000	1.080
26.5	28.6	----	73.0	82.0	67.5	3.55	11.34	0.157	0.008	0.435	0.000	1.080
26.5	28.6	----	72.1	82.4	57.1	3.58	11.33	0.158	0.008	0.435	0.000	1.080
26.1	28.2	----	71.7	80.7	64.7	3.44	11.21	0.158	0.008	0.435	0.000	1.080
26.4	28.1	----	72.2	79.7	67.1	3.36	11.19	0.158	0.008	0.435	0.000	1.080
26.5	28.8	----	71.9	80.8	67.2	3.35	11.36	0.158	0.008	0.435	0.000	1.080
25.9	28.6	----	70.8	80.5	66.6	3.46	11.33	0.158	0.008	0.435	0.000	1.080
25.9	29.0	----	71.7	82.2	67.5	3.32	11.51	0.158	0.009	0.435	0.000	1.080

Table A2.6 (continued) Raw experimental performance data for the operating characteristics of the ammonia-water absorption system at Cerro Prieto.

date
10/11/88

time	T1	T2	T3	T4	T5	T6	T7	T8	T9	T10	T11	T12
10:30:30	101.0	128.0	77.1	48.7	39.2	31.7	111.0	0.5	0.7	2.1	21.6	1.1
10:46:15	100.7	127.0	75.9	49.6	40.0	32.2	110.7	0.8	1.0	2.2	21.7	1.2
11:00:28	100.6	126.3	75.2	49.7	40.5	32.2	110.6	0.5	0.6	2.0	22.7	1.2
11:15:43	101.2	127.7	75.1	49.7	40.0	32.3	111.2	0.3	0.5	1.9	23.2	1.1
11:30:38	100.8	126.7	74.7	49.7	39.9	32.0	110.8	0.5	0.9	1.8	23.0	1.7
11:46:15	100.6	125.6	74.4	49.5	39.3	31.6	110.5	0.0	0.4	1.6	23.1	1.2
12:00:59	100.7	127.2	75.7	50.0	39.7	31.6	110.7	0.2	0.4	1.4	23.5	0.8
12:15:45	101.6	128.5	76.4	50.2	40.4	32.3	111.6	0.8	0.8	1.7	24.6	1.3
12:30:41	101.2	126.4	75.4	50.5	40.7	32.6	110.8	1.1	1.3	2.3	24.1	1.9
12:45:13	101.5	126.1	75.0	50.8	41.2	32.7	111.1	1.0	1.2	2.2	25.8	1.6
13:00:46	102.1	127.3	76.2	50.7	41.7	33.2	111.3	1.1	1.3	2.5	25.3	2.3
13:15:29	101.8	127.2	76.3	51.5	42.2	33.5	111.1	1.6	2.0	3.0	27.5	2.8
13:30:47	101.2	124.6	74.7	50.5	41.3	33.3	110.1	1.7	2.1	3.1	24.8	3.1
13:45:35	100.8	124.8	75.3	50.1	41.5	32.9	109.9	1.9	2.1	2.9	25.3	2.9
14:01:32	101.0	124.6	74.7	50.1	41.3	33.1	109.9	1.5	1.7	2.7	25.7	3.1

date
11/11/88

10:01:03	97.9	118.9	69.7	45.6	36.3	25.7	109.2	-3.8	-3.6	-2.0	22.1	-3.2
10:15:51	95.6	116.0	71.0	46.5	36.0	27.3	108.0	-2.0	-1.8	-0.9	22.6	-1.3
10:30:42	96.3	118.7	71.5	46.2	37.0	28.0	110.6	-1.7	-1.7	-0.3	22.8	-0.9
10:45:13	95.5	116.5	69.1	46.9	35.8	27.8	109.0	-2.2	-2.1	-0.7	22.8	-0.9
11:01:46	96.8	120.4	70.8	46.3	35.8	27.7	111.6	-2.2	-1.8	-0.7	23.4	-1.1
11:15:32	97.0	123.9	72.9	46.2	36.6	27.9	111.2	-1.8	-1.6	-0.4	23.5	-0.8
11:30:30	97.5	126.2	72.7	47.5	37.1	28.6	111.2	-1.4	-1.4	-0.3	23.6	-0.9
11:15:35	97.4	118.3	71.0	47.7	37.0	----	110.7	-1.8	-1.6	-0.2	23.5	-0.8
12:00:29	98.2	121.1	71.5	47.6	36.7	28.8	111.3	-1.7	-1.3	-0.3	23.7	-0.5
12:17:00	97.5	120.2	72.3	46.3	37.3	28.7	111.2	-1.4	-1.2	0.0	24.2	-0.4
12:31:02	97.6	118.8	72.9	46.8	37.4	28.7	111.1	-1.2	-1.0	0.0	24.3	-0.2
12:45:50	97.8	121.4	73.2	47.8	37.7	29.0	111.3	-1.1	-0.9	0.1	24.5	-0.3
13:00:46	97.0	117.3	71.2	47.3	37.4	28.9	110.0	-1.2	-1.2	0.0	24.5	-0.2
13:15:33	97.9	118.8	71.0	47.3	37.5	29.3	110.9	-1.6	-1.4	-0.2	26.0	-0.6
13:30:27	98.8	123.3	71.4	47.3	37.7	29.4	111.2	-1.8	-1.6	-0.2	25.6	-0.4
13:45:43	98.1	117.6	70.8	47.7	37.3	29.2	110.8	-1.4	-1.0	-0.1	25.0	0.1
14:00:52	97.3	120.5	70.9	47.0	38.0	29.0	110.6	-1.3	-0.9	0.3	25.5	-0.3

date
14/11/88

10:31:50	113.0	129.1	84.1	49.0	40.5	27.1	118.3	-5.4	-5.2	-3.4	21.8	-5.0
10:45:37	103.3	128.3	78.2	49.1	40.3	29.1	112.9	-1.6	-1.6	-0.6	22.9	-1.0
11:01:23	101.4	128.6	76.8	50.1	40.2	30.6	112.3	1.3	1.1	1.7	23.4	1.7
11:15:57	101.5	128.1	76.1	50.6	39.9	31.0	112.5	1.0	1.2	2.4	23.9	1.8
11:30:17	101.1	128.3	75.9	50.2	39.1	30.8	112.5	0.4	0.6	1.8	23.5	0.8
11:45:37	101.6	128.8	76.6	50.0	38.5	31.0	112.9	0.0	0.2	1.3	23.8	0.7
12:00:34	102.3	130.4	77.9	49.5	38.2	31.3	113.4	-0.3	-0.3	1.1	24.4	0.3
12:16:07	103.0	131.8	78.6	49.3	39.9	31.7	113.9	0.3	0.3	1.3	25.5	0.9
12:31:00	104.4	130.9	79.9	51.9	41.0	32.6	114.8	1.2	1.2	2.2	25.0	2.8
12:46:39	96.9	116.1	70.1	47.4	37.6	29.7	108.7	-0.7	0.2	1.2	22.0	1.8
13:01:40	95.4	115.3	67.5	46.4	35.7	27.8	107.2	-2.7	-2.1	-0.8	21.9	-0.8
13:16:18	92.8	113.9	64.5	43.2	34.4	26.3	105.6	-3.9	-3.5	-1.9	21.2	-2.1

Table A2.6 (continued) Raw experimental performance data for the operating characteristics of the ammonia-water absorption system at Cerro Prieto.

date
10/11/88

T13	T14	T15	T16	T17	T18	T19	T20	T21	T22	T23	T24	T25
49.3	71.5	96.2	26.1	29.4	76.6	76.7	39.4	31.5	33.2	1.7	0.9	26.8
50.2	72.2	96.4	----	30.0	76.7	77.0	40.0	26.0	33.7	2.1	1.2	27.3
49.9	72.0	96.5	26.4	29.7	76.3	77.1	40.1	17.1	33.5	2.2	0.8	27.0
50.1	72.8	97.1	26.5	29.8	77.5	78.1	40.1	12.8	33.6	1.6	0.6	27.2
50.4	73.0	96.1	26.1	29.5	77.3	77.7	40.0	6.5	33.3	2.0	0.8	26.7
49.8	72.6	95.9	25.8	29.1	76.7	77.3	39.8	3.9	32.9	1.5	0.7	26.5
50.0	72.3	96.1	26.0	29.3	76.9	77.2	39.8	5.6	33.2	1.5	0.3	26.7
51.3	73.8	97.2	26.9	30.2	78.1	78.5	40.1	10.1	33.8	2.0	1.1	27.8
51.4	73.6	96.7	27.6	30.7	77.9	78.4	40.8	13.3	34.1	2.5	1.6	28.3
51.5	74.0	97.4	27.5	30.8	78.3	78.9	41.1	19.8	34.2	2.4	1.3	28.2
52.0	74.3	97.5	28.4	31.5	79.2	79.6	41.4	27.1	34.6	2.5	1.5	29.0
52.5	74.0	97.9	28.9	32.0	78.9	79.1	41.9	25.9	34.9	3.4	2.1	29.5
52.2	74.0	96.0	28.6	31.7	78.9	78.9	42.0	30.9	34.5	3.4	2.2	29.3
52.0	74.0	96.6	----	31.5	78.5	78.5	41.8	25.6	34.1	3.2	2.6	29.1
51.7	74.0	96.0	28.3	31.3	78.9	78.9	41.8	21.8	34.6	2.8	2.0	29.0

date
11/11/88

47.1	70.8	92.9	21.1	24.4	74.2	74.7	36.7	-2.6	25.5	-3.4	-3.6	21.8
45.3	67.0	90.8	21.3	24.8	70.6	71.3	36.1	26.3	28.8	-0.3	-1.7	22.2
45.5	67.1	91.5	21.4	25.1	71.1	71.8	36.2	7.3	29.7	0.2	-1.6	22.3
44.8	67.2	90.4	21.3	24.8	71.0	71.7	36.2	1.0	29.3	-0.6	-2.0	22.1
45.5	67.8	91.7	21.5	25.0	71.7	72.3	36.0	18.8	29.1	-0.6	-1.6	22.1
46.2	68.2	92.0	21.9	25.4	72.3	72.7	36.4	25.9	29.6	0.0	-1.4	22.7
46.9	68.9	93.0	22.2	25.7	73.0	73.6	36.8	6.6	30.3	0.1	-1.3	22.9
47.0	69.7	92.6	22.5	25.8	73.5	74.1	37.3	1.1	30.1	-0.3	-1.5	23.2
47.6	70.7	93.2	22.6	25.9	74.3	74.9	37.1	1.7	30.0	-0.4	-1.2	23.4
47.5	69.7	92.9	22.7	26.1	73.6	74.2	37.4	22.3	30.1	-0.2	-0.9	23.3
47.3	69.5	92.8	22.9	26.4	73.7	74.2	37.4	28.0	30.3	0.3	-0.9	23.6
47.4	69.8	93.0	23.0	26.3	73.9	74.3	37.5	12.9	30.6	0.4	-0.8	23.6
47.2	69.4	92.2	22.9	26.2	73.3	73.9	37.7	3.5	30.4	0.1	-1.1	23.6
47.9	70.4	93.3	22.9	26.4	74.4	75.0	37.7	1.3	30.5	-0.5	-1.5	23.8
48.0	71.2	93.8	23.0	26.3	75.3	75.9	37.8	0.3	30.5	-0.9	-1.5	23.7
48.4	71.3	93.2	23.2	26.5	74.9	75.5	38.0	1.4	30.5	-0.3	-0.9	23.9
48.2	70.5	93.0	23.4	26.7	73.9	74.9	38.1	17.4	30.4	0.0	-0.6	24.0

date
14/11/88

50.3	78.1	106.7	24.6	27.8	88.7	90.1	41.3	-4.0	26.9	-4.6	-5.2	25.2
51.7	75.6	98.5	25.4	28.5	80.2	80.4	40.5	-0.2	28.5	-1.0	-1.4	26.0
50.9	74.2	95.3	25.3	28.8	77.7	77.9	39.8	5.1	32.7	1.9	1.3	25.9
50.4	74.0	96.3	24.6	28.3	77.8	77.8	39.4	2.7	32.7	1.9	1.1	25.2
49.2	72.1	95.5	24.0	----	76.3	76.6	39.2	6.4	32.3	1.9	0.5	24.7
49.0	71.2	96.2	23.8	27.5	76.3	76.3	39.0	5.6	32.6	1.5	0.3	24.5
49.5	72.1	96.6	24.4	28.2	77.1	77.5	38.4	19.2	33.0	1.0	0.0	25.1
50.6	73.7	97.8	25.3	28.6	78.6	78.8	39.1	10.0	33.3	1.6	0.6	26.0
52.7	75.9	99.1	26.4	29.9	80.6	81.2	40.4	6.2	34.2	2.5	1.3	27.1
47.0	68.2	92.4	23.3	26.8	72.9	73.9	38.9	9.4	31.0	2.2	0.4	24.4
44.1	65.2	90.5	21.2	24.7	70.3	71.1	36.5	6.4	29.0	0.1	-2.0	21.9
42.0	63.2	88.2	19.5	23.0	68.3	69.2	34.8	2.5	27.5	-1.8	-3.4	20.5

Table A2.6 (continued) Raw experimental performance data for the operating characteristics of the ammonia-water absorption system at Cerro Prieto.

date
10/11/88

T26	T27	T28	T29	T30	T31	PEV	PCO	FSOL	FREF	FWRE	FWCO	FWAB
26.3	32.1	----	75.8	96.9	27.6	4.27	12.53	0.189	0.019	0.000	0.555	0.978
26.9	32.3	----	75.5	96.6	28.1	4.36	12.60	0.189	0.016	0.000	0.555	0.978
26.6	32.4	----	74.8	96.5	27.7	4.28	12.58	0.189	0.016	0.000	0.555	0.978
26.6	32.4	----	74.8	97.0	28.0	4.26	12.65	0.189	0.016	0.000	0.555	0.978
26.4	32.2	----	74.8	96.2	27.7	4.26	12.61	0.189	0.016	0.000	0.555	0.978
25.9	31.7	----	74.2	96.0	27.3	4.22	12.42	0.189	0.017	0.000	0.555	0.978
26.1	31.9	----	74.9	96.6	27.4	4.23	12.47	0.189	0.017	0.000	0.555	0.978
27.2	32.6	----	76.5	97.8	28.6	4.34	12.74	0.189	0.016	0.000	0.555	0.978
27.7	32.9	----	76.1	96.8	29.1	4.36	12.84	0.189	0.015	0.000	0.555	0.978
27.8	33.0	----	75.8	97.3	29.0	4.37	12.88	0.189	0.015	0.000	0.555	0.978
28.5	33.5	----	77.0	98.1	29.8	4.44	13.03	0.189	0.015	0.000	0.555	0.978
29.0	33.8	----	76.9	98.0	30.1	4.48	13.16	0.186	0.014	0.000	0.555	0.978
28.7	33.6	----	76.1	96.5	30.1	4.53	12.86	0.189	0.014	0.000	0.555	0.978
28.5	33.2	----	75.8	96.5	29.9	4.55	12.91	0.189	0.015	0.000	0.555	0.978
28.4	33.2	----	75.8	96.9	29.7	4.47	12.94	0.189	0.015	0.000	0.555	0.978

date
11/11/88

21.3	26.9	----	68.3	92.3	22.8	3.64	10.83	0.189	0.019	0.000	0.555	1.010
21.6	27.4	----	67.5	90.2	23.0	3.89	10.94	0.189	0.020	0.000	0.555	1.010
21.7	28.1	----	68.0	90.7	23.1	3.94	11.18	0.189	0.017	0.000	0.555	1.010
21.5	27.9	----	66.0	89.4	23.1	3.87	11.14	0.189	0.016	0.000	0.555	1.010
21.5	27.7	----	68.2	91.2	23.1	3.90	11.10	0.189	0.020	0.000	0.555	1.010
22.1	28.1	----	70.2	91.4	23.4	3.99	11.16	0.189	0.020	0.000	0.555	1.010
22.4	28.8	----	70.7	92.4	23.9	3.99	11.40	0.189	0.016	0.000	0.555	1.010
22.6	28.8	----	70.4	92.1	24.0	3.93	11.43	0.189	0.016	0.000	0.555	1.010
22.8	28.8	----	70.4	92.7	24.2	3.97	11.42	0.189	0.018	0.000	0.555	1.010
22.7	28.7	----	71.4	92.8	24.3	4.05	11.35	0.189	0.018	0.000	0.555	1.010
23.2	29.0	----	70.4	92.1	24.5	4.00	11.49	0.187	0.018	0.000	0.555	1.010
23.1	29.1	----	70.8	92.7	24.6	4.06	11.51	0.188	0.016	0.000	0.555	1.010
23.0	29.0	----	69.5	91.4	24.4	4.03	11.49	0.189	0.015	0.000	0.561	0.997
23.2	29.2	----	70.6	92.6	24.5	3.97	11.67	0.189	0.015	0.000	0.555	0.997
23.2	29.4	----	70.7	93.4	24.7	3.92	11.65	0.189	0.015	0.000	0.555	0.997
23.3	29.3	----	69.8	93.2	24.7	3.97	11.59	0.189	0.018	0.000	0.555	0.997
23.5	29.3	----	70.8	92.9	25.0	4.06	11.53	0.187	0.018	0.000	0.555	1.000

date
14/11/88

24.8	32.5	----	80.4	108.1	26.3	3.44	12.48	0.177	0.021	0.000	0.568	1.010
25.6	30.6	----	77.8	99.1	27.0	3.89	12.00	0.183	0.020	0.000	0.568	1.010
25.5	30.9	----	75.1	96.6	26.9	4.40	12.11	0.189	0.015	0.000	0.568	1.010
25.0	31.0	----	73.8	96.4	26.3	4.33	12.25	0.189	0.014	0.000	0.568	1.010
24.4	30.7	----	73.6	96.0	25.7	4.26	12.19	0.189	0.017	0.000	0.568	1.010
24.1	30.9	----	73.9	96.3	25.7	4.19	12.20	0.189	0.018	0.000	0.568	1.010
24.5	31.4	----	75.2	97.4	26.0	4.16	12.34	0.188	0.019	0.000	0.568	1.010
25.4	31.8	----	76.7	98.5	26.9	4.22	12.52	0.189	0.018	0.000	0.568	1.010
26.7	32.7	----	79.0	99.4	28.1	4.34	12.85	0.186	0.018	0.000	0.568	1.010
23.6	29.8	----	68.4	89.7	25.2	4.08	11.77	0.183	0.018	0.000	0.568	1.010
21.3	27.9	----	66.4	87.8	22.8	3.80	11.11	0.180	0.018	0.000	0.568	0.990
19.7	26.3	----	63.2	85.0	21.3	3.63	10.62	0.180	0.018	0.000	0.561	1.000

Table A2.6 (continued) Raw experimental performance data for the operating characteristics of the ammonia-water absorption system at Cerro Prieto.

time	T1	T2	T3	T4	T5	T6	T7	T8	T9	T10	T11	T12
						date 15/11/88						
12:31:50	97.3	122.2	70.3	47.8	38.2	30.1	106.3	-1.7	-1.3	-0.3	21.0	-0.7
12:46:47	96.4	121.9	70.8	47.5	39.5	30.2	105.9	-0.8	-0.4	0.6	21.1	0.0
13:01:10	96.7	121.3	70.9	49.3	39.8	30.7	106.2	-0.3	-0.5	0.7	22.4	0.3
13:15:35	96.2	118.7	69.5	48.0	38.8	30.2	106.2	-0.5	-0.1	0.9	21.5	0.5
13:30:25	95.2	116.5	68.3	48.3	39.2	29.7	105.2	-0.5	-0.1	0.9	21.8	0.7
13:45:58	95.7	119.7	68.4	48.3	39.1	30.0	105.3	-0.4	-0.2	0.8	21.7	0.6
14:00:58	96.5	122.1	69.7	49.2	39.7	30.3	105.9	-0.6	0.0	1.0	23.3	0.4
14:15:49	96.6	120.6	69.3	48.5	40.1	30.4	105.9	-0.4	0.0	0.8	21.7	1.0
14:30:52	96.3	119.5	67.6	47.9	39.1	29.8	105.3	-1.2	-0.6	0.2	21.1	1.0
14:45:59	95.1	119.5	67.2	48.3	38.7	28.9	105.0	-1.2	-0.8	0.2	22.1	0.2
15:00:31	94.8	118.6	66.7	47.7	38.1	28.7	104.6	-1.4	-1.0	0.0	21.3	0.2
15:15:30	96.4	121.9	68.0	46.9	38.3	29.1	106.3	-1.8	-1.6	-0.6	22.3	-0.4
15:30:20	96.4	122.4	69.4	48.2	39.4	29.2	105.8	-1.1	-1.1	-0.1	23.8	-0.3
						date 16/11/88						
12:45:25	90.0	117.6	59.2	42.8	34.2	23.8	100.3	-5.8	-5.0	-2.3	20.7	1.3
13:00:10	89.8	118.3	61.8	43.4	34.4	24.7	100.6	-4.3	-4.3	-2.5	20.8	-3.9
13:15:34	90.4	115.5	61.8	44.5	34.7	25.5	101.1	-4.1	-3.5	-2.3	21.2	-2.7
13:30:53	89.6	114.7	60.4	43.9	34.3	25.4	100.0	-4.4	-3.8	-2.8	21.1	-3.0
13:48:48	89.9	113.1	60.6	44.2	35.4	26.1	99.8	-4.4	-4.2	-2.6	21.3	0.6
14:01:42	89.7	114.9	60.6	44.2	35.2	26.0	100.0	-4.0	-4.0	-2.6	21.3	-2.8
14:15:30	90.7	114.0	59.3	43.5	34.8	26.2	100.7	-3.8	-4.0	-2.8	21.5	0.0
14:31:31	91.2	115.4	61.7	44.2	35.6	26.3	101.0	-3.6	-3.6	-2.4	22.2	-2.0
14:45:47	91.8	115.7	62.2	45.2	36.6	27.0	101.8	-3.2	-2.8	-2.0	22.5	-1.4
15:00:16	91.7	110.9	60.7	43.9	36.5	27.4	101.1	-3.1	-2.7	-1.7	22.8	-0.5
15:15:44	91.0	106.2	61.1	45.1	37.3	27.4	100.2	-2.5	-2.5	-1.5	22.4	0.5
15:30:17	91.4	106.4	60.8	46.5	37.9	27.9	100.5	-2.2	-1.8	-1.1	22.2	2.9
						date 17/11/88						
10:01:04	85.8	104.4	53.2	42.3	33.9	23.1	96.1	-6.3	-2.2	-2.2	17.2	12.4
10:33:43	85.9	103.4	56.0	42.2	34.0	24.9	95.8	-5.1	-4.5	-3.5	17.3	-2.3
10:46:07	85.4	103.1	55.5	42.1	34.0	24.8	95.5	-5.2	-4.8	-3.6	18.0	-3.0
11:00:10	85.7	103.2	55.2	42.2	33.6	24.7	95.8	-5.3	-4.9	-3.7	18.7	-2.7
11:16:34	84.9	103.1	54.3	41.6	33.3	24.4	95.1	-6.2	-5.4	-4.4	18.8	-4.2
11:30:10	85.9	103.6	55.0	40.7	33.0	23.9	96.0	-6.4	-6.0	-4.9	19.3	-4.7
11:45:26	86.4	103.6	55.9	41.9	33.5	24.6	96.2	-6.4	-6.0	-5.0	20.1	-4.4
12:00:17	85.8	103.1	57.0	41.8	33.9	25.0	95.5	-5.7	-5.7	-4.5	21.3	-4.0
12:15:16	85.7	103.0	56.1	41.6	34.1	25.1	95.4	-5.3	-5.1	-4.1	21.2	-2.7
12:30:23	86.3	103.1	56.2	43.0	34.8	25.3	96.0	-5.0	-4.6	-3.8	21.8	-1.5
12:45:44	86.6	103.4	56.9	43.0	34.5	25.5	96.3	-4.5	-4.3	-3.5	21.8	-1.1
13:00:19	86.0	102.4	56.3	43.1	35.4	25.8	95.5	-4.6	-4.2	-3.2	22.1	0.2
13:16:05	84.9	102.2	53.8	41.9	34.5	25.0	94.4	-5.2	-4.6	-3.4	22.1	0.8
13:30:19	85.8	102.9	54.0	42.1	33.7	---	95.1	-5.6	-4.8	-4.0	22.5	0.8
13:45:12	85.1	102.3	54.0	41.9	33.9	24.4	94.9	-5.8	-5.4	-4.2	22.5	0.4
14:00:18	83.9	102.4	52.1	41.0	32.5	23.6	94.2	-6.4	-5.8	-4.8	22.9	-0.8

Table A2.6 (continued) Raw experimental performance data for the operating characteristics of the ammonia-water absorption system at Cerro Prieto.

date
15/11/88

T13	T14	T15	T16	T17	T18	T19	T20	T21	T22	T23	T24	T25
48.7	68.6	92.8	24.9	27.8	73.5	73.7	38.3	4.1	30.8	-0.5	-1.2	25.5
49.0	67.8	92.3	25.4	28.5	72.5	72.9	38.9	19.2	31.8	0.8	-0.2	26.0
49.5	68.7	92.8	25.7	29.0	73.2	73.8	39.3	27.0	32.0	0.8	-0.4	26.4
49.5	69.5	92.3	25.5	28.6	73.4	74.2	39.5	28.7	31.4	1.0	0.0	26.2
49.7	68.8	91.3	25.1	28.4	72.4	73.4	39.4	29.5	31.1	1.3	0.3	25.7
49.6	68.9	91.6	25.4	28.5	73.1	73.6	39.2	19.7	31.2	0.7	-0.1	25.9
50.2	69.2	92.4	26.2	29.3	73.7	73.9	39.4	30.4	31.4	1.5	0.4	26.7
50.6	69.9	92.4	26.4	29.5	74.4	74.6	40.0	16.4	31.7	1.1	0.3	27.1
50.2	70.1	91.8	25.4	28.5	74.4	74.6	39.6	1.3	30.9	-0.1	-0.5	26.1
49.8	69.5	91.4	24.8	28.1	73.3	73.8	39.2	2.5	30.2	0.1	-0.7	25.5
49.0	68.9	90.9	24.0	27.5	72.9	73.5	38.8	0.7	29.8	-0.1	-0.9	24.7
50.4	70.6	92.2	24.4	27.7	74.2	75.0	38.4	-0.3	30.2	-1.1	-1.5	24.9
50.7	70.4	92.5	25.5	28.4	74.3	74.7	39.1	27.5	30.6	-0.2	-0.8	26.2

date
16/11/88

41.9	61.1	85.4	18.7	22.0	65.3	65.7	33.7	-3.2	24.0	-0.3	-4.6	19.3
42.6	61.5	85.2	19.5	22.8	65.3	65.8	34.0	17.5	25.9	-3.1	-4.1	20.1
43.7	63.0	85.7	20.4	23.5	66.5	67.1	34.3	8.7	26.4	-2.1	-3.5	21.2
43.9	62.5	84.9	20.6	23.7	66.3	66.7	34.5	-2.2	26.2	-3.0	-3.6	21.3
43.8	62.7	85.1	21.5	24.4	66.7	67.4	35.0	0.1	27.3	-2.6	-4.0	22.1
44.1	62.7	85.3	21.5	24.4	66.7	67.2	35.0	18.2	27.3	-2.6	-4.0	22.0
45.0	64.6	86.0	21.5	24.4	68.0	68.6	35.4	-1.9	26.9	-3.1	-3.8	22.0
45.7	64.9	86.3	22.6	----	68.7	69.3	35.6	24.5	27.4	-2.6	-3.5	23.1
47.0	65.9	87.7	23.1	26.2	69.5	70.1	36.3	1.1	27.8	-1.7	-2.7	23.7
47.6	66.9	87.4	23.9	26.8	70.3	70.9	36.9	-2.3	28.0	-2.3	-2.7	24.5
47.0	66.0	86.7	24.5	27.4	69.8	70.2	37.5	25.9	28.4	-1.5	-2.3	25.1
48.0	67.2	87.5	25.0	27.7	70.6	71.0	37.7	-0.4	28.7	-0.8	-1.4	25.6

date
17/11/88

41.4	58.4	81.9	----	22.5	62.0	62.5	32.6	11.7	23.0	8.9	2.6	20.0
43.4	60.0	82.2	21.8	24.5	63.6	63.7	34.1	24.6	25.6	-3.2	-4.2	22.3
43.1	59.6	81.7	21.5	24.4	62.9	63.2	34.2	24.5	25.7	-3.5	-4.7	22.2
43.4	60.1	82.2	21.2	24.1	63.5	63.9	34.1	-1.8	25.4	-3.8	-4.6	21.7
42.1	58.7	81.3	20.3	23.2	62.1	62.7	33.5	-4.3	25.0	-4.7	-5.3	21.0
43.2	60.0	82.2	20.5	23.2	63.8	64.1	33.4	-5.4	24.5	-5.6	-5.8	21.0
43.7	60.8	82.6	21.1	23.8	64.6	64.8	33.6	-5.4	25.3	-5.6	-6.0	21.8
43.7	59.9	81.9	21.9	24.6	63.7	63.9	34.0	4.5	25.7	-4.8	-5.4	22.5
43.9	60.1	81.8	22.2	24.9	63.9	64.1	34.5	14.1	26.0	-4.2	-4.7	22.9
44.2	60.9	82.8	22.4	25.1	64.7	65.1	34.8	-3.1	26.1	-3.7	-4.3	23.0
45.1	61.4	82.7	22.9	25.5	65.2	65.4	34.9	12.8	26.2	-3.3	-3.9	23.5
44.6	61.0	82.3	23.3	26.0	64.8	65.2	35.2	24.8	26.6	-2.8	-3.8	23.8
43.3	59.7	81.3	21.9	24.6	63.8	63.8	35.0	7.3	25.8	-3.2	-4.2	22.7
43.7	61.0	81.5	21.5	24.2	64.6	64.8	34.5	-3.2	25.6	-4.0	-4.5	22.1
43.1	59.8	81.3	21.3	24.0	64.0	64.2	34.3	-2.6	25.4	-4.0	-5.2	21.9
42.1	59.1	80.2	20.1	22.9	62.7	62.9	33.5	-4.3	24.3	-4.9	-5.5	20.8

Table A2.6 (continued) Raw experimental performance data for the operating characteristics of the ammonia-water absorption system at Cerro Prieto.

date
15/11/88

T26	T27	T28	T29	T30	T31	PEV	PCO	FSOL	FREF	FWRE	FWCO	FWAB
25.2	30.4	----	70.4	92.7	26.3	3.97	11.93	0.186	0.019	0.000	0.568	1.010
25.6	30.4	----	71.0	92.5	26.7	4.11	11.96	0.189	0.014	0.000	0.568	1.010
26.0	30.8	----	71.4	92.6	27.2	4.15	12.06	0.189	0.015	0.000	0.568	1.010
25.8	30.6	----	69.3	92.0	26.9	4.20	11.93	0.188	0.015	0.000	0.568	1.010
25.3	30.1	----	69.0	90.8	26.4	4.19	11.80	0.189	0.015	0.000	0.568	1.010
25.5	30.2	----	68.5	91.6	26.7	4.16	11.87	0.189	0.014	0.000	0.568	1.010
26.3	30.6	----	70.4	92.9	27.5	4.20	11.94	0.189	0.015	0.000	0.568	1.010
26.5	30.8	----	70.6	92.7	27.7	4.20	12.01	0.189	0.015	0.000	0.568	1.010
25.5	30.0	----	69.4	92.3	26.7	4.08	11.82	0.189	0.013	0.000	0.568	1.010
24.9	29.2	----	68.5	91.0	26.1	4.07	11.53	0.189	0.013	0.000	0.568	1.010
24.4	29.0	----	67.9	90.6	25.3	4.06	11.35	0.189	0.013	0.000	0.568	1.010
24.5	29.2	----	68.5	92.1	25.7	3.95	11.66	0.189	0.013	0.000	0.568	1.010
25.6	29.5	----	70.3	92.6	26.8	4.10	11.70	0.189	0.014	0.000	0.568	1.010

date
16/11/88

18.9	24.6	----	56.2	85.0	20.1	3.36	10.10	0.189	0.016	0.000	0.568	1.010
19.7	24.7	----	60.0	84.8	20.9	3.58	10.25	0.189	0.017	0.000	0.568	1.010
20.6	25.5	----	60.7	84.2	21.8	3.65	10.43	0.189	0.016	0.000	0.568	1.010
20.8	25.4	----	62.0	84.9	21.9	3.62	10.34	0.189	0.016	0.000	0.568	1.010
21.7	26.1	----	61.7	84.3	22.6	3.61	10.59	0.189	0.009	0.000	0.568	1.010
21.7	26.1	----	61.5	84.7	22.8	3.66	10.57	0.189	0.013	0.000	0.568	1.010
21.6	26.1	----	60.9	85.6	22.8	3.64	10.57	0.189	0.011	0.000	0.568	1.010
22.7	26.6	----	62.0	86.0	23.7	3.74	10.71	0.189	0.012	0.000	0.568	1.010
23.2	27.2	----	63.2	87.2	24.1	3.80	10.88	0.189	0.013	0.000	0.568	1.010
24.2	27.6	----	63.4	87.1	24.9	3.80	11.06	0.126	0.009	0.000	0.568	1.010
24.7	27.6	----	64.0	87.1	25.5	3.88	11.01	0.189	0.011	0.000	0.568	1.010
25.0	28.1	----	63.9	87.5	26.0	3.95	11.25	0.189	0.009	0.000	0.568	1.010

date
17/11/88

19.8	23.9	----	51.6	81.6	20.6	3.36	9.98	0.189	0.011	0.000	0.568	1.010
22.1	25.2	----	58.2	81.7	22.9	3.55	10.21	0.189	0.013	0.000	0.568	1.010
21.8	25.1	----	58.1	81.6	22.6	3.52	10.24	0.189	0.011	0.000	0.568	1.010
21.3	24.8	----	58.3	82.1	22.3	3.49	10.10	0.189	0.011	0.000	0.568	1.010
20.6	24.5	----	57.2	81.0	21.6	3.39	10.00	0.189	0.010	0.000	0.568	1.010
20.6	24.3	----	57.5	82.2	21.6	3.33	9.97	0.189	0.010	0.000	0.568	1.010
21.5	24.8	----	58.5	83.0	22.2	3.38	10.14	0.189	0.010	0.000	0.568	1.010
22.1	25.2	----	58.9	82.4	22.8	3.41	10.23	0.189	0.009	0.000	0.568	1.010
22.5	25.4	----	59.1	81.9	23.3	3.52	10.30	0.189	0.009	0.000	0.568	1.010
22.6	25.5	----	59.4	82.2	23.6	3.52	10.39	0.189	0.009	0.000	0.568	1.010
23.1	25.6	----	59.9	83.5	23.9	3.61	10.34	0.189	0.009	0.000	0.568	1.010
23.5	26.0	----	57.6	81.7	24.2	3.58	10.44	0.189	0.009	0.000	0.568	1.010
22.3	25.2	----	55.5	80.0	23.1	3.52	10.22	0.189	0.008	0.000	0.568	1.010
21.7	24.8	----	55.1	81.2	22.7	3.45	10.17	0.189	0.009	0.000	0.568	1.010
21.5	24.6	----	54.9	80.4	22.3	3.42	10.12	0.189	0.009	0.000	0.568	1.010
20.4	23.7	----	54.2	79.5	21.1	3.36	9.80	0.189	0.009	0.000	0.568	1.010

Table A2.6 (continued) Raw experimental performance data for the operating characteristics of the ammonia-water absorption system at Cerro Prieto.

date
18/11/88

time	T1	T2	T3	T4	T5	T6	T7	T8	T9	T10	T11	T12
10:15:24	79.4	101.2	41.9	35.6	29.8	15.4	90.6	-14.2	-7.4	-8.2	15.4	9.6
10:30:13	80.3	101.5	42.6	35.5	29.5	15.1	91.1	-15.1	-11.3	-11.3	16.1	8.3
10:45:32	79.5	100.9	41.6	34.1	29.3	15.3	90.3	-15.3	-14.9	-12.9	16.5	-7.5
11:00:29	78.5	101.1	42.4	33.9	27.9	15.5	89.8	-15.5	-15.1	-13.5	16.7	-13.9
11:16:12	78.1	101.0	42.3	33.7	27.7	16.0	89.7	-15.4	-15.0	-13.4	17.0	-13.8
11:31:22	77.6	101.5	41.2	32.8	27.7	16.5	89.8	-15.1	-14.9	-13.5	17.5	-13.7
11:45:21	77.5	101.7	41.1	33.0	28.0	16.7	89.2	-14.7	-14.5	-13.3	17.3	-13.5
12:00:14	78.2	102.1	42.8	33.0	28.0	17.5	90.4	-14.0	-14.0	-12.8	17.7	-13.0
12:15:54	76.2	101.6	40.9	32.9	27.8	17.8	89.7	-14.2	-14.0	-12.8	18.0	-12.6
12:30:23	77.6	102.0	41.4	32.5	27.3	17.6	89.9	-14.1	-14.1	-12.7	18.0	-13.1
12:45:38	77.1	101.7	41.6	32.6	27.4	18.1	90.0	-13.6	-13.8	-12.4	17.5	-12.8
13:00:40	77.4	102.2	42.3	31.9	27.1	18.2	90.1	-13.6	-13.4	-12.2	17.8	-12.2
13:16:10	78.4	101.9	43.4	33.6	26.4	18.9	90.9	-13.1	-13.1	-11.9	18.1	-10.3
13:30:24	74.9	101.1	40.6	33.1	26.0	18.0	88.6	-12.3	-12.3	-11.1	18.2	-11.7
13:45:42	78.3	101.7	41.3	34.4	25.9	19.1	90.8	-12.6	-12.6	-11.4	17.7	-9.0
14:00:15	77.8	101.5	42.2	34.5	26.0	18.2	90.5	-12.9	-12.5	-11.5	18.6	-10.3

date
21/11/88

11:15:50	108.8	132.6	86.2	44.4	33.9	28.1	116.7	-5.2	-5.4	-4.4	18.4	-4.8
11:30:26	109.7	133.3	82.2	44.3	35.1	28.8	116.5	-5.5	-5.5	-4.1	18.7	-5.5
11:45:09	102.7	132.3	81.7	42.5	35.2	28.8	114.5	-4.0	-4.2	-3.2	19.0	-3.8
12:00:42	104.6	133.8	84.0	41.8	35.2	28.9	116.0	-4.0	-4.2	-3.4	20.0	-3.8
12:16:10	104.0	132.5	84.3	42.0	34.5	28.3	115.3	-3.8	-4.0	-3.2	20.0	-3.2
12:31:07	105.3	132.3	84.3	42.3	32.5	28.1	115.8	-4.4	-4.2	-3.4	20.5	-3.6
12:46:08	109.8	133.6	81.3	45.6	35.8	29.1	116.0	-4.8	-4.8	-3.2	20.5	-4.6
13:00:23	104.7	133.0	82.2	43.8	35.6	28.8	114.8	-3.8	-3.8	-2.9	20.3	-3.4
13:15:24	105.2	133.6	83.8	44.1	34.9	28.2	115.7	-3.3	-3.3	-2.7	20.4	-2.9
13:30:31	106.2	132.8	83.7	42.7	33.8	28.2	115.6	-4.0	-3.6	-2.8	20.9	-3.0
13:45:30	109.8	133.4	84.0	46.0	36.0	28.9	117.1	-4.6	-4.4	-3.0	20.7	-4.0
14:00:15	104.3	133.1	82.9	44.3	37.0	29.1	114.4	-2.9	-2.9	-2.0	21.4	-2.5
14:16:06	105.2	133.6	83.6	44.3	35.9	28.7	115.7	-3.1	-3.1	-2.3	21.8	-2.5

date
22/11/88

11:01:38	94.3	114.6	66.2	32.8	28.8	21.4	99.3	-9.2	-9.0	-7.5	16.7	-9.0
11:15:22	96.0	116.3	68.7	30.9	28.2	23.8	100.3	-7.6	-7.6	-6.4	17.5	-7.6
11:30:17	98.2	114.1	70.6	35.2	30.0	24.9	100.8	-6.6	-6.6	-5.4	18.0	-6.6
11:45:39	97.1	104.9	69.6	33.2	30.5	24.9	99.9	-6.2	-6.2	-5.0	18.5	-6.2
12:00:37	97.4	105.4	69.2	33.2	30.5	25.8	100.2	-5.7	-5.7	-4.7	19.2	-5.5
12:15:19	98.4	105.7	70.4	34.2	31.0	26.5	100.3	-5.0	-5.0	-4.0	19.7	-5.0
12:30:11	99.6	106.1	71.1	30.9	30.9	26.8	101.3	-4.7	-4.5	-3.7	20.2	-4.7
12:47:06	97.7	104.8	70.3	34.5	31.4	27.3	100.1	-4.4	-4.4	-3.4	20.7	-4.4
13:02:00	98.0	105.0	70.3	33.9	30.6	27.9	100.4	-4.1	-4.1	-3.3	21.2	-4.1
13:15:13	98.9	105.3	69.7	32.2	31.4	28.3	100.3	-4.2	-4.2	-3.2	21.3	-4.2
13:30:16	98.9	105.4	70.7	33.7	31.8	28.7	100.7	-3.9	-3.9	-2.9	21.7	-3.9
13:45:26	97.8	105.0	70.3	36.6	32.4	29.7	100.0	-3.6	-3.6	-2.6	22.3	-3.6
14:00:14	97.3	104.7	70.2	33.8	31.9	30.4	99.7	-2.8	-2.8	-2.0	22.4	-3.0
14:15:44	97.8	104.9	69.6	37.3	32.5	30.7	99.9	-2.7	-2.7	-1.7	22.6	-2.7
14:30:35	96.9	104.6	69.7	34.5	31.4	30.9	99.8	-2.3	-2.3	-1.3	22.5	-2.3

Table A2.6 (continued) Raw experimental performance data for the operating characteristics of the ammonia-water absorption system at Cerro Prieto.

date
18/11/88

T13	T14	T15	T16	T17	T18	T19	T20	T21	T22	T23	T24	T25
34.8	51.8	76.0	13.5	16.2	53.7	54.3	29.6	-11.8	15.6	1.5	-1.5	14.2
35.1	52.3	77.1	13.8	16.3	54.4	55.0	29.6	-13.4	15.4	-1.6	-7.0	14.3
35.0	52.1	76.7	13.9	16.3	54.2	54.7	29.5	-14.3	15.7	-11.5	-14.7	14.3
34.7	51.3	75.7	13.7	16.3	53.2	53.6	28.7	-14.6	15.9	-14.6	-15.0	14.3
34.4	50.7	75.3	13.9	16.4	52.6	53.0	28.2	-181.5	16.1	-14.7	-14.9	14.4
34.1	50.4	75.0	13.9	16.3	51.9	52.7	27.8	11.3	16.8	-14.4	-14.8	14.6
34.0	50.2	74.3	13.8	16.1	52.0	52.3	27.9	-13.8	17.0	-14.0	-14.2	14.3
34.2	50.5	74.7	13.8	16.2	52.4	52.6	28,1	-13.4	17.8	-13.8	-14.0	14.3
34.0	49.9	73.8	13.7	16.2	51.4	52.0	27.7	-13.5	17.8	-13.5	-13.9	14.5
33.9	49.8	74.0	13.7	16.1	51.5	51.9	27.6	-13.4	18.1	-13.6	-13.8	14.4
33.8	49.7	73.7	13.8	16.3	51.2	51.8	27.5	-12.9	18.4	-13.5	-13.7	14.5
33.9	49.8	73.8	13.7	16.2	51.5	52.0	27.4	-12.9	18.7	-13.1	-13.3	14.4
34.5	50.8	74.8	14.0	16.7	52.9	53.7	27.3	-12.6	19.4	-12.8	-13.0	14.9
33.5	49.0	72.3	14.1	16.8	50.5	51.3	26.3	-11.8	18.5	-11.8	-12.0	14.8
34.4	50.5	74.5	14.0	16.6	53.3	53.9	26.2	-12.1	19.6	-12.3	-12.5	14.7
34.7	51.0	74.1	14.2	16.9	53.8	54.2	26.3	-12.2	18.5	-12.2	-12.2	14.8

date
21/11/88

37.1	64.2	103.4	17.0	19.9	78.3	79.1	34.2	10.2	30.4	-4.0	-5.2	18.2
36.5	62.2	102.8	17.7	20.4	76.6	77.9	33.9	-1.6	30.6	-4.2	-5.5	18.8
37.1	60.2	98.8	18.2	21.1	69.5	70.2	33.3	-1.6	31.0	-3.1	-4.1	19.2
37.7	62.9	100.5	18.6	21.3	73.5	73.6	34.1	5.0	31.2	-2.9	-3.9	19.6
38.9	64.6	100.0	18.8	21.3	75.2	75.2	34.3	20.0	30.7	-2.5	-3.5	19.8
38.7	68.8	101.3	19.0	21.7	79.3	79.5	34.7	18.8	30.3	-2.7	-3.9	20.0
38.7	65.2	103.1	19.0	21.9	78.5	79.8	35.1	-0.2	30.8	-3.2	-4.7	20.0
39.8	65.7	100.1	19.1	21.8	76.4	77.1	35.2	3.3	30.9	-2.0	-3.8	20.1
40.7	67.7	100.8	19.4	22.0	78.4	78.6	35.3	25.8	30.5	-2.1	-3.1	20.4
39.8	71.0	101.6	19.7	22.4	80.7	81.3	35.7	24.5	30.2	-2.5	-3.5	20.7
40.0	72.3	103.9	19.8	22.5	83.6	84.7	35.6	4.5	30.8	-2.6	-4.4	20.7
40.6	65.6	100.2	19.8	22.7	75.6	76.1	35.6	1.5	31.4	-1.4	-2.8	20.7
42.0	69.0	101.1	20.0	22.7	79.0	79.7	35.6	2.6	31.0	-2.0	-3.0	20.9

date
22/11/88

24.5	46.6	90.8	17.7	19.1	57.5	57.7	30.9	-7.6	21.2	-8.4	-9.0	18.5
25.3	47.4	90.6	18.7	19.9	59.4	59.4	30.1	-6.3	23.3	-7.3	-7.5	19.5
26.3	49.0	91.7	19.7	20.9	62.6	63.4	29.9	-4.7	24.7	-5.9	-6.5	20.4
27.3	49.9	93.2	----	21.6	64.3	64.9	30.5	-4.7	24.9	-5.7	-6.1	21.2
27.4	50.2	92.4	----	22.2	64.3	64.5	31.0	-4.2	25.5	-5.2	-5.6	21.7
27.9	50.5	91.9	21.1	22.4	64.9	65.3	31.2	-3.3	26.2	-4.5	-4.9	22.0
28.2	51.4	92.2	21.6	22.7	66.5	66.9	31.3	-3.2	26.7	-4.2	-4.4	22.2
28.7	51.7	93.1	21.9	23.1	66.1	66.3	32.0	-2.7	27.2	-3.9	-4.3	22.7
28.7	51.5	93.1	21.9	23.1	66.5	66.3	32.2	-3.1	27.8	-3.9	-4.1	22.8
28.7	51.9	92.9	22.1	----	66.7	67.1	32.2	-2.7	28.2	-3.7	-3.9	22.7
29.1	52.1	93.3	22.3	----	66.9	67.1	32.4	-2.5	28.5	-3.5	-3.7	23.1
29.3	51.9	93.3	22.5	23.9	65.7	66.3	32.8	-1.8	29.3	-3.2	-3.3	23.3
29.0	51.5	92.1	22.4	23.6	65.9	65.9	32.5	-1.2	30.2	-2.4	-2.6	23.2
29.0	51.4	92.5	22.4	23.8	65.8	66.4	32.6	-0.7	30.5	-2.3	-2.7	23.2
29.1	51.4	92.2	22.7	23.9	65.8	65.6	32.6	-1.0	30.9	-1.9	-2.1	23.5

Table A2.6 (continued) Raw experimental performance data for the operating characteristics of the ammonia-water absorption system at Cerro Prieto.

date
18/11/88

T26	T27	T28	T29	T30	T31	PEV	PCO	FSOL	FREF	FWRE	FWCO	FWAB
13.7	18.1	----	41.1	73.6	14.8	2.36	8.28	0.189	0.010	0.000	0.568	1.010
13.9	18.0	----	42.3	74.7	14.9	2.28	8.30	0.189	0.010	0.000	0.568	1.010
14.0	17.7	----	43.5	74.4	14.9	2.27	8.15	0.189	0.011	0.000	0.568	1.010
13.9	17.6	----	43.1	73.8	14.9	2.27	8.20	0.189	0.011	0.000	0.568	1.020
14.0	17.9	----	43.2	73.2	15.0	2.30	8.22	0.189	0.011	0.000	0.568	1.010
14.0	18.1	----	40.3	70.7	15.2	2.31	8.32	0.189	0.011	0.000	0.568	1.020
13.9	18.0	----	40.6	72.1	15.0	2.35	8.28	0.189	0.012	0.000	0.568	1.020
13.9	18.6	----	40.8	72.3	15.1	2.42	8.44	0.189	0.011	0.000	0.568	1.020
13.9	18.6	----	39.7	69.1	15.1	2.40	8.36	0.189	0.011	0.000	0.568	1.010
14.0	18.5	----	40.3	70.7	15.2	2.40	8.41	0.189	0.011	0.000	0.568	1.020
13.9	18.8	----	40.0	69.7	15.3	2.44	8.47	0.189	0.012	0.000	0.568	1.010
14.0	18.9	----	40.5	70.3	15.2	2.49	8.46	0.189	0.012	0.000	0.568	1.020
14.3	19.2	----	40.6	70.4	15.7	2.55	8.62	0.189	0.012	0.000	0.568	1.020
14.4	18.1	----	40.5	68.7	15.6	2.64	8.21	0.189	0.011	0.000	0.568	1.020
14.2	18.8	----	40.5	71.1	15.3	2.60	8.46	0.189	0.010	0.000	0.568	1.020
14.5	18.4	----	41.9	72.7	15.4	2.57	8.44	0.189	0.010	0.000	0.568	1.020

date
21/11/88

17.2	28.2	----	77.3	101.8	19.5	3.35	11.20	0.126	0.029	0.000	0.568	1.010
18.0	28.5	----	76.7	99.8	20.2	3.28	11.42	0.189	0.025	0.000	0.568	1.010
18.4	28.3	----	77.1	96.7	20.6	3.49	11.50	0.126	0.022	0.000	0.568	1.010
18.8	28.7	----	77.4	99.3	21.0	3.50	11.49	0.126	0.023	0.000	0.568	1.010
19.0	28.3	----	78.2	98.9	21.2	3.54	11.27	0.126	0.024	0.000	0.568	1.010
19.2	28.5	----	75.6	100.6	21.2	3.52	11.20	0.126	0.026	0.000	0.568	1.010
19.2	28.9	----	75.5	100.5	21.3	3.40	11.47	0.126	0.025	0.000	0.568	1.010
19.3	28.6	----	75.8	99.0	21.3	3.59	11.47	0.126	0.023	0.000	0.568	1.010
19.6	28.4	----	77.7	100.0	21.6	3.61	11.13	0.126	0.025	0.000	0.568	1.010
19.9	28.6	----	75.8	101.2	21.6	3.61	11.16	0.126	0.025	0.000	0.568	1.010
19.9	29.2	----	78.1	103.3	21.9	3.45	11.39	0.126	0.025	0.000	0.568	1.010
20.1	29.0	----	77.2	98.8	22.1	3.67	11.63	0.126	0.020	0.000	0.568	1.010
20.2	28.7	----	76.3	99.6	22.1	3.64	11.43	0.126	0.023	0.000	0.568	1.010

date
22/11/88

17.9	25.1	----	65.3	89.8	19.5	2.90	10.34	0.063	0.019	0.000	0.568	1.010
18.9	26.8	----	65.6	91.9	20.6	3.10	10.97	0.063	0.020	0.000	0.568	1.010
19.9	28.2	----	67.5	93.9	21.6	3.23	11.36	0.063	0.019	0.000	0.568	1.010
20.6	28.3	----	67.8	92.6	22.1	3.30	11.44	0.063	0.019	0.000	0.568	1.010
21.1	28.8	----	66.6	92.5	22.6	3.40	11.60	0.063	0.020	0.000	0.568	1.010
21.4	29.1	----	67.3	93.1	22.9	3.45	11.66	0.063	0.020	0.000	0.568	1.010
21.7	29.6	----	68.1	94.5	23.2	3.52	11.88	0.063	0.020	0.000	0.568	1.010
22.2	29.7	----	68.2	93.5	23.7	3.54	11.91	0.063	0.019	0.000	0.568	1.010
22.2	29.7	----	67.9	93.4	23.7	3.60	11.90	0.063	0.018	0.000	0.568	1.010
22.3	29.7	----	67.7	93.7	23.7	3.60	11.90	0.063	0.018	0.000	0.568	1.010
22.5	30.1	----	68.6	94.3	24.1	3.61	12.03	0.063	0.018	0.000	0.568	1.010
22.7	30.3	----	68.4	93.3	24.3	3.69	12.02	0.063	0.020	0.000	0.568	1.010
22.6	30.4	----	67.6	92.7	24.2	3.77	12.21	0.063	0.020	0.000	0.568	1.010
22.6	30.5	----	67.2	92.6	24.1	3.82	12.11	0.063	0.020	0.000	0.568	1.010
22.9	30.7	----	67.3	92.8	24.5	3.89	12.22	0.063	0.020	0.000	0.568	1.010

Table A2.6 (continued) Raw experimental performance data for the operating characteristics of the ammonia-water absorption system at Cerro Prieto.

time	T1	T2	T3	T4	T5	T6	T7	T8	T9	T10	T11	T12
						date 23/11/88						
11:14:56	104.1	122.9	79.3	35.3	33.0	30.7	106.1	-0.3	-0.3	0.7	20.4	-0.1
11:30:26	103.1	122.3	78.9	37.6	33.7	30.8	105.2	0.0	0.0	1.0	21.7	0.2
11:45:14	103.3	122.6	78.3	37.7	33.7	30.8	105.3	-0.1	0.1	1.1	22.6	0.1
12:00:12	103.9	122.3	79.0	40.3	34.0	30.9	105.4	-0.1	0.1	1.1	23.0	0.1
12:16:48	103.2	122.7	79.0	37.1	34.0	31.1	105.4	0.3	0.3	1.3	23.7	0.5
12:31:04	103.6	122.4	78.5	39.6	33.7	30.8	105.7	0.0	0.2	1.1	23.8	0.2
12:45:21	103.2	121.0	78.0	36.8	33.2	30.1	105.2	-0.4	-0.4	0.8	23.3	-0.2
13:00:13	104.9	121.8	78.0	38.0	33.0	29.9	106.0	-1.1	-0.9	0.3	23.9	-0.9
13:16:02	104.7	122.2	79.0	38.8	32.8	29.9	106.0	-1.7	-1.5	-0.1	24.7	-1.5
13:30:29	103.5	121.9	78.9	36.4	32.6	29.7	105.7	-2.0	-2.0	-0.8	24.7	-1.8
13:45:23	103.3	121.9	78.0	36.6	32.7	29.6	105.3	-2.2	-2.2	-0.8	25.2	-2.0
14:00:28	102.5	121.9	77.2	34.0	32.1	29.8	105.1	-1.8	-1.8	-0.6	25.9	-1.6
14:15:27	103.4	122.7	77.7	39.6	32.3	29.9	105.6	-1.9	-1.7	-0.5	26.1	-1.7
14:30:49	103.4	122.5	78.0	37.2	32.0	30.1	105.6	-1.5	-1.3	-0.3	26.0	-1.3
						date 24/11/88						
11:01:39	95.7	103.9	71.4	33.2	29.5	24.9	97.8	-1.7	-1.7	-0.6	14.9	-1.6
11:15:50	94.6	102.8	65.2	37.8	31.6	24.9	95.9	-2.9	-2.7	-1.2	14.6	-2.5
11:30:23	90.7	101.3	65.6	35.5	30.5	24.1	95.0	-4.7	-4.3	-3.1	14.8	-4.1
11:45:32	88.9	101.4	63.4	34.2	30.3	24.4	93.8	-5.6	-5.8	-4.2	14.8	-5.6
12:02:12	103.4	105.6	63.0	37.6	30.5	24.5	102.3	-7.7	-7.3	-5.7	15.2	-7.5
12:15:17	94.2	101.8	62.1	37.3	31.4	25.6	95.9	-7.8	-7.2	-5.8	15.1	-7.2
12:30:08	91.3	101.3	60.3	35.5	31.3	25.5	94.7	-7.5	-7.3	-6.1	15.4	-7.5
12:45:52	88.8	100.9	58.3	35.6	29.8	25.0	93.6	-7.6	-7.6	-6.4	14.9	-7.4
13:00:14	93.6	101.5	60.7	35.3	29.4	24.7	96.0	-9.0	-9.2	-7.6	15.0	-8.6
13:15:23	87.9	100.7	56.5	31.6	28.9	24.1	93.1	-9.1	-8.9	-7.7	15.3	-8.5
13:30:36	85.8	100.6	53.1	33.4	28.4	23.4	91.5	-8.8	-8.6	-7.6	15.0	-8.2
13:45:23	95.4	101.9	58.0	31.8	26.8	23.3	96.3	-9.3	-9.1	-7.9	16.3	-8.7
14:00:20	97.7	102.7	63.4	31.7	26.3	22.6	98.4	-10.4	-10.2	-9.0	16.6	-10.0
14:15:22	94.9	101.6	63.8	33.8	26.9	22.4	95.8	-12.0	-11.8	-10.2	16.4	-11.4
14:30:20	83.7	99.9	53.3	28.4	25.7	21.8	90.8	-12.2	-11.8	-10.8	16.7	-11.2
						date 25/11/88						
11:00:59	86.0	99.4	51.3	32.3	26.2	15.9	89.7	-15.1	-14.3	-12.5	14.9	-12.1
11:16:08	82.0	99.4	45.0	30.2	25.3	16.4	88.2	-15.6	-15.2	-13.4	16.6	-14.6
11:30:43	81.3	99.9	45.7	29.2	24.9	17.4	88.7	-15.4	-15.0	-13.6	17.8	-15.0
11:45:34	83.9	103.6	46.3	27.5	24.2	18.4	89.7	-14.6	-14.4	-13.2	17.6	-14.2
12:00:50	81.7	104.2	48.9	25.6	23.3	19.8	89.4	-12.7	-12.7	-11.9	17.8	-12.7
12:15:29	85.5	102.0	49.1	26.6	24.1	21.0	90.5	-11.7	-11.7	-10.7	18.6	-11.7
12:30:46	84.4	101.7	51.0	30.7	25.9	21.4	90.2	-11.2	-11.2	-10.1	18.9	-11.0
12:45:15	82.2	101.5	49.1	30.5	25.9	21.2	89.1	-10.4	-10.4	-9.4	19.1	-10.0
13:00:14	82.9	103.7	49.5	29.9	26.4	21.4	89.4	-9.7	-9.7	-8.7	20.0	-9.5
13:15:37	86.4	104.8	52.7	30.7	26.2	22.1	91.5	-9.5	-9.3	-8.3	20.4	-9.3
13:30:26	81.5	100.3	50.7	31.6	27.1	----	89.0	-8.9	-8.9	-8.0	20.0	-8.5
13:45:06	92.1	101.5	51.6	31.9	27.2	----	93.0	-10.0	-9.8	-8.4	21.0	-9.4
14:00:32	81.9	99.8	50.0	31.8	26.4	21.2	88.3	-10.3	-10.1	-8.9	21.0	-10.1
14:15:10	82.0	99.7	49.2	31.5	27.1	21.3	89.1	-11.0	-10.8	-9.6	21.6	-10.0
14:30:23	87.4	100.7	51.2	33.5	28.0	22.1	91.3	-11.5	-11.3	-9.9	21.6	-10.1

Table A2.6 (continued) Raw experimental performance data for the operating characteristics of the ammonia-water absorption system at Cerro Prieto.

date
23/11/88

T13	T14	T15	T16	T17	T18	T19	T20	T21	T22	T23	T24	T25
27.6	52.5	97.6	21.0	22.6	68.4	68.8	33.9	2.2	32.3	0.4	0.0	21.9
27.7	52.7	98.0	21.4	22.9	68.2	68.6	34.2	3.7	32.5	0.9	0.1	21.9
27.5	52.4	97.7	21.1	22.6	68.1	68.5	34.3	4.2	32.4	1.0	0.3	21.8
27.4	52.4	98.0	21.2	22.6	67.9	68.7	34.3	3.9	32.4	1.4	0.0	21.7
27.6	51.8	97.6	21.4	23.0	67.9	68.1	34.3	3.3	32.7	1.0	0.4	22.1
27.9	53.2	98.3	20.9	22.5	69.1	69.5	34.4	3.6	32.2	1.1	0.3	21.6
27.4	52.7	97.4	20.4	22.1	68.8	69.4	34.0	2.5	31.7	0.3	-0.3	20.9
26.8	52.3	97.6	20.0	21.8	69.4	70.0	33.6	1.5	31.3	-0.3	-0.9	20.7
26.6	51.6	98.4	20.0	21.6	68.5	69.0	33.2	1.7	31.5	-0.7	-1.5	20.7
27.2	52.7	98.5	20.0	21.7	69.2	69.4	33.2	0.7	31.3	-1.1	-1.9	20.6
27.1	51.9	97.7	20.2	21.9	67.8	68.4	33.3	0.6	31.2	-1.4	-2.0	20.6
27.1	51.5	97.7	20.3	21.9	67.2	67.6	33.5	0.6	31.4	-1.2	-1.6	20.9
26.9	51.0	97.7	20.1	21.8	67.5	67.9	33.3	1.3	31.5	-0.9	-1.6	20.7
26.6	50.8	98.0	20.2	22.0	67.5	67.9	33.0	0.9	31.7	-0.9	-1.3	20.8

date
24/11/88

23.9	49.5	83.6	17.3	18.6	62.4	62.2	29.7	3.4	26.5	-0.7	-1.7	17.7
23.9	49.3	86.1	17.7	19.2	63.3	63.9	30.7	3.0	26.1	-1.1	-2.7	17.9
24.5	50.8	87.9	17.9	19.5	64.5	63.5	30.9	24.0	25.3	-2.5	-4.2	18.1
25.3	49.0	86.3	18.3	19.7	60.7	60.9	31.0	18.8	25.6	-4.2	-5.8	18.8
26.8	56.5	88.9	19.5	----	73.4	73.2	31.3	-3.5	25.3	-6.5	-7.3	20.0
26.9	51.3	88.6	20.1	21.5	64.6	65.9	31.3	0.7	26.5	-5.6	-7.0	20.7
27.0	49.7	87.6	20.2	21.6	61.5	62.4	31.4	10.8	26.4	-5.9	-7.1	20.8
26.2	49.0	86.4	19.6	20.9	59.5	60.4	31.0	-3.0	25.7	-6.8	-7.6	20.3
26.3	51.0	88.3	19.1	20.5	63.7	64.9	30.3	-7.5	25.6	-8.5	-9.1	19.6
25.2	47.7	85.7	18.6	20.0	58.2	58.9	30.0	-6.4	24.8	-8.0	-8.8	19.4
24.4	45.7	82.6	18.1	19.5	55.4	56.2	29.5	-5.1	24.1	-7.4	-8.6	18.9
23.7	49.1	84.0	17.1	18.3	62.6	64.1	28.4	-8.1	24.1	-8.9	-9.1	17.7
23.6	50.7	86.7	16.2	17.6	67.0	67.4	27.5	-9.1	22.5	-9.9	-10.3	17.1
24.0	50.9	88.4	16.4	17.7	67.2	67.5	27.6	-10.1	22.3	-11.1	-11.7	17.3
22.8	44.3	82.5	16.1	17.5	54.4	54.2	27.1	-10.7	21.9	-11.5	-11.9	16.8

date
25/11/88

23.3	51.1	81.1	14.7	16.3	63.5	63.6	26.6	-13.3	16.1	-12.1	-14.1	15.1
22.2	47.1	79.4	14.8	16.0	58.3	57.3	26.3	-14.2	16.6	-14.2	-15.0	15.1
22.0	44.4	79.2	14.6	16.0	53.9	53.3	25.8	-13.9	17.2	-14.3	-14.9	15.1
21.3	42.7	78.1	14.7	15.8	52.0	51.8	25.2	-13.5	18.2	-13.9	-14.3	15.1
21.5	42.4	78.9	14.9	16.1	51.3	51.0	24.9	-11.8	19.9	-12.2	-12.6	15.2
22.0	44.1	78.9	15.1	16.3	55.4	55.4	24.7	-10.8	21.4	-11.2	-11.4	15.6
22.6	45.1	79.2	15.8	16.9	56.0	56.0	25.3	-9.6	22.0	-10.4	-11.0	16.0
22.6	44.1	79.0	16.0	17.3	54.1	54.3	26.3	-8.4	21.9	-9.2	-10.2	16.4
22.8	44.3	78.2	16.3	17.5	54.2	54.2	27.1	-7.2	22.0	-8.6	-9.4	16.6
23.7	47.0	80.6	16.7	17.9	58.8	58.6	27.2	-8.3	22.7	-8.7	-9.3	17.1
23.6	45.4	79.5	16.8	18.2	55.5	55.1	27.7	-6.3	22.3	-7.9	-8.7	17.4
24.1	48.9	81.1	17.0	18.3	62.2	63.2	27.8	-8.2	22.6	-9.0	-9.6	17.4
24.3	46.4	79.9	17.3	18.4	57.4	57.4	28.1	11.8	21.7	-9.1	-10.1	17.7
24.4	46.7	80.0	17.4	18.5	57.1	56.8	28.0	20.3	22.0	-8.8	-10.6	17.7
24.7	47.7	81.0	17.7	19.0	59.3	59.3	28.1	-7.5	22.7	-9.3	-10.9	18.1

Table A2.6 (continued) Raw experimental performance data for the operating characteristics of the ammonia-water absorption system at Cerro Prieto.

date
23/11/88

T26	T27	T28	T29	T30	T31	PEV	PCO	FSOL	FREF	FWRE	FWCO	FWAB
21.3	30.6	----	75.1	99.8	23.1	4.13	12.03	0.063	0.023	0.000	0.568	1.010
21.5	30.8	----	75.1	98.8	23.2	4.20	12.11	0.063	0.023	0.000	0.568	1.010
21.4	30.5	----	74.3	98.5	23.1	4.21	12.15	0.063	0.023	0.000	0.568	1.010
21.3	30.6	----	75.2	99.1	23.1	4.20	12.19	0.063	0.023	0.000	0.568	1.010
21.7	30.8	----	74.8	98.9	23.5	4.20	12.31	0.063	0.023	0.000	0.568	1.010
21.2	30.5	----	74.1	98.9	23.0	4.17	12.13	0.063	0.023	0.000	0.568	1.010
20.7	30.0	----	74.4	98.8	22.4	4.12	11.88	0.063	0.023	0.000	0.568	1.010
20.3	29.6	----	74.0	99.2	22.0	4.01	11.77	0.063	0.022	0.000	0.568	1.010
20.3	29.8	----	75.3	99.5	22.0	3.89	11.89	0.063	0.022	0.000	0.568	1.010
20.2	29.5	----	75.2	99.5	22.2	3.87	11.75	0.063	0.022	0.000	0.568	1.010
20.4	29.5	----	74.6	98.5	22.1	3.87	11.77	0.063	0.022	0.000	0.568	1.010
20.5	29.6	----	73.8	98.1	22.3	3.93	11.80	0.063	0.022	0.000	0.568	1.010
20.3	29.8	----	74.0	99.0	22.0	3.90	11.85	0.063	0.022	0.000	0.568	1.010
20.4	29.9	----	74.5	98.9	22.2	3.96	11.97	0.063	0.022	0.000	0.568	1.010

date
24/11/88

17.3	24.7	----	65.6	92.1	18.9	3.89	10.13	0.063	0.021	0.000	0.568	1.010
17.7	24.5	----	63.4	88.7	19.1	3.73	10.11	0.063	0.019	0.000	0.568	1.010
18.1	24.2	----	62.3	88.9	19.3	3.52	9.99	0.063	0.020	0.000	0.568	1.010
18.4	24.2	----	61.7	85.8	19.6	3.38	10.07	0.063	0.016	0.000	0.568	1.010
19.7	24.5	----	62.2	97.1	21.0	3.12	10.04	0.063	0.015	0.000	0.568	1.010
20.3	25.5	----	62.7	88.4	21.3	3.14	10.43	0.063	0.013	0.000	0.568	1.010
20.4	25.2	----	58.6	86.1	21.4	3.18	10.40	0.063	0.013	0.000	0.568	1.010
19.7	24.8	----	54.9	83.2	21.1	3.17	10.01	0.063	0.012	0.000	0.568	1.010
19.2	24.7	----	56.7	87.0	20.6	2.98	10.16	0.063	0.015	0.000	0.568	1.010
18.8	23.8	----	53.6	82.1	20.1	2.99	9.89	0.063	0.015	0.000	0.568	1.010
18.5	23.4	----	50.1	79.7	19.7	3.04	9.76	0.063	0.015	0.000	0.568	1.010
17.1	23.1	----	53.7	86.8	18.7	2.96	9.72	0.063	0.015	0.000	0.568	1.010
16.5	22.3	----	60.6	90.9	18.0	2.79	9.48	0.063	0.014	0.000	0.568	1.010
16.5	22.1	----	63.7	88.8	17.9	2.59	9.41	0.063	0.014	0.000	0.568	1.010
16.5	21.5	----	56.4	78.5	17.6	9.24	0.00	0.014	0.000	0.568	1.010	1.010

date
25/11/88

14.9	18.4	----	53.2	82.6	15.7	2.31	8.31	0.063	0.011	0.000	0.568	1.010
15.1	18.2	----	48.6	78.9	15.7	2.27	8.24	0.063	0.011	0.000	0.568	1.010
14.9	19.0	----	47.3	78.7	15.9	2.31	8.47	0.063	0.011	0.000	0.568	1.010
14.9	19.6	----	46.2	79.7	15.9	2.36	8.66	0.063	0.012	0.000	0.568	1.010
15.2	20.3	----	47.8	78.4	16.2	2.56	8.87	0.063	0.015	0.000	0.568	1.010
15.4	20.9	----	48.2	81.1	16.6	2.70	9.05	0.063	0.014	0.000	0.568	1.010
15.8	21.1	----	50.3	80.7	17.0	2.73	9.12	0.063	0.014	0.000	0.568	1.010
16.2	21.1	----	49.4	78.7	17.2	2.87	9.07	0.063	0.014	0.000	0.568	1.010
16.4	21.1	----	49.0	78.8	17.4	2.94	9.14	0.063	0.014	0.000	0.568	1.010
16.7	22.0	----	51.8	83.3	17.9	2.97	9.36	0.063	0.014	0.000	0.568	1.010
17.1	21.5	----	51.1	78.5	18.0	3.01	9.23	0.063	0.014	0.000	0.568	1.010
17.2	22.0	----	51.6	86.3	18.1	2.91	9.27	0.063	0.014	0.000	0.568	1.010
17.5	21.2	----	52.3	78.4	18.2	2.85	9.05	0.063	0.011	0.000	0.568	1.010
17.6	21.2	----	50.7	79.2	18.3	2.80	9.02	0.063	0.012	0.000	0.568	1.010
17.9	22.1	----	51.3	83.8	18.6	2.73	9.35	0.063	0.013	0.000	0.568	1.010

Table A2.6 (continued) Raw experimental performance data for the operating characteristics of the ammonia-water absorption system at Cerro Prieto.

date 6/10/88		date 25/10/88		date 1/11/88		date 7/11/88	
time	FGS	time	FGS	time	FGS	time	FGS
13:00	62.4	12:30	39.8	10:30	55.8	11:30	31.2
13:30	52.9	13:00	29.8	11:00	55.4	12:00	33.5
14:00	51.7	13:30	35.3	11:30	51.7	12:30	33.2
14:30	52.3	14:00	37.2	12:00	52.6	13:00	32.9
15:00	52.0	14:30	37.1	12:30	49.7	13:30	33.2
15:30	46.9			13:00	50.1	14:00	34.9
16:00	47.5	26/10/88		13:30	48.6	14:30	33.1
						15:00	39.6
7/10/88		10:00	34.3	2/11/88			
		10:30	35.1			10/11/88	
10:00	66.9	11:00	23.6	11:00	43.8		
10:30	60.9	11:30	26.0	11:30	46.1	10:00	69.4
11:00	66.6	12:00	28.2	12:00	43.8	10:30	71.9
11:30	63.3	12:30	27.4	12:30	47.2	11:00	69.0
12:00	63.3	13:00	27.4	13:00	47.5	11:30	70.1
12:30	61.4	13:30	23.1	13:30	42.6	12:00	68.8
13:00	58.4	14:00	25.0	14:00	48.1	12:30	66.9
13:30	63.4			14:30	48.0	13:00	67.8
14:00	66.6	28/10/88				13:30	64.5
				3/11/88		14:00	64.8
10/10/88		10:00	60.2				
		10:30	61.2	11:00	49.4	11/11/88	
11:30	70.9	11:00	64.5	11:30	50.2		
12:00	72.7	11:30	66.4	12:00	43.7	10:00	64.1
12:30	67.0	12:00	63.0	12:30	41.7	10:30	65.8
13:00	68.5	12:30	64.1	13:00	44.1	11:00	69.1
13:30	68.4	13:00	64.0	13:30	45.4	11:30	72.9
14:00	68.1	13:30	64.0	14:00	45.3	12:00	71.5
		14:00	63.7	14:30	40.0	12:30	71.5
24/10/88						13:00	69.9
		31/10/88		4/11/88		13:30	70.7
11:30	42.0					14:00	69.1
12:00	42.5	11:30	58.6	10:30	45.8		
12:30	42.0	12:00	62.8	11:00	46.9	14/11/88	
13:00	41.9	12:30	44.4	11:30	44.7		
13:30	42.3	13:00	50.1	12:00	43.5	10:30	53.1
14:00	39.9	13:30	48.4	12:30	43.7	11:00	72.5
		14:00	46.4	13:00	39.4	11:30	75.4
		14:30	46.1	13:30	37.2	12:00	74.4
		15:00	45.4	14:00	38.0	12:30	73.6
				14:30	37.2	13:00	69.7

Table A2.6 (continued) Raw experimental performance data for the operating characteristics of the ammonia-water absorption refrigerator at the Cerro Prieto geothermal field.

date 15/11/88		date 18/11/88		date 24/11/88	
time	FGS	time	FGS	time	FGS
12:30	66.5	10:00	62.0	11:00	50.9
13:00	62.4	10:30	49.8	11:30	37.1
13:30	60.8	11:00	49.5	12:00	38.2
14:00	61.1	11:30	48.5	12:30	38.6
14:30	59.5	12:00	52.5	13:00	40.7
15:00	60.2	12:30	49.7	13:30	42.4
15:30	60.8	13:00	50.2	14:00	43.3
		13:30	46.6	14:30	36.1
16/11/88		14:00	49.1		
				25/11/88	
13:00	67.4	21/11/88			
13:30	57.8			11:00	21.5
14:00	57.9	11:30	75.2	11:30	27.1
14:30	55.4	12:00	74.7	12:00	25.8
15:00	54.6	12:30	71.2	12:30	32.4
15:30	52.5	13:00	73.4	13:00	32.8
		13:30	70.9	13:30	31.2
17/11/88		14:00	71.8	14:00	25.4
				14:30	31.0
10:00	53.6	22/11/88			
10:30	41.9				
11:00	50.0	11:00	50.4		
11:30	50.2	11:30	55.4		
12:00	49.0	12:00	51.6		
12:30	42.8	12:30	47.4		
13:00	46.8	13:00	43.7		
13:30	48.5	13:30	45.0		
14:00	47.8	14:00	43.5		
		14:30	45.9		
		23/11/88			
		11:00	50.7		
		11:30	53.1		
		12:00	61.0		
		12:30	59.3		
		13:00	50.8		
		13:30	53.1		
		14:00	59.7		
		14:30	57.0		

Table A2.6 (continued) Raw experimental performance data for the operating characteristics of the ammonia-water absorption refrigerator at the Cerro Prieto geothermal field.

BIBLIOGRAPHY

Absorption heat pumps congress, Paris, 20-22 March 1985, Published by the Commission of the European Communities, EUR 10007, (1985).

J.E. Aker, R.G. Squires and L.F. Albright, An evaluation of alcohol-salt mixtures as absorption refrigeration solution, ASHRAE Journal, 7, 90-92 (1965).

G. Alefeld, A high temperature absorption heat pump as topping process for power generation. Energy, 3(5) 649-656 (1978).

G. Alefeld, P. Maier-Laxhuber and M. Rothmeyer, Zeolite heat pump and heat transformer for load management, Proceedings of the 16th intersociety energy conversion engineering conference, I, pp 855-860 (1981).

G. Alefeld, What needs to be known about fluid pairs to determine heat ratios of absorber heat pumps and heat transformers, Heat pumps, prospects in heat pump technology and marketing, Proceedings of the 1987 IEA heat pump conference, K.H. Zimmerman (Ed.), Lewis Publishers Inc., Chapter 26, 375-387 (1987).

R.R. Al-hindi, A.M.A. Khalifa and M. Akyurt, Simulation studies of the behaviour of a heat pipe-assisted solar absorption refrigerator Applied Energy, 30(1), 61-80 (1988).

K. Badarinarayana, S.S. Murthy and M.V.K. Murthy, Thermodynamic analysis of R21-DMF vapour absorption refrigeration systems for solar energy applications, Int. J. Refrig., 5(2), 115-119 (1982).

M. Balakumar, S.S. Murthy and M.V.K. Murthy,. A comparative thermodynamic study of metal hydride heat transformers and heat pumps, J. Heat Recovery Systems, 5(6), 527-534 (1985).

H. Bokelmann and F. Steimle, Development of advanced heat transformers utilizing new working fluids, Int. J. Refrig., 9(1), 51-59 (1986).

H. Bokelmann and P. Paikert, Experience gained with industrial heat transformers. Development of new systems, Chem. Ing. Tech., 60(6) p. 489 (1988).

H. Bokelmann, Advanced absorption systems, Proceedings of a workshop held in London, Zeger and Miriam (Ed.), Commission of the European Communities, pp 332-341 (1988).

G.C. Blytas and F. Daniels, Concentrated solutions of sodium thiocyanate in liquid ammonia: solubility, density, vapor pressure, viscosity, thermal conductance, heat of solution and heat capacity, J. Am. Chem. Soc., 84(7), 1075-1083 (1962).

P. Bourseau and R. Bugarel, Absorption-diffusion machines: comparison of the performances of NH_3 - H_2O and NH_3 - NaSCN, Int. J. Refrig., 9(4), 206-214 (1986).

D. Butz and K. Stephan, Dynamic behaviour of an absorption heat pump, Int. J. Refrig., 12(4), 204-212 (1989).

P. Ciambelli and V. Tufano, A simplified model for water-sulfuric acid absorption heat transformer, Heat and Technology (calore e tecnologia), 5(1-2), 69-83 (1987).

P. Ciambelli and V. Tufano, The upgrading of waste heat by means of water-sulphuric acid absorption heat transformers, J. Heat Recovery Systems and CHP, 7(6), 517-524 (1987).

P. Ciambelli and V. Tufano, On the performance of advanced absorption heat transformer-I. The two stage configuration, J. Heat Systems and CHP, *(5), 445-450 (1988).

P. Ciambelli and V. Tufano, On the performance of advanced absorption heat transformer-II. The double absorption configuration, J. Heat Recovery Systems and CHP, 8(5), 451-457 (1988).

S.K. Chaudhari, D.V. Paranjape, M.A.R. Eisa and F.A. Holland, A study of the operating characteristics of a water-lithium bromide absorption heat pump, J. Heat Recovery Systems, 5(4), 285-297 (1985).

S.K. Chaudhari, D.V. Paranjape, M.A.R. Eisa and F.A. Holland, A comparative study of the operating characteristics of water-lithium chloride absorption heat pumps, J. Heat Recovery Systems, 6(1), 39-46 (1986).

L. Chen, A new ejector-absorber cycle to improve the COP of an absorption refrigeration system, Applied Energy, 30(1), 37-52 (1988).

E.C. Clark and O. Morgan, Chemical heat pumps for industry, Proceedings of the 16th intersociety energy conversion engineering conference, I pp 866-870 (1981).

S. Devotta and F.A. Holland, Comparison of theoretical rankine heat pump cycle-performance data for twenty-one working fluids, J. Heat Recovery Systems, 5(3), 225-231 (1985).

R.T. Ellington, G. Kunst, R.E. Peck and J.F. Reed, The absorption cooling process, Inst. of Gas Technology, Chicago, Res. Bull. No. 14 (1957).

M.A.R. Eisa, S.K. Chaudhari, D.I. Paranjape and F.A. Holland, Classified reference for absorption heat pump systems from 1975 to May 1985, J. Heat Recovery Systems, 6(1), 47-61 (1986).

M.A.R. Eisa and F.A. Holland, A study of the optimum interaction between the working fluid and the absorbent in absorption heat pump systems, J. Heat Recovery Systems, 7(2), 107-117 (1987).

K. Eriksson and A. Jernquist, Heat transformer with self-circulation: design and preliminary operational data, Int. J. Refrig., 12(1), 15-20 (1989).

J.M. George and S.S. Murthy, Influence of heat exchanger effectiveness of performance of vapour absorption heat transformers, Int. J. of Energy Research, 13, 455-475 (1989).

V.W. Goldschmidt and R.W. Henrick, Heat pumps (Basics, types and performance characteristics). Ann Rev. Energy, 9, 447-472 (1984).

K. Gommed and G. Grossman, Process steam generation by temperature boosting from solar ponds, Solar Energy 41(1), 81-89 (1988).

Ph. Grenier, J.J. Guilleminot, F. Meunier and M. Pons, Solar powered solid adsorption cold store, J. of Solar Energy Engineering, 110(3), 192-197 (1988).

G.S. Grover, M.A.R. Eisa and F.A. Holland, Thermodynamic design data for absorption heat pump systems operating on water-lithium chloride part one. Cooling. J. Heat Recovery Systems and CHP, 8(1), 33-41 (1988).

G.S. Grover, S. Devotta and F.A. Holland, Thermodynamic design data for absorption heat pump systems operating on water-lithium chloride-part II. Heating. J. Heat Recovery Systems and CHP, 8(5), 419-423 (1988).

G.S. Grover, S. Devotta and F.A. Holland, Thermodynamic design data for absorption heat transformers-part III. Operating on water-lithium chloride. J. Heat Recovery Systems and CHP, 8(5), 425-431 (1988).

G. Grossman and H. Perez Blanco, Conceptual design and performance analysis of absorption heat pumps for waste heat utilization, Int. J. Refrig., 5(6) 361-370 (1982).

G. Grossman and K.W. Childs, Computer simulation of a lithium bromide-water absorption heat pump for temperature boosting. ASHRAE Transactions, 89(1), Paper AC-83-05, No. 4 (1983).

R.L. Harris, G.K. Olson, C.S. Mah and J.H. Bujalski, Geothermal absorption refrigeration for food processing industries, Final report, Aerojet energy conversion company, prepared for the Department of Energy, (1977).

S. Hasaba, T. Uemura and H. Narita, Some physical properties of monomethylamine-water solutions at various temperatures, Refrigeration, 36(405), 619-623 (1961).

H.T. Haukas, Design of a plate-type evaporator for heat pumps, Int. J. Refrig., 7(1) 59-63 (1984).

Heat pumps and heat transformers, The Chemical Engineer, (41-43), July (1989).

K.E. Herold and R. Radermacher, Absorption heat pumps, Mechanical Engineering, 68-73, August (1989).

D.L. Hodgett, E. Chalmers and A.A. Mitchell, A steam heat pump for increasing the energy efficiency in distillation, ECRC/M2184, Electric Council Research Centre, (1987).

D.L. Hodgett and L. Aahlby, Compression-absorption heat pumps, Proceedings of a workshop held in London, Zeger and Miriam (Ed.), Commission of the European Communities, 204-215 (1988).

G. Holldorf, Revisions of absorption refrigeration efficiency, Hydrocarbon Processing, 149-155, July (1979).

S. Iyoki and T. Uemura, Physical and thermal properties of the water-lithium bromide-zinc chloride-calcium bromide system, Int. J. Refrig., 12(5), 272-277 (1989).

M.R. Jeday and P.Le Goff, Search for an optimal sorbent for absorption heat pumps and mechanical mixing machines, Part 2: application to solutions in liquid ammonia, Int. J. Refrig., 11(3), 164-172 (1988).

S.I. Kaplan (Ed.), A survey and assessment of chemical heat pumps, ORNL/TM-9544, Oak Ridge National Laboratory (1985).

S.C. Kaushik, C.S. Tomar and S. Chandra, Coefficient of performance of an ideal absorption cycle, Applied Energy, 14, 115-121 (1983).

K.F. Knoche, K. Molitov, C.W. Seltz, H. Zerres and M. Saghafi, Progress in development of the periodically operating absorption heat pump, IEA-HPC Newsletter, 6(4), 17-20 (1988).

J.F. Kreider and F. Kreith, Solar heating and cooling, Engineering-practical design and economics, McGraw Hill, New York, pp 161-172 (1977).

V.M. Kripalani, S.S. Murthy and M.V.K. Murthy, Performance analysis of a vapour absorption heat transformer with different working fluid combinations, J. Heat Recovery Systems, 4(3), 129-140 (1984).

W. Koebbeman and J. Wagner, Hybrid heat pump application study, EM-4654, Research Project 2220-1, Final Report, July (1986).

D.A. Kouremenos, K.A. Antonoupoulos and E. Rogdakis, Performance of solar NH_3/H_2O absorption cycles in the Athens area, Solar Energy, 39(3), 187-195 (1987).

D.A. Kouremenos and E.D. Rogdakis, Thermodynamic cicles for refrigeration and heat transformer units H_2O/LiBr, Forschung im Ingenieruwesen, 54(2), 39-47 (1988).

P. Kumar and S. Devotta, Modelling of the thermal behaviour of a solar regenerator for open-cycle cooling systems, Applied Energy, 34(4), 287-296 (1989).

R.M. Lazzarin, Commercially available absorption heat pumps: some experimental test, Int. J. Refrig., 11(2), 96-99 (1988).

G.O.F. Löf, G. Cler and T. Brisbane, Performance of a solar dessicant cooling system, J. of Solar Energy Engineering, 110(3), 165-171 (1988).

C.H.M. Machielsen, J.J. Westra and H. Becker, Compact heat and mass exchangers in sorption systems, IEA-HPL Newsletter, 6(4), 20-23 (1988).

R.A. Macriss, Selecting refrigerant-absorbent fluid systems for solar energy utilization, ASHRAE Transactions, 82(1), 975-986 (1976).

R.A. Macriss, Recommended thermodynamic data for NH_3-H_2O in the temperature range of -50°C to 316°C and pressure range of 0.05 to 170 bar, IEA Newsletter, 7(2), 48-53 (1989).

V.S. Maisotsenko, Systems for cooling natural gas in regions of hot and dry climate, Applied Solar Energy (Gelio tekhnika), 23(4), 56-60 (1987).

G.A. Mansoori and V. Patel, Thermodynamic basis for the choice of working fluids for solar absorption cooling systems, Solar Energy, 22(6), 483-491 (1979).

L. Mattarolo, Solar powered air conditioning systems: a general survey, Int. J. Refrig., 5(6), 371-375 (1982).

A.J. Morrissey and J.P. O'Donnell (Fellow), Endothermic solutions and their application in absorption heat pumps, Chem. Eng. Res. Des., 64, 404-406 (1986).

M. Narodoslawsky, G. Ottey and F. Moser, New working pairs for medium and high temperature industrial absorption heat pumps, J. Heat Recovery Systems and CHP, 8(5), 459-468 (1988).

K.R. Patil, M.N. Kim, M.A.R. Eisa and F.A. Holland, Experimental evaluation of aqueous lithium halides as single-and double-salt systems in absorption heat pumps, Applied Energy, 34, 99-111 (1989).

S.I. Pereira Duarte and R. Bugarel, Optimal working conditions for an absorption heat transformer-analysis of the H_2O/LiBr theoretical cycle, J. Heat Recovery Systems and CHP, 9(6), 521-532 (1989).

E.H. Perry, The theoretical performance of the lithium bromide-water intermittent absorption refrigeration cycle, Solar Energy, 17, 321-323 (1975).

M. Pflugal and F. Moser, Behaviour of absorbers with falling films of salt solutions in heat pumps applications, Paper G1, Proceedings of the 3rd international symposium on the large scale applications of heat pumps, published by BHRA, pp 141-148 (1987).

U. Plocker, U. Preussner und B. Brandt, Absorption heat transformers for the chemical industry as seen from a users point of view, Chem. Ing. Tech., 60(2), 103-108 (1988).

M. Pons and Ph. Grenier, Experimental data on a solar-powered icemaker using activated carbon and methanol adsorption pair, J. of Solar Energy Engineering, 109(4), 303-310 (1987).

R. Radermacher, Arbeitsstoffkombination en für absorptionswärme pumpen, Ph.D Thesis, Technishe Universität München, (1981).

H. Raheman and C.P. Gupta, Development of a solar-energy operated vapour-absorption-type refrigerator, Applied Energy, 34(2), 89-98 (1989).

J.P. Roberson, C.Y. Lee, R.G.S. Squires and L.F. Albright, Vapor pressure of ammonia and methylamines in solutions for absorption refrigeration systems, ASHRAE Transactions, 72(1), 198-208 (1966).

F.E. Swallow and I.E. Smith, Vapour absorption into liquid films on rotating discs, Int. J. Refrig., 12(5), 291-294 (1989).

K.P. Tyagi, Water-ammonia heat transformers, J. Heat Recovery Systems and CHP, 7(5), 423-433 (1987).

K.P. Tyagi, S. Mathur, A. Sinch, A. Srinivas and G. Mathur, Working fluids for heat transformers, J. Heat Recovery Systems and CHP, 9(2), 175-181 (1989).

S.C.G. Schulz, Equations of state for the system ammonia-water for the use with computers, reprint from the Proceedings of the VIIth International Congress of Refrigeration, Washington, D.C., (1971).

K. Stephan, Heat transformer: Principles and applications, Chem. Ing. Tech., 60(5), 335-348 (1988).

W.F. Stoecker and L.D. Reed, Effect of operating temperatures on the coefficient of performance of aqua ammonia refrigerant systems, ASHRAE Transactions, 77(1), 163-170 (1971).

N.A. Schchetinina, S.Z. Zhadan and V.A. Petrenko, Experimental investigation of a solar-ejector freon refrigerating machine, Applied Solar Energy (Geliotekhnika), 23(3), 66-74 (1987).

K. Stephan and D. Seher, Heat transformer cicles-II. Thermodynamic analysis and optimization of a single-stage absorption heat transformer, J. Heat Recovery Systems, 4(5), 371-375 (1984).

M. Renz and F. Steimle, Thermodynamic properties of the binary system methanol-lithium bromide, Int. J. Refrig., 4(2), 97-101 (1981).

G. Restuccia, G. Cacciola and R. Quagliata, Identification of zeolites for heat transformer chemical heat pump and cooling systema, Int. J. Energy Research, 12, 101-111 (1988).

R. Gorman and P. Moritz, Comparative economics and energy consumption of chemical heat pumps and competitive systems, Proceedings of the 16th intersociety energy conversion engineering conference I, pp 861-865 (1981).

K. Stephan and D. Seher, Heat transformer cycles-I. One-and two-stages processes, J. Heat Recovery Systems, 4(5), 365-369 (1984).

U. Stuven, Development and testing of a new substance system for use in absorption heat transformer, Chem. Ing. Tech., 61(6), 492-493 (1989).

H. Uddholm and F. Setterwall, Model for dimensioning a falling film absorber in an absorption heat pump, Int. J. of Refrig., 11(1), 41-46 (1988).

E.P. Whitlow, Relationship between heat source, temperature, heat sink temperature and coefficient of performance for solar-powered absorption air conditioners, ASHRAE Transactions, 82(1), 950-958 (1976).

B. Ziegler and Ch. Trepp, Equations of state for ammonia-water mixtures, Int. J. Refrig., 7(2), 101-106 (1984).

AUTHOR'S PUBLICATIONS

1. R. Best, C.L. Heard, H. Fernández and J. Siqueiros, Developments in geothermal energy in Mexico-Part five: The commissioning of an ammonia/water absorption cooler operating on low enthalpy geothermal energy, J. Heat Recovery Systems, 6(3), 209-216 (1986).

2. M.A.R. Eisa, R. Best and F.A. Holland, Working fluids for high temperature heat pumps, J. Heat Recovery Systems, 6(4), 305-311 (1986).

3. M.A.R. Eisa, R. Best and F.A. Holland, Thermodynamic design data for absorption heat transformers: Part I, Operating on water-lithium bromide, J. Heat Recovery Systems, 6(5), 421-432 (1986).

4. M.A.R. Eisa, R. Best and F.A. Holland, Thermodynamic design data for absorption heat transformers: Part 2, Operating on water-calcium chloride, J. Heat Recovery Systems, 6(6), 443-450 (1986).

5. M.A.R. Eisa, R. Best, P.J. Diggory and F.A. Holland, Heat pump assisted distillation: Part 5, A feasibility study on absorption heat pump assisted distillation systems, Int. J. Energy Research, 11, 179-191 (1987).

6. M.A.R. Eisa, R. Best and F.A. Holland,
Open and closed cycle mechanical vapour compression heat pump assisted sea-water purification systems. Applied Energy, 2, 203-208 (1987).

7. M.A.R. Eisa, R. Best and F.A. Holland,
Heat pump assisted water purification systems, Proceedings of the 3rd BHRA International Symposium on the Large Scale Applications of Heat Pumps, Oxford, England, paper B2, pp 35-44 (1987).

8. M.A.R. Eisa, R. Best and F.A. Holland,
Thermodynamic design data for absorption heat pump systems operating on water-calcium chloride, Applied Energy, 28, 69-81 (1987).

9. R. Best, M.A.R. Eisa and F.A. Holland,
Thermodynamic design data for absorption heat pump systems operating on ammonia-water: Part I, Cooling, J. Heat Recovery Systems and CHP, 7(2), 167-175 (1987).

10. R. Best, M.A.R. Eisa and F.A. Holland,
Thermodynamic design data for absorption heat pump systems operating on ammonia-water: Part 2, Heating, J. Heat Recovery Systems and CHP, 7(2), 177-185 (1987).

11. R. Best, M.A.R. Eisa and F.A. Holland,
Thermodynamic design data for absorption heat pump systems operating on ammonia-water: Part 3, Simultaneous heating and cooling, J. Heat Recovery Systems and CHP, 7(2), 187-194 (1987).

12. R. Best, M.A.R. Eisa and F.A. Holland,
Thermodynamic design data for absorption heat transformers: Part 3, Operating on ammonia-water, J. Heat Recovery Systems and CHP, 7(3), 259-272 (1987).

13. R. Best, C.L. Heard and F.A. Holland,
Developments in geothermal energy in Mexico-Part sixteen: the potential for heat pump technology, J. of Heat Recovery Systems and CHP, 8(3), 185-202 (1988).

14. M.A.R. Eisa, R. Best, P.J. Diggory and F.A. Holland,
Heat pump assisted distillation: Part 7, A feasibility study on heat transformer assisted distillation systems, Int. J. Energy Research, 12, 1-10 (1988).

15. R. Best, C.L. Heard, P. Peña, H. Fernández and Prof. F.A. Holland,
Developments in geothermal energy in Mexico-Part twenty six: Experimental assessment of an ammonia/water absorption cooler operating on low enthalpy geothermal energy, J. of Heat Recovery Systems and CHP, 10(1), 61-70 (1990).

16. R. Best, C.L. Heard, J. Siqueiros, D. Barragán and H. Fernández,
Heat pump developments in Mexico, Handbook on heat pump technology, F.A. Holland and C.L. Heard (Ed.), Instituto de Investigaciones Eléctricas, Cuernavaca, México, 8.1-8.19 (1990).

17. R. Best and F.A. Holland,
A study of the operating characteristics of an experimental absorption cooler using ternary systems, Int. J. Energy Research (in press).

18. R. Best, W. Rivera, I. Pilatowsky and F.A. Holland,
Thermodynamic design data for absorption heat transformers: Part 4, operating on ammonia-lithium nitrate, J. Heat Recovery Systems and CHP, (in press).

19. M. Martínez and R. Best,
Developments in geothermal energy in Mexico-Part thirty: Supply and demand perspectives for the year 2000, J. Heat Recovery Systems and CHP, (in press).

20. R. Best, L. Porras and F.A. Holland,
Thermodynamic design data for absorption heat pump systems operating on ammonia-lithium nitrate, Part 1: Cooling, J. Heat Recovery Systems and CHP, (in press).

21. R. Best, W. Rivera, I. Pilatowsky and F.A. Holland,
Thermodynamic design data for absorption heat pump systems operating on ammonia-lithium nitrate, Part 11: Heating, J. Heat Recovery Systems and CHP, (in press).

22. R. Best, W. Rivera, I. Pilatowsky and F.A. Holland,
Thermodynamic design data for absorption heat pump systems operating on ammonia-lithium nitrate, Part 111: Simultaneous cooling and heating, J. Heat Recovery Systems and CHP, (in press).